AD-A007 886

REINFORCED CONCRETE CONSTITUTIVE RELATIONS

S. Adham, et al

Agbabian Associates

Prepared for:

Air Force Weapons Laboratory
Defense Nuclear Agency

February 1975

AFWL-TR-74-72

AFWL-TR
74-72

REINFORCED CONCRETE CONSTITUTIVE RELATIONS

S. Adham, A. Bhaumik, J. Isenberg

Agbabian Associates

El Segundo, CA 90245

February 1975

Final Report for Period 6 March 1973 - 6 March 1974

Approved for public release; distribution unlimited.

This research was sponsored by the Defense Nuclear Agency under Subtask Y99QAXSC157, Work Unit 04, Strategic Structures Vulnerability/Hardening.

Prepared for

Director
DEFENSE NUCLEAR AGENCY
Washington, D.C. 20305

AIR FORCE WEAPONS LABORATORY
Air Force Systems Command
Kirtland Air Force Base, NM 87117

REPORT DOCUMENTATION PAGE

READ INSTRUCTIONS BEFORE COMPLETING FORM

1. REPORT NUMBER: AFWL-TR-74-72	2. GOVT ACCESSION NO.
3. RECIPIENT'S CATALOG NUMBER	
4. TITLE (and Subtitle): REINFORCED CONCRETE CONSTITUTIVE RELATIONS	5. TYPE OF REPORT & PERIOD COVERED: Final Report, 6 March 1973-8 March 1974
6. PERFORMING ORG. REPORT NUMBER	
7. AUTHOR(s): S. Adham, A. Bhaumik, J. Isenberg	8. CONTRACT OR GRANT NUMBER(s): F29601-73-C-0070
9. PERFORMING ORGANIZATION NAME AND ADDRESS: Agbabian Associates, 250 N. Nash Street, El Segundo, CA 90245	10. PROGRAM ELEMENT, PROJECT, TASK AREA & WORK UNIT NUMBERS: Program Element 61102H, Project WDNS, Subtask Y990AXSC157
11. CONTROLLING OFFICE NAME AND ADDRESS: Defense Nuclear Agency, Washington, DC 20305	12. REPORT DATE: February 1975
	13. NUMBER OF PAGES: 358
14. MONITORING AGENCY NAME & ADDRESS (if different from Controlling Office): Air Force Weapons Laboratory, Kirtland Air Force Base, NM 87117	15. SECURITY CLASS. (of this report): UNCLASSIFIED
	15a. DECLASSIFICATION/DOWNGRADING SCHEDULE

16. DISTRIBUTION STATEMENT (of this Report)

Approved for public release; distribution unlimited.

17. DISTRIBUTION STATEMENT (of the abstract entered in Block 20, if different from Report)

18. SUPPLEMENTARY NOTES

19. KEY WORDS (Continue on reverse side if necessary and identify by block number)

Reinforced concrete	Cracking
Constitutive relations	Rebonding
Stress strain	Bond slip relations
Finite element	Dynamics

20. ABSTRACT (Continue on reverse side if necessary and identify by block number)

A mathematical model of reinforced concrete is derived from stress/strain relations of reinforcing steel and plain concrete, and from considering slip in bond between them. The stress/strain relations are nonlinear due to inelasticity of the concrete and steel and to cracking. They are presented in the form of a variable modulus model for use in a finite-element code. The stress/strain relations for plain concrete are based on experimental data

(over)

ABSTRACT (cont'd)

obtained under uniaxial, biaxial and triaxial states of stress. Additional laboratory experiments were performed under this contract to investigate the bond-slip relation in tension and in compression. The model stress/strain relation in each principal stress direction is affected by the other two principal stresses. The form of the stress/strain relation and the manner in which it is affected by the lateral principal stresses is different in tension and compression. Until cracking occurs, properties of the model depend on the entire stiffness of steel and concrete. After cracking, a composite modulus is used which reflects the combined stiffness of steel and concrete and takes into account the extent to which bond between steel and concrete is broken. This model is incorporated in a dynamic inelastic finite-element code and is used to analyze the response of reinforced concrete members such as beams, deep beams, beam columns, and ring beams, subjected to static and dynamic loading. The results of analysis are in general agreement with available experimental observations. Recommendations for improvement in the material model are made as a result of the correlation studies.

This final report was prepared by Agbabian Associates, El Segundo, California, under Contract F29601-73-C-0070, Job Order WDNS3417 with the Air Force Weapons Laboratory, Kirtland Air Force Base, New Mexico. Captain Jerry S. Doughty (DEV) was the Laboratory Project Officer-in-Charge.

When US government drawings, specifications, or other data are used for any purpose other than a definitely related Government procurement operation, the Government thereby incurs no responsibility nor any obligation whatsoever, and the fact that the Government may have formulated, furnished, or in any way supplied the said drawings, specifications, or other data, is not to be regarded by implication or otherwise, as in any manner licensing the holder or any other person or corporation, or conveying any rights or permission to manufacture, use, or sell any patented invention that may in any way be related thereto.

This technical report has been reviewed and is approved for publication.

JERRY S. DOUGHTY
Captain, USAF
Project Officer

FOR THE COMMANDER

JOHN J. OSBORN
Lt Colonel, USAF
Chief, Facility Survivability Branch

WILLIAM B. LIDDICOET
Colonel, USAF
Chief, Civil Engineering Research Division

DO NOT RETURN THIS COPY. RETAIN OR DESTROY.

CONTENTS

CONTENTS (continued)

CONTENTS (continued)

ILLUSTRATIONS

ILLUSTRATIONS (continued)

ILLUSTRATIONS (continued)

ILLUSTRATIONS (continued)

ILLUSTRATIONS (continued)

ILLUSTRATIONS (continued)

ILLUSTRATIONS (concluded)

TABLES

LIST OF SYMBOLS

A, B	Transformation matrices (in Eq. 91 ff.)
$\overline{A}$	Coefficient of dowel action
$A_1, A_2, \ldots, A_6$	Coefficients used in incremental stress-strain relations (Ref. 51)
A_s	Cross sectional area of steel
$A_{s_I}, A_{s_{II}}$	Areas of steel reinforcement in concrete (Ref. 1)
A_i^c	Effective concrete ratio in the i-direction
A_i^s	Effective steel ratio in the i-direction
C	Matrix for stress/strain relations
$C_{ijk\ell}$	Elastic stress/strain relationships
D	Intact bonded length of concrete after cracking (Ref. 1)
D	Poisson's ratio multiplier
E	Tangent modulus in uniaxial loading
E_1, E_2	Tangent moduli in direction 1, 2
E'_{1b}	Initial tangent modulus in biaxial compression
E_c	Initial tangent modulus for concrete
E_i, E_j	Tangent moduli in direction i, j
E_s	Young's modulus of steel
E_s	Secant modulus of concrete at ultimate load (Ref. 53)
$\overline{E}_i$	Effective composite modulus
E_{oc}	Initial tangent modulus for concrete in unconfined compression

LIST OF SYMBOLS (continued)

E_{os}	Elastic Young's modulus of steel bars (Ref. 1)
E_{pc}	Tangent modulus for concrete in the inelastic range
E_{ps}	Plastic Young's modulus of steel bars (Ref. 1)
E_{sc}	Secant modulus based on ultimate stress and corresponding strain
E_i^c	Effective concrete modulus
F_1, F_2	Yield surface functions (ref. 51)
G	Dowel shear modulus
G_{12}	Composite shear modulus (Ref. 1)
G_s	Shear modulus of steel
G_{ij}	Biaxial shear modulus of concrete
H	Axial force
$I_2'^p$	Second invariant of the plastic-strain deviator (Ref. 51)
J_1	First invariant of stress (Ref. 51)
J_2'	Second invariant of stress deviator (Ref. 51)
K_1, K_2	Hardening parameters (Ref. 51)
K_h	Axial stiffness
K_v	Transverse stiffness
L	Length of specimen or element
M	Moment (Ref. 58)

N	Axial tension force of bar (Ref. 65)
N_y	Axial tensile force inducing yield in pure tension (Ref. 65)
P	Applied load
P_x, P_y	Load applied in x and y directions, respectively (Ref. 4, 20, 21)
T	Tension force (Ref. 58)
T_f	Failure load of dowel shear
V	Transverse force
V_s	Transverse shear (Ref. 58)
W	Unit weight of concrete (ACI Code 318-71)
W_{ave}	Crack width (Ref. 33)
X, Y, Z	Global coordinate for entire structure
X, Y, Z	Submatrices of C matrix (Eq. 71 - 76)
Z_c	Shear contribution of concrete
Z_s	Shear contribution of steel
a^*	Effective length of longitudinal cracked zone (Ref. 58)
d	Unbonded (cracked) length of concrete (Ref. 1)
$d\varepsilon_{k\ell}$	Total strain increment
$d\sigma_i$	Stress increment in the i-direction
$d\sigma_{ij}$	Incremental stress
f	Maximum stress at which idealized stress-strain curves change slope

LIST OF SYMBOLS (continued)

f_c'	Unconfined compressive strength of concrete
$\overline{f}_c$	Experimental parameter for the unconfined compressive strength of concrete
f_o	Concrete stress (Ref. 84)
$f_o(max)$	Max concrete stress (Ref. 84)
f_s	Yield strength of steel (Ref. 1)
f_t	Unconfined tensile strength of concrete
f_t'	Biaxial tensile strength of concrete
f_y	Yield stress of steel in a uniaxial tension test
$g_1(J_1)$	Function of J_1 (Ref. 51)
h_1, h_2	Functions of the stress and plastic strain invariants (Ref. 51)
n	Dowel coefficient of local compression of concrete (Ref. 65)
p_{xs}, p_{ys}, p_{zs}	Steel ratios in steel directions
r	Constant for plastic capped model (Ref. 51)
t	Thickness of concrete cover (Ref. 33)
x, y, z	Local coordinates for element
x_s, y_s, z_s	Steel directions
y_1 -- y_{25}	Constants used for yield surfaces (Ref. 51)
Δ	Displacement (Ref. 58)
α	Dowel factor
α_x, β_x, γ_x	Angles between x-axis and X-, Y-, and Z axes, respectively

LIST OF SYMBOLS (continued)

$\bar{\alpha}$	Dowel factor multiplier
β	An experimental parameter corresponding to angle of internal friction
β_l	Ratio of principal stress in the orthogonal direction to the principal stress in the direction considered
γ	Dowel constant (Ref. 65)
γ_{shear}	Dowel shear strain
δ	Angle of stirrups in degrees (Ref. 65)
ε_1	Concrete strain in the 1-direction
ε_h	Relative displacement parallel to steel reinforcement
ε_i	Strain in direction i
ε_p	Peak strain
ε_s	Steel strain
ε_v	Relative displacement perpendicular to steel
ε^p_{ij}	Elastic strain increments
ε^p_{vc}	Volumetric plastic strain
η	Slope of cracking envelope
θ	Cracking angle (extent of bond deterioration (Ref. 1))
λ	Ratio of concrete contributing to overall stiffness
λ'	Biaxial compression factor (Ref. 53)
$\bar{\lambda}$	Bond-slip parameter in compression
ν	Poisson's ratio
ν_{ij}	Poisson's ratio of concrete in biaxial directions

LIST OF SYMBOLS (concluded)

ν_{st}	Poisson's ratio for steel (Ref. 1)
ρ	Dowel action coefficient (Ref. 65)
σ_1	Concrete stress in the i-direction
σ_c	Cube strength of concrete (Ref. 65)
σ_h	Axial stress
σ_i	Effective average stress in i-direction
σ_o	Unconfined compressive strength of concrete (Ref. 53)
σ_p	Peak stress
σ_s	Stress in steel reinforcing bar
σ_v	Transverse stress
σ_y	Yield stress of steel (Ref. 65)
σ_i^c	Stress in concrete in i-direction
τ_f	Failure stress of dowel shear
ϕ	Bar size (Ref. 65)
φ	Inclination of steel reinforcement to global coordinates (Ref. 1)

SECTION I

INTRODUCTION

The purpose of this study was to include a number of recent advances in theoretical and experimental behavior of reinforced and plain concrete in a computer program for analyzing plain or reinforced concrete structures. The properties of reinforced concrete are represented by variable moduli that combine the stiffness of steel and concrete and can change due to (1) cracks, (2) progressive failure of bond, (3) orthotropy due to different tangent moduli in different directions, (4) general orthotropy due to inelasticity of concrete in compression and cracks in tension, (5) confining effects, and (6) inelasticity of steel.

Although a model of this type was originally developed by Isenberg and Adham in 1969 (Ref. 1), the present study aims at specific types of improvements as follows:

- Improved constitutive properties of plain concrete, especially in multiaxial compression
- Improved representation of dowel action
- Improved representation of bond slip, including review of previous work and some new experiments
- Inclusion of rebonding capability
- Development of a computer program that incorporates the constitutive properties and that can be inserted with few or no changes into a wide variety of continuum finite element and finite difference programs

The present study was carried in four primary steps as follows:

STEP 1. The purpose of this step was to refine the formulation of the material model proposed by Isenberg and Adham (Ref. 1) on the basis of experimental and analytical data that became available after this model was proposed

in 1969. The work included: (1) literature review, (2) evaluation of data that are pertinent to the improvement of the Isenberg-Adham model, (3) modification of the model based on the above pertinent data.

STEP 2. The purpose of this step was to develop a set of subroutines for the plain and reinforced concrete models developed under Step 1. The subroutines are designed to be used with finite element or finite difference codes and can handle plane stress, plane strain, axisymmetric, and three-dimensional states of stress or strain.

In the intended application a solution is obtained by the step-by-step method of integration. The subroutines calculate stress and strain at the end of the current step, based on the current strain increment. However, the capability of calculating strains from a known state of stress was also included.

STEP 3. The purpose of this step was to obtain new experimental data on bond slip and to compare the results with the assumptions contained in the mathematical model. Cylindrical specimens of concrete were each cast with one reinforcing bar cast concentrically. Strain gages were placed on the inner surface of the bar and the outer surface of the concrete. One experiment was performed on bond slip in tension, while another experiment was performed on bond slip in compression. Each experiment used two instrumented specimens and one noninstrumented specimen on which only total elongation/contraction were measured. Auxiliary tests were made on noninstrumented specimens to determine the physical properties of concrete.

STEP 4. The purpose of this step was to incorporate the computer package developed under Step 2 into an existing dynamic, inelastic, two-dimensional continuum finite element code (FEDIA), which has been developed by Agbabian Associates. The new version of FEDIA, which includes the new material package, is called FEDRC. The FEDRC code was used to analyze several reinforced concrete structures in order to demonstrate the capabilities of the material model developed under this study. Five static cases and four dynamic cases were analyzed, for a total of nine demonstration cases. Cases 1 and 2 represented static behavior of deep beams, while static cases 3, 4, and 5 were aimed at

representing the extreme condition of beam columns under static loads. The first dynamic case was a deep beam subjected to impact loading, while the second case demonstrated dynamic beam column response. The third dynamic case was aimed at demonstrating the capability of the code to model the behavior of reinforced concrete silos. The fourth dynamic case represented the behavior of reinforced concrete beams under impact loading. The results of these demonstration cases were compared with available experimental data.

The main application of the present work is to the analysis of the static or dynamic response of reinforced concrete structures. Although the examples reported are two-dimensional, the computer program is capable of analyzing three-dimensional structures.

Section II of this report is a review of current approaches to analyzing composite models of reinforced concrete.

Section III is a discussion of the recent data on parameters to construct a composite reinforced concrete model.

Section IV describes the method of analysis used in this project. The fundamental assumptions and the formulation of the model are given.

Section V includes a description of the experimental studies.

Section VI contains a detailed description of the cases studied and discussion of the results.

Sections VII and VIII provide a summary and conclusions, derived from this study, and offer recommendations.

The computer package MATPAC (Material Package), used in this study, is described in Appendix I. The procedure for setting up input for the analytical model is given in Appendix II.

Units of measurement are given throughout in both English and System International units.

SECTION II

REVIEW OF CURRENT APPROACHES USED TO FORMULATE COMPOSITE MODELS

1. BACKGROUND AND SCOPE OF REVIEW

A rigorous analysis of a reinforced concrete structure requires the idealization of the structure as a composite model. The formulation of such a model is complicated by the following factors.

- The reinforced concrete member is composed of two materials: steel and concrete.
- The stress/strain relationship for reinforced concrete is nonlinear.
- The data on confining effects and failure theory for concrete under biaxial or three-dimensional states are limited.
- The influence of creep and shrinkage may need to be accounted for.
- The inception and propagation of cracks, the associated bond-slip relationships, and change in topology* are difficult to model.
- The effect of stirrups, dowel action, and aggregate interlock at cracks on shear transfer mechanism is not clearly understood.
- The orthotropy due to reinforcement, cracks, material nonhomogeneity, and anisotropy may change the effective properties during a solution updating, thus requiring successive evaluation and transformation of composite properties.

Significant progress has recently been made in developing analytical methods to examine reinforced concrete structures. The finite element method has provided the basis for most of the new analytical methods.

There are presently two distinct types of constitutive equations that are used in finite element or finite difference models of reinforced concrete. The discrete cracking element approach, advanced by Ngo and Scordelis (Ref. 2) and

*Topography of the surface.

by Nilson (Ref. 3), uses a special linkage element to represent the bond between steel and concrete. A different approach, proposed by Isenberg and Adham (Ref. 1), develops a composite modulus from individual properties of concrete and steel, and the bond between them.

As a result of the differences in techniques used to account for composite behavior, the two approaches have developed along different lines. The discrete cracking element approach allows a much simpler model of concrete properties to be formulated because the cracks occur between finite elements rather than within them. The equivalent continuum approach requires the crack directions to be computed and stored on an element-by-element basis. The properties of the continuum elements become orthotropic as cracking and inelasticity progress.

Both the scope of application and formulation of the discrete cracking element approach have been expanded and refined by several authors (Ref. 4) to include beams and shear walls subjected to static loading. The equivalent continuum approach has been applied to cylindrical concrete silos embedded in rock through which the static equivalent of dynamic ground shock loading is applied (Ref. 5). The finite element method has provided the basis for most of the analytical solutions that use these two approaches.

2. BASIC FINITE ELEMENT MODELS USED FOR THE ANALYSIS OF REINFORCED CONCRETE STRUCTURES

The finite element method has provided an extremely powerful tool for the analysis of complex structures and continuous media (Refs. 6-11). This method has been used to solve an extensive range of elastostatic, as well as elastodynamic, problems (Refs. 11-14). The method proved successful also in the solution of elastic-plastic problems (Refs. 15-17).

A comprehensive survey of the literature on application of the finite element method to the analysis of reinforced concrete structures was made by Scordelis (Ref. 4). The following material presents a summary of finite element models based on the linkage element and continuum approaches. In addition, brief summaries are included of some pertinent applications of the finite element method which are not necessarily based on the two approaches under discussion.

a. Original Linkage--Element Model

The first finite element model for the analysis of a reinforced concrete beam was described by Ngo and Scordelis (Ref. 2). Simple beams were represented by two-dimensional triangular finite elements. A special linkage element was developed to represent bond-slip phenomena. This element, which is illustrated in figure 1, links continuum elements representing steel reinforcing to those representing concrete at discrete points. The linkage element has two degrees of freedom corresponding to relative displacement between steel and concrete along the reinforcement (ε_h) and perpendicular to the reinforcement (ε_v). The bond stress-strain relationship is given by

$$\begin{Bmatrix} \sigma_h \\ \sigma_v \end{Bmatrix} = \begin{bmatrix} K_h & 0 \\ 0 & K_v \end{bmatrix} \begin{Bmatrix} \varepsilon_h \\ \varepsilon_v \end{Bmatrix} \tag{1}$$

The axial and transverse stiffness, K_h and K_v, are prescribed in the natural coordinate system, which is parallel and perpendicular to the axis of the bar. The strains and displacements are related by the displacement transformation illustrated in figure 1. In order to add the stiffness of the linkage element to the global stiffness matrix, transformation to global coordinates is performed.

With the aid of the linkage element, it was possible to construct an analytical model for the study of reinforced concrete beams. A typical result from this analysis method is shown in figures 2 and 3. The result agrees with intuition in that stress in the steel bar is maximum at a crack, the bond force is zero at the crack and reaches maximum of opposite sign on either side of a crack.

b. Refined Linkage Element Model

Ngo, Scordelis, and Franklin (Ref. 18) extended the work of reference 2. Shear in beams with diagonal tension cracks was studied as illustrated by the example given in figures 4 and 5. The model was refined by representing the concrete and main longitudinal reinforcement by quadrilateral elements

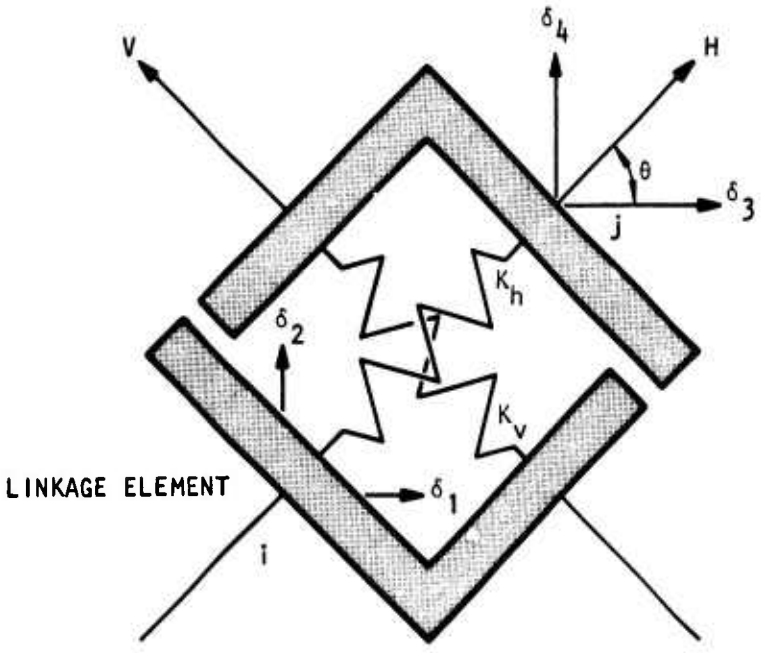

$$\begin{Bmatrix} \varepsilon_h \\ \varepsilon_v \end{Bmatrix} = \begin{bmatrix} -C & -S & C & S \\ S & -C & -S & C \end{bmatrix} \begin{Bmatrix} \delta_1 \\ \delta_2 \\ \delta_3 \\ \delta_4 \end{Bmatrix}$$

$C = \cos\theta \qquad S = \sin\theta$

$\delta_{1,2,3,4}$ = ABSOLUTE DISPLACEMENTS, EXPRESSED IN LOCAL COORDINATES, OF NODAL POINTS OF CONTINUUM ELEMENTS TO WHICH LINKAGE IS ATTACHED

Figure 1. Linkage Element (Ref. 2)

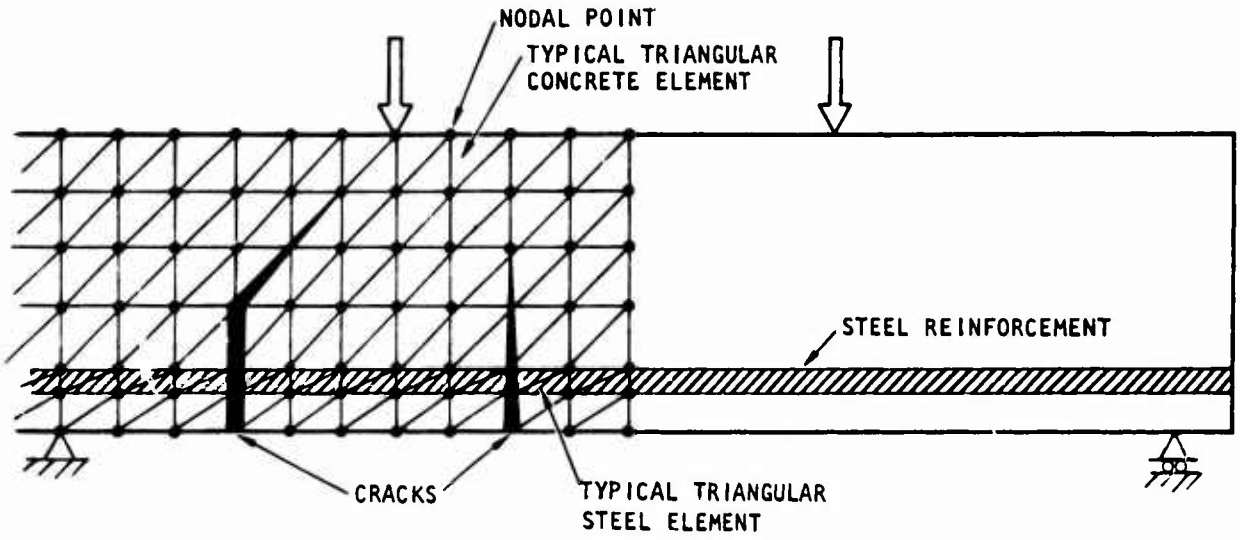

(a) Finite element mesh

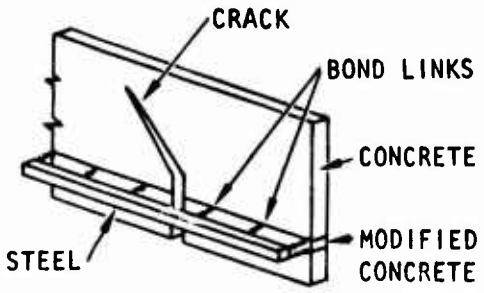

(b) Analytical model

Figure 2. Finite Element Mesh and Analytical Model (Ref. 2)

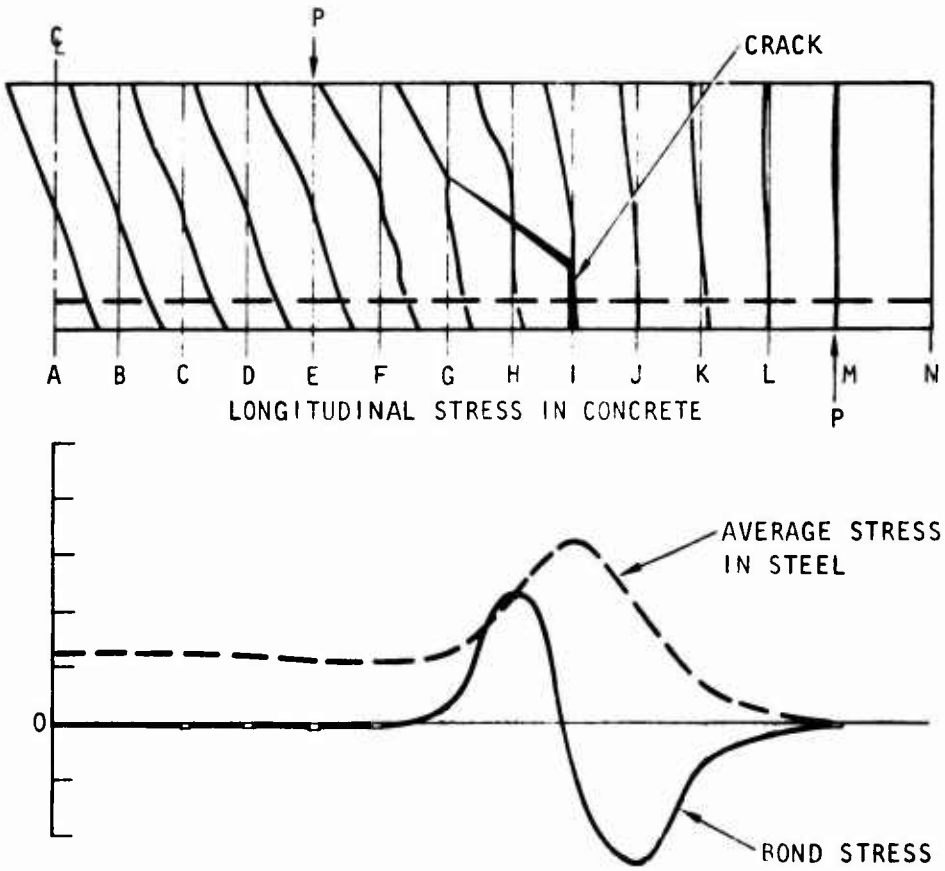

Figure 3. Variation in Bond and Steel Stresses in Beam (Ref. 2)

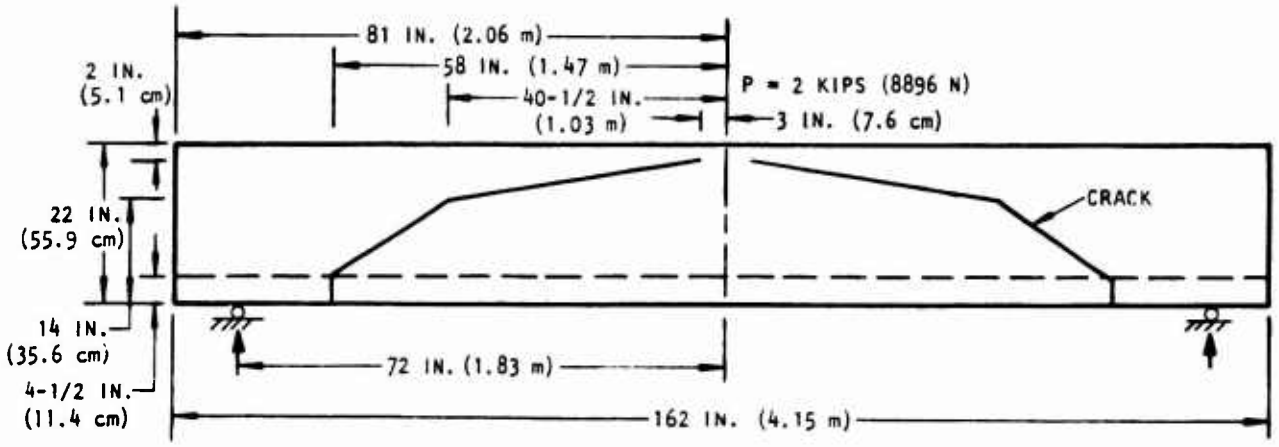

(a) Symmetrical idealized single diagonal crack (beam width = 9 in. [22.86 cm])

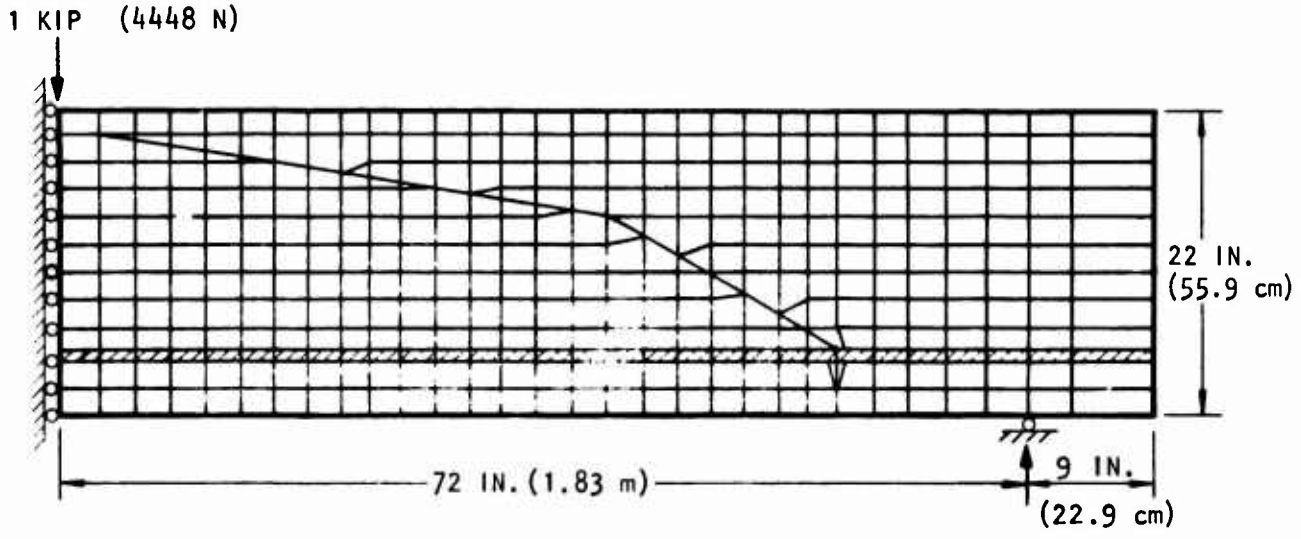

(b) Finite element mesh layout

Figure 4. Linear Analysis of a Beam with a Predefined Crack (Ref. 18)

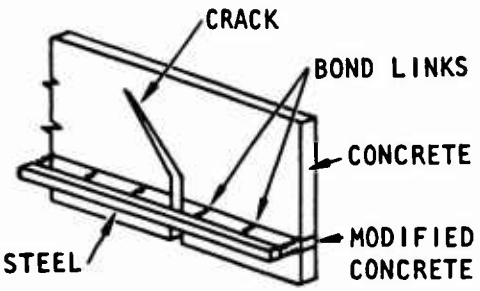

(a) Analytical model

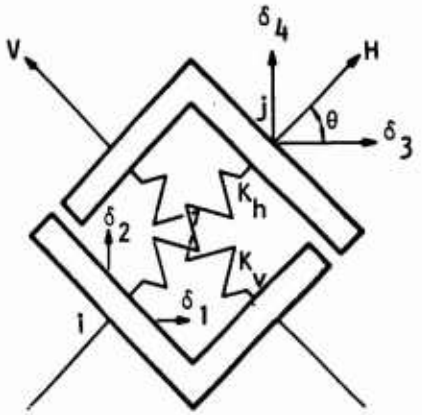

(b) Linkage element

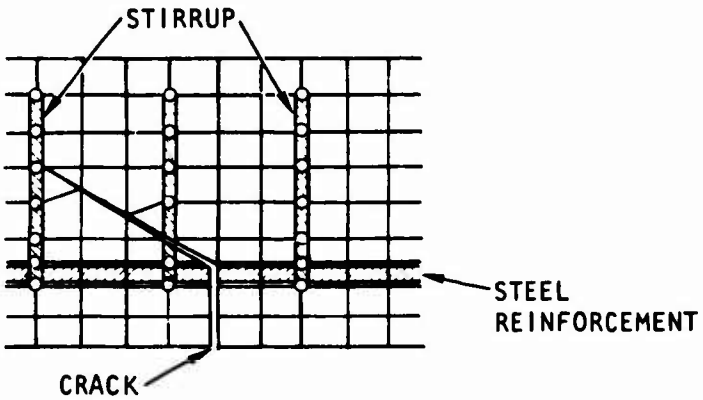

(c) Reinforcement representation

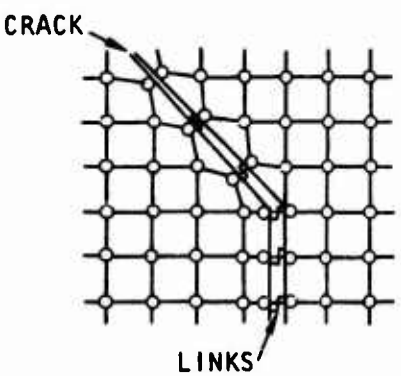

(d) Crack and aggregate interlock

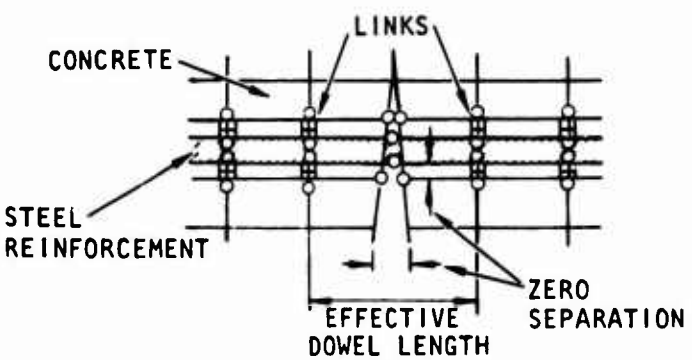

(e) Effective dowel length

Figure 5. Analytical Models and Linkage Elements (Ref. 18)

consisting of two constrained linear-strain triangles (Ref. 14), and the influence of stirrups, dowel shear, aggregate interlock and horizontal splitting along reinforcement near the support were considered. One-dimensional bar elements were used for the vertical stirrups.

c. Nonlinear Model

Nilson (Refs. 3 and 19) refined the work of reference 2 by introducing nonlinear material properties and a nonlinear bond-slip relationship into the model. He accounted for these nonlinearities by applying the load in small increments (Figs. 6 and 7). Improved quadrilateral plane stress finite elements were used. Cracking was accounted for by stopping the solution when an element indicated a tensile failure. The new cracked structure was redefined, the revised information was then input into the computer, and the structure was reloaded incrementally. The method was applied to concentric and eccentric reinforced tensile members that were subjected to loads applied longitudinally through the reinforcing bars, and the results were checked against experimental data. Nilson found bond stress patterns that are similar to those found by Ngo and Scordelis (Ref. 2).

The main shortcoming of Nilson's work, besides approximate treatment of constitutive properties of plain concrete, is the difficulty of handling tensile cracking. While it may be possible to terminate a static calculation, remesh, and begin loading again from the beginning, it is extremely difficult to do this in a dynamic calculation.

d. Refined Nonlinear Models

Franklin (Ref. 20) performed a nonlinear analysis of the beam, as shown in figure 8, in which cracking within the finite elements and redistribution of stresses was automatically accounted for, so that the response from initial loading to failure was obtained in one continuous computer analysis. Incremental loading, with iterations within each increment, were used to account for cracking and nonlinear material properties. Unlike the preceding studies, the crack is not predefined, and progressive cracking is assumed to occur over an entire element normal to a principal stress direction rather than along a

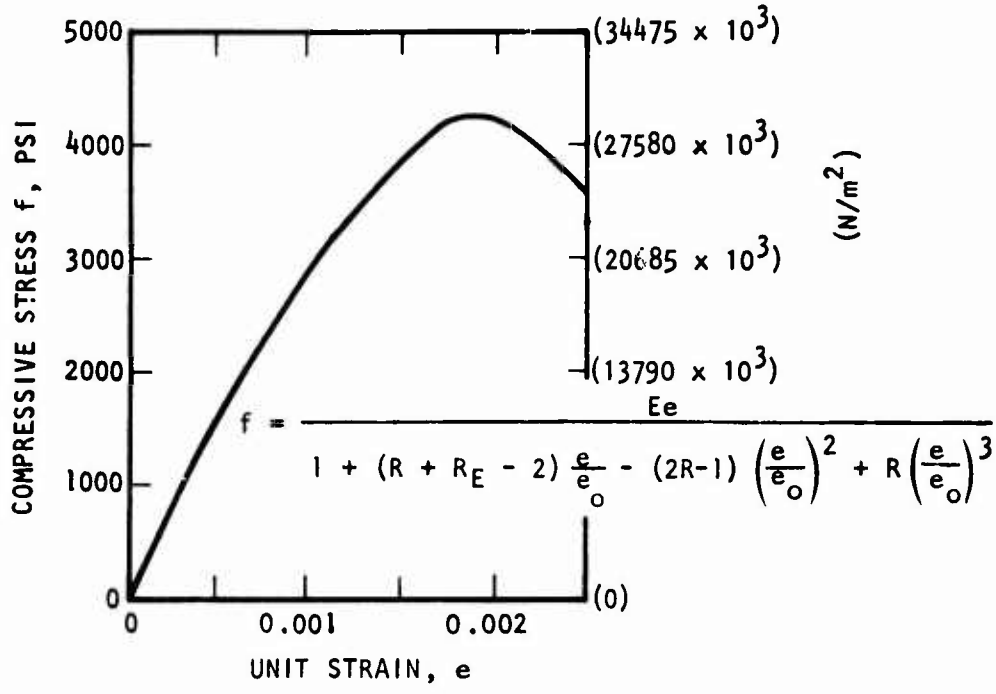

TERMS

f = STRESS AT STRAIN e

f_f = FAILURE STRESS AT FAILURE STRAIN e_f

e_o = STRAIN CORRESPONDING TO MAXIMUM STRESS f_o

E = THE INITIAL TANGENT MODULUS

E_s = THE SECANT MODULUS = $\frac{f_o}{e_o}$

$R_E = \frac{E}{E_s}$

$R_f = \frac{f_o}{f_f}$

$R_e = \frac{e_f}{e_o}$

$R = \frac{R_E(R_f - 1)}{(R_e - 1)^2} - \frac{1}{R_e}$

Figure 6. Concrete Uniaxial Stress/Strain Relations in Compression (Saenz Equation, Ref. 19)

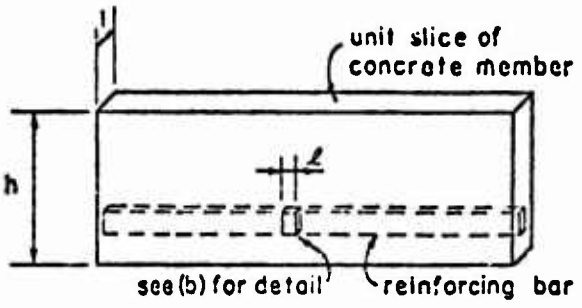

(a) Model of reinforced concrete member

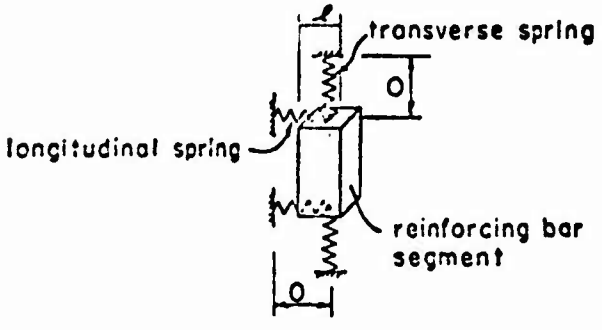

(b) Detail of bond linkage

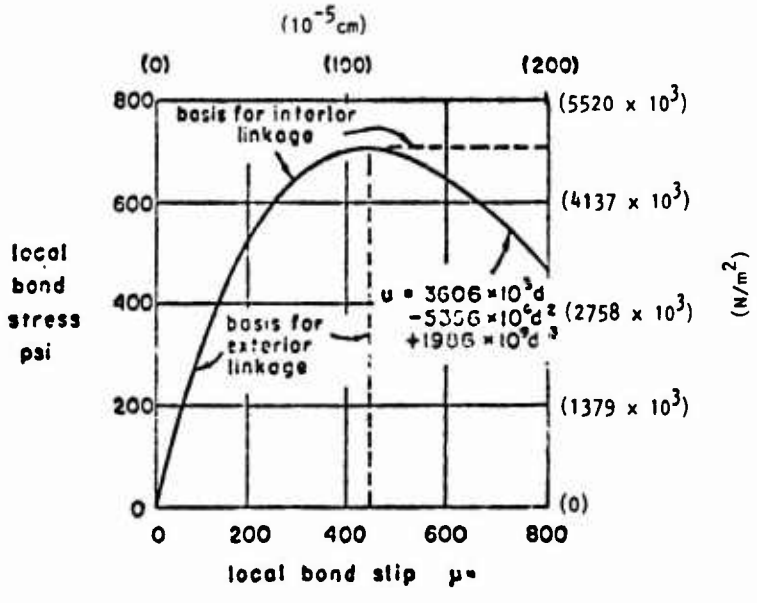

(c) Bond-slip curves used in analysis

Figure 7. Bond-Slip Model (Ref. 19)

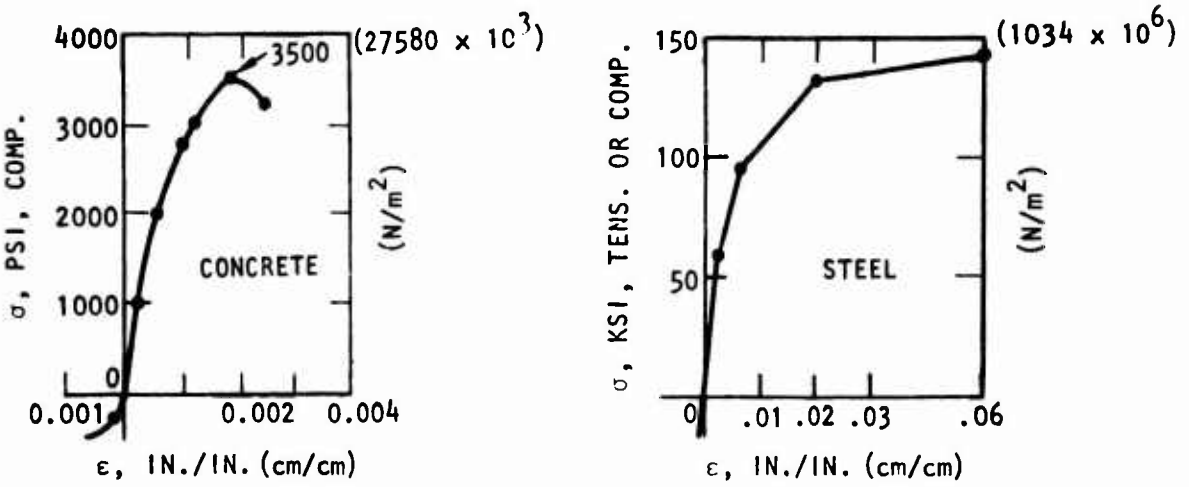

(a) Material uniaxial stress/strain curves in tension

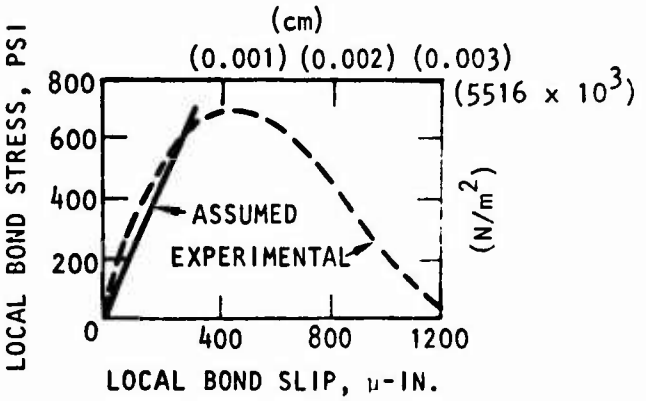

(b) Bond stress vs. slip curve

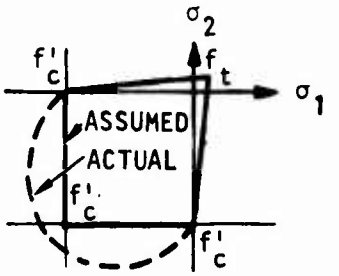

(c) Concrete failure criteria

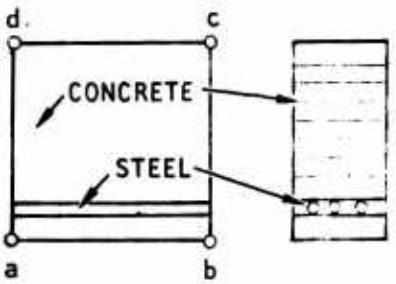

(d) One-dimensional layered frame element

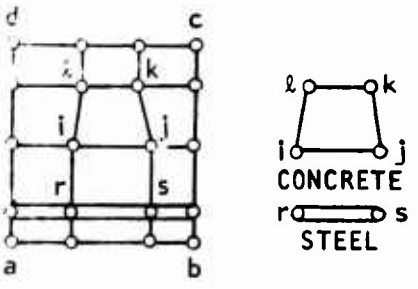

(e) Two-dimensional quadrilateral elements and rod elements

Figure 8. Nonlinear Analysis of a Beam with Progressive Cracking (Refs. 4 and 20)

single line. This permits the use of the same structural nodal point topology throughout the solution, rather than the necessity for splitting the nodes after cracking and establishing a new topology, as would be required by Nilson's nonlinear approach.

The segmental material uniaxial stress-strain curves used for the concrete, steel, and bond stress/slip are shown in figures 8(a) and (b). Two different modeling schemes used in the analysis are shown in figures 8(d) and (e).

In the first scheme, figure 8(d), the beam is divided longitudinally into a series of "frame elements," each having a total depth equal to that of the beam. The frame element is subdivided into ten concrete layers and may have reinforcement at up to four layers over the depth. Utilizing an assumption of plane sections remaining plane at sections a-d and b-c, the stiffness of the frame element subjected to axial force, shear, and moment at each section can be evaluated for material properties that may vary vertically from layer to layer, but are constant over the length of the element. For this purpose, each layer is assumed to be in a state of uniaxial stress. The nonlinear analysis proceeds in the usual manner with the modulus of elasticity of each concrete or steel layer, taken from the stress-strain curves of figure 8(a), being dependent on the strain existing at the start of the load increment. When a concrete layer cracks in tension, its modulus is set to zero and the stress is redistributed to the remaining structure. Obviously, for this idealization only vertical cracks can occur in the beam. Also, no account is taken of bond slip.

For plane stress systems in which diagonal cracks occur and the two-dimensional stress state dominates the behavior, the second scheme (shown in Fig. 8(e)) is more realistic. Here the beam segment a-b-c-d is subdivided into series of concrete quadrilateral plane stress elements i-j-k-ℓ, made up of two constrained linear strain triangles and one-dimensional steel bar elements r-s. Bond may be simulated by adding linkage elements between double nodes introduced at points such as r. In the present example, Franklin (Ref. 20) assumed isotropic behavior during each increment of loading prior to cracking.

He used a single tangent modulus E taken from the uniaxial stress-strain curve (Fig. 8(a)) as the smaller of the tangent moduli E_1 and E_2 corresponding to the two current principal strains. The modulus E is used to define his isotropic two-dimensional constitutive relation. On the other hand, Nilson (Refs. 3 and 19) treated the material as orthotropic and used tangent moduli E_1 and E_2. Franklin assumed a modified biaxial failure envelope for the concrete which approximates the actual envelope (Fig. 8(c')). When tensile cracking failure occurs, the element is cracked normal to the principal stress direction, and this stress is redistributed to the remaining structure. Subsequently, the element is assumed to be anisotropic and to have zero modulus of elasticity normal to the crack.

Experimental and analytical load versus midspan deflection curves are shown in figure 9. It can be seen that the analytical cracking load is lower in all cases than the experimental load, indicating that the actual tensile strength of the concrete was higher than assumed, or that at low loads the "tension stiffening" effect of the concrete between cracks in an element, which was ignored, cannot be neglected. All analytical curves indicate a stiffer model after cracking than found experimentally. Only the analytical model with a low bond link failure limit produced a failure load less than the experimental value, all others being much higher. Scordelis (Ref. 4) concluded that for beams that fail primarily because of diagonal tension cracking, the bond, dowel shear, and aggregate interlock must be modeled more accurately before a reliable finite element prediction can be made of the failure load.

e. Wall Panel Study

In this example, the response of a wall panel specimen was studied experimentally and analytically by Cervenka (Ref. 21) and also analytically by Franklin (Ref. 20). Dimensions, loading, reinforcing scheme, and method of loading are shown in figure 10. Because of symmetry, each half of the deep beam test specimen can be considered similar to a wall panel subjected to a single transverse load.

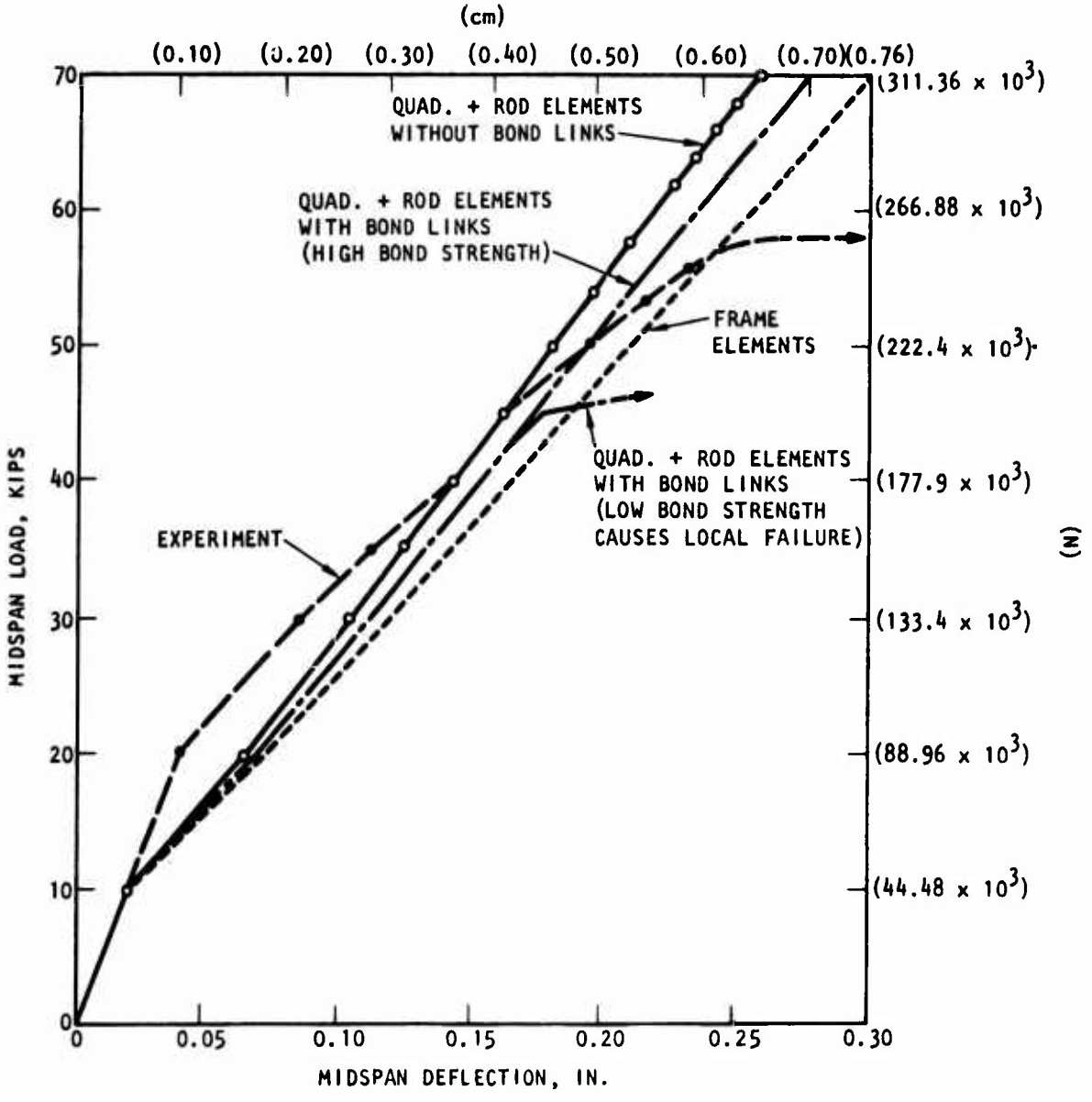

Figure 9. Experimental and Analytical Load versus Deflection Curves (Refs. 4 and 20)

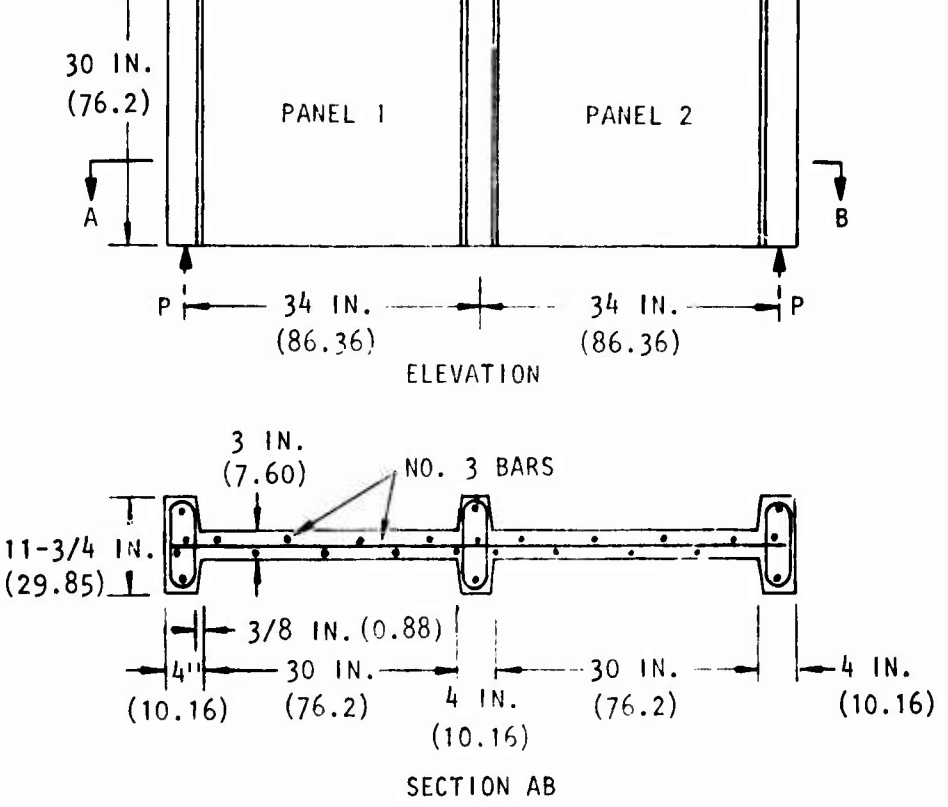

(a) Dimensions and loading of test specimen

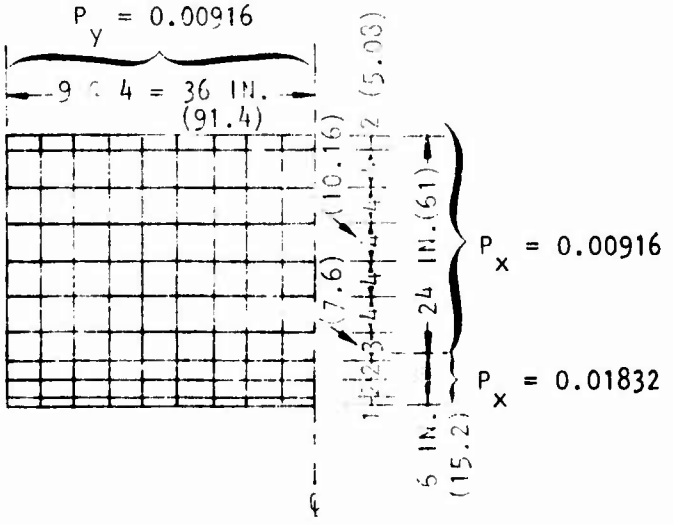

(b) No. 3 reinforcement for test specimen

Figure 10. Wall Panel Study (Refs. 4, 20, 21)

In Cervenka's analysis, constant-strain triangular finite elements were used to model the concrete and steel reinforcement. The steel was assumed to be uniformly distributed over the element in two orthogonal directions, and a composite material constitutive relation was developed in order to determine the element stiffness matrix. Both the concrete and steel were assumed to have elastic-perfectly plastic stress/strain curves (Figs. 11(a), 11(b)). For the concrete, f'_c = 3880 psi (26753 x 10^3 N/m^2), f_t = 529 psi (3647 x 10^3 N/m^2), E_c = 2900 ksi (19996 x 10^6 N/m^2); and for the steel, f_y = 51,200 psi (353024 x 10^3 N/m^2), E_s = 27,300 ksi (188233 x 10^6 N/m^2). The assumed biaxial stress failure criteria shown in figure 11(c) was adopted for the concrete. An incremental nonlinear analysis was used which accounted for tensile cracking and subsequent stress redistribution. Plasticity of the uncracked concrete, which is in a biaxial state of stress, was assumed to obey the von Mises yield condition and associated flow rule, and was used in the finite element analysis to account for plastic deformations under biaxial compressive yielding. No account was taken, either in this analysis or the one that follows, of bond slip, aggregate interlock, or tension stiffening of concrete in the cracked zone. Cervenka compared his analytical results with Peter's experimental studies on reinforced concrete wall panels and spandrel beams (Ref. 22). He concluded that reasonable correlation with experimental results can be obtained in problems by monotonically increasing the loading. However, in the problems with cyclic loading, nonlinear effects of bond slip and crack surface deterioration should be properly accounted for, in order to achieve good correlation with experimental measurements.

In the analysis using Franklin's program (Ref. 20), quadrilateral elements made up of two constrained linear strain triangles (Ref. 14) were used for the concrete and one-dimensional bar elements were used for the steel reinforcement. The same uniaxial stress/strain curves (Figs. 11(a) and 11(b)) were used for the concrete and steel, while a slightly different failure criterion (Fig. 8(c)) was assumed for the concrete under biaxial stress. Tensile cracking was accounted for and the concrete was assumed to have failed when it reached f'_c in compression with no subsequent plasticity.

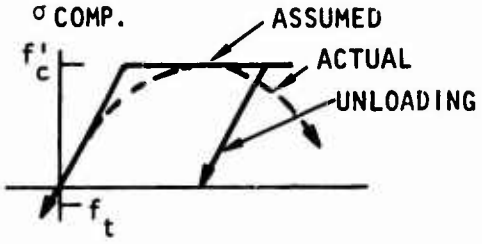

(a) Uniaxial stress/strain curve for concrete

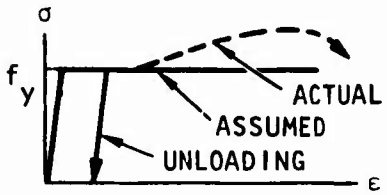

(b) Uniaxial stress/strain curve for steel

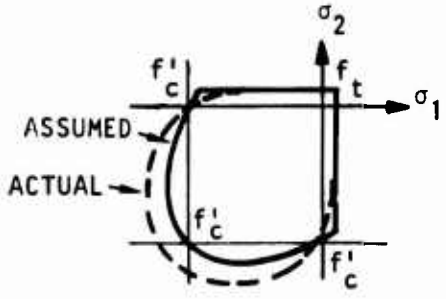

(c) Concrete failure criteria

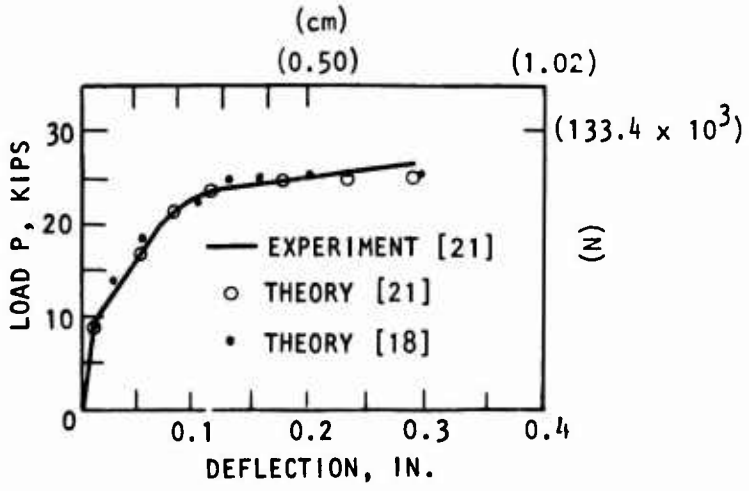

(d) Experimental and analytical load vs. deflection curves

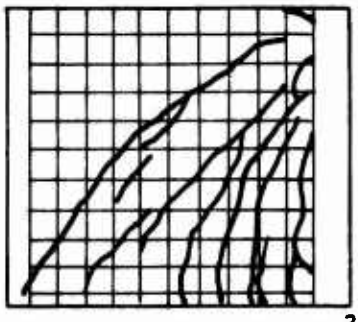

P = 25.5 KIPS (113.4 x 10^3 N)

(e) Experimental crack pattern

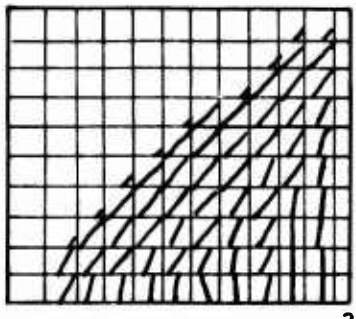

P = 25.5 KIPS(113.4 x 10^3 N)

(f) Analytical crack pattern

Figure 11. Material Idealization and Selected Results (Ref. 21)

The two analyses both seemed to predict experimental load-deflection curve and crack pattern quite well (see Figs. 11(d), 11(e), and 11(f), respectively). From these results it appears that for wall panels in which the reinforcement is distributed rather uniformly over the entire wall panel, the effects of bond slip, dowel shear, aggregate interlock, and tension stiffening of the concrete in a cracked zone are of much less importance than for the case of a beam in which the major reinforcement is concentrated along a single line.

3. CONTINUUM METHOD

General constitutive equations that consider the following aspects of reinforced concrete behavior were developed by Isenberg and Adham (Ref. 1).

- Inelastic stress/strain properties of plain concrete including tensile cracking and compressive crushing
- Inelastic stress/strain properties of steel
- Progressive deterioration of bond
- Anisotropy (different effective moduli in different directions) due to cracking and crushing

These equations have been adapted to a plane strain, static finite element code, which was applied to determine quasi-static aspects of hardened structure response in the SAMSO RockTest II program.* Comparison between predictions and measurements, reported in reference 5, was encouraging.

The continuum approach requires composite moduli to be defined. Due to the tendency for concrete to develop large-scale, discrete cracks under tensile stress, these models must be capable of representing anisotropy. Thus, tensile stress/strain properties perpendicular to a crack should be different from those parallel to the crack. A central problem is to define the principal directions of anisotropy--that is, directions in the material for which fundamental stress/strain properties can be derived and subsequently transformed to

*The RockTest II program sponsored by the U.S. Air Force included design and validation testing under a HEST/DIHEST environment of facility subsystems for an advanced fixed-base, large payload missile system.

other directions. A fundamental assumption of the Isenberg and Adham approach is that the principal directions of anisotropy coincide with the principal axes of stress until tensile cracking occurs. Thereafter, principal directions of anisotropy are assumed to be parallel and perpendicular to the direction of first cracking. Within this framework of orthotropy, tangent moduli for the composite material are defined in the principal directions of orthotropy. These moduli depend on the tangent stiffnesses of the concrete and steel and on the state of bond between them. A variable modulus model, described below, was developed to represent data available in 1968 (Ref. 1). A variable modulus model of the reinforcing steel was also defined. These two contributions are combined, using area-averaging as modified by the bond-slip relation, into composite moduli of a section. The development of this model includes:

a. Compressive-Stress/Strain Relations for Plain Concrete (Tangent Modulus)

The relation between increments of stress and strain for increasing compressive stress was considered. Experimental data from which the tangent modulus could be obtained were available at that time for the following states of stress:

- Uniaxial Compressive Stress ($\sigma_1 < 0$; $\sigma_2 = \sigma_3 = 0$)*
  (Barnard, Ref. 23 and Kabaila, Ref. 24)
- Triaxial Compressive Stress ($\sigma_1 < \sigma_2 = \sigma_3 < 0$)
  (Balmer, Ref. 25)
- Biaxial Tensile and Compressive Stress ($\sigma_1 < 0$; $\sigma_2 > 0$; $\sigma_3 = 0$)
  (Isenberg, Ref. 26, 27)

*Throughout this report the stress will be compressive if preceded by a negative sign.

The relevant data from these experiments are illustrated in figure 12. The stress/strain (σ_1/ε_1) relation for unconfined compression, figure 12(a), is nonlinear before maximum stress is reached and, when testing is performed in a stiff machine, the curve has a falling branch.

The triaxial compression experiments, figure 12(b), were performed in the usual way, whereby an initial all-around confining pressure is applied to solid cylindrical specimens. This is followed by applying additional stress (additional σ_1) in the direction of the long axis of the specimen. The data of interest are the σ_1/ε_1 curves developed during application of the additional stress. Balmer's experiments apparently were not performed in a stiff testing machine. Hence there is no reason to expect a falling branch in the σ_1/ε_1 curves that he measured. The existence of a falling branch under triaxial compressive stress has been neither proved nor disproved.

The biaxial tension and compression experiments were performed by subjecting tubular specimens to combined torsion and compression. The technique is reported in reference 27. The data indicate that the shape of the σ_1/ε_1 curves are roughly similar to those measured in unconfined compression and triaxial compression. However, the magnitude of stress at a particular strain and the maximum value of σ_1 depend heavily on the state of stress. Although the σ_1/ε_1 curves in figure 12(c) contain a small Poisson's-ratio effect because of the fact that ε_2 is changing, the effect is small and

$$\varepsilon_1 \approx \varepsilon_1 - \nu\varepsilon_2 \tag{2}$$

These data suggest that, if an ideal series of tests covering a wide range of stress states could be performed on a group of identical specimens, the σ_1/ε_1 curves shown in figure 13(b) might be obtained. These curves represent loading conditions where the lateral stresses σ_2 and σ_3 are held constant. Hence, the slope of the σ_1/ε_1 curve at any point is the tangent modulus

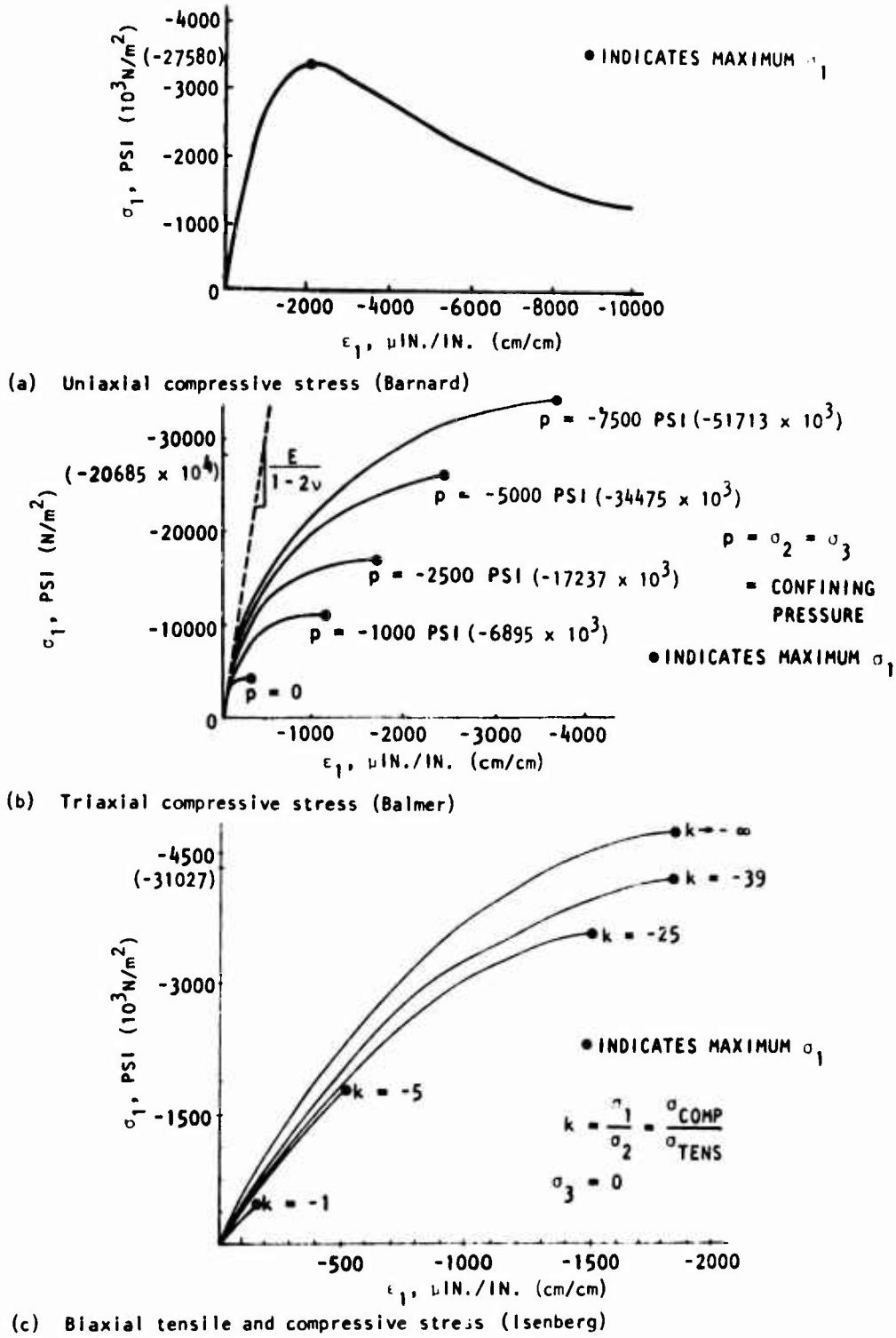

Figure 12. Experimental Compressive Stress/Strain Curves for Three States of Stress

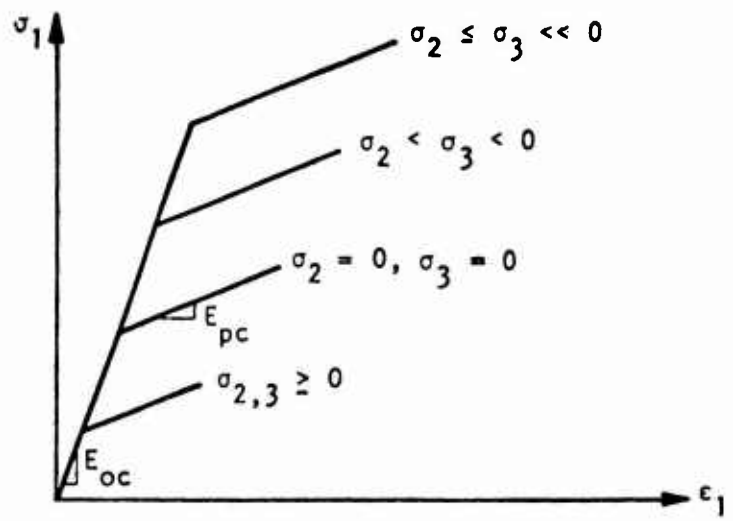

(a) Bilinear model

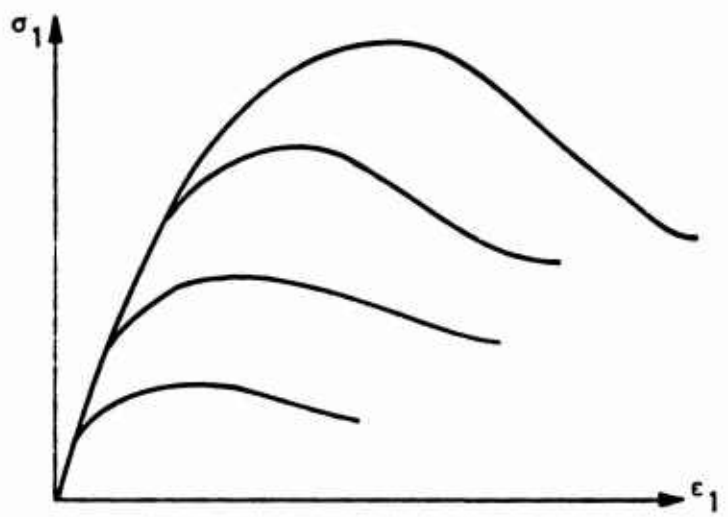

(b) Model based on modified Kabaila equation

Figure 13. Idealized Stress/Strain Curves for Plain Concrete

$$\left(\frac{\partial \sigma_1}{\partial \varepsilon_1}\right)_{\sigma_2,\sigma_3 = \text{const}} = E_1 \tag{3}$$

which is prescribed as a function of the current values of σ_1, σ_2 and σ_3.

The bilinear model shown in figure 13(a) is attractive because it is simple and represents the broad characteristics of the experimental curves up to maximum stress. The state of stress at which the model σ_1/ε_1 curves change slope is given by

$$f = \bar{f}_c + \beta\left(\frac{\sigma_2 + \sigma_3}{2}\right) \tag{4}$$

The tangent modulus E_1 is defined as follows:

$$\begin{aligned} &\text{if } \sigma_1 > f \quad , \quad E_1 = E_{oc} \\ &\quad\ \sigma_1 < f \quad , \quad E_1 = E_{pc} \end{aligned} \tag{5}$$

where E_{oc} and E_{pc} are the tangent moduli for concrete in the elastic and inelastic regimes, respectively, and

β = An experimental parameter corresponding to angle of internal friction

$\bar{f}_c$ = An experimental parameter related to the unconfined compressive cylinder strength of concrete, with the value of $\bar{f}_c$ considered to lie between 0.85 and 1.0 times the unconfined compressive strength f'_c.

Values of β and $\bar{f}_c$ may be obtained for a specific type of concrete by plotting maximum σ_1 versus $(\sigma_2 + \sigma_3)/2$ and finding the slope and intercept. This has been done for the maximum combined stress data shown in figure 12 and some additional data obtained in biaxial compression, reference 28 ($\sigma_1 = \sigma_2 < 0$; $\sigma_3 = 0$). The result is shown in figure 14, where an attempt has

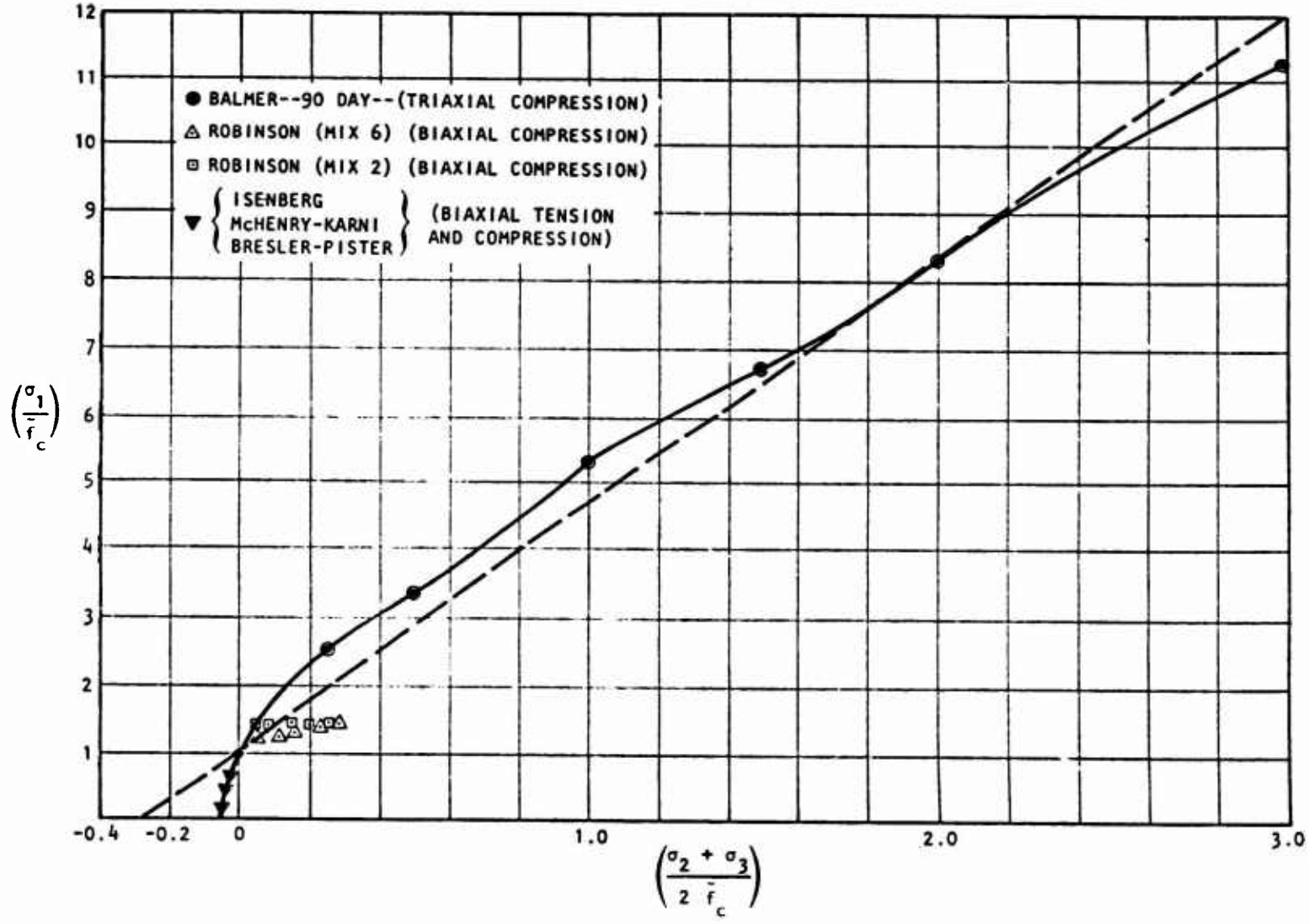

Figure 14. Maximum Compressive Stress (σ_1) as a Function of the Other Compressive Stresses (σ_2, σ_3)

been made to take into account the different properties of test specimens used by the various investigators. In each individual test series, the companion values of σ_1 and $(\sigma_2 + \sigma_3)/2$, are divided by $\bar{f}_c$, where $\bar{f}_c$ is here defined as 1.0 times unconfined compressive strength in that test series. The results of tests in biaxial tensile and compressive stress are so closely grouped in a small area of the graph that they are represented by only three symbols.

In determining the parameter β from experimental data, more weight is given to the results of triaxial compression tests than to biaxial compression tests. This is done when the model is being applied to plane strain situations, where the most frequent states of stress are closer to triaxial than to biaxial compression. For plane stress analyses, β should be evaluated on the basis of biaxial compression tests.

b. Tensile Stress/Strain Relations for Plain Concrete (Tangent Modulus)

The relation between increments of stress and strain for increasing tensile stress is considered next. The states of stress for which data on the tangent modulus are available are:

- Uniaxial tensile stress, reference 29
- Biaxial tensile and compressive stress, reference 27

These data indicate that the tensile stress/strain relations are approximately linear up to maximum combined stress, although they are not exactly linear. It was decided to represent the tangent modulus in tension by a constant

$$\left(\frac{\partial \sigma_1}{\partial \varepsilon_1}\right)_{\sigma_2, \sigma_3} = E_{oc} \text{ (a constant)} \qquad (6)$$

where E_{oc} is equal to the initial tangent modulus in unconfined compression.

In addition to tensile stress/strain relations, it is also necessary to have a criterion of maximum tensile stress or cracking stress. The sense and magnitude of the lateral stresses σ_2, σ_3 affect the maximum tensile stress, as experiments under biaxial tensile and compressive tests show (Refs. 27, 30, and 31). However, at the time of conducting the study reported in reference 1, there were no data on maximum tensile stress as a function of two lateral compressive stresses ($\sigma_2 < 0$, $\sigma_3 < 0$) or as a function of one lateral tensile stress ($\sigma_2 > 0$) and one lateral compressive stress ($\sigma_3 < 0$). In the absence of such experimental data, a criterion based on data from the biaxial tensile and compressive stress state was assumed. The mathematical statement of the tensile strength criterion is as follows:

For $\sigma_2 < 0$ and $\sigma_2 < \sigma_3$

$$\sigma_1 \leq f'_t ,$$

where $$f'_t = f_t - \eta \sigma_2 \tag{7}$$

and

f_t = Unconfined tensile strength of concrete (> 0)

η = Slope of cracking envelope

If $\sigma_1 = f'_t$, maximum tensile stress has been reached and cracking is said to have occurred.

For both $\sigma_2, \sigma_3 > 0$

$$f'_t = f_t \tag{8}$$

The graphical representation of this criterion is illustrated in figure 15. The projection of this criterion in σ_1/σ_2 plane is shown for convenience in the same figure and correlates well with the actual criterion shown in figure 8(c).

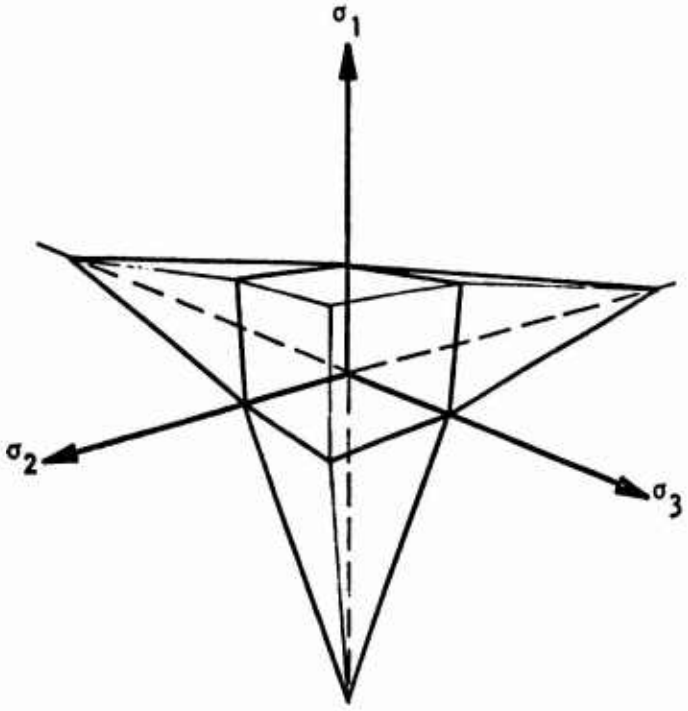

(a) Three-dimensional cracking criteria

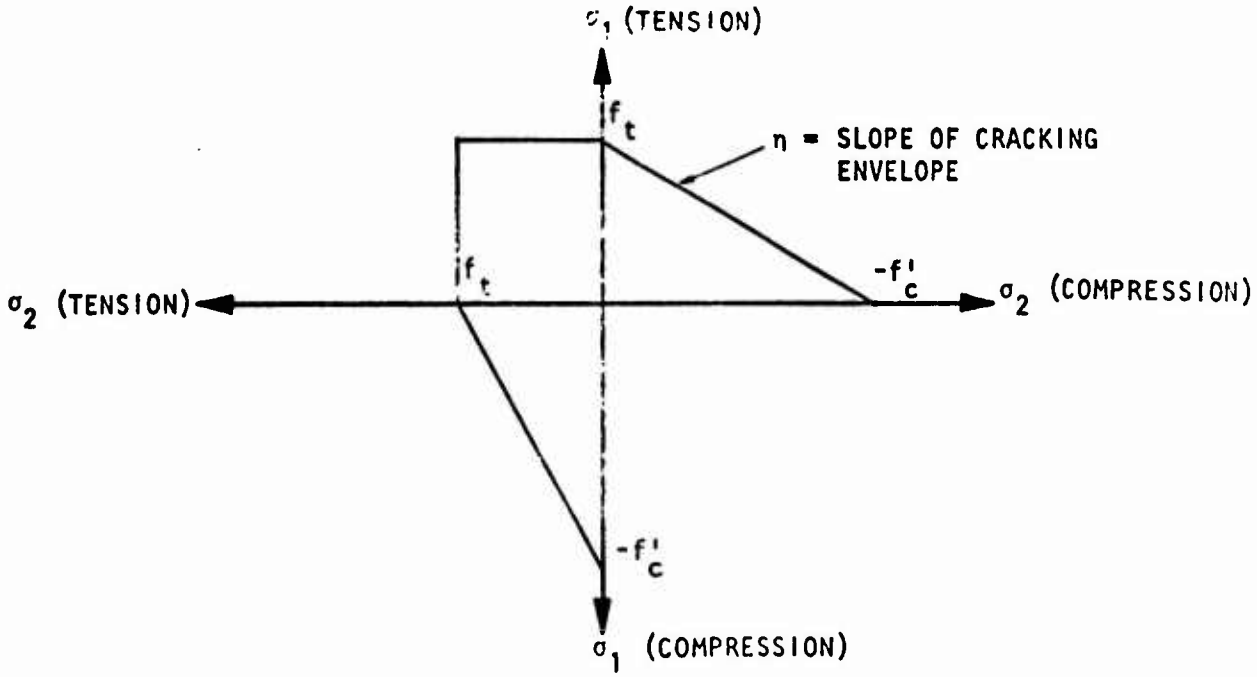

(b) Projection of tensile cracking criterion in the $\sigma_1 - \sigma_2$ plane

Figure 15. Tensile Cracking Criteria

c. Poisson's Ratio

Experimental data on Poisson's ratio are available mainly from tests in triaxial compressive stress. The data in reference 32 clearly show that under this state of stress, Poisson's ratio is approximately a constant up to 50 to 90 percent of maximum combined stress and that it increases rapidly as maximum stress is approached.

No attempt has been made to represent this type of variation in Poisson's ratio. Instead, it has been assumed to be initially constant, equal in all directions and equal to the value measured in unconfined compression near zero stress. This assumption is justifiable because the model is intended to apply in situations of plane strain or nearly uniaxial strain. These situations differ sufficiently from triaxial compressive stress, where lateral expansion is not prevented.

The initial value of Poisson's ratio for plain concrete is used for the composite material. When inelasticity occurs, one or more tangent moduli decrease. Consequently, in order to preserve the symmetry of the finite element stiffness matrix, one or more Poisson's ratios of the composite material are also decreased. This procedure is justified mathematically but does not necessarily represent physical processes. The steps required to maintain a symmetric stiffness matrix are described below.

d. Properties of Steel

The required properties of the steel are the tangent modulus, the yield stress, and Poisson's ratio. These properties are assumed to be the same in tension and compression. It is also assumed that yielding of a steel bar is governed only by the stress in the direction of the bar. The influence on yielding of stresses perpendicular to the bar is neglected.

No specific experimental data were used in the Isenberg/Adham model (Ref. 1) to define the properties of the steel. Engineering handbook values of elastic Young's modulus, Poisson's ratio, and yield strength were used. The experimental tensile stress/strain curve of the steel bars were idealized

as shown in figure 16. The broken line is the stress/strain curve used in the model. The parameters which characterize the model are:

E_{o_s} = Elastic Young's modulus

E_{ps} = Plastic Young's modulus

f_s = Yield strength of steel

In addition, Poisson's ratio for steel, ν_{st} should be specified.

e. Composite Behavior

The composite model combines the variations in steel and concrete properties discussed above and accounts for:

- The combined properties of steel and concrete
- The change in principal directions of stresses and the orientation of cracks
- Progressive bond failure between steel and concrete
- Material orthotropy
- Mechanical orthotropy
- Orthotropy due to cracking

The present model considers the finite element system as a continuum in which properties are uniform within an element. To demonstrate the method, the linear strain triangle is used in the present analysis.

f. Idealization of a Reinforced Concrete Structure

A typical finite element idealization of a reinforced concrete structure and the surrounding medium is shown in figure 17. The external loads act in the x-y plane, which is also the plane of primary reinforcement (Fig. 18). For a reinforced concrete element the reinforcement areas A_{s_I} and $A_{s_{II}}$ in an arbitrary orthogonal orientation are given. The angle γ, is the inclination of the reinforcement relative to the global x-axis as shown in figure 18(b).

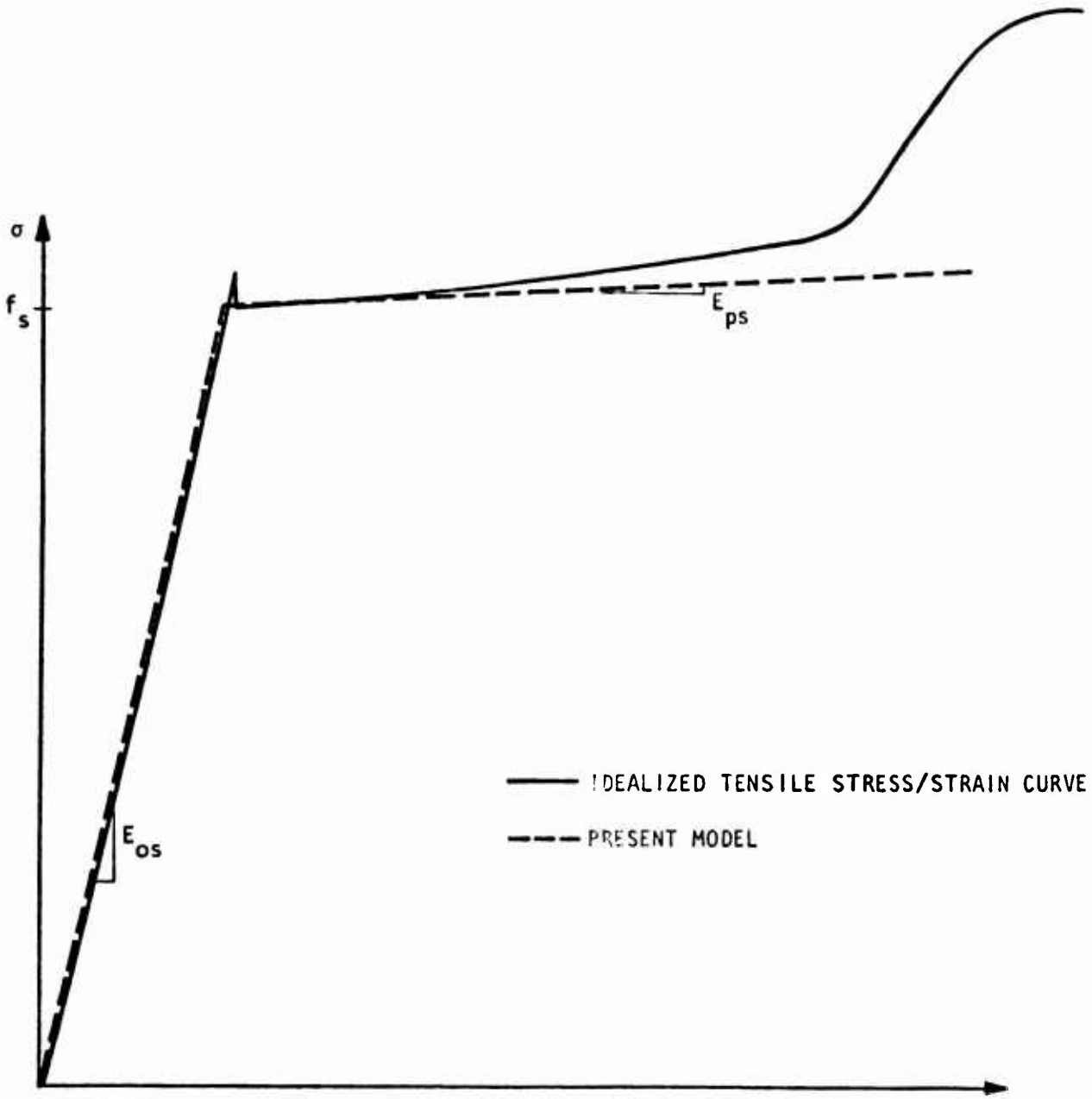

Figure 16. Tensile Stress/Strain Curves for Reinforcing Steel

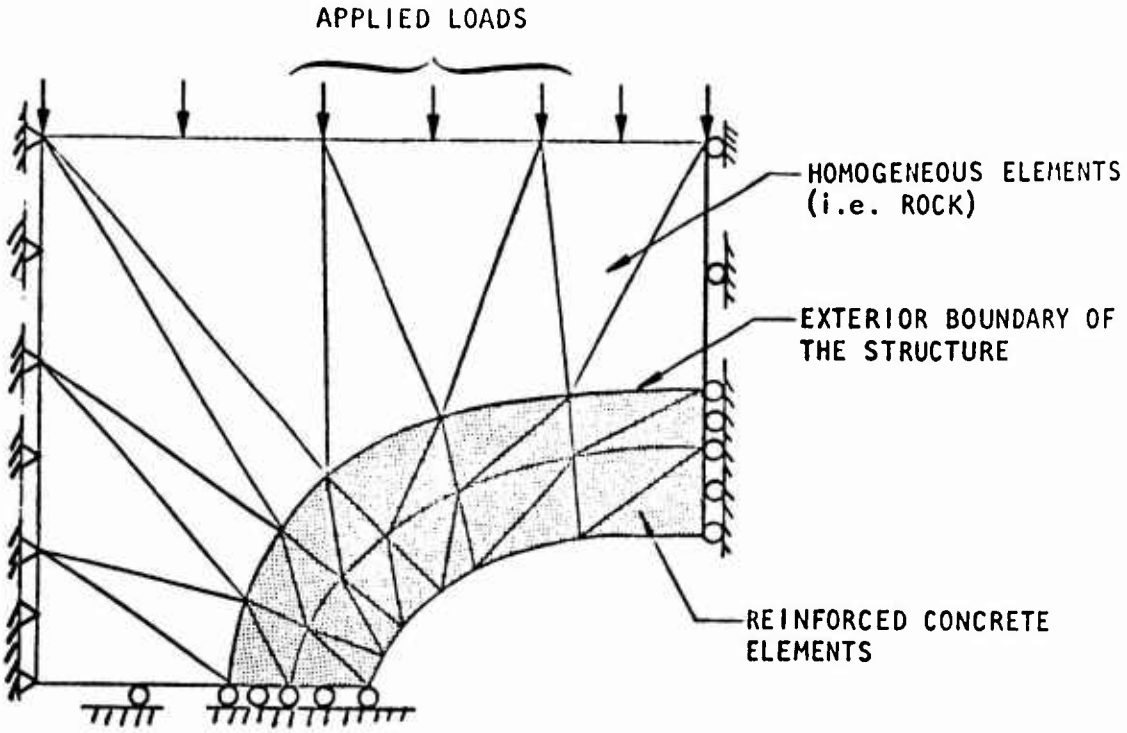

Figure 17. Simplified Finite-Element Representation of a Reinforced Concrete Structure Embedded in a Homogeneous Medium (i.e., Rock)

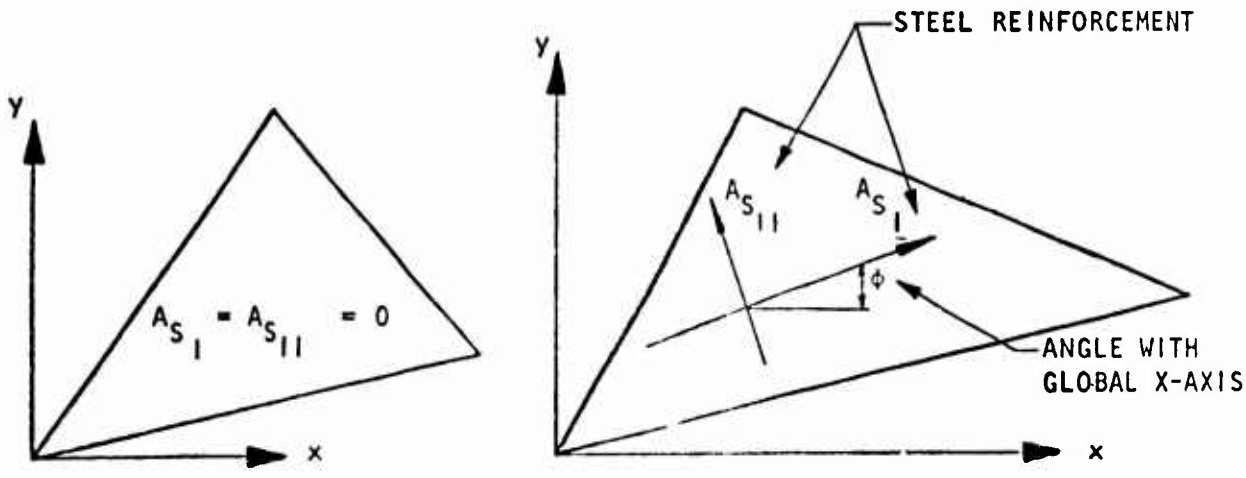

(a) Homogeneous material

(b) Reinforced concrete

Figure 18. Finite Elements

Both A_{s_1}, $A_{s_{11}}$, and ϕ may vary from element to element. While the method is addressed to reinforced concrete elements, it can also be applied to homogeneous elements of plain concrete or rock, etc., by eliminating from the analysis the terms corresponding to the reinforcement as shown in figure 18(a). The objective of the reference 1 investigation is illustrated by figure 19. The compressive paths (1-2-3), (1-2'-3'), etc., of figure 19(a) are applicable for defining the tangent moduli for compressive states of stress for both composite and homogeneous elements, as discussed above. The tensile path (1-4-5) in figure 19(a) applies to homogeneous elements only. The composite behavior of a reinforced concrete element in tension is illustrated in figure 19(b). In this figure, the portion (1'-4') shows the composite behavior before cracking. After primary cracks occur, a reinforced concrete element behaves differently. The bond between steel and concrete allows the concrete to continue adding a portion of its stiffness to that of the reinforcing steel, resulting in a composite tensile modulus as illustrated by the segment (4'-5') in figure 19(b). The portion (5'-6') of figure 19(b) represents the condition when bond is completely broken and the composite modulus is determined by the plastic modulus of steel. At this stage, strains may become excessive.

Upon application of load, three components of stress develop in the element. The average element stresses σ_1, σ_2, and σ_3 in the principal directions of orthotropy are used to check and update the properties of the entire element. At the end of each load step, a check is performed in each of the three orthotropic directions, and the properties of the elements are changed according to the stress magnitudes, the loading/unloading history, and the orthotropic properties along the three directions. The three-way check can be summarized as follows.

If σ_1 is compressive, the modulus E_1 is obtained as shown above. However, if σ_1 is tensile and does not exceed cracking stress f'_t (see equations 7 and 8), an initial tensile modulus equal to the initial unconfined compressive modulus E_{oc} is used. In this case, the principal axes of orthotropy coincide with principal axes of stress. This behavior is represented by segments (1'-4') of figure 19(b), and the principal axes of orthotropy

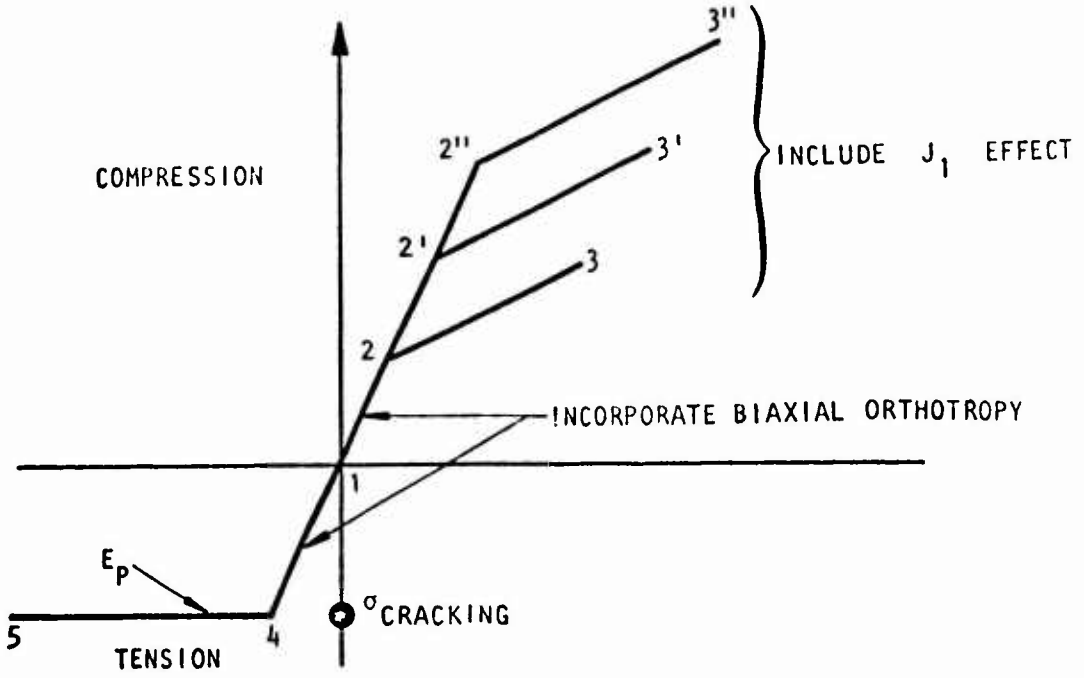

(a) Idealized stress/strain relations for concrete (homogeneous material)

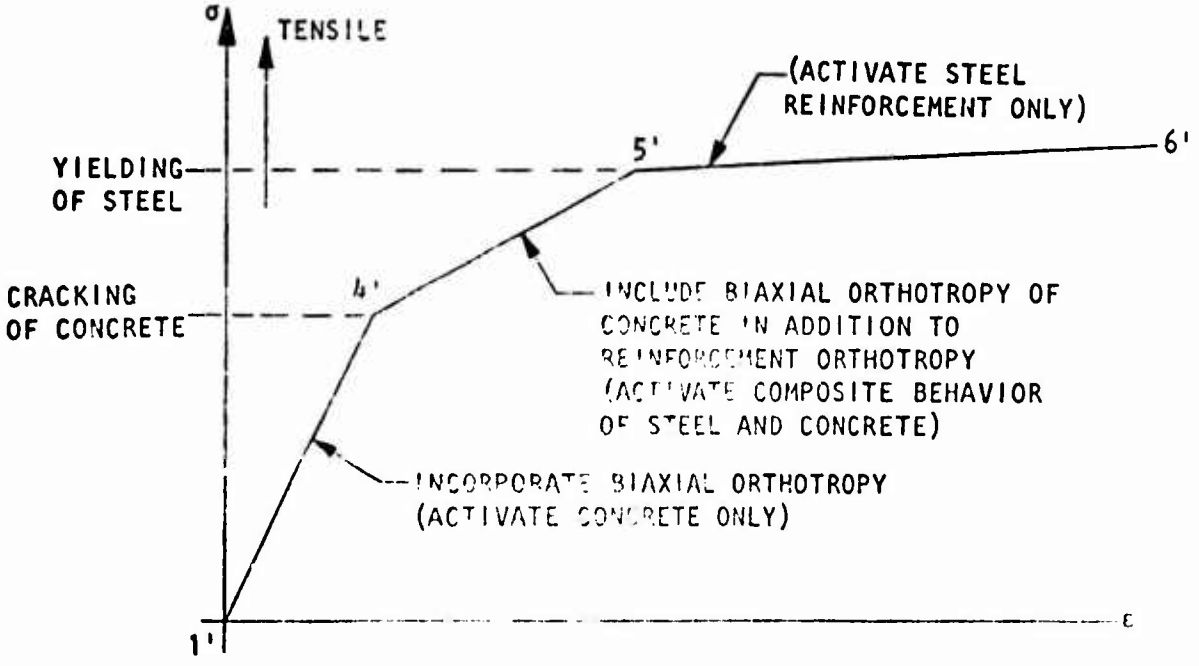

(b) Composite concrete tensile stress/strain relation

Figure 19. Composite Stress/Strain Relations

still coincide with the principal axes of stress. If, however, σ_1 exceeds the cracking stress f'_t, the principal directions of stresses are recorded as the initial cracking directions. The effective areas of steel A_{s_1} and A_{s_2} are found by resolving A_{s_I} and $A_{s_{II}}$ to the cracked direction and the cracking angle θ is recorded, as illustrated in figure 20. The cracking directions are thus recorded and used as a permanent reference for calculating and updating the orthotropic properties of the element. After cracking, the principal axes of stress may differ from the cracking axes. The present analysis assumes that these deviations are small and that fixing the cracking directions approximates the actual behavior of the structure under consideration. The check on cracking is repeated again for the σ_2 and σ_3 stresses, following similar steps.

For increased stresses, a postcracking hypothesis is adopted. The present analysis used available experimental data (Ref. 33) on the extension of cracks in reinforced concrete members subjected to tension loads. It is based on the premise that, after initial cracking, the concrete contributes to the overall stiffness of the section by an amount proportional to the bonded length D, and that a variable λ can be used to estimate the reduced stiffness of the section at various stages of loading. The variable λ is defined as

$$\lambda = \frac{D}{d+D} \tag{9}$$

where D is the bonded length of concrete, and d is the unbonded cracked length of concrete.

The variable λ is used to compute the composite stiffness E_1 of the section, which is given by:

$$E_1 = \frac{1}{\left[\frac{1-\lambda_1}{E_s A'_{s_1}} + \frac{\lambda_1}{E_s A'_{s_1} + E_{c_1}}\right]} \tag{10}$$

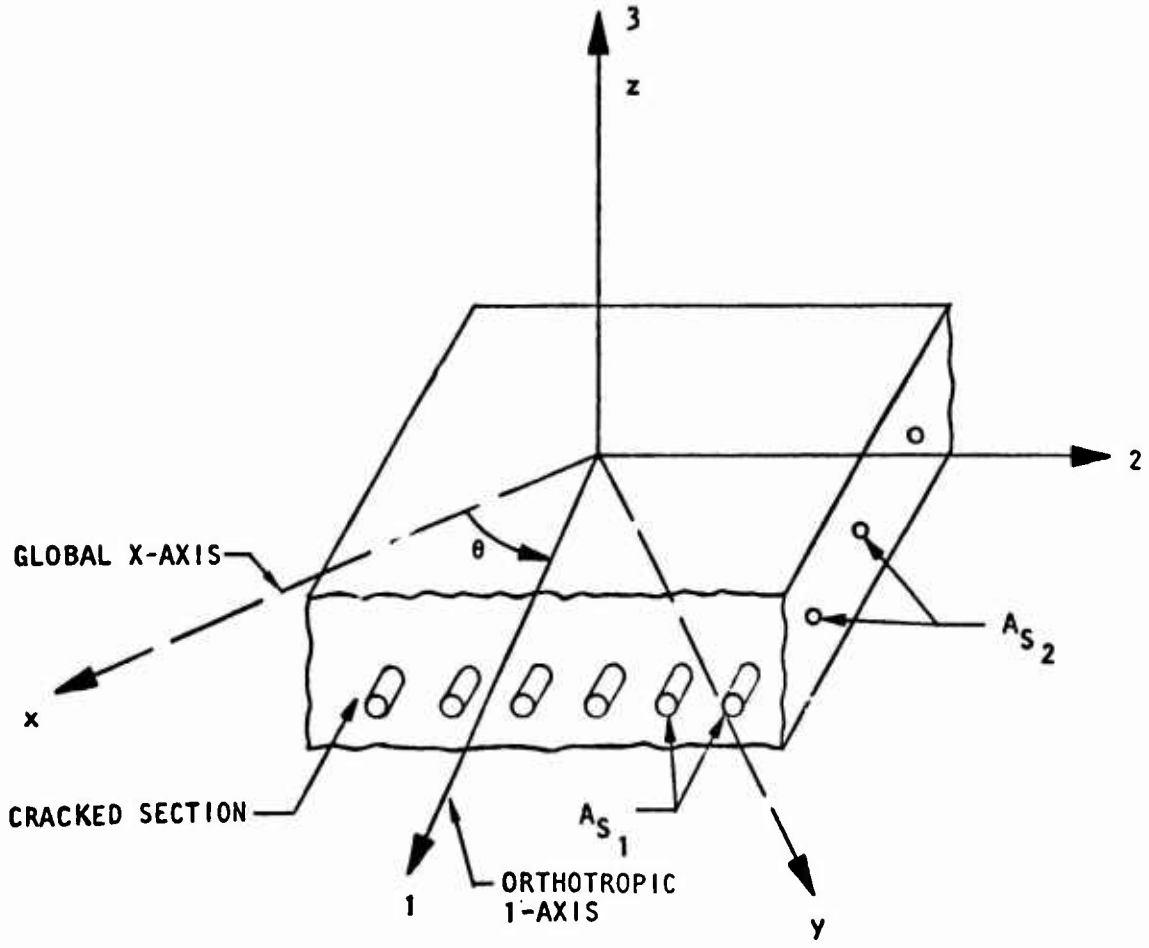

x,y,z ≡ GLOBAL COORDINATE SYSTEM

1 ≡ COORDINATE PERPENDICULAR TO THE CRACKING PLANE (WEAK DIRECTION)

θ ≡ ANGLE BETWEEN 1 AND x AXES. (POSITIVE COUNTERCLOCKWISE)

A_{S_1}, A_{S_2} ≡ REINFORCING STEEL IN THE DIRECTION AND PERPENDICULAR TO THE CRACKS

(a) Orientation of orthotropic axes 1, 2, 3 as defined by the initial cracking

Figure 20. Initiation of Cracks and Bond Slip in the Principal Direction

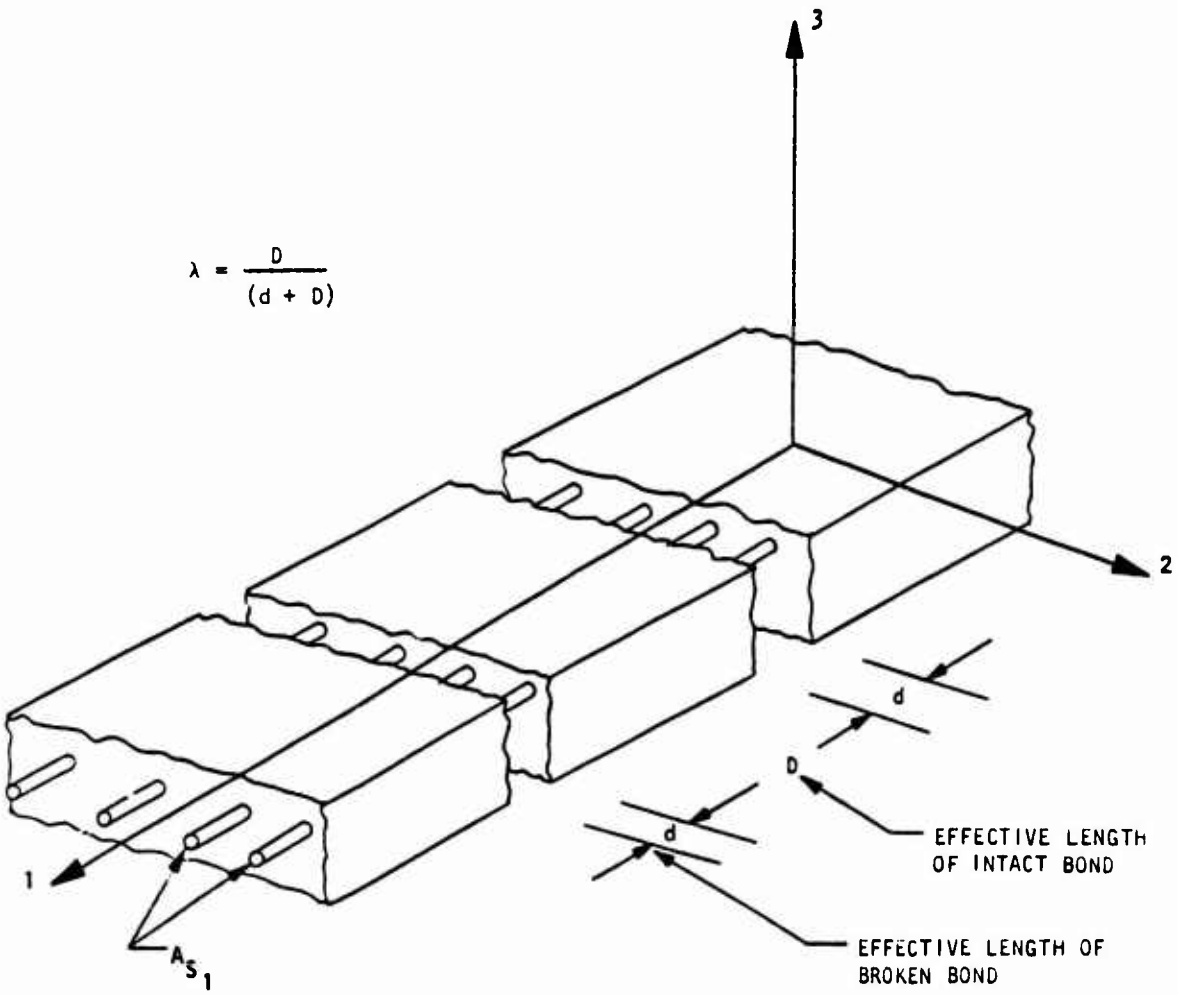

(b) Deterioration of bond produces decrease in λ

Figure 20. Initiation of Cracks and Bond Slip in the Principal Direction (concluded)

where

E_s = Modulus of steel (E_{os} or E_{ps})

A'_{s_1} = Percentage of steel in the 1-direction

E_{c_1} = Concrete initial modulus in tension (E_{oc})

λ_1 = Cracking variable as computed for direction 1

The above formula was used successively to compute the composite moduli E_1, E_2 and E_3 in the three orthotropic directions.

Before cracking, the value of λ is one and the concrete and steel contribute all their respective stiffnesses. However, after cracks occur, the first term in the denominator of equation 10 increases with the decrease of λ, while the second term decreases with decrease of λ. When bond becomes entirely broken, $\lambda = 0$, the second term disappears and the composite stiffness becomes the stiffness of the steel bars. Thus continuous change of λ accounts for the continuous loss of bond due to increased loads and provides a simple way for updating the composite properties of the element.

The variable λ describes the extent of bond deterioration. Bond begins to deteriorate at the onset of cracking of concrete and ends when the concrete ceases to add any stiffness to the assemblage. This range varies among materials and should be part of the input to the problem. The onset of yielding of reinforcing steel is the upper bound for the cracking range.

The composite shear modulus G_{12} was computed in a similar manner.

$$G_{12} = \frac{1}{2}\left\{\left[\lambda_1 \frac{E_{c_i}}{2(1+\nu_{21})} + \frac{E_s}{2(1+\nu_s)} A'_{s_1}\right] + \left[\lambda_2 \frac{E_{c_2}}{2(1+\nu_{12})} + \frac{E_s}{2(1+\nu_s)} A'_{s_2}\right]\right\} \qquad (11)$$

For a homogeneous element (plain concrete, rock, etc.), the second and fourth terms in the above equation vanish.

The form of equation 11 is somewhat analogous to the equation for shear modulus of an isotropic material, $G = \frac{E}{2(1 + \nu)}$. Equation 11 has two basic parts. First, a shear modulus is calculated as if the element isotropically possessed the effective E and ν in the 1-1 direction. A second calculation is made using the effective E and ν in the 2-2 direction. The average of the two shear moduli is assumed to be the effective shear modulus for the element. In several practical calculations of structural response, G_{12} based on equation 11 varied from 0.75 to 1.0 times the shear modulus for plain concrete near zero stress.

4. SUMMARY OF BASIC MODELS

A summary of the models that are discussed above is given in table 1.

From this summary it was concluded that the advantage of the discrete cracking element approach is its simplicity for computer programming and its ability to represent detailed bond-slip behavior at the exact position of the reinforcing. Disadvantages of this approach are the following:

- The parameters of the cracking element do not have a clear physical meaning and are therefore difficult to evaluate.
- The independent degrees of freedom of the cracking elements are the absolute displacements. It would therefore be possible for continuum elements on either side of the cracking element to move past each other if there were a reversal in sign of the load.
- In order for the cracking direction to be completely general, it is necessary to supply a cracking element for every nodal point in the assemblage.

Table 1. Summary of Basic Models

Model	Linkage Element (a)	Refined Linkage Element (b)	Nonlinear Model (c)	Refined Nonlinear Model (d)		Wall Panel Studies (e)		Continuum (f)
	Ngo & Scordelis	Ngo, Scordelis, & Franklin	Nilson	Franklin's 1st Scheme	Franklin's 2nd Scheme	Cervenka	Franklin	Isenberg & Adham
Finite Element	CST	CLS	CST	Frame	Q + Rod	Lattice	Q + Rod	LST
Linkage Element	Yes	Yes	Yes	No	Yes	No	No	No
Bond Slip	Linear--crude	Linear--crude	Nonlinear	No	Linear	No	No	Linear
Concrete Stiffness after Cracks	Crude	Crude	Yes	0	0 Normal to cracks	0	0	Yes
State of Stress	Uniaxial	Uniaxial	Biaxial	Uniaxial	Uniaxial	Biaxial	Biaxial	Plain strain
Basis of Stress-Strain Relation	Linear	Linear	Nonlinear Uniaxial	Nonlinear	Nonlinear	Nonlinear Uniaxial	Nonlinear Uniaxial	Bilinear Triaxial
Cracks	Predefined	Predefined	Calculated and remeshed	Vertical	Diagonal	Calculated	Calculated	Calculated
Dowel Shear	No	Crude	No	No	No	No	No	Linear
Aggregate Interlock	No	Crude	No	No	No	No	No	No
Unloading	No	No	No	No	No	Yes	No	Yes
Experimental Correlation	Fair (beam)	Fair (beam)	Fair (axial)	Poor (beam)	Poor (beam)	Good (wall panel)	Good (wall panel)	Good for adequate reinforcing

The advantage of the equivalent continuum approach is that it offers complete generality with respect to directions of cracking and orthotropy and with respect to the constitutive properties of plain concrete. A disadvantage is complexity of computer programming that is needed due to the orthotropic formulation of composite stress/strain relations.

5. OTHER MODELS OF REINFORCED CONCRETE

A brief summary of other studies of reinforced concrete behavior are included here for completeness. Bresler and Bertero (Ref. 34) studied the effects of repeated loads on reinforced concrete members. Selna (Refs. 35 and 36) developed a method of analyzing one-dimensional beams and frames as layered systems, assuming linear elastic behavior up to tensile cracking or perfectly plastic yielding. Time-dependent shrinkage and creep effects were included. Sandhu, Wilson, and Raphael (Ref. 37) performed two-dimensional stress analyses of plain concrete dams, including the effect of creep. Similar studies have been undertaken by several other investigators. Valiappan and Doolan (Ref. 38) made two-dimensional stress studies that included the effects of tensile cracking and elastic-plastic behavior in compression using an initial stress approach. The postcracking stiffness of cracked finite elements was set equal to zero.

In a recent report Yuzugullu and Schnobrich (Ref. 39) used the finite element method to study the inelastic behavior of shear wall-frame systems. They assumed that cracked concrete does not carry any tensile forces perpendicular to the cracks, but maintains some amount of shear stiffness because of the irregular surface of the crack. Uniaxial, perfectly plastic behavior was assumed for both the cracked concrete and reinforcing steel. A linkage element similar to that developed by Ngo and Scordelis (Ref. 2) was used.

Taylor et al. (Ref. 40) presented a finite element analysis that used an incremental, iterative solution to predict the nonlinear behavior of reinforced and prestressed concrete structures subject to cracking. The initiation and propagation of cracks were accounted for by redefining (within

each iteration) the finite element grid lines so that they more nearly coincided with the predicted crack paths. Linear strain elements were used to model the reinforcement. A linkage element (Ref. 2) was used to model the bond/slip mechanism. The solution is path-independent, and no attempt was made to discuss cyclic stress-strain states.

Studies of reinforced concrete slabs by the finite element method have been presented by Jofriet and McNiece (Ref. 41) and by Bell and Elms (Ref. 42), which incorporate progressive cracking in triangular or quadrilateral plate bending elements. Changes in the bending stiffness of elements due to cracking normal to the principal moment direction are accounted for by using a reduced flexural rigidity in forming the element stiffnesses. Comparisons between computed and experimental results are presented.

Wahl and Kasiba (Ref. 43) applied the finite element method to the analysis of prestressed concrete nuclear reactor structures, which were treated as axisymmetric solids. Rashid (Ref. 44) discussed an analysis method (more refined than that of Wahl and Kasiba) that accounts for cracking, temperature effects, creep, and load history.

A study was undertaken by Endebrock and Traina (Ref. 45) to determine the behavior of plain concrete under combined stresses and to formulate computer-oriented constitutive relations for concrete. One nominal concrete strength was tested under various loading combinations. The loading combinations included the uniaxial, biaxial, and triaxial states of stress with various combinations of compressive and tensile stresses. The test specimens were three-inch cubes. The test information was obtained as stress/strain records for the three principal directions of the cubical test specimens.

During the testing program it was noted that somewhat different strength values were obtained depending upon the orientation of the cube with respect to the applied loads and the direction of casting. The uniaxial compressive strength was not greatly affected by the orientation of the cubes; however, the biaxial and triaxial test results were noticeably affected by the cube

orientation. The failure mode of the cubes was identical to that described by several investigators. It was noted that the slightest confinement of a test cube in an intended uniaxial test would noticeably affect the maximum strength.

In triaxial compressive tests, it was noted that the maximum stress was greatly affected by the magnitude of the minor stress and somewhat affected by the intermediate stress. The strains were generally affected in the same manner.

The test results from this investigation were compared to available test results reported by other investigators. The scatter in results reported is rather large; however, many of the investigators used different testing procedures, equipment, and different shaped test specimens. The results of this investigation were bounded by the results reported by other investigators.

A model to predict concrete behavior was developed. The mathematical development of the model was theoretical; however, empirical results were incorporated into the model such that the test results were simulated. The model was used to predict the constitutive relations for concrete subjected to combined loads. The loads can be tensile or compressive. The model solution was incorporated in a computer program.

The experimental data generated by this study represent a substantial addition to the information available on multiaxial loading. However, the model developed uses one concrete strength only and does not account for the effect of loading and unloading under combined stresses.

SECTION III

RECENT DEVELOPMENT IN METHODS OF OBTAINING PARAMETERS OF A COMPLETE MODEL

One of the greatest difficulties in any attempt to analyze a reinforced concrete member is to select a material model general enough to allow good correlation with data from various types of loading tests and to evaluate the parameters appearing in such a model. Recently reported progress, summarized below, indicates that suitable descriptions of the behavior of plain concrete and of the influence of reinforcing are available. These elements will be combined in Section IV to obtain a model of reinforced concrete.

1. CONSTITUTIVE PROPERTIES OF PLAIN CONCRETE

Considerable work has been conducted on uniaxial behavior of plain concrete. However, most of this work does not account for the combined stress states encountered in refined analysis by the finite element method. The paper by Popovics (Ref. 46) on stress/strain relationships for concrete under uniaxial loading provides an excellent review of the literature. Information on the response of concrete under combined stresses is much more meager (Refs. 1, 4, 45, and 47 through 51), particularly with respect to general stress/strain relationships. Significant experimental work was reported by Kupfer, Hilsdorf and Rusch (Ref. 50). Buyokozturk, Nilson, and Slate (Ref. 52) have used the finite element method to develop an analytical model of plain concrete composed of aggregate elements and paste elements to study its behavior under two-dimensional combined stress states. Liu, Nilson, and Slate (Ref. 53) proposed an analytical form of stress/strain relationship of concrete in biaxial compression. In addition, orthotropic constitutive relationships were stated in a matrix form adapted to finite element models. They also compared their biaxial relation to those developed by Saenz (Ref. 54) and by Desayi and Krishnan (Ref. 55).

The following constitutive relations developed by Liu, Nilson, and Slate for concrete in biaxial compression are adopted.

$$\sigma_1 = \frac{\varepsilon_1 E}{(1 - \nu\beta_1)\left[1 + \left(\frac{1}{1 - \nu\beta_1}\frac{E}{E_{sc}} - 2\right)\left(\frac{\varepsilon_1}{\varepsilon_p}\right) + \left(\frac{\varepsilon_1}{\varepsilon_p}\right)^2\right]} \qquad (12)$$

where secant modulus at ultimate load $E_{sc} = \sigma_p/\varepsilon_p$, and σ_p, ε_p are the peak stresses and strains in biaxial compression respectively, and

σ_1 = Stress in the 1-direction

ε_1 = Strain in the 1-direction

$\beta_1 = \dfrac{\sigma_2}{\sigma_1}$

E = Initial tangent modulus in uniaxial loading for unconfined compression

ν = Poisson's ratio in uniaxial loading for unconfined compression

The value of E can be computed from the equation of Pauw (Ref. 56) as recommended in the American Concrete Institute Code (318-71):

$$E = 33\, W^{3/2} \sqrt{f'_c} \text{ psi} \qquad (13)$$

$$\left(E = 42.7\, W^{3/2} \sqrt{f'_c} \text{ N/m}^2\right)$$

in which W is the unit weight of the hardened concrete, in pounds per cubic foot (kg/m^3); and f'_c = ultimate cylinder strength of concrete in uniaxial compression, in pounds per square inch (Newton/m^2).

Pauw (Ref. 56) examined Poisson's ratio ν in a series of tests and found values near 0.20. Liu, Nilson, and Slate (Ref. 53) found that the ultimate strength σ_p could be computed from:

$$\left.\begin{array}{lll} \beta < 0.2 & \dfrac{\sigma_p}{\sigma_o} = 1 + \dfrac{\beta}{1.2 - \beta} \\ 1.0 \geq \beta \geq 0.2 & \dfrac{\sigma_p}{\sigma_o} = 1.2 \\ 5.0 \geq \beta \geq 1.0 & \dfrac{\sigma_p}{\sigma_o} = \dfrac{1.2}{\beta} \\ \beta > 5.0 & \dfrac{\sigma_p}{\sigma_o} = \dfrac{1}{\beta}\left(1 + \dfrac{1}{1.2\beta - 1}\right) \end{array}\right\} \qquad (14)$$

and

$\beta = \beta_1 = \sigma_2/\sigma_1$ if the 1-direction is considered,

and ε_p is computed from

$$\left.\begin{array}{lll} \beta \leq 1 & \varepsilon_p = 0.0025 & \\ \beta > 1 & \varepsilon_p = (-500 + 0.55\,\sigma_p) \times 10^{-6}, & \sigma_p \text{ in psi} \\ & (\quad = (-500 + 7.98 \times 10^{-5}\,\sigma_p) \times 10^{-6}, & \sigma_p \text{ in } N/m^2) \end{array}\right\} \quad (15)$$

where

σ_o = Unconfined compressive strength

In addition to Young's moduli, which must be computed for each of the three orthotropic directions, three Poisson's ratios must be computed: $\nu_{12} = \nu_{21}$, $\nu_{23} = \nu_{32}$, and $\nu_{31} = \nu_{13}$.

When cracking occurs, a simplification can be made. For example, for cracking in the plane perpendicular to the 1-direction, the coupling effects are removed and

$$\nu_{21} = \nu_{31} = 0 \quad (16a)$$

For simplicity it is assumed that

$$\nu_{23} = \nu_{32} = 0 \quad (16b)$$

Three concrete shear moduli are also required. Assuming that the 1-2 plane is uncracked,

$$G_{12} = \frac{E'_{1b} E'_{2b}}{E'_{1b} + E'_{2b} + 2E'_{2b}\,\nu} \quad (17)$$

in which

$$E'_{1b} = \frac{E\left[1 - \left(\frac{\varepsilon_1}{\varepsilon_p}\right)^2\right]}{\left[1 + \left(\frac{1}{1 - \nu\beta_1}\frac{E}{E_{sc}} - 2\right)\left(\frac{\varepsilon_1}{\varepsilon_p}\right) + \left(\frac{\varepsilon_1}{\varepsilon_p}\right)^2\right]^2} \quad (18)$$

where

$$\nu_{12} = \nu_{21} = \nu_{31} = \nu_{13} = \nu_{23} = \nu_{32} = \nu \tag{19}$$

for biaxial compression and is equal to E for biaxial tension and tension-compression cases (for concrete in tension, it can be assumed without significant loss of accuracy that linear behavior is obtained up to failure; the elastic slope will be taken equal to the initial tangent modulus in compression)

and

$$E'_{2b} = \frac{E\left[1 - \left(\frac{\varepsilon_2}{\varepsilon_p}\right)^2\right]}{\left[1 + \left(\frac{1}{1 - \nu\beta_2}\frac{E}{E_{sc}} - 2\right)\left(\frac{\varepsilon_2}{\varepsilon_p}\right) + \left(\frac{\varepsilon_2}{\varepsilon_p}\right)^2\right]^2} \tag{20}$$

for biaxial compression, and is equal to E for biaxial tension, and to E_2 for tension-compression case, where

E_2 = E in the 2-direction

$\beta_1 = \sigma_2/\sigma_1$ for biaxial compression

$\beta_2 = \sigma_1/\sigma_2$ for tension/compression

Assuming that there is a crack in the plane perpendicular to the 3-direction,

$$G_{13} = G_{23} = 0 \tag{21}$$

It follows that

$$\begin{bmatrix} \sigma_1 \\ \sigma_2 \\ \sigma_{12} \end{bmatrix} = \begin{bmatrix} \lambda' \frac{E'_{1b}}{E'_{2b}} & \lambda'\nu & 0 \\ \lambda'\nu & \lambda' & 0 \\ 0 & 0 & \frac{E'_{1b}E'_{2b}}{E'_{1b} + E'_{2b} + 2E'_{2b}\nu} \end{bmatrix} \begin{bmatrix} \varepsilon_1 \\ \varepsilon_2 \\ \varepsilon_{12} \end{bmatrix} \text{.....} \tag{22}$$

where

$$\lambda' = \frac{E_1' b}{\frac{E_1' b}{E_2' b} - \nu^2} \tag{23}$$

Liu, Nilson, and Slate (Ref. 53) recommended equation 22 for the constitutive relation of concrete in biaxial loading and indicated that it produces results that compare well with experimental data as illustrated in figures 21 and 22. However, they also indicated that no experimental data are presently available to check the shear term in the proposed relationship.

2. DOWEL ACTION OF REINFORCEMENT CROSSING CRACKS IN CONCRETE

If a shear force acts on the cracked specimen, the cracked surfaces may slip, the force being counteracted only by the crosswise bars. During slipping, the bars develop shears that cause flexural stresses. This resistance of the bars to slipping is called "dowel action."

Dowel action has been studied by several investigators. Jones (Ref. 57), Parmelee (Ref. 58), Krefeld and Thurston (Ref. 59), and Lorensten (Ref. 60) have studied dowel action in reinforced concrete beams.

Parmelee (Ref. 58) proposed that the transverse force-displacement relationship of reinforcement at an inclined crack can be approximated by considering a semi-infinite elastic rod subjected to tension, T, and transverse shear, V_s, and restrained at the end of the gap by embedment in an elastic medium (Fig. 23). The displacement, Δ, of such a rod depends to some extent on the effective width, a*, of the longitudinal cracked zone (Fig. 24).

A brief summary of the previous work on dowel action has been presented by Bresler and MacGregor (Ref. 61).

The studies reported above have neglected the action of the stirrups and the effect of horizontal cracking of the concrete cover. No consideration has been given to the dowel action in the postcracking stage.

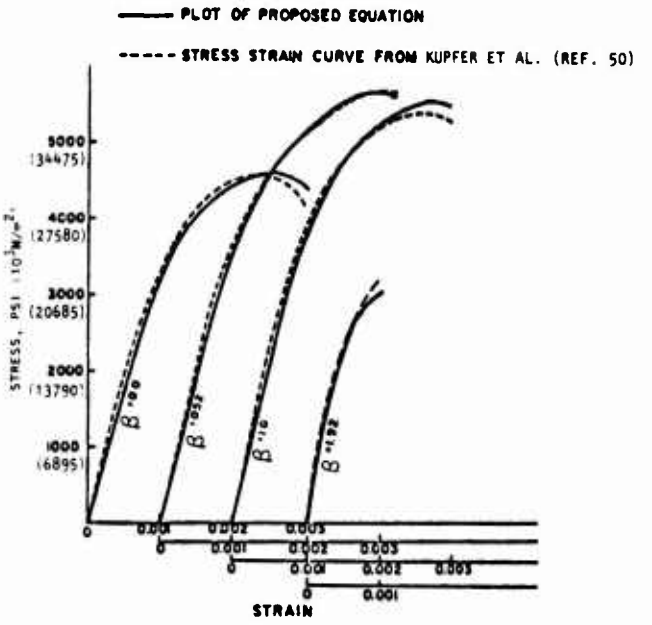

Figure 21. Comparison of Plot of Proposed Equation with Those Obtained from Biaxial Compression Tests (Ref. 50)

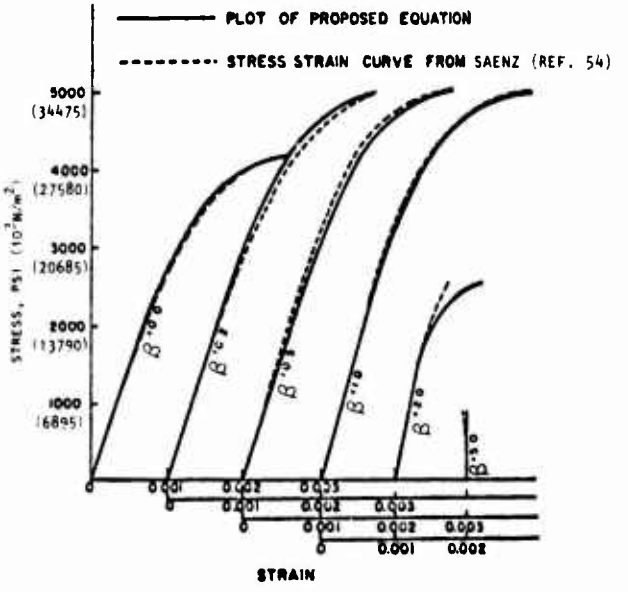

Figure 22. Comparison of Plot of Proposed Equation with Those Obtained from Biaxial Compression Tests (Ref. 54)

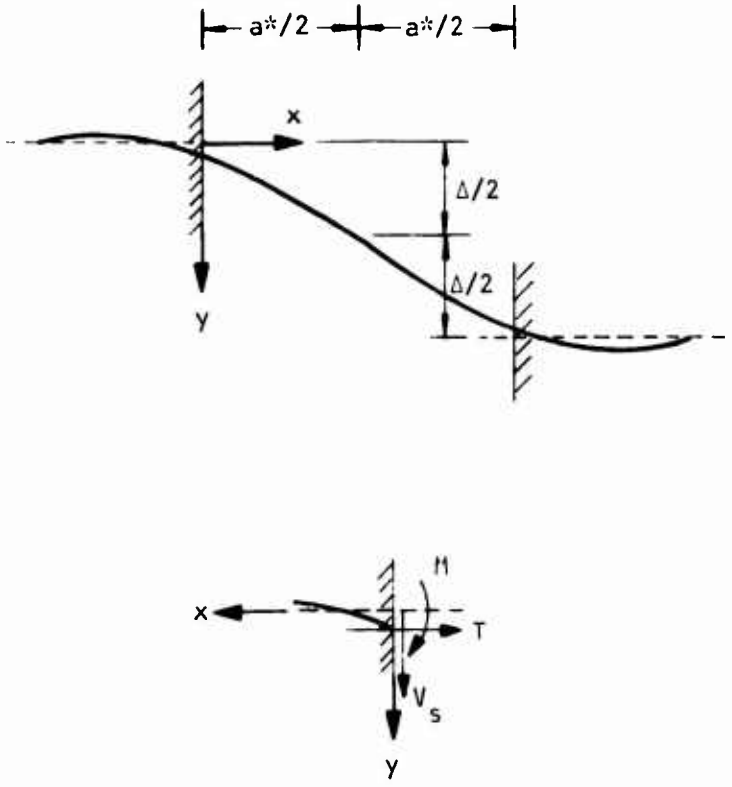

Figure 23. Dowel Action-Displacement

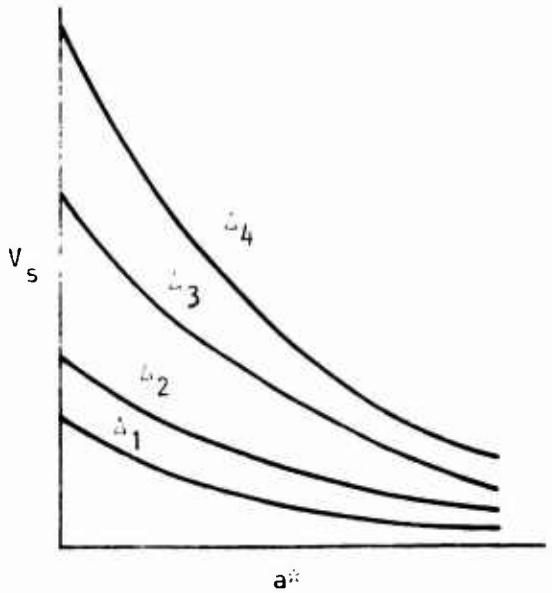

Figure 24. Dowel Force-Displacement Relationships (after Parmelee--Ref. 58)

Dowel action in precracked and uncracked specimens was studied by Hofbeck, et al. (Ref. 62), Johnston and Zia (Ref. 63), and Peter (Ref. 22). It was also discussed in the ACI-ASCE Joint Committee 426 report (Ref. 64).

In a recent paper Dulacska (Ref. 65) conducted a test program to examine the phenomenon of dowel action in order to establish theoretical load-deformation relationships. The Dulacska tests were made using specimens designed as shown in figure 25. To simulate cracks, two layers of 0.0078-in.-thick (0.019812 cm) sheet brass, which were connected in the middle by a skewed steel stirrup, were embedded in the test specimens. During testing, relative slip along the simulated crack and opening of the crack perpendicular to the direction of the load were recorded.

Experimental results for the failure load in the bar were found to correlate well with the following relationship:

$$T_f = \rho\phi^2 \gamma \sigma_y n \sin\delta \left[\sqrt{\left(1 + \frac{\sigma_c}{3\rho\gamma^2 \sigma_y n \sin^2\delta}\right)} - 1 \right] \qquad (24)$$

where

T_f = Failure load of dowel shear

ϕ = Bar size

δ = Angle of stirrups in degrees

σ_y = Yield stress of steel

σ_c = Cube strength of concrete

n = Coefficient of local compression of concrete

γ = Constant

$\rho = 1 - N^2/N_y^2$

N = Axial tension force of bar

N_y = Axial tensile force inducing yield in pure tension

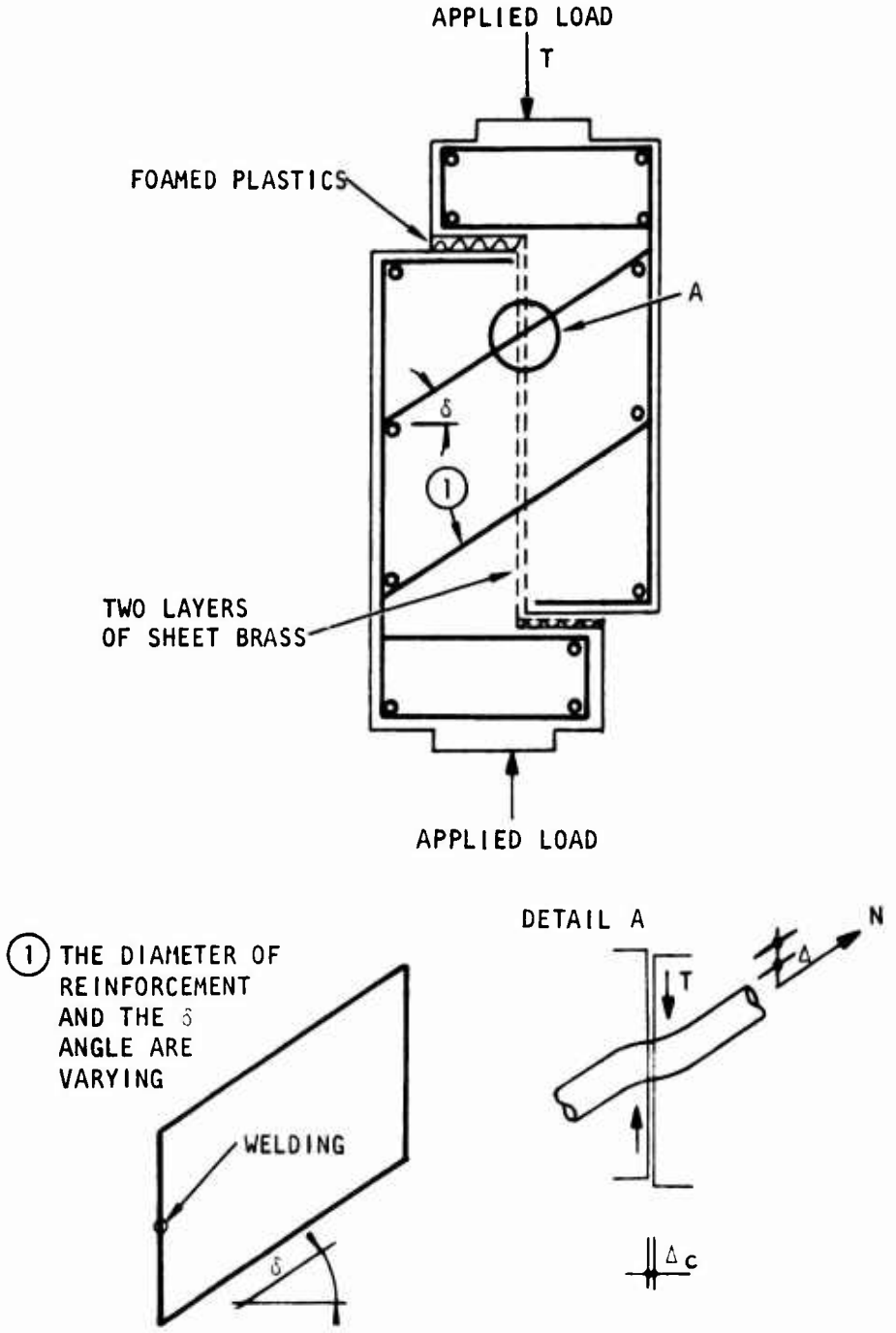

Figure 25. Details of Test Specimen Construction (Ref. 65)

From test results, it was found that slip in inches (cm) can be predicted by the approximate expression:

$$\Delta = \frac{\bar{A}T}{\phi}\sqrt{\frac{1}{\sigma_c}\tan\left(\frac{T}{T_f}\frac{\pi}{2}\right)} \qquad (25)$$

where

$\bar{A}$ = Constant

T = Dowel shear load

T_f = Failure load of dowel shear calculated from equation 24

ϕ = Bar size

σ_c = Cube strength of concrete

when T, ϕ, and σ_c are in consistent units.

Equation 25 was plotted as a function of T and Δ for two values of $\delta = 10^{o}$ and 40^{o} respectively, as shown in figure 26.

The results indicate that an increase in the angle δ results in a decrease of the dowel shear force T and increase in the bar's normal force N. Also, an increase in the concrete strength σ_c results in an increase of dowel shear capacity T_f.

3. BOND SLIP

Bond slip enters constitutive equations for reinforced concrete through the effective moduli of the composite material. It may be defined quantitatively as the percentage of its own stiffness that concrete contributes to the stiffness of a composite element.

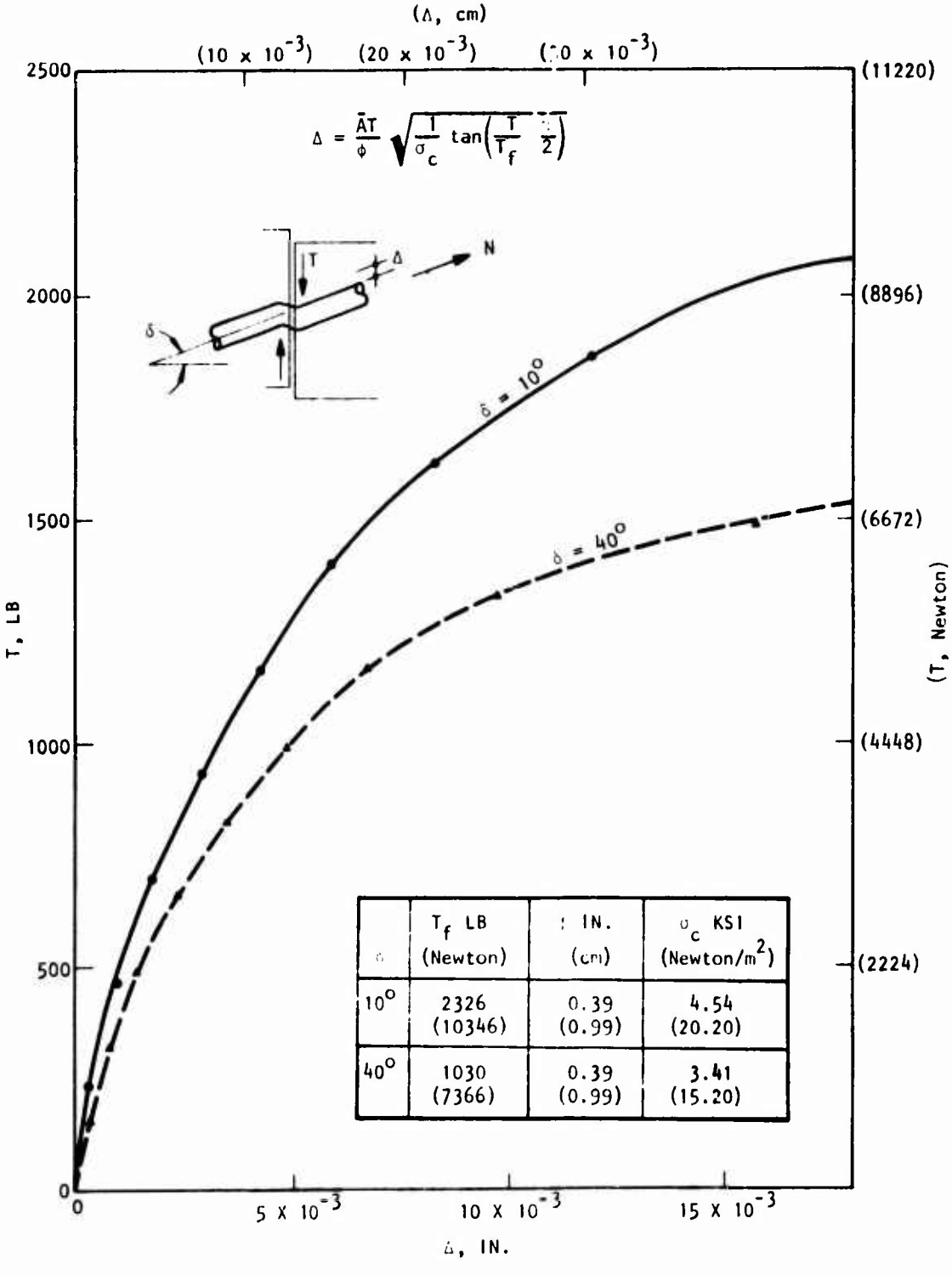

δ	T_f LB (Newton)	Δ IN. (cm)	σ_c KSI (Newton/m^2)
10°	2326 (10346)	0.39 (0.99)	4.54 (20.20)
40°	1030 (7366)	0.39 (0.99)	3.41 (15.20)

Figure 26. Dowel Shear Force-Slip Relationship (Ref. 65)

The new work bearing on this subject is that of Ismail and Jirsa (Ref. 66). An expression for λ, the ratio of concrete contributing to overall stiffness of the section was defined as follows:

$$\lambda = 1 - \frac{\int_0^L \varepsilon_s \, dx}{\frac{TL}{A_s E_s}} \tag{26}$$

where

ε_s = Steel strain

T = Tensile force

A_s = Cross-sectional area of steel

E_s = Young's modulus for steel

L = Length of specimen

The length of test specimen was 16 in. (40.6 cm), selected to limit the formation of secondary cracks between the ends and the primary crack at the midlength. The location of the primary crack was determined by inserting greased sheet metal strips (crack formers) in the form prior to casting, as illustrated in figure 27(a). The concrete strength f'_c was 4.75 ksi (32751 x 10^3 N/m^2) for two specimens and 3.25 ksi (22409 x 10^3 N/m^2) for the other two. Data from this work are shown in figure 27 as a relationship between λ and σ_s/σ_y, where σ_s is the stress in the steel reinforcing bar and σ_y is yield stress of this bar. The data indicate that λ can be presented as a function of

- Concrete strength
- Steel stress (fraction of yield strength)
- Cycle of loading/unloading

The experimental work by Tanner (Ref. 67) represents a valuable addition to the data on bond slip. The concentric pullout specimen, figure 27(b), was used to simulate conditions obtained in the constant moment region of a

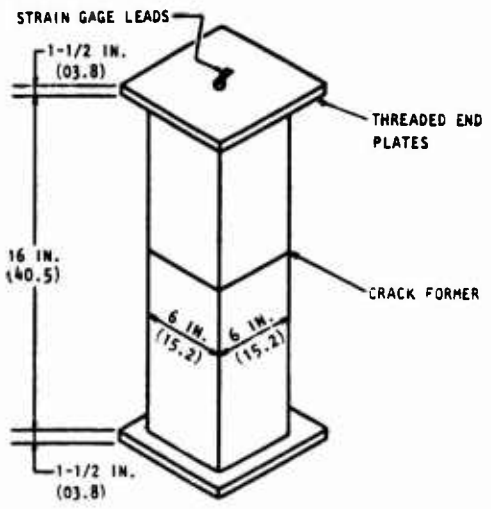

(a) Dimensions of test specimen used by Ismail and Jirsa (Ref. 66)

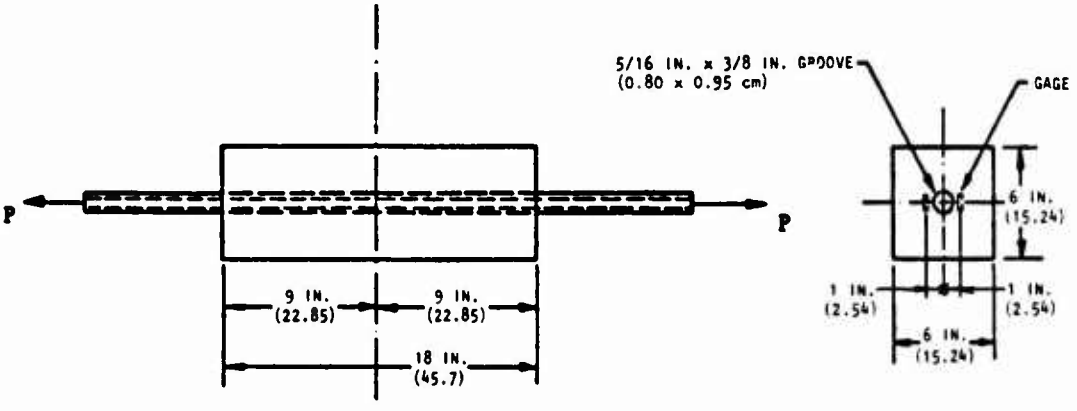

(b) Specimen used in test series II by Tanner (Ref. 67)

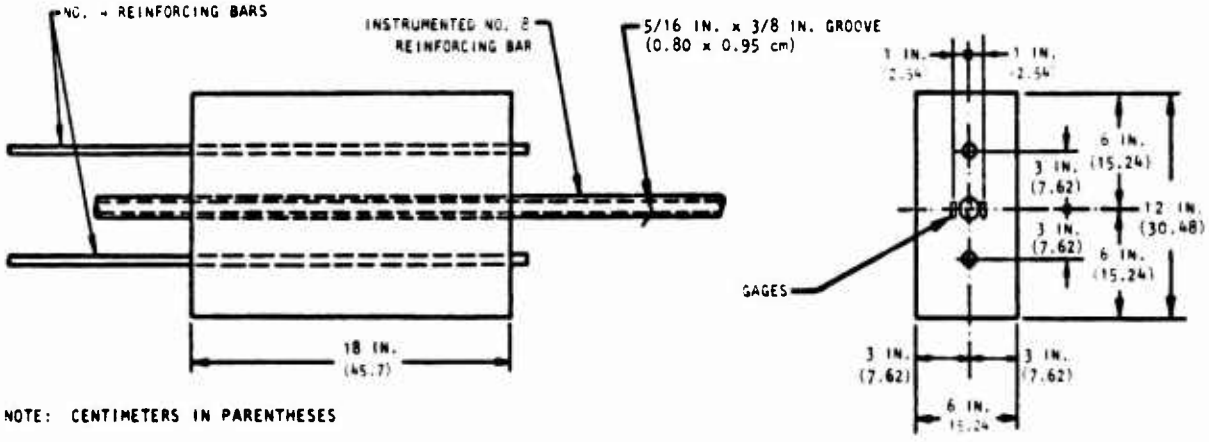

(c) Specimen used in test series III by Tanner (Ref. 67)

Figure 27. Test Specimens of Bond Slip (Refs. 66, 67)

reinforced concrete beam between tensile cracks. The lapped-splice specimen, figure 27(c), was designed to simulate spliced reinforcement in a constant moment region of a beam between tensile cracks.

Data from both tests are plotted for different concrete strength in figure 28. The results of Tanner's concentric pullout tests (II-B) are bounded by the results of Ismail and Jirsa (Ref. 66). However, the results of Tanner's lapped-splice specimens were considerably higher than those obtained from concentric pullout tests performed both by Tanner and by Ismail and Jirsa.

The linear bond-slip relation used by Isenberg and Adham (Ref. 1) is also indicated in figure 28.

The effect of loading and unloading on λ was studied by Ismail and Jirsa (Ref. 66) and indicates that λ is reduced by cyclic loading whenever the peak moments in the preceding cycle are greater than in any previous cycle.

4. CRACK WIDTH AND CRACK SPACING

Extensive investigations have been carried out concerning crack widths and crack spacing in reinforced concrete members (Refs. 33 and 68-84) and several theoretical and empirical formulas have been developed (Refs. 68-69, 75-76, and 84-86).

One of the simplest and most useful studies found in the references cited above is the one conducted by Broms (Ref. 33). Data on crack widths were obtained from flexural and tensile tests of members reinforced with steel bars, figures 29 through 33.

A tension member is shown in figure 29(a). The crack spacing at the level of the reinforcement was observed to decrease rapidly with increasing applied load. After the axial stress in the reinforcement had reached a certain critical value, the spacing of visible cracks remained approximately constant. It has been shown by Broms (Ref. 33) that high calculated axial tensile stress will be present within an area located inside a circle that is inscribed between

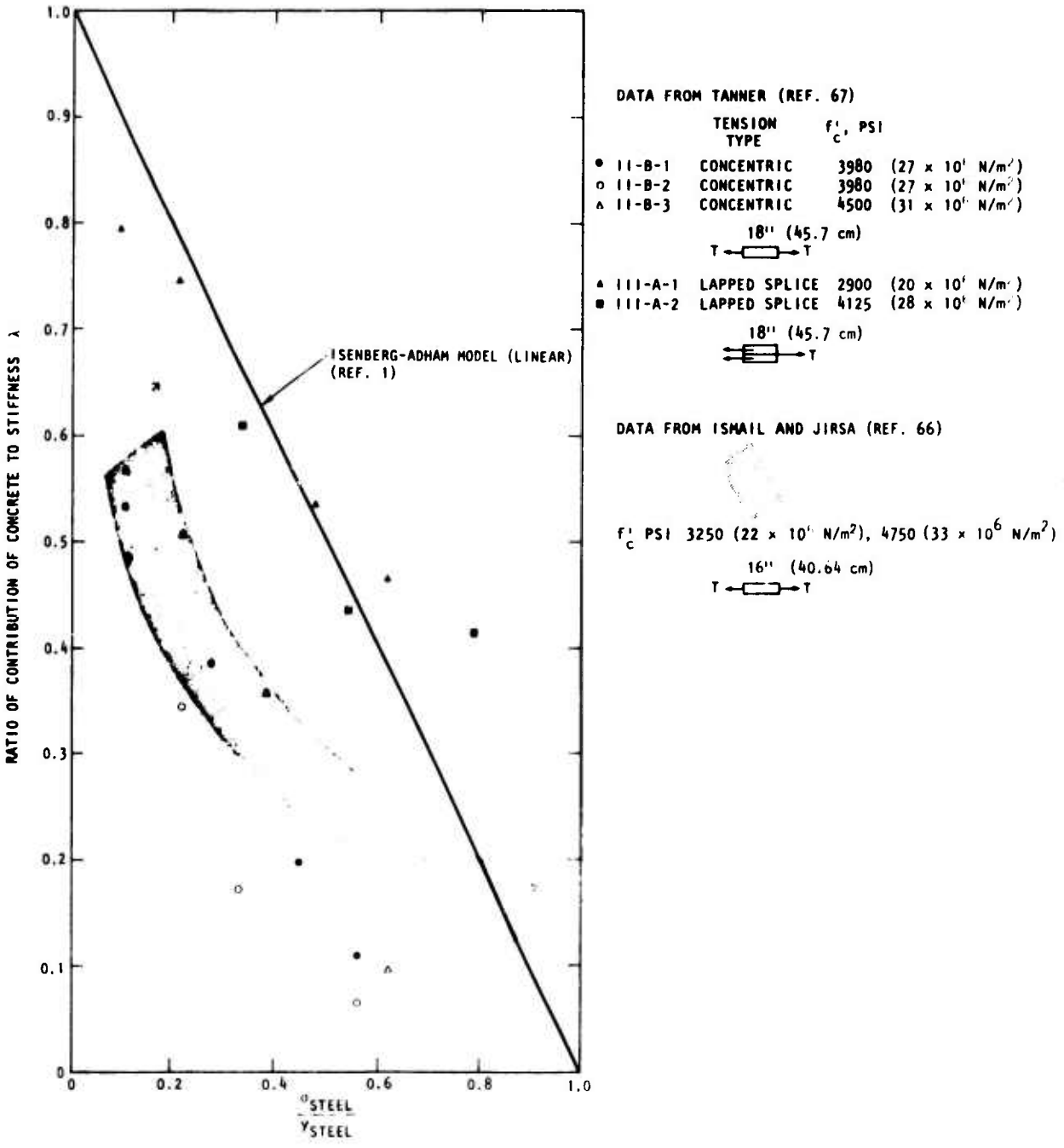

Figure 28. Experimental Bond-Slip Results (Refs. 66, 67) Compared with Analytical Results (Ref. 1)

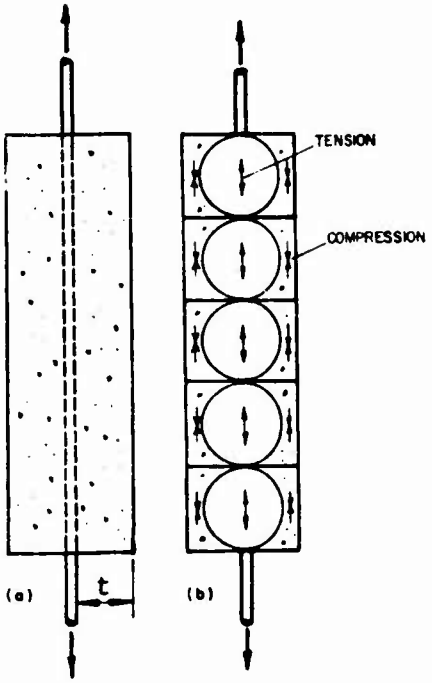

Figure 29. Tension Members (Ref. 33)

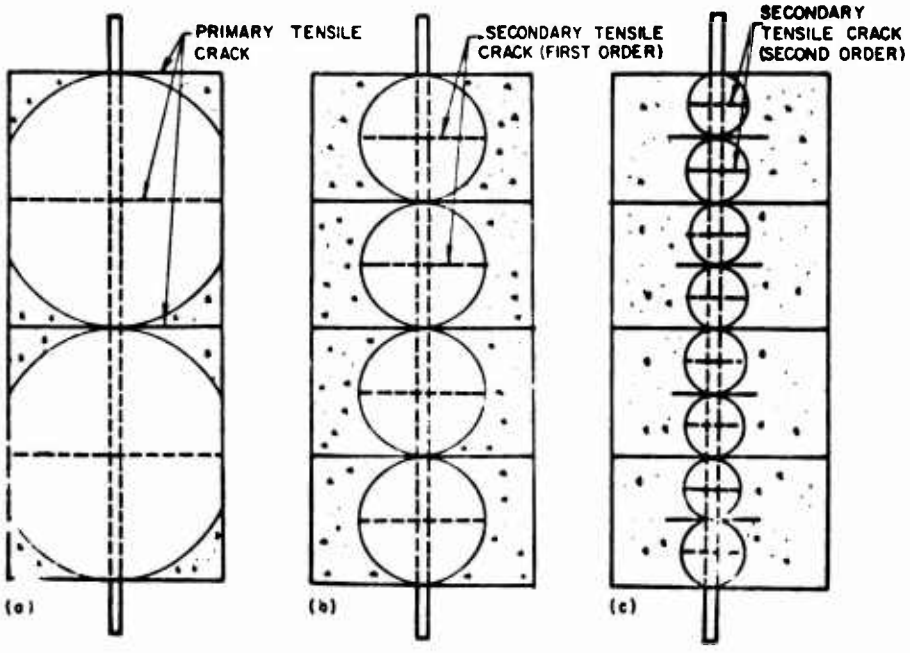

Figure 30. Mechanism of Tension Cracking (member reinforced with one bar) (Ref. 33)

two adjacent preexisting cracks. Outside this stress circle, compressive stresses or very small tensile stresses will be present, as illustrated in figure 29(b).

According to Broms (Ref. 33),

> When the maximum tensile stress within any one stress circle exceeds the tensile crack strength of the concrete, a new tensile crack develops. This tensile crack will spread laterally until the average tensile stress at the root of the crack decreases to a value smaller than the tensile strength of the concrete. This appears to occur when the crack approaches the periphery of the corresponding inscribed circle. For the case when the member is reinforced with a single reinforcing bar, the length of this new tensile crack will be governed by the diameter of the circle inscribed between two adjacent preexisting cracks and thus, by the crack spacing. If the diameter of the inscribed circle is equal to or larger than the total width of the member shown in figure 30(a), then the normal crack will traverse the total section of the member. Such a crack is defined as a primary crack. If on the other hand, the diameter of the inscribed circle is less than the total width as shown in figure 30(b), then the new crack (which forms halfway between two existing primary cracks) will extend over only part of the total member width. This crack will be defined as a secondary crack. Therefore as cracking proceeds, the length of subsequent cracks will decrease in proportion to the crack spacing as shown in figure 30(c).
>
> The length of the new cracks that develop in a member reinforced with several bars will depend on the spacing of the individual bars and on the primary crack spacing. In the case when the primary crack spacing is larger than the spacing of the reinforcement (Figs. 31(a) and 31(b)), the individual stress circles corresponding to each reinforcing bar overlap. As a result, the tensile cracks that develop at each individual bar join into a single crack that extends over part or all of the width of the member. The new tensile crack will extend to the unloaded vertical sides of the member (and will become a primary crack) if the stress circle corresponding to the bar located closest to the side of the member reaches the side of the member (Fig. 31(a)). This condition occurs when primary crack spacing is larger than twice the thickness of the side cover. When the primary crack spacing is less than twice the concrete cover (Fig. 31(b)), then the new tensile crack will not reach the surface of the member and will become a secondary crack.
>
> The preceding analysis suggests that the absolute minimum visible crack spacing will be equal to the distance from the surface to the center of the bar located closest to the surface of the member. This distance is defined as the distance t. Thus, it is suggested that the theoretical minimum crack spacing will be equal to the thickness of the concrete cover (measured from the center of the reinforcing bar located closest to the considered face).

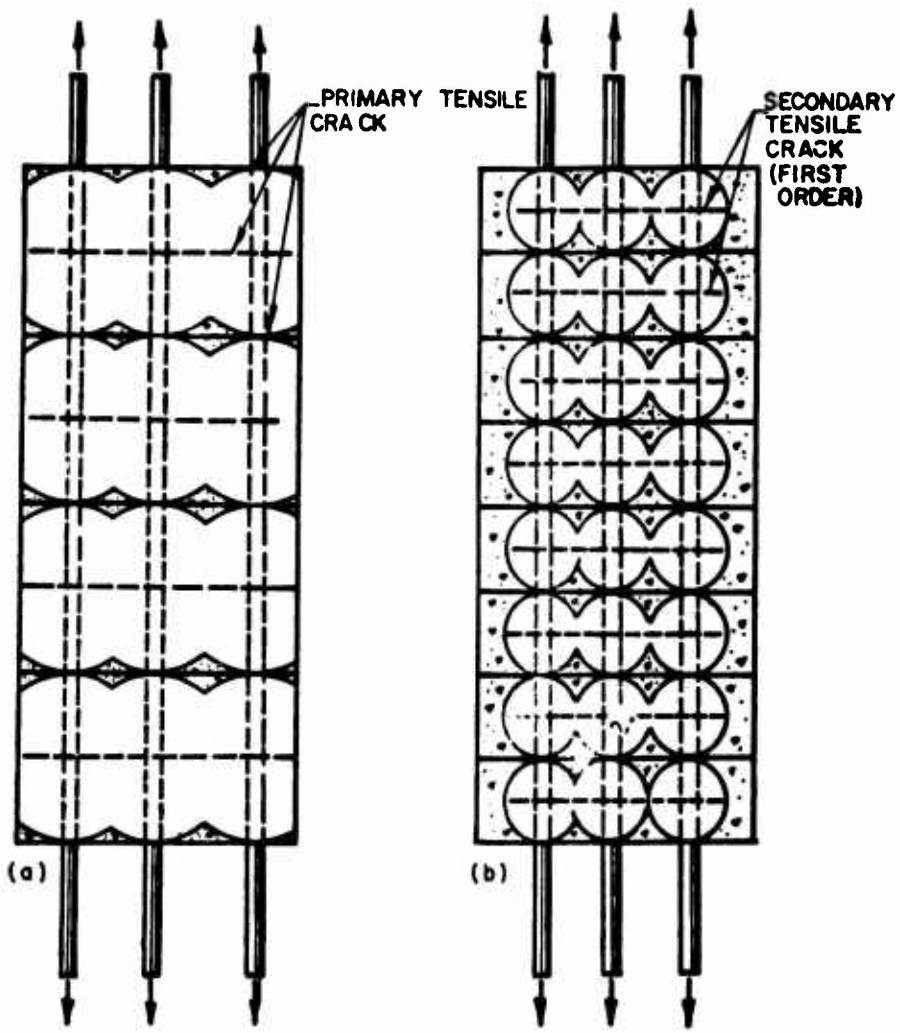

Figure 31. Mechanism of Tension Cracking (member reinforced with several bars) (Ref. 33)

The formation of flexural cracks affects the longitudinal stress distribution in flexural members. The stress distribution within a cracked flexural member can be calculated approximately from theory of elasticity. It can be shown that high tensile stresses will be present within the circular area located between two adjacent cracks, as illustrated in figure 32. Outside this circular area, compression stresses or small tensile stresses will be present. The stress circles governing the stress distribution for the tension zone have been redrawn in figure 33(a). When a set of cracks occurs approximately halfway between existing primary cracks, the new cracks will spread laterally until they reach the periphery of the corresponding stress circles where the intensity of the average axial tensile stress is low. If the primary crack spacing is less than twice the distance from the level of the reinforcement to the neutral axis, then the length of the new cracks will be less than that of the original primary flexural cracks (which extend to the neutral axis) and the new flexural cracks will become secondary flexural cracks.

The secondary flexural cracks (shown in figure 33(b)) will cause a stress redistribution in the immediate vicinity of the reinforcement. A new set of cracks, secondary flexural cracks of the second order, develops when the maximum tensile stress in the concrete exceeds the tensile strength of the concrete. The lengths of these new tensile cracks will be governed by the diameter of the corresponding stress circles (the distance between two adjacent tensile cracks). If the crack spacing for adjacent cracks is less than twice the thickness of the bottom cover of the flexural members, then the corresponding stress circles and the new set of tensile cracks will not reach the bottom face of the member, as shown in figure 33(b).

In summary, the work of Broms indicated that the assumption of a uniform linear stress distribution in cracked reinforced concrete may lead to large errors when the calculated crack spacing of the main cracks approaches twice the thickness of the concrete cover or the spacing of the individual reinforcing bars. The absolute minimum visible cracking spacing was found to be equal to the thickness of the concrete cover. The average minimum crack spacing will be larger than the absolute minimum crack spacing given above.

$$t < \text{crack spacing} < 2t \qquad (27)$$

where t is the thickness of the concrete cover as indicated in figures 29 and 33.

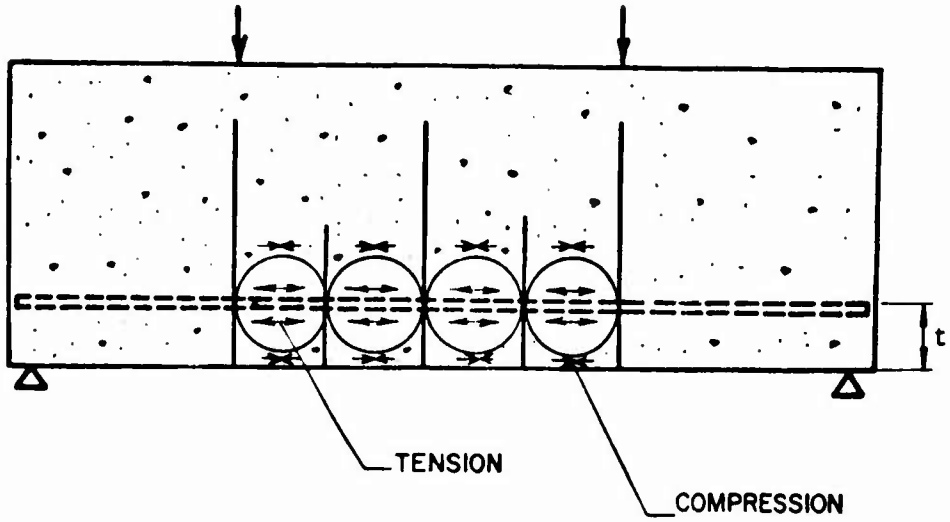

Figure 32. Flexural Members (Ref. 33)

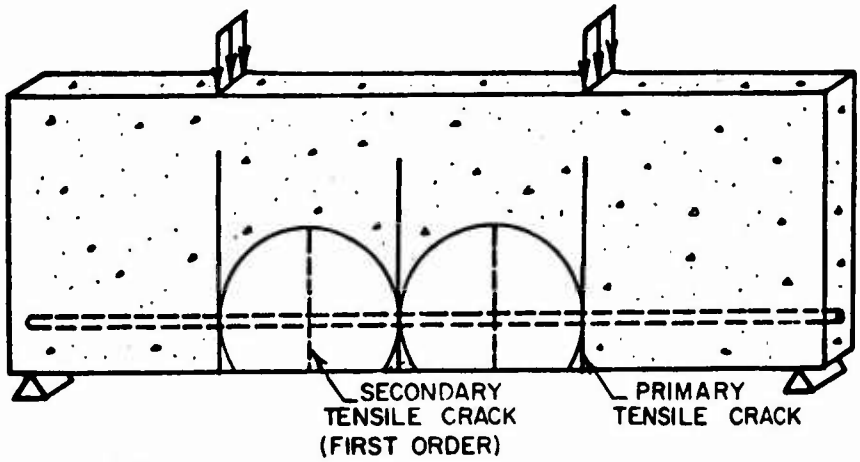

(a) Primary and first order second cracks

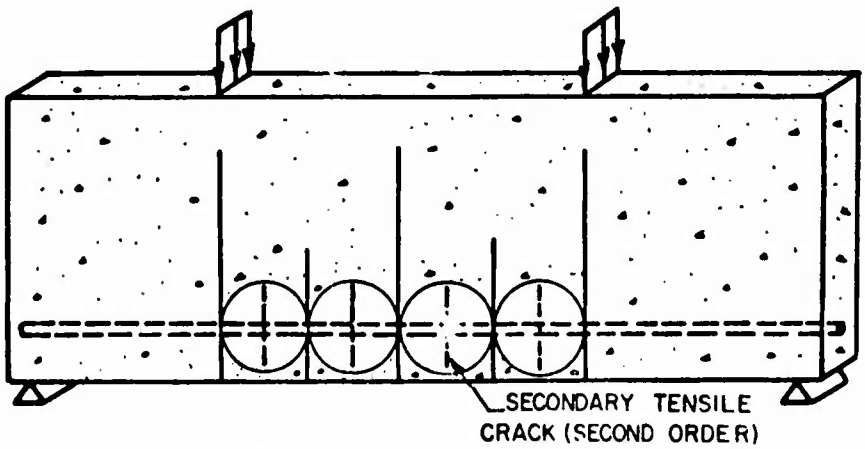

(b) Second order secondary cracks

Figure 33. Mechanism of Tension Cracking (flexural members) (Ref. 33)

From the observation that the average crack spacing is approximately equal to twice the distance t, Broms (Ref. 33), found that the crack width can be calculated from the relation

$$W_{ave} = 2t\varepsilon_s \tag{28}$$

where W_{ave} = crack width or the total elongation of the reinforcement, and ε_s = is the average steel strain.

SECTION IV

FORMULATION OF PRESENT MODEL

This section summarizes the formulation of the mathematical model developed under the present contract. This model is essentially an improved version of the Isenberg/Adham model (Ref. 1). The improvements were based on pertinent studies reviewed at the beginning of this contract. No new development of fracture theory or nonlinear constitutive relations was included in the scope of the present work. Some features of the model such as concrete stress/strain relations were discussed in previous sections, and their details are not repeated. Other features such as the dowel action formula are modified and their details are included in this section. The model was formulated in steps that are summarized below.

1. STEPS TO FORMULATION OF THE MODEL

The model was formulated in two basic steps:

STEP 1. This step establishes the stress/strain relations in principal directions of orthotropy. The formulation includes the following elements:

- Concrete stress/strain relations
- Steel properties
- Bond-slip relations
- Dowel action
- Composite moduli of reinforced concrete

The principal directions of orthotropy were defined as follows:

- Before cracking, principal directions of orthotropy are defined by principal directions of stress.
- Direction of first cracking defines principal direction of orthotropy, while second and third principal direction of orthotropy are directions of the largest stress and its normal.

STEP 2. This step involved matrix transformation from principal directions of orthotropy to global directions and included:

- Formulation of matrix of direction cosines
- Assembling global stiffness matrix

The details of the above steps are given below.

2. CONCRETE STRESS/STRAIN RELATIONS

Two types of plain concrete stress/strain models are incorporated in the present analysis:

a. Variable Modulus Model

The virgin loading stress/strain relations incorporated in this model are those suggested by Liu, Nilson, and Slate in reference 53 and described in detail in Section III. In these relations the moduli of elasticity in orthogonal directions are expressed as functions of strain and confinement. The moduli E_i and G_{ij} are functions of the state of stress and strain and take the form

$$E_i = \frac{E_c \left[1 - \left(\frac{\varepsilon_i}{\varepsilon_p}\right)^2\right]}{\left[1 + \left(\frac{1}{1 - \nu\beta_i}\frac{E_c}{E_{sc}} - 2\right)\left(\frac{\varepsilon_i}{\varepsilon_p}\right) + \left(\frac{\varepsilon_i}{\varepsilon_p}\right)^2\right]^2} \tag{29}$$

$$G_{ij} = \frac{E_i E_j}{(1 + \nu)(E_i + E_j)} \tag{30}$$

where

E_i, E_j = Tangent moduli in directions i, j

E_c = Initial tangent modulus for concrete

ε_i = Strain in direction i

ε_p = Strain at peak stress

ν = Poisson's ratio for concrete

E_{sc} = Secant modulus based on ultimate stress and corresponding strain

β_i = Ratio of principal stress in the direction normal to the principal stress in the direction considered

The peak stress, σ_p, due to combined loading is expressed as

$$\left.\begin{aligned} \sigma_p &= \left[1 + \frac{\beta_i}{1.2 - \beta_i}\right] \sigma_o && \text{for } \beta_i < 0.2 \\ &= 1.2\, \sigma_o && \text{for } 1.0 \geq \beta_i \geq 0.2 \\ &= \frac{1.2\, \sigma_o}{\beta_i} && \text{for } 5.0 \geq \beta_i \geq 1.0 \\ &= \frac{\sigma_o}{\beta_i}\left(1 + \frac{1}{1.2\beta_i - 1}\right) && \text{for } \beta_i > 5.0 \end{aligned}\right\} \quad (31)$$

where

σ_o = f'_c, the unconfined cylinder strength in uniaxial compression.

The strain ε_p corresponding to σ_p is given as

$$\begin{aligned} \varepsilon_p &= 0.0025 \text{ for } \beta_i < 1 \\ &= (-500 + 0.55\, \sigma_p) \times 10^{-6} \\ &= (-500 + 7.98 \times 10^{-1}\, \sigma_p) \times 10^{-4} \end{aligned} \quad \left.\begin{aligned} &\text{for } \beta_i > 1 \\ &\sigma_p \text{ in psi} \\ &\sigma_p \text{ in N/m}^2 \end{aligned}\right. \quad (32)$$

The secant modulus E_{sc} is given by

$$E_{sc} = \frac{\sigma_p}{\varepsilon_p} \tag{33}$$

The corresponding incremental stress/strain relation is given by

$$d\sigma_i = \frac{E_i \, d\varepsilon_i}{1 - \nu\beta_i} \tag{34}$$

where $d\sigma_i$ is the stress increment in the i-direction, and ν has a constant value equal to Poisson's ratio for concrete.

The descending branch of the stress/strain relation in unconfined compression is not represented in the model. The reason is that including it would require either a negative tangent modulus or complete reliance on the load vector correction method of integrating equations of motion. The first requirement leads to numerical difficulties with implicit integration methods, while the second demands the capability for iteration in the main code. Since this would tend to produce a material property package which works for some codes and not for others, the falling branch is excluded. However, to include the descending branch of the stress/strain relation in a future model, general equations 12, and/or 29, should be modified to incorporate the point of failure or some other point on the descending branch of the curve.

Observation of the numerator in equation 29 reveals that the tangent modulus E_i becomes negative whenever ε_i exceeds ε_p. When this occurs, an arbitrary small value is substituted for E_i. This value is usually taken as 1 percent of E_c.

Another difficulty encountered is that equation 29 becomes singular when

$$\nu\beta_i = 1 \tag{35}$$

This problem was avoided by arbitrarily setting $\beta_i = 0.0$. Therefore, in the present model no additional strength is obtained under biaxial or triaxial confinement.

Figure 34 shows the stress/strain relations for plain concrete in compression, used in the present model. Unloading and reloading occurs with the initial tangent modulus E_c.

The concrete modulus in tension is assumed to have a constant value E_c until cracking. However, after cracking, the concrete modulus is set to a minimal value to avoid numerical difficulties, while the stress is set to zero (Fig. 35). In the event of rebonding, after tension cracks have been closed, the modulus is set to a user specified fraction α of the initial modulus, E_c. Rebonding is indicated in the code by a change of the sign of strain.

The cracking strength of concrete f_t' in any given direction was discussed in Section II and can be expressed as

$$f_t' = f_t - \eta\sigma_2 \qquad (36a)$$

for $\sigma_2 < 0$ and $\sigma_2 < \sigma_3$

where

f_t = Unconfined tensile strength of concrete

η = Slope of cracking envelope to be determined experimentally (Fig. 15)

σ_2 = Mirimum nonpositive stress normal to the tension axis

Equation 36(a) can also be expressed as

$$f_t' = f_t \left[1 - \frac{\sigma_2}{f_c'}\right] \qquad (36b)$$

where

f_c' = Unconfined compressive cylinder strength of concrete

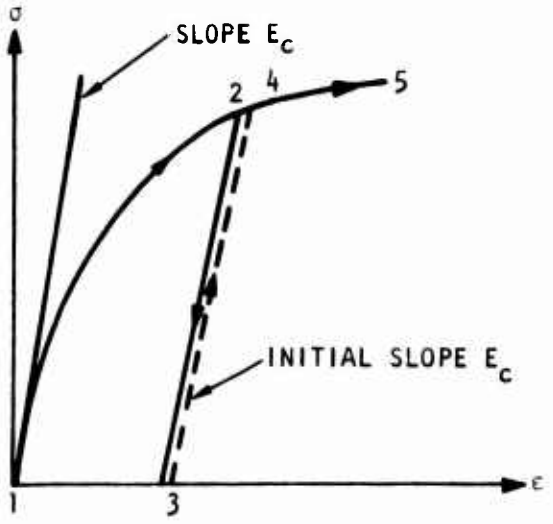

(a) Virgin loading and unloading/reloading behavior of present model

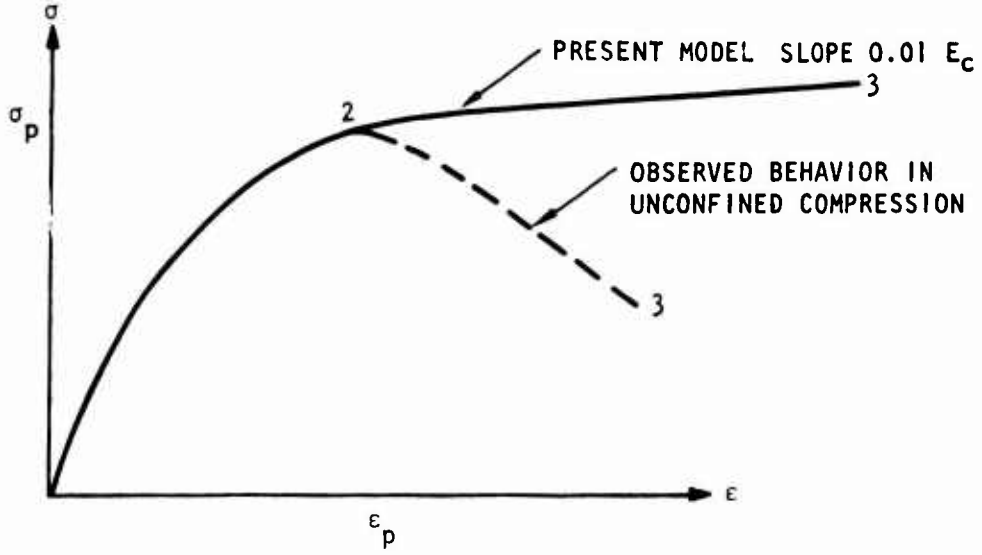

(b) Present model does not account for descending portion of compressive stress/strain relations for plain concrete

Figure 34. Stress/Strain Relations for Plain Concrete

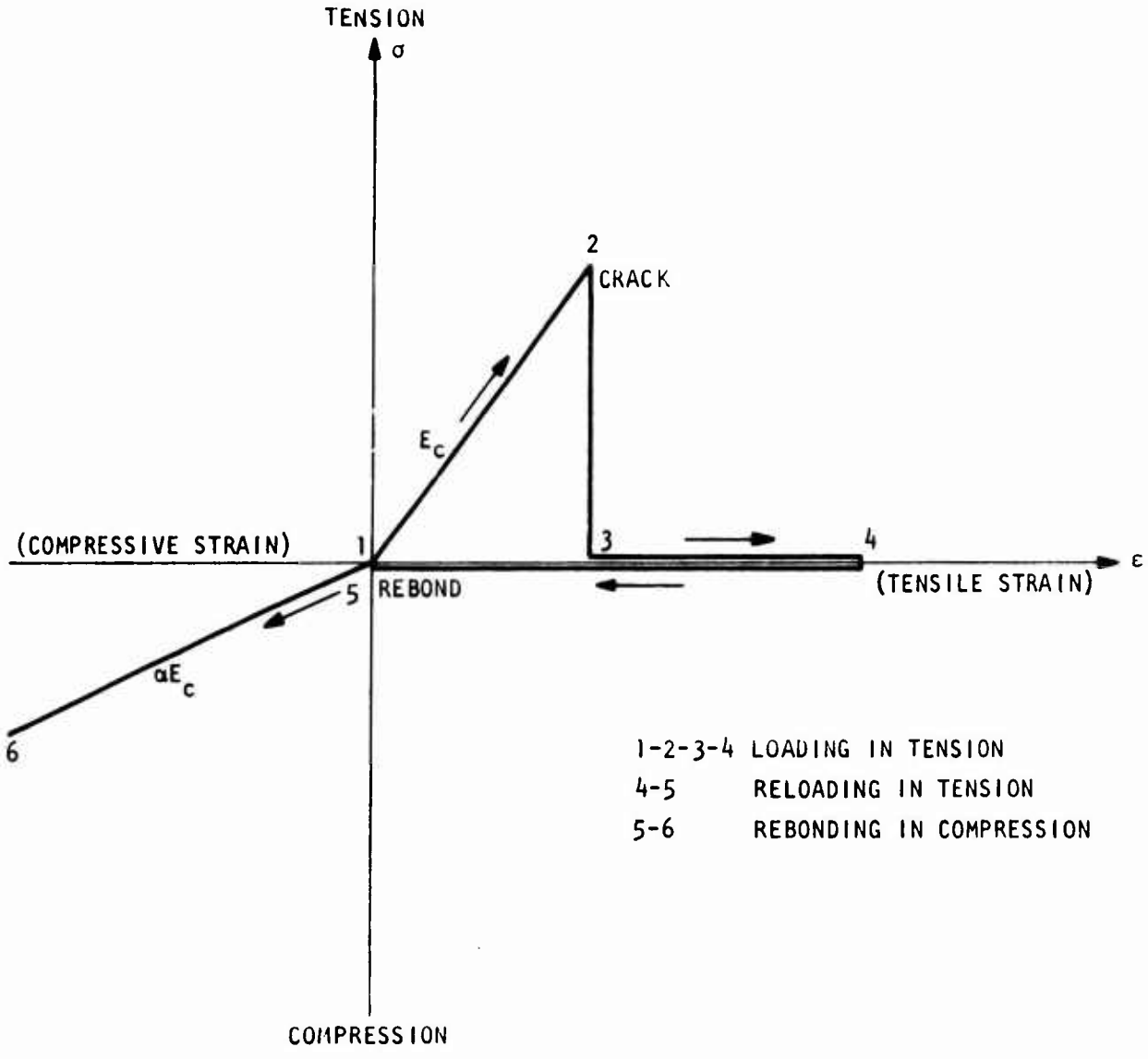

Figure 35. Stress/Strain Relations for Plain Concrete in Tension for Variable Modulus Model

Equation 36(a, b) accounts for the change in ultimate tensile strength due to the interaction of perpendicular stress components.

b. Plastic Capped Model

In addition to the variable moduli stress/strain relations used in composite moduli, stress/strain relations based on a strain-hardening theory of plasticity are also included in the computer program. These relations were developed under a separate project (Ref. 51). This type of mathematical formulation does not readily lend itself to the composite moduli approach, and hence it is included in the computer program for those cases where steel is absent or can be neglected.

The yield surface consists of two segments F_1 and F_2 defined as

$$\left.\begin{aligned} F_1 &= \sqrt{J_2'} + g_1(J_1) - K_1 \\ F_2 &= \frac{\left(\sqrt{J_2'}\right)^2}{2} + r^2 \frac{J_1^2}{2} - K_2 \end{aligned}\right\} \qquad (37)$$

where

J_1 = First invariant of stress

J_2' = Second invariant of stress deviator

$g_1(J_1)$ = A function of J_1

r = Constant

K_1, K_2 = Hardening parameters

The hardening laws used are

$$d\sqrt{I_2'}^{\,p} = h_1\, dF_1 \qquad (38)$$

and

$$d\,\varepsilon_{vc}^{p} = h_2\, dF_2 \qquad (39)$$

where $I_2^{'P}$ is the second invariant of the plastic-strain deviator and ε_{vc}^{P} is the volumetric plastic strain associated with compaction only. The variables h_1 and h_2 are functions of the stress and plastic strain invariants.

The yield surface and the hardening rules are used in conjunction with the flow rule

$$d\varepsilon_{ij}^{P} = \frac{\partial F_1}{\partial \sigma_{ij}} \lambda_1 + \frac{\partial F_2}{\partial \sigma_{ij}} \lambda_2 \tag{40}$$

where $d\varepsilon_{ij}^{P}$ are the plastic strain increments and λ_1 and λ_2 are factors to be determined.

The incremental stress/strain relations are expressed as

$$d\sigma_{ij} = C_{ijk\ell}\left(d\varepsilon_{k\ell} - d\varepsilon_{k\ell}^{P}\right) \tag{41}$$

where $d_{\sigma ij}$ is the stress increment, $d\varepsilon_{k\ell}$ is the total strain increment and $C_{ijk\ell}$ are the coefficients of the elastic stress/strain relationship.

Substitution of equation 40 in equation 41 yields

$$d\sigma_{ij} = C_{ijk\ell}\ d\varepsilon_{k\ell} - C_{ijk\ell}\left(\frac{\partial F_1}{\partial \sigma_{k\ell}} \lambda_1 + \frac{\partial F_2}{\partial \sigma_{k\ell}} \lambda_2\right) \tag{42}$$

The values of λ_1 and λ_2 are obtained from the solution of

$$A_1 \lambda_1 + A_2 \lambda_2 = A_3 \tag{43}$$

$$A_4 \lambda_1 + A_5 \lambda_2 = A_6 \tag{44}$$

where

$$A_1 = \frac{\partial F_1}{\partial \sqrt{J_2'}} + 2\, h_1 \frac{\partial F_1}{\partial \sigma_{ij}} C_{ijk\ell} \frac{\partial F_1}{\partial \sigma_{k\ell}} \tag{45}$$

$$A_2 = \frac{\partial F_2}{\partial \sqrt{J_2'}} + 2\, h_1 \frac{\partial F_1}{\partial \sigma_{ij}} C_{ijk\ell} \frac{\partial F_2}{\partial \sigma_{k\ell}} \tag{46}$$

$$A_3 = 2\, h_1 \frac{\partial F_1}{\partial \sigma_{ij}} C_{ijk\ell}\, d\varepsilon_{k\ell} \tag{47}$$

$$A_4 = \frac{h_2}{3} \frac{\partial F_2}{\partial \sigma_{ij}} C_{ijk\ell} \frac{\partial F_1}{\partial \sigma_{k\ell}} \tag{48}$$

$$A_5 = \frac{\partial F_2}{\partial J_1} + \frac{h_2}{3} \frac{\partial F_2}{\partial \sigma_{ij}} C_{ijk\ell} \frac{\partial F_2}{\partial \sigma_{k\ell}} \tag{49}$$

and

$$A_6 = \frac{h_2}{3} \frac{\partial F_2}{\partial \sigma_{ij}} C_{ijk\ell}\, d\varepsilon_{k\ell} \tag{50}$$

It should be noted however that if yielding occurs on F_1 only

$$A_2 = A_4 = A_5 = A_6 = 0$$

Consequently

$$\lambda_2 = 0$$

$$\lambda_1 = A_3/A_1$$

Similarly, if yielding occurs on F_2 only

$$A_1 = A_2 = A_3 = A_4 = 0$$

and

$$\lambda_1 = 0$$

$$\lambda_2 = A_6/A_5$$

For an elastic case both λ_1 and λ_2 are zero.

Substitution of λ_1 and λ_2 in equation 41 results in the desired incremental stress/strain relations.

The actual functions used by the authors of reference 51 are detailed below, where the constants (y_1 through y_{25}) are model fitting parameters.

The yield surfaces are given by

$$F_1 = \sqrt{J_2'} - y_1\left[y_2 - y_3\, e^{J_1/y_4}\right]\left[1 - e^{(J_1 - y_5)/y_6}\right] - K_1 \tag{51}$$

and

$$F_2 = \frac{J_2'}{2} + y_7\, J_1^2 - K_2 \tag{52}$$

with initial values of K_1 and K_2 given by

$$K_1 = y_{24} \tag{53}$$

$$K_2 = y_{25} \tag{54}$$

The hardening rules are given by

$$h_1 = y_8\, \frac{1 - y_9\left[1 - e^{y_{10}\sqrt{I_2'}^{\,p}/(1 - y_{11}J_1)}\right]}{y_{12} - y_{13}\, J_1} \tag{55}$$

and

$$h_2 = y_{14}\sqrt{J_2'}\left[1 - e^{-\sqrt{J_2'}/y_{15}}\right]\frac{e^{-J_2'^2/y_{16}}}{1 - y_{20}J_1} - y_{17}\left[1 - e^{J_1/y_{18}}\right]e^{J_1/y_{19}} \qquad (56)$$

where

y_1 through y_{25} = Constants

Coefficients Y_1 through Y_{23} were assumed in reference 51 to have the following values (Table II)

Table II. Values of Coefficients Used in Model (Ref. 51)*

$Y_1 = 1000$	$Y_2 = 12.2$	$Y_3 = 11.0$	$Y_4 = 40{,}000$	$Y_5 = 800$
$Y_6 = 700$	$Y_7 = 2$	$Y_8 = 0.1\times10^{-5}$	$Y_9 = 100$	$Y_{10} = 120$
$Y_{11} = 0.0001$	$Y_{12} = 2$	$Y_{13} = 0.7\times10^{-4}$	$Y_{14} = -0.24\times10^{-3}$	$Y_{15} = 4000$
$Y_{16} = 0.8\times10^{16}$	$Y_{17} = -0.70^2\times10^{-11}$	$Y_{18} = 0.135\times10^{-14}$	$Y_{19} = 60{,}000$	$Y_{20} = 0.0005$
$Y_{21} = 0$	$Y_{22} = 0$	$Y_{23} = 0$		

These values were based on concrete cylinder strength $f_c' = 7000$ psi (483×10^5 N/m^2). Guidelines for selecting these coefficients for different concrete strengths are included in Appendix I.

3. STEEL PROPERTIES

The main properties of reinforcing steel treated are the area fraction of the steel and its stress/strain relationship. Both of these are originally prescribed by the user in so-called "steel coordinates"; that is, in directions parallel to the axes of the bars. These areas are then transformed to the principal directions of orthotropy where they are incorporated together with the tangent moduli of the steel into the composite moduli.

*Valid only for English units.

a. Steel Transformation

The number of reinforcing "steel sets" for the structure being analyzed is specified by input to the computer program. Each "steel set" is defined as steel reinforcement in any three directions that are not necessarily orthogonal; the three directions are specified by direction cosines with respect to the global coordinates. The actual steel ratios involved in the three directions are left as variables from element to element. Thus, the steel reinforcement in an element is completely specified by specifying the steel set involved. The steel set defines the reinforcement directions and the three steel ratios that set the amounts of reinforcement in the three directions.

In each load step, for each individual element the code determines coordinates based on the principal directions of orthotropy. The code then determines the equivalent amount of steel reinforcement in the principal directions of orthotropy by transforming the actual steel ratios.

Let X, Y, and Z represent the global coordinates for the entire structure; x, y, and z the local coordinates for the element; x_s, y_s and z_s the actual steel directions; and p_{xs}, p_{ys}, and p_{zs} the accompanying steel ratios as shown in figure 36.

Further, let the direction cosines of coordinate directions x, y, and z with respect to coordinates X, Y, and Z be represented by the array

$$\begin{bmatrix} \cos \alpha_x & \cos \beta_x & \cos \gamma_x \\ \cos \alpha_y & \cos \beta_y & \cos \gamma_y \\ \cos \alpha_z & \cos \beta_z & \cos \gamma_z \end{bmatrix} \tag{57}$$

where α_x, β_x, and γ_x, for example, denote the angles between the x-axis and the X-, Y-, and Z-axes, respectively. Similarly, let the array

$$\begin{bmatrix} \cos \alpha_{xs} & \cos \alpha_{ys} & \cos \alpha_{zs} \\ \cos \beta_{xs} & \cos \beta_{ys} & \cos \beta_{zs} \\ \cos \gamma_{xs} & \cos \gamma_{ys} & \cos \gamma_{zs} \end{bmatrix} \tag{58}$$

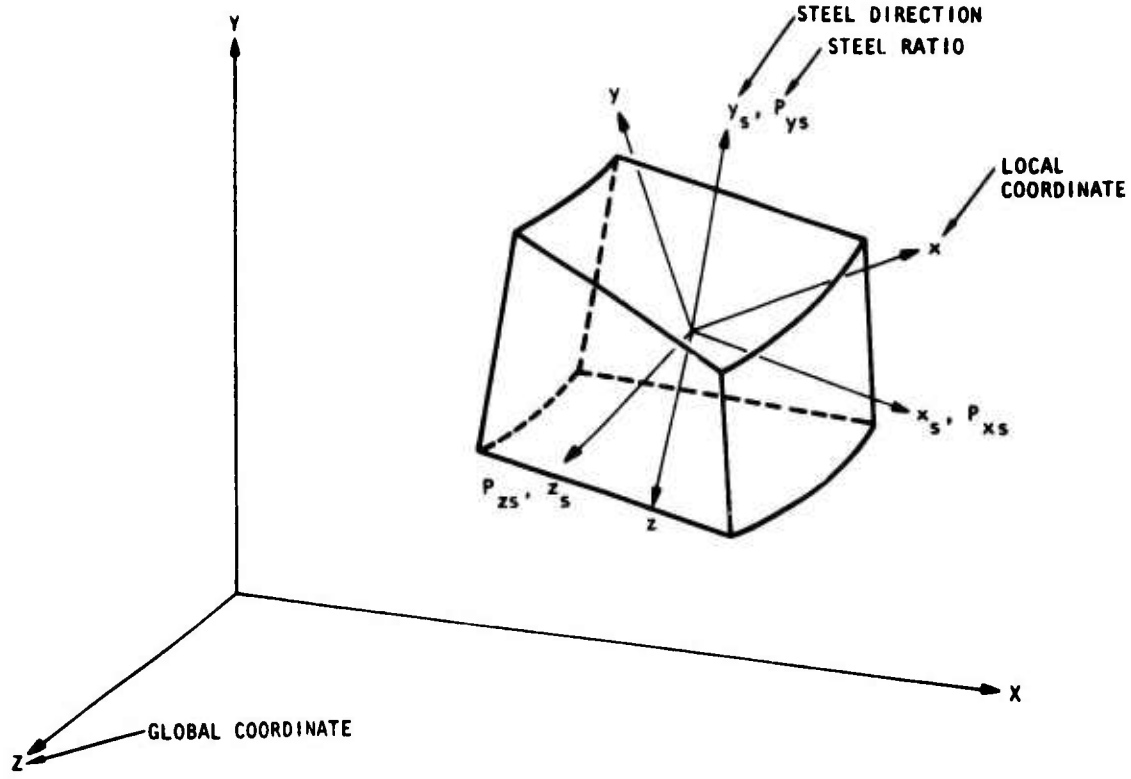

Figure 36. Coordinates System for Transforming Steel Areas

represent the direction cosines of steel directions x_s, y_s, and z_s with respect to the global coordinates X, Y, and Z. The first set of direction cosines as given by equation 57 are calculated internally by the code following the establishment of the local coordinates, while the second set of direction cosines as given by equation 58 are available as part of the input.

The direction cosines of the steel directions x_s, y_s, and z_s with respect to the local coordinates x, y, and z are then easily obtained as the scalar product of equations 57 and 58. Thus,

$$\begin{bmatrix} \cos\bar{\alpha}_{xs} & \cos\bar{\alpha}_{ys} & \cos\bar{\alpha}_{zs} \\ \cos\bar{\beta}_{xs} & \cos\bar{\beta}_{ys} & \cos\bar{\beta}_{zs} \\ \cos\bar{\gamma}_{xs} & \cos\bar{\gamma}_{ys} & \cos\bar{\gamma}_{zs} \end{bmatrix} = \begin{bmatrix} \cos\alpha_x & \cos\beta_x & \cos\gamma_x \\ \cos\alpha_y & \cos\beta_y & \cos\gamma_y \\ \cos\alpha_z & \cos\beta_z & \cos\gamma_z \end{bmatrix} \begin{bmatrix} \cos\alpha_{xs} & \cos\alpha_{ys} & \cos\alpha_{zs} \\ \cos\beta_{xs} & \cos\beta_{ys} & \cos\beta_{zs} \\ \cos\gamma_{xs} & \cos\gamma_{ys} & \cos\gamma_{zs} \end{bmatrix} \quad (59)$$

where $\bar{\alpha}_{xs}$, $\bar{\beta}_{xs}$ and $\bar{\gamma}_{xs}$, for example, represent the angles between the x_s-axis and the x-, y-, and z-axes, respectively.

In FEDRC* code, the original steel ratios specified by the user in the steel directions, x_s, y_s, and z_s, are transformed into equivalent steel ratios in the local coordinate directions x, y, and z, using the direction cosines obtained in equation 59 as follows:

$$\begin{Bmatrix} p_x \\ p_y \\ p_z \end{Bmatrix} = \begin{bmatrix} \cos^2\alpha_{xs} & \cos^2\alpha_{ys} & \cos^2\alpha_{zs} \\ \cos^2\beta_{xs} & \cos^2\beta_{ys} & \cos^2\beta_{zs} \\ \cos^2\gamma_{xs} & \cos^2\gamma_{ys} & \cos^2\gamma_{zs} \end{bmatrix} \begin{Bmatrix} p_{xs} \\ p_{ys} \\ p_{zs} \end{Bmatrix} \quad (60)$$

The justification for this transformation is that it does not give rise to negative steel areas and that it conserves the total steel area. The latter follows from the fact that the sum of squares of a set of direction cosines is unity.

*FEDRC is a modified version of Agbabian Associates FEDIA code, which is a dynamic, inelastic, two-dimensional continuum finite element code. The modification consisted of incorporating the present material package in FEDIA code.

b. Steel Stress/Strain Relations

The tensile and compressive stress/strain relations are linearly elastic, perfectly plastic as shown in figure 37. Instead of assuming perfect plasticity, the user of the present computer program may specify hardening by means of a nonzero slope.

4. BOND-SLIP RELATION

The bond-slip is accounted for by the quantity λ in equation 26, which is assumed to vary from 1.0 to 0 as the strain in the steel reaches the yield strain. The variation of λ in the present model is shown in figure 38. This relation is based on data from previous experiments. (These are compared to the experiments conducted as part of the present study in Sec. V). Further refinements in this relation, including taking into account the spacing between cracks, the effect of cyclic loading, and the strength of concrete used, are probably desirable from a theoretical point of view. However, in the author's opinion, they were not justified in view of other uncertainties that were encountered at the beginning of this study.

5. DOWEL ACTION

Dowel action was discussed in Section III and refers to the shear stiffness afforded to cracked sections by the reinforcing bars that span the cracks. Dowel action is represented by a variable shear modulus that relates incremental shear stress to incremental shear strain in the principal directions of orthotropy as follows:

$$d\tau_o = G_o d\gamma_o \tag{61}$$

The formula for the shear modulus, used in the present computer program, is similar to that suggested by Dulacska (Ref. 65) and summarized in Section III in equations 24 and 25. However, the present formulation is simplified by the assumption that the angle between the stirrup and the crack direction is assumed to be 90^o. This assumption follows directly from transforming the steel from its natural coordinates to the principal directions of orthotropy.

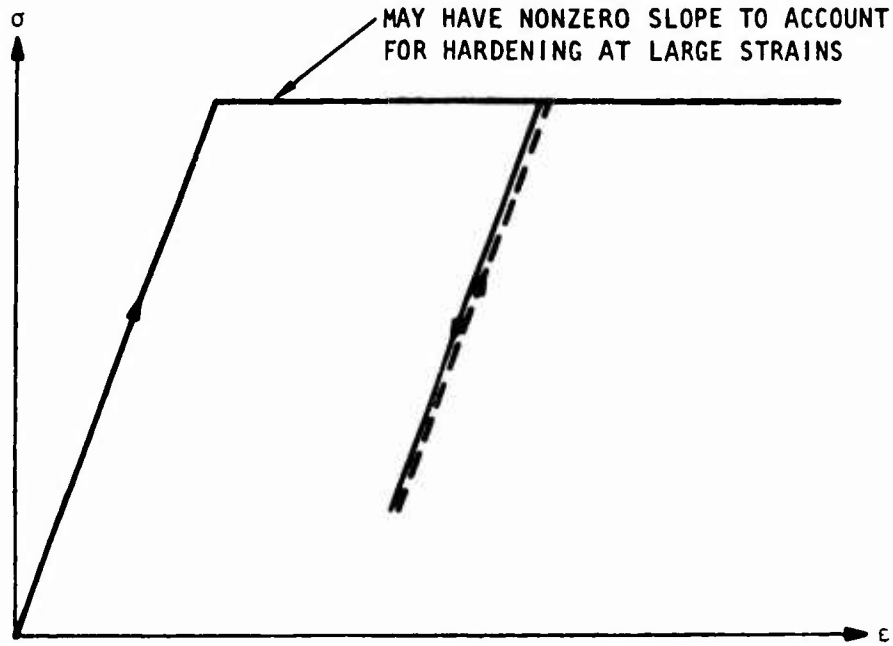

Figure 37. Stress/Strain Relations for Reinforcing Steel

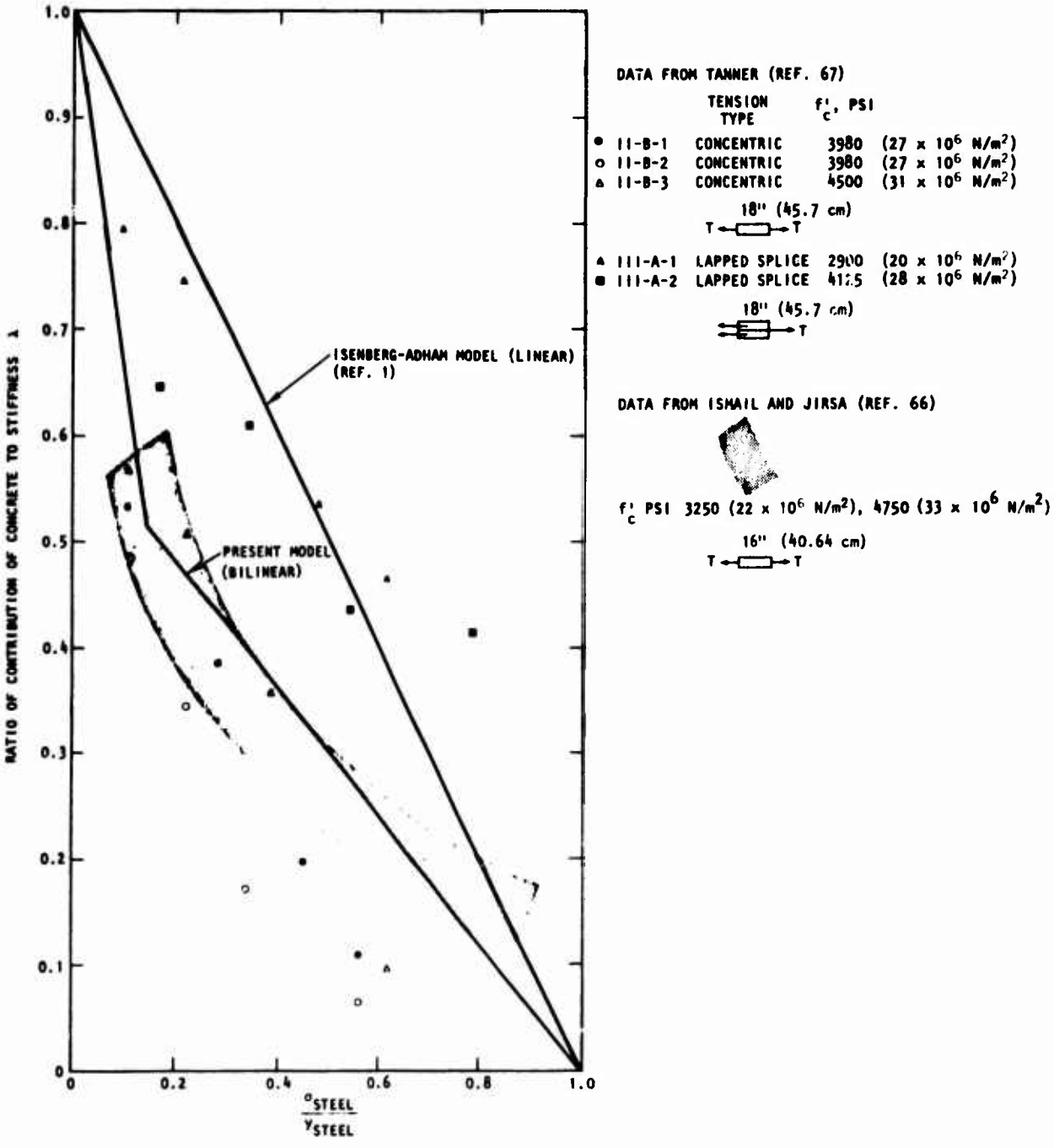

Figure 38. Experimental Bond-Slip Results (Refs. 66, 67) Compared with Two Sets of Analytical Results (Ref. 1 and present study)

For $\delta = 0$, Dulacska's relationship, equation 24, reduces to the simple form

$$T_f = \phi^2 \sqrt{\frac{\sigma_c \rho \sigma_y n}{3}} \tag{62}$$

where

T_f = Failure force

ϕ = Bar size

σ_c = Cube strength of concrete

σ_y = Tension yield stress of bar

n = Coefficient of local compression of concrete

$\rho = 1 - \frac{N^2}{N_y^2}$

N = Axial tension force of bar

N_y = Axial tensile force inducing yield in pure tension

and the maximum shear stress τ_f that the bar is capable of withstanding is as follows:

$$\tau_f = \frac{4}{\pi} \sqrt{\frac{\sigma_c \rho \sigma_y n}{3}} \tag{63}$$

The relation between the dowel shear force T and the displacement Δ given by equation 25 was also simplified to the form

$$\frac{T}{T_f} = 1 - e^{-\alpha \Delta} \tag{64}$$

where α is a constant.

The validity of the present simplified relation was demonstrated by comparing it with Dulacska's relation, which agrees well with experimental data. Five different cases involving different stirrup angles, diameters and yield strengths were performed as shown in table III. The value of the parameter α in equation 64 was selected in order to match the relation of Dulacska. The results obtained by both relations are compared in figure 39.

Equation 64 can be written in terms of stresses in the form

$$\frac{\tau}{\tau_f} = 1 - e^{-\bar{\alpha}\gamma_{shear}} \tag{65}$$

where

$\bar{\alpha}$ = $L\,\alpha$

L = Length of element

γ_{shear} = Dowel shear strain

The dowel shear modulus can be calculated from equation 65 by differentiation

$$\frac{1}{\tau_f}\frac{d\tau}{d\gamma} = \bar{\alpha} e^{-\bar{\alpha}|\gamma_{shear}|} \tag{66}$$

or

$$G = \tau_f \bar{\alpha} e^{-\bar{\alpha}|\gamma_{shear}|} \tag{67}$$

and for

$$\gamma_{shear} = 0 \quad G = G_o \tag{68}$$

Substituting equation 68 into equation 67, the constant $\bar{\alpha}$ can be calculated from

$$\bar{\alpha} = \frac{G_o}{\tau_f} \tag{69a}$$

Table III. Dulacska's Cases Used to Match Present Simplified Relationship

Case No.	Stirrup Angle δ degrees	Stirrup Diameter ℓ in. (cm)	Stirrup Yield σ_y ksi (10^3 N/m^2)	Concrete Strength σ_c ksi (N/m^2)	Theoretical Strength T_{max} lb (N)	α
1	10	0.39 (0.99)	41.89 (288831)	4.54 (31303)	2249 (10004)	146.5
2	20	0.2535 (0.64)	35.07 (241807)	4.26 (29373)	794 (3532)	261.3
3	20	0.39 (0.99)	41.89 (288831)	1.42 (9791)	1014 (4510)	181.7
4	20	0.39 (0.99)	41.89 (288831)	4.54 (31303)	2072 (9216)	159.0
5	20	0.546 (1.39)	36.49 (251598)	4.26 (29373)	3682 (16378)	121.4

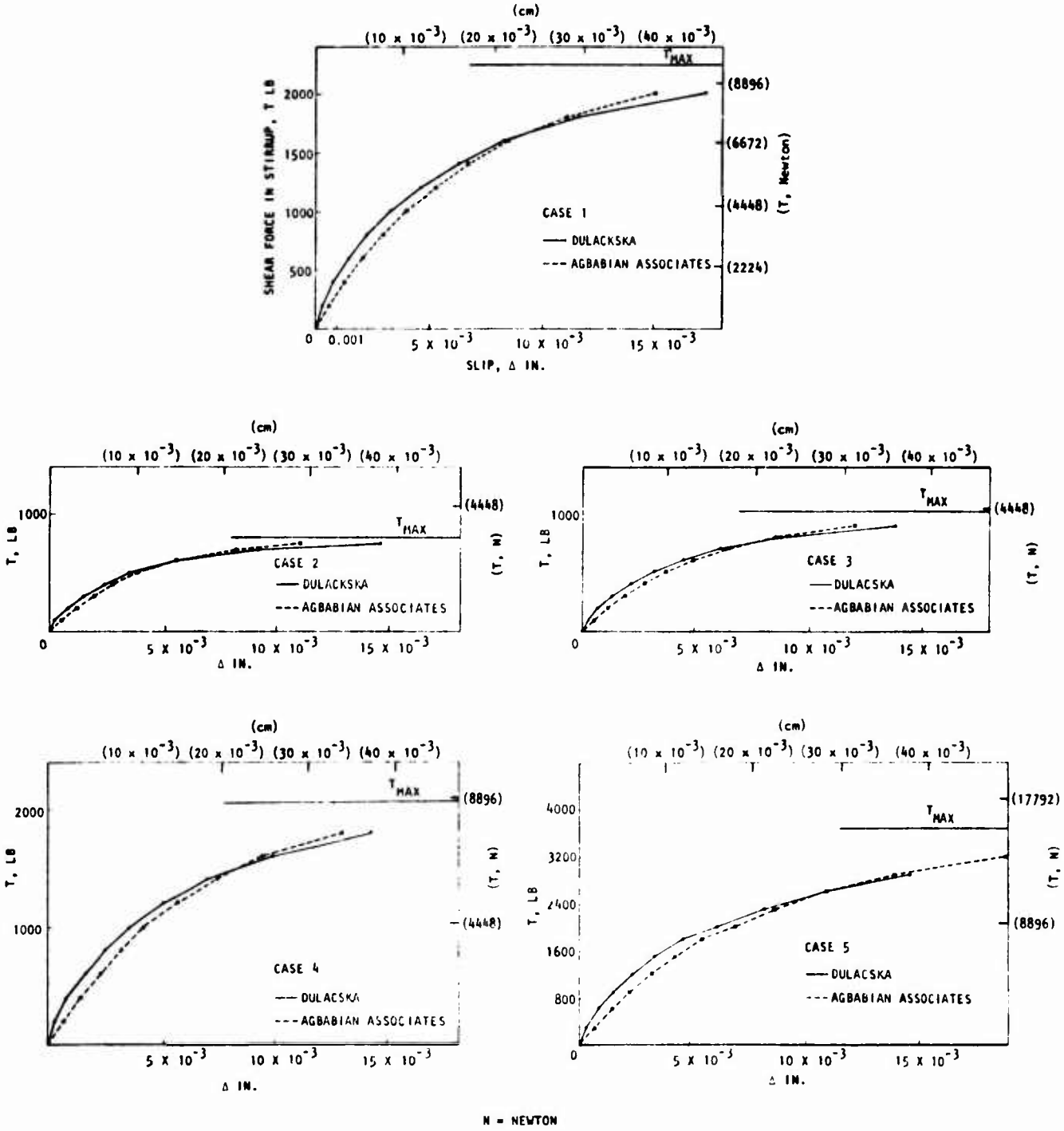

Figure 39. Comparison of Dowel Action Relationships

Thus equation 67 can be used to calculate the dowel shear modulus for various stages of loading. Substituting equation 69(a) in equation 67, we get

$$G = G_o \, e^{-\bar{\alpha} |\gamma_{shear}|} \tag{69b}$$

6. COMPOSITE MODULI OF REINFORCED CONCRETE

The purpose of this subsection is to introduce a method that incorporates, in a composite model, the variations in steel and concrete properties discussed above. The composite model accounts for

- The combined properties of steel and concrete
- The change in principal directions of stresses and the orientation of cracks

The combined properties of steel and concrete at various phases of loading will be discussed in the next paragraphs, while the matrix transformation from principal and orthotropic directions to global directions will be given in the next subsection.

a. Composite Moduli for Uncracked Reinforced Concrete

The composite moduli for the uncracked reinforced concrete elements are given by

$$\bar{E}_i = E_i^c A_i^c + E_{st} A_i^s \tag{70}$$

where

$\bar{E}_i$ = Effective composite moduli

$$E_i^c = \begin{cases} E_i \text{ (from equation 29)} & \text{for loading in compression} \\ E_c & \text{for unloading or reloading in compression} \\ E_c & \text{for loading in tension} \end{cases}$$

E_{st} = Modulus of steel

A_i^s = Effective steel ratio in direction i (area fraction)

A_i^c = $1 - A_i^s$ = effective concrete ratio in direction i

The composite tangent moduli matrix is 6 x 6. For convenience it is partioned in 3 x 3 blocks as follows:

$$C = \left[\begin{array}{c|c} X & Y \\ \hline Y & Z \end{array}\right] \tag{71}$$

In the principal orthotropic directions there is no coupling between normal and shear components. Hence

$$Y = \begin{bmatrix} 0 & 0 & 0 \\ 0 & 0 & 0 \\ 0 & 0 & 0 \end{bmatrix} \tag{72}$$

and X can be defined as follows:

$$X = \frac{1}{D}\begin{bmatrix} \bar{E}_1(1 - \nu_{23}\nu_{32})A_1^c & \bar{E}_1(\nu_{12} + \nu_{13}\nu_{32})A_1^c & \bar{E}_1(\nu_{13} + \nu_{12}\nu_{23})A_1^c \\ & \bar{E}_2(1 - \nu_{13}\nu_{31})A_2^c & \bar{E}_2(\nu_{23} + \nu_{21}\nu_{13})A_2^c \\ & & \bar{E}_3(1 - \nu_{12}\nu_{21})A_3^c \end{bmatrix} \tag{73}$$

where

$D = 1 - \nu_{23}\nu_{32} - \nu_{12}\nu_{21} - \nu_{13}\nu_{31} - \nu_{12}\nu_{23}\nu_{31} - \nu_{13}\nu_{21}\nu_{32}$

ν_{ij} = Poisson's ratio of concrete taken as a constant ν in this study

and

$$[Z] = [Z_c + Z_s] \tag{74}$$

where

$$Z_s = \begin{bmatrix} G_s A_1^s & 0 & 0 \\ 0 & G_s A_2^s & 0 \\ 0 & 0 & G_s A_3^s \end{bmatrix} \tag{75}$$

where

G_s = Shear modulus of steel

A_1^s, A_2^s, A_3^s = Projected steel ratios in the principal stress directions

and

$$Z_c = \begin{bmatrix} G_{12} A_1^c & 0 & 0 \\ 0 & G_{23} A_2^c & 0 \\ 0 & 0 & G_{31} A_3^c \end{bmatrix} \tag{76}$$

where G_{12}, G_{23}, G_{31} have already been defined by equation 30, and $A_i^c = 1 - A_i^s$.

The possibility of yielding of steel in uncracked concrete is not included in the present model.

b. Onset of Cracking

In order to check for cracking, it is necessary to calculate the stress carried by concrete. This is done by the following equation:

$$\sigma_i^c = \frac{E_c \, \sigma_i}{E_c \, A_i^c + E_{st} \, A_i^s} \tag{77}$$

where

σ_i = Effective average stress

σ_i^c = Stress in concrete

Cracking occurs whenever

$$\sigma_i^c > f_t' \tag{78}$$

The value of f_t' can be calculated from equation 36.

In order to simulate the sudden increase in strain without additional loading at the onset of cracking, the stress σ_i is reduced by the amount $\sigma_i^c A_i^c$ at that point. This implies that the force in the element at this instant is carried by steel alone.

c. Composite Tensile Modulus After Cracking

The composite modulus after cracking is given by

$$\bar{E}_i = \frac{(E_c A_i^c + E_{st} A_i^s) E_{st} A_i^s}{E_{st} A_i^s + (1 - \lambda) E_c A_i^c} \tag{79}$$

where λ defines the bond-slip relation shown in figure 38 and can be expressed in the form

$$\lambda = \begin{cases} 1 - \frac{10x}{3} & \text{for } x \leq 0.15 \\ \frac{10(1 - x)}{17} & \text{for } 0.15 < x \leq 1.0 \end{cases} \tag{80}$$

where

$$x = \frac{\text{tensile stress in steel}}{\text{yield stress of steel}}$$

For a crack in the 1-direction (Fig. 20) the first row and column of combined tangent moduli X and Z of equation 71 are altered to

$$X = \left[\begin{array}{c|cc} \bar{E}_1 & 0 & 0 \\ \hline 0 & & \\ 0 & & \text{unaltered} \end{array}\right] \tag{81}$$

$$Z = \left[\begin{array}{c|cc} G\,A_1^s & 0 & 0 \\ \hline 0 & & \\ 0 & & \text{unaltered} \end{array}\right] \tag{82}$$

For cracks in both the 1- and 2-directions, the alterations in X are:

$$X = \left[\begin{array}{cc|c} \bar{E}_1 & 0 & 0 \\ 0 & \bar{E}_2 & 0 \\ \hline & & \text{unaltered} \\ 0 & 0 & \end{array}\right] \tag{83}$$

For cracks in all 3 directions

$$X = \begin{bmatrix} \bar{E}_1 & 0 & 0 \\ 0 & \bar{E}_2 & 0 \\ 0 & 0 & \bar{E}_3 \end{bmatrix} \tag{84}$$

where $\bar{E}_1$ is calculated from equation 79 and G is the dowel shear modulus calculated from equation 67.

For unloading/reloading in uncracked direction

$$E_i^c = E_c \tag{85}$$

For unloading/reloading for cracked element in cracked directions

$$\bar{E}_I = E_{st} A_i^s + 0.01\, E_c A_i^c \qquad \text{for} \qquad \varepsilon_i \geq 0 \tag{86}$$

d. Composite Modulus for Postyielding of Steel

When steel yields, $\bar{E}_i$ is set to a nominal minimum value to avoid numerical difficulties, the value presently used is

$$\bar{E}_i = 0.01\, E_c\, A_i^c + 0.05\, E_{st}\, A_i^s \tag{87}$$

However, the stress is not allowed to exceed the yield stress of steel.

For unloading/reloading, the steel modulus is used. Thus

$$\bar{E}_I = E_{st}\ A_i^s \tag{88}$$

e. Composite Moduli for Rebonding Behavior

If unloading causes the strain to be negative (i.e., compression), rebonding occurs. During rebonding a user-specified fraction of the concrete stiffness is used in the composite modulus. Thus

$$\bar{E}_I = \alpha\, E_c\, A_i^c + E_{st}\ A_i^s \tag{89}$$

where α is a user-specified quantity. A value not to exceed 0.5 is recommended by the authors. The rebonding was illustrated in figure 35 by the portion 5-6 of the stress/strain path. The rebonding relations included in the code are base' on adjusting the stiffness of the element to avoid any instability in the solution.

7. COORDINATE TRANSFORMATION PRINCIPLES

Various coordinate transformations are carried out in the program. The procedure and principles of these transformations are discussed in this section.

a. Definition of Direction Cosines

Let (x, y, z) be one orthogonal system of coordinates and (x', y', z') be another system of coordinates obtained by rotating the system (x, y, z). The direction cosine table for the system is defined in table IV, where ℓ_1, m_1, n_1 are the cosines of the angles between the positive x'-axis and the positive x, y and z axes respectively. Similarly, ℓ_2, m_2, n_2 are the direction cosines of y' with respect to x, y, and z and ℓ_3, m_3, n_3 are the direction cosines of z' with respect to x, y, and z.

Table IV. Direction Cosine for Rotation of Axes

	x'	y'	z'
x	ℓ_1	ℓ_2	ℓ_3
y	m_1	m_2	m_3
z	n_1	n_2	n_3

b. Stress and Strain Transformation

Let σ and σ^1 be the stress components in the (x, y, z) and (x', y', z') coordinate systems, respectively. In expanded form these are

$$\sigma = \begin{Bmatrix} \sigma_x \\ \sigma_y \\ \sigma_z \\ \tau_{xy} \\ \tau_{yz} \\ \tau_{zx} \end{Bmatrix} \qquad \sigma' = \begin{Bmatrix} \sigma'_x \\ \sigma'_y \\ \sigma'_z \\ \tau'_{xy} \\ \tau'_{yz} \\ \tau'_{zx} \end{Bmatrix}$$

Since stress is a tensor quantity, the transformation due to rotation of axes is represented by

$$\begin{bmatrix} \sigma_x & \tau_{xy} & \tau'_{zx} \\ \tau'_{xy} & \sigma_y & \tau'_{yz} \\ \tau'_{zx} & \tau_{yz} & \sigma'_z \end{bmatrix} = \begin{bmatrix} \ell_1 & m_1 & n_1 \\ \ell_2 & m_2 & n_2 \\ \ell_3 & m_3 & n_3 \end{bmatrix} \begin{bmatrix} \sigma_x & \tau_{xy} & \tau_{zx} \\ \tau_{xy} & \sigma_y & \tau_{yz} \\ \tau_{zx} & \tau_{yz} & \sigma_z \end{bmatrix} \begin{bmatrix} \ell_1 & \ell_2 & \ell_3 \\ m_1 & m_2 & m_3 \\ n_1 & n_2 & n_3 \end{bmatrix} \tag{90}$$

or in expanded form

$$\begin{Bmatrix} \sigma'_x \\ \sigma'_y \\ \sigma'_z \\ \tau'_{xy} \\ \tau'_{yz} \\ \tau'_{zx} \end{Bmatrix} = \begin{bmatrix} \ell_1^2 & m_1^2 & n_1^2 & 2\,\ell_1 m_1 & 2\,n_1 m_1 & 2\,\ell_1 n_1 \\ \ell_2^2 & m_2^2 & n_2^2 & 2\,\ell_2 m_2 & 2\,n_2 m_2 & 2\,\ell_2 n_2 \\ \ell_3^2 & m_3^2 & n_3^2 & 2\,\ell_3 m_3 & 2\,n_3 m_3 & 2\,\ell_3 n_3 \\ \ell_1\ell_2 & m_1 m_2 & n_1 n_2 & m_1\ell_2 + \ell_1 m_2 & n_1 m_2 + m_1 n_2 & \ell_1 n_2 + n_1 \ell_2 \\ \ell_2\ell_3 & m_2 m_3 & n_2 n_3 & m_2\ell_3 + \ell_2 m_3 & n_2 m_3 + m_2 n_3 & \ell_2 n_3 + n_2 \ell_3 \\ \ell_1\ell_3 & m_1 m_3 & n_1 n_3 & m_1\ell_3 + \ell_1 m_3 & n_1 m_3 + n_3 m_1 & \ell_1 n_3 + \ell_3 n_1 \end{bmatrix} \begin{Bmatrix} \sigma_x \\ \sigma_y \\ \sigma_z \\ \tau_{xy} \\ \tau_{yz} \\ \tau_{zx} \end{Bmatrix} \tag{91}$$

Symbolically, equation 91 is written as

$$\sigma' = A\,\sigma \tag{92}$$

where A is the transformation matrix in equation 91.

In a similar manner, the transformation from σ' to σ is obtained as

$$\sigma = B\,\sigma' \tag{93}$$

where

$$B = \begin{bmatrix} \ell_1^2 & \ell_2^2 & \ell_3^2 & 2\,\ell_1\ell_2 & 2\,\ell_2\ell_3 & 2\,\ell_1\ell_3 \\ m_1^2 & m_2^2 & m_3^2 & 2\,m_1m_2 & 2\,m_2m_3 & 2\,m_1m_3 \\ n_1^2 & n_2^2 & n_3^2 & 2\,n_1n_2 & 2\,n_2n_3 & 2\,n_1n_3 \\ \ell_1m_1 & \ell_2m_2 & \ell_3m_3 & \ell_2m_1 + m_2\ell_1 & \ell_3m_2 + m_3\ell_2 & \ell_1m_3 + m_1\ell_3 \\ m_1n_1 & m_2n_2 & m_3n_3 & m_1n_2 + n_1m_2 & m_2n_3 + n_2m_3 & n_1m_3 + m_1n_3 \\ \ell_1n_1 & \ell_2n_2 & \ell_3n_3 & \ell_2n_1 + \ell_1n_2 & \ell_3n_2 + n_3\ell_2 & \ell_1n_3 + n_1\ell_3 \end{bmatrix} \tag{94}$$

If the strain components ε, ε' correspond to σ and σ' respectively, the strain transformations can be obtained from the conservation of energy.

$$\sigma'^{T}\varepsilon' = \sigma^{T}\varepsilon \tag{95}$$

Substituting equation 93 for σ into equation 95 results in

$$\sigma'^{T}\varepsilon' = \sigma'^{T}B^{T}\varepsilon$$

Hence

$$\varepsilon' = B^{T}\varepsilon \tag{96}$$

or substituting equation 92 for σ' into equation 95 results in

$$\sigma^{T}A^{T}\varepsilon' = \sigma^{T}\varepsilon$$

Hence

$$\varepsilon = A^{T}\varepsilon' \tag{97}$$

c. Transformation of Matrix of Stress-Strain Relations

In order to transform the matrix relating stress and strain the following procedure is followed. C and C' interrelate stress with strain in the respective coordinate systems. Thus

$$\sigma = C\varepsilon \tag{98}$$

and

$$\sigma' = C'\varepsilon' \tag{99}$$

Premultiplying equation 99 by B and substituting for ε' from equation 96 results in

$$B\sigma' = BC'B^T\varepsilon \tag{100}$$

Substituting equation 93 into equation 100 results in

$$\sigma = BC'B^T\varepsilon \tag{101}$$

Comparison of equation 98 and 101 results in the designed transformation of the stress-strain relationship matrix. Thus

$$C = BC'B^T \tag{102}$$

Similarly, it can be shown that

$$C' = ACA^T \tag{103}$$

8. WIDTH OF FINITE ELEMENTS IN CRACKING ZONE

When a reinforced concrete member is subjected to tensile stresses, the first cracks (primary cracks) will be developed when the stresses exceed the allowable tensile stresses of the concrete. When a crack forms, the tensile stress in the concrete immediately adjacent to it must drop to zero (Refs. 3, 84, and 85), as illustrated in figure 40. However, the reinforcement, which is bonded to the concrete, retains its tensile stress and therefore strain. Thus tensile stress must continue to exist in the concrete along the reinforcement and will spread throughout the portion between cracks. At the same time, the concrete stress f_o, along the bars, must increase gradually from zero at the crack to a maximum value $f_{o\ (max)}$ (Fig. 40).

When the forces on the reinforced concrete member are increased above those causing the primary cracks, the steel stresses will increase; and the portion of bond remaining after slip will cause the longitudinal concrete stresses to also increase. The maximum tensile stress in the concrete, $f_{o\ (max)}$, may then somewhere well exceed the tensile strength of the concrete, and a new crack will be started. The same mechanism may result in several cycles of cracks. Broms (Ref. 33) indicated that crack spacing is usually stabilized when the crack spacing is approximately equivalent to the thickness of the cover. The bond-slip relation used in the model is based on initial perfect bond. This perfect bond requires enough length to develop. Therefore, the width of the finite element in the expected cracking regions must be enough to develop this bond. However, the element size in areas of stress concentration should be small enough to provide reasonable approximation of the exact stress gradient. Therefore the analyst should select the element size based on these two requirements and should interpret the results on the basis of this selection. This subject is addressed further in section V.

9. ASSUMPTIONS AND LIMITATIONS OF THE MODEL

a. The deformations (displacements, rotations, and strains) are assumed to be small and, accordingly, the analysis utilizes the initial, undeformed geometry of the system.

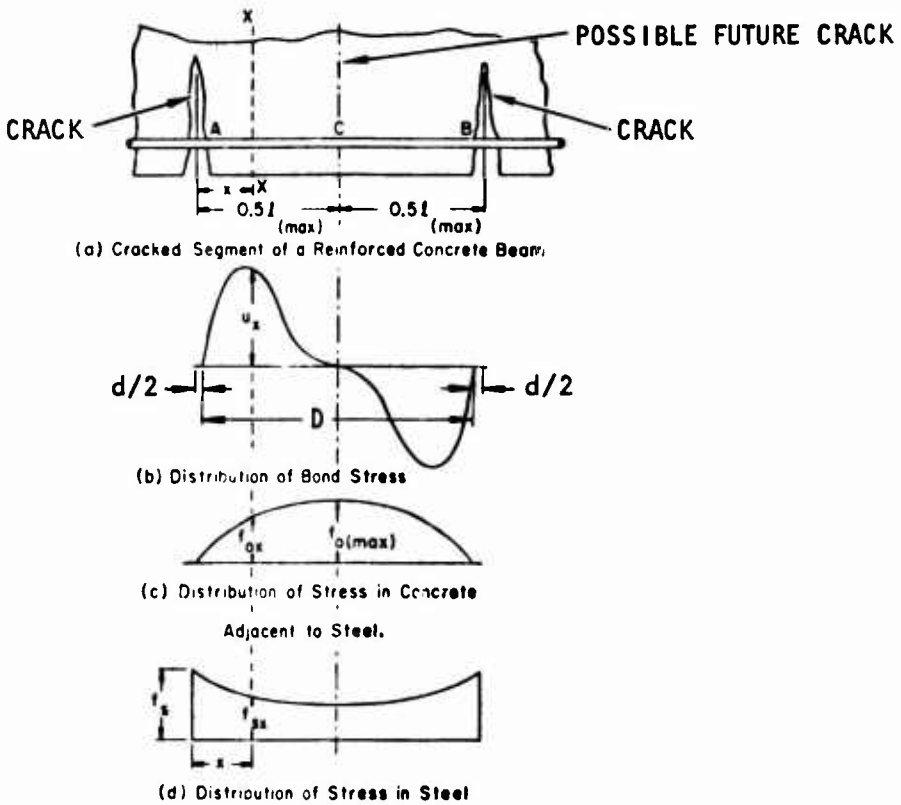

U_x = bond stress at distance x from crack

f_{ox} = Stress in concrete at distance x from crack

f_{sx} = Stress in steel at distance x from crack

Figure 40. Stress Distributions in Cracked Segment (Refs. 3, 84, 85)

b. The geometry can be two- or three-dimensional.

c. The continuum can be approximated by a system of two- or three-dimensional finite elements.

d. The material properties are homogeneous within each element.

e. The directions of first cracks in an element define the directions of orthotropy in this element.

f. The continuum is divided into elements that are long enough to provide full bond at the beginning of loading in tension.

g. The bond is perfect between steel and concrete in compression.

h. The mechanical properties of reinforced concrete elements can be approximated by composite variable moduli.

i. The steel bars are allowed to yield only in tension.

j. The rebonding capability is based on adjusting the stiffness properties of the element.

k. The creep effects are neglected.

l. The value of Poisson's ratio in uncracked elements is assumed constant throughout the solution.

m. Poisson's ratio is assumed zero after cracking.

n. Confining effects were not activated in the present model.

o. The strains in a cracked element represent the average value of the strains in the bonded and debonded zones of the element.

SECTION V

EXPERIMENTAL STUDIES

1. INTRODUCTION

Experimental studies of bond slip were performed as part of the present project to add to the data that are presented by Mains (Ref. 87). These data indicate the average strength contributed by the concrete to a composite section subjected to uniaxial tensile stress. The concrete contribution is expressed as a fraction λ varying from 1.0 to zero. The value of λ is known to be a function of several variables:

a. Strain in the steel

b. Length of uncracked section

c. Concrete strength, bar deformations, and other material parameters

In the present experiments, factors *b* and *c* are held constant.

In the composite model explained in Section IV the function of λ is to facilitate forming a composite modulus from the concrete and steel moduli, as follows:

$$E = \frac{1}{\frac{1-\lambda}{E_s A_s} + \frac{\lambda}{E_s A_s + E_c A_c}} \qquad (104)$$

Experimental data by Ismail and Jirsa (Ref. 66) and Tanner (Ref. 67) were shown in figure 38 and were reduced to a form that expresses λ as a function of average steel strain in a finite element. In addition to exploring the variation of λ in tension, the present experiments also investigated bond slip in compression.

Cylindrical specimens with a coaxial piece of reinforcing bar were subjected to tension and compression, as illustrated in figure 41. Strain gages were attached to the reinforcing bar as shown in figure 42. Strains were also measured on the surface of the concrete. The approximate load/deflection properties of the specimens are shown in figure 41.

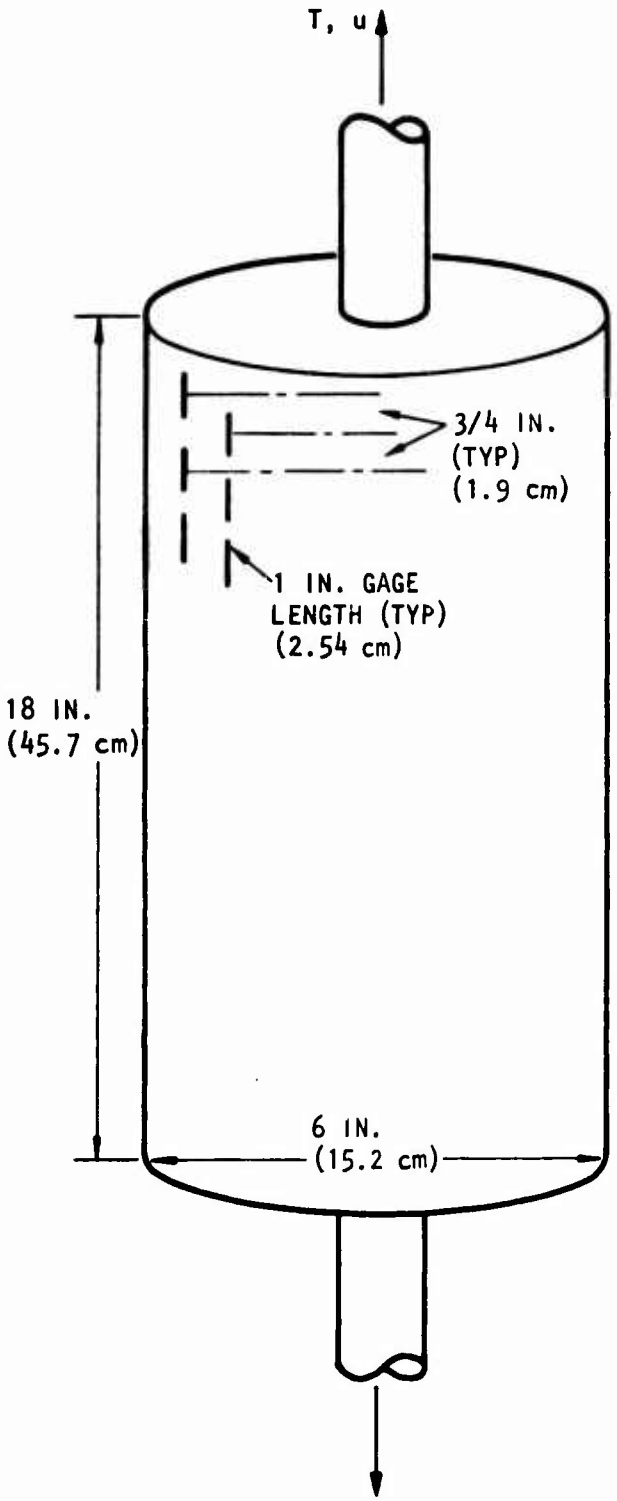

(a) Test specimens

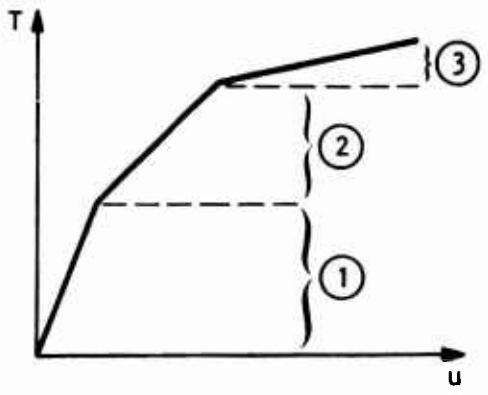

REGION	EVENT
(1)	STEEL IN ELASTIC CONCRETE IS NEARLY ELASTIC. BOND IS BROKEN ONLY AT THE ENDS OF THE SPECIMEN
(2)	STEEL IS ELASTIC. CONCRETE IS CRACKED AT SEVERAL POINTS. BOND IS BROKEN OVER AN APPRECIABLE LENGTH
(3)	STEEL YIELDS. BOND MAY BE BROKEN OVER A LARGE PERCENT OF LENGTH OF SPECIMEN

(b) Tension test

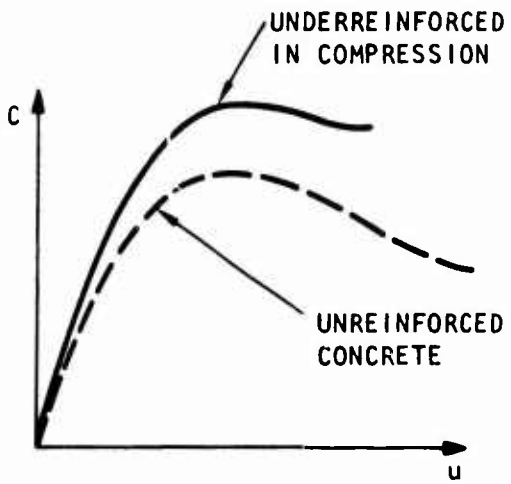

(c) Compression test

Figure 41. Test Specimen Configuration and Loading

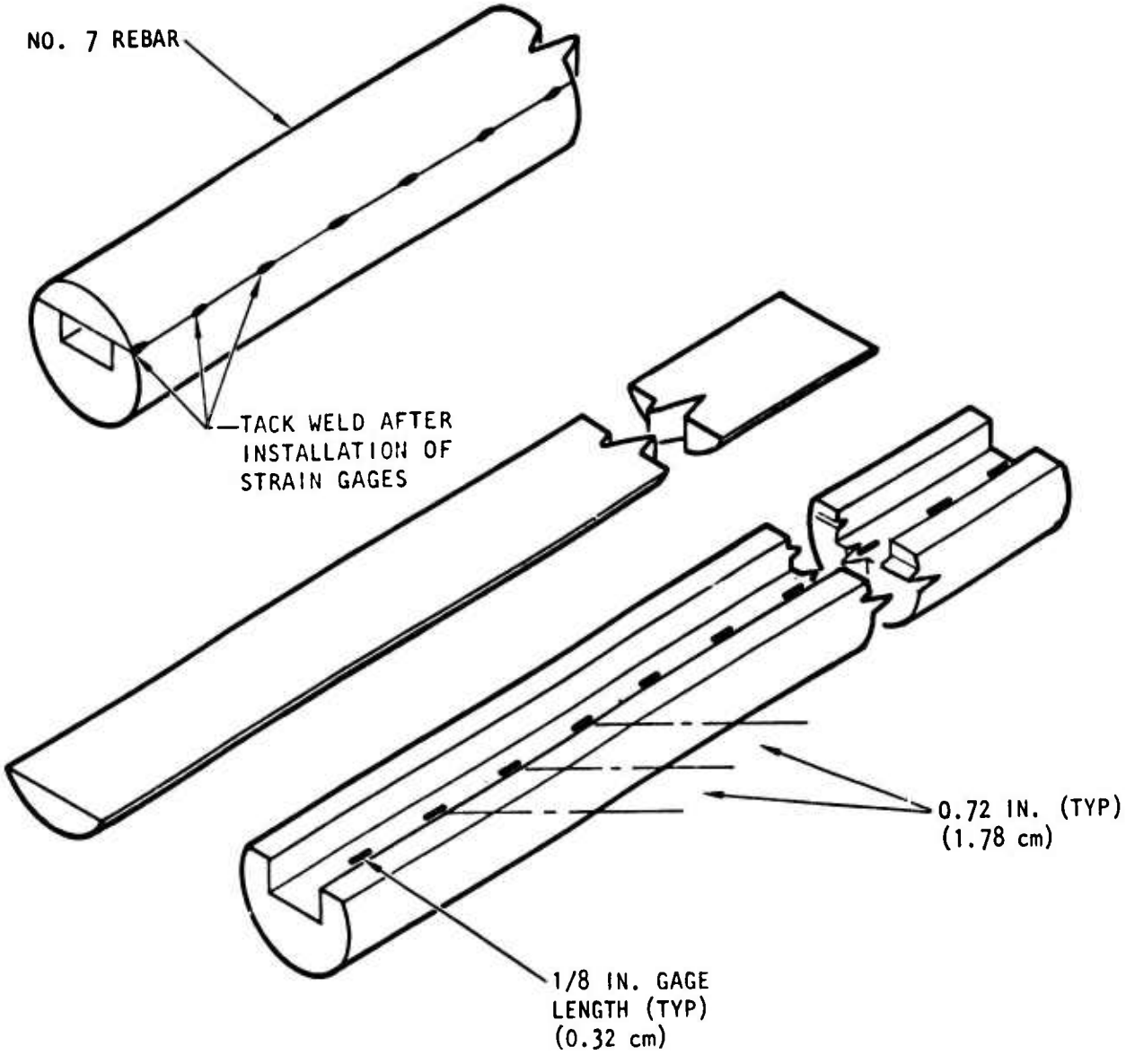

Figure 42. Instrumented Rebar Details

The specimens were tested in unconfined compression and tension in a universal testing machine. The tension specimens were tested by applying tensile forces to the ends of the reinforcing bar (Fig. 41(a)). The compression specimens were tested by applying compressive stress to the concrete only; one end of the bar was cut slightly above the level of the bottom end of the concrete cylinder, and the other end passed through a hole in the crosshead of the testing machine (Fig. 43).

Automatic recording of data from the strain gages and load cells facilitated the processing of results.

2. MANUFACTURE OF SPECIMENS

a. Strain Gaging of the Specimen

The major task in preparing specimens was the gaging of the reinforcing bars. To increase survivability, the strain gages were installed inside the rebar by machining a ground-finish flat surface on two 18-in. (81.28 cm) long pieces of rebar in order to combine them as a pair for each specimen. When the two flat surfaces were matched, the pair formed a bar with the same diameter as in the unmodified condition. Figure 4[illegible]s the cross section of the specimen rebar.

Prior to welding the two parts together, a slot with a ground-surface bottom was first machined into the flat side of the larger piece of rebar. Foil strain gages (Micro-Measurements, Type SA-06-125-DP-350) were installed with AE-15 adhesive in the bottom of the slot at a spacing of 0.72 in. (1.78 cm) center to center, for a total of 25 gages over the 18-in. (45.7 cm) concrete specimen length. The gages were cured two hours at 150°F. Hook-up wires were No. 30 AWG magnet wire with double Formvar insulation. Gages were wired for the 3-wire hook-up method (3 wires to each gage). When all the gages had been installed and wired with the leads extending out one end of the slot, a wash coat of epoxy was used as waterproofing over the gages.

The next step in the processing was to weld the two pieces of rebar together to form a single piece again. The steel was chilled in dry ice and

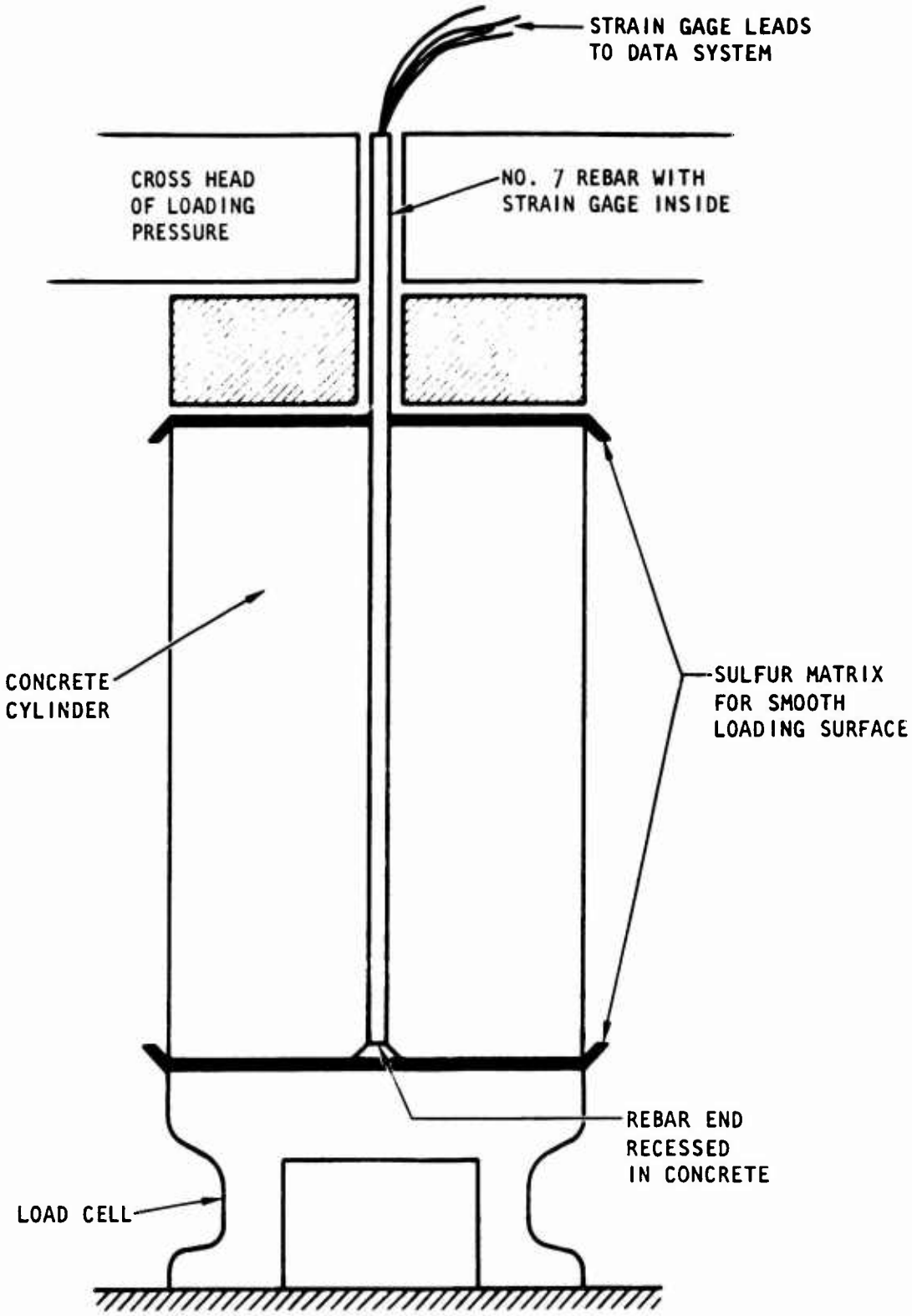

Figure 43. Configuration of Compression Test Specimen

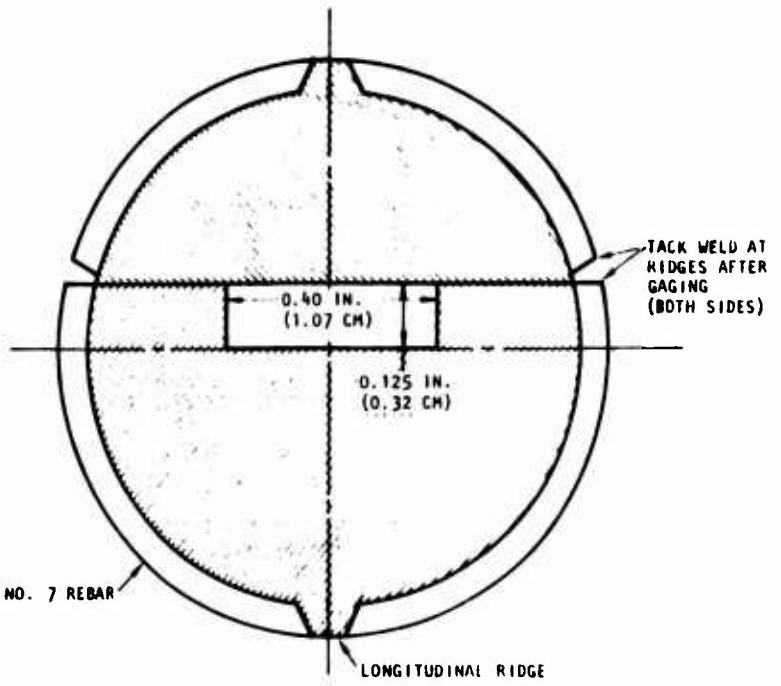

Figure 44. Cross Section of Strain-Gaged Rebar

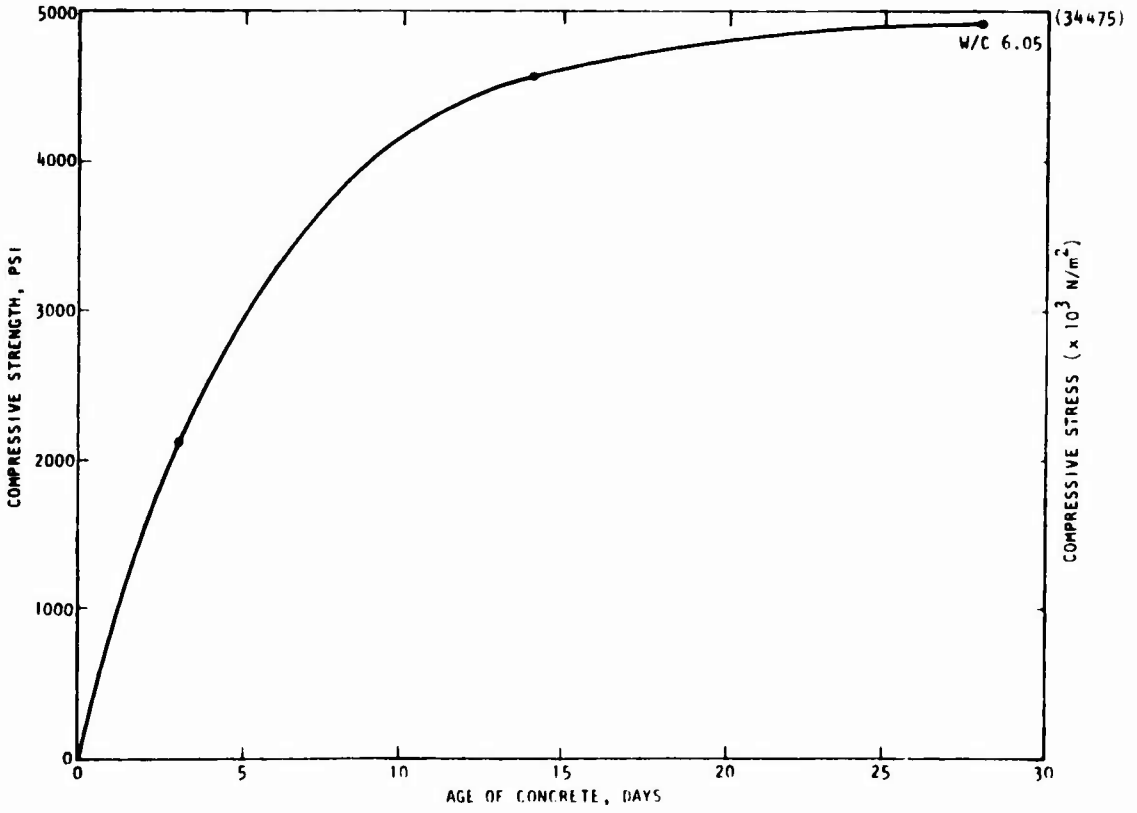

Figure 45. Concrete Strength versus Cure Time

spot welded along the length. The prechilling successfully prevented heat damage to the installed gages since the temperature of the bars remained well below room ambient temperature. Finally, the central slot was filled with epoxy to preclude concrete entry.

When all four rebars had been welded, they were installed in a testing machine and exercised three times to 60 percent of yield to minimize "first cycle off-set" that is common in strain gage work. At this time the load cell built into the tensile specimens just above the "concrete line" was calibrated. After the exercisings, the bottom portions of the two compression specimen rebars were cut off adjacent to the last strain gage. (The compression specimen rebar was originally the same length as the tensile specimen rebars, to facilitate the exercising after gage installation.)

The next step was to cast the specimens, and after the concrete was cured a minimum of 35 days, the specimens were taken out of cure and dried sufficiently to install the surface gages. The concrete surface was sanded lightly in the gage installation area and the vicinity neutralized with phosphoric acid. Washed and redried, the area was coated with A-10 epoxy to provide a smooth surface for gage installation. After the surface was cured overnight, sanded and cleaned, the gages were installed with Eastman 910 adhesive. These outside gages (except for end gages) had a gage length of one inch to attempt to average around any aggregate inclusions near the surface. The center-to-center spacing of these gages was the same as the spacing on the rebar. In order to accommodate this spacing, two changes were required:

1. The gages were staggered in two lines the length of the specimen.

2. The end gages used were the 1/8-in. (0.32 cm) length used on the rebar, in order to get the required center spacing close to the end. The external gages were postyield foil gages, Micro-Measurements type EP-08-10CBE-120.

The outside gages were also wired in the 3-wire method using No. 30 AWG magnet wire. The finished installation was given a coating of AE-15 adhesive as waterproofing.

b. Pouring Concrete Specimens

Pouring of the specimens was done after the reinforcing bars were gaged and waterproofed. In pouring the specimens, the reinforcing bars were centered in molds of polyvinyl tubing. Concrete was poured in three lifts, and each lift was vibrated for about 10 sec. In the tension specimens the bars were centered by drilling a center hole in the bottom cap, which aligned the bottom of the bar. The top was aligned using a jig with a central hole. In the compression specimens, the bottom of the bar rested on a cardboard plug centered in the bottom of the mold and covered with masking tape, which held the bar centered while concrete was poured and vibrated. The top of the bar was positioned with a jig. The cardboard plug caused the bar to be recessed about 1/4 in. (0.63 cm) relative to the concrete surface. This recess prevented the rebar from shunting compressive load around the concrete and directly into the testing machine base.

3. MIX PROPORTIONS OF CONCRETE

The mix proportions and aggregate grading are shown in table V. The strengths of 6-x-12-in. (15.2-x-30.4 cm) cylinders, cured according to ASTM standards, are shown in figure 45. These samples were poured as a trial batch. When the specimens with reinforcing bars were cast, companion 6-x-12-in. (15.2-x-30.4 cm) cylinders and 6-x-18-in. (15.2-x-45.6 cm) cylinders were also cast. They were tested on the same day as the reinforced specimens.

4. STEEL PROPERTIES

The reinforcing bars used in this investigation are No. 7 deformed bars, ASTM Grade 60. They conformed to standard specifications for "Deformed Billet-Steel Bars for Concrete Reinforcement," ASTM Designation A615-68 (Ref. 88). The minimum yield strength is 60,000 psi (4137×10^5 N/m^2).

5. SPECIMEN TESTING AND DATA RECORDING

After 35 days of curing in a 100-percent-humidity environment, the four instrumented test specimens and the five noninstrumented specimens were removed from the curing room. The exterior gages were applied to the four test specimen as detailed in Section 1(a). The data recording system was readied and the testing began.

Table V. Mix Proportions and Aggregate Grading of Concrete Used for Test Specimens

PHYSICAL CHEMICAL
RESEARCH NON DESTRUCTIVE
SOILS ENGINEERING

Osborne LABORATORIES, INC.

Testing and Inspection Services

2636 SOUTH GRAND AVENUE
LOS ANGELES, CALIF. 90007
PHONE: (213) 749-3111

1601 SO. SINCLAIR ST. BLDG. E
ANAHEIM, CALIF. 92806
PHONE: (714) 639-9793

STATEMENT OF MIX DESIGN FOR CONCRETE

PROJECT	Agbabian Associates
ADDRESS	250 North Nash St., El Segundo
ARCHITECT	
ENGINEER	
GEN. CONTR.	
CONC. SUB-CONTR.	
CONC. SUPPLIER	

MIX DESIGN NO. OT 3719-1
DATE

DESIGN STRENGTH Trial Batch
MAX. AGGR. SIZE 3/4"
MAX. SLUMP
WATER / CEMENT 6.45
DESIGN METHOD
WSD USD

AVERAGE COMPRESSIVE STRENGTH OF PREVIOUSLY EVALUATED CYLINDERS psi

DESIGN FOR ONE CUBIC YARD OF CONCRETE SATURATED, SURFACE DRY

MATERIAL		BATCH WEIGHT	SP. GR.	ABSOLUTE VOLUME
CEMENT	TYPE II 5.4lb sks	513	3.15	2.61
AGGREGATE 1.	W C Sand	1300	2.64	7.88
AGGREGATE 2.	Gravel No. 4	265	2.65	1.60
AGGREGATE 3.	Gravel No. 3 (regraded)	1695	2.65	10.23
AGGREGATE 4.				
WATER	35.2 gals	293	1.0	4.68
ADMIXTURE	None			

GRADING ANALYSIS PERCENT PASSING U.S. STANDARD SIEVE

	%	1 1/2	1	3/4	1/2	3/8	4	8	16	30	50	100	200	F.M.
AGGR. 1.	40					100	99	86	66	48	22	7		2.70
AGGR. 2.	8				100	92	13	3	2					5.89
AGGR. 3.	52			100	56	21	6							6.73
AGGR. 4.														
COMBINED				100	77	58	44	34	26	19	9	3		5.07
SPECIFIED LIMITS														

CEMENT BRAND Victor TYPE II

AGGREGATE SOURCE Conrock - San Gabriel

RESPECTFULLY SUBMITTED,
OSBORNE LABORATORIES, INC.

R.C.E. No

a. Plain Specimen Testing

The nongaged sample specimens were tested prior to the gaged specimens to determine basic strength of the concrete, and to determine the fracture characteristics of samples with rebar included, when tested in the same manner as that to be used on the strain-gaged specimens. The five tests were all run the same day (October 5, 1973). The samples were 53 days old at that time. The results are summarized below:

- Sample 1: Split cylinder test on a 6-in. dia. by 12-in.-long (15.2 x 30.4 cm) cylinder (compressive loading on side of cylinder, roller bearing fashion). Ultimate load: 75,750 lb (337×10^3 N). Tensile strength: 715 psi (4930×10^3 N/m^2).

- Sample 2: Compressive test, end loading of 6 in. dia. by 12-in. (15.2 x 30.4 cm) long cylinder. Ultimate load: 183,000 lb (814×10^3 N). Compressive strength: 6470 psi (4461×10^4 N/m^2).

- Sample 3: Compressive test, end loading of 6-in. dia. by 18-in.-long (15.2 x 45.6 cm) cylinder. Ultimate load: 168,000 lb (747×10^3 N). Compressive strength: 5960 psi (4109×10^4 N/m^2).

- Sample 4: Compressive test, 6-in. dia. by 18-in.-long (15.2 x 45.6 cm) cylinder with coaxial No. 7 rebar protruding 11 in. (27.94 cm) from top of specimen only. Capping compound partially removed from lower end of rebar to prevent load transfer to rebar. Ultimate load: 135,000 lb (600×10^3 N).

- Sample 5: Tensile test, 6-in. dia. by 18-in.-long (15.2 x 45.6 cm) cylinder with coaxial No. 7 rebar through specimen and protruding from each end. Tensile load applied to rebar. Ultimate load: 34,000 lb (151×10^3 N) to first circumferential crack, continued to 46,000 lb (205×10^3 N), by which time cracking was extensive over entire specimen.

b. Instrumented Specimen Testing

Instrumented tests took longer to set up than did tests of the plain samples. The four specimens were tested on the following schedule:

- Compressive Test (Sample No. 2) tested 10/18/73 to a load of 154,500 lb (687×10^3 N). Sample was 66 days old.
- Tensile Test (Sample No. 3) tested 10/24/73 to a load of 44,000 lb (196×10^3 N). Sample was 72 days old.
- Compressive Test (Sample No. 1) tested 10/29/73 to a load of 160,000 lb (712×10^3 N). Sample was 77 days old.
- Tensile Test (Sample No. 4) tested 10/29/73 to a load of 43,000 lb (191×10^3 N). Sample was 77 days old.

Physically, the evidence of failure of these specimens looked similar to the failure modes of the nongaged samples. Photographs of all samples are shown in figures 46 and 47.

c. Data Logging System

The data from the strain gages were sequentially sampled and routed to an analog-to-digital converter (ADC) and then recorded on 7-track magnetic computer tape. The tape was directly computer-compatible, which greatly facilitated data processing.

The data system consisted of 50 channels of bridge completion and balancing system, bridge excitation, a 50-channel reed-relay scanner, a 12-bit ADC and a digital magnetic-tape recorder, all interconnected as indicated on the block diagram shown in figure 48. This system scanned through all 50 channels in 1/4 sec. These scans were conducted every 5 to 20 sec, as indicated in

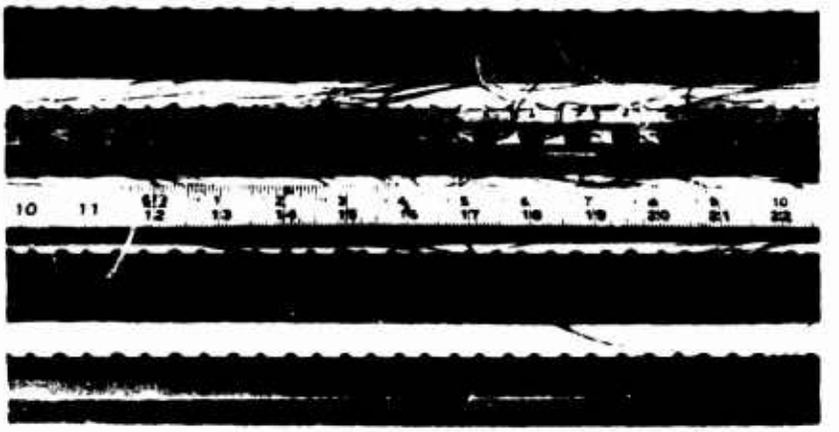

(a) A rebar preparation. Bottom: Internal groove.
Next to bottom: Strain gages installed in groove.
Next to top: Leads attached to gages.
Top: Rebar welded together.

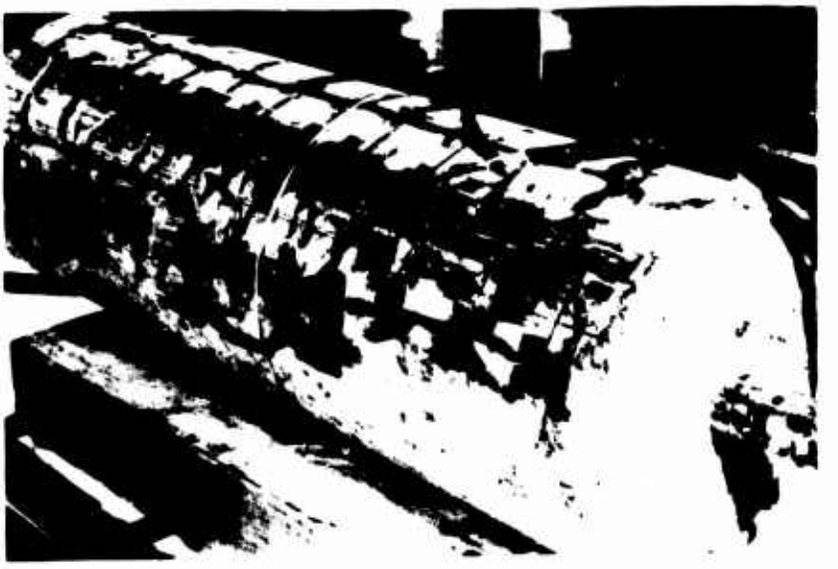

(b) A view showing external strain gages prior to testing

Figure 46. Specimen Preparation

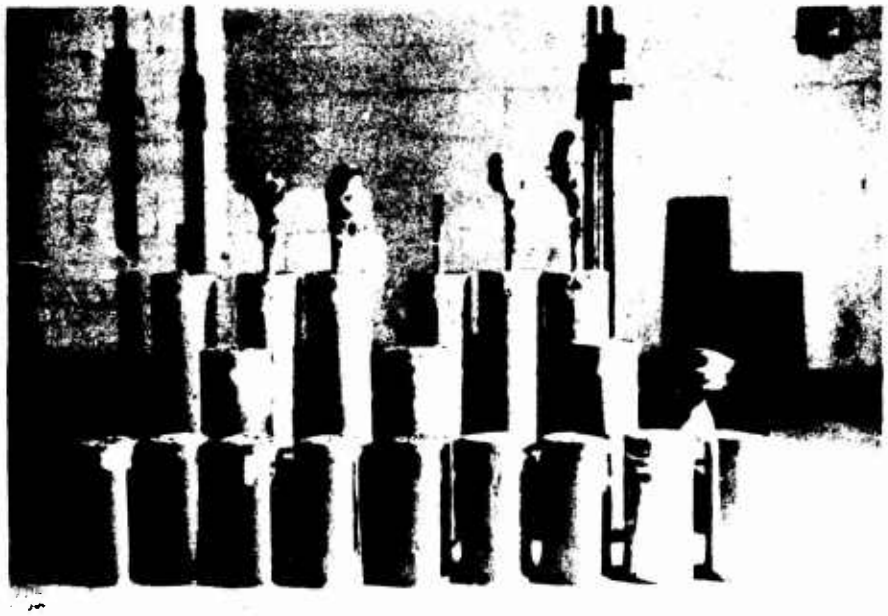

(c) Test specimens and batch test samples prior to curing

(d) Same as above, top view

Figure 46. Specimen Preparation (concluded)

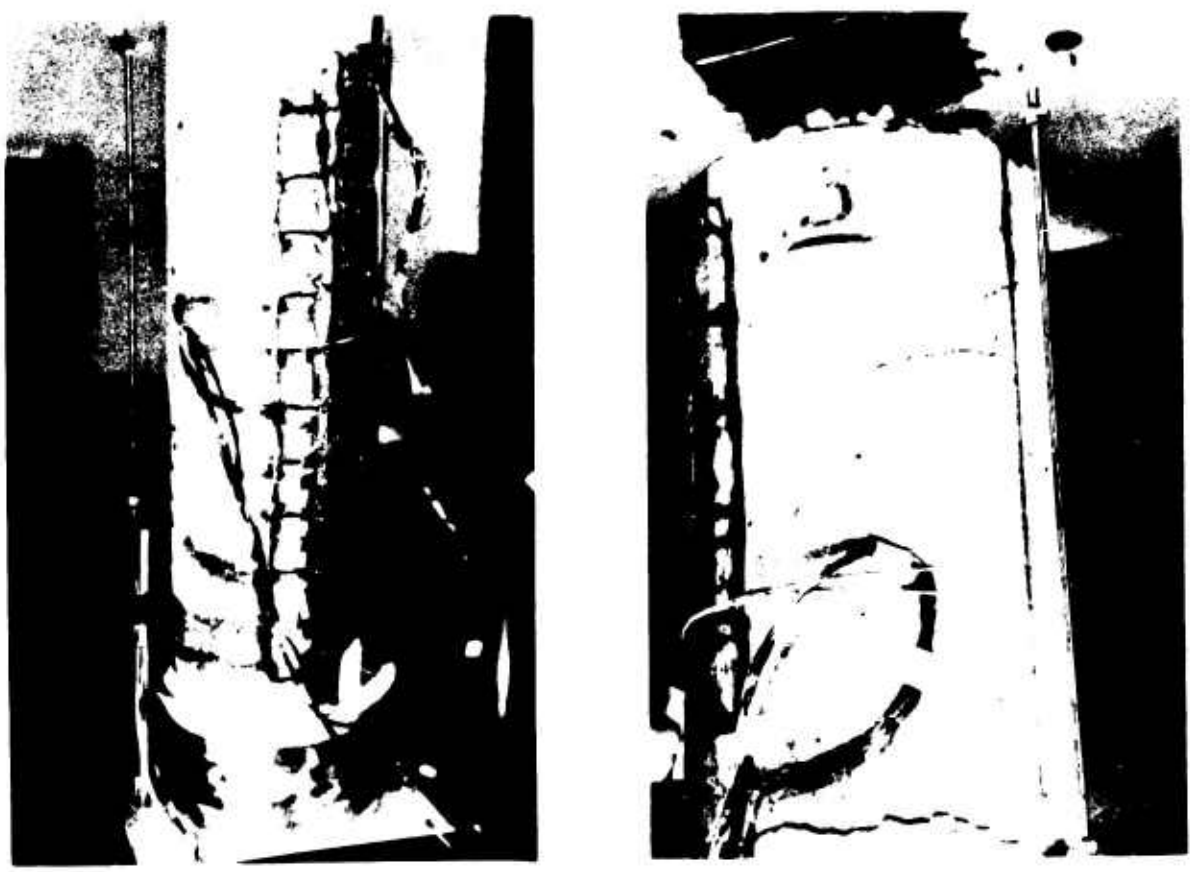

(a) Specimen No. 2 during compression testing

(b) Specimen No. 3 during tension testing. Note cracks.

Figure 47. Specimen Testing and Results

(c) 12 in. x 6 in. (30.48 x 15.24 cm) diameter split test specimen. Failure at 75,750 (337×10^3 Newton) lb equal to tensile strength of 715 psi (4930×10^3 N/m^2)

(d) Split test specimen showing interior

Figure 47. Specimen Testing and Results (continued)

(e) 18 in. x 6 in. (45.6 x 15.24 cm) diameter specimen with non-instrumented rebar, after compression test

(f) 18 in. x 6 in. (45.6 x 15.24 cm) diameter batch sample after compression test

Figure 47. Specimen Testing and Results (continued)

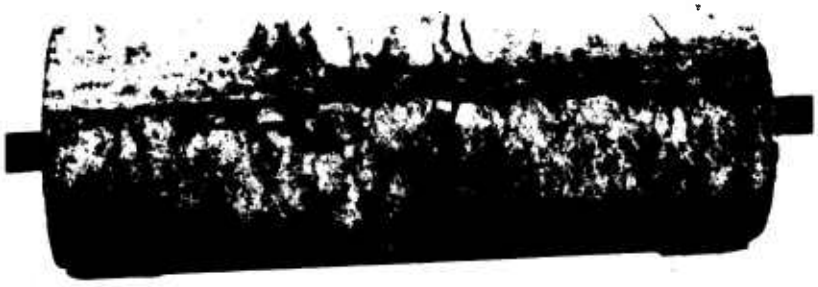

(g) Noninstrumented specimen with rebar, after tension test. Note cracking pattern.

(h) Back side of above specimen

Figure 47. Specimen Testing and Results (continued)

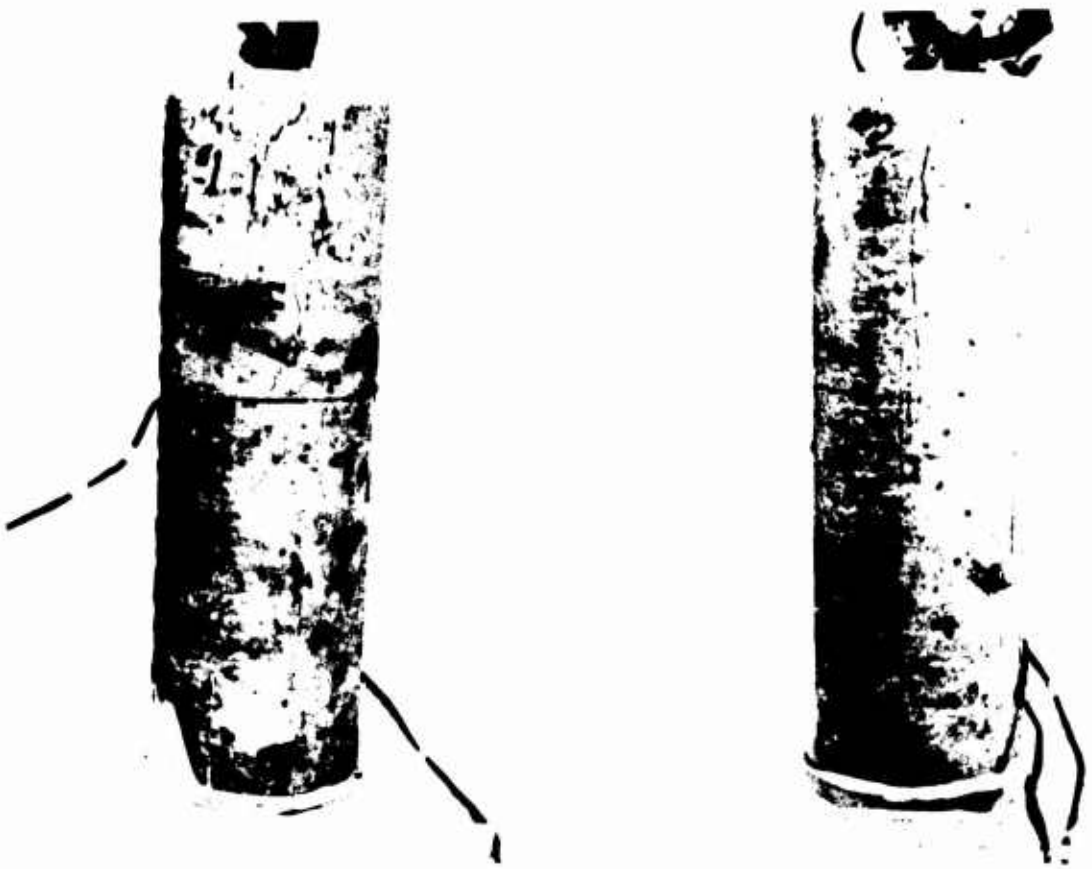

(i) Instrumented specimen No. 1, after compression test. Cracking at upper end

(j) Instrumented specimen No. 2, after compression test

Figure 47. Specimen Testing and Results (continued)

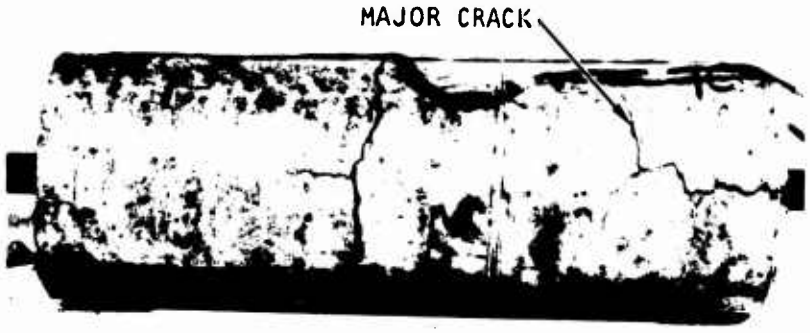

(k) Instrumented specimen No. 3, after tension test, showing cracking pattern

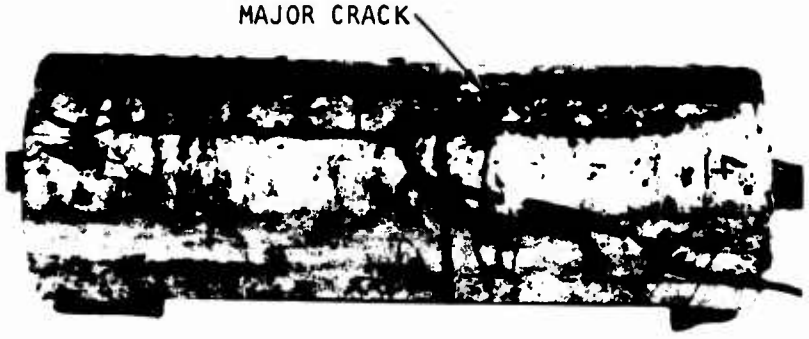

(l) Instrumented specimen No. 4, after tension test, showing cracking pattern

Figure 47. Specimen Testing and Results (concluded)

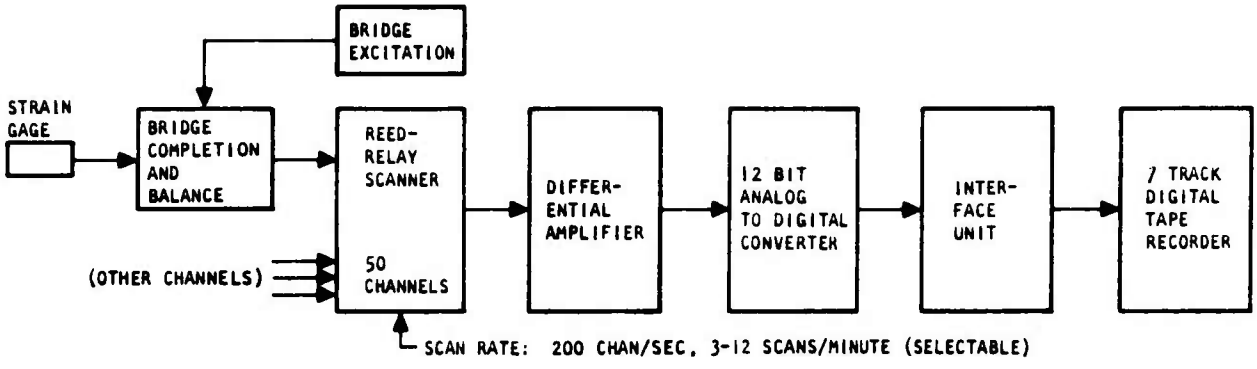

Figure 48. Block Diagram of Data Logging System

the testing summary above. Because of the essentially steady-state, bandwidth-limited nature of the data, no antialiasing filters* were used ahead of the scanner.

The specimens were hooked up in pairs, a compressive specimen with a tensile specimen, each serving in turn as temperature-compensating dummy to the other. The gage factor desensitization effect of the resistance of the long leads of small gage wire was compensated mathematically. When a step-function increase in the strain level of some channels was found much later in processing, the effect was confirmed and quantified by ECAP† computer analysis of the circuit; one of the double lead wires was broken. Thus, correction factors were incorporated as needed.

6. EXPERIMENTAL RESULTS

For the tensile tests, specimens of the type shown in figure 41(a) were subjected to tensile forces applied directly to the reinforcing bar, as shown. An idealization of the load/deflection curve to be expected from such a test is shown in figure 41(b), where the three regions of differing stiffnesses are explainable in terms of cracking of the concrete and yielding of the steel. Before cracking occurs, the tensile forces are resisted by the composite stiffness of the concrete/steel specimen. As the bond between the concrete and steel deteriorates, through cracking of the concrete, the participation of the concrete in resisting the tensile forces diminishes, eventually leaving only the steel to carry the load. The variable composite Young's modulus resulting from such a model is expressed through equation 104, in which λ is the bond strength parameter. Ismail and Jirsa (Ref. 66) have defined λ for a test specimen similar to that of figure 41(a), loaded in tension, according to the formula

---

*Sampled data systems usually require antialiasing filter ahead of the scanner to prevent errors caused by the sampling (scanning) process. However, the bandwidth limited nature of the essentially steady state data collected on this test precluded the need for such filtering.

†Electronic Circuit Analyses Program, developed by IBM.

$$\lambda = 1 - \frac{\int_0^L \varepsilon_s \, dx}{\frac{TL}{A_s E_s}} \qquad (105a)$$

where

ε_s = The steel strain

T = The tensile force

A_s = The steel cross-sectional area

E_s = Young's modulus for steel

L = The length of the specimen

before cracking $\lambda = 1$, which indicates strong bond between concrete and steel and results in full participation of concrete stiffness in equation 104. However, after cracks occur, the first term in the denominator of equation 104 increases with the decreases of λ, while the second term decreases with the decrease of λ. When bond becomes entirely broken, $\lambda = 0$, and the second term disappears while the first term equals the stiffness of the steel bars. Continuous change of λ thus accounts for the continuous loss of bond due to increased loads and provides a simple way for updating the composite properties of the element.

Equation 105(a) can also be expressed in the form

$$\lambda = 1 - \frac{\int_0^L \varepsilon_s \, dx}{\bar{\varepsilon}_s \, L} \qquad (105b)$$

where $\varepsilon_s/\bar{\varepsilon}_s$ for a unit length of the specimen can be regarded as the ratio of the strain ε_s in a steel bar totally or partially bonded to concrete and the strain $\bar{\varepsilon}_s$ in a steel bar free of any bond with concrete. It should be noted that

$$\frac{\varepsilon_s}{\bar{\varepsilon}_s} = \frac{\varepsilon_s A_s E_s}{T} = 1 \qquad (106)$$

for the case where bond between concrete and steel bar is completely broken.

Figure 49 shows an idealization of the strain distribution to be expected in the reinforcing bar at various stages of loading of the specimen. The area of the shaded portion of each figure is equal to λ. Figure 49(a) shows the strain distribution at an early stage of loading, before any major cracks have developed. Throughout most of the length of the reinforcing bar, the strain is but a small fraction of the strain which would prevail if there were no concrete. At the ends of the specimen, however, since the load beyond the concrete portion of the specimen is carried entirely by the reinforcing bar, the strain in the reinforcing bar approaches the value it would have if there were no concrete. Thus, local bond deterioration near each end of the specimen has reduced the role of the concrete in supporting the tensile load. Figure 49(b) shows the strain distribution in the reinforcing bar after a crack has developed. The value of the strain at the site of the crack is the "no-concrete" strain value. Comparison with figure 49(a) shows that the formation of a crack results in a large reduction in the value of λ. Figure 49(c) shows the strain distribution in the reinforcing bar after the steel/concrete bond has completely deteriorated. Note that the strain is the no-concrete strain throughout the specimen and that the value of λ is zero.

Test specimens 3 and 4 were tested in tension. Strain gages distributed along the reinforcing bar were used to obtain plots of the strain distribution. Figure 49 shows plots of the strain distribution in the reinforcing bar of specimen 4 during each of the three stages illustrated in figure 49. The strains at each end of the reinforcing bar are higher than the no-concrete

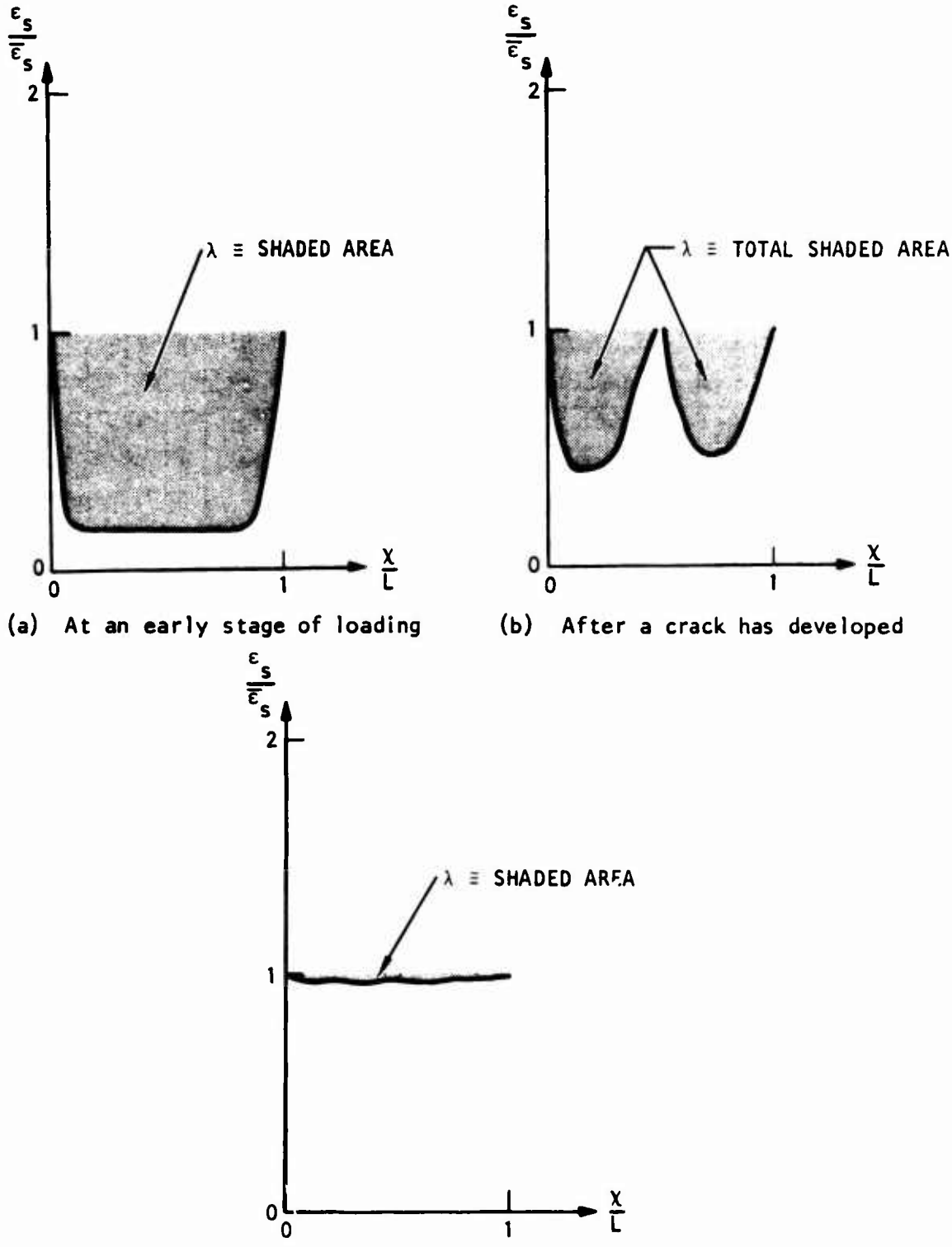

(a) At an early stage of loading

(b) After a crack has developed

(c) Bond completely broken

Figure 49. Idealization of the Strain Distribution in a Tensile Specimen at Three Stages of Loading

strain. As described in subsection 2, the reinforcing bars were split in order to install strain gages. An error was caused by the local failure of the weld joining the two parts of the reinforcing bar. Therefore, strain measurements near each end of the specimen were disregarded in computing λ. Curve (a) of figure 50 shows the strain distribution in specimen 4 during the load stage corresponding to (a) of figure 49. Curve (b) of figure 50 shows the strain distribution after cracks had developed. Unlike (b) of figure 49, cracking in specimen 4 resulted in the total loss of bond strength over almost half the length of the specimen. Curve (c) of figure 50 shows the strain distribution in specimen 4 during the final stages of loading. The strain throughout the specimen is approximately the no-concrete strain.

Figure 51 shows the strain distribution in specimen 3 during the three load stages. Curve (a) is the strain distribution prior to cracking, curve (b) shows the postcracking strain distribution, and curve (c) shows the strain distribution after total deterioration of the bond. The strain at one end of the specimen is abnormally high, due to splitting of the reinforcing bar during load stages (a) and (b). By load stage (c), both ends had split.

Equation 105 was used to evaluate λ at each load step of the tensile tests. The close spacing of the strain gages along the reinforcing bar made possible the evaluation of the integral of equation 105 by numerical integration. Due to the fact that a typical load step contained several bad strain gage readings, which had to be ignored in the analysis, an integration routine capable of variable step size was required. For this reason the trapezoidal rule was used. Figure 52(a) shows λ, as obtained from the tensile tests, plotted against fraction of ultimate load. Ultimate load, in the case of tensile specimens, is taken to be the product of the yield stress and the cross-sectional area of the reinforcing bar.

The sudden drop in λ, occurring once for each specimen, signals the onset of cracking. Although in both cases this drop occurred at a load fraction of 0.4, it should be emphasized that the two specimens were identical. Hence, agreement between the specimens on such matters as cracking stress is to be expected.

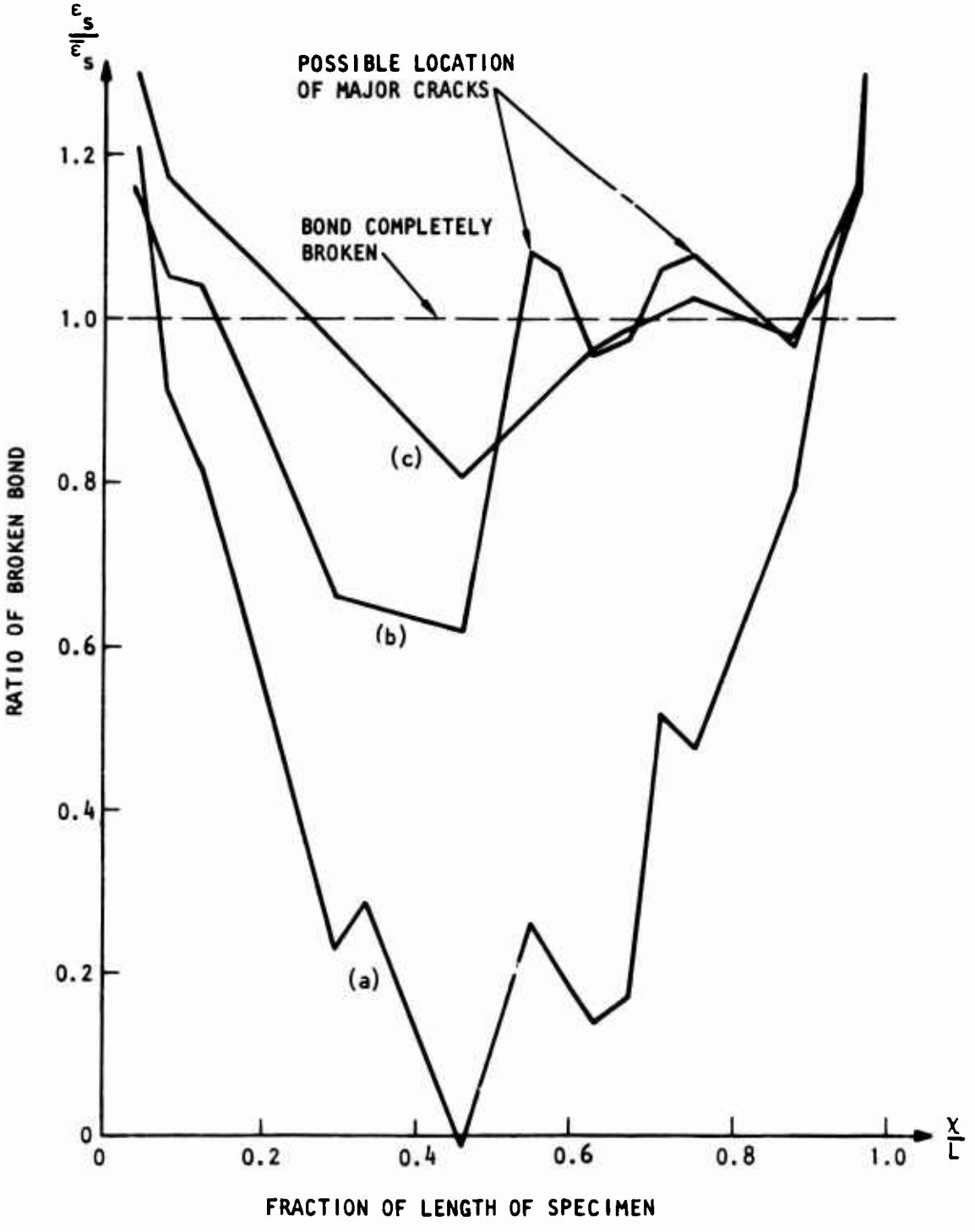

Figure 50. Strain Distribution in the Reinforcing Bar of Specimen 4 for Load Fractions (a) 0.356, (b) 0.533, (c) 0.828

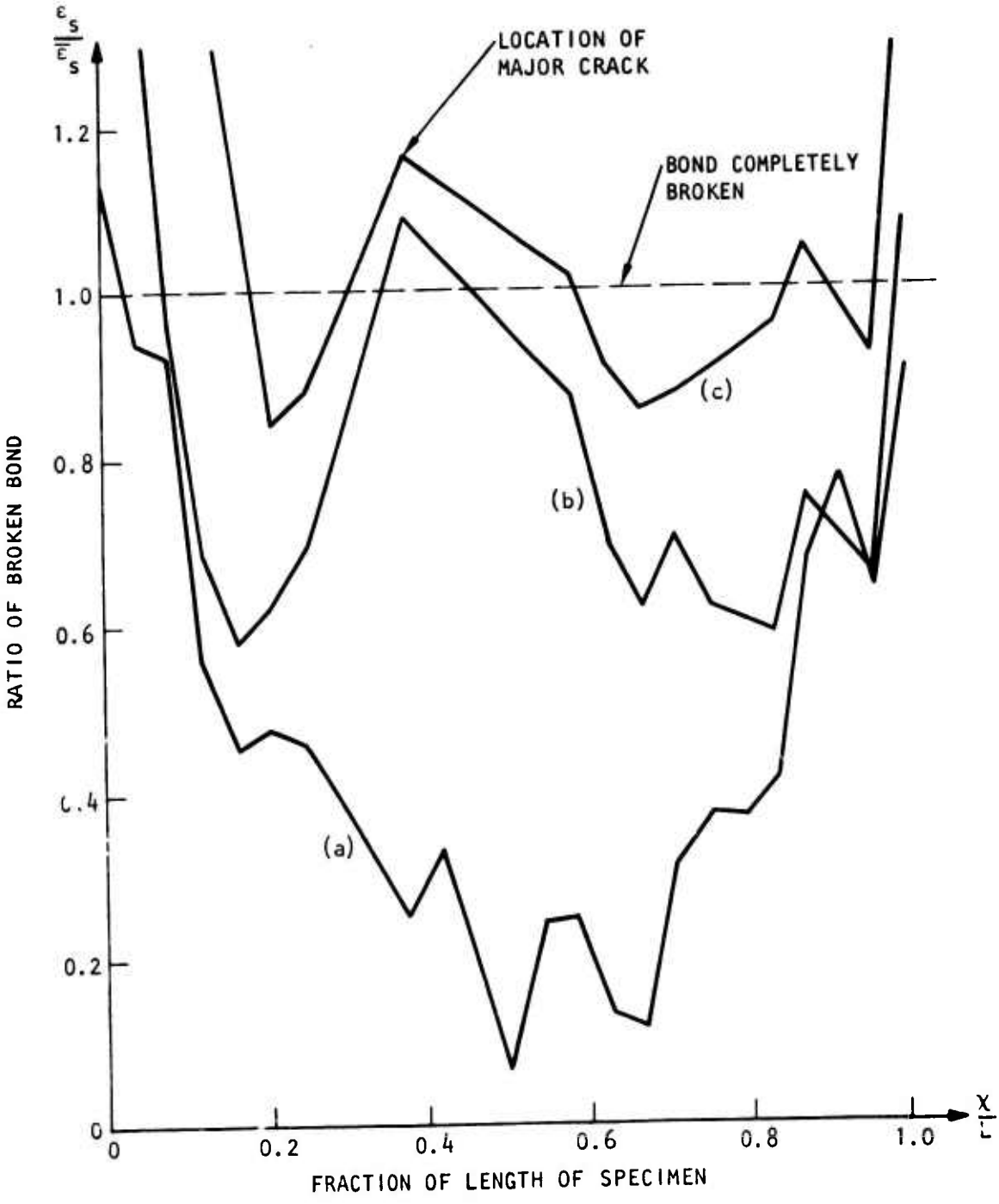

Figure 51. Strain Distribution in the Reinforcing Bar of Specimen 3 for Load Fractions (a) 0.325, (b) 0.455, (c) 0.795

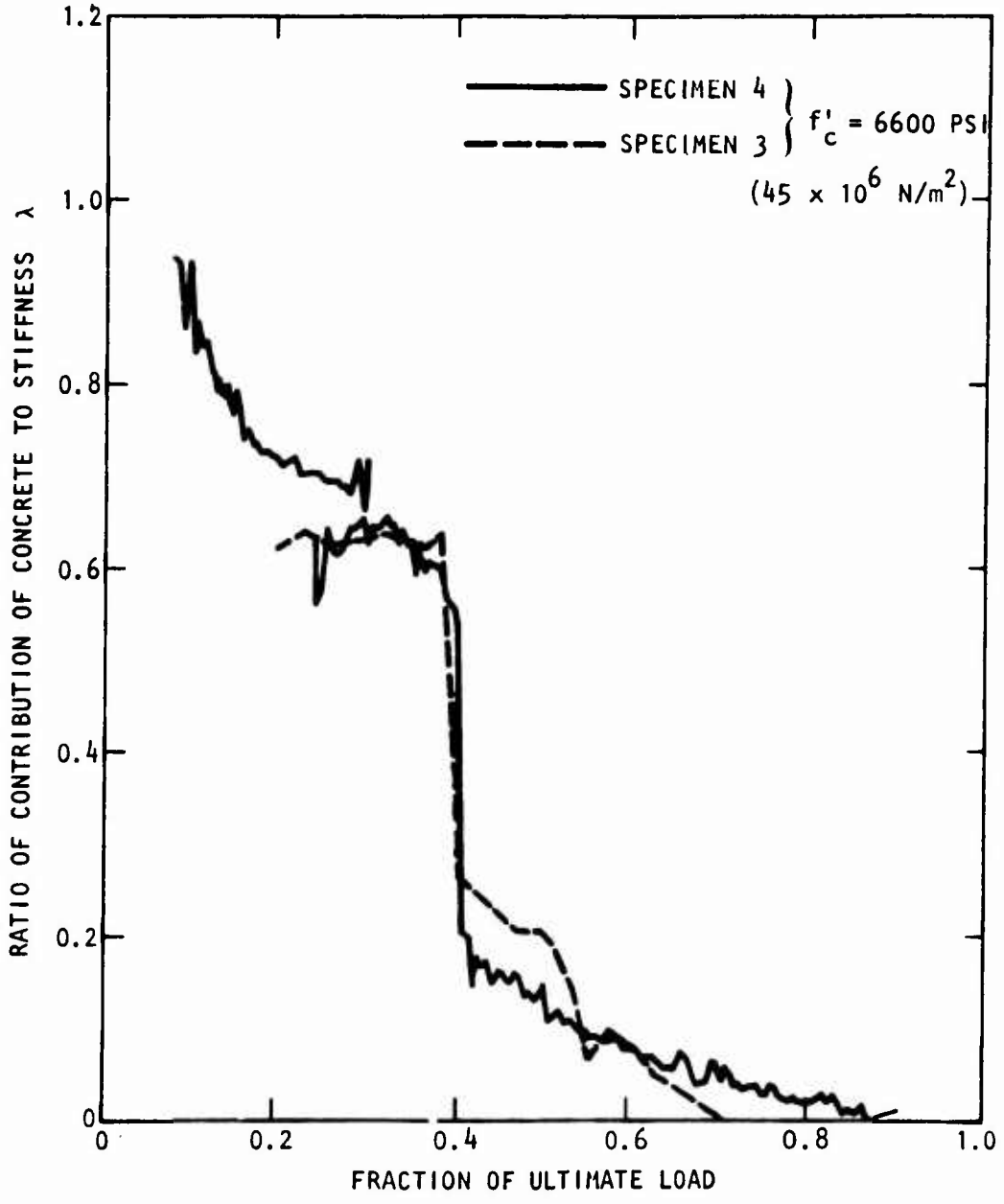

(a) Present experimental results, bond-slip relations in tension

Figure 52. Bond-Slip Relations

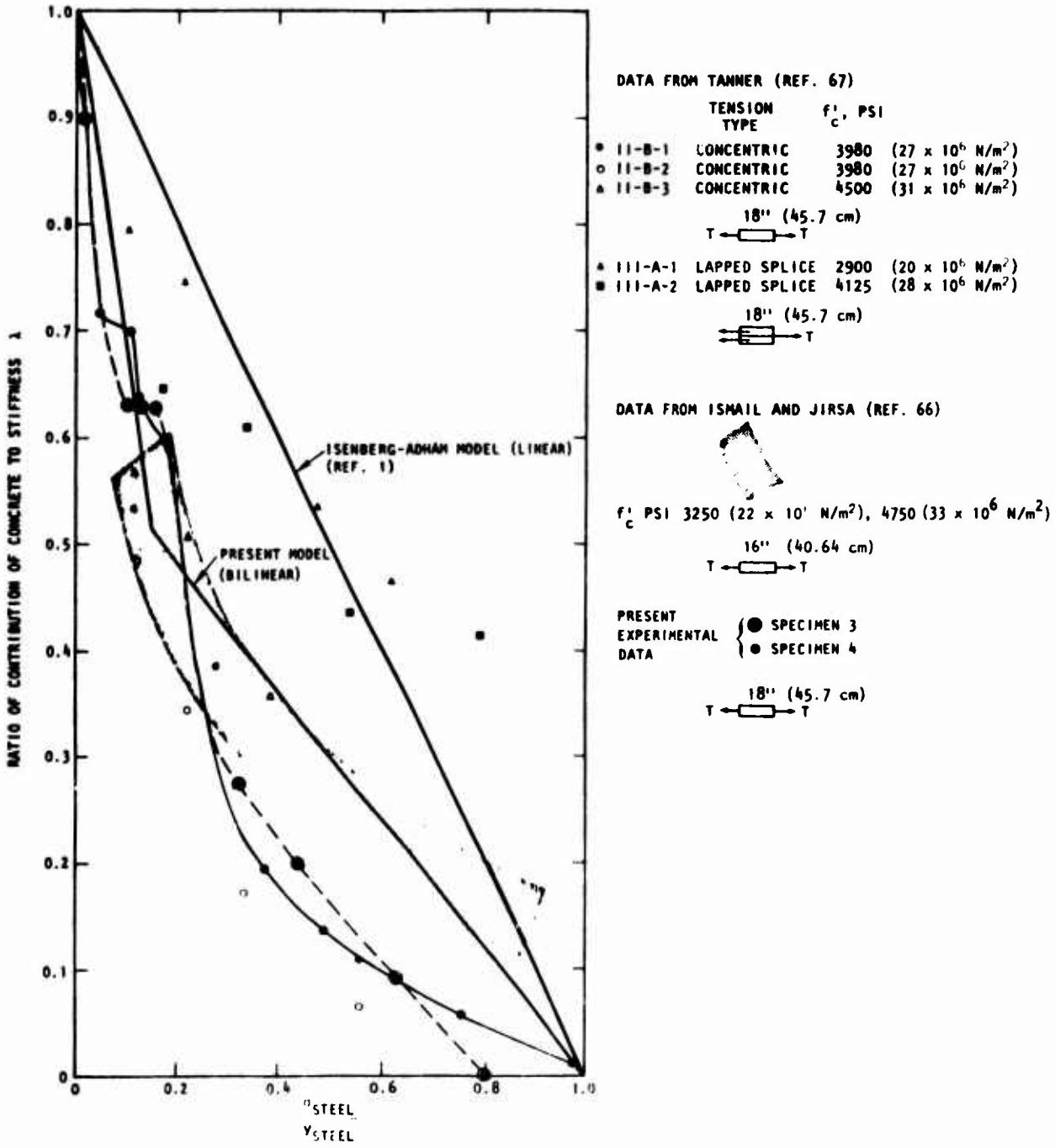

(b) Experimental results (Refs. 66, 67, and present study) compared with analytical results (Ref. 1 and present study)

Figure 52. Bond-Slip Relations (concluded)

An interruption in the testing of specimen 4 is evident in figure 52. After the specimen had been loaded to a load fraction of 0.30, a power failure occurred, causing the load fraction to drop to 0.24. The test was resumed from there. The deterioration of the bond that took place prior to the power failure could not be recovered. Therefore, when the test was resumed, λ retained its value from before the power failure. During reloading, further destruction of the bond was minimal until the specimen had been reloaded to a load fraction of 0.30, the value at which the power failure had occurred. At this point, destruction of the bond at the original rate was resumed. A similar interruption of the testing of specimen 3 occurred. This interruption was caused by a failure of the load cell to operate properly. Hence, no data are available for the portion of the test prior to the interruption. The curve shown in figure 52(a) is the portion of the specimen 3 test after the interruption. The left-hand portion of the curve is flat, indicating reloading rather than virgin loading.

Ismail and Jirsa (Ref. 66) conducted similar tests, using tensile specimens with No. 9 reinforcing bars, whereas No. 7 bars were used in the present study. They used concrete of 3.25 ksi (224×10^5 N/m^2) and 4.75 ksi (328×10^5 N/m^2) ultimate strength, while concrete of 6.6 ksi (455×10^5 N/m^2) ultimate strength was used in the present study. The primary effort of the tests of Ismail and Jirsa was to study the bond deterioration under cyclic loading. They obtained the result that unloading and reloading up to the previous maximum load did little damage to the bond. Loading beyond the previous maximum was detrimental to the bond. The path of the λ versus load fraction curve observed during the power failure of specimen 4 in the present study is consistent with this finding.

Other bond-slip data were discussed in sections III and IV. The choice of the bond-slip relation used in this study was based mainly on the experimental data by Ismail and Jirsa (Ref. 66) and Tanner (Ref. 67), as illustrated in figure 38. The experimental results obtained from specimens 3 and 4,

superimposed on bond-slip data of figure 38, are presented in figure 52(b). Several observations on this figure follow:

- There is a good agreement between experimental results of specimens 3 and 4 of the present study and specimens II-B of Tanner (Ref. 67). Both tests were performed under similar conditions where cracks were allowed to develop arbitrarily during testing.

- The bilinear bond-slip relation used in the present model correlates well with the experimental data of the crack-controlled specimens of Ismail and Jirsa (Ref. 66) and falls in between experimental results of Tanner (Ref. 67) and specimens 3 and 4 of this study.

- The Isenberg-Adham model (Ref. 1) correlates well with the experimental results of specimens III-A of Tanner (Ref. 67).

- The results of specimens 3 and 4 of this study and specimens II-B of Tanner, which had a total length less than the 30 bar diameter required to develop full bond, can be considered representative of bond-slip behavior of short samples pulled from both ends. The behavior can be characterized by three stages: (1) gradual deterioration of bond caused by end effects, (2) sudden loss of bond when major cracks occur, (3) some recovery due to aggregate interlock followed by gradual deterioration of bond.

- The results of specimens III-A of Tanner, where the bar was pulled only from one side, can be considered representative of behavior of samples which are long enough to develop full bond. Behavior of such samples is characterized by deterioration of bond.

Specimens 1 and 2 were tested in compression, the load being applied directly to the concrete, rather than to the steel, as was the case with the tension specimen. A bonding parameter, $\bar{\lambda}$, applicable to these tests, and for which the values 1.0 and 0.0 have meanings similar to those described for concrete in the tension specimens, can be defined for steel in the compression specimens through

$$\bar{\lambda} = \frac{\int_0^L \varepsilon_s \, dx}{\int_0^L \varepsilon_c \, dx} \qquad (107)$$

where ε_c is the strain in the concrete. If the bond were perfect, the strain in the steel would equal the strain in the concrete. The value of $\bar{\lambda}$ obtained from equation 107 would, therefore, be 1.0. If the bond had partially deteriorated, the strain in the concrete would exceed the strain in the steel, since the load bears directly on the concrete. In this case $\bar{\lambda}$ would be less than 1.0. A value of $\bar{\lambda} = 0.0$ would result if the bond were so ineffective that no strain could be transmitted from the concrete to the steel.

Figure 53 shows the strain distribution in the steel and in the concrete of specimen 1 at various stages of loading. At each stage the strain in the concrete exceeds the strain in the steel. Evident in figure 53 is a trend for the strain in the concrete to exceed the strain in the steel by a proportion that increases with load, although the trend is not rapid. There appears to be no sudden deterioration of the bond as there was in the tensile tests when cracks appeared. Figure 54 shows a similar sequence of strain distributions for specimen 2. These curves invite the same observations made in connection with specimen 1, except that the steel and concrete strains recorded during the early stages of loading are in less agreement than in the case of specimen 1.

Figure 55 shows $\bar{\lambda}$, calculated through numerical integration by trapezoidal rule, plotted against fraction of ultimate load. In the case of the compression specimens, ultimate load was taken to be the experimentally measured load at which failure occurred. The observation from figures 53 and 54 that the bond for small load fractions was weaker in specimen 2 than in specimen 1 is reconfirmed in figure 55. Note that the compression data contain no striking features, such as the sudden deterioration of the bond due to cracking. However, due to bad placing of the bearing cap in the compression test, symmetry of the concrete strain from both ends was not preserved (Figs. 53 and 54) and some irregularities of strains were observed

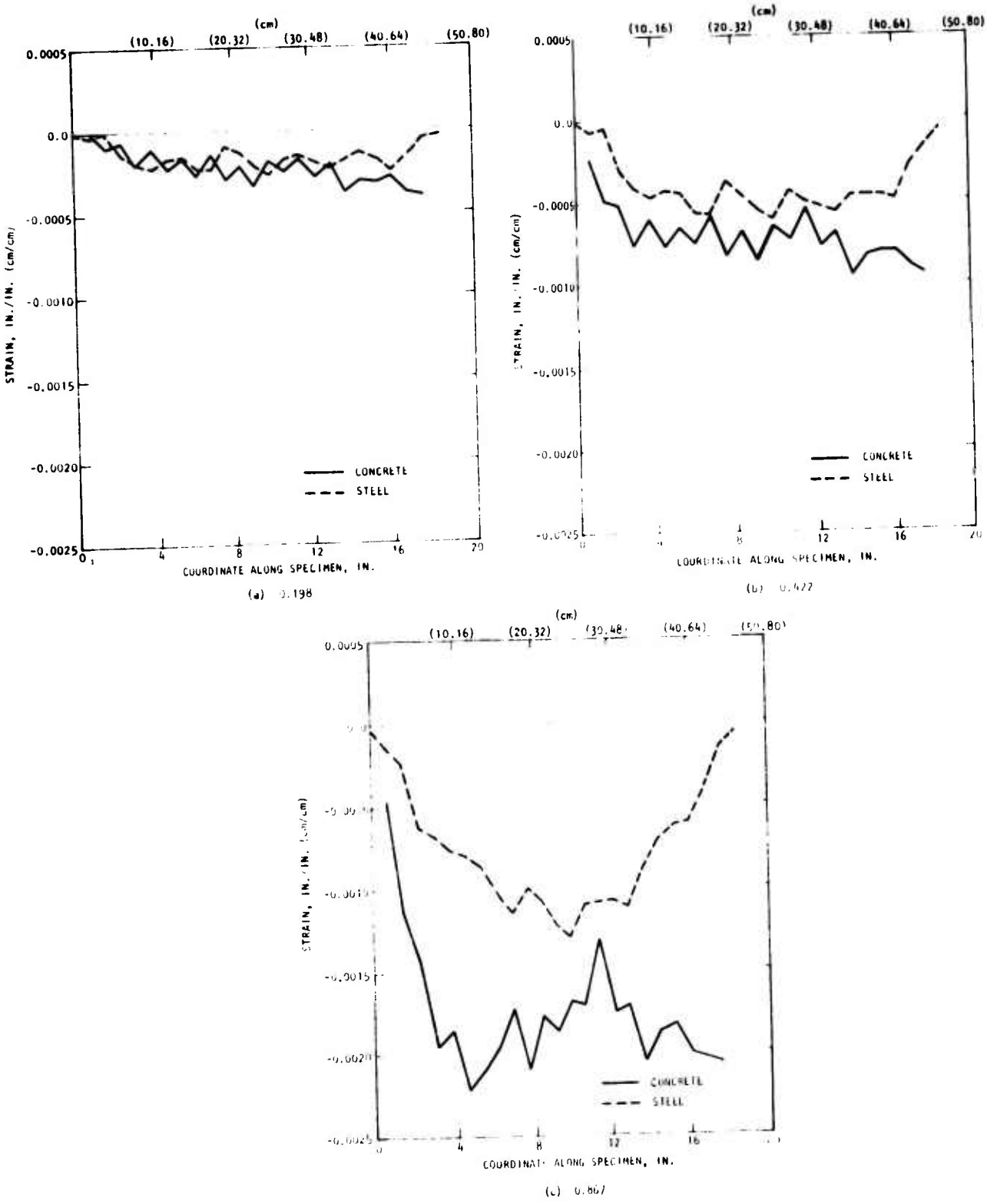

Figure 53. Strain Distribution in Specimen 1 for Load Fractions

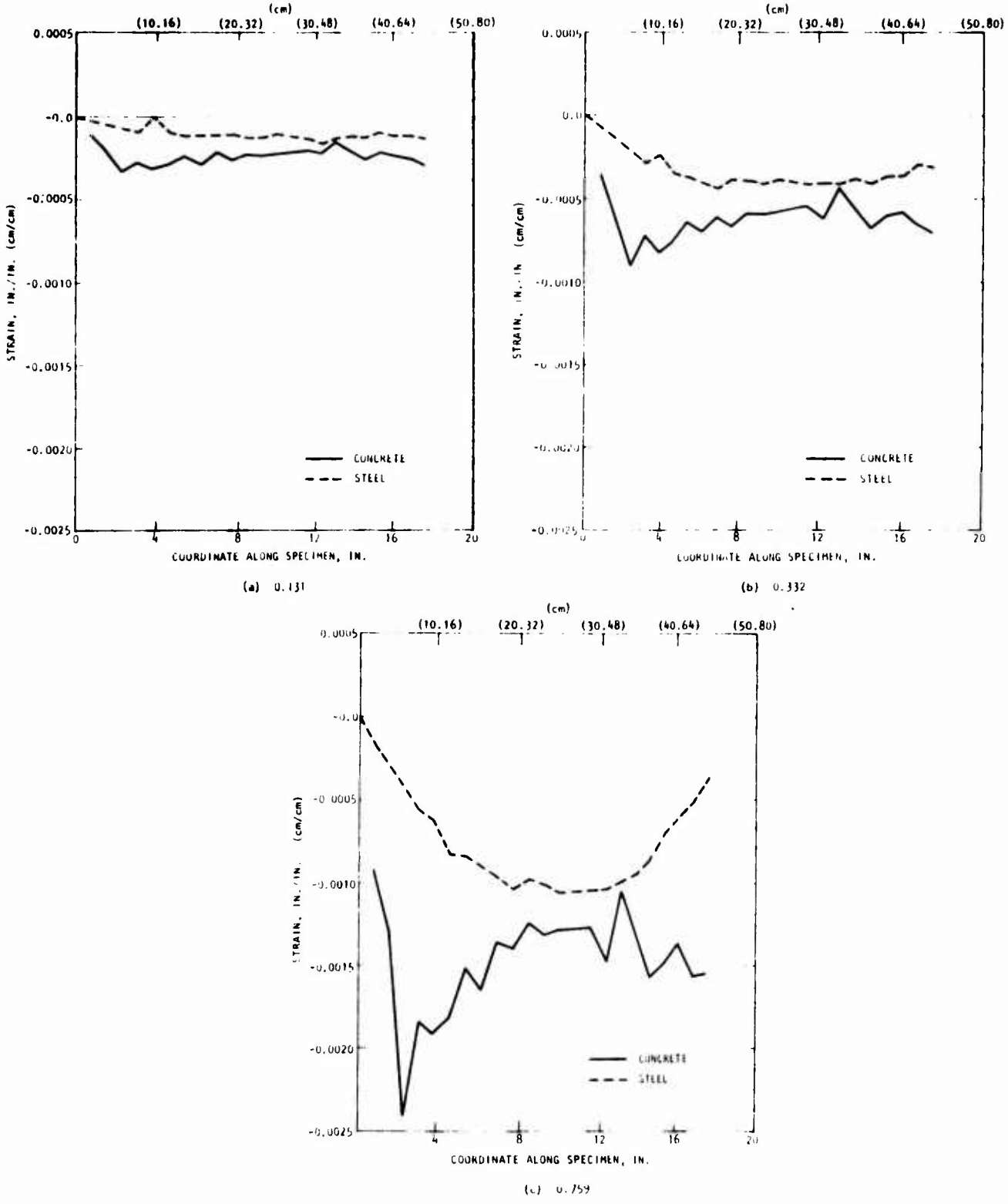

Figure 54. Strain Distribution in Specimen 2 for Load Fractions

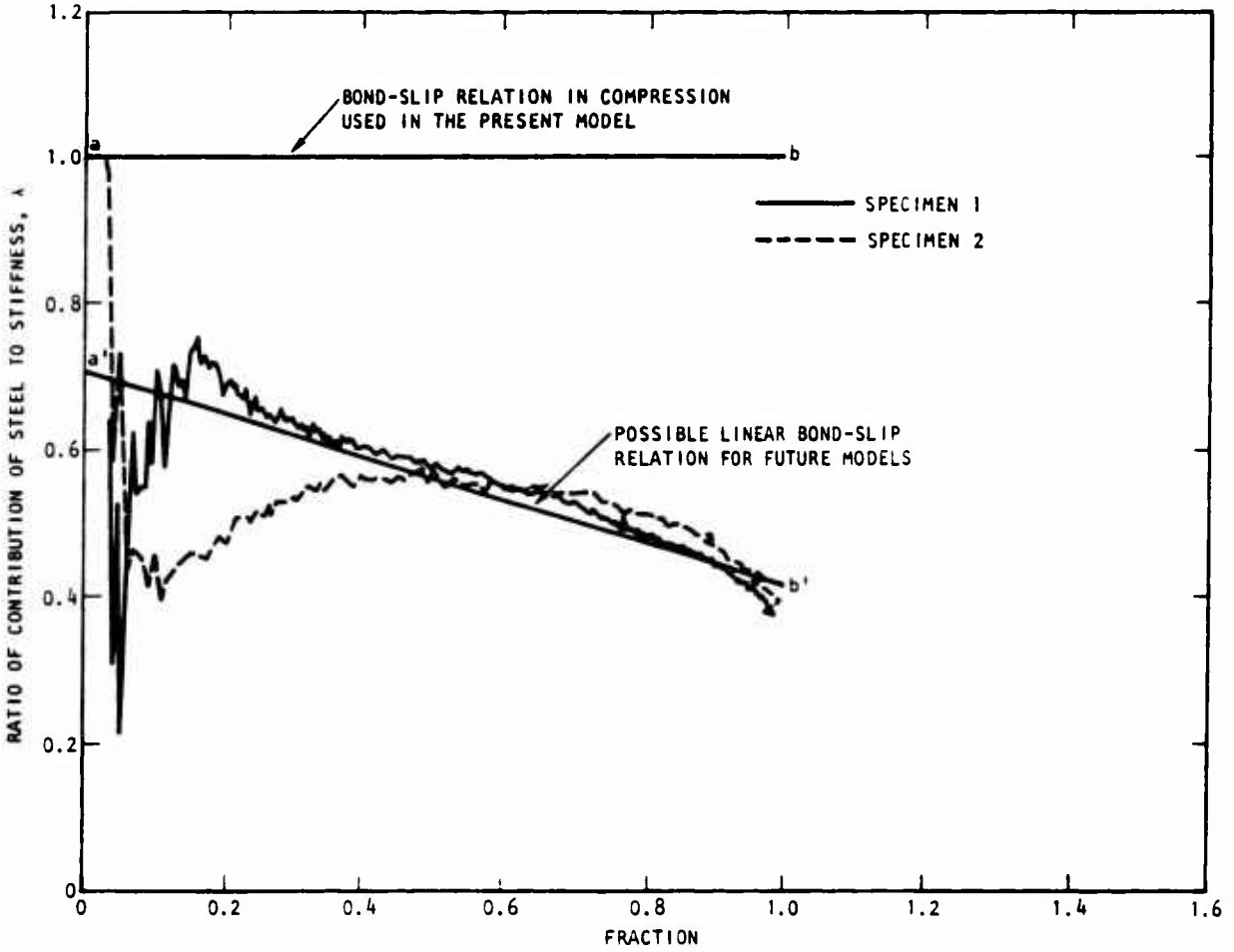

Figure 55. Bond-Slip Relation in Compression

at early stages of the loading. This irregularity has apparently caused the unrealistic drop in bond between steel and concrete at the beginning of the loading (Fig. 55). Therefore a reasonable correction of figure 55 would be to let a' represent the start of the test with full bond, i.e., $\bar{\lambda} = 1$. A possible linear relation for bond slip in compression, a' - b', based on the present experimental data is postulated in figure 55. This relation indicates that the effective stiffness of steel can be reduced by as much as 36 percent by application of the ultimate load in compression.

7. CONCLUSIONS

From the above observations on bond slip in tension, it can be concluded that the bilinear bond-slip relation used in this study follows a course approximately through the middle of the experimental data for both short and long samples shown in figure 52(b). However, the use of very short finite elements may reduce the accuracy of the model. The dependence of bond slip on other parameters, such as concrete strength or number of loading cycles, requires additional study.

In compression, the computer model assumes perfect bonding. Since compressive loads are carried primarily by the concrete, and since figure 55 indicates that the contribution of steel in compression remains high throughout most of the range of loading, this approximation seems reasonable. However, for heavily reinforced concrete structures with a dominant compression mode of behavior, a refinement of the compression bond-slip relation included in the present model may be justified.

SECTION VI

DEMONSTRATION OF CONSTITUTIVE PROPERTIES IN RESPONSE OF STRUCTURAL ELEMENTS

1. INTRODUCTION

This section describes the application of the orthotropic model of reinforced concrete to the response of structural elements such as shallow and deep beams, circular arches, and beam columns. The analyses were performed with an existing two-dimensional axisymmetric finite element computer program, FEDIA,* into which the constitutive equations were inserted as a module. Both static and dynamic calculations were performed. In many of the nine demonstration cases, comparison was made between experimental measurements and the results of analysis. In fact, the reason for performing static analyses was that there were many more published results of static experiments than of dynamic experiments. Hence, there were greater opportunities for validating the model through static than through dynamic calculations. A summary of the demonstration cases is given in table VI.

One of the main difficulties in performing these analyses was that some details of the concrete and steel properties required for the model were not measured. Among these were the Young's modulus, Poisson's ratio, tensile strength, slope of the cracking envelope for concrete, and dowel action parameter n. Where these were not available from experiments, they were assumed on the basis of previous measurements on similar concrete. A summary of the properties used in each of the cases is given in table VII.

2. CASE S-1 (DEEP BEAM 2S1.6-1 OF CRIST, REF. 89)

The static analysis of deep beam 2S1.6-1 was performed using the finite element mesh shown in figure 56. Sizes and locations of the elements were chosen such that the refinement was greatest in regions of high stress gradients (for example, compression zone) so that reinforcing bars were approximately in the center of the elements. The area of tension steel in Elements 1

*FEDIA is a dynamic, inelastic, two-dimensional, continuum finite element code developed by Agbabian Associates.

Table VI. Summary of Example Problems

Case Number	Loading	Type of Structure	Experimental Source Data
S-1	Static	Deep beam	Crist (Ref. 89)
S-2	Static	Deep beam	Crist (Ref. 89)
S-3	Static	Beam column	Lane (Ref. 90)
S-4	Static	Beam column	Lane (Ref. 90)
S-5	Static	Beam column	Lane (Ref. 90)
D-1	Dynamic	Deep beam	Crist (Ref. 89)
D-2	Dynamic	Beam column	Lane (Ref. 90)
D-3	Dynamic	Circular arch	
D-4	Dynamic	Beam	Feldman, et al. (Ref. 91)

Table VII. Summary of Properties Used in Example Problems

Case No.	E_c, 10^6 psi (10^6N/m^2)	E_s, 10^6 psi (10^6N/m^2)	f'_c, 10^3 psi (10^3N/m^2)	f_s, 10^3 psi (10^3N/m^2)	ν_c	f_t conc, psi (10^3N/m^2)	Slope of Cracking Envelope,* η	Dowel Action Parameters† n	G_{steel}, 10^6 psi (10^6N/m^2)
S-1	3.00 (20685)	30.0 (206850)	4.16 (28683)	48.0 (330960)	0.2	365.0 (2517)	-0.083	4.0	12 (82740)
S-2	3.72 (25649)	30.0 (256490)	5.02 (34612)	50.0 (344750)	0.2	365.0 (2517)	-0.083	4.0	12 (82740)
S-3	3.00 (20685)	30.0 (206850)	4.05 (27925)	62.0 (427490)	0.2	320.0 (2206)	-0.080	4.0	12 (82740)
S-4	3.00 (20685)	30.0 (206850)	4.40 (30338)	62.0 (427490)	0.2	350.0 (2413)	-0.080	4.0	12 (82740)
S-5	3.00 (20685	30.0 (206850)	5.00 (34475)	62.0 (427490)	0.2	400.0 (2758)	-0.080	4.0	12 (82740)
D-1	3.00 (20685)	30.0 (206850)	4.16 (28683)	48.0 (330960)	0.2	365.0 (2517)	-0.083	4.0	12 (82740)
D-2	3.00 (20685)	30.0 (206850)	5.00 (34475)	62.0 (427490)	0.2	400.0 (2758)	-0.080	4.0	12 (82740)
D-3	7.00 (48265)	30.00 (482650)	7.00 (48265)	50.0 (344750)	0.2	500.0 (3447)	-0.083	4.0	12 (82740)
D-4	3.74 (25787)	30.0 (257870)	3.26 (22478)	45.8 (315791)	0.2	450.0 (3103)	-0.08	4.0	12 (82740)

* See equation 36(a).

† n is the empirical dowel shear constant of equation 63.

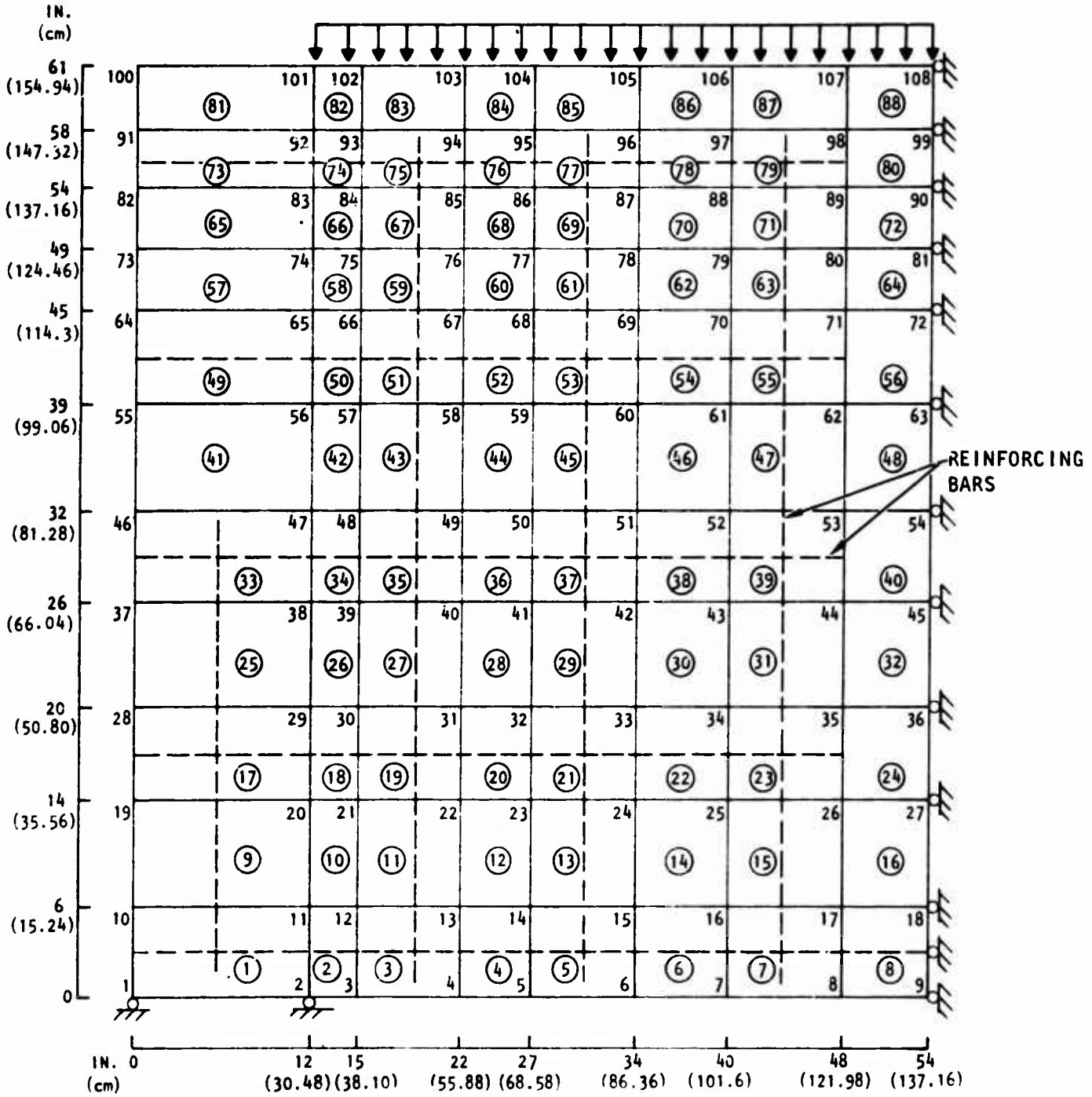

Figure 56. Finite Element Representation of Beams 2S1.6-1 and 2D1.6-1 for Cases S-1 and D-1 (Crist, Ref. 89)

through 8 was about 5 percent of the cross-sectional areas of the elements. Stirrups in other parts of the beam had areas ranging between 0.15 percent to 0.4 percent of the cross-sectional areas of elements in which they were located.

Several different methods of applying uniform pressure loading were investigated. These include:

a. Applying the full value of the experimentally measured collapse load in one step and then iterating until equilibrium is reached

b. Applying increments of load, reforming the global stiffness matrix and iterating for equilibrium at every step

c. Applying increments of load, reforming the global stiffness matrix at every step, and accepting some degree of disequilibrium at each step

The results presented below were obtained with procedure *b*.

The main results of the analysis are shown in figures 57 through 59. Figure 57 shows that the analysis overestimates both stiffness and strength of the beam, as indicated by the curve of external load versus midpoint deflection. The steel yields at 570 kips (2535×10^3 N) external load in the analysis and 470 kips (2091×10^3 N) in the experiment. Figure 58 compares measured and calculated distribution of steel strain and beam displacement at the onset of yielding and at the collapse load. As figure 57 shows, these are not the same loads for analysis and experiment. There is a general agreement between calculated and measured strains and displacements except for the measured displacement at L/4, which was not reported in reference 89. The present writers consider that it is more meaningful to compare strains at the onset of similar phenomena than at the same load levels in the event these are different. Figure 59 compares measured and calculated crack patterns at the collapse load. The model results appear to predict most of the cracked regions. However, the absence of cracks from some elements such as 19, 29, 30, 38, 55, and 63 is an indication that the analytical model is stiffer than the experimental model.

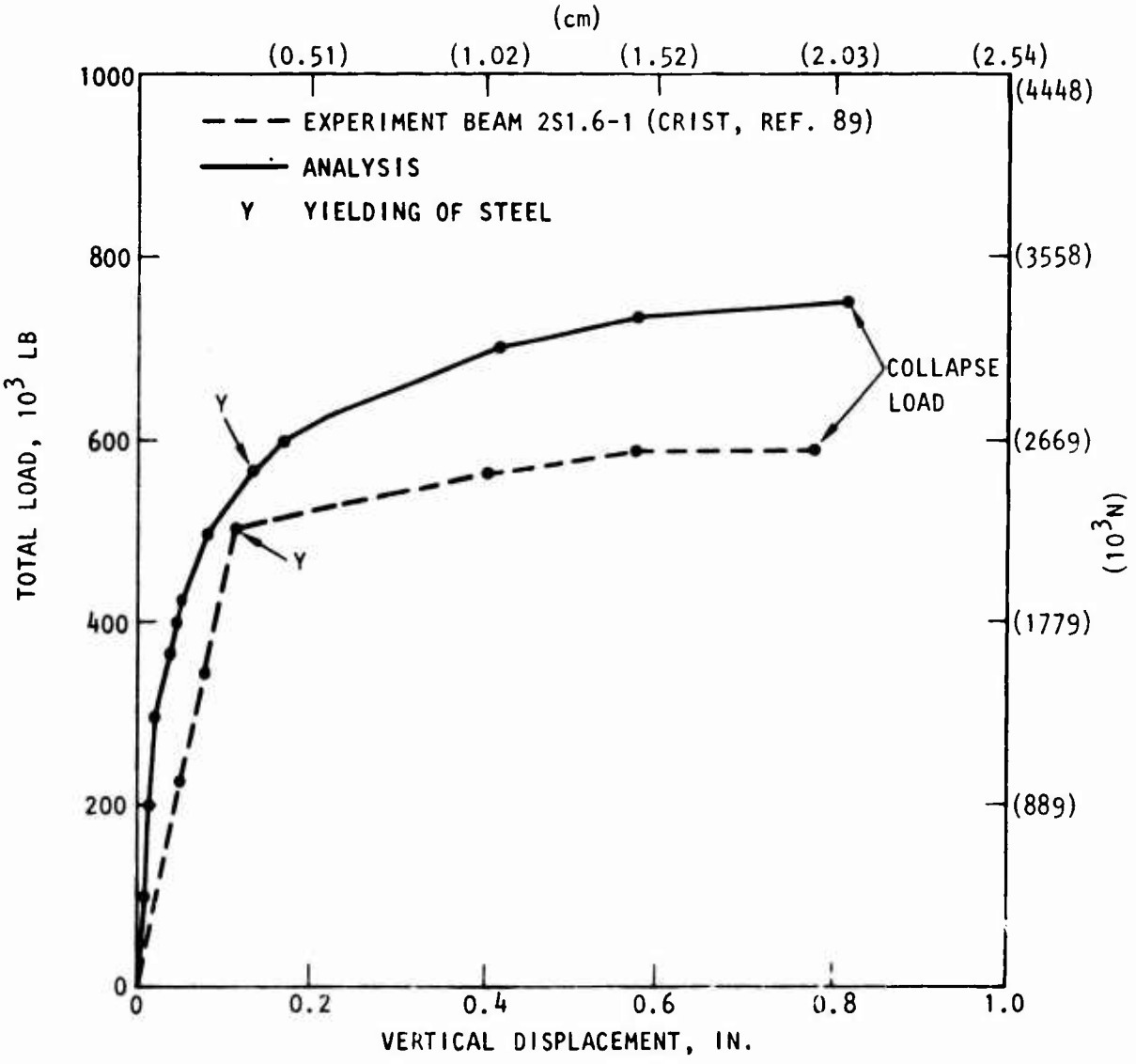

Figure 57. Comparison of Measured and Calculated Vertical Displacements at Middle of Beam 2S1.6-1, Case S-1 (Crist, Ref. 89)

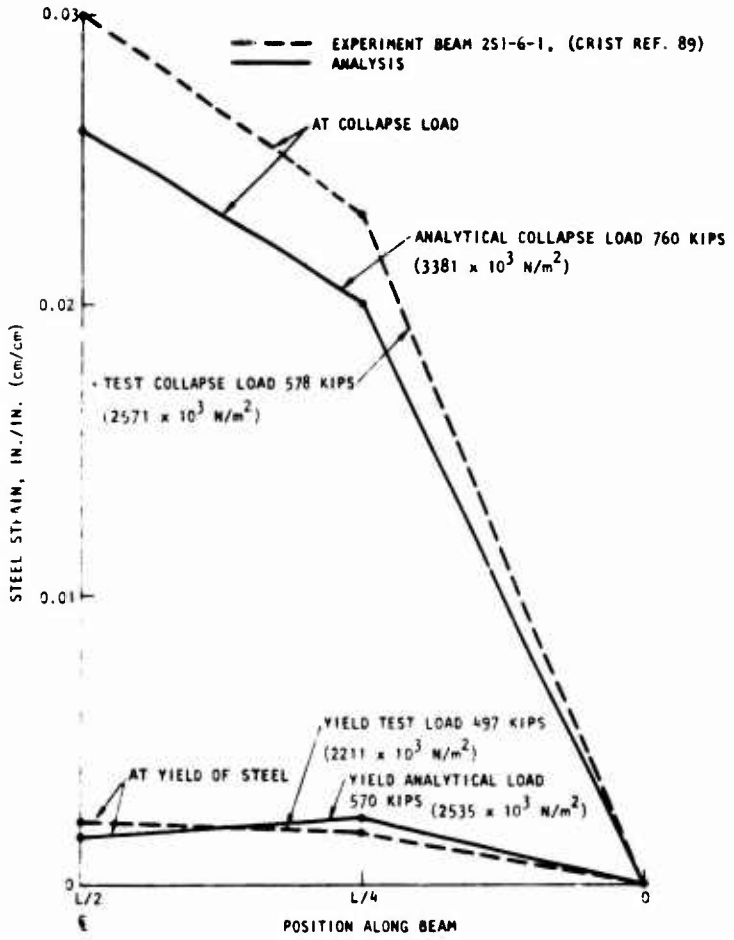

(a) Comparison of measured and calculated strains

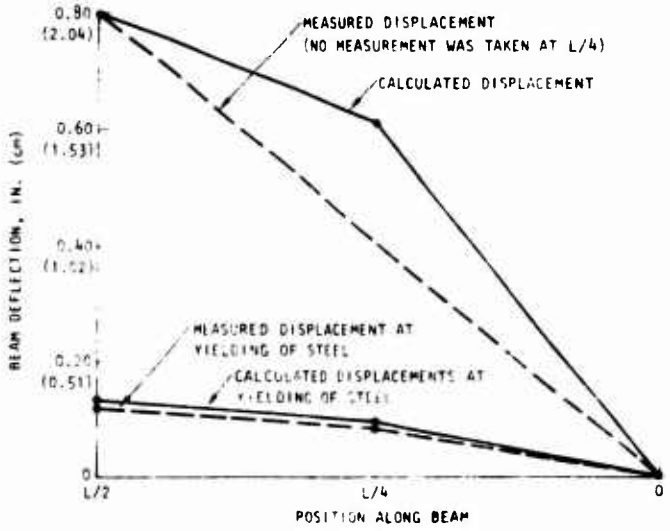

(b) Comparison of measured and calculated displacements

Figure 58. Displacements and Strains in Tension Steel, Beam 2S1.6-1, Case S-1 (Crist, Ref. 89)

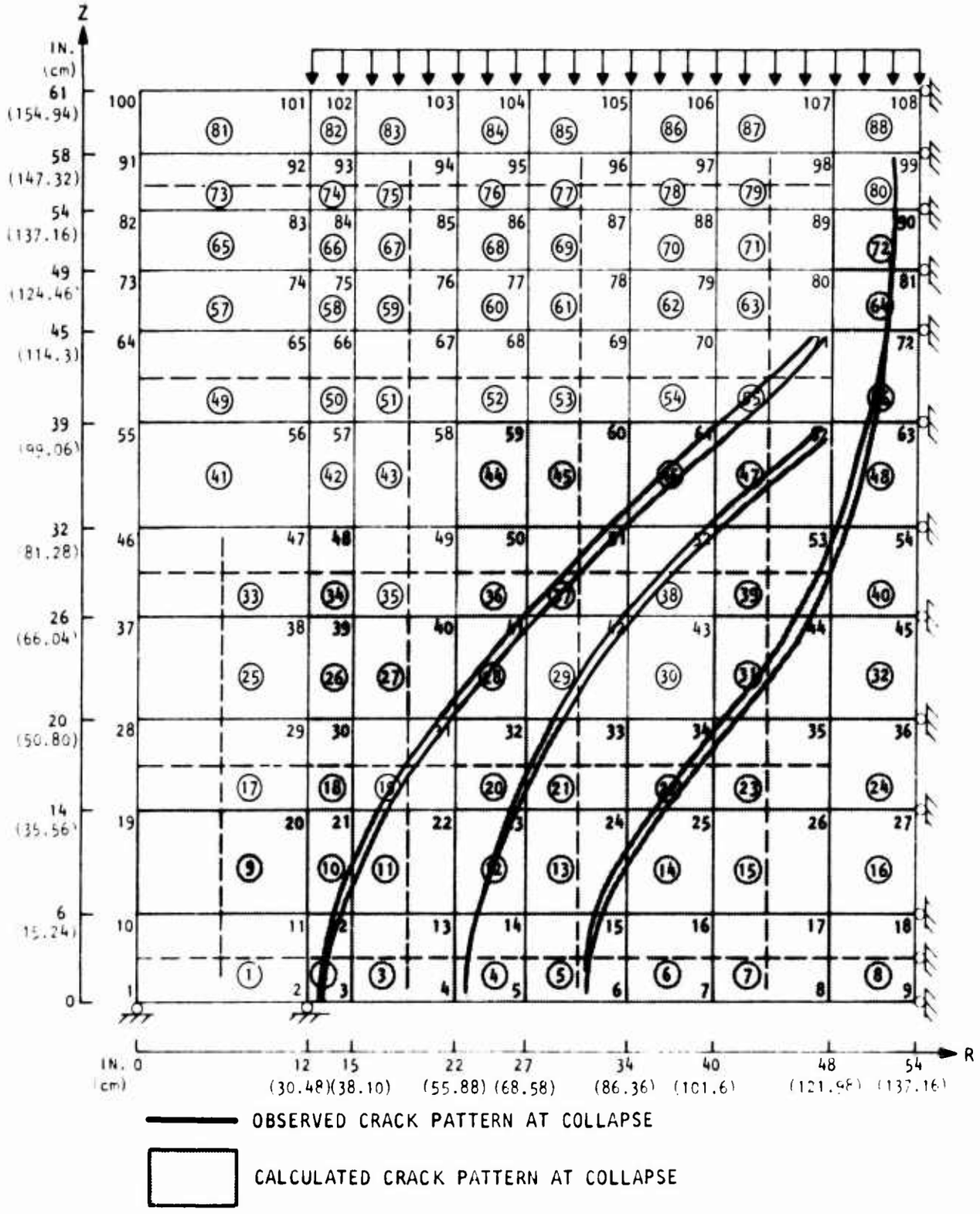

Figure 59. Comparison of Calculated and Observed Crack Patterns at Collapse of Beam 2S1.6-1, Case S-1 (Crist, Ref. 89)

3. CASE S-2 (DEEP BEAM 2S1.6-3 of CRIST, REF. 89)

The static analysis of deep beam 2S1.6-3 was performed using the finite element mesh shown in figure 60. The refinement of the finite elements and their arrangement with respect to the reinforcing is similar to the mesh for Case S-1, except that there are fewer elements in the compression zone in Case S-2. The tension steel is 5 percent of the cross-sectional area of the concrete. The steel percentage elsewhere is about 0.15 percent.

The main results of the analysis are shown in figures 61 through 63. Figure 61 shows that the analysis overestimates the stiffness and collapse load, as was the case for S-1. Reasonable agreement between measurements and calculations of steel strains at yielding of steel and collapse load is shown in figure 62(a). There is a general agreement between calculated and measured displacements as illustrated in figure 62(b). However, since the collapse load is taken as the load at which the solution begins to be unstable, both calculated strains and displacements should be considered as approproximate values. As in Case S-1, it is found that nodal point forces are in disequilibrium following yielding of the steel. This contributed to overestimating the collapse load in the analysis. The model appears to predict well the crack patterns in the bottom and center of the beam. However, the absence of cracks from elements such as 27, 35, 36, 43, 44, 45, 51, 52, 53, 59, 60, 61, 62, and 71 indicates that the analytical model is stiffer than the experimental model.

4. STATIC CASES S-3, S-4, S-5 (BEAM COLUMNS 5-3-1, 5-2-1, 5-0-1 OF LANE, REF. 90)

An analysis was performed of beam columns subjected to different ratios of transverse to axial load. The geometry, properties, and loading correspond to those used in physical experiments performed by Lane (Ref. 90). The geometry and arrangement of reinforcing is the same in each case. Three values of the ratio of axial load (P) to lateral load (F) were treated: 3.18, 1.9, and 0 (transverse load only). The finite element representation of the beam column is shown in figure 64. A plane of symmetry was assumed at midspan in order to conserve computer time.

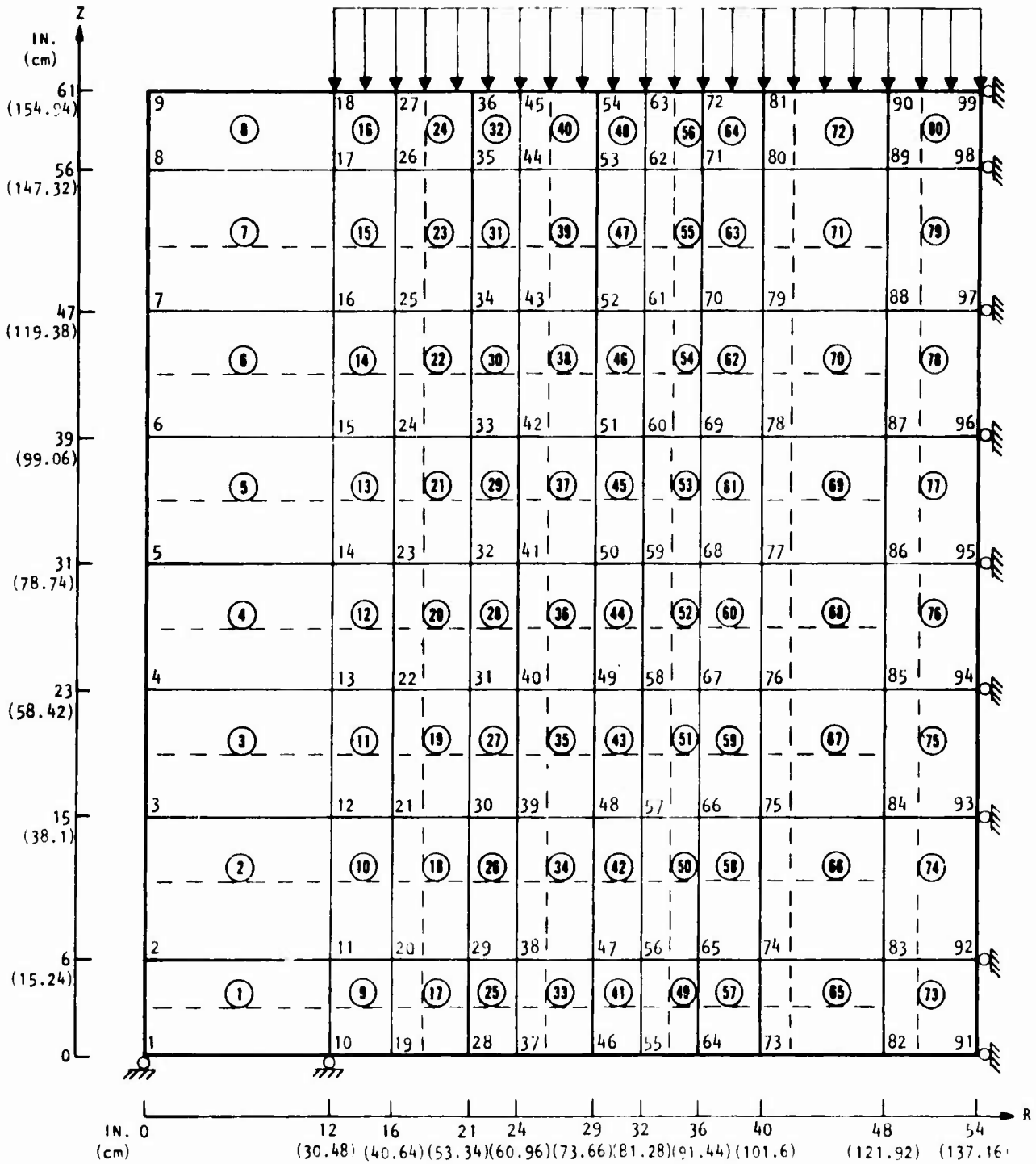

Figure 60. Finite Element Representation of Beam 2S1.6-3, Case S-2 (Crist, Ref. 89)

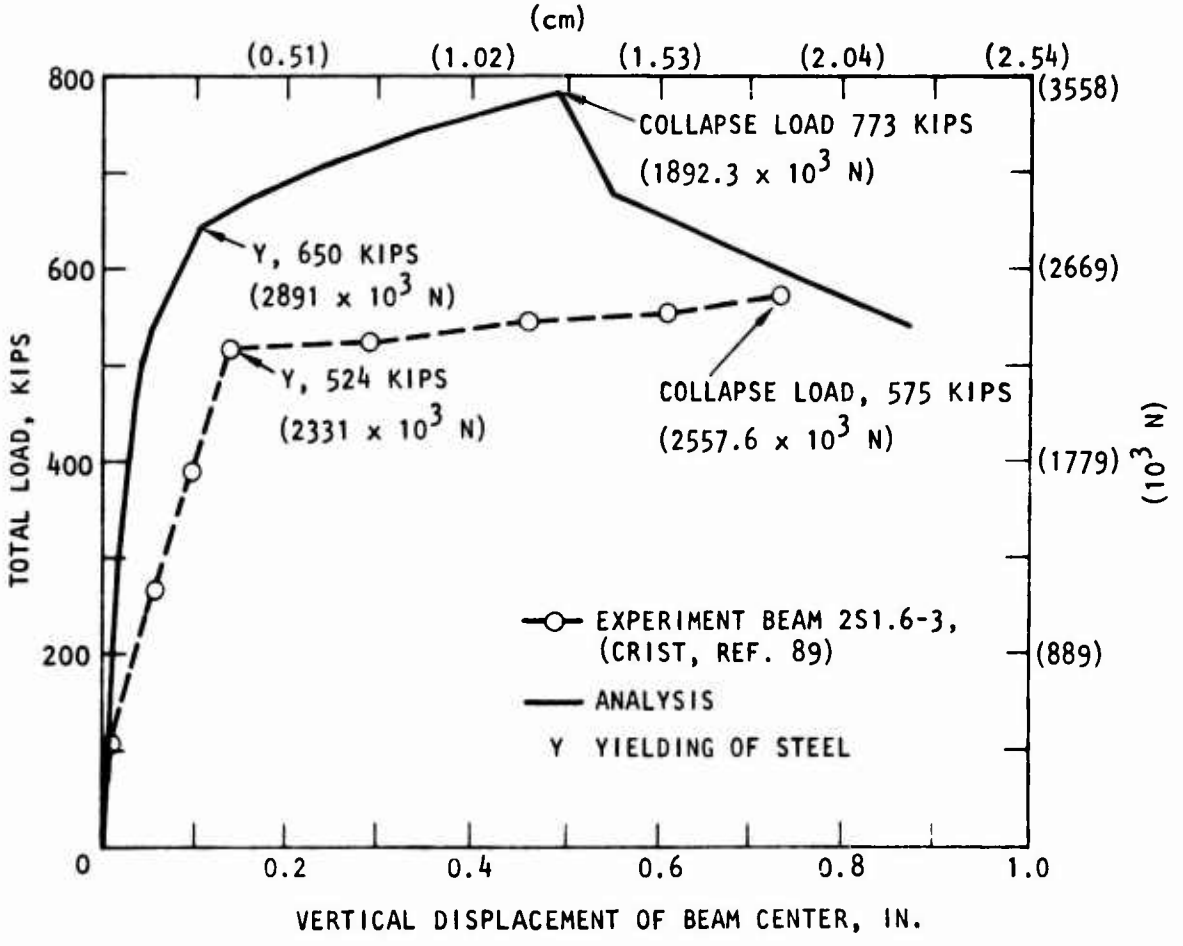

Figure 61. Comparison of Measured and Calculated Vertical Displacements at Middle of Beam 2S1.6-3, Case S-2 (Crist, Ref. 89)

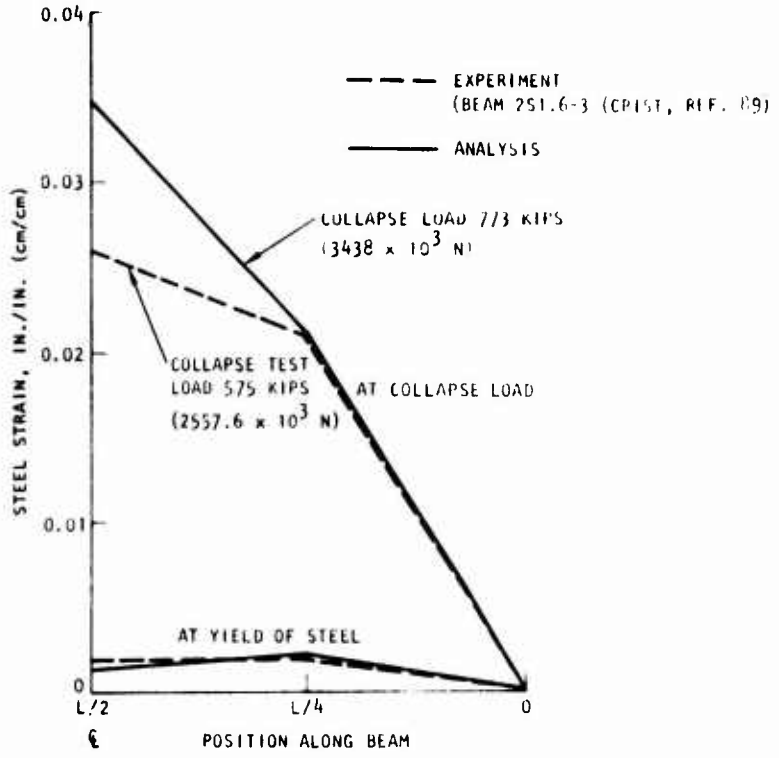

(a) Comparison of measured and calculated strains

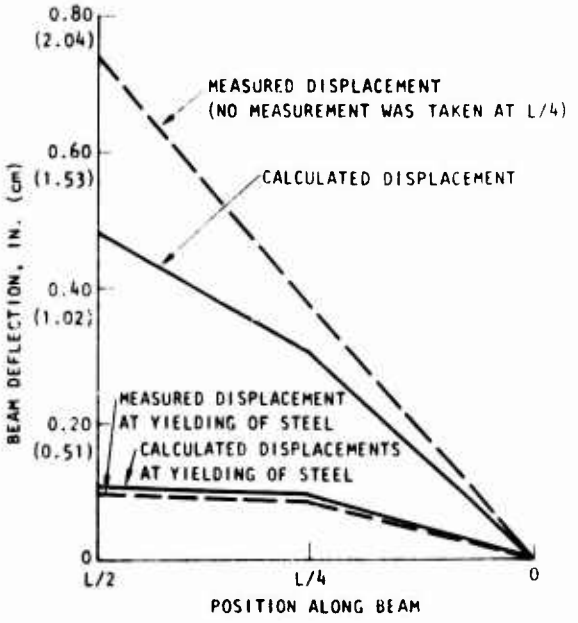

(b) Comparison of measured and calculated displacements

Figure 62. Displacements and Strains in Tension Steel, Beam 2S1.6-3, Case S-2 (Crist, Ref. 89)

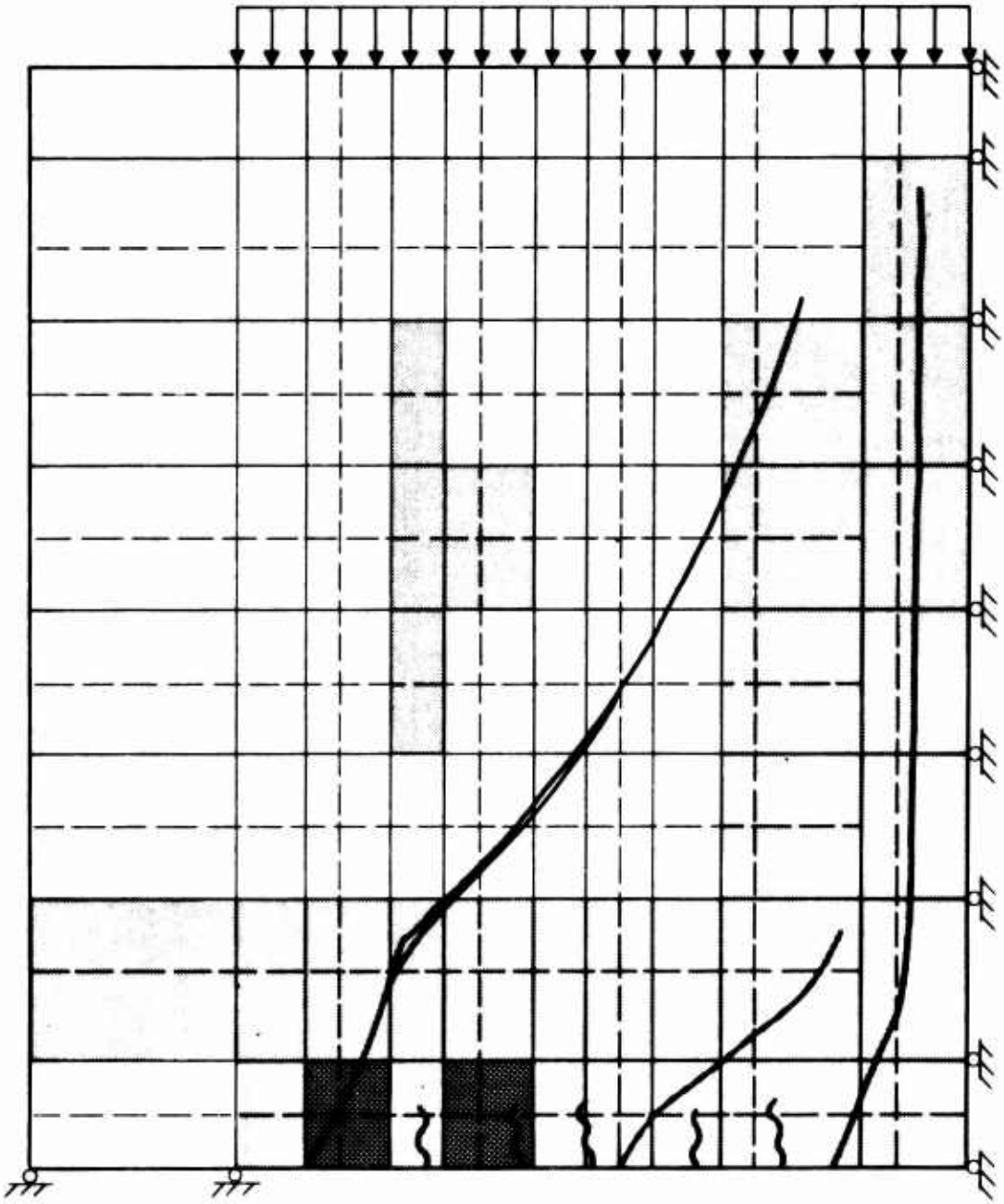

Figure 63. Comparison of Calculated and Observed Crack Patterns at Collapse of Beam 2S1.6-3, Case S-2 (Crist, Ref. 89)

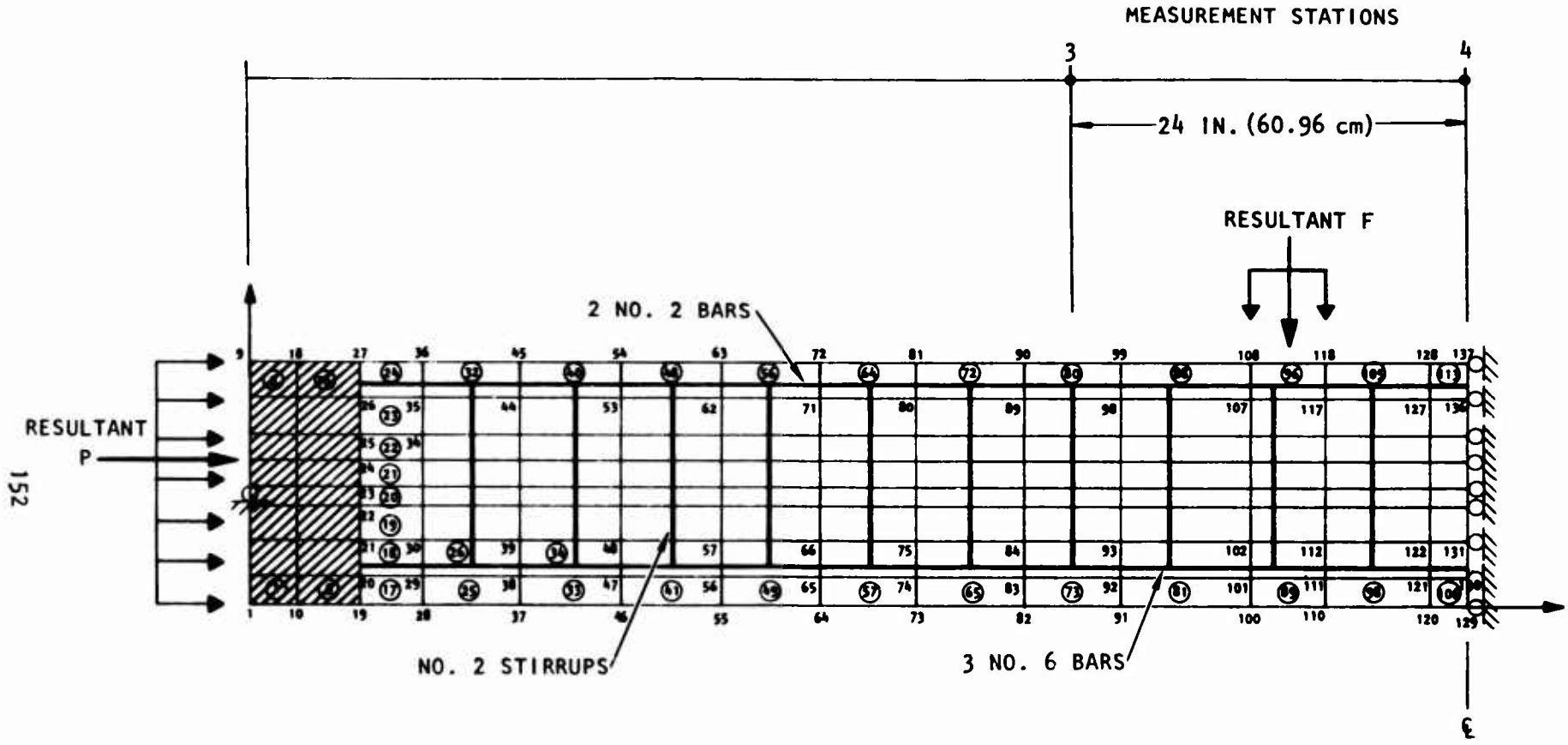

Figure 64. Finite Element Mesh used in Static Analysis of Beam Column of Cases S-3, S-4, S-5 (Lane, Ref. 90) and Dynamic Analysis Case D-2.

As in the case of other static analyses, the collapse load must be approached slowly, with iteration at each load step to assure that nodal point equilibrium is reached at each step. The onset of collapse is detected by observing that displacements increase while external load is held fixed. This signifies that nodal point equilibrium cannot be satisfied, and that collapse eventually will occur if enough iterations are performed. This procedure leads to an upper bound on collapse load. In the following analyses, an attempt was made to find the collapse load through the procedure of incrementing external load in small steps and iterating at each step.

Results of the three beam-column analyses are compared in figures 65 through 70 with experimental measurements. The general indication of the results is that the analytical model overestimates the collapse load of the beam. Figures 65, 67, and 69 indicate that before yielding, the analytical model is stiffer than the experiment. However, after yielding, the analytical model results in displacements that are higher than the measured values. The same trend was observed in the comparison of strains at the bottom of beam 5-3-1 of case S-3 where the calculated strains in Element 107 were compared to the measured steel strain as illustrated in figure 66(a). Since the strains in the element after propagation of cracks are essentially those of the steel embedded in the element, the comparison between element strain and steel strain is justified in this case.

The average strain calculated in Element 80 at top of beam 5-3-1 (Station 3) was compared to strains measured in both concrete and steel (Fig. 66(b)). The results reveal good correlation except in the postyielding regime, where the calculated strains appear to exceed the measured values.

The strain in steel at the bottom of the middle of beam 5-2-1 of case S-4 was compared to the strain in Element 107 at the same location of the beam as illustrated in figure 68(a). The comparison reveals a trend similar to that observed for case S-3 where the analytical model appeared to be stiffer than the experimental beam at the early stages of the loading.

The strain calculated at the top of beam 5-2-1 was compared to the strain measured in both steel and concrete at this location as illustrated in figure 68(b). The comparison reveals that the calculated element strain exceeds

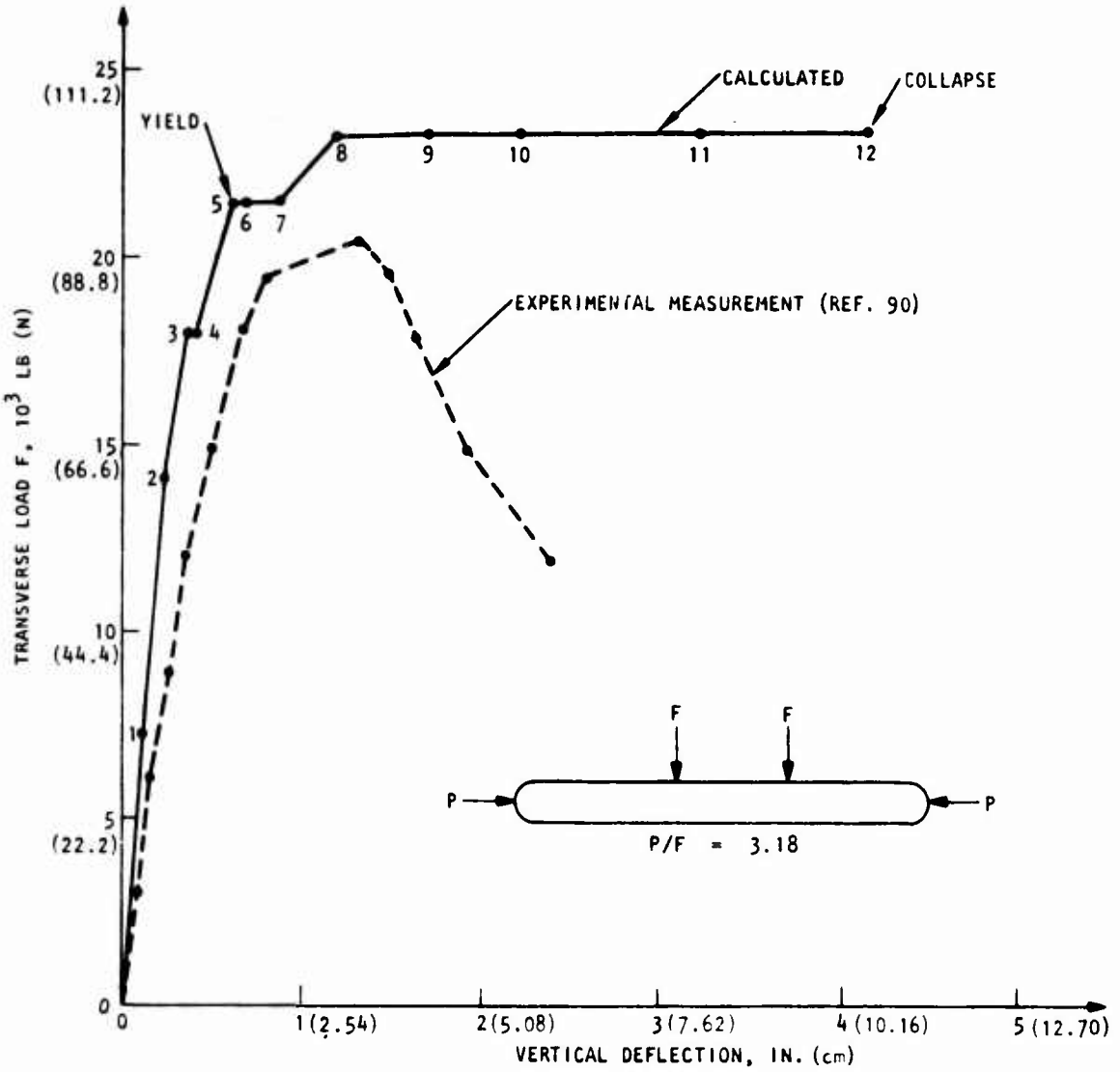

Figure 65. Measured and Calculated Vertical Load/Deflection Relationship at Middle of Beam Column 5-3-1, Case S-3 (Lane, Ref. 90)

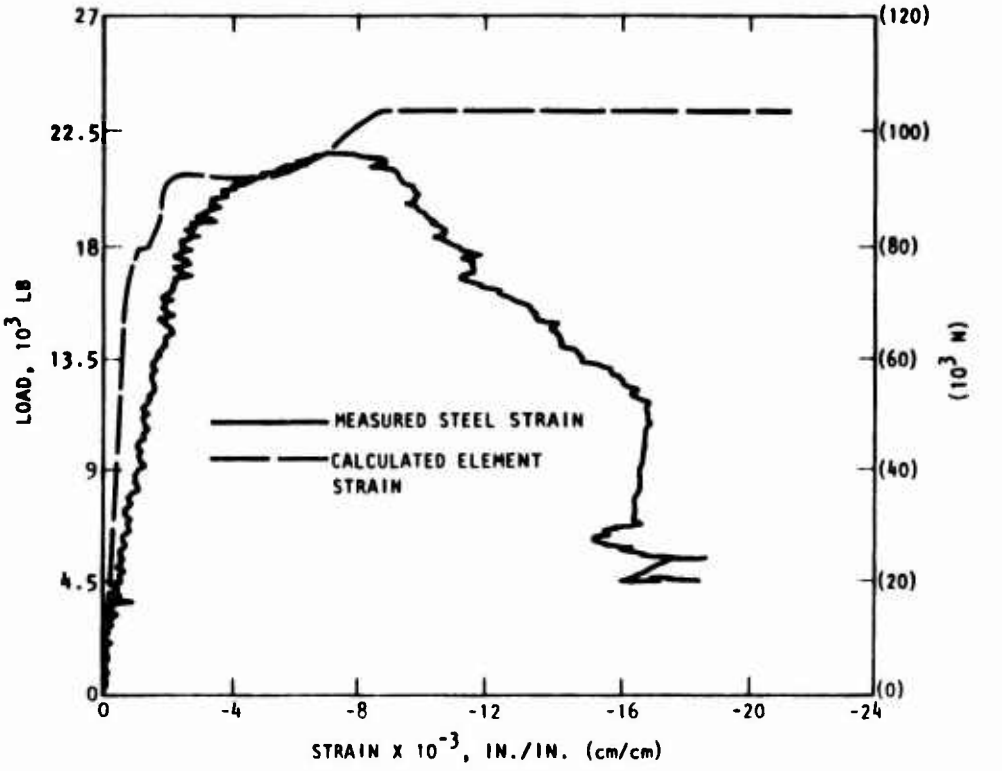

(a) Strains calculated for Element 107 and strains measured in steel at bottom of the middle (Station 4) of the beam

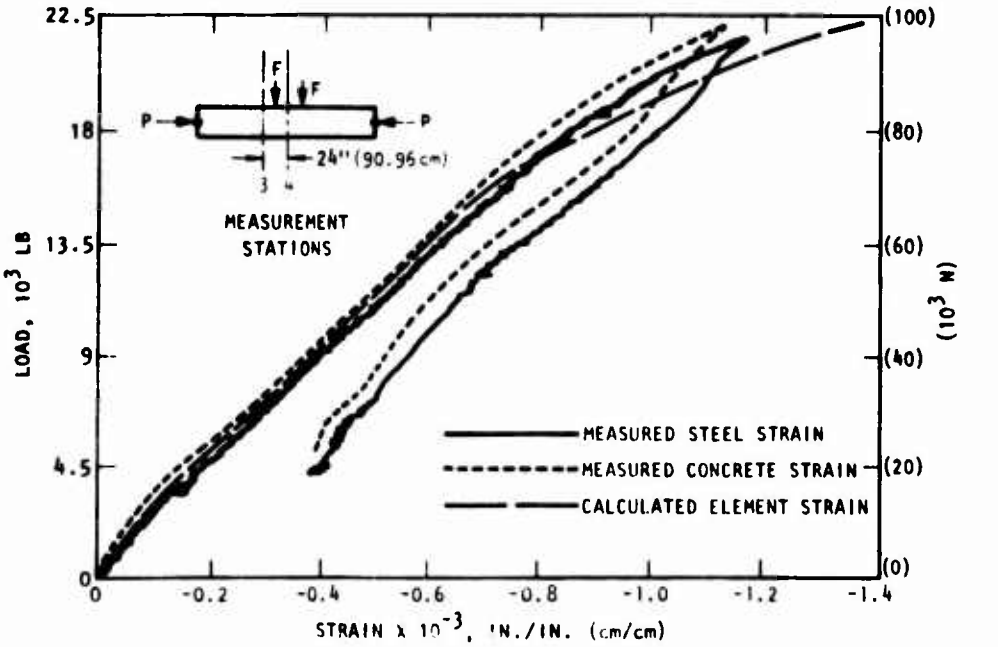

(b) Strains calculated for Element 80 at top of beam (Station 3) and strains measured in both steel and concrete

Figure 66. Comparison of Measured and Calculated Strains, Beam 5-3-1, Case S-3 (Lane, Ref. 90)

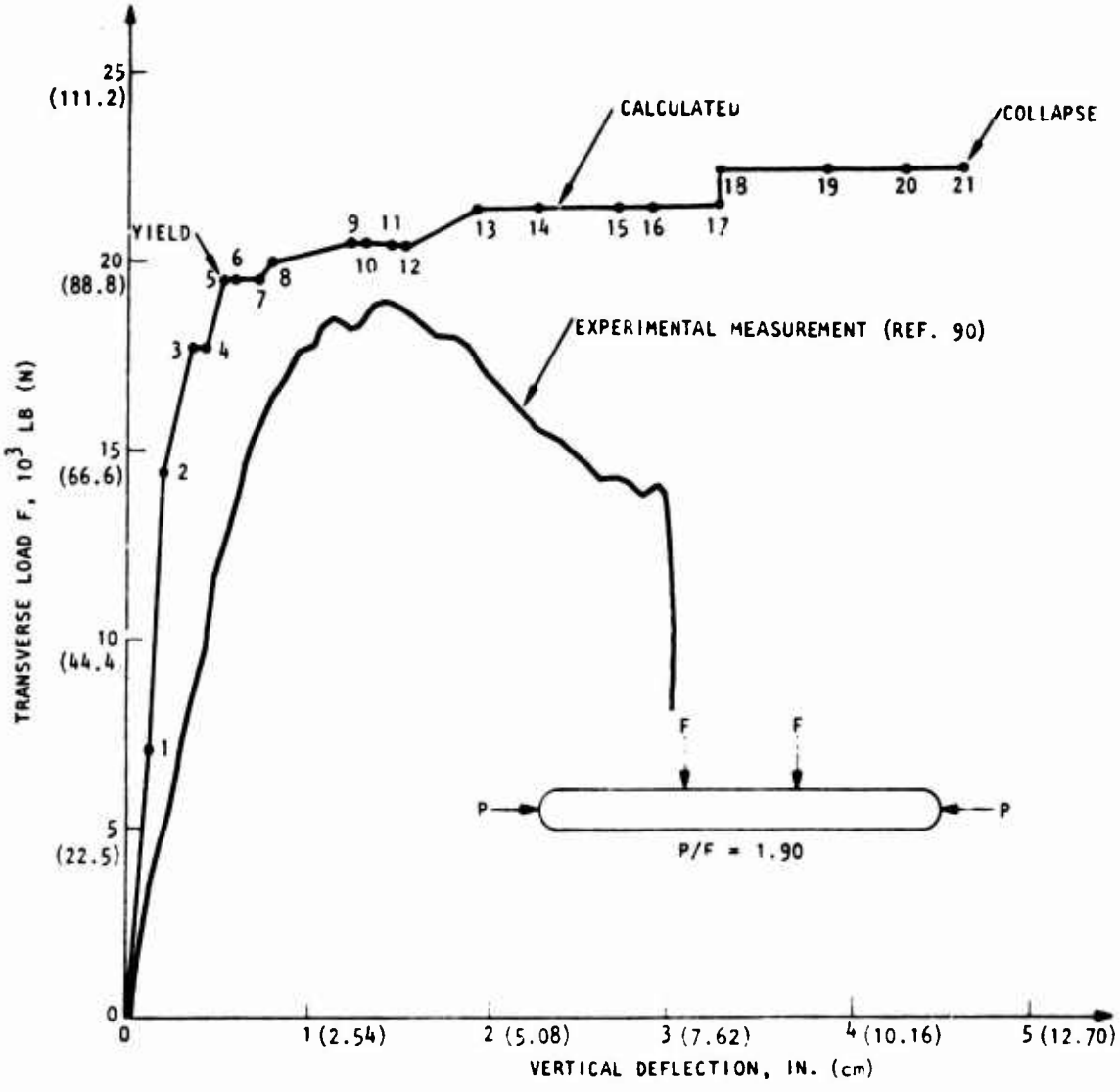

Figure 67. Measured and Calculated Vertical Load/Deflection Relationship for Beam Column 5-2-1, Case S-4 (Lane, Ref. 90)

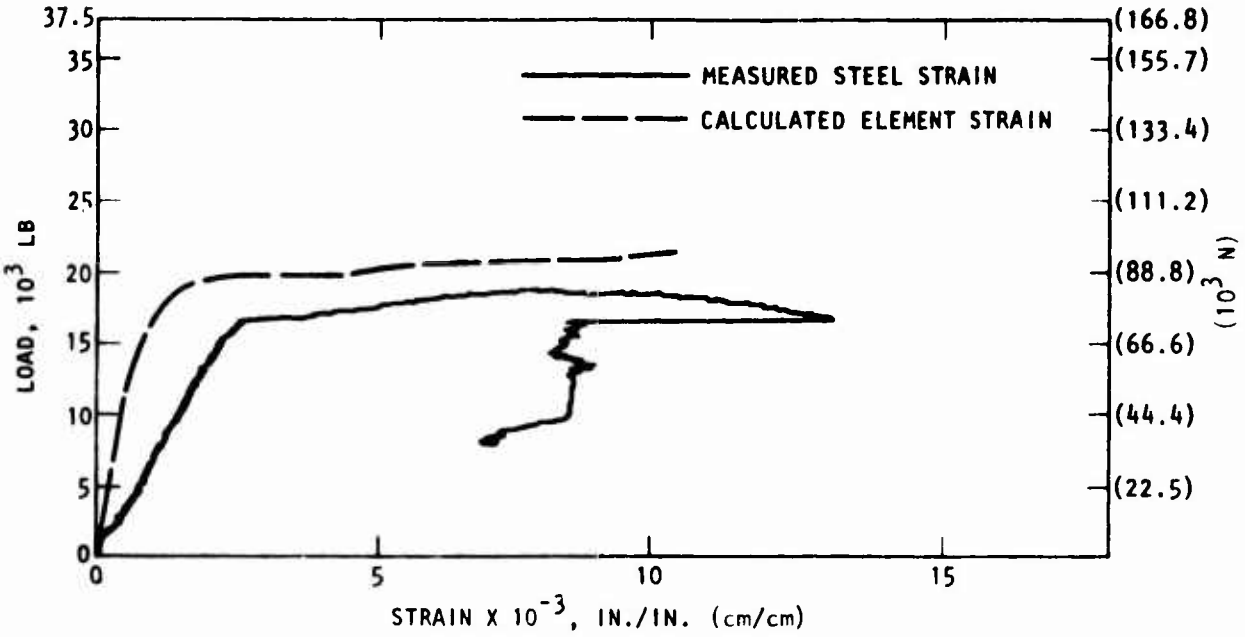

(a) Strains calculated for Element 107 and strains measured in steel at bottom of middle of the beam (Station 4)

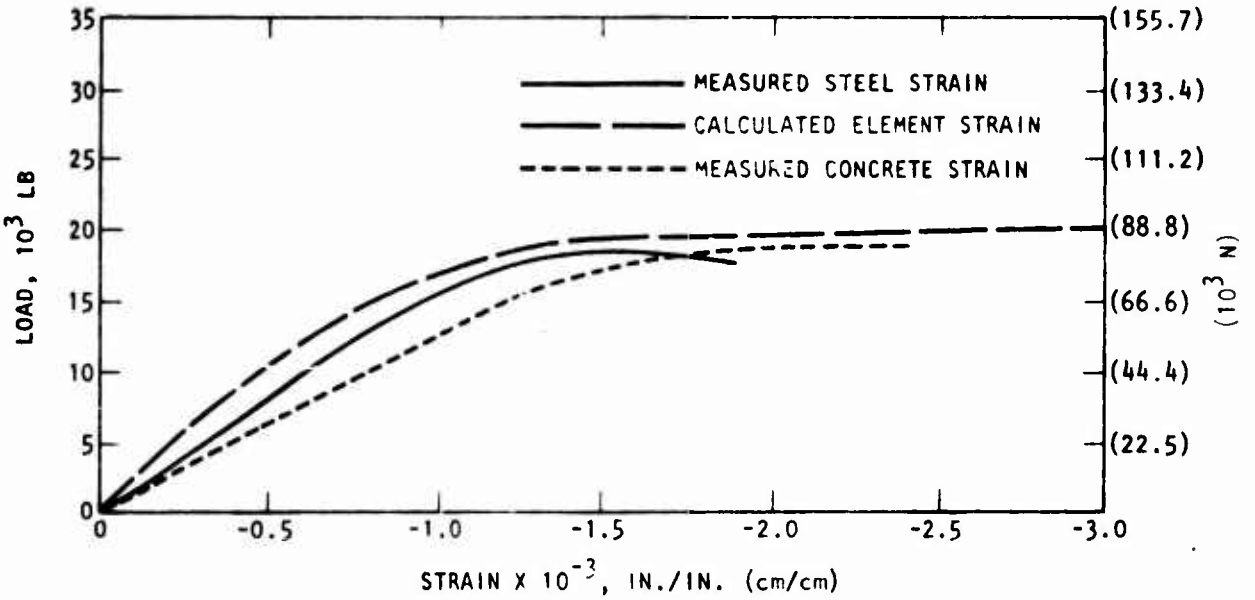

(b) Strains calculated in Element 113 at top of middle of the beam (Station 4)

Figure 68. Comparison of Measured and Calculated Strains, Beam 5-2-1, Case S-4 (Lane, Ref. 39)

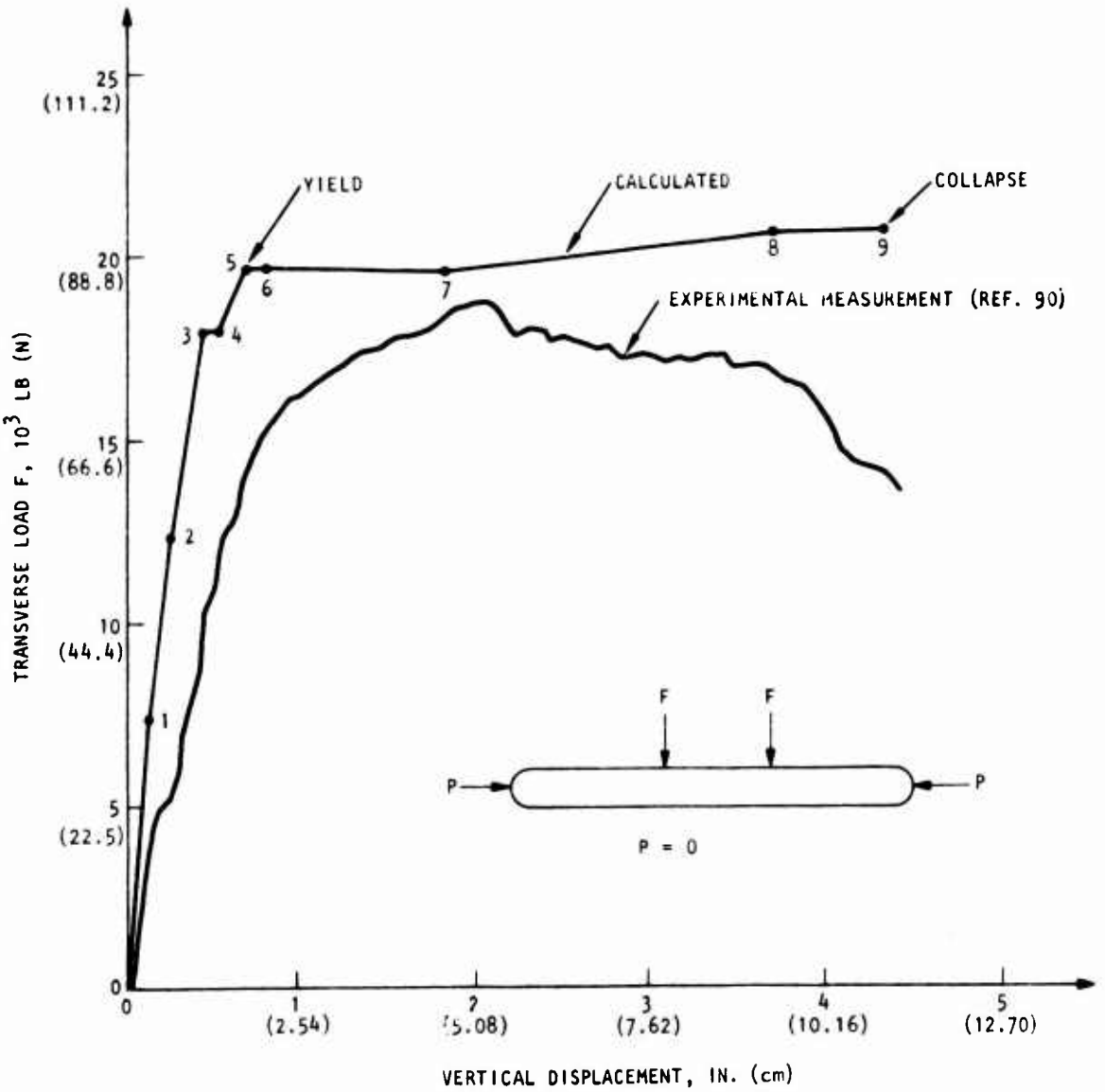

Figure 69. Measured and Calculated Vertical Load/Deflection Relationship at Middle of Beam Column 5-0-1, Case S-5 (Lane, Ref. 90).

the steel strain indicating that the analytical model overestimates the stiffness. The same trend was revealed in figures 70(a) and 70(b) for beam 5-0-1 of case S-5.

In each of the above discussed cases, the analysis slightly overestimated the collapse load. This appears to be partially due to applying too large a load increment.

5. CASE D-1 (DYNAMIC ANALYSIS OF BEAM 2D1.6-1 OF CRIST, REF. 89)

The dynamic analysis of beam 2D1.6-1 is performed using the finite element mesh shown in figure 56. Dynamic loading pulse L1, shown in figure 71, is applied to this model. There are two main differences between the dynamic analysis and the physical experiment. In the analysis the pressure load is assumed to be stationary, whereas in the physical experiment it is a traveling wave applied by a shock tube. This detail is omitted from the analysis for economy. The second difference is that the analytic model is assumed to rest on fixed supports, whereas the physical beam rests on flexible supports. This detail is omitted because it is irrelevant to the properties of the model being investigated but would affect comparisons.

The measured deflection/time history of the midpoint of the beam (Ref. 89) is compared with the computation in figure 72. The mathematical model underestimates the displacement of the physical beam, and has a fundamental period which is slightly longer. The time to the maximum measured centerline deflection of 0.32 in. (0.81 cm) was 8.5 msec. The maximum calculated centerline deflection of 0.19 in. (0.48 cm) occurred at 12 msec.

The above results are in general agreement with the previous static results which indicate that the analytical model is stiffer than the experimental model. However, since the test apparatus used (Ref. 89) allows the supports to move, which complicates the response of the test beam, the test results should be interpreted in the gross sense. The model beam undergoes a great deal of localized yielding, as is illustrated in figure 73, when measured and computed steel strains are plotted as a function of length along the beam. The comparison is made at two different times to allow for the possibility that the model and physical beams do not reach their maximum

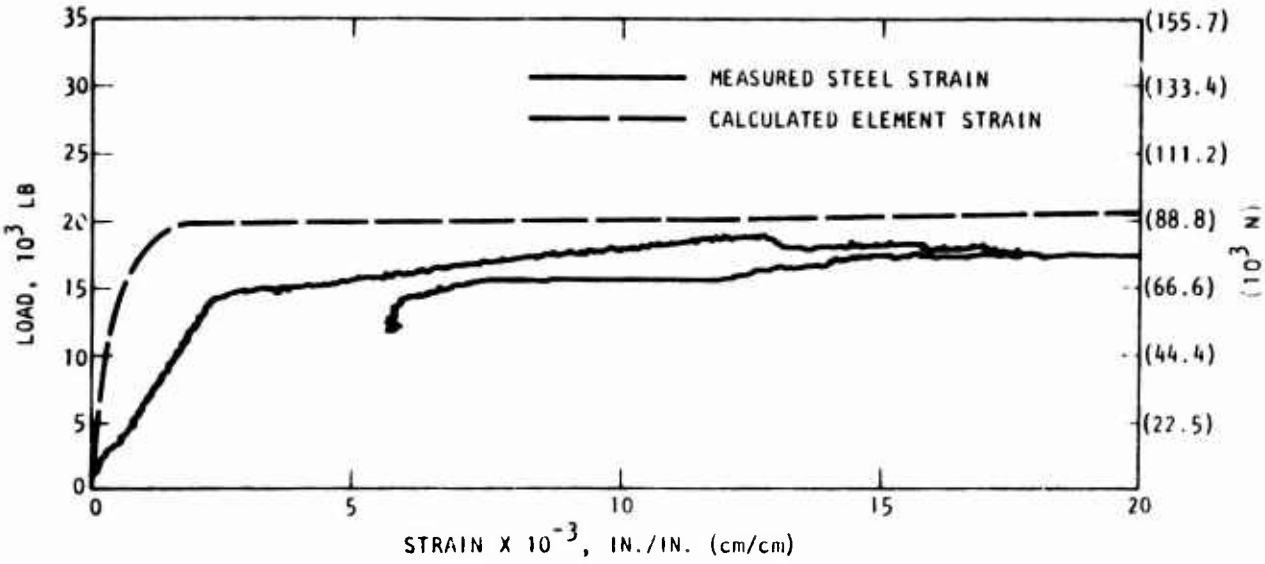

(a) Strains calculated for Element 107 and strains measured in steel at bottom of the middle of the beam (Station 4)

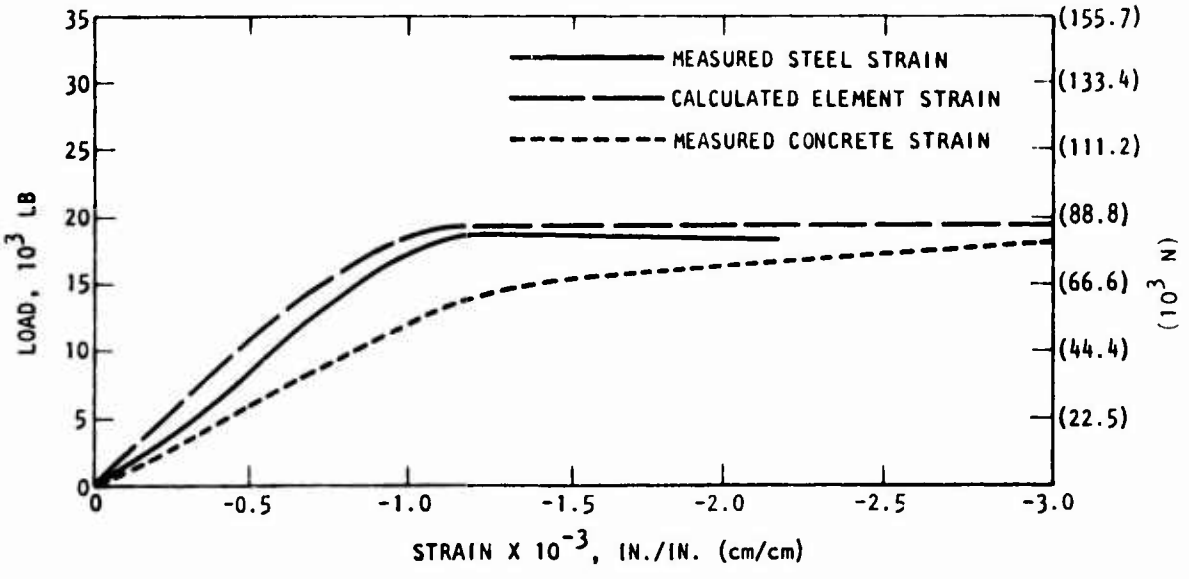

(b) Strains calculated in Element 113 at top of middle of the beam (Station 4)

Figure 70. Comparison of Measured and Calculated Strains, Beam 5-0-1, Case S-5 (Lane, Ref. 90)

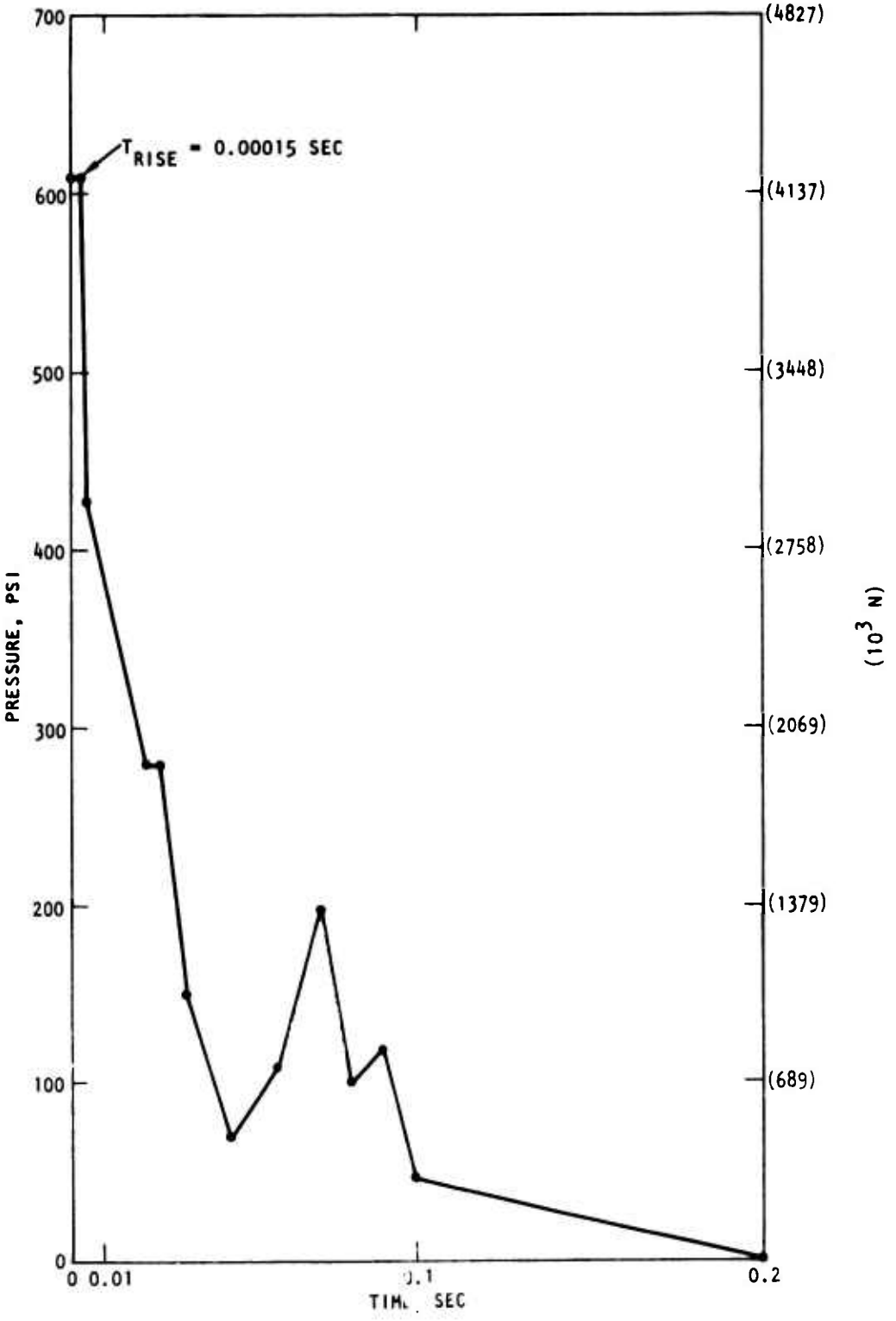

Figure 71. Pressure Loading for Beam 2D1.6-1, Case D-1, Loading L1 (Crist, Ref. 89)

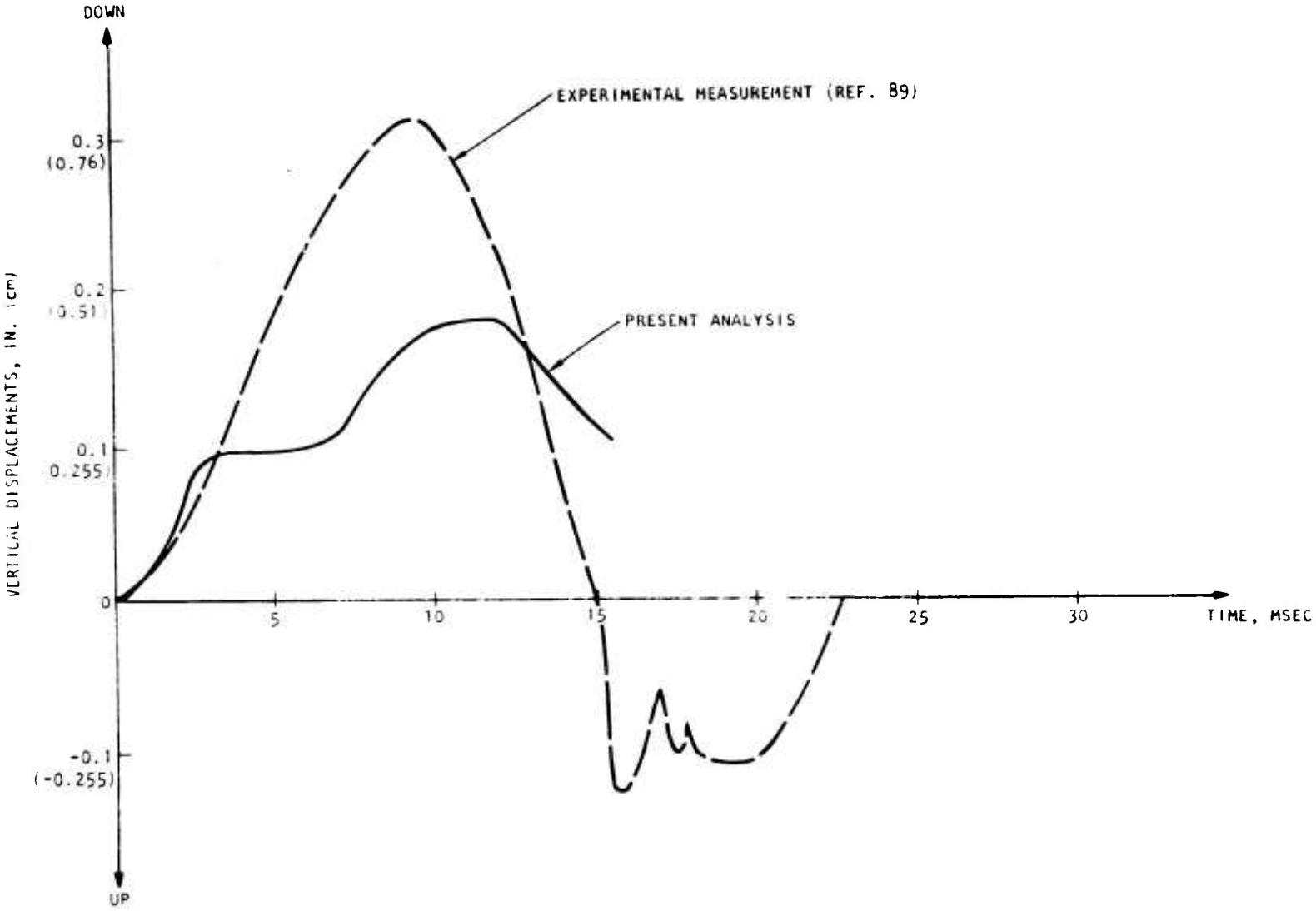

Figure 72. Comparison of Measured and Calculated Vertical Displacements at Middle of Beam 2D1.6-1, Case D-1

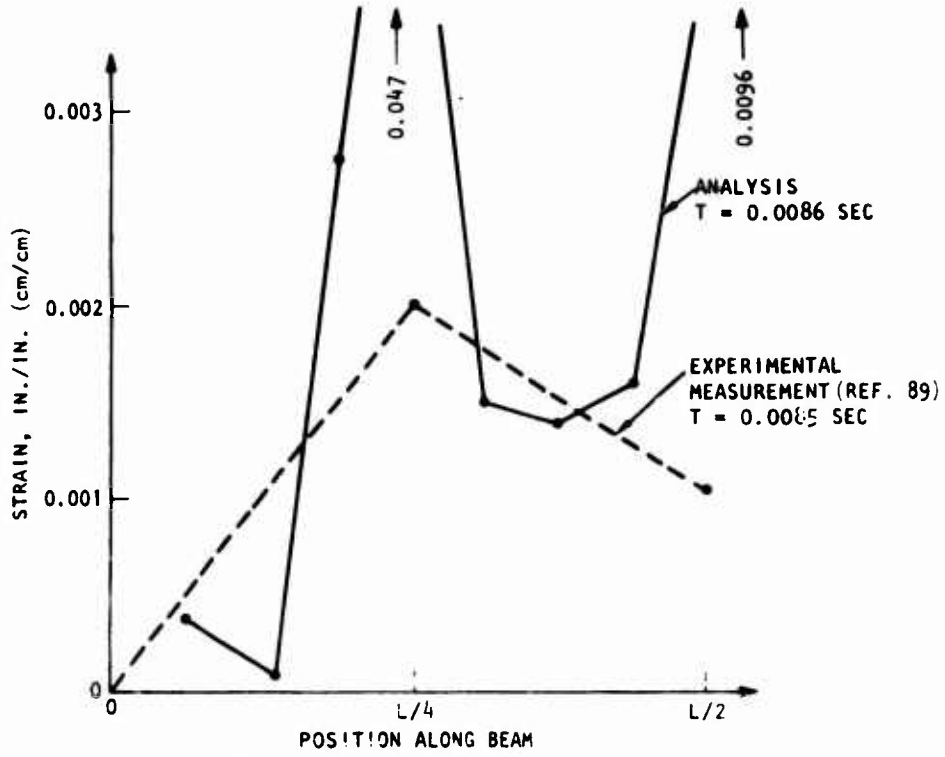

(a) T = 0.0085 sec for both physical and model beam

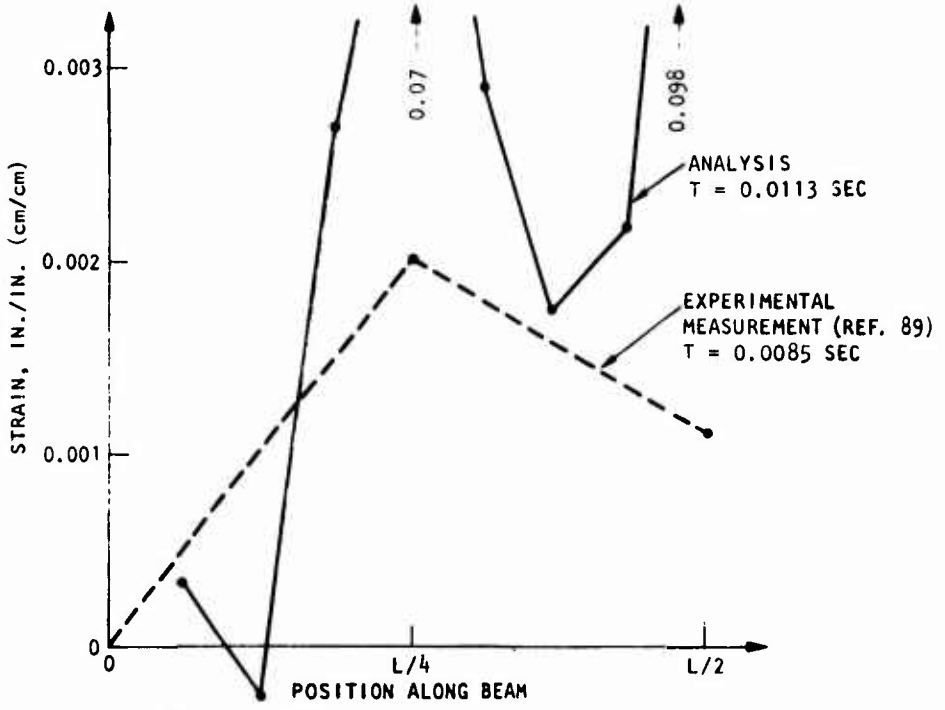

(b) T = 0.0085 sec for physical beam and
T = 0.01131 sec for model beam

Figure 73. Comparison of Strains in Tension Steel in Analysis and Physical Experiment, Beam 2D1.6-1, Case D-1

responses at the same time. The comparison is favorable except that the analysis greatly exaggerates the strain concentration at several points. Figure 73(a) indicates that the strains calculated at 0.0086 sec correlate well with the measured strains in the middle of the range between L/4 and L/2 of the beam length. For the range of length between 0 and L/4, the calculated strains appear to fluctuate above and below the measured strains for approximately one-third of the length of the beam. After that point the calculated strains exceed the measured strains by a very large margin. The discrepancy between calculated and measured strains for the first one-third of the length of the beam may be due to the difference in end-support conditions. While the analytical model assumes rigid end supports, the experimental model rests on flexible supports.

The comparison of calculated strains at a later time of 0.0113 sec, with measured strains for t = 0.0085 sec, illustrated in figure 73(b), indicate a trend similar to that observed in figure 73(a). The strains obtained from the analysis are the average strains of the cracked and uncracked regions of the element. Since the strains in the cracked regions increase drastically with the increase in response, the average value of strain is expected to jump to a very high value also. Crist (Ref. 89) indicated that the experimental data were not complete because of gage damage, and there appeared to be radical deviation of steel strain in some cases. However, Crist indicated that this can be attributed to the proximity of the strain gages to the cracks. Therefore, conclusions should not be based on comparison of results at middle points or quarter points of the beam where both analytical and experimental mental results appear to be least reliable.

Comparison is made in figure 74 of measured and observed crack patterns. Although the calculations stop at about T = 0.017 sec, the computed cracks do not extend after about T = 0.012 sec. Hence, comparison with the final observed crack pattern is valid. The absence of cracks from elements 28, 29, 38, 45, 46, 47, 53, 54, 63, 70, and 71 indicates that the analytical model is stiffer than the experimental model. The overcracking in the compression zone that is observed in figure 74 requires additional investigation and has been discussed at the end of this section.

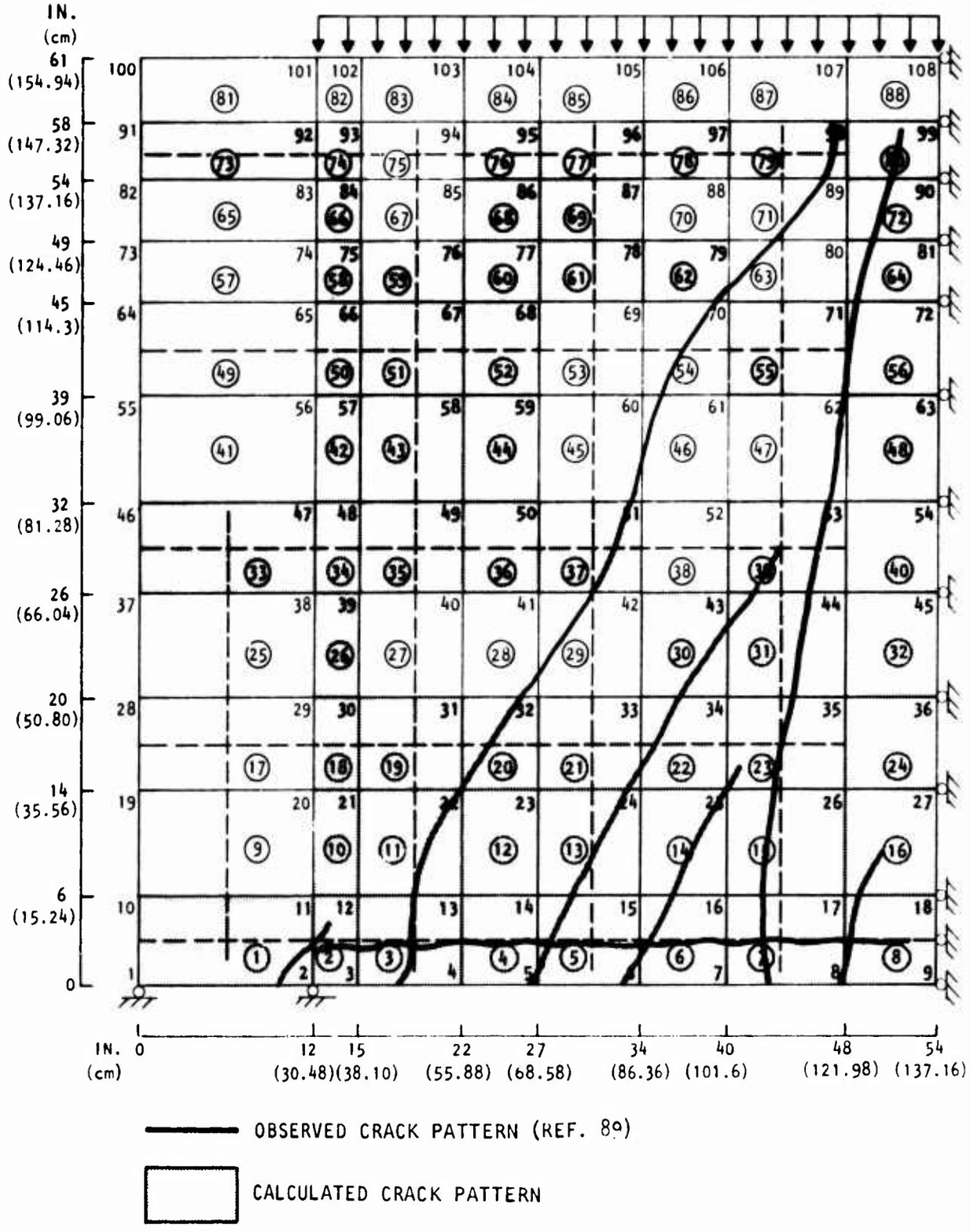

Figure 74. Comparison of Calculated and Observed Crack Patterns for Beam 2D1.6-1, Case D-1

6. CASE D-2 (DYNAMIC ANALYSIS OF BEAM COLUMN 5-3-1 OF LANE, REF. 90)

The dynamic analysis of a beam column was performed using the finite element mesh shown in figure 64. Dynamic loading, shown in figure 75, was applied simultaneously as axial and transverse forces. There is no physical experiment corresponding to this analysis.

The results of the analysis are presented in terms of velocity/ and displacement/time histories and in terms of stresses in the compression zone and along the tension steel. Figures 76 and 77 show the midspan displacement and velocity up to the time of collapse and numerical instability at $t = 0.025$ sec. Figure 78 shows the extreme fiber stress in the compression zone at midspan (Element 113). In the present case, onset of instability is signaled by a reduction in the compressive stress in Element 113, even though vertical load and rotation are increasing. Figure 79 shows the extreme fiber stress in the tension zone at midspan (Element 106). Cracking occurs at $t = 0.007$ sec. There is no longitudinal steel in this element, and hence the longitudinal stress drops abruptly to zero. Figure 80 shows longitudinal stress, normalized to stress at the yield point of steel in several elements containing tension steel. Near the center of the span, represented by Elements 90 and 107, the stress rises to the yield point. In other locations, represented by Element 58, the stress rises to a maximum value which is considerably less than the yield point and then fluctuates as a hinge forms in the center span of beam and redistribution takes place.

7. CASE D-3 (DYNAMIC ANALYSIS OF A REINFORCED CONCRETE RING)

The dynamic analysis of a reinforced concrete ring subjected to a traveling pressure pulse was performed using the finite element mesh shown in figure 81. The analysis simulates the behavior of an underground reinforced concrete silo when subjected to a pressure pulse traveling in the surrounding soil or rock.

Only half of the ring is modeled because of symmetry. The concrete is reinforced only in the circumferential direction, with 1 percent steel in the inner layer of elements and 0.37 percent in the outer layer of elements.

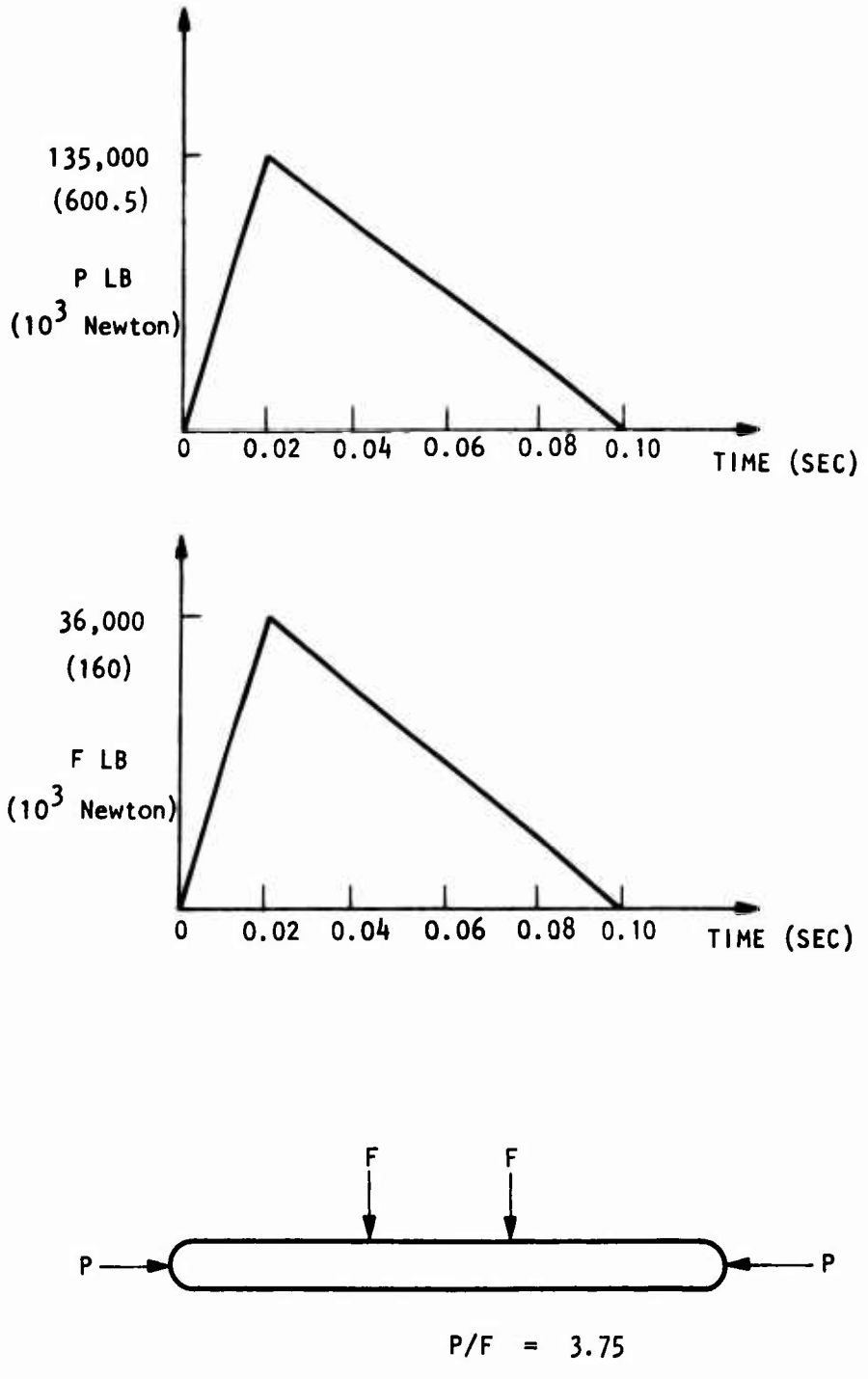

Figure 75. Axial and Transverse Loading for Beam Column 5-3-1, Case D-2, Having P/F = 3.75 (Lane, Ref. 90)

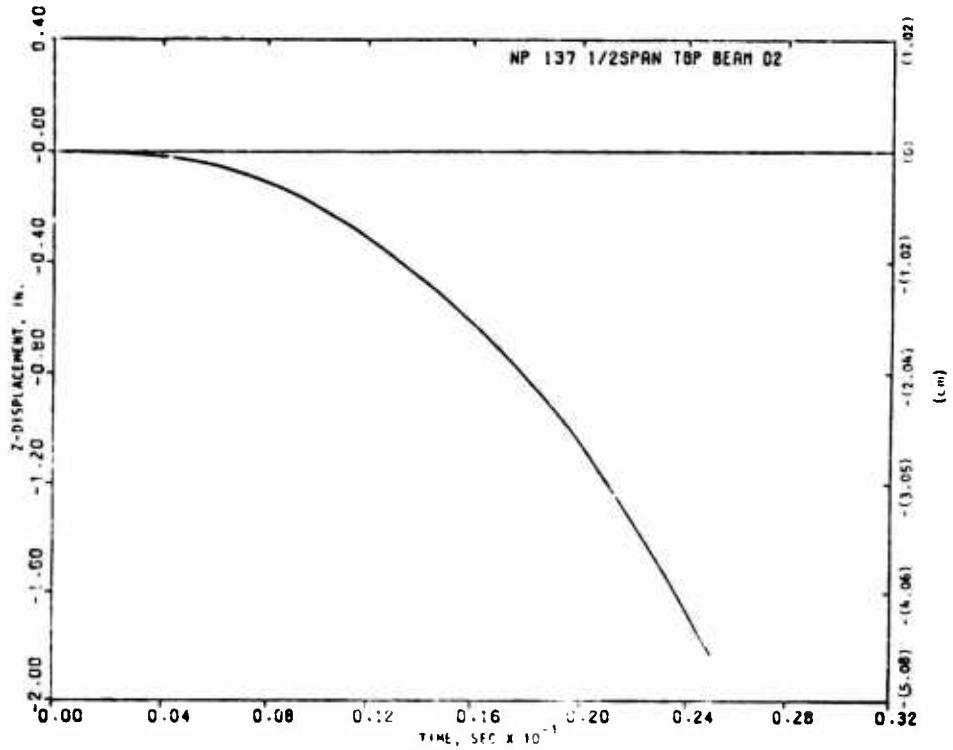

Figure 76. Calculated Midspan Displacement, Case D-2

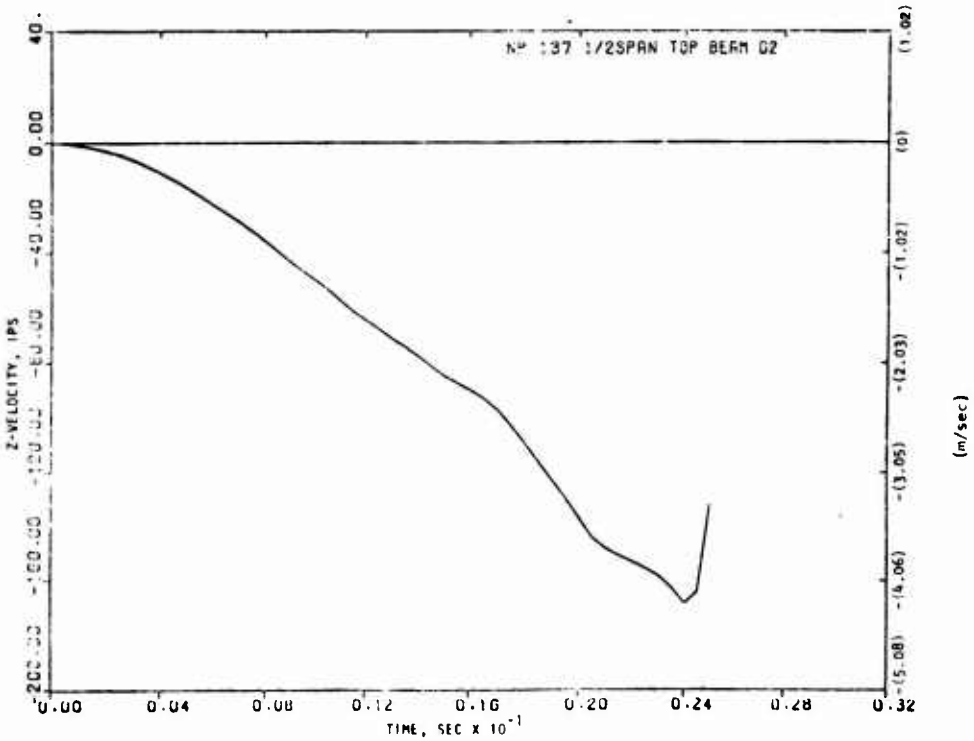

Figure 77. Calculated Midspan Velocity, Case D-2

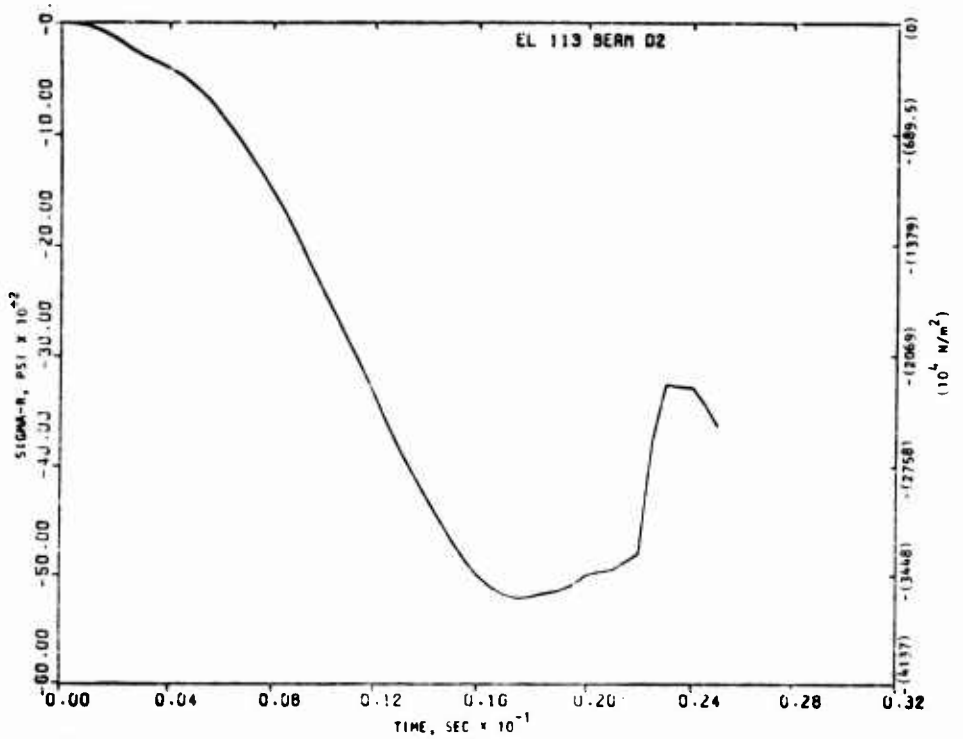

Figure 78. Extreme Fiber Stress in the Compression Zone at Midspan, Element 113, Case D-2

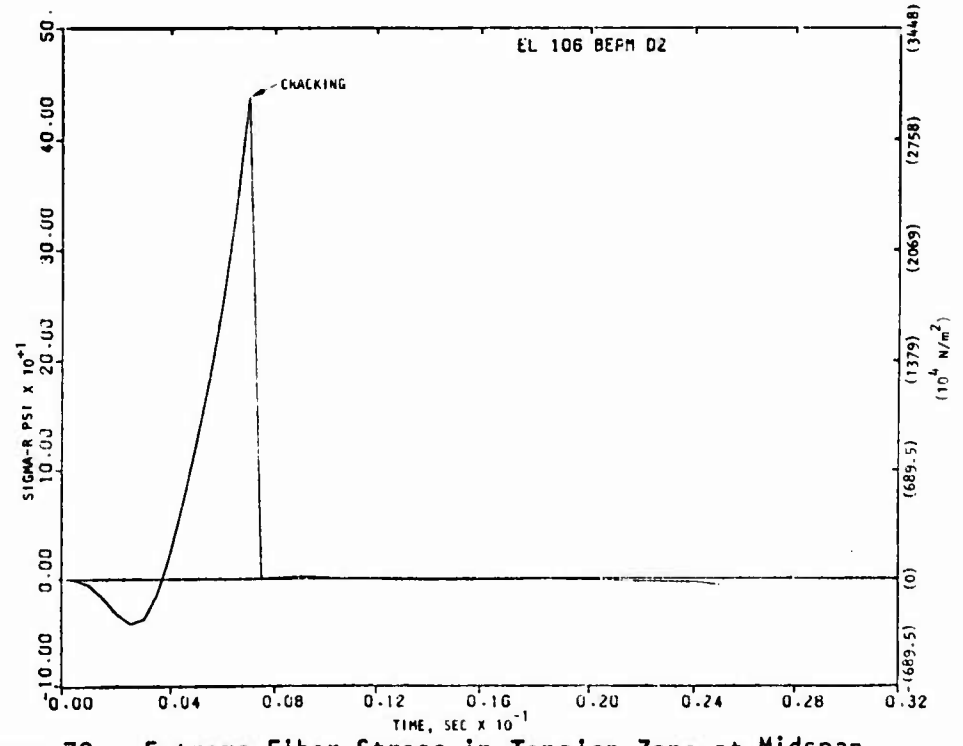

Figure 79. Extreme Fiber Stress in Tension Zone at Midspan, Element 106, Case D-2

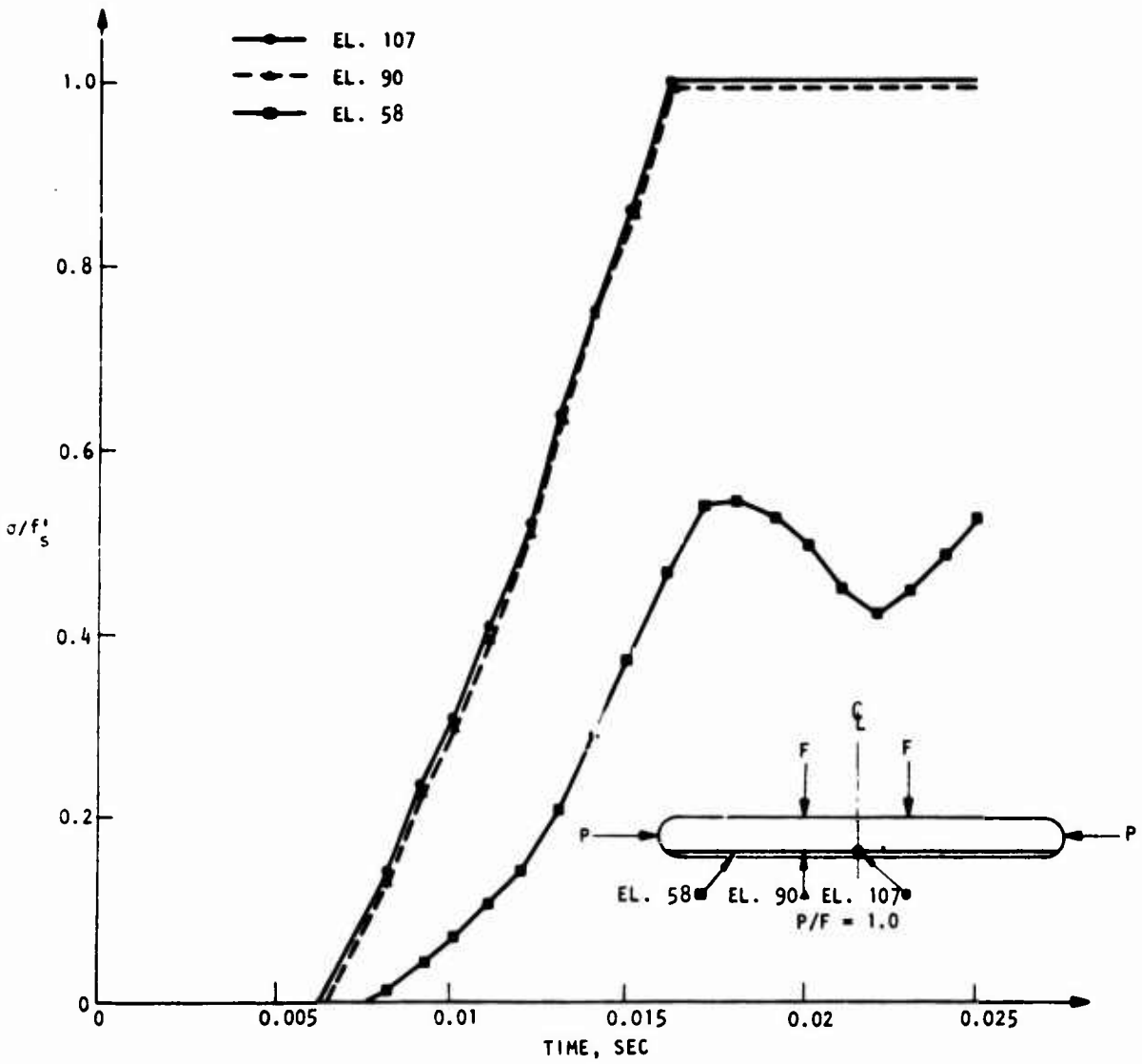

Figure 80. Steel Stress, Expressed as Fraction of Yield Stress, Versus Time Calculated for Beam Column, Case D-2

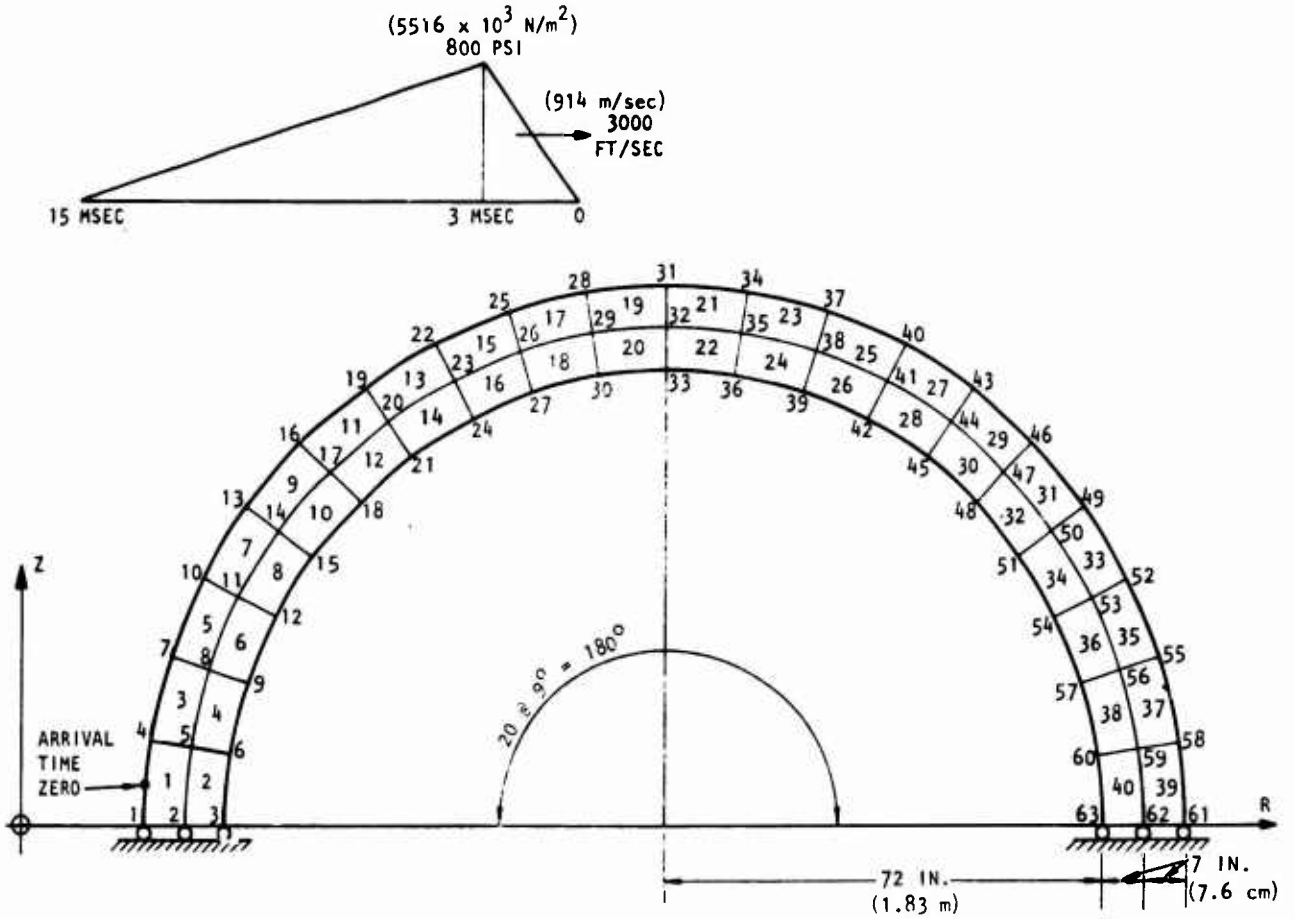

Figure 81. Finite Element Mesh for a Reinforced Concrete Ring and the Associated Traveling Pressure Pulse, Case D-3

The pressure pulse, which is triangular in shape as shown in figure 81, is assumed to travel at a constant velocity of 3000 ft/sec (914 m/sec) in the R-direction. The rise time is 0.003 sec with a peak pressure of 800 psi (5516×10^3 N/m^2). The pressure is applied normal to the outer surface of the ring. The arrival time for the midpoint of side 1-4 of Element 1 (Fig. 81) is taken as zero, and the arrival times for other loaded sides are determined on the basis of the 3000-ft/sec (914 m/sec) traveling speed and the differences between the R-coordinates of the midpoints of the loaded sides and that of the reference point with zero arrival time. Figure 82 shows the loading conditions at t sec.

A total of 240 integration time steps of 0.00005 sec each were taken for the inelastic analysis, resulting in 0.012 sec of response history. Figures 83 through 86 show the time histories of stress components (effectively, hoop stress) in four selected elements. There is, however, no experimental data for comparison.

The curves presented show that Element 1 cracks in tension at about 0.0108 sec while Element 40 cracks at about 0.0044 sec. In both cases, the stress level drops instantaneously to that corresponding to the 50,000 psi (345×10^6 N/m^2) yield point assumed for the reinforcing steel. This is because the steel percentages assigned to the outer and the inner element layers are both so low that the transfer of stress from concrete to steel accompanying the concrete cracking throws large enough load on the reinforcing steel to cause it to yield instantaneously. Notice that in the case of Element 40, the yielding of steel in tension is followed by a period of unloading and reloading of the element. The stiffness assigned to the steel during this period corresponds to the elastic modulus, while that assigned to the cracked concrete is taken as 5 percent of its initial tangent modulus--a more-or-less arbitrarily selected value.

Other elements which develop tension cracks and yielding of steel during the response are indicated in figure 87 together with the times at which the cracks first develop. The element which develops the largest compressive stress is Element 39. The time history of the stress σ_z in this element, which is almost directed in the circumferential direction, is given in figure 85.

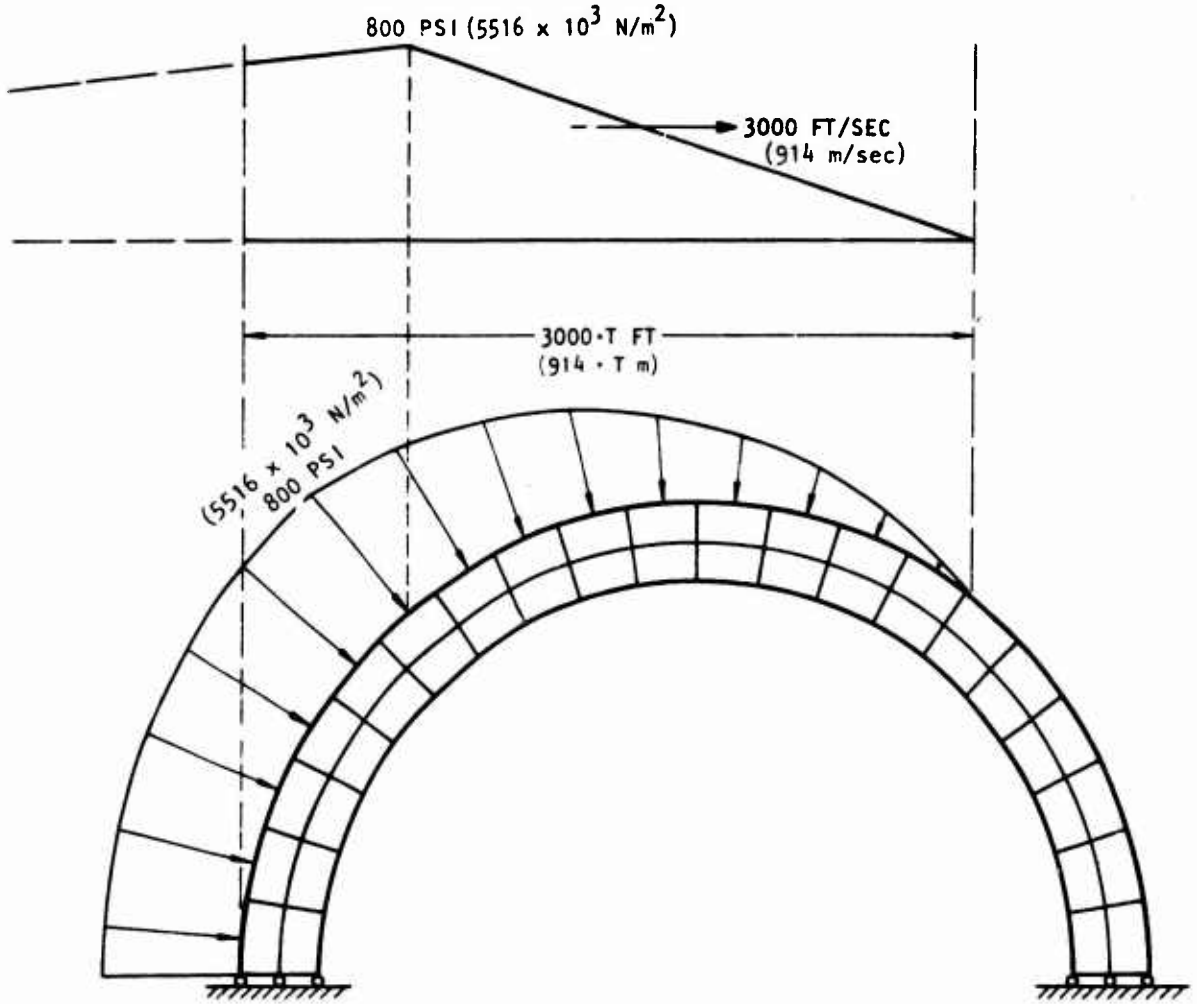

Figure 82. Loading Condition on the Ring at T Seconds, Case D-3

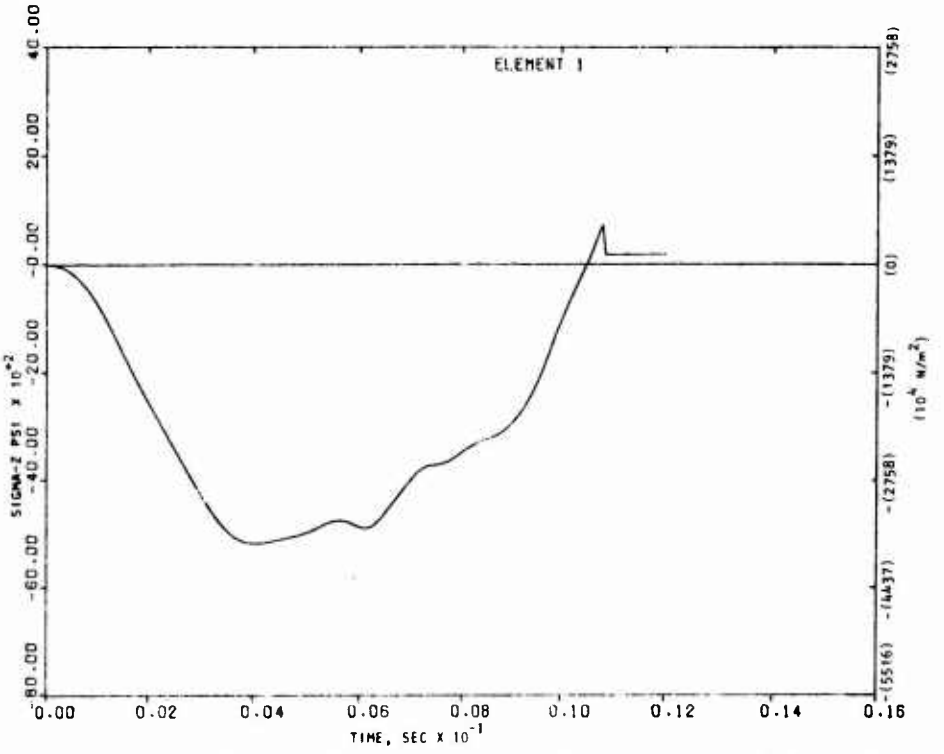

Figure 83. σ_z in Element 1 due to Traveling Pressure Pulse, Case D-3

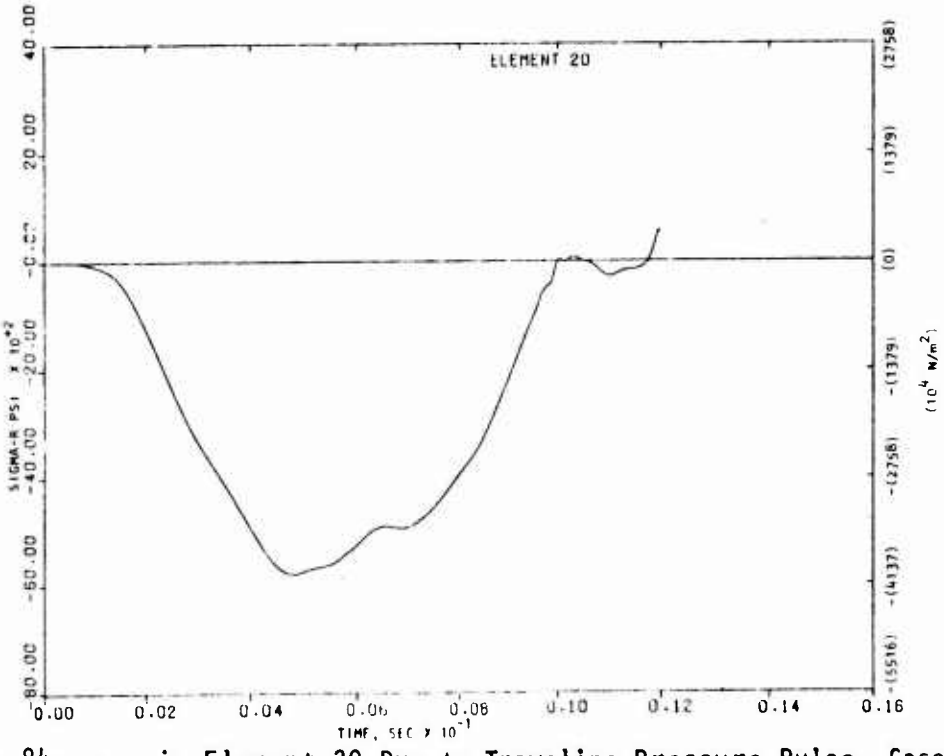

Figure 84. σ_R in Element 20 Due to Traveling Pressure Pulse, Case D-3

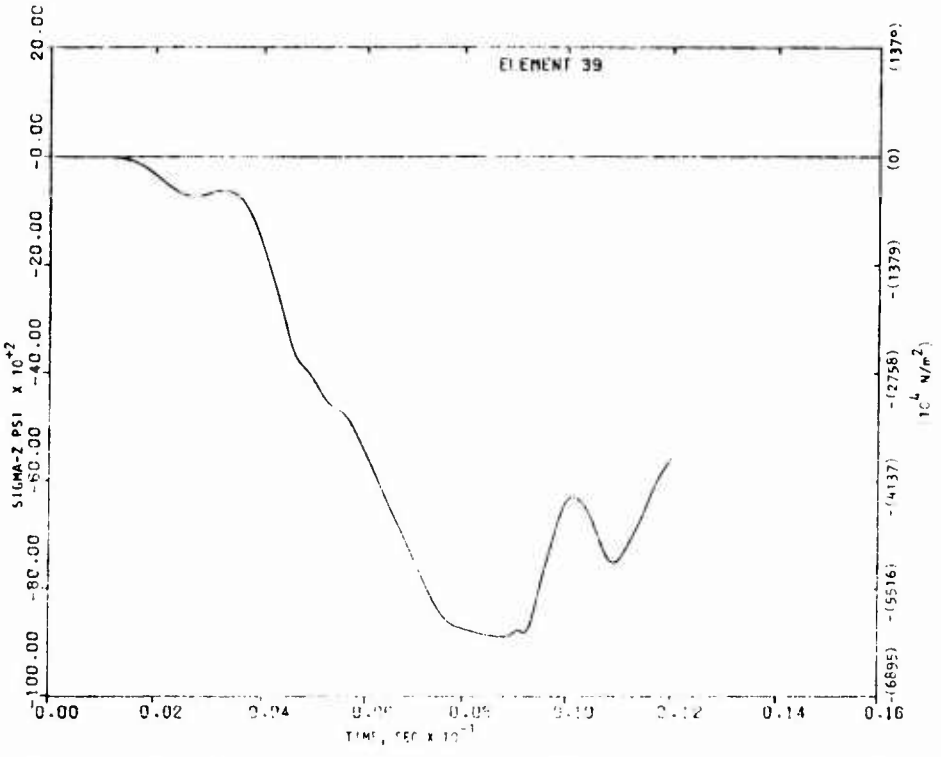

Figure 85. σ_z in Element 39 Due to Traveling Pressure Pulse, Case D-3

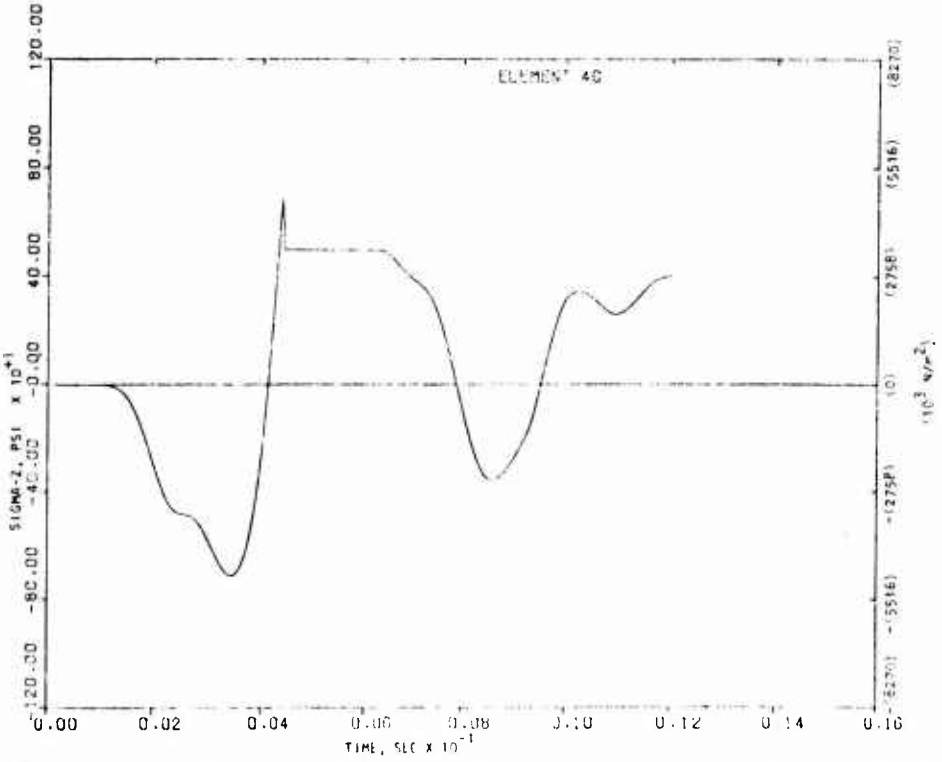

Figure 86. σ_z in Element 40 Due to Traveling Pressure Pulse, Case D-3

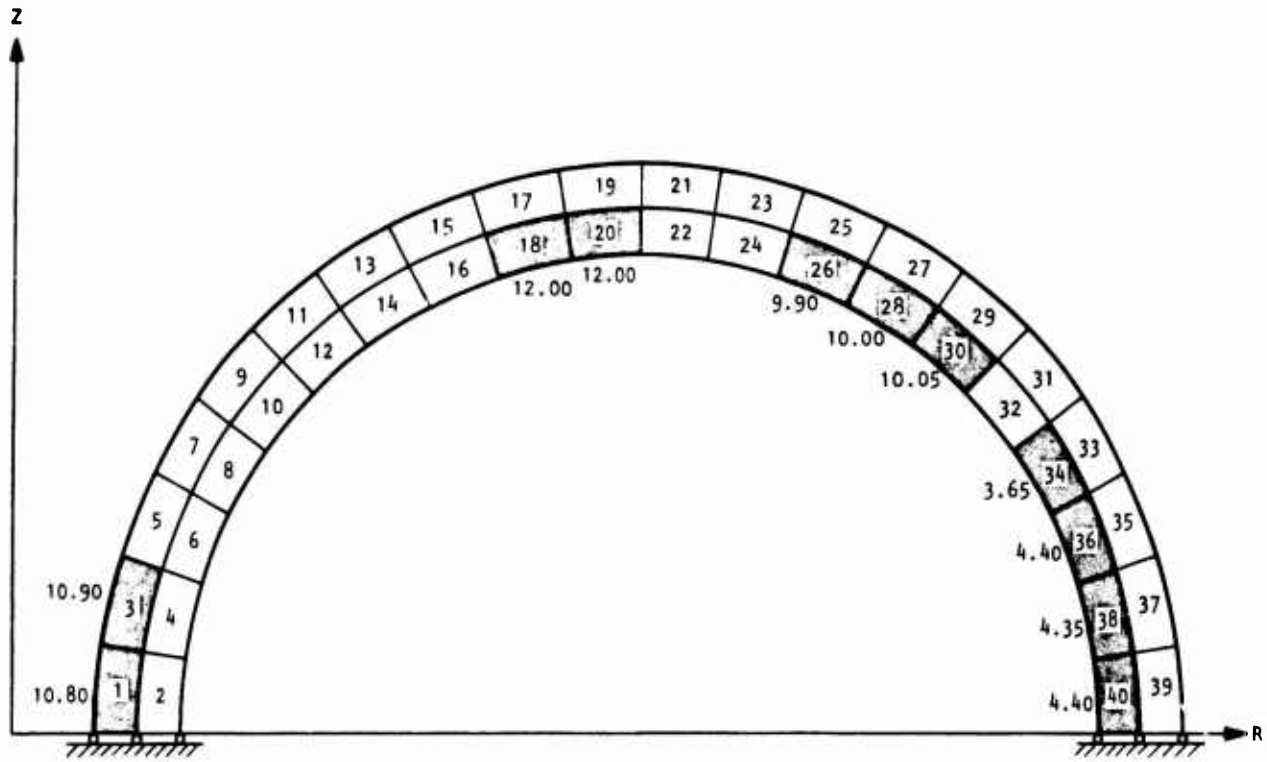

Figure 87. Elements Developing Tension Cracks and the Times in Milliseconds at Which the Cracks Develop, Case D-3

Figure 88 shows the deformed shape of the central axis of the ring at various times during the dynamic response. For convenience, the deformed shapes have been drawn with Nodal Point 62 considered stationary. It must be emphasized, however, that since the displacements are magnified 40 times in this figure, the deformed shapes are considerably distorted. Care must therefore be exercised in interpreting this figure. As an example, the figure suggests that some tension should develop in Element 33. The reason that no tension is indicated in the output may be due to the fact that Element 34 cracks in one direction very early in the history at 3.65 msec. Then at 5.05 msec, it cracks in a second direction perpendicular to the first. With Element 34 rendered almost useless structurally, only Element 33 remains in the locale to carry the load. Since a stress component calculated for an element is the average stress across that element, a single element is inadequate for determining bending stresses or the variation of stresses across an element. The absence of tensile stress in the output for Element 33, therefore, seems reasonable.

8. CASE D-4 (DYNAMIC ANALYSIS OF REINFORCED CONCRETE BEAM 3b2 OF FELDMAN, REF. 91)

a. Introduction

The dynamic behavior of a double-reinforced concrete beam under dynamic loads is investigated in this sample problem. The beam has a span length of 9 ft (2.7 m) and a cross section of 12 in. by 6 in. (30.4 x 15.2 cm), as shown in figure 89. The beam has two No. 9 bars as tension reinforcement, two No. 7 bars as compression reinforcement and No. 2 stirrups spaced at a constant interval of 4-1/4 in. (10.78 cm). The effective depth is 9.925 in. (50.5 cm). The ultimate strength of concrete (f'_c) as reported in reference 91 is 3.26 ksi (22 x 10^6 N/m^2), the initial tangent modulus (E_c) is 3.74 ksi (26 x 10^6 N/m^2), and the reinforcing steel has an average yield point of 45.8 ksi (316 x 10^6 N/m^2).

The beam is simply supported and is subjected to two concentrated loads symmetrically placed at a distance of 18 in. (45.7 cm) from the midspan. The loads are derived from explosive sources, and each of them has a time variation as shown in figure 90. Since the load-time curve is very nearly triangular, it is idealized into what is shown in figure 90 for the actual numerical

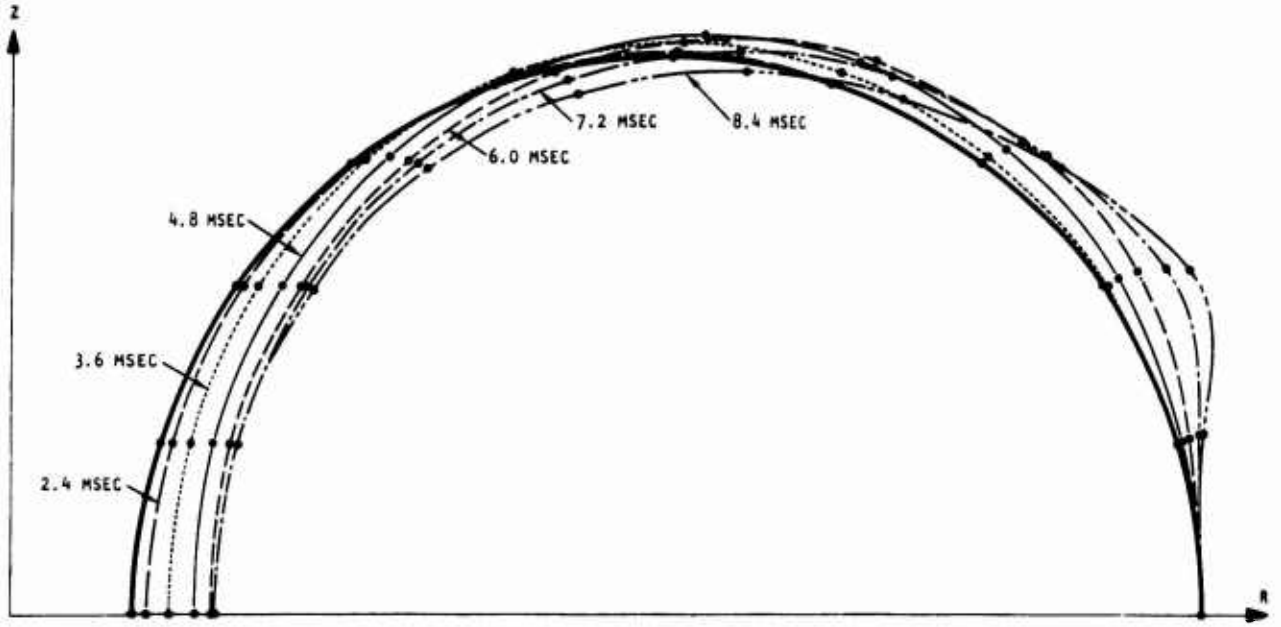

Figure 88. Deformed Shape of Ring at Various Times in Milliseconds (displacements magnified 40 times), Case D-3

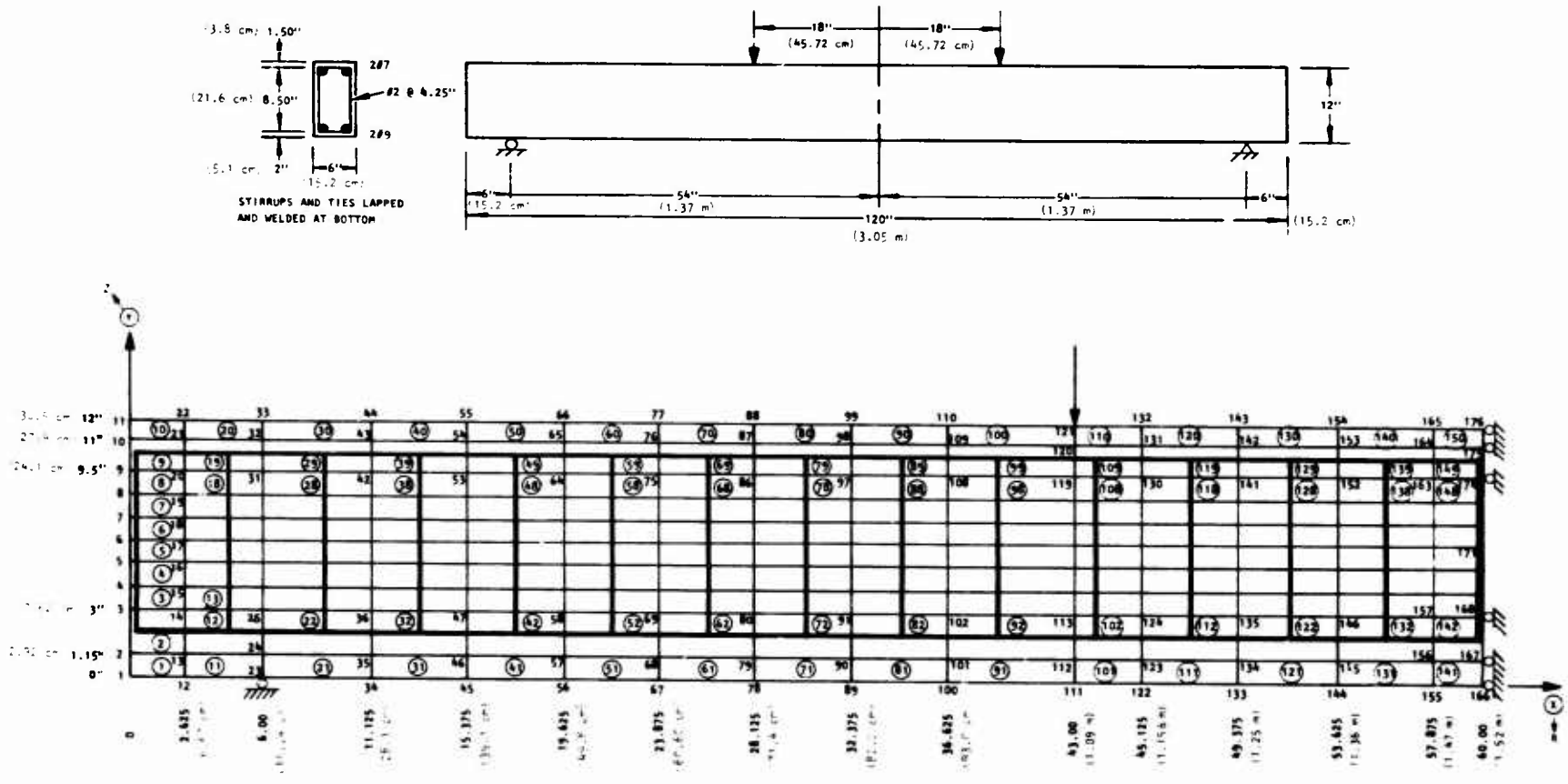

Figure 89. Finite Element Representation of Beam 3b2, Dynamic Case D-4

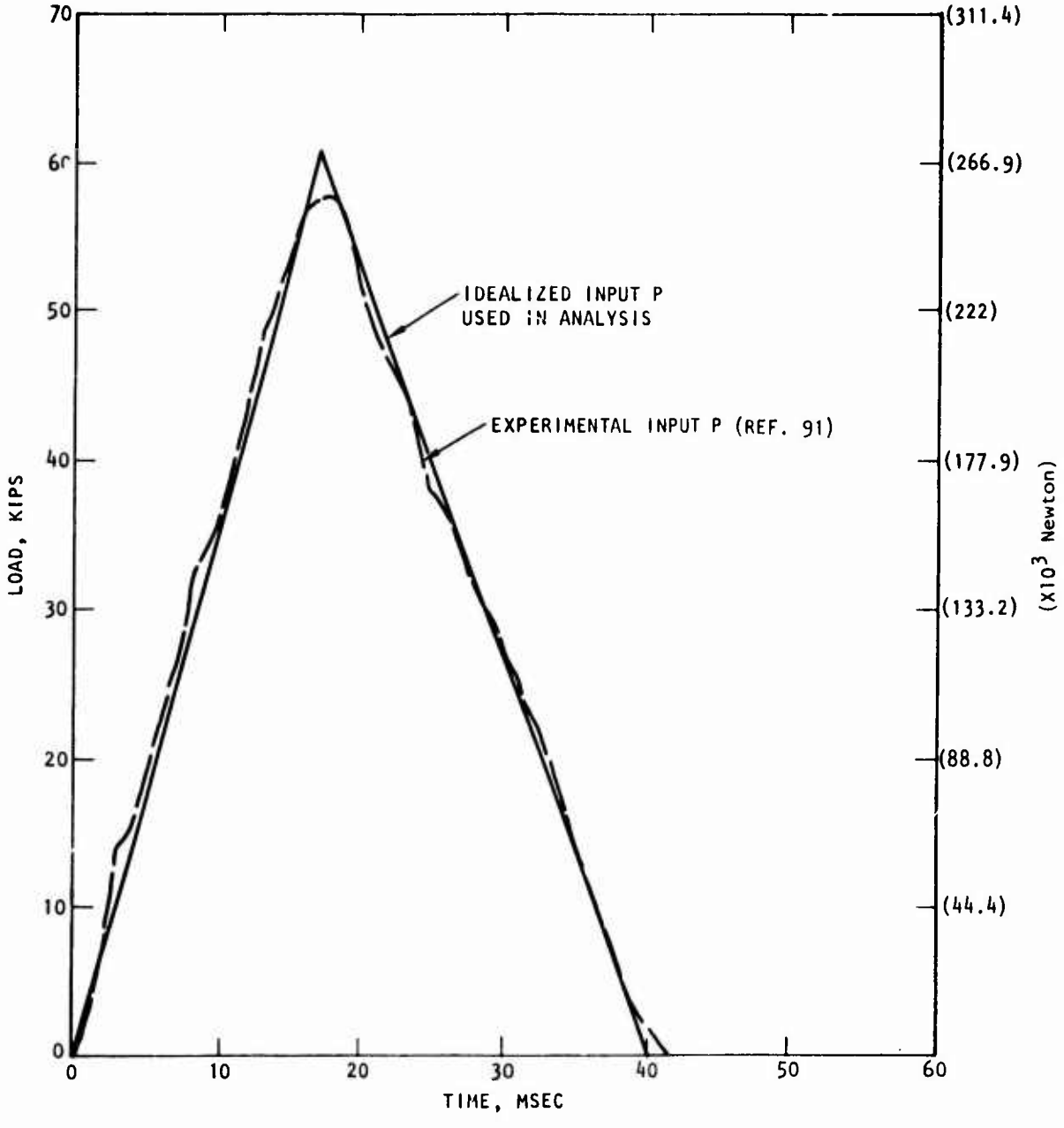

Figure 90. Load-Time History, Blow 1, Beam 3b2, Case D-4

calculation. In the actual test the beam is subjected to two additional force pulses (blows). However, only the first pulse is considered in the following analysis.

The finite element mesh used in the analysis is shown in figure 89. It is a 10 by 15 rectangular mesh with 176 nodal points and 150 elements. The right boundary corresponding to the midspan section is rollered to reflect the beam symmetry. Any element crossed by steel--whether tension steel, compression steel or a stirrup--is considered reinforced, with the steel percentage calculated as the steel area divided by the cross-sectional area of the element perpendicular to the steel reinforcement.

A total of 50 one-msec steps are taken, resulting in 50 msec of response history. The FEDRC code was used for the dynamic analysis, and the results are discussed in the following section.

b. Case D-4: Original Results and Modifications Required to Improve These Results

The dynamic analysis of Case D-4 was performed first using the original version of FEDRC code. Selected portions of the analysis are shown in figures 91(a), 92(a), 93(a), and 94. Figure 91(a) reveals that the beam started to crack at 4 msec. However, cracks were initiated in the second row in a heavily reinforced group of elements rather than at the lower tension fibers of the beam. An examination of the cracking criteria in the original version of the code indicated that the cracking of an element was established on the basis of overall element stress. Since the heavily reinforced elements have more stiffness, they developed higher stresses and therefore cracked first. To avoid this condition the cracking criteria were modified in such a manner that the onset of cracking would be decided by the concrete stress rather than the average element stress. The result of this modification is illustrated in figure 91(b). A similar comparison, at 5 msec, is shown in figures 91(c) and 91(d).

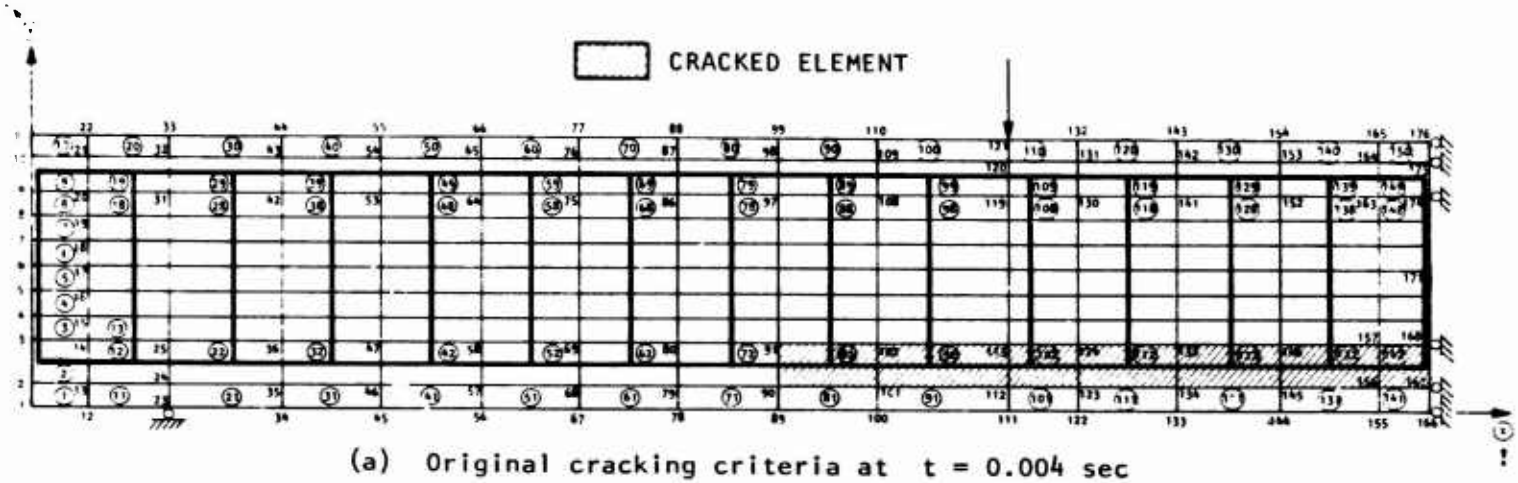

(a) Original cracking criteria at t = 0.004 sec

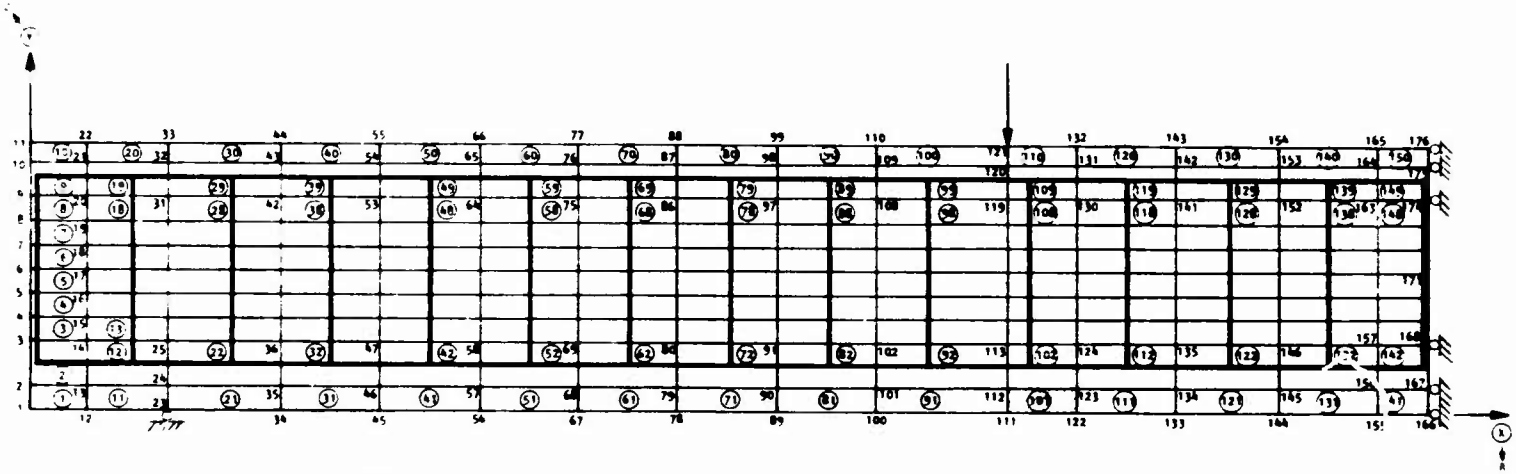

(b) Modified cracking criteria at t = 0.004 sec

Figure 91. Comparison of Initial Crack Patterns Obtained from Original and Modified Cracking Criteria, Dynamic Case D-4

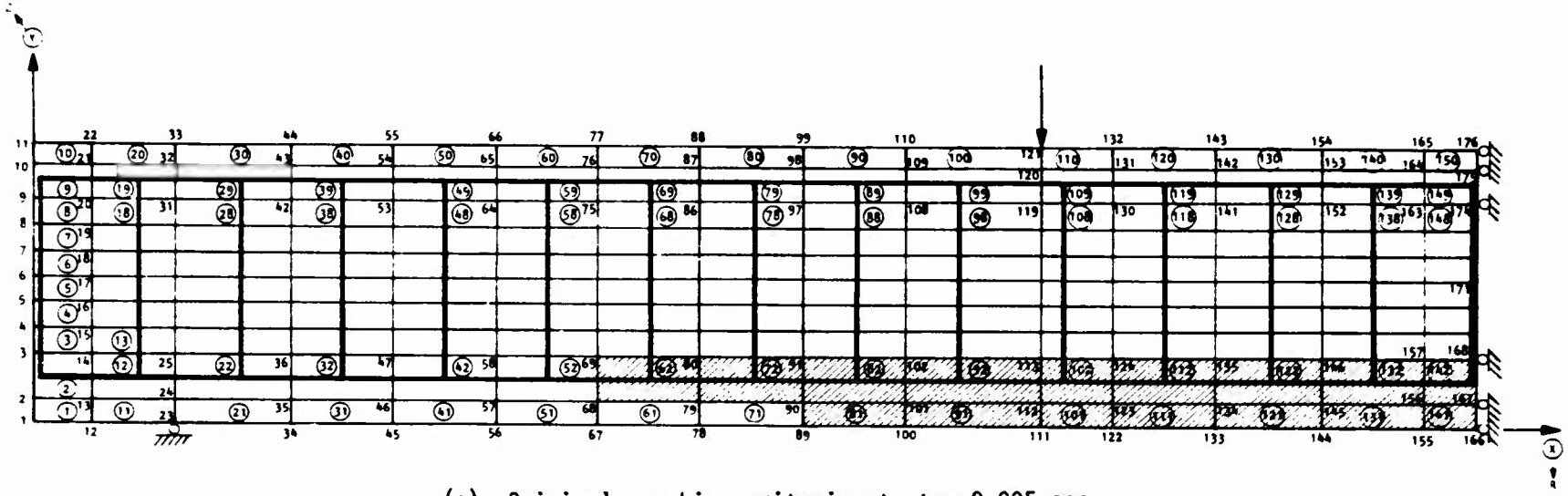

(c) Original cracking criteria at t = 0.005 sec

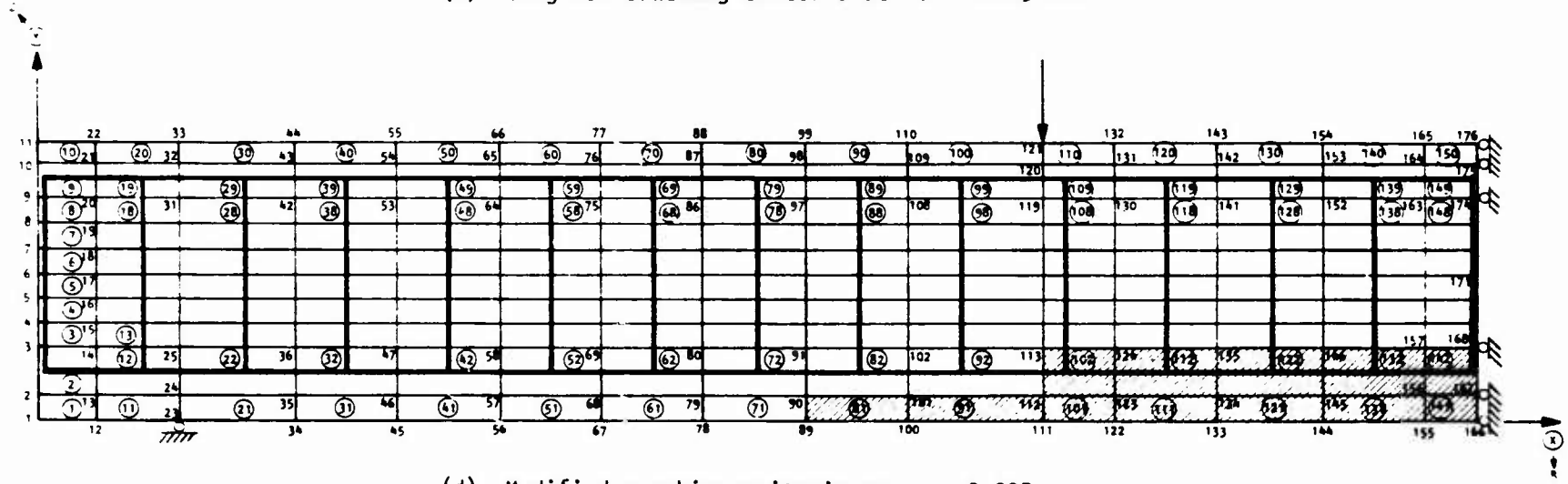

(d) Modified cracking criteria at t = 0.005 sec

Figure 91. Comparison of Initial Crack Patterns Obtained from Original and Modified Cracking Criteria, Dynamic Case D-4 (concluded)

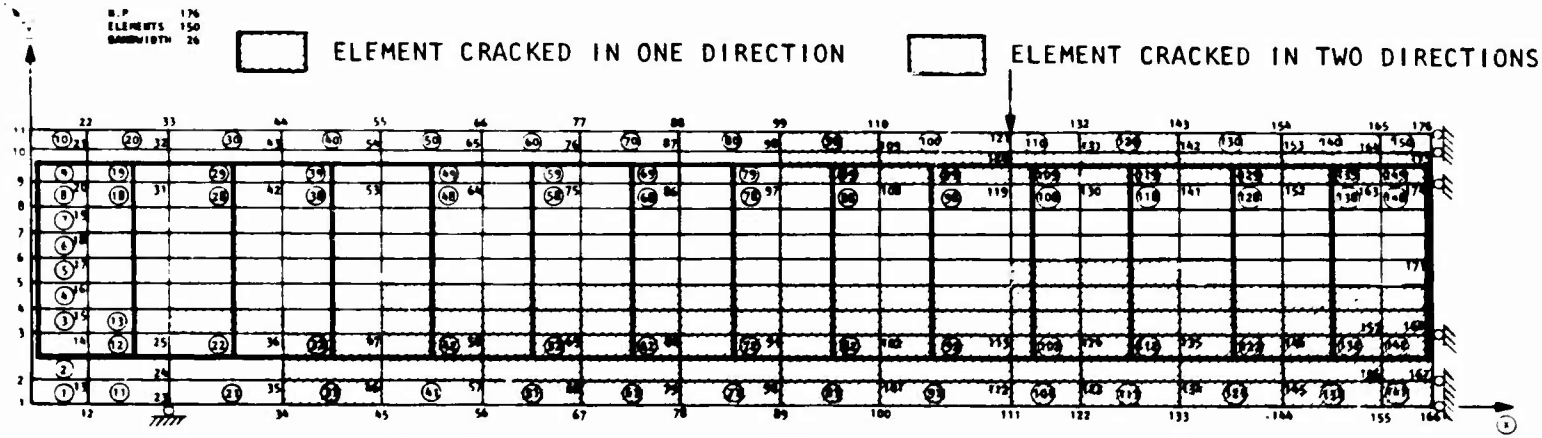

(a) Original cracking criteria at t = 0.012 SEC

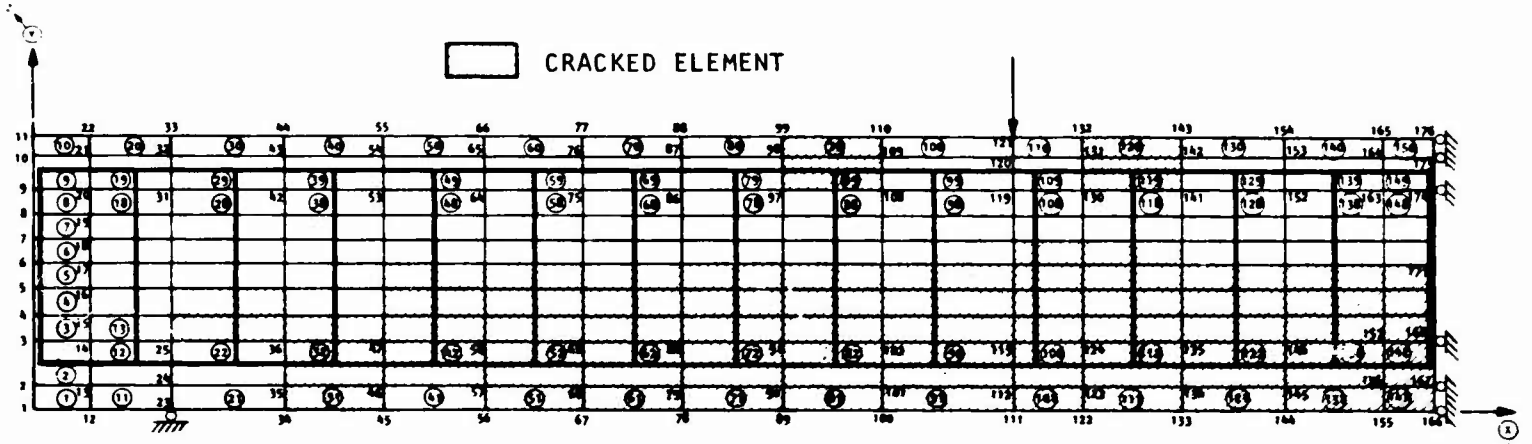

(b) Modified cracking criteria at t = 0.012 SEC

Figure 92. Comparison of Propagation of Cracks in Compression Zone Obtained by Original and Modified Cracking Criteria, Dynamic Case D-4

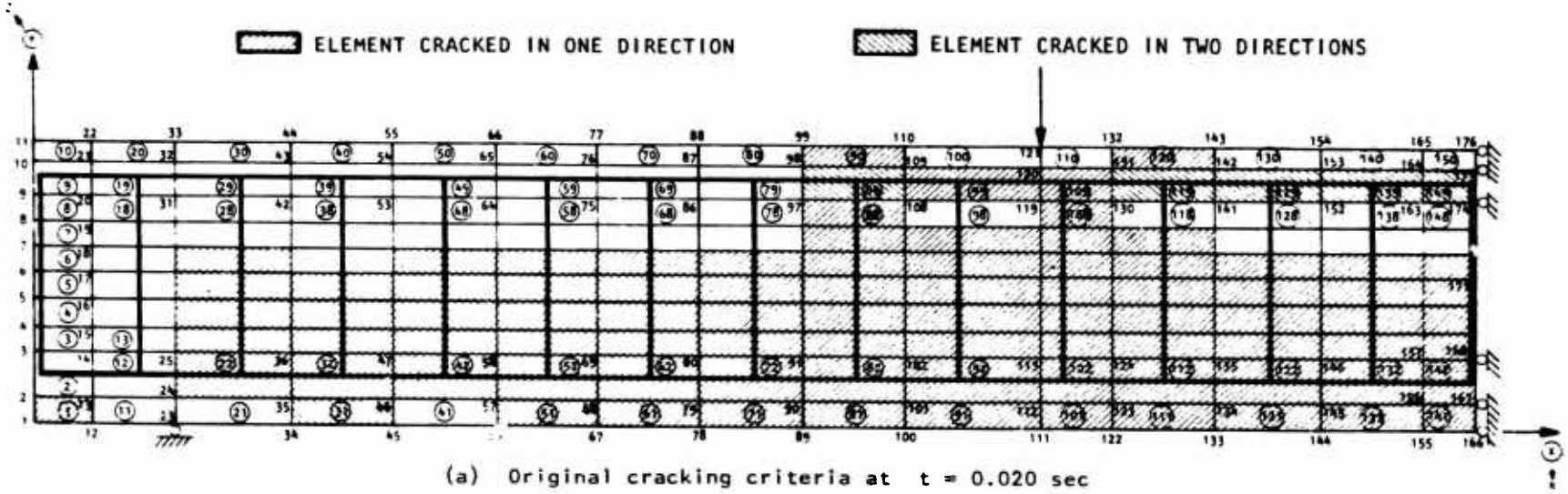

(a) Original cracking criteria at t = 0.020 sec

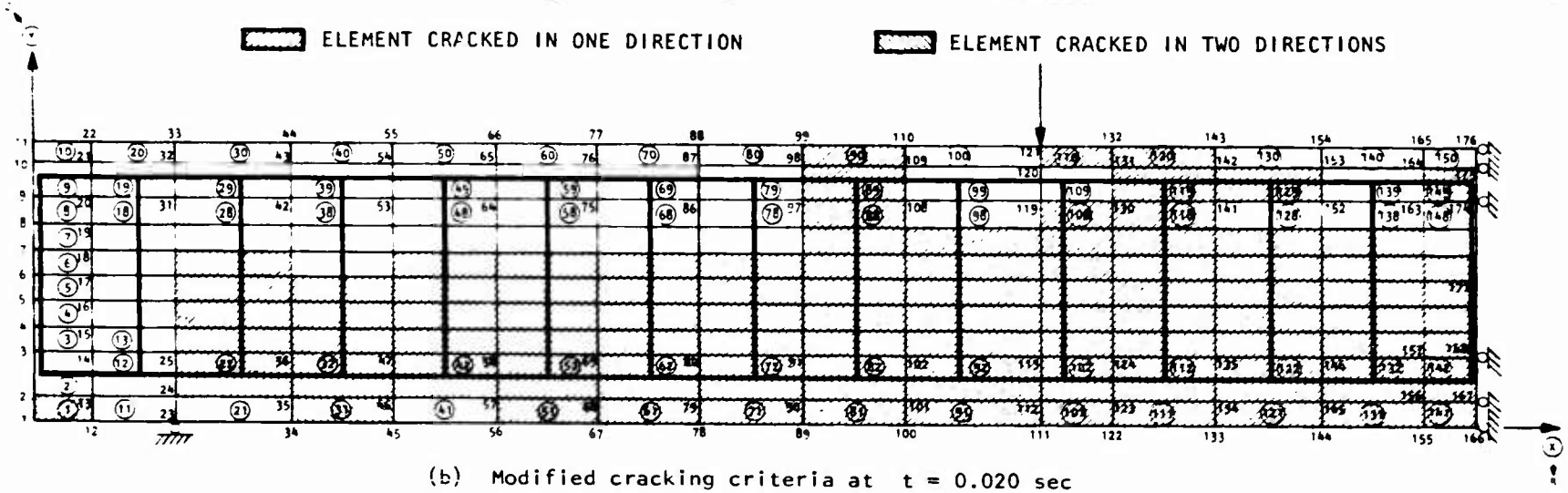

(b) Modified cracking criteria at t = 0.020 sec

Figure 93. Comparison of Propagation of Cracks in Compression Zone Obtained by Original and Modified Cracking Criteria, Dynamic Case D-4

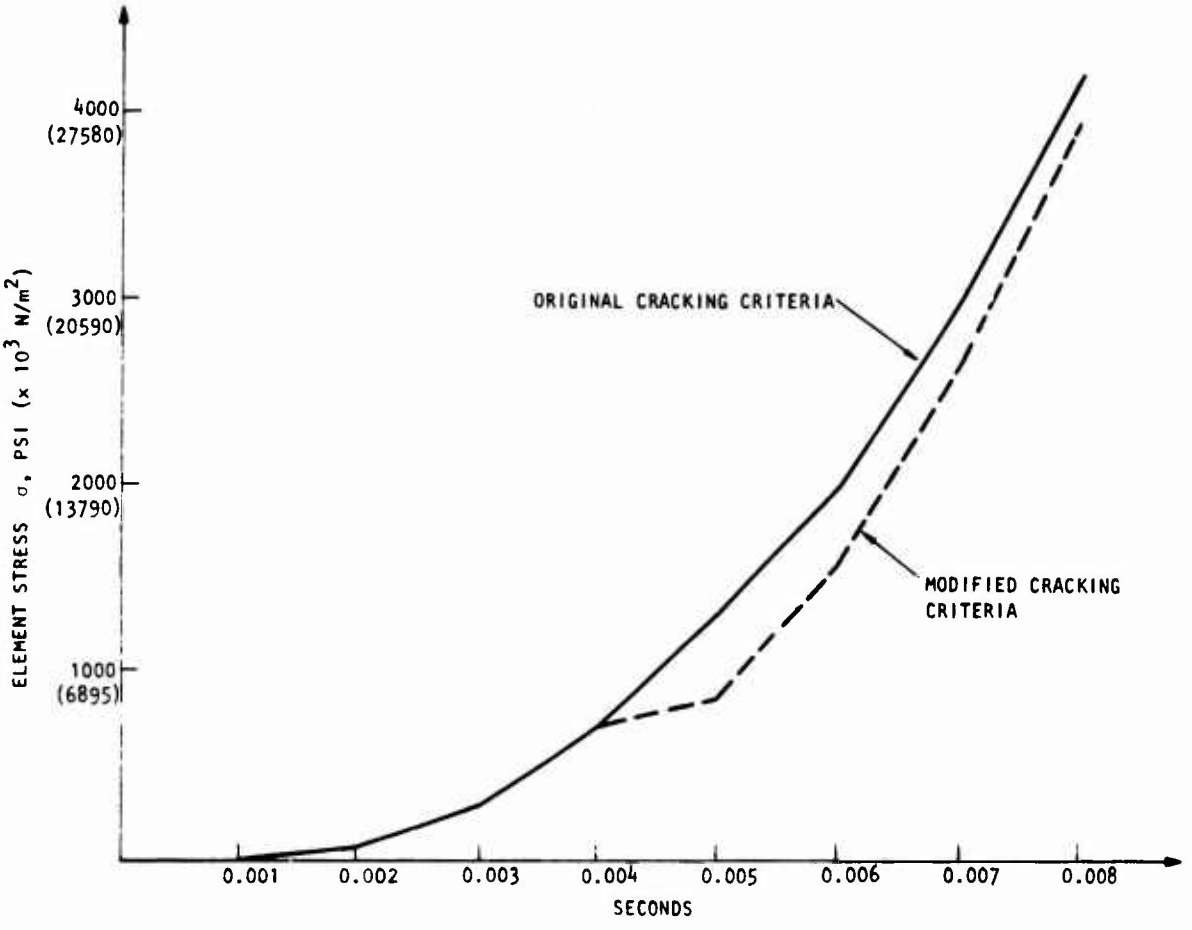

Figure 9. Comparison of Stresses in Tension-Reinforced Element 142 Obtained by the Original and Modified Cracking Criteria, Case D-4

Another discrepancy was observed in the propagation of cracks in the beam at 12 msec, as shown in figures 92(a) and 93(a). Double cracks were developed in the top compression zone, implying that tension stresses were developed in both directions.

An examination of the interaction formula (36a) for cracking (Fig. 15)

$$f_t' = f_t - \eta\sigma_2$$

where

f_t' = Tension cracking stress

f_t = Unconfined tensile stress of concrete (>o)

η = Sloping of cracking envelope (<o)

σ_2 = Minimum nonpositive stress normal to tension axis

indicates that if large compressive stress σ_2 is applied, f_t' will approach zero stress and cracks will be initiated at almost zero-tension stress (Fig. 15). Therefore, a slight numerical noise in the solution, which is almost unavoidable in any numerical solution, would trigger cracks in the compression zone.

To prevent the contaminating of crack patterns with unrealistic cracks, a 5-percent threshold was used as a numerical noise filter. As a result, only tension stresses that are above 0.05 f_t are allowed to produce tension cracks. The results of this modification are shown in figures 92(b) and 93(b).

Another feature that was added to the material package is the capability to simulate the sudden increase of strain at the onset of cracking. This is achieved by dropping the concrete stress level in the element immediately after cracks. The result of such modification is shown in figure 94.

The material package was further improved by including rebonding capability. With all the above improvements incorporated in the material package, a modified version of FEDRC became available. This version was first used to rerun the analysis of dynamic case D-4 and later to recalculate the static response of beam S-1. Both these calculations will be discussed in the following pages.

c. Case D-4: Results of Modified Dynamic Analysis

The results of case D-4 are shown in figures 95, 96, 97, 98, and 99. An examination of the displacement time-history plots (Fig. 95) reveals good agreement between calculated and measured displacements for the first 20 msec. This time almost coincides with the end of the loading part of the triangular pulse and the beginning of the unloading portion of this pulse (Fig. 90). However, for longer times, the calculated displacements are nigher than the observed displacements. A maximum displacement of 2.40 in. (6.1 cm) was calculated at the middle of the beam, as compared to 1.25 in. (3.2 cm) obtained from experimental measurements (Ref. 91). Both velocity and acceleration time-history at the middle of the beam are shown in figure 96. The displacement time-history of nodal point 116, located 18 in. (45.6 cm) away from the center of the beam, is shown in figure 97. There is a general agreement between the shapes of the displacement time-histories obtained from analysis and experimental measurements as illustrated in figures 95 and 97.

The results recorded in figure 98 reveal good correlation between calculated and measured strains for a range that extends to 20 or 25 msec. This range again coincides with the ascending part of the input pulse given in figure 90. However, for the descending part of the loading (beyond 20 or 25 msec), calculated strains are larger than measured strains.

The stress time histories for selected elements are shown in figure 99. Figures 99(a), (e), and (h) indicate that the stress drops to a zero value immediately after cracks occur in unreinforced concrete elements. However, rebonding can be observed in figures 99(a), and (e), where a buildup of compression stress occurs beyond 45 msec.

An examination of figure 99(b) reveals that Element 52 cracked at approximately 7 msec, whereas steel bars yielded at approximately 15 msec. A similar trend was observed in figures 99(f) and 99(i). The stresses in elements at the top of the beam are illustrated in figures 99(d), (g), and (k). The rapid fluctuations of stresses from loading to unloading reflect the effect of waves and undamped oscillations on the response.

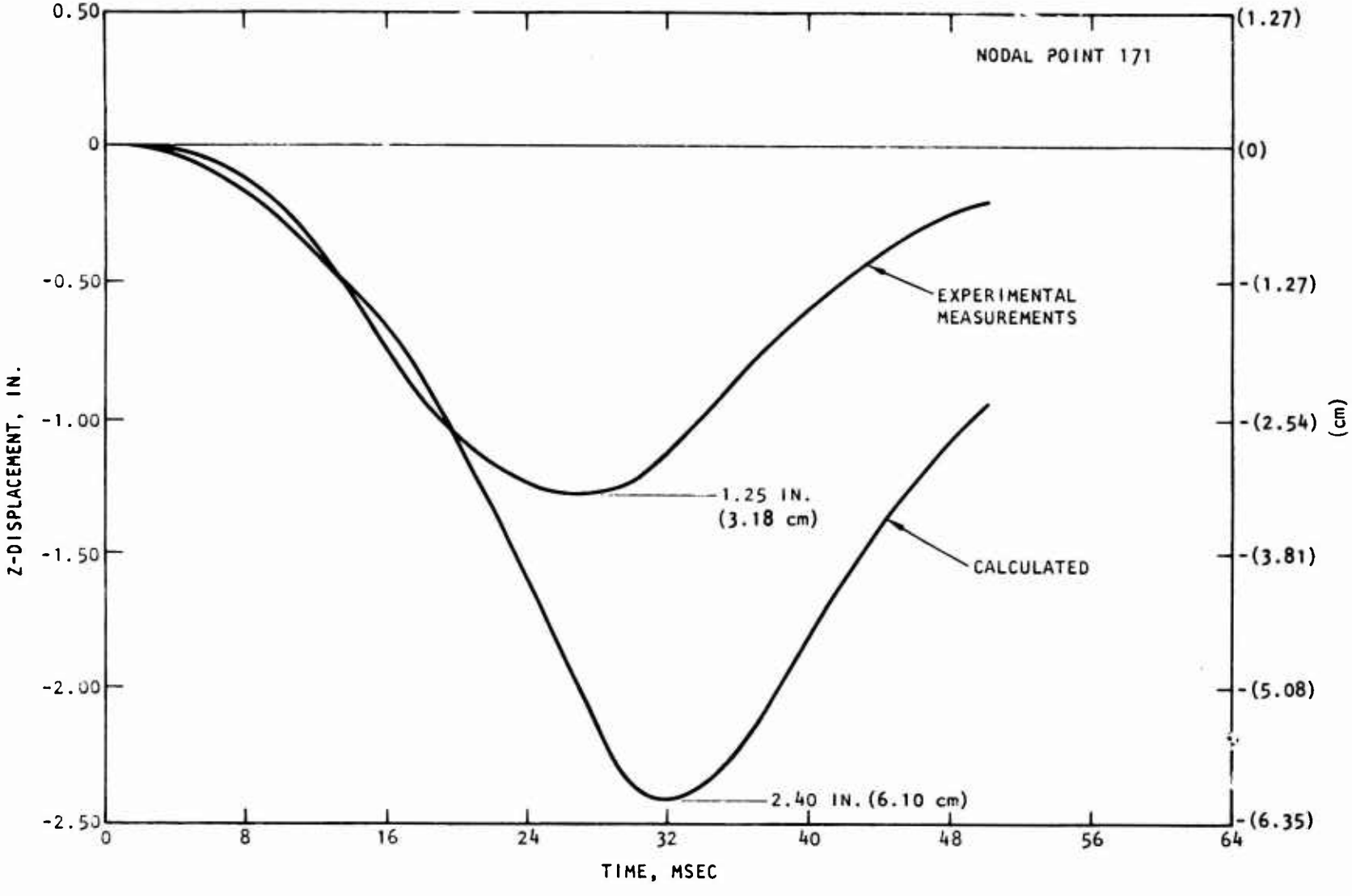

Figure 95. Vertical Displacement Time History at the Middle of the Beam Obtained from Experimental Measurements and Calculations, Case D-4

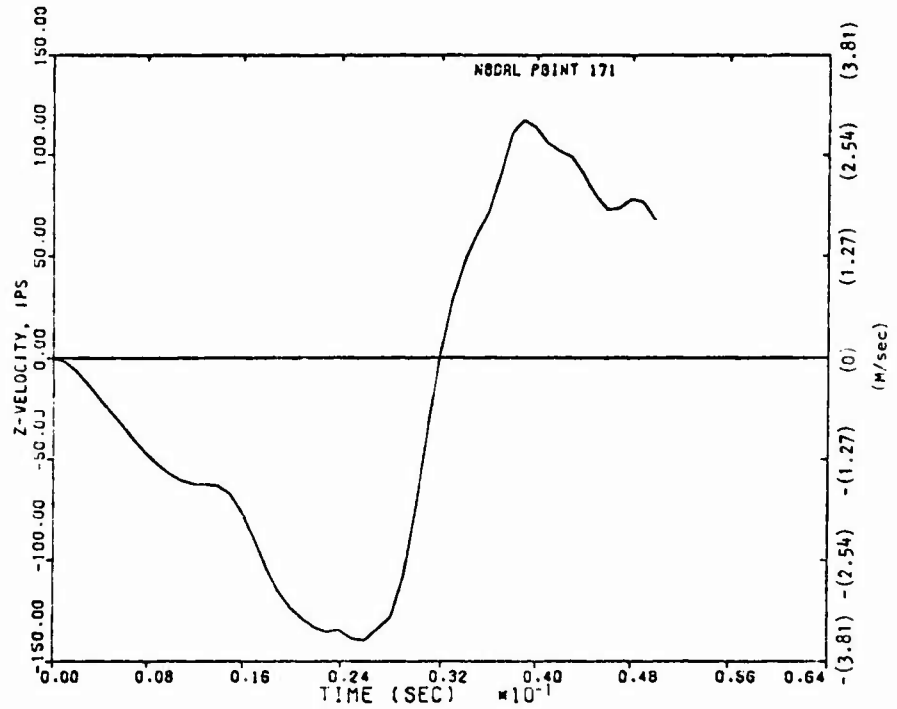

(a) Velocity time history

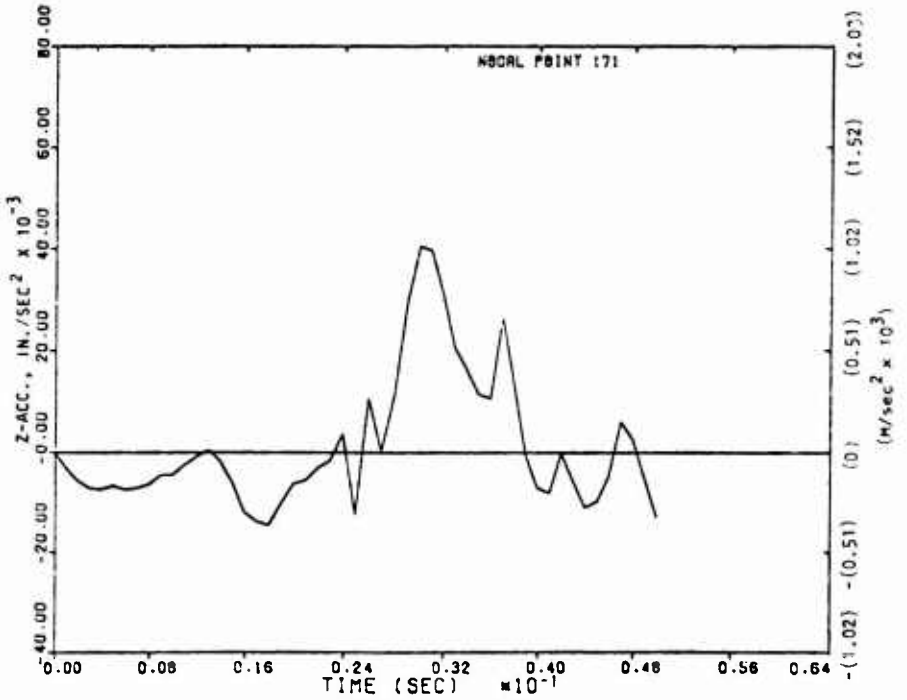

(b) Acceleration time history

Figure 96. Calculated Response at the Middle of the Beam, Nodal Point 171, Dynamic Case D-4

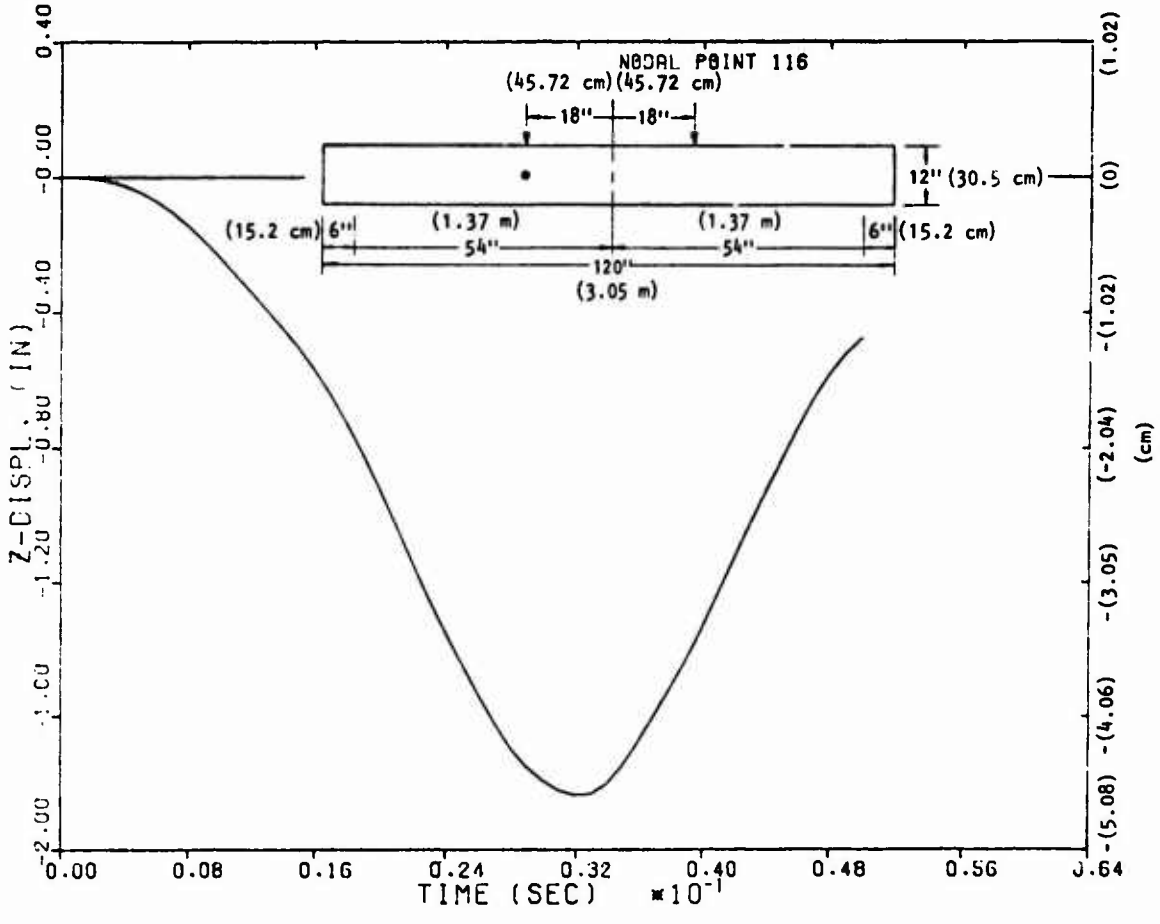

Figure 97. Calculated Vertical Displacement Time History at Nodal Point 116, Dynamic Case D-4

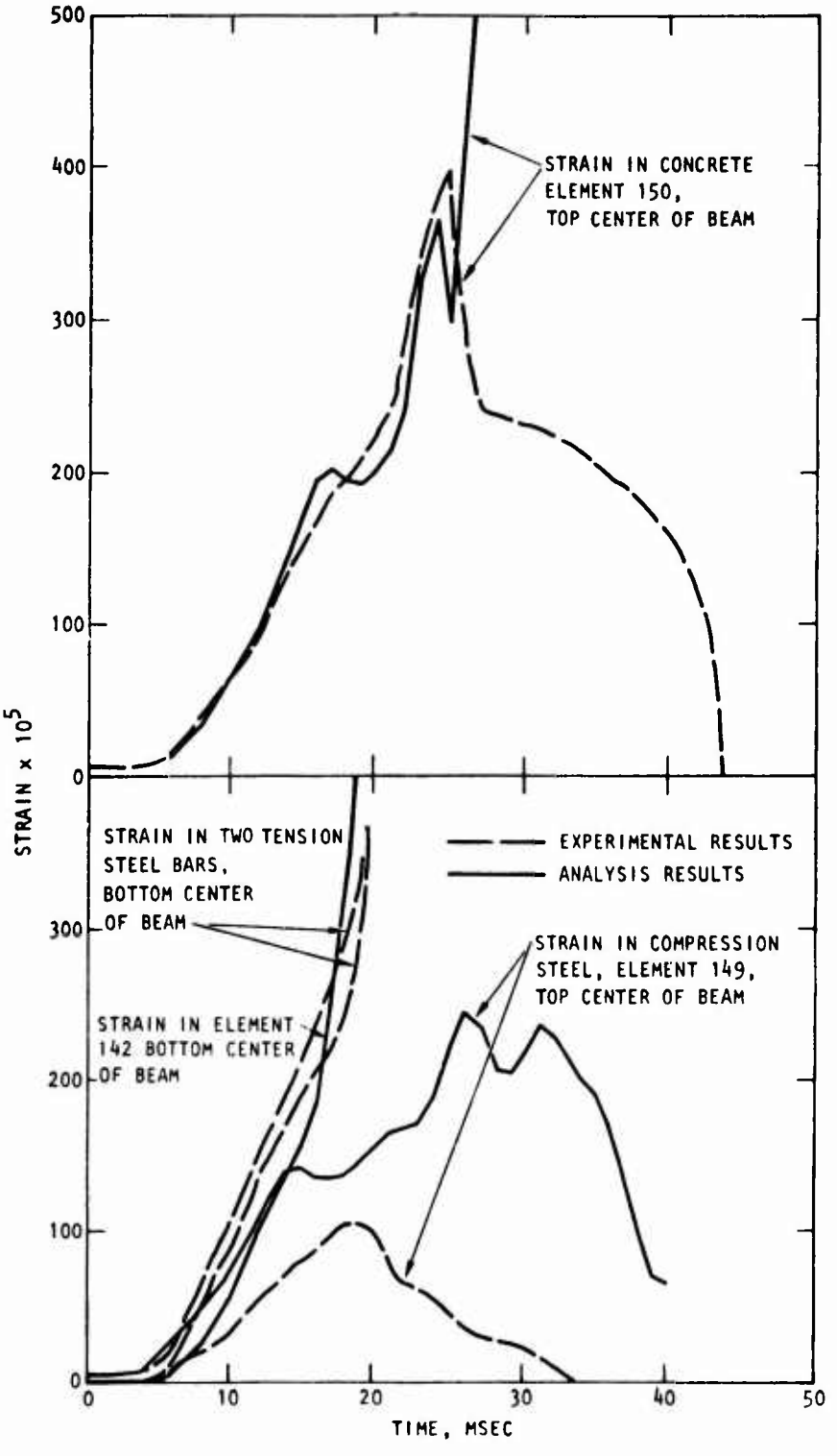

Figure 98. Comparison of Calculated and Observed Strain Histories, Blow 1, Beam 3b2, Case D-4

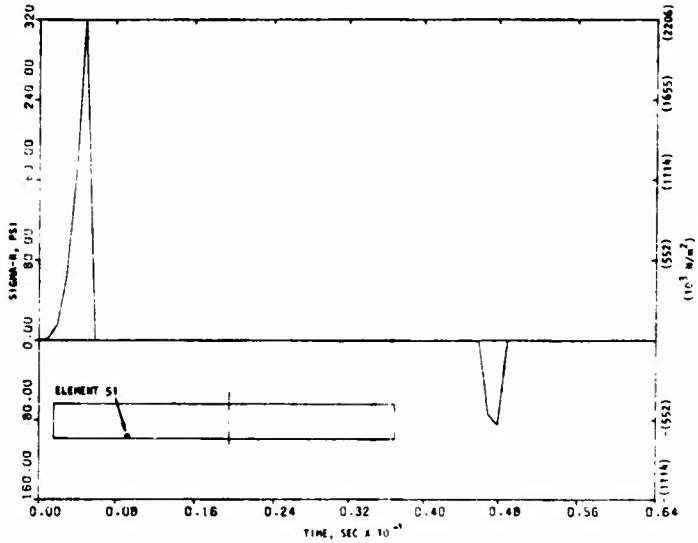

(a) Element 51

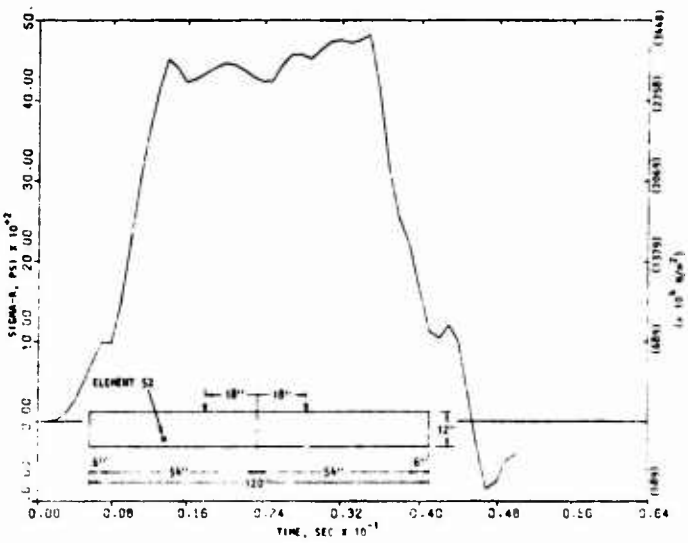

(b) Element 52 (tension reinforcement)

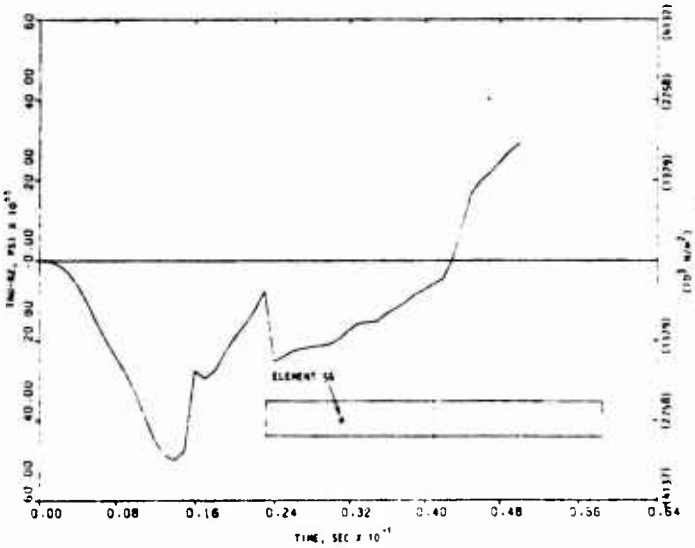

(c) Element 56

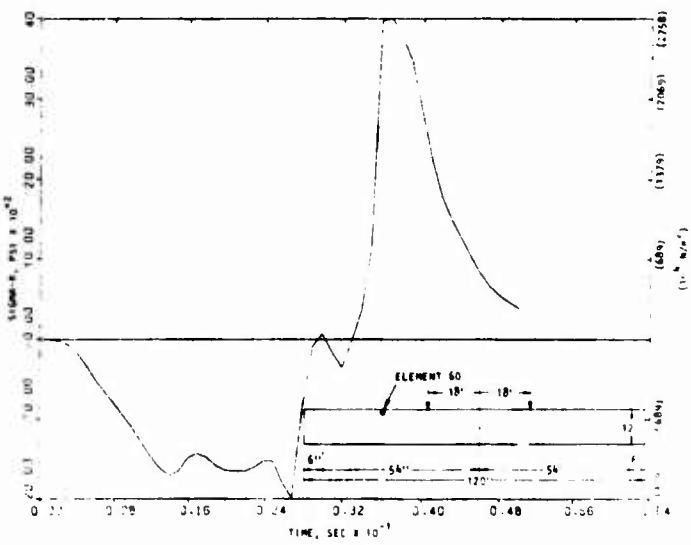

(d) Element 60

Figure 99. Dynamic Case D-4: Stresses in Beam 3b2

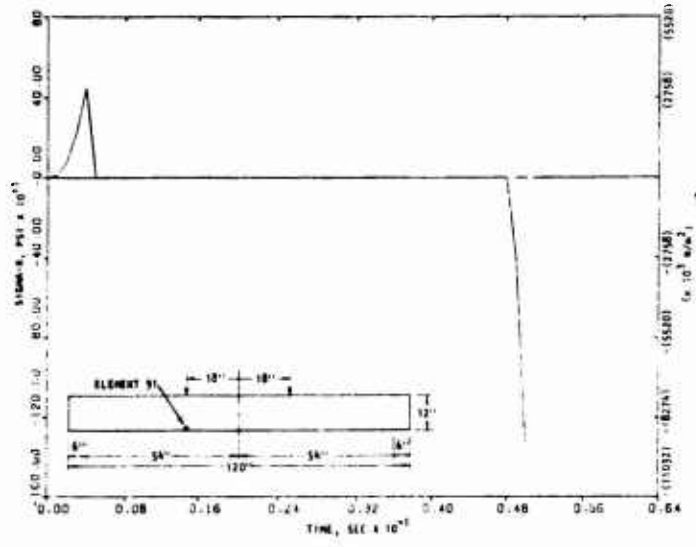

(e) Element 91

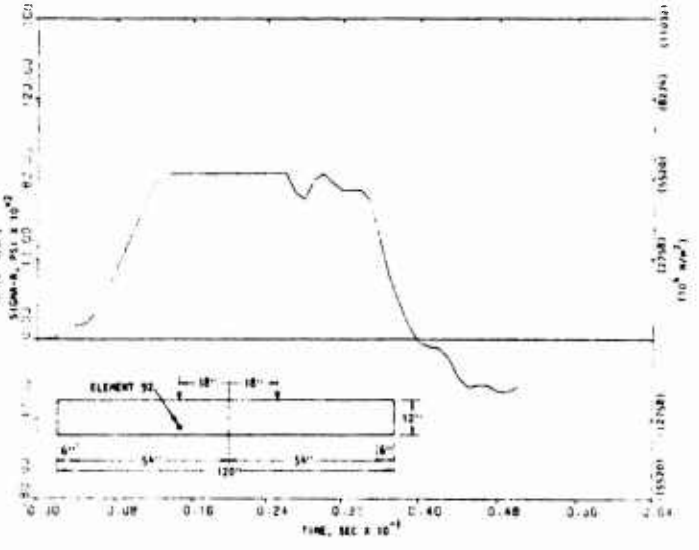

(f) Element 92

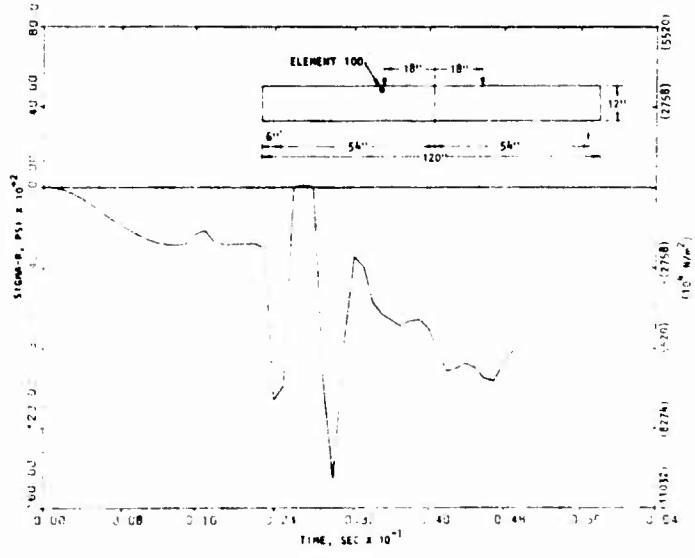

(g) Element 100

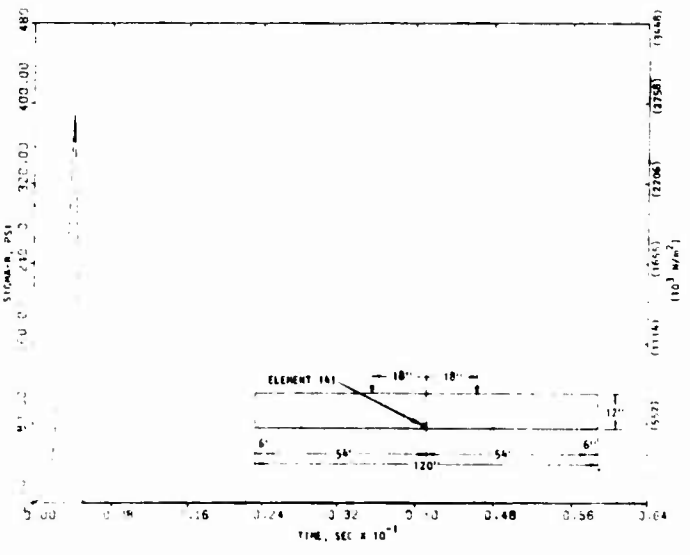

(h) Element 141

Figure 99. Dynamic Case D-4: Stresses in Beam 3b2 (continued)

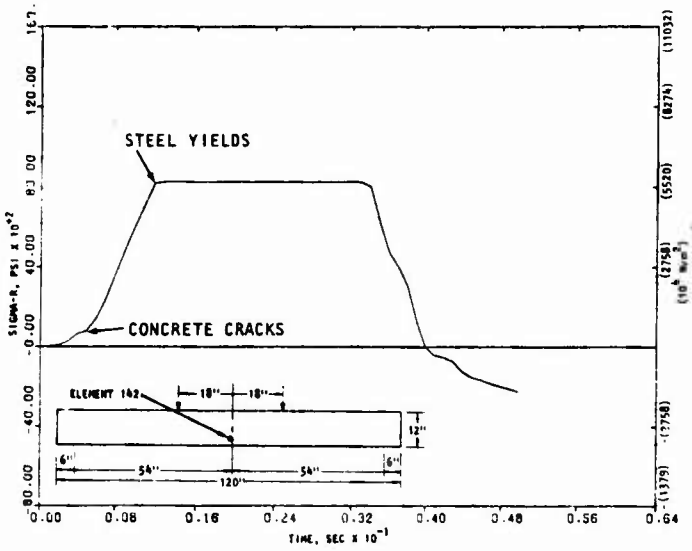

(i) Element 142 (tension reinforcement)

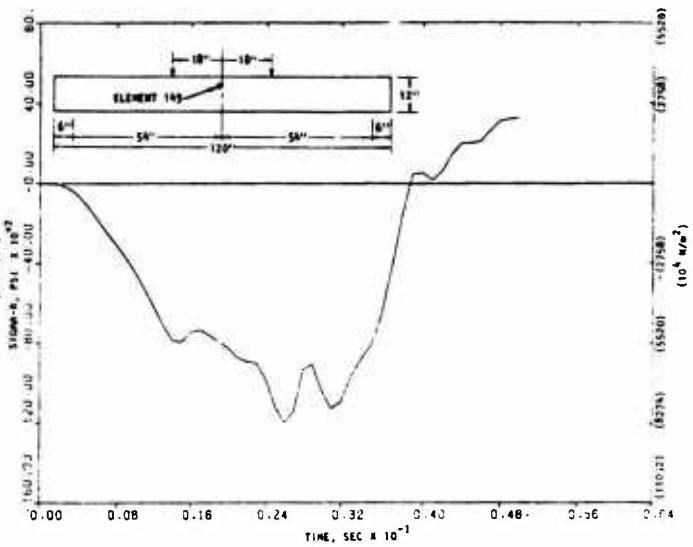

(j) Element 149 (compression reinforcement)

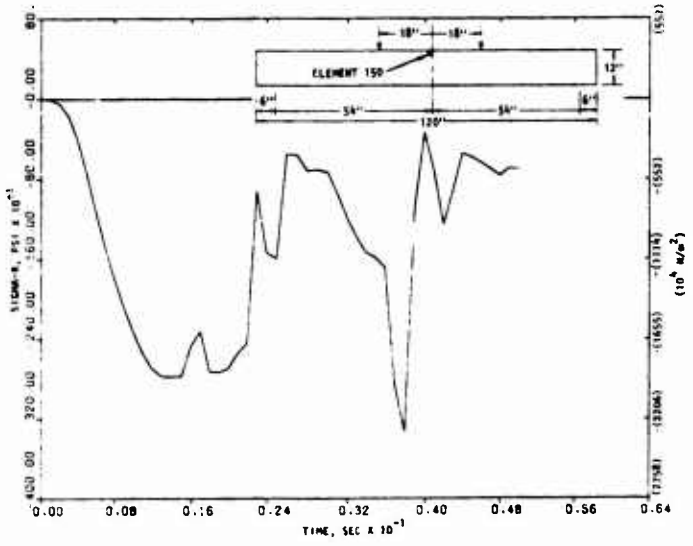

(k) Element 150

Figure 99. Dynamic Case D-4: Stresses in Beam 3b2 (concluded)

It should be emphasized that the calculated strains are the average strains in the element. Higher strains would be expected in the cracked portion of the element while lower strains would be expected in the portion of the element where the bond is still intact. As a result the calculated strains would be higher than the strains measured at the same points on the beam where the bond is still intact. In addition reference 91 has indicated that strain damage occurred in some cases such as steel bars of element 142 (Fig. 98). It should also be observed that in the compression zone the concrete strain may exceed the steel strain, as clearly illustrated in the experimental work reported in section V (Figs. 52, 53, and 54). Therefore the average strain in element 149 near the top of the middle of the beam should be higher than the strain in the compression steel of the same element as revealed by figure 98.

The crack pattern calculated at the end of the 50 msec of the first blow is shown in figure 100. This figure indicates that cracks cover almost the entire beam.

d. Discussion of Results of Case D-4

From the preceding results it can be concluded that the modified analytical model can predict the response of beam 3b2 (case D-4) in the ascending portion of the loading, but overestimates the response in the unloading and free-vibration periods.

Since the dynamic behavior of a beam is more affected by damping in the unloading and free vibration portions of the response, a discussion of the damping mechanism is necessary.

The present material package accounts only for the hysteretic damping generated by the inelastic material behavior. Another type of damping that can be incorporated in a dynamic model is viscous damping. This type of damping is important at later stages of loading and would participate in damping of the free vibrations of a beam. Therefore, the absence of the viscous portion of the damping appears to contribute to the overestimation of the free vibration response of the beam.

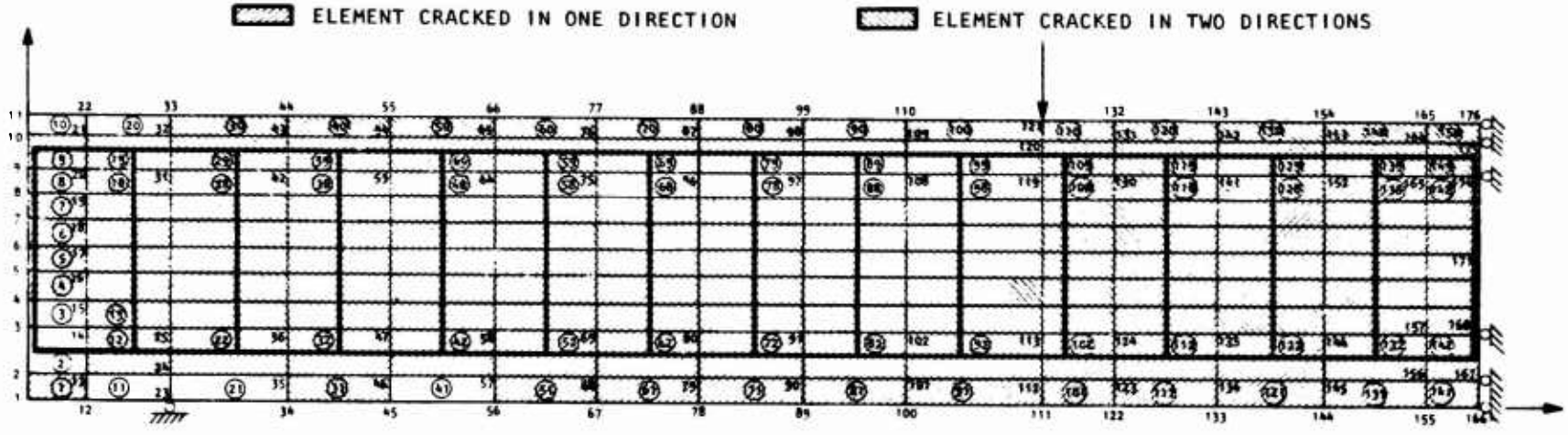

Figure 100. Dynamic Case D-4: Cracking Pattern at End of 50 msec

9. CASE S-1 (MODIFIED STATIC ANALYSIS OF REINFORCED CONCRETE BEAM 2S1.6-1 OF CRIST, REF. 89)

a. Introduction

The static response of beam S-1 (Fig. 56) was recalculated using the modified material package that was used earlier for the final dynamic analysis of case D-4. These results are also compared with both experimental measurements and original analysis results. Conclusions and recommendations are given at the end of this section.

b. Results of Modified Analysis

The results are shown in figure 101 and are compared to those obtained from both the original analysis and experiment (Ref. 89).

Figure 101 reveals that the modified analysis represents a considerable improvement over the original analysis. Collapse loads predicted by the modified analysis appear to correlate well with the experiment. Yielding occurs at approximately the same level of loading. Better correlation between calculated and measured displacements was also found in the postyielding range.

Figure 102 compares measured and calculated distribution of steel strain at the onset of yielding and at the collapse load. There is a general agreement between calculated and measured strains. However, since the analytical collapse load is taken as the load at which the solution begins to be unstable, the calculated strains must be interpreted within this approximation. The propagation of cracks in the deep beam is shown in figures 103 through 107. Figures 103 and 104 show the crack patterns calculated at 200 kips (890×10^3 N) loading by the original and modified versions respectively. The modified package appears to provide a better control of the cracks at this early stage of loading. However, figures 105, 106, and 107 indicate that the modified analytical model is affected by cracks over a wider area. Thus, it responds as a softer system, allowing better correlation between calculated and measured displacements.

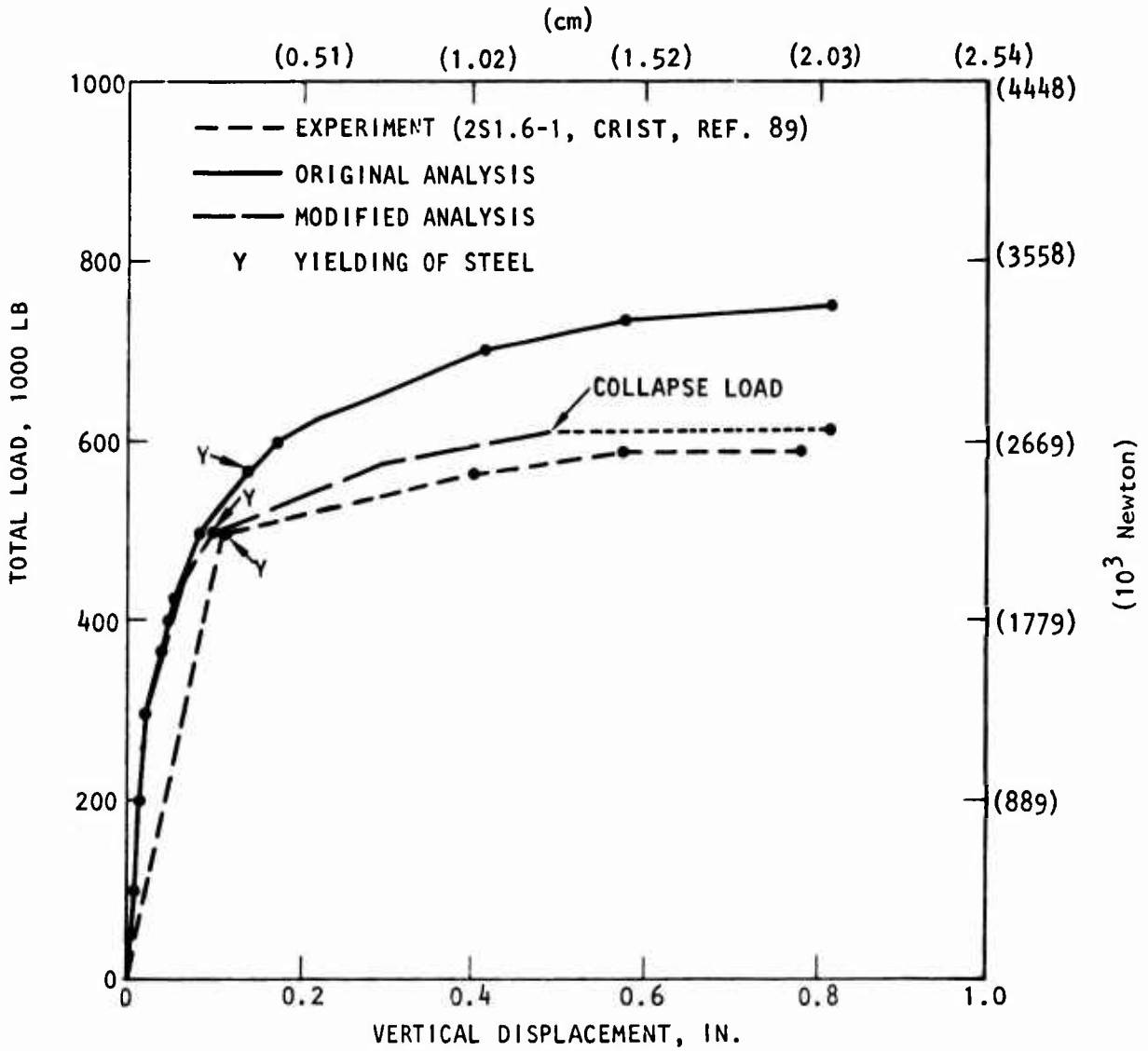

Figure 101. Comparison of Measured and Calculated (original and modified) Vertical Displacements at Midpoint of Beam 2S1.6-1, Case S-1

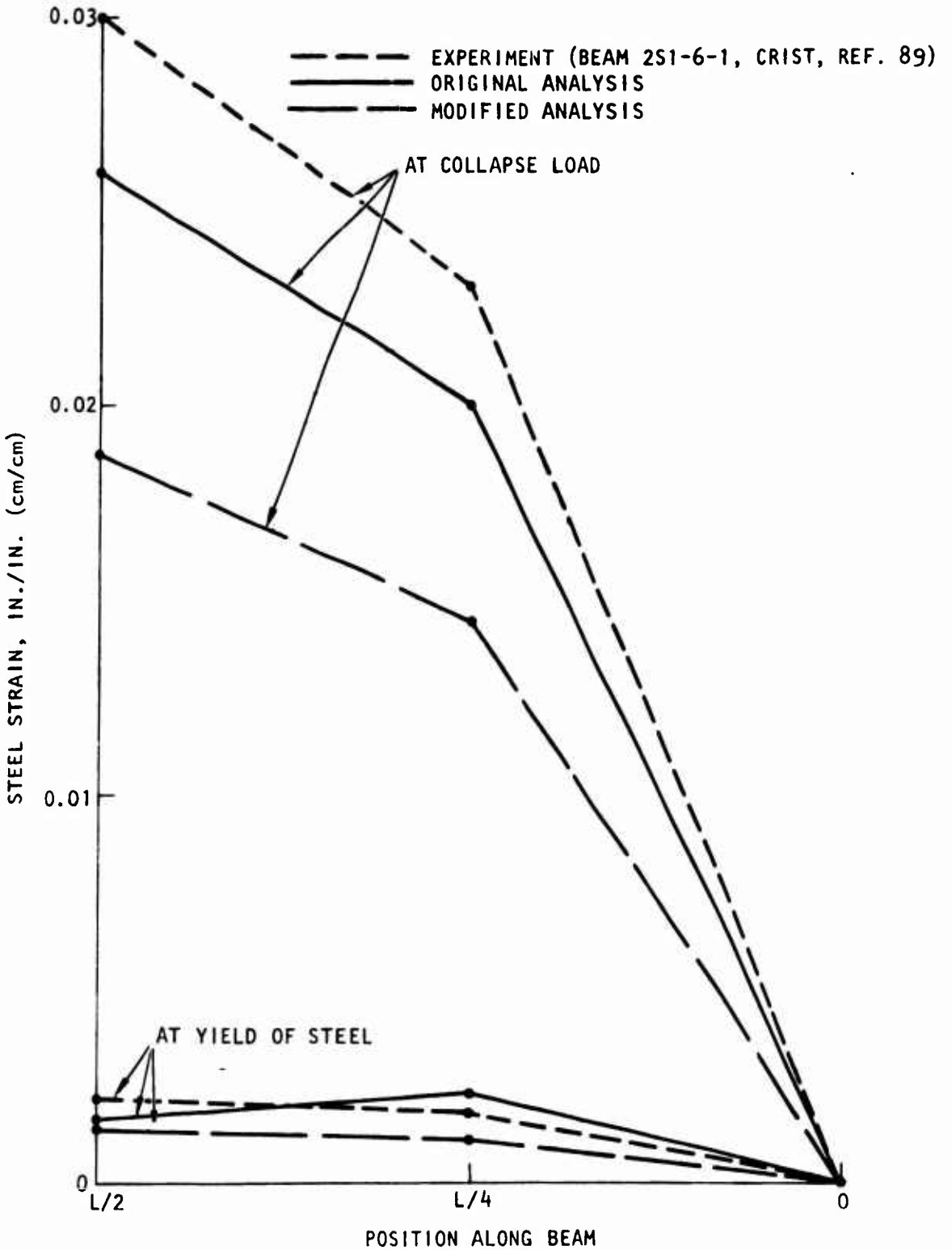

Figure 102. Comparison of Measured and Calculated (original and modified) Strains in Tension Steel, Beam 2S1.6-1, Case S-1

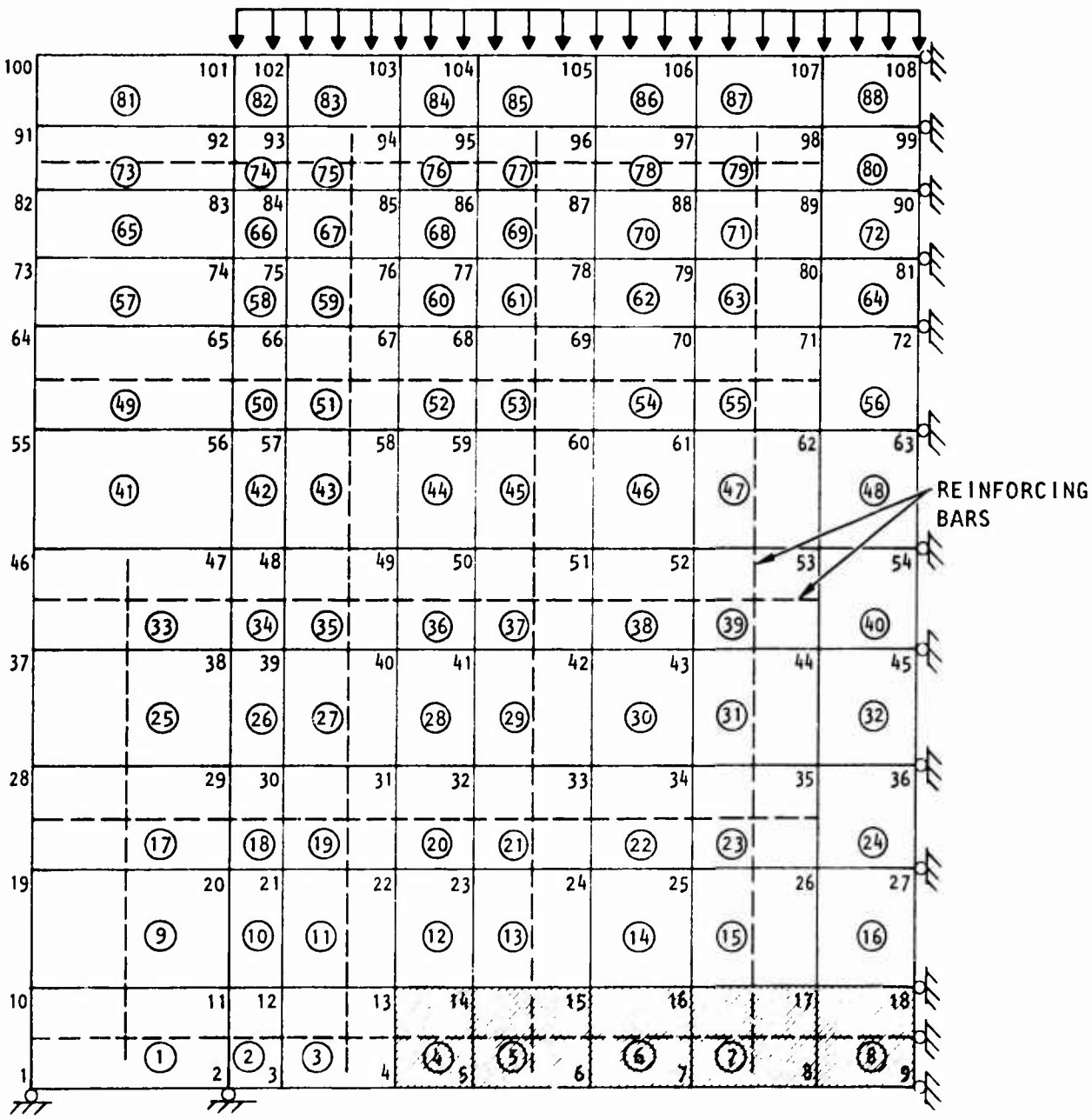

Figure 103. Crack Pattern Calculated by Original Version for Step 2 (200 kips), (890 x 10^3 N), Case S-1

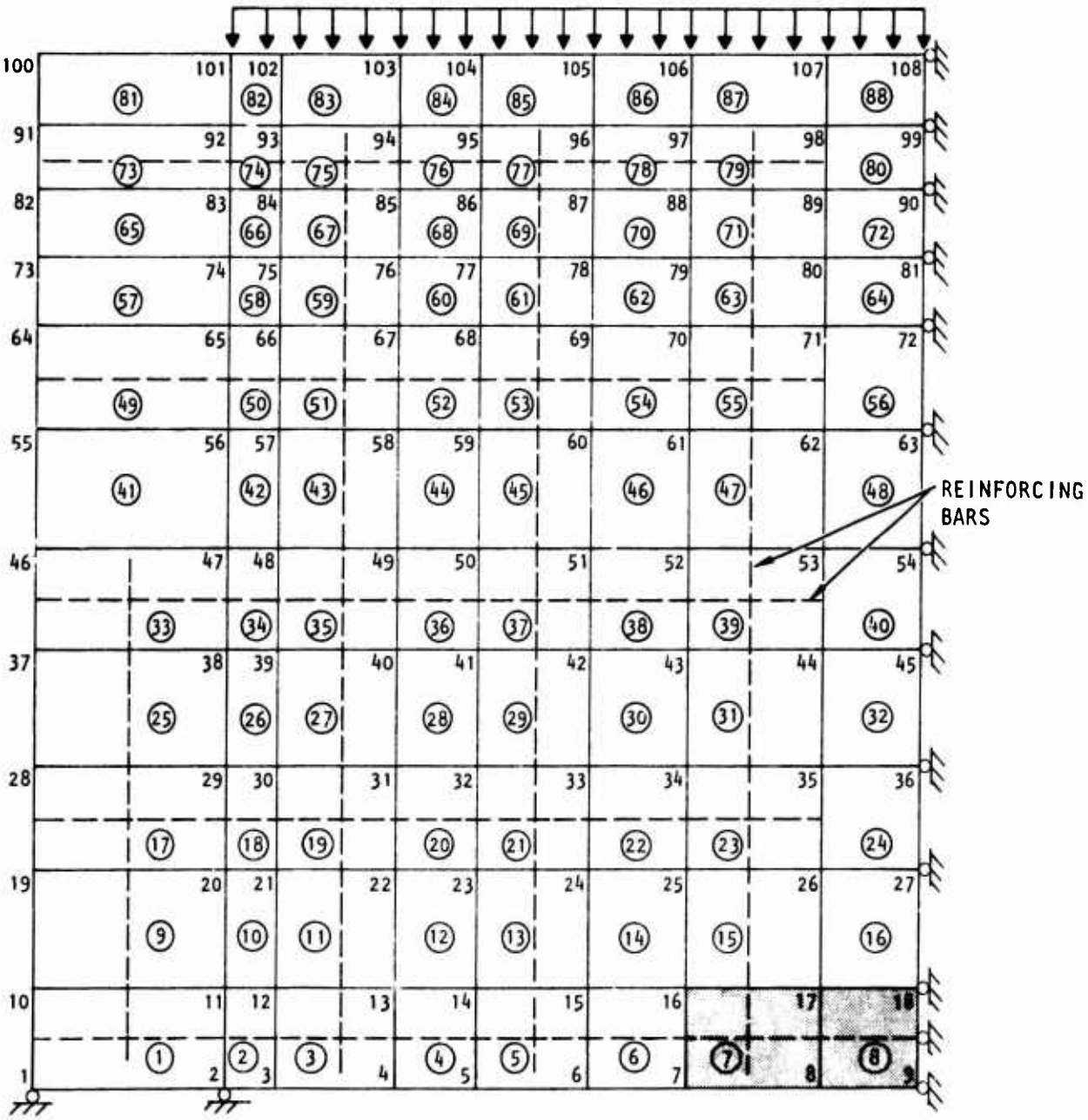

Figure 104. Crack Pattern Calculated by Modified Version for Step 2 (200 kips) (890×10^3 N), Case S-1

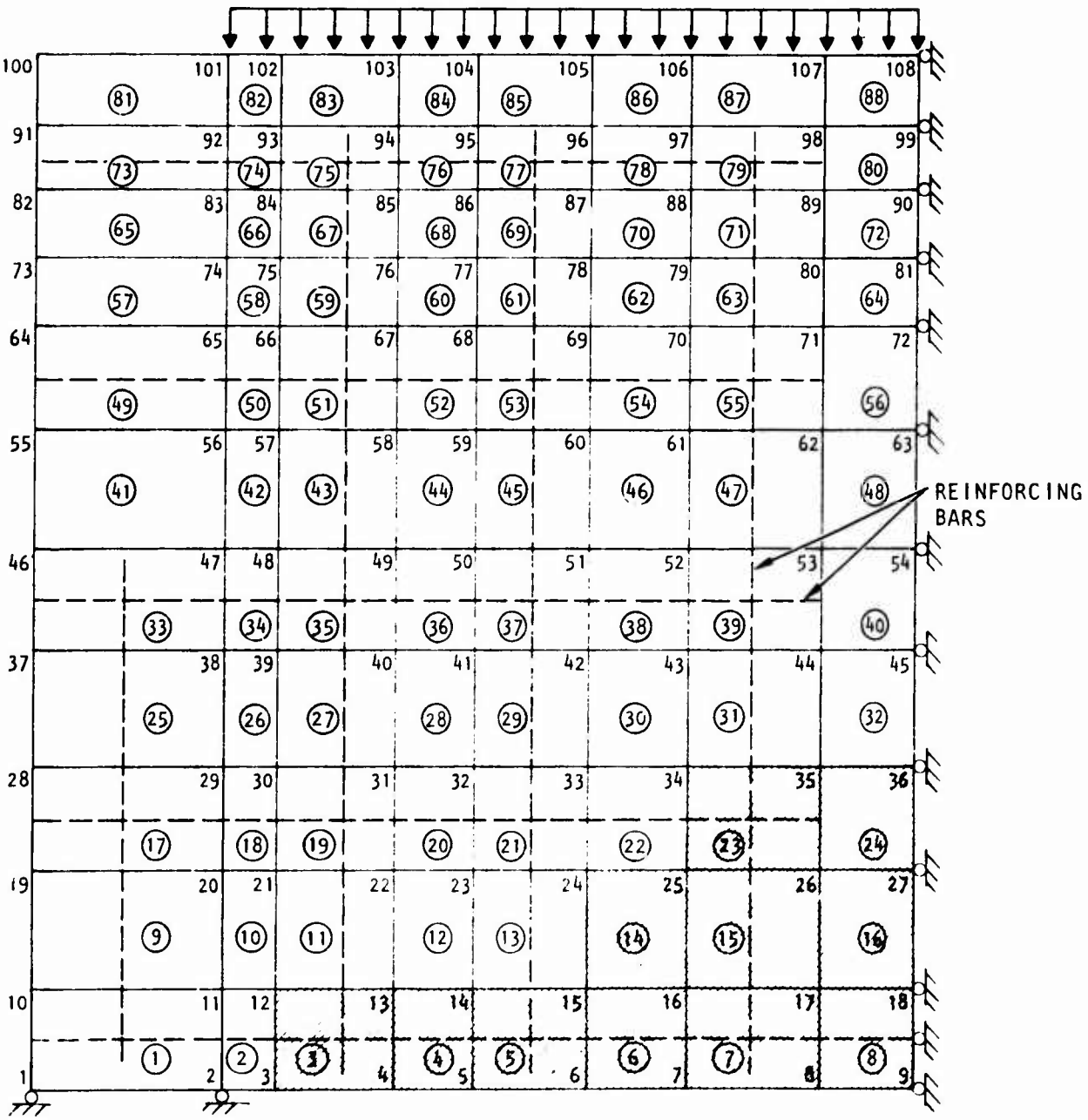

Figure 105. Crack Pattern Calculated by Original Version for Step 2 (300 kips) (1334 x 10^3 N), Case S-1

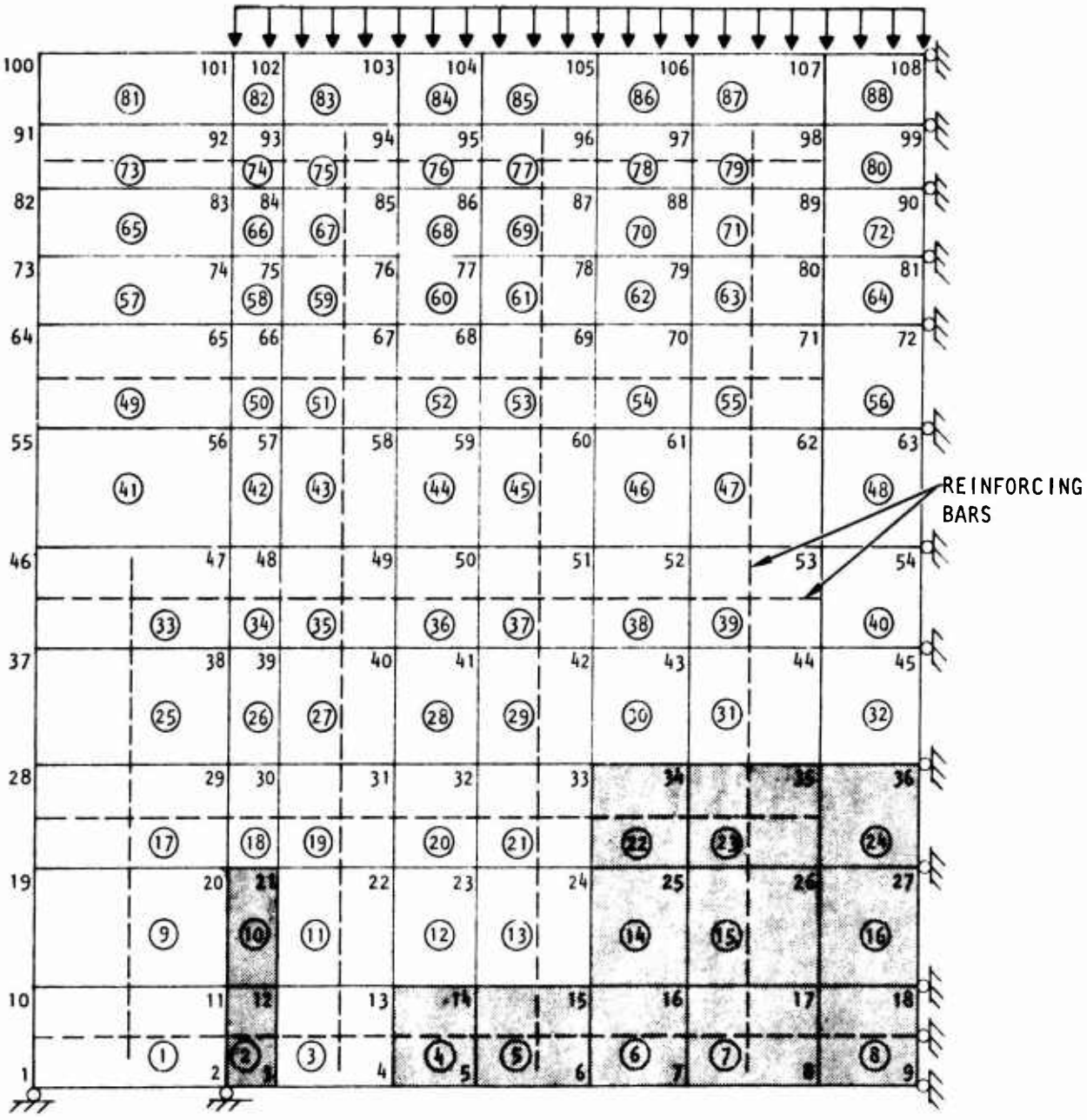

Figure 106. Crack Pattern Calculated by Modified Version for Step 2 (300 kips) (1334 x 10^3 N), Case S-1

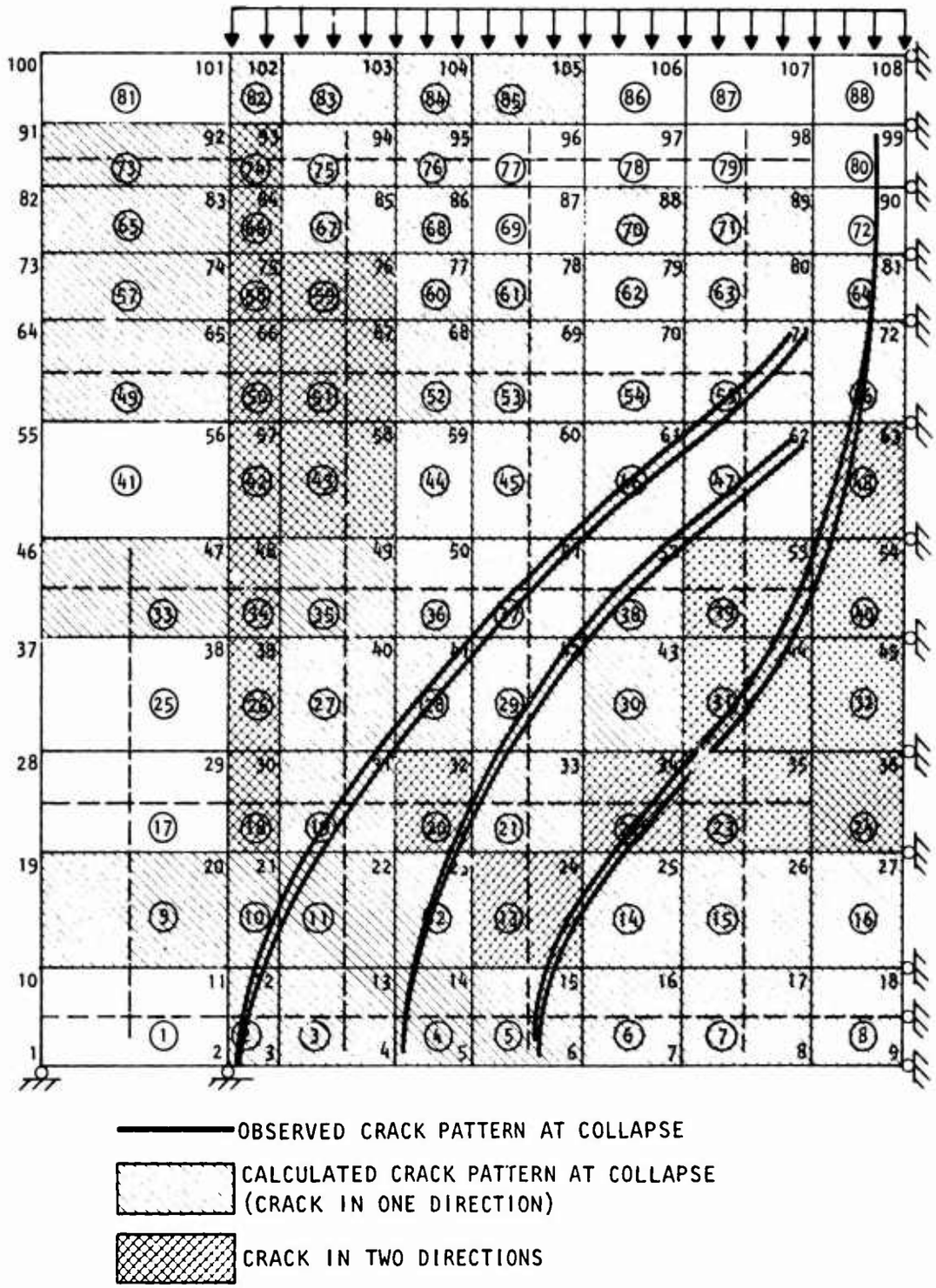

Figure 107. Comparison of Calculated (modified analysis) and Observed Crack Patterns at Collapse of Beam 2S1.6-1, Case S-1 (Crist, Ref. 89)

The results indicate that the modified model provides a better tool for predicting collapse load and deflection of static cases. However, overcracking was observed in the compression zone. Additional investigation of cracking under lateral confinement should be conducted, including comparative analysis for static and dynamic cases treated here. This will improve the prediction of crack formation and postcracking behavior.

SECTION VII

SUMMARY

The primary study objective was to incorporate recent advances in describing the behavior of plain and reinforced concrete in a computer program for analyzing plain or reinforced concrete structures. This objective was achieved in a three-step approach.

a. Pertinent analytical and experimental data that became available after the development of the original Isenberg/Adham model were reviewed and evaluated (Secs. II and III).

b. A material behavior package was prepared for incorporation in computer programs for analyzing typical reinforced concrete structures (Sec. IV and App. I).

c. A matrix of cases was considered to validate the material behavior package by comparing the analytical results with the experimental data obtained from different sources (Sec. VI).

Secondary objectives were satisfied by a test program conducted to support the development of a model of bond slip incorporated in the material behavior package. A final objective was the provision of guidelines for performing analyses of typical reinforced concrete structures with the computer package developed in this study.

1. ANALYTICAL MODEL

The analytical model developed under this contract is essentially an improved version of the Isenberg/Adham model (Ref. 1). The improvements were based on pertinent studies reviewed at the beginning of this contract. Two types of plain concrete stress/strain models were incorporated in the present model: (a) variable modulus model and (b) plastic-capped model. The virgin stress/strain relations incorporated in the variable modulus model were based

on those suggested by Liu, Nilson, and Slate (Ref. 53). However, only the ascending branch of the stress/strain relations was activated in this study. The steel reinforcement is specified as a number of steel sets in any three arbitrary directions. The pertinent experimental data on bond slip were fitted by a bilinear relation. The dowel action was accounted for by a simplified relation based on the work of Dulacska (Ref. 65). The properties of steel and concrete were combined to represent composite behavior at various phases of loading. Rebonding capability was incorporated in the code and was based on adjusting the stiffness of the element to avoid numerical instability of the solution.

2. EXPERIMENTAL STUDIES

Experimental studies on bond slip were performed under this contract to add to the sparse data that were available, to verify analysis assumptions on bond slip and, in addition, to provide some guidance for element size selection. Four cylindrical specimens, each reinforced with a coaxial piece of rebar, were subjected to tension and compression. Strain gages were attached to the reinforcing bar and to the surface of the concrete.

Results of tension tests were compared to those of Ismail and Jirsa (Ref. 66) and Tanner (Ref. 67). The results were also compared to the analytical relationships of reference 1 and the bilinear relationship used in this study.

The two specimens tested for bond slip in tension had a total length less than the 30-bar diameter required to develop full bond. Their behavior was characterized by three stages: (a) gradual deterioration of bond caused by end effects, (b) sudden loss of bond when major cracks occur, and (c) some recovery due to aggregate interlock, followed by gradual deterioration of bond.

The two specimens tested in compression indicated that the effective stiffness of steel can be reduced by as much as 36 percent by application of the ultimate load in compression. The analytical model developed under this study assumes full contribution of steel in compression.

3. RESULTS OF DEMONSTRATION CASES

The material package developed for this contract was incorporated in FEDIA, a dynamic inelastic, two-dimensional continuum, finite element code developed by Agbabian Associates. The demonstration of the capabilities of this package included nine cases. Static cases were completed for two uniformly loaded, reinforced-concrete deep beams (cases S-1 and S-2) and for three reinforced-concrete beam columns (cases S-3, S-4, and S-5). Four dynamic cases were completed. Case D-1 was performed with the deep beam of static case S-1. Case D-2 was for the beam column configuration of case S-3. The third dynamic case, D-3, was designed to demonstrate the capability of the code to model the behavior of buried, reinforced concrete silos. Case D-4 represents the behavior of reinforced-concrete beams under impact loading. In addition, one static and one dynamic case were repeated using a modified version of the reinforced concrete model. The results of these demonstration cases were compared to available experimental data.

The results of the original analyses for the static cases appear to predict most of the cracked regions. However, the general results indicate that the analytical model is stiffer than the experimental model. The analysis appears also to overestimate the collapse load by about 20 percent. The modified material package behavior, which incorporated changes in the criteria for the onset of tensile cracking, showed marked improvement in predicting both initial cracking and the collapse load in the reanalysis of case S-1.

The results of case D-1, the dynamic analysis of the deep beam, indicate general agreement with test results, except that the analysis greatly exaggerates the strain concentration at the points corresponding to cracking and plastic hinge development, i.e., the points at one-fourth, and three-fourths of the length of the beam. It should be noted that the strains obtained from the analysis are the average strains of the cracked and uncracked regions of the element. Since the strains in the cracked regions increase drastically with the increase in response, the average value of strain is expected to jump to a very high value. Comparable deviation of steel strain

was observed in the experimental work of Crist (Ref. 89). The proximity of the strain gages to the cracks was suggested as one of the causes of this deviation. Therefore, both analytical and experimental results appear to be least reliable at the cracks. Peak dynamic deflection was underestimated by a factor of about two. Crack patterns in the tensile region were in reasonable agreement with test results, but excessive cracking was predicted for the compression zone. No direct experimental data were available for comparison with the results of dynamic cases D-2 and D-3. However, the general character of the results indicates that the analytical model is applicable to both the beam column and buried structure configurations treated.

Overestimation of collapse loads, already evident from the static cases, and observation of anomalous crack initiation during the early stages of calculating the dynamic response of case D-4, led to modification of the composite model of reinforced concrete behavior. The results of the modified dynamic analysis of case D-4, indicated favorable agreement with experimental data in the ascending portion of the loading. Strain in the tensile steel and compressive strain in the concrete were in excellent agreement during this stage. However, the analysis was found to overestimate the response in the unloading and free-vibration phases. This was attributed to the higher effective stiffness of finite elements with higher steel ratios, which attracted higher stresses.

The original test for cracking, which predicted crack initiation in reinforced elements on the basis of average element stress, was replaced by a criterion based on concrete stress above. This produced initial cracking at the beam edge, in agreement with experimental observation. Also, cracking in the compression region was found to be sensitive to the interaction of lateral stresses. Therefore, the criteria were modified to eliminate unrealistic cracks in the compression zone. Case D-4 was then reexamined using the improved reinforced concrete model.

The design of finite element meshes for the nine demonstration cases was guided by factors that included (a) uniform distribution of compression and tension steel, as well as stirrups in all elements, (b) elements wide enough to provide full bond at the start of the loading and to allow primary cracks to develop within the element, (c) elements small enough to allow for adequate description of stress and/or strain gradients, (d) integration time-step in a dynamic solution small enough to allow resolution of the dynamic input with sharp rises, and (e) budget limitations on size of problem and the number of integration time steps.

SECTION VIII

CONCLUSIONS AND RECOMMENDATIONS

1. CONCLUSIONS

From the previous discussion, the following conclusions can be summarized.

a. The experiments performed as part of this study presented additional data for the interpretation of the bond-slip behavior of reinforced concrete members. Concrete strength and load history appear to have a significant effect on bond-slip relations in tension. For bond-slip in compression, the present experimental results indicate that perfect bonding may not exist. Some reduction in the effective stiffness of steel in compression is expected.

b. The composite material model that was incorporated in a finite element computer program provided numerical solutions that were in general agreement with experimental results. In general the numerical solutions overestimated the stiffness and collapse loads. Agreement between analytical and experimental results was better for static than for dynamic cases.

c. In the two examples for which a more refined material model was used for comparison with earlier analyses of this study, considerable improvement was observed. The refined static analysis of case S-1 resulted in improved prediction of collapse load, while the refined dynamic analysis of case D-4 resulted in good correlation with measured displacements for the loading portion of the input. The refined model incorporates the following changes: (1) onset of cracking is described by the concrete stress rather than the average element stress, (2) initiation of cracking by numerical noise in regions of compressive confining stresses was avoided by introducing a "noise" filter, (3) sudden increase of strain at the onset of cracking was incorporated by dropping the concrete stress level in the element immediately after cracks are initiated, (4) rebonding capability was included.

d. The authors feel that without introducing additional damping mechanisms, the model is incapable of providing good correlation with experimental observations of dynamic behavior in the unloading and free-vibration portions of the response.

e. Onset of cracking and propagation of cracks depend to some extent on the distribution of finite elements and percent of steel in these elements.

f. Long elements in the tensile region allow better description of the bond at the beginning of loading, while shorter elements may underestimate the role of the concrete prior to cracking.

g. Smaller size elements allow better description of the response in regions of high stress or strain gradient.

h. Shorter integration time steps would allow more accurate description of the initial response to short rise-time dynamic input.

2. RECOMMENDATIONS

The results of the matrix of demonstration cases indicate that several areas need further study. It is recommended that improvements be made in the material package that would lead to better correlation between computed response and experimental observations. The recommended improvements and studies are summarized in the following:

a. Additional dynamic cases for which experimental measurements are available should be studied with the modified material package to determine the importance of damping mechanisms not presently accounted for.

b. The effects of finite element size and distribution and steel percent on the analysis results need more detailed examination.

c. The details of concrete strength under multiaxial loading, dowel action, bond slip, variation of Poisson's ratio, and rebonding need further experimental and analytical investigation.

d. The feasibility of using other elements in the composite model to describe (a) crack initiation and (b) failure under multiaxial stress conditions, as well as alternative forms of the basic constitutive relations that avoid limitations of the Liu, Nilson, and Slate formulation (Ref. 53) adopted here, should be investigated.

APPENDIX I

USER'S GUIDE AND DESCRIPTION OF THE COMPUTER PROGRAM MATPAC

1. INTRODUCTION

A material model package consisting of a set of subroutines has been developed for plain and reinforced concrete. Two types of models defining the constitutive properties of concrete have been incorporated in this package. These two types of models are

- Variable modulus model
- Capped plastic model

The routines are designed to be used with finite element or finite difference codes and can handle plane stress, plane strain, axisymmetric, and three-dimensional solids. Both models are capable of handling plain concrete. However, only the variable modulus model is equipped to handle cracked reinforced concrete.

The code calculates stress and strain at the end of the current step based on the current strain as stress increment. Incremental tangent stress/strain relations are also calculated.

The code is accessed by call to subroutine MATPAC with proper arguments whenever stress or tangential stress/strain relationships are necessary. The code operates on stress or strain increments.

The important options of the code are tabulated below.

a. Variable modulus model or plastic-capped model controlled by variable ICOMPS

b. Plane stress, plane strain, axisymmetric or three-dimensional state of stress controlled by variable NELTYP

c. Steel orientation in global or prescribed directions controlled by variable NRB

d. Stress increment input or strain increment input options controlled by the sign of variable NSPLIT

e. Splitting of stress or strain increments for better accuracy controlled by the magnitude of variable NSPLIT

The controlling variables are defined in section 2, with suggested guidelines for choice of material properties. Guidelines for variable initialization and storage are also included.

A brief description of each subroutine and its functions is included in section 3. Section 4 contains the program flow charts. The listings of the routines are given in section 5.

Examples using the stress increment option and the strain increment option are shown in section 6. Section 7 contains the listing of the main program for testing the MATPAC program.

2. DEFINITION OF VARIABLES

The variables used as arguments of the material package (MATPAC) are described in detail below and in table VIII on page 221.

STRESS The six components of stress are stored in this location. In rectangular coordinate system the stress components are stored in the following order: $[\sigma_x, \sigma_y, \sigma_z, \tau_{xy}, \tau_{yz}, \tau_{zx}]$. In plane stress and plane strain problems the last two components are not used. In cylindrical coordinate system (r, z, θ) the stress components are arranged as follows: $[\sigma_r, \sigma_z, \sigma_\theta, \tau_{rz}, \tau_{z\theta}, \tau_{\theta r}]$. For axisymmetric problems the last two components are not used.

STRAIN The six strain components are stored in this location. The strain components are arranged in the same order as STRESS.

STRINC The incremental stress (NSPLIT $>$ 0) or the incremental strain (if NSPLIT $<$ 0) components are stored in this location. The components are arranged in the same order as STRESS.

EPSEL For the plastic-capped model the elastic strain components are stored in this location. For the variable modulus model strain components are stored in this location to indicate loading or unloading paths.

COEFF Fifteen constants defining material property for reinforced concrete for the variable modulus model are stored in this location. The arrangement of the properties is as follows:

CØEFF(1) = E_c, initial modulus of elasticity for concrete

CØEFF(2) = E_s, modulus of elasticity for steel

CØEFF(3) = $|f'_c|$, ultimate compressive strength of concrete

CØEFF(4) = f_y, yield strength of steel

CØEFF(5) = ν, Poisson's ratio for concrete

CØEFF(6) = f_t, cracking strength of unconfined concrete in tension

CØEFF(7) = n, a constant reflecting change in cracking stress due to confinement ($\sigma_{crack} = f'_t - n*\sigma$, σ = nonpositive confinement) = f_t/f'_c = negative quantity

CØEFF(8) = n, dowel coefficient of local compression for shear (usually of the order 4.0) see equation 62

CØEFF(9) = G_s, shear modulus for steel

CØEFF(10) = Fraction of E_c during rebonding after crack (recommended value $\leq$ 0.5)

CØEFF(11 through 15) = Currently not used

BLKMOD Bulk modulus for concrete (used only for plastic-capped model)

SHRMOD Shear modulus for concrete (used only for plastic-capped model)

YCOF Twenty-five material constants defining the plastic-capped model are stored in this location. The values suggested for these material

parameters for a concrete with an ultimate unconfined compressive strength of f'_c (in psi, or English units) are as follows:

YCØF(1) = $\left|\frac{f'_c}{7}\right|$

YCØF(2) = 12.2

YCØF(3) = 11.0

YCØF(4) = 40000.0

YCØF(5) = 800.0

YCØF(6) = 700.0

YCØF(7) = 2.0

YCØF(8) = 1.0×10^{-6}

YCØF(9) = 100.0

YCØF(10) = 120.0

YCØF(11) = 1.0×10^{-4}

YCØF(12) = 2.0

YCØF(13) = 7.0×10^{-5}

YCØF(14) = $-2.4 \times 10^{-4} \times \left|\frac{f'_c}{7000}\right|$

YCØF(15) = 4000.0

YCØF(16) = 8.0×10^{15}

YCØF(17) = $-7.02 \times 10^{-12} \times \left|\frac{f'_c}{7000}\right|$

YCØF(18) = 1.35×10^{13}

YCØF(19) = 6.0×10^{4}

YCØF(20) = 0.0005

YCØF(21), YCØF(22), YCØF(23) = 0 (not currently used)

YCØF(24) = 0

YCØF(25) = 5.0×10^{7}

DC A 3 x 3 direction cosine table indicating principal orthotropic or cracked directions (for variable modulus model only)

DCS A 3 x 3 direction cosine table indicating steel orientation if different from global coordinate directions (for variable modulus model only).

1st column	direction cosine of 1st steel direction
2nd column	direction cosine of 2nd steel direction
3rd column	direction cosine of 3rd steel direction

The steel directions need not be mutually orthonormal.

AST Steel ratios $\left(\frac{\text{Steel area}}{\text{Total cross-sectional area}}\right)$

AST(1) Steel ratio in direction 1

AST(2) Steel ratio in direction 2

AST(3) Steel ratio in direction 3

(for variable modulus model only)

NRB A flag. If NRB $\leq$ 0, the steel directions are assumed to be in the global coordinate directions. If NRB > 0, steel is oriented in specified directions indicated by DCS (for variable modulus only).

ZK1,ZK2 Cap parameters to be stored for the plastic-capped model.

SI2P Second plastic deviatoric strain invariant to be stored for the plastic-capped model.

ICOMPS A flag.

ICØMPS = 1 for variable modulus model

ICØMPS = 2 for plastic-capped model

NELTYP Type of problem

NELTYP =	+3	for plane stress problem
=	-3	for plane strain problem
=	4	for axisymmetric problem
>	4	for general 3-D problem

C — A 6 x 6 incremental stress/strain transformation matrix.

$$-d\sigma = C\, de$$

For plane stress, plane strain, and axisymmetric problems the first 4 x 4 block of the C-matrix is used.

ICRACK — A counter designating number of cracked planes for variable-modulus model.

ICRACK = 0 (uncracked concrete)
= 1 (1 plane cracked)
= 2 (2 $\perp$ planes cracked)
= 3 (3 $\perp$ planes cracked)

NSPLIT — A flag designating stress increment or strain increment input. The flag also designates the number of splits made to the stress or strain increment (for variable modulus model only).

If NSPLIT < 0, strain increment input and
|NSPLIT| = Number of splits

If NSPLIT > 0, stress increment input and
|NSPLIT| = Number of splits

The following quantities must be initialized to zero. The material package updates these quantities.

STRESS, STRAIN, EPSCL, DC*, ZK1**, ZK2**, SIZP**, ICRACK*

The following quantities must be stored for each element (or points where stress is calculated).

STRESS, STRAIN, EPSEL, DC*, ZK1**, SI2P**, ICRACK*, AST*, DCS*, NRB*

---

*Applicable for variable modulus model only.

**Applicable for plastic-capped model only.

Table VIII. Definition of Arguments of Program MATPAC

Argument	Size	Definition
STRESS	6	Stress components. The routine updates the stress.
STRAIN	6	Strain components. The routine updates the strains.
STRINC	6	Strain increments or stress increments based on NSPLIT
EPSEL	6	Elastic strains.** The routine updates the elastic strains.
CØEFF*	15	Coefficients defining material property (see next page).
BULKMØD**	1	Bulk modulus of concrete.
SHRMØD**	1	Shear modulus of concrete.
YCØF**	25	Yield coefficients defining capped yielding of concrete
DC*	3 x 3	Direction cosines of cracked directions. (If NRB > 0)
DCS*	3 x 3	Direction cosines for steel directions.
AST*	3	Steel ratios as fraction of cross-sectional area
NRB*	1	A flag. NRB ≤ 0 steel in global coordinates (DCS not necessary). NRB > 0 steel in direction DCS.
ZK1**	1	Constant in first yield surface.
ZK2**	1	Constant in second yield surface.
SI2P**	1	Second plastic deviatoric strain invariant.
IØOMPS	1	A flag. ICØMPS = 2, for capped plastic model. ICØMPS = 1, for variable modulus model.
NELTYP	1	Type of problem. NELTYP = 3 for plane stress = -3 for plane strain = 4 for axisymmetric > 4 for 3-dimensional stress
C	6 x 6	Tangent stiffness relating stress/strain increments ($d\sigma = Cd\varepsilon$).
ICRACK*		A counter designating number of cracked planes.
NSPLIT	1	A flag. NSPLIT < 0, strain increment input option NSPLIT > 0, stress increment input option The stress or strain increments are subdivided by |NSPLIT|. For better accuracy |NSPLIT| may be increased.

*Applicable for variable modulus model only.

**Applicable for plastic capped model only.

The following quantities must be stored for each different material.

COEFF*, BLKMOD**, SHRMOD**, YCOF**

The following flags must be appropriately set.

ICOMPS to exercise the variable modulus model or the plastic-capped model

NSPLIT to exercise the stress increment input or the strain increment input options

3. SUBROUTINES AND THEIR FUNCTIONS

The material property package contains 22 subroutines. The functions of each of these routines are described below. The routines appear in alphabetical sequence.

(1) Subroutine CADJST

CADJST adjusts the C-matrix defining incremental stress/strain relationship for plane-stress problems. CADJST is called from subroutine ELFUNN.

(2) Subroutine CHANGE

CHANGE interchanges orthotropic coordinate axes such that axis normal to cracked planes always precede axis normal to uncracked planes. CHANGE is called from subroutine CRACKS.

(3) Subroutine COMPOS

COMPOS calculates composite modulus of steel and concrete in directions normal to cracks according to equation 79. COMPOS is called from subroutine VARMOD.

---

*Applicable for variable modulus model only.

**Applicable for plastic-capped model only.

(4) Subroutine COMPUT

COMPUT computes incremental stress by premultiplying incremental strains by the C-matrix. It then updates the stress vector. COMPUT is called from subroutine ELFUNN.

(5) Subroutine CRACKS

CRACKS checks for crack-initiation in principal orthotropic directions. CRACKS calls subroutine CHANGE to reorder coordinate system. CRACKS is called from subroutine ELFUNN.

(6) Subroutine CTRANF

CTRANF transforms C-matrix from orthotropic to global coordinate directions. Transformation procedures are described in section IV. CTRANF is called from ELFUNN.

(7) Subroutines DOWEL1 and DOWEL2

DOWEL1 and DOWEL2 calculate shear stiffness due to dowel action. These routines are called from subroutine VARMOD.

(8) Subroutine ELFUNN

ELFUNN is a major subroutine of the package. ELFUNN calls PRNSTR to evaluate principal stresses and directions, calls TRANSF to evaluate coordinate transformation matrices, calls MATPLY to convert stress and strain from one coordinate system to another, calls MAXMIN to evaluate principal stress directions in a plane, calls CRACKS to determine cracked planes if any, calls STLTRN to transform steel ratios from steel directions to principal orthotropic directions, calls VARMOD to evaluate the C-matrix in principal orthotropic directions, calls CTRANF to convert C-matrix from principal orthotropic direction to global direction, calls COMPUT to compute incremental stress from incremental strains, and calls PLASTK for the capped plastic model computations. ELFUNN is called from MATPAC.

(9) Subroutine FORMC

FORMC formulates the C-matrix (Eq. 71) in the principal orthotropic directions. FORMC is called from subroutine VARMOD.

(10) Subroutine JACOBI

JACOBI is a standard subroutine to find eigenvalues and eigenvectors. It is used here to find the principal stresses and their directions. JACOBI is called from subroutine PRNSTR.

(11) Subroutine LODUN

LODUN determines loading or unloading/reloading in directions normal to cracked planes. LODUN is called from subroutine VARMOD.

(12) Subroutine MATPAC

MATPAC controls the material package program. It bifurcates the program for the stress and strain increment options. It calls ELFUNN to obtain stress from strain increment and SOLVEX to convert stress increment to corresponding strain increments.

(13) Subroutine MATPLY

MATPLY is a matrix multiplication routine used to transform stress and strain from one coordinate system to another. MATPLY is called from subroutine ELFUNN.

(14) Subroutine MAXMIN

MAXMIN calculates the principal stress directions in a plane. MAXMIN is called from subroutine ELFUNN.

(15) Subroutine MODULI

MODULI calculates the tangent modulus of uncracked concrete in compression according to equation 29. MODULI is called from subroutine VARMOD.

(16) Subroutine PLASTK

PLASTK calculates stress increments from strain increments based on the plastic capped model. PLASTK is called from subroutine ELFUNN.

(17) Subroutine PRNSTR

PRNSTR evaluates principal stresses and directions. PRNSTR calls JACOBI to solve the general eigenvalue problem. PRNSTR is called from ELFUNN.

(18) Subroutine REBOND

REBOND checks for rebonding after a crack is intiated. If rebonding occurs, the concrete modulus is set to a user-specified fraction of the initial concrete modulus. REBOND is called from VARMOD.

(19) Subroutine SOLVEX

SOLVEX is an equation-solver routine using Gaussian reduction techniques. SOLVEX converts stress increments to corresponding strain increments. SOLVEX is called from MATPAC.

(20) Subroutine STLTRN

STLTRN transforms steel ratios from original steel directions to the principal directions of orthotropy. Transformation principles are discussed in section IV. STLTRN is called from ELFUNN.

(21) Subroutine TRANSF

TRANSF evaluates transformation matrices for stress and strain in order to change from one coordinate system to another. Transformation principles are discussed in section IV. TRANSF is called from subroutine ELFUNN.

(22) Subroutine VARMOD

VARMOD computes the tangent stress-strain relationship for the variable modulus model.

VARMOD calls LODUN to check loading/unloading in cracked directions; calls COMPOS to obtain composite modulus in directions normal to cracked planes, calls MODULI for tangent moduli in directions normal to uncracked planes, calls DOWEL1 and DOWEL2 for shear stiffness due to dowel action, and finally calls FORMC to assemble the C-matrix defining incremental stress-strain relationship. VARMOD is called from ELFUNN.

4. FLOW CHARTS FOR MATPAC PROGRAM

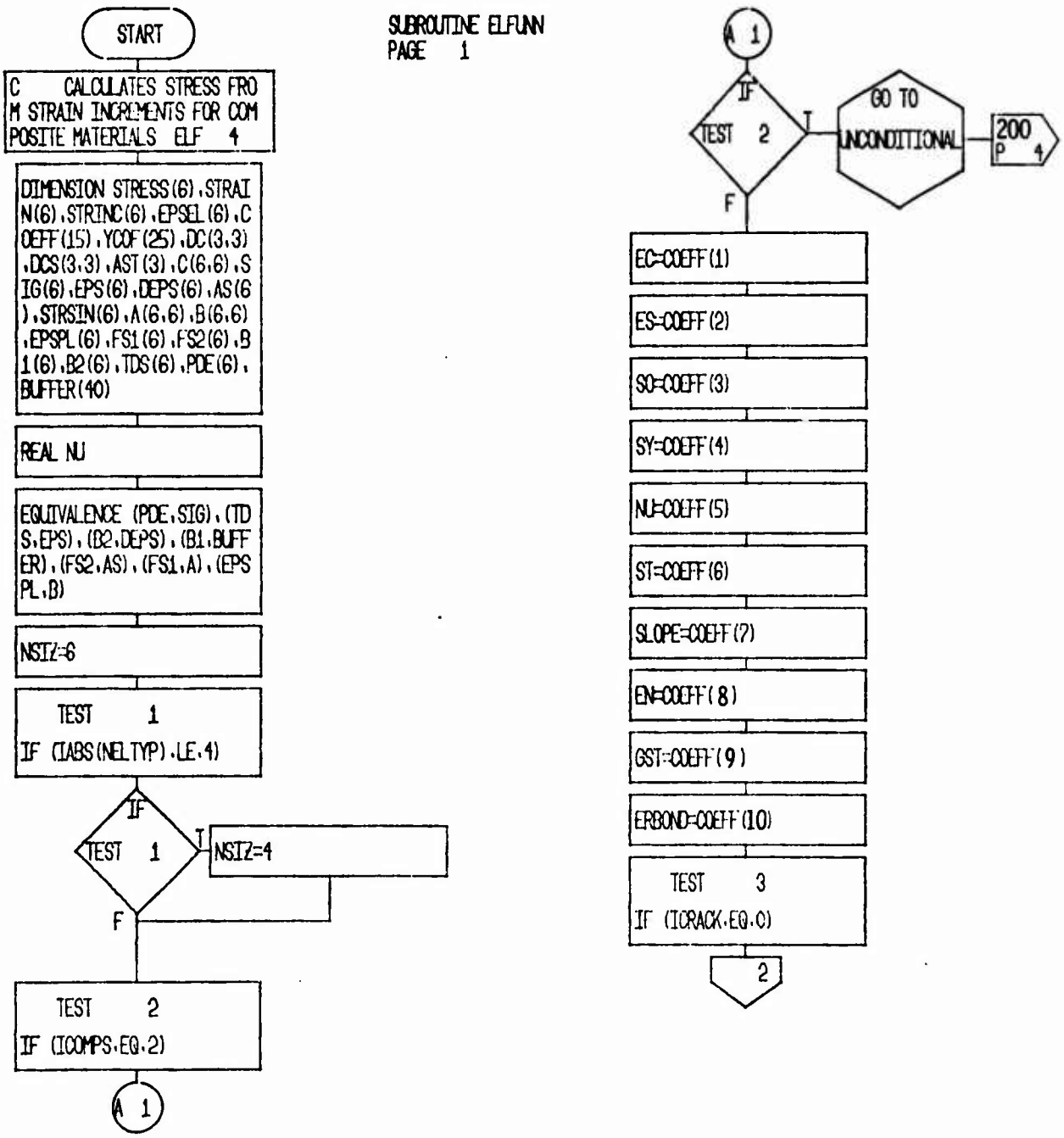

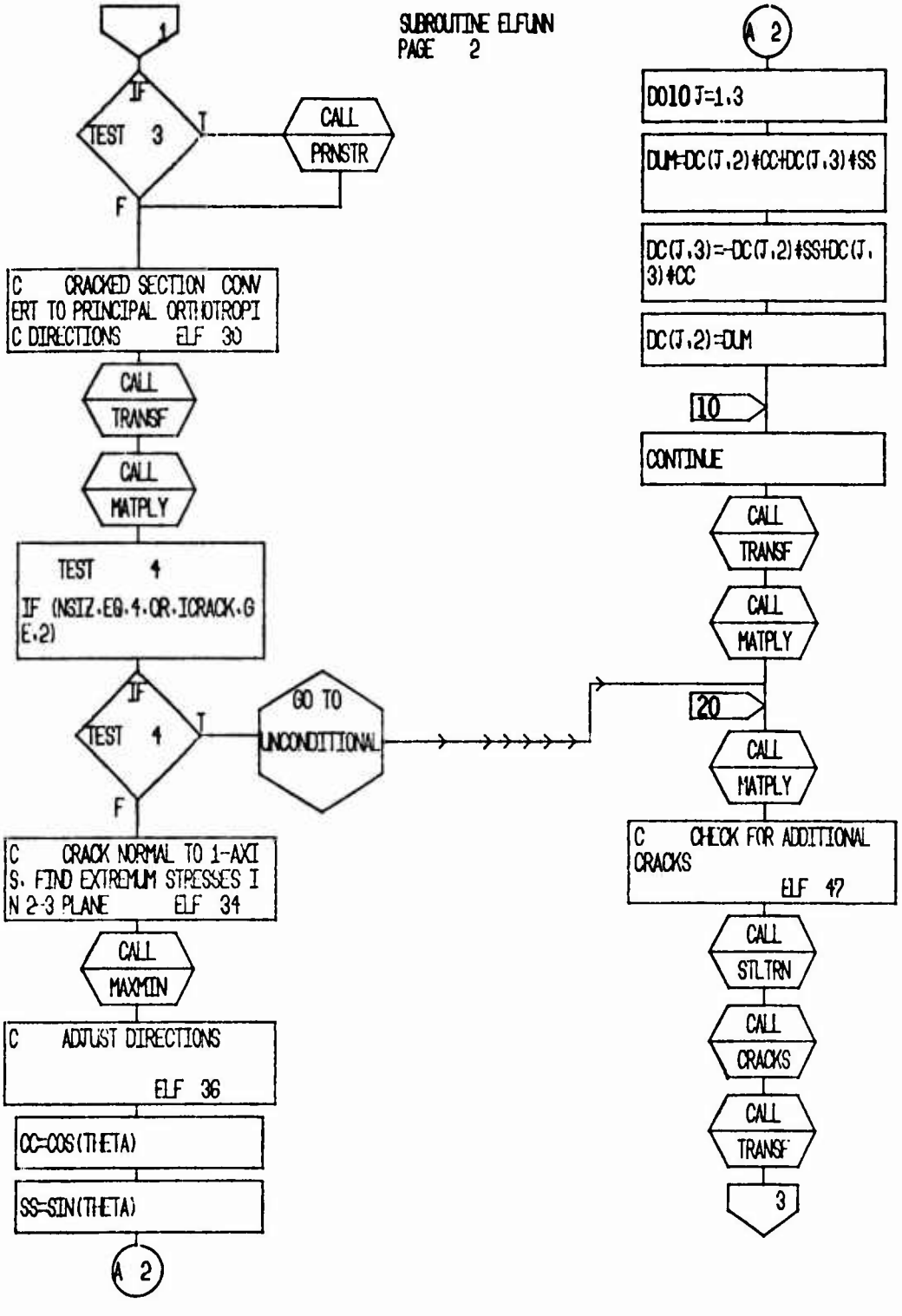
SUBROUTINE ELFUNN
PAGE 2
1
IF
TEST 3
T
CALL
PRNSTR
F
C CRACKED SECTION CONV
ERT TO PRINCIPAL ORTHOTROPI
C DIRECTIONS ELF 30
CALL
TRANSF
CALL
MATPLY
TEST 4
IF (NSIZ.EQ.4.OR.ICRACK.G
E.2)
IF
TEST 4
T
GO TO
UNCONDITIONAL
F
C CRACK NORMAL TO 1-AXI
S. FIND EXTREMUM STRESSES I
N 2-3 PLANE ELF 34
CALL
MAXMIN
C ADJUST DIRECTIONS
ELF 36
CC=COS(THETA)
SS=SIN(THETA)
A 2
A 2
DO10 J=1,3
DUM=DC(J,2)*CC+DC(J,3)*SS
DC(J,3)=-DC(J,2)*SS+DC(J,
3)*CC
DC(J,2)=DUM
10
CONTINUE
CALL
TRANSF
CALL
MATPLY
20
CALL
MATPLY
C CHECK FOR ADDITIONAL
CRACKS
ELF 47
CALL
STLTRN
CALL
CRACKS
CALL
TRANSF
3

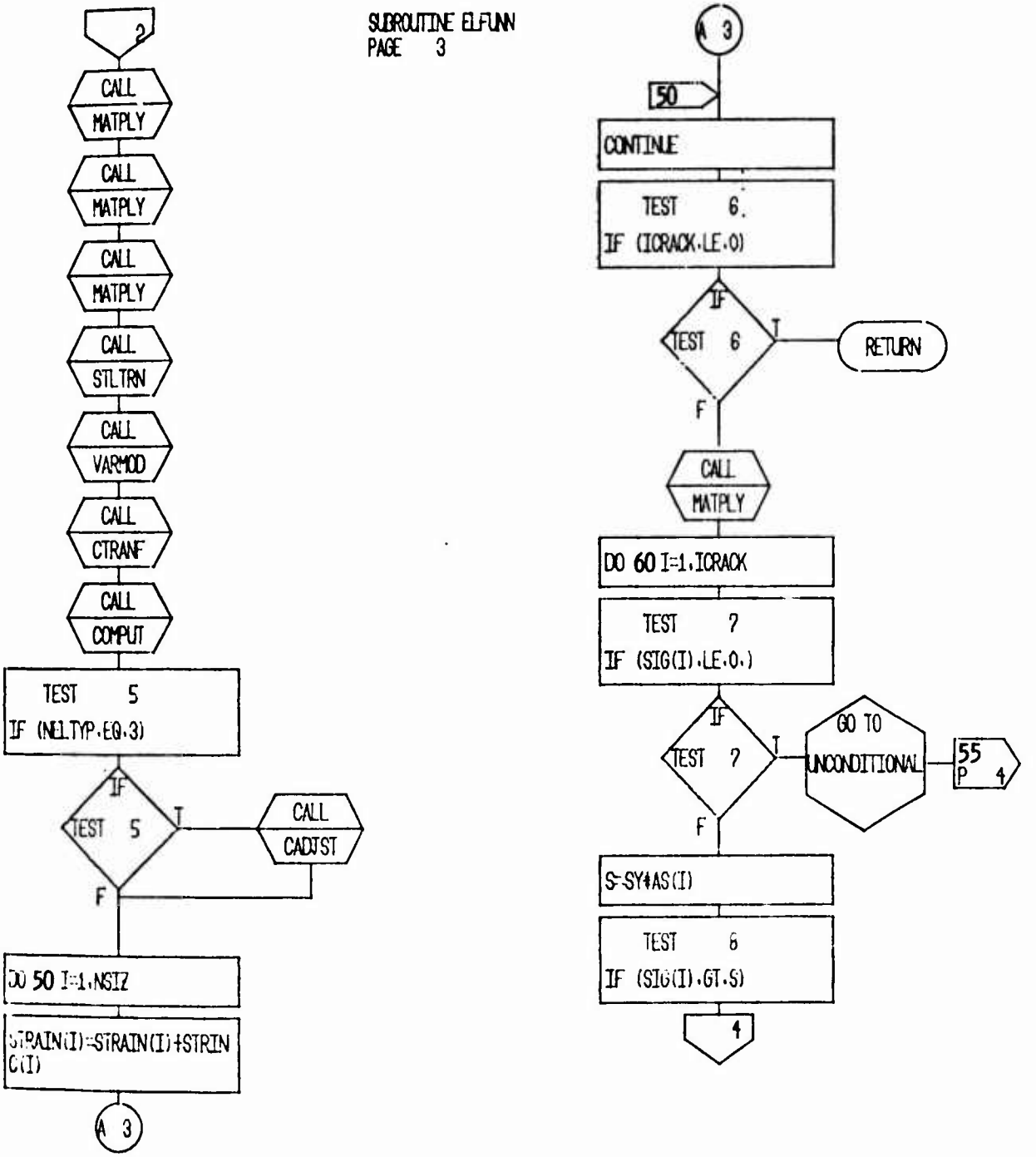
2
CALL MATPLY
CALL MATPLY
CALL MATPLY
CALL STLTRN
CALL VARMOD
CALL CTRANF
CALL COMPUT
TEST 5
IF (NELTYP.EQ.3)
IF TEST 5
T
CALL CADJST
F
DO 50 I=1,NSIZ
STRAIN(I)=STRAIN(I)+STRIN C(I)
A 3
A 3
50
CONTINUE
TEST 6.
IF (ICRACK.LE.0)
IF TEST 6
T
RETURN
F
CALL MATPLY
DO 60 I=1,ICRACK
TEST 7
IF (SIG(I).LE.0.)
IF TEST 7
T
GO TO UNCONDITIONAL
55 P 4
F
S=SY*AS(I)
TEST 6
IF (SIG(I).GT.S)
4

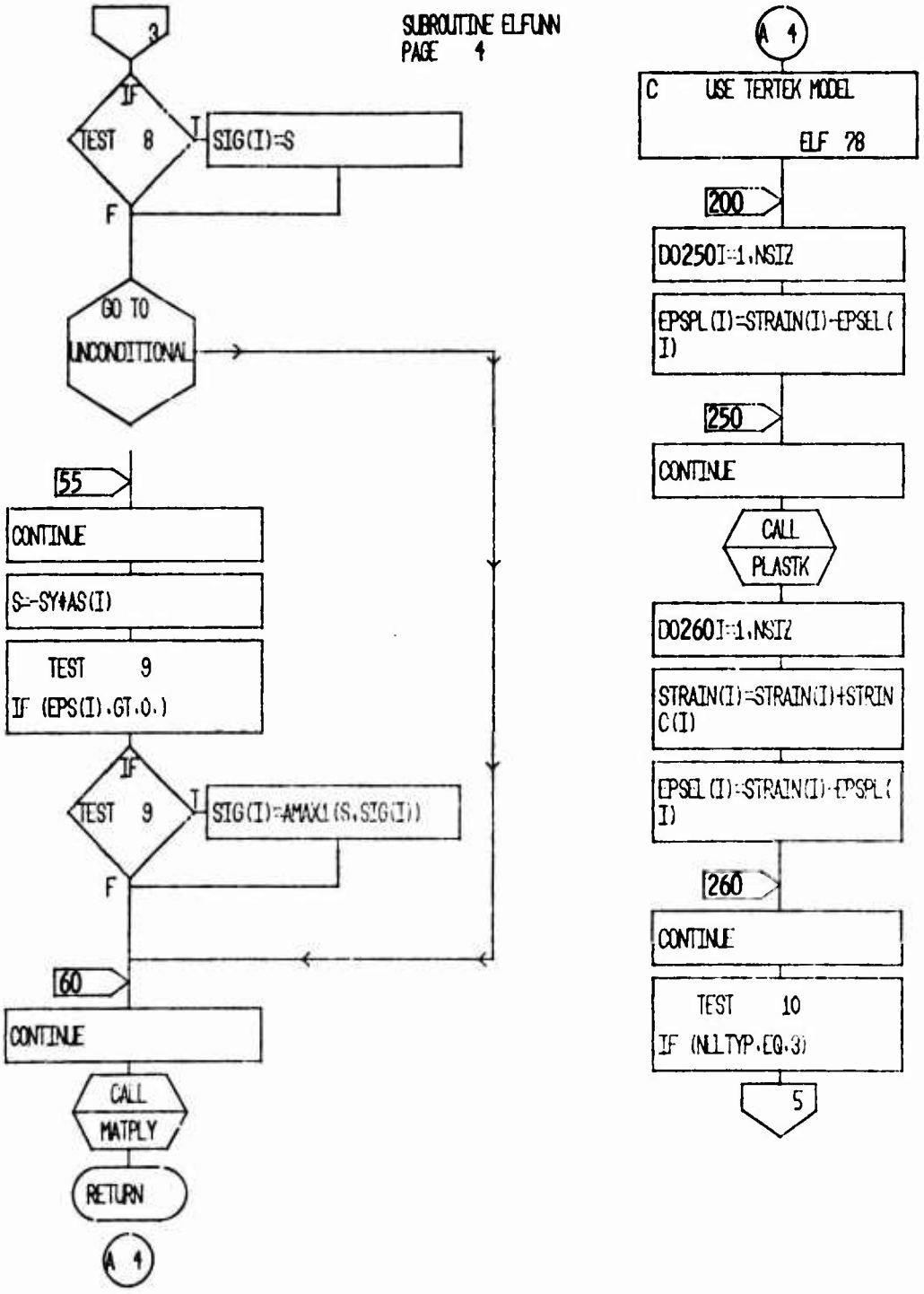
SUBROUTINE ELFUNN
PAGE 4
3
IF
TEST 8
I
SIG(I)=S
F
GO TO
UNCONDITIONAL
55
CONTINUE
S=-SY*AS(I)
TEST 9
IF (EPS(I).GT.0.)
IF
TEST 9
I
SIG(I)=AMAX1(S,SIG(I))
F
60
CONTINUE
CALL
MATPLY
RETURN
A 1
A 1
C USE TERTEK MODEL
ELF 78
200
DO250I=1,NSIZ
EPSPL(I)=STRAIN(I)-EPSEL(
I)
250
CONTINUE
CALL
PLASTK
DO260I=1,NSIZ
STRAIN(I)=STRAIN(I)+STRIN
C(I)
EPSEL(I)=STRAIN(I)-EPSPL(
I)
260
CONTINUE
TEST 10
IF (NLTYP.EQ.3)
5

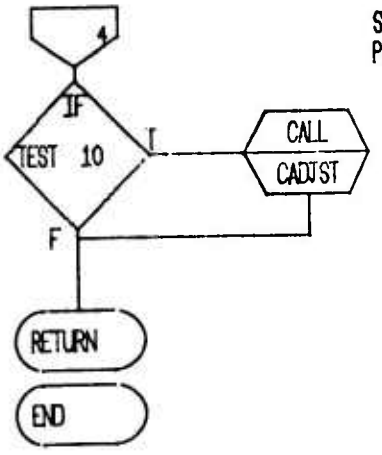
4
IF
TEST 10
T
CALL
CADJST
F
RETURN
END

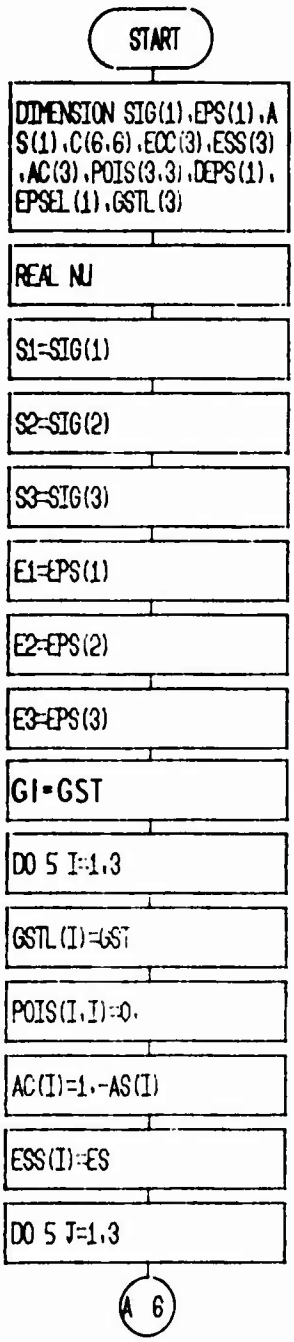
START
DIMENSION SIG(1),EPS(1),AS(1),C(6,6),ECC(3),ESS(3),AC(3),POIS(3,3),DEPS(1),EPSEL(1),GSTL(3)
REAL NU
S1=SIG(1)
S2=SIG(2)
S3=SIG(3)
E1=EPS(1)
E2=EPS(2)
E3=EPS(3)
GI=GST
DO 5 I=1,3
GSTL(I)=GST
POIS(I,I)=0.
AC(I)=1.-AS(I)
ESS(I)=ES
DO 5 J=1,3
A 6

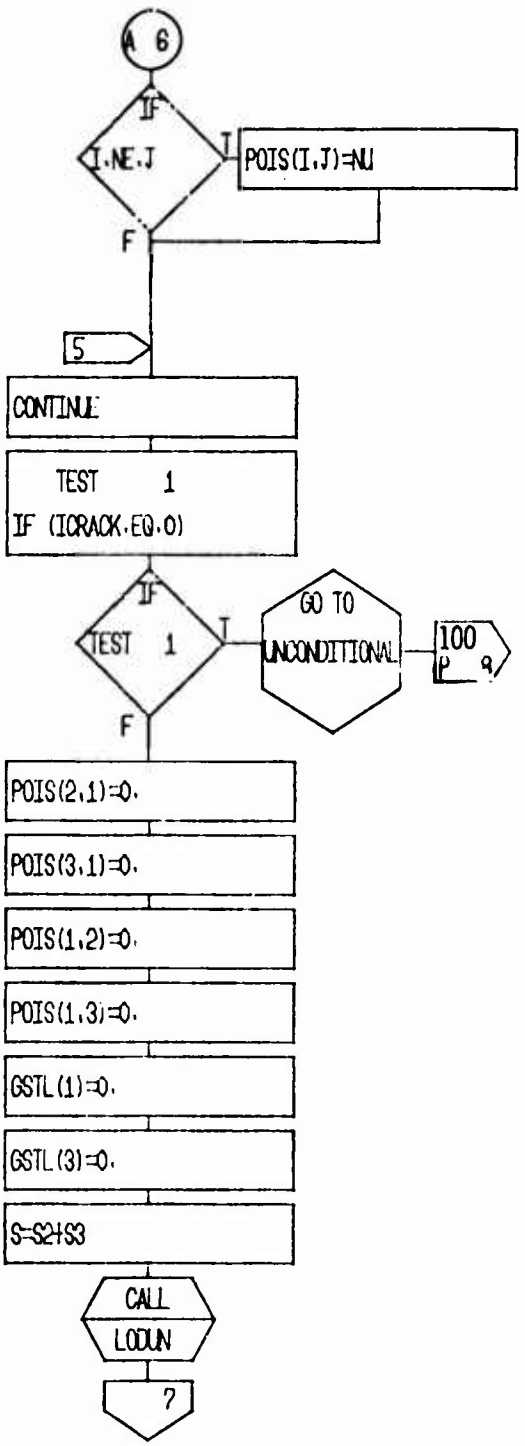
A 6
IF
I.NE.J
T
POIS(I,J)=NU
F
5
CONTINUE
TEST 1
IF (ICRACK.EQ.0)
IF
TEST 1
T
GO TO
UNCONDITIONAL
100
P 9
F
POIS(2,1)=0.
POIS(3,1)=0.
POIS(1,2)=0.
POIS(1,3)=0.
GSTL(1)=0.
GSTL(3)=0.
S=S2+S3
CALL
LODUN
7

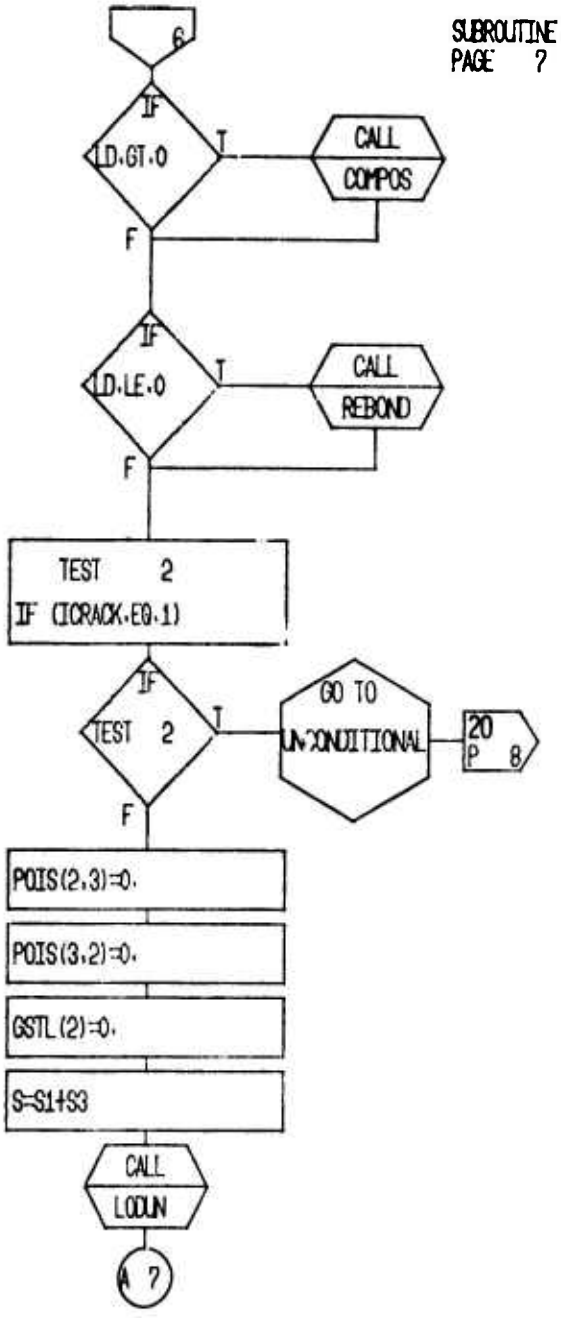
6
IF
LD.GT.0
T
CALL
COMPOS
F
IF
LD.LE.0
T
CALL
REBOND
F
TEST 2
IF (ICRACK.EQ.1)
IF
TEST 2
T
GO TO
UNCONDITIONAL
20
P 8
F
POIS(2,3)=0.
POIS(3,2)=0.
GSTL(2)=0.
S=S1+S3
CALL
LOCUN
A 7

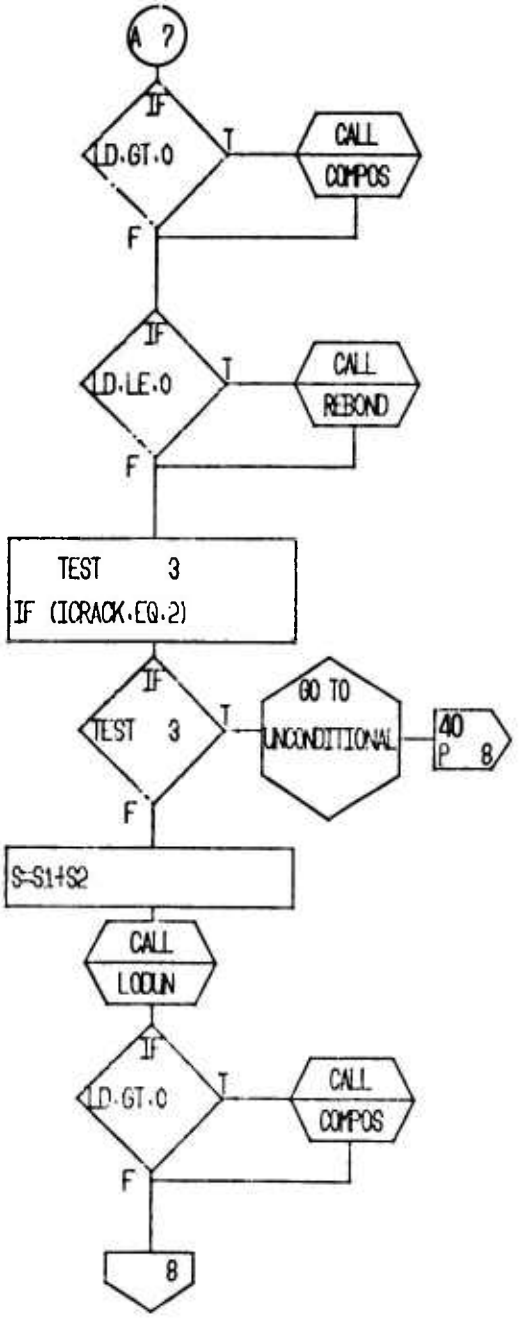
A 7
IF
LD.GT.0
T
CALL
COMPOS
F
IF
LD.LE.0
T
CALL
REBOND
F
TEST 3
IF (ICRACK.EQ.2)
IF
TEST 3
T
GO TO
UNCONDITIONAL
40
P 8
F
S=S1+S2
CALL
LOCUN
IF
LD.GT.0
T
CALL
COMPOS
F
8

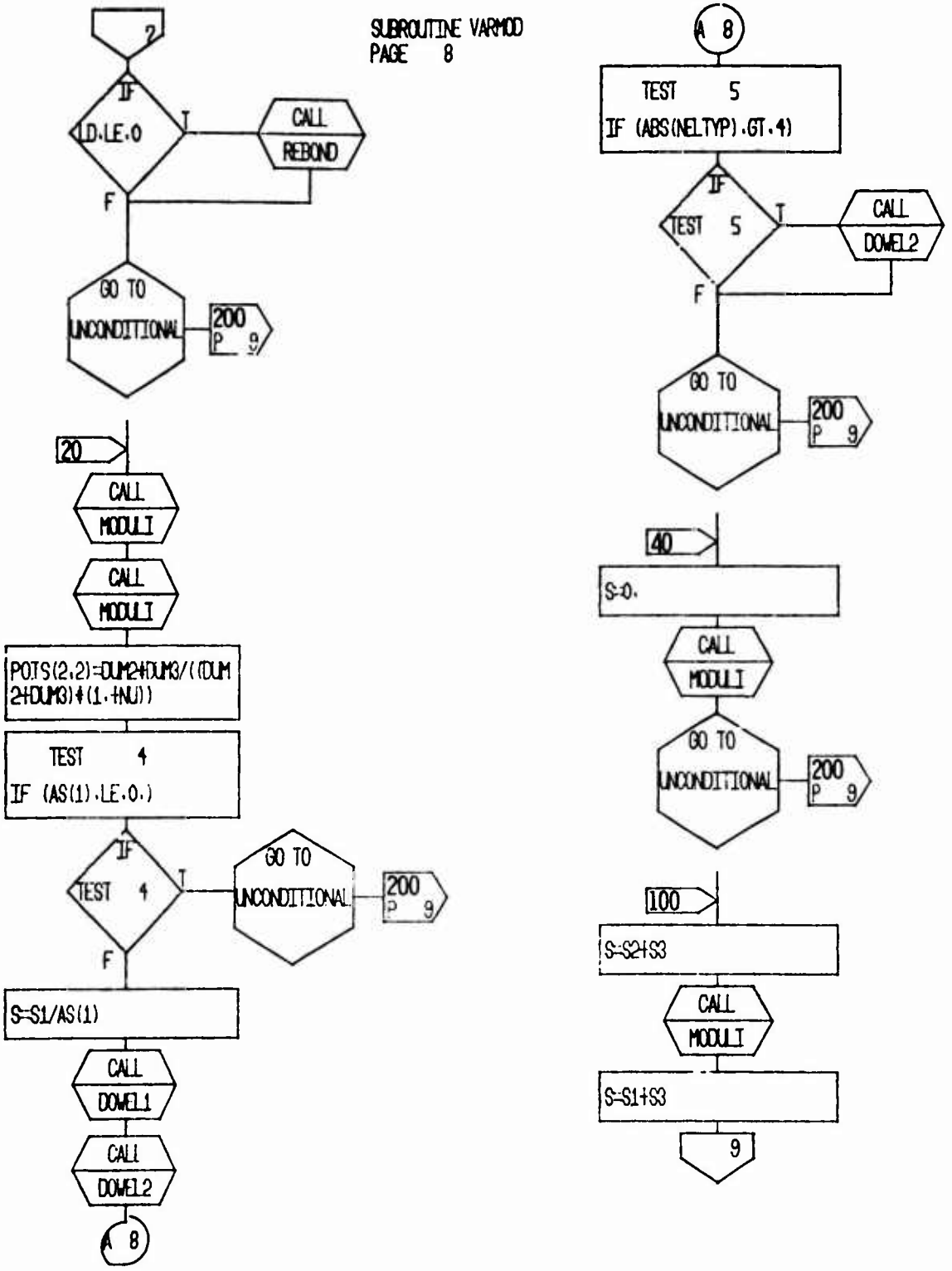
SUBROUTINE VARMOD
PAGE 8
2
IF
LD.LE.0
T
CALL
REBOND
F
GO TO
UNCONDITIONAL
200
P 9
20
CALL
MODLI
CALL
MODLI
POTS(2,2)=DUM2+DUM3/((DUM
2+DUM3)*(1.+NU))
TEST 4
IF (AS(1).LE.0.)
IF
TEST 4
T
GO TO
UNCONDITIONAL
200
P 9
F
S=S1/AS(1)
CALL
DOWEL1
CALL
DOWEL2
A 8
A 8
TEST 5
IF (ABS(NELTYP).GT.4)
IF
TEST 5
T
CALL
DOWEL2
F
GO TO
UNCONDITIONAL
200
P 9
40
S=0.
CALL
MODLI
GO TO
UNCONDITIONAL
200
P 9
100
S=S2+S3
CALL
MODLI
S=S1+S3
9

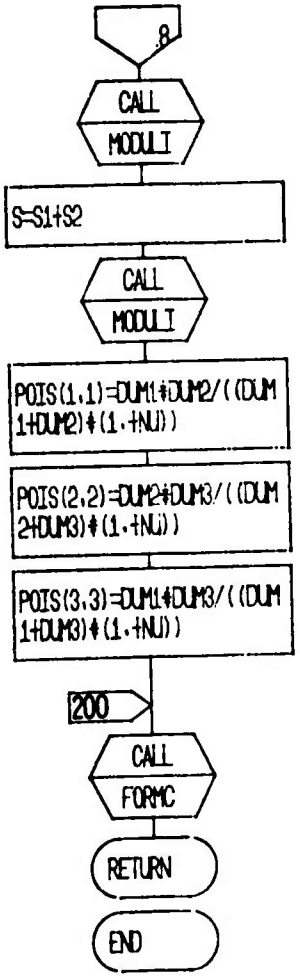
8
CALL
MODLI
S=S1+S2
CALL
MODLI
POIS(1,1)=DUM1+DUM2/((DUM
1+DUM2)+(1.+NU))
POIS(2,2)=DUM2+DUM3/((DUM
2+DUM3)+(1.+NU))
POIS(3,3)=DUM1+DUM3/((DUM
1+DUM3)+(1.+NU))
200
CALL
FORMC
RETURN
END

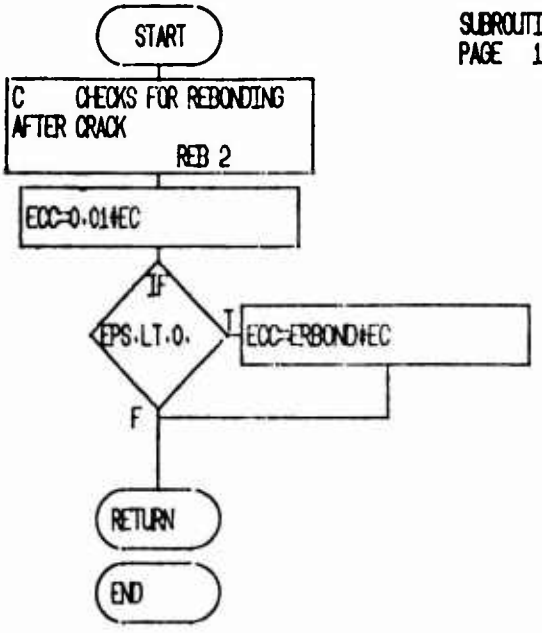

SUBROUTINE REBOND
PAGE 10

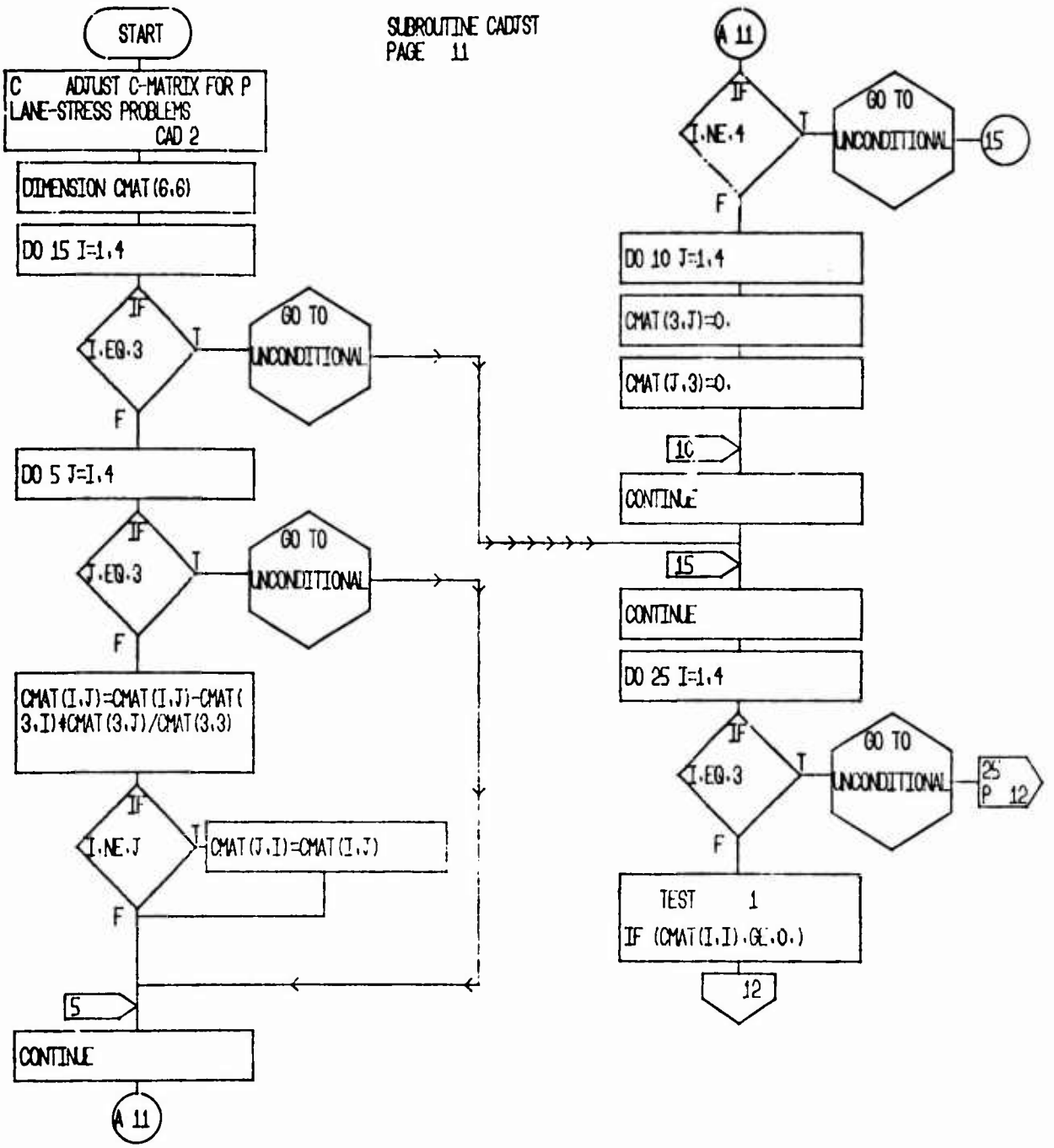
SUBROUTINE CADJST
PAGE 11
START
C ADJUST C-MATRIX FOR P
LANE-STRESS PROBLEMS
CAD 2
DIMENSION CMAT(6,6)
DO 15 I=1,4
IF
I.EQ.3
T
GO TO
UNCONDITIONAL
F
DO 5 J=1,4
IF
J.EQ.3
T
GO TO
UNCONDITIONAL
F
CMAT(I,J)=CMAT(I,J)-CMAT(
3,I)*CMAT(3,J)/CMAT(3,3)
IF
I.NE.J
T
CMAT(J,I)=CMAT(I,J)
F
5
CONTINUE
A 11
A 11
IF
I.NE.4
T
GO TO
UNCONDITIONAL
15
F
DO 10 J=1,4
CMAT(3,J)=0.
CMAT(J,3)=0.
10
CONTINUE
15
CONTINUE
DO 25 I=1,4
IF
I.EQ.3
T
GO TO
UNCONDITIONAL
25
P 12
F
TEST 1
IF (CMAT(I,I).GE.0.)
12

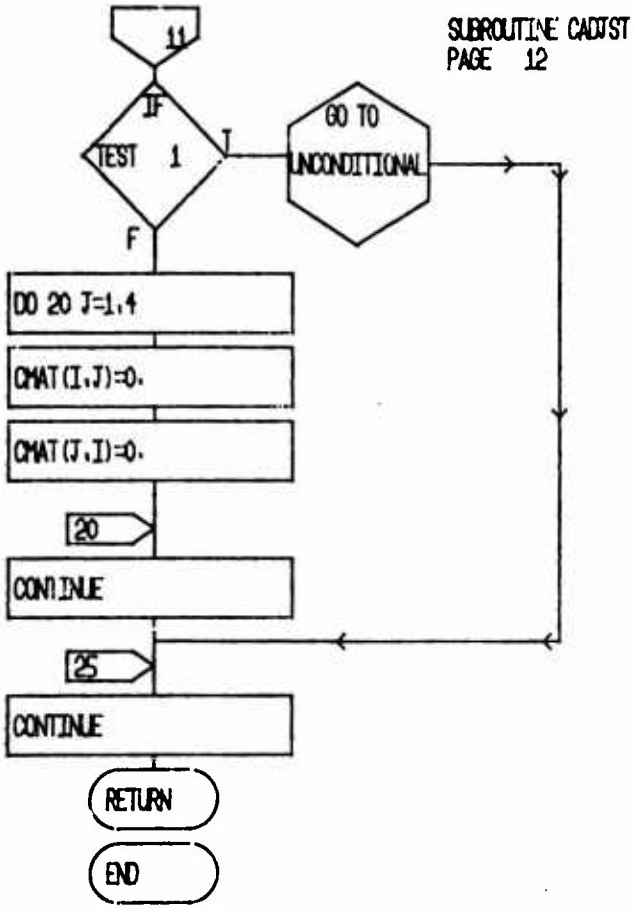
11
IF
TEST 1
T
GO TO
UNCONDITIONAL
F
DO 20 J=1,4
CMAT(I,J)=0.
CMAT(J,I)=0.
20
CONTINUE
25
CONTINUE
RETURN
END

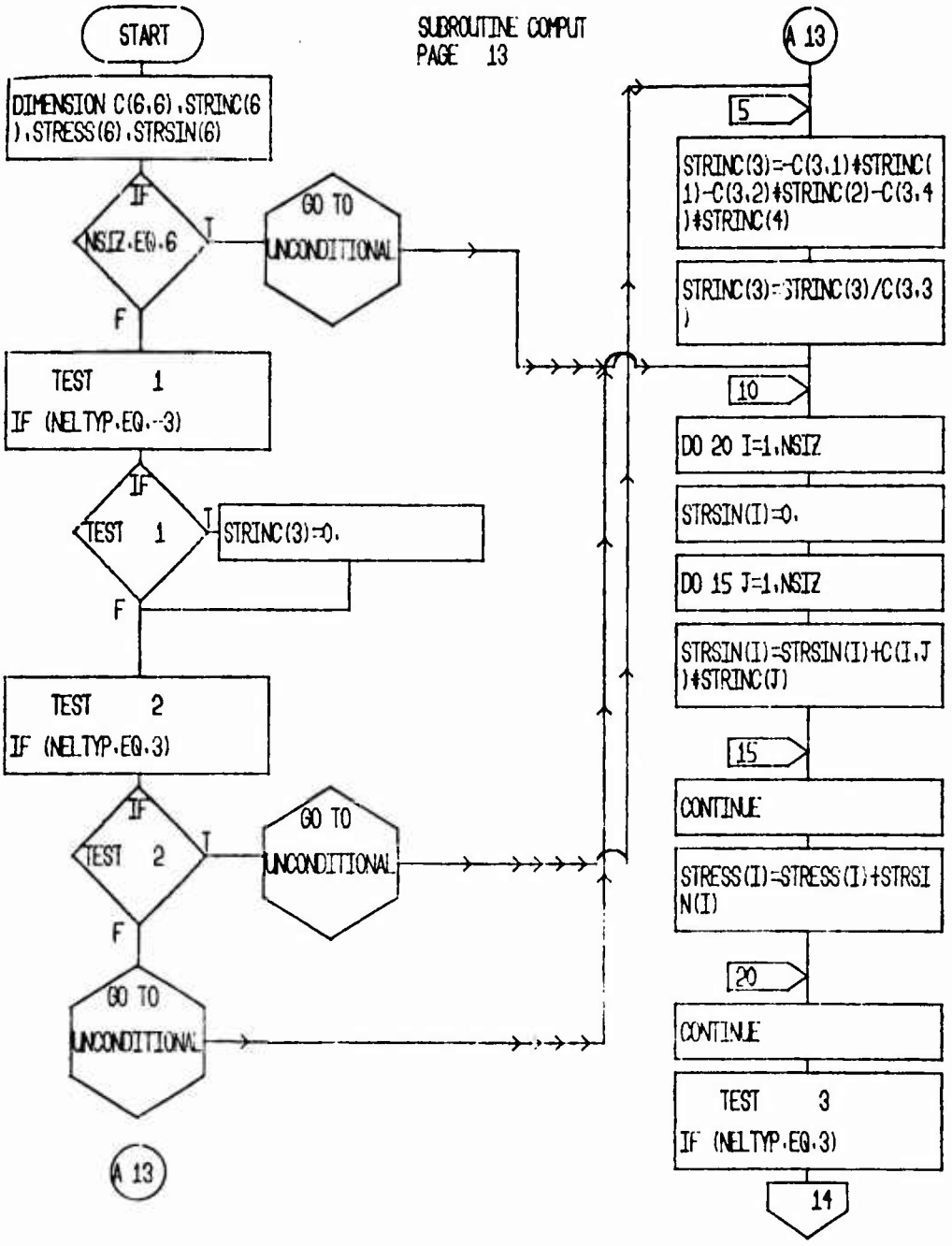
START
SUBROUTINE COMPUT
PAGE 13
A 13
DIMENSION C(6,6),STRINC(6),STRESS(6),STRSIN(6)
IF NSIZ.EQ.6
T
GO TO UNCONDITIONAL
F
TEST 1
IF (NELTYP.EQ.-3)
IF TEST 1
T
STRINC(3)=0.
F
TEST 2
IF (NELTYP.EQ.3)
IF TEST 2
T
GO TO UNCONDITIONAL
F
GO TO UNCONDITIONAL
A 13
5
STRINC(3)=-C(3,1)*STRINC(1)-C(3,2)*STRINC(2)-C(3,4)*STRINC(4)
STRINC(3)=STRINC(3)/C(3,3)
10
DO 20 I=1,NSIZ
STRSIN(I)=0.
DO 15 J=1,NSIZ
STRSIN(I)=STRSIN(I)+C(I,J)*STRINC(J)
15
CONTINUE
STRESS(I)=STRESS(I)+STRSIN(I)
20
CONTINUE
TEST 3
IF (NELTYP.EQ.3)
14

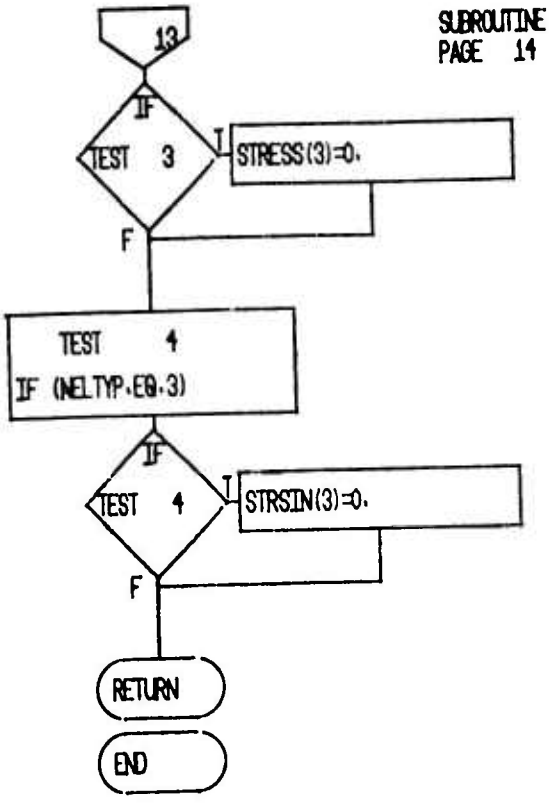
13
IF
TEST 3
T
STRESS(3)=0.
F
TEST 4
IF (NELTYP.EQ.3)
IF
TEST 4
T
STRSIN(3)=0.
F
RETURN
END

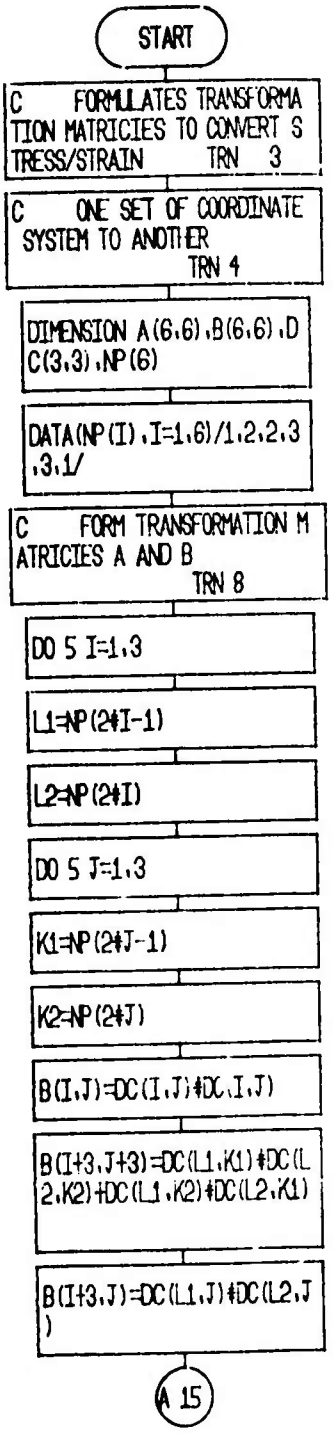

SUBROUTINE TRANSF
PAGE 15

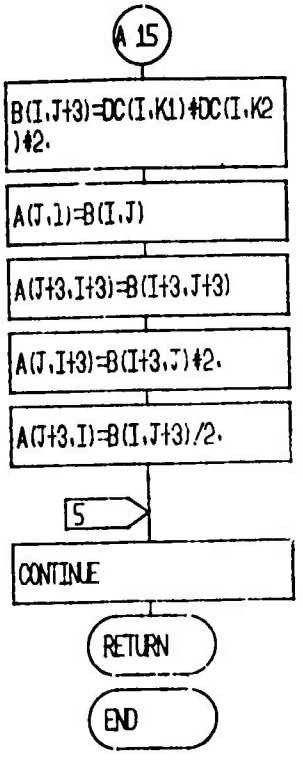

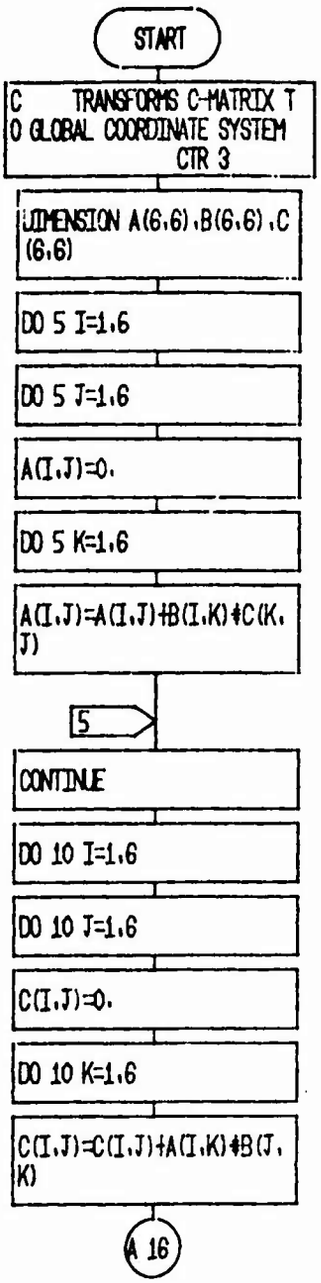

SUBROUTINE CTRANF
PAGE 16

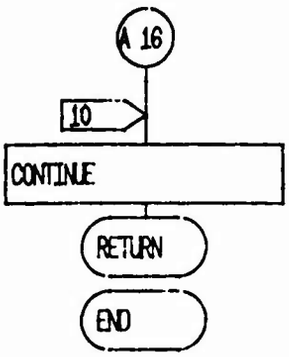

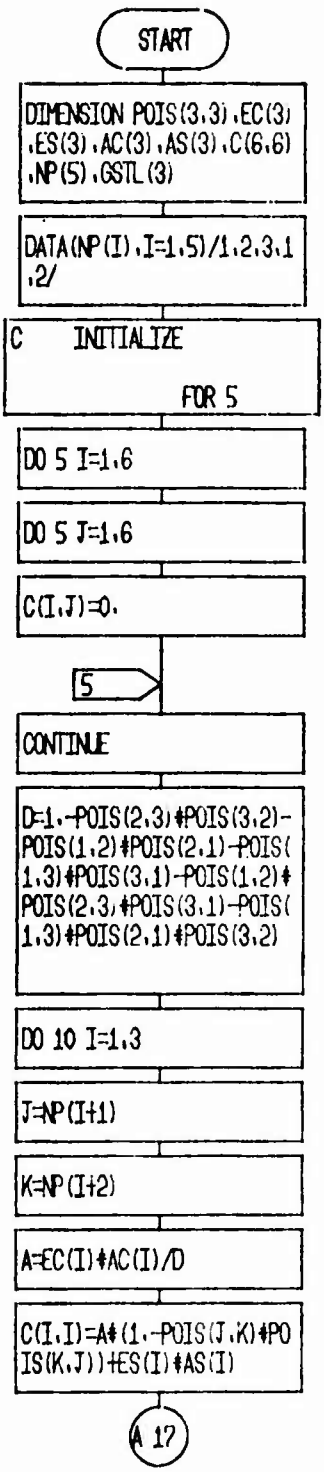
START
DIMENSION POIS(3,3),EC(3),ES(3),AC(3),AS(3),C(6,6),NP(5),GSTL(3)
DATA(NP(I),I=1,5)/1,2,3,1,2/
C INITIALIZE FOR 5
DO 5 I=1,6
DO 5 J=1,6
C(I,J)=0.
5
CONTINUE
D=1.-POIS(2,3)*POIS(3,2)-POIS(1,2)*POIS(2,1)-POIS(1,3)*POIS(3,1)-POIS(1,2)*POIS(2,3)*POIS(3,1)-POIS(1,3)*POIS(2,1)*POIS(3,2)
DO 10 I=1,3
J=NP(I+1)
K=NP(I+2)
A=EC(I)*AC(I)/D
C(I,I)=A*(1.-POIS(J,K)*POIS(K,J))+ES(I)*AS(I)
A 17

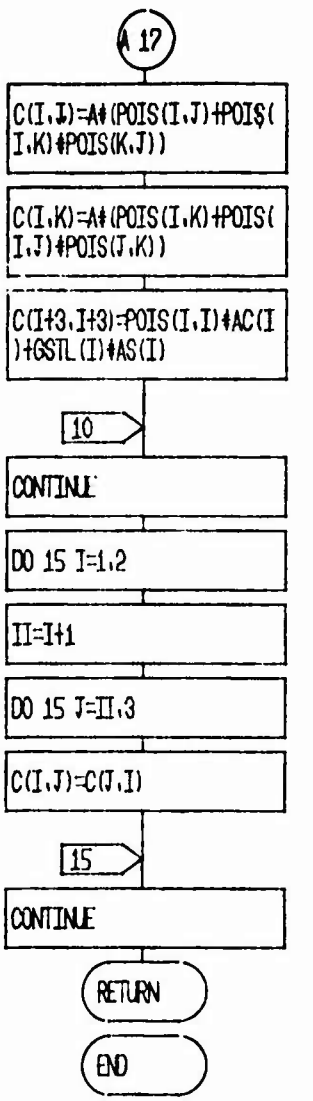
A 17
C(I,J)=A*(POIS(I,J)+POIS(I,K)*POIS(K,J))
C(I,K)=A*(POIS(I,K)+POIS(I,J)*POIS(J,K))
C(I+3,I+3)=POIS(I,I)*AC(I)+GSTL(I)*AS(I)
10
CONTINUE
DO 15 I=1,2
II=I+1
DO 15 J=II,3
C(I,J)=C(J,I)
15
CONTINUE
RETURN
END

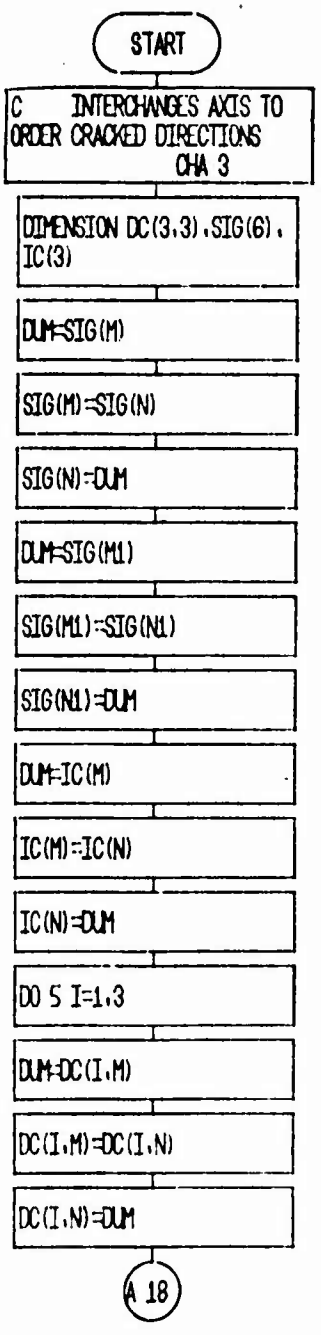

SUBROUTINE CHANGE
PAGE 18

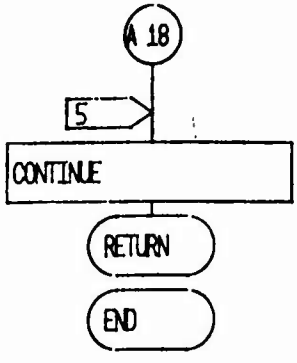

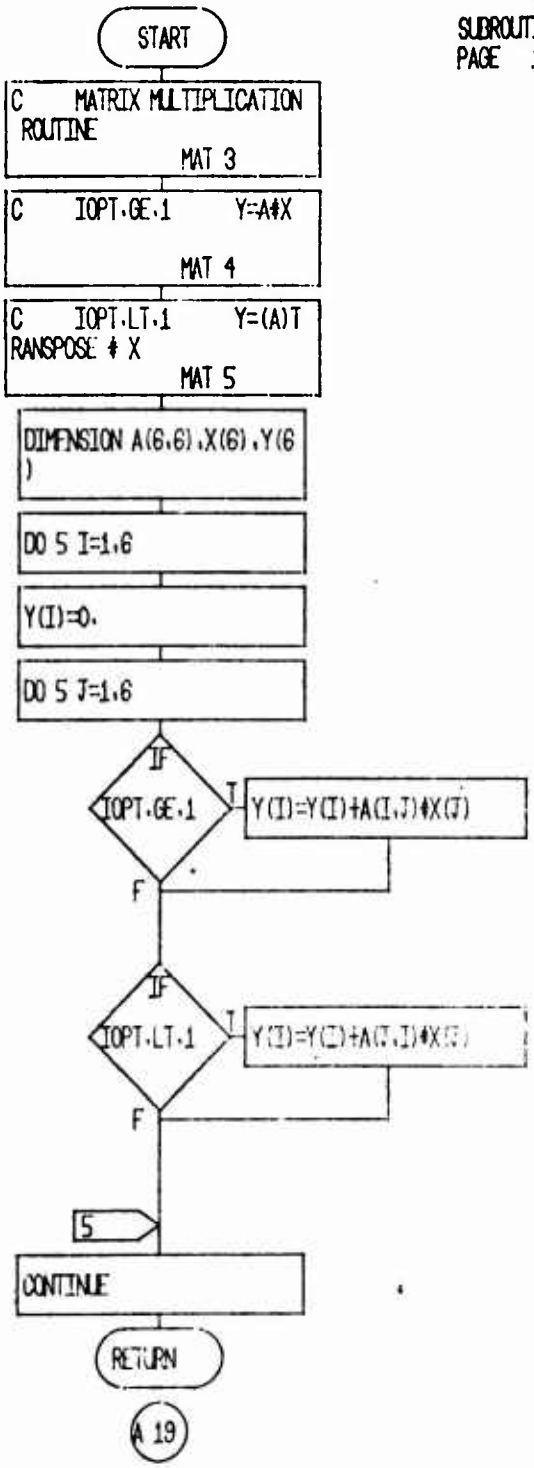

SUBROUTINE MATPLY
PAGE 19

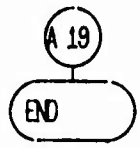

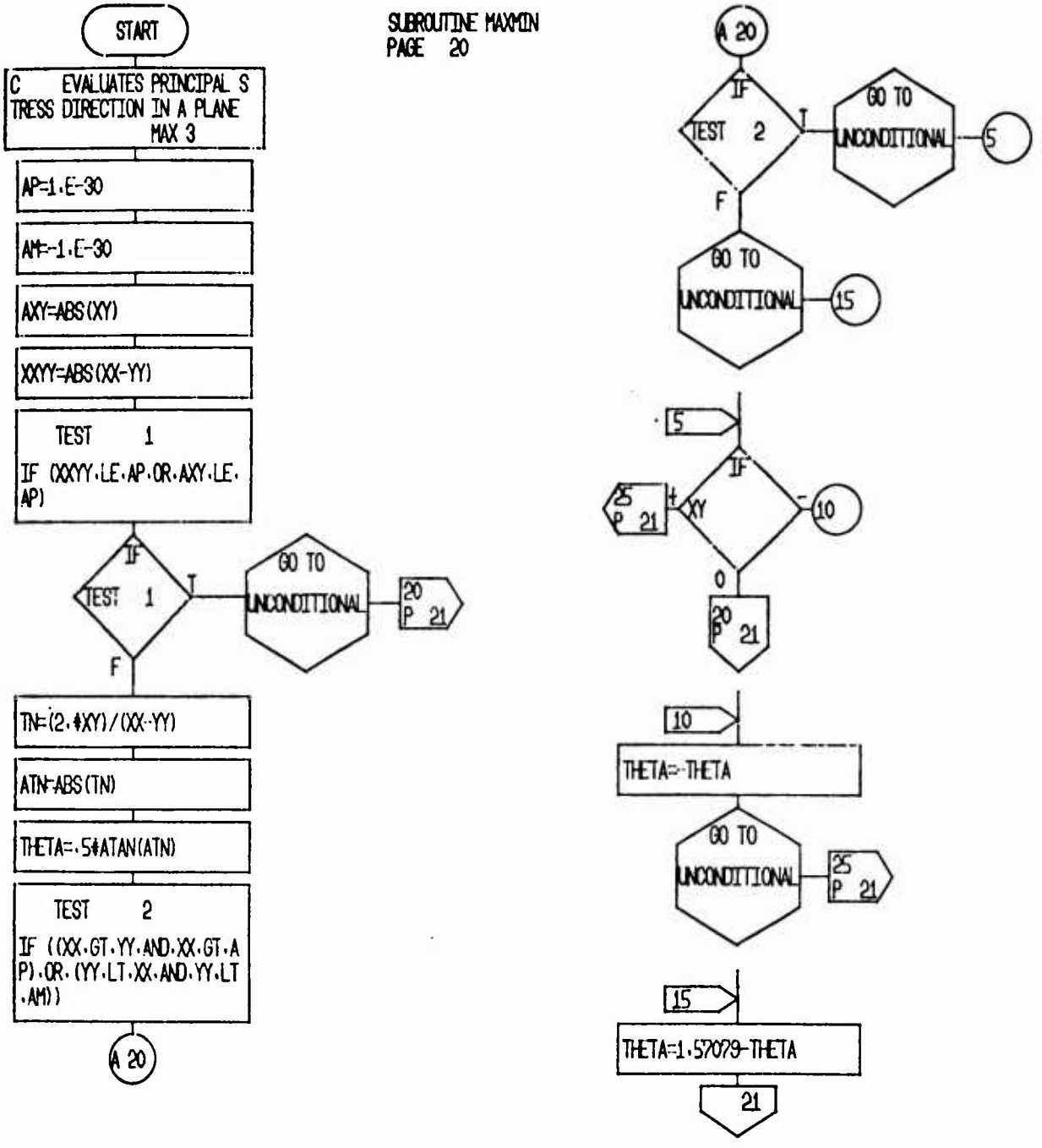
SUBROUTINE MAXMIN
PAGE 20
START
C EVALUATES PRINCIPAL S
TRESS DIRECTION IN A PLANE
MAX 3
AP=1.E-30
AM=-1.E-30
AXY=ABS(XY)
XXYY=ABS(XX-YY)
TEST 1
IF (XXYY.LE.AP.OR.AXY.LE.
AP)
IF
TEST 1
T
GO TO
UNCONDITIONAL
20
P 21
F
TN=(2.*XY)/(XX-YY)
ATN=ABS(TN)
THETA=.5*ATAN(ATN)
TEST 2
IF ((XX.GT.YY.AND.XX.GT.A
P).OR.(YY.LT.XX.AND.YY.LT
.AM))
A 20
A 20
IF
TEST 2
T
GO TO
UNCONDITIONAL
5
F
GO TO
UNCONDITIONAL
15
5
IF
25
P 21
+
XY
-
10
0
20
P 21
10
THETA=-THETA
GO TO
UNCONDITIONAL
25
P 21
15
THETA=1.57079-THETA
21

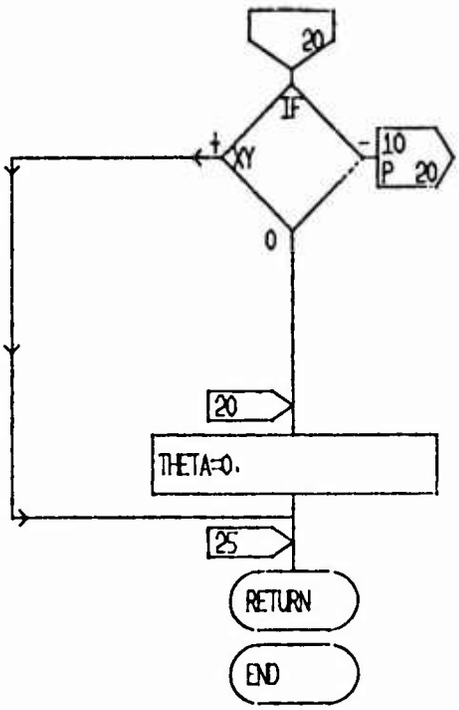
20
IF
+
XY
-
10
P 20
0
20
THETA=0.
25
RETURN
END

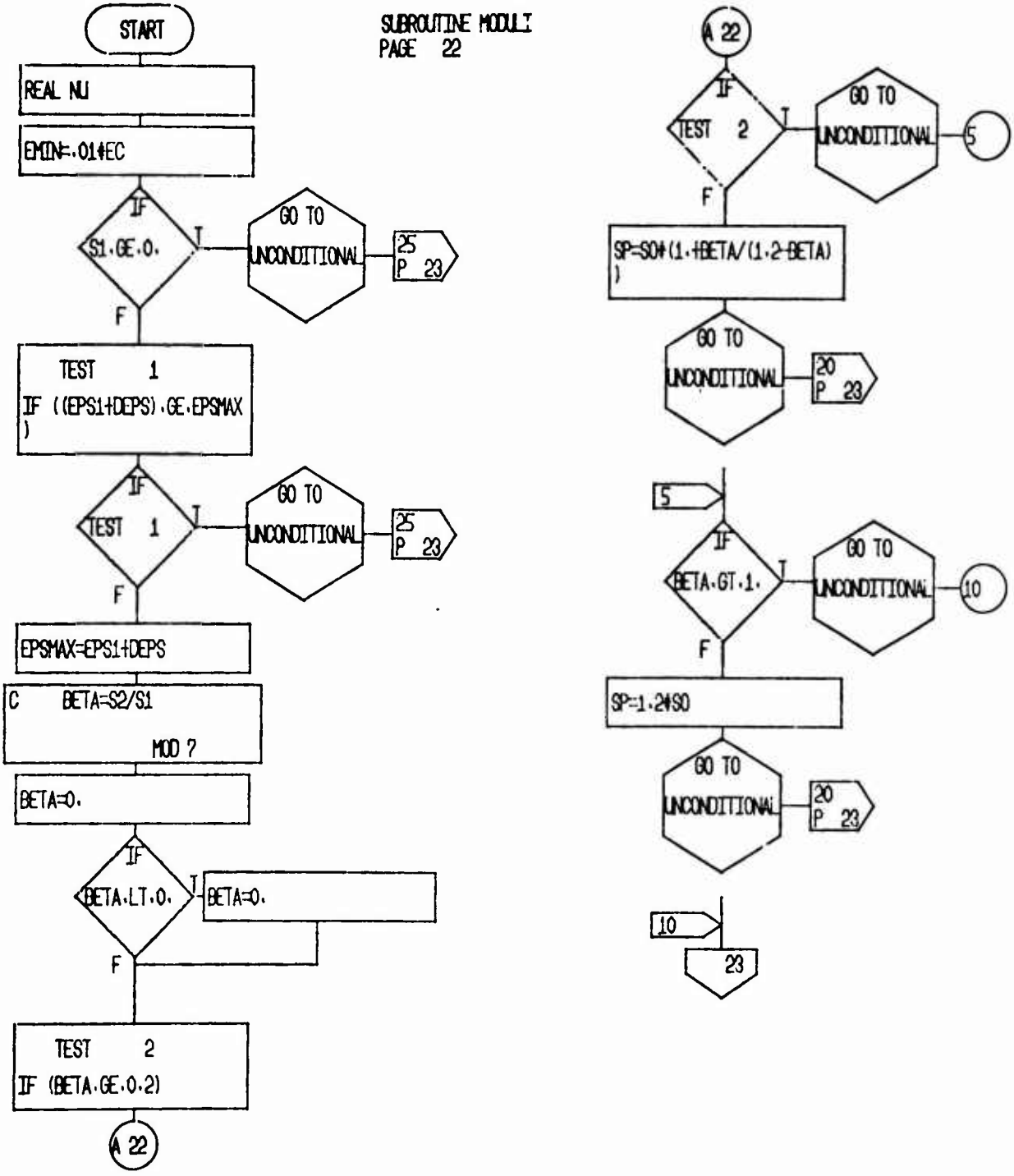
SUBROUTINE MODLI
PAGE 22
START
REAL NU
EMIN=.01*EC
IF
S1.GE.0.
T
GO TO
UNCONDITIONAL
25
P 23
F
TEST 1
IF ((EPS1+DEPS).GE.EPSMAX
)
IF
TEST 1
T
GO TO
UNCONDITIONAL
25
P 23
F
EPSMAX=EPS1+DEPS
C BETA=S2/S1
MOD ?
BETA=0.
IF
BETA.LT.0.
T
BETA=0.
F
TEST 2
IF (BETA.GE.0.2)
A 22
A 22
IF
TEST 2
T
GO TO
UNCONDITIONAL
5
F
SP=S0*(1.+BETA/(1.-BETA)
)
GO TO
UNCONDITIONAL
20
P 23
5
IF
BETA.GT.1.
T
GO TO
UNCONDITIONAL
10
F
SP=1.2*S0
GO TO
UNCONDITIONAL
20
P 23
10
23

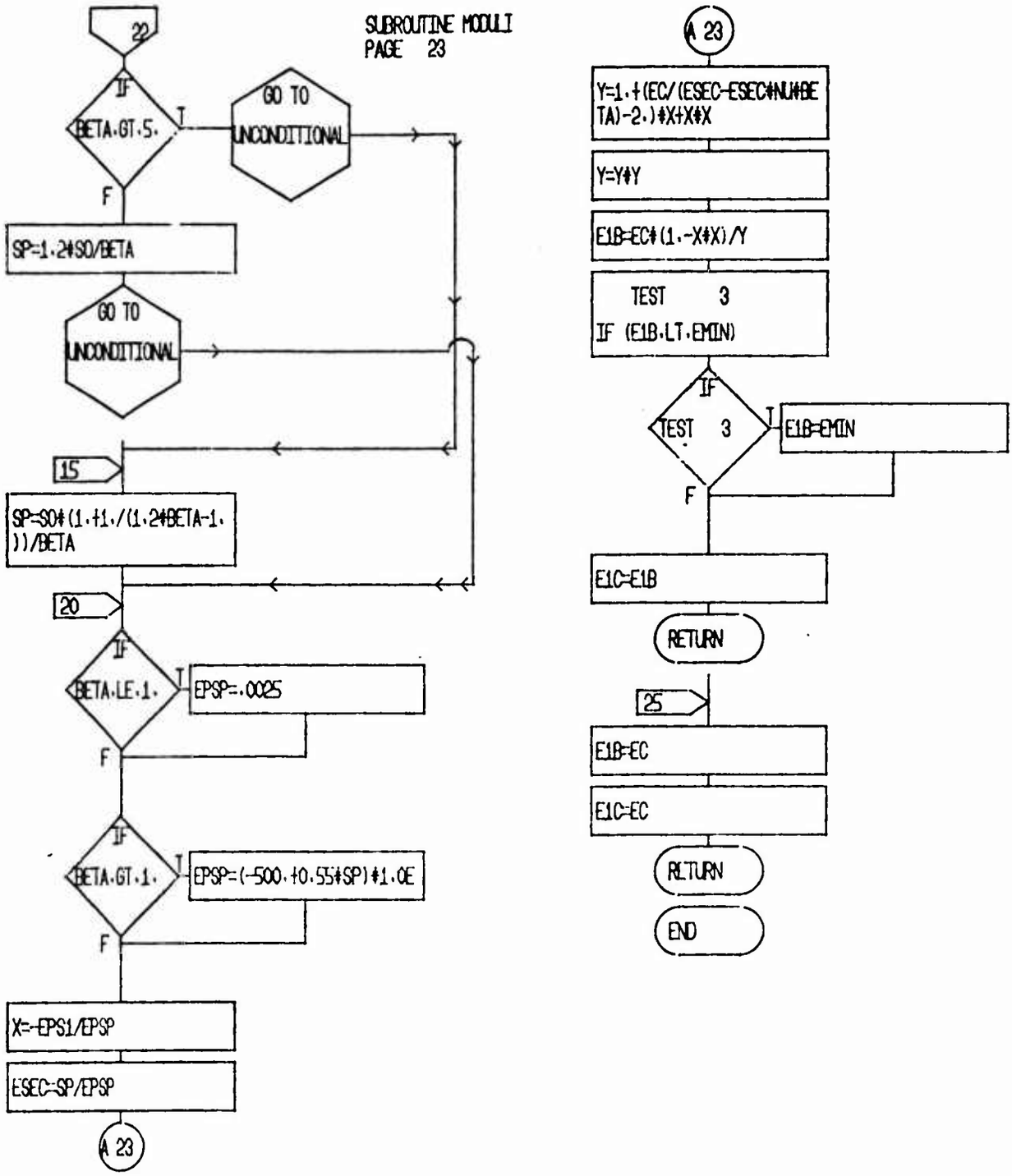
SUBROUTINE MODULI
PAGE 23
22
IF
BETA.GT.5.
T
GO TO
UNCONDITIONAL
F
SP=1.2*SO/BETA
GO TO
UNCONDITIONAL
15
SP=SO*(1.+1./(1.2*BETA-1.
))/BETA
20
IF
BETA.LE.1.
T
EPSP=.0025
F
IF
BETA.GT.1.
T
EPSP=(-500.+0.55*SP)*1.0E
F
X=-EPS1/EPSP
ESEC=SP/EPSP
A 23
A 23
Y=1.+(EC/(ESEC-ESEC*NU*BE
TA)-2.)*X+X*X
Y=Y*Y
E1B=EC*(1.-X*X)/Y
TEST 3
IF (E1B.LT.EMIN)
IF
TEST 3
T
E1B=EMIN
F
E1C=E1B
RETURN
25
E1B=EC
E1C=EC
RETURN
END

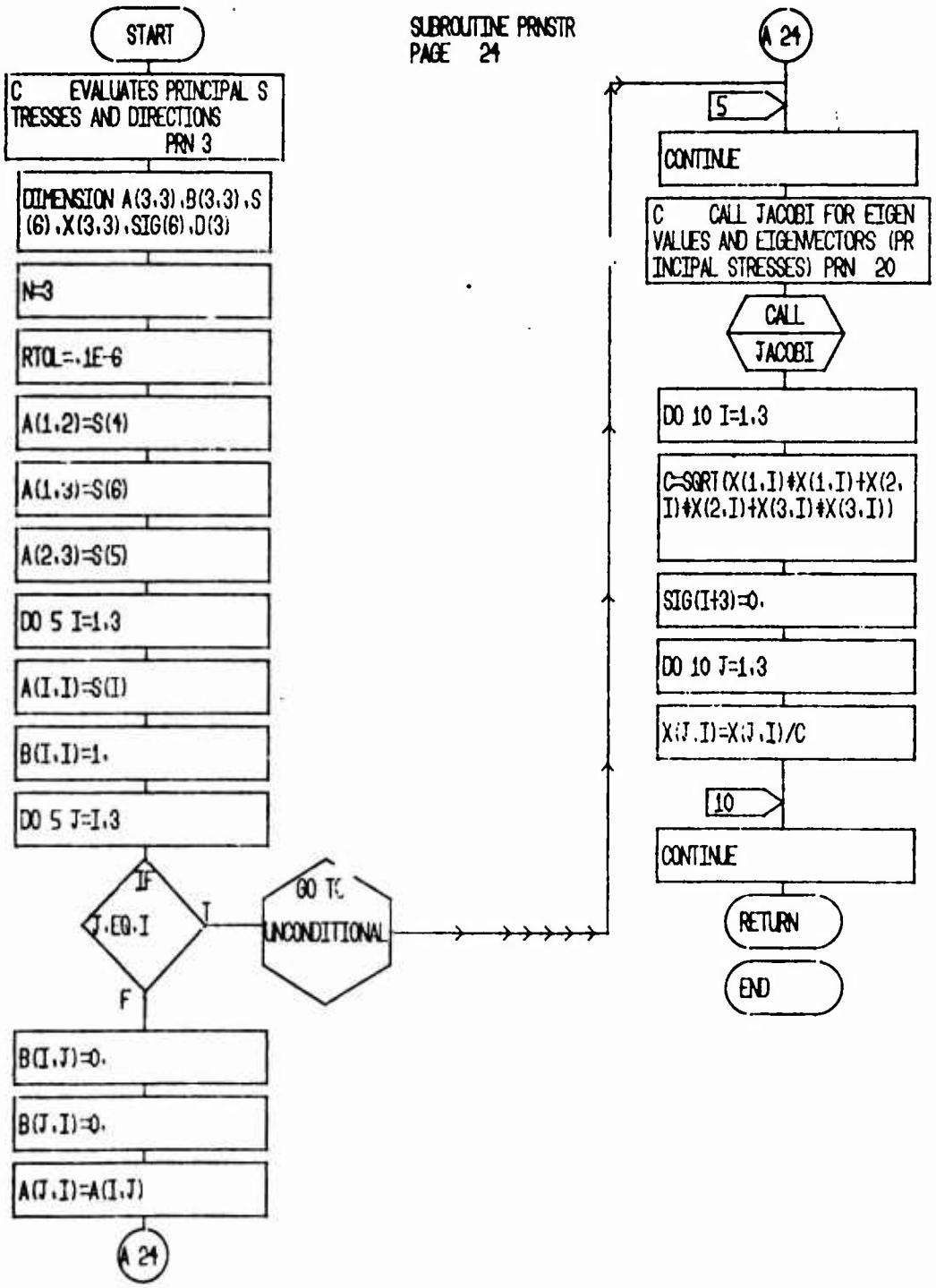
SUBROUTINE PRNSTR
PAGE 24
START
C EVALUATES PRINCIPAL S TRESSES AND DIRECTIONS PRN 3
DIMENSION A(3,3),B(3,3),S (6),X(3,3),SIG(6),D(3)
N=3
RTOL=.1E-6
A(1,2)=S(4)
A(1,3)=S(6)
A(2,3)=S(5)
DO 5 I=1,3
A(I,I)=S(I)
B(I,I)=1.
DO 5 J=I,3
IF
J.EQ.I
T
GO TO
UNCONDITIONAL
F
B(I,J)=0.
B(J,I)=0.
A(J,I)=A(I,J)
A 24
A 24
5
CONTINUE
C CALL JACOBI FOR EIGEN VALUES AND EIGENVECTORS (PR INCIPAL STRESSES) PRN 20
CALL
JACOBI
DO 10 I=1,3
C=SQRT(X(1,I)*X(1,I)+X(2, I)*X(2,I)+X(3,I)*X(3,I))
SIG(I+3)=0.
DO 10 J=1,3
X(J,I)=X(J,I)/C
10
CONTINUE
RETURN
END

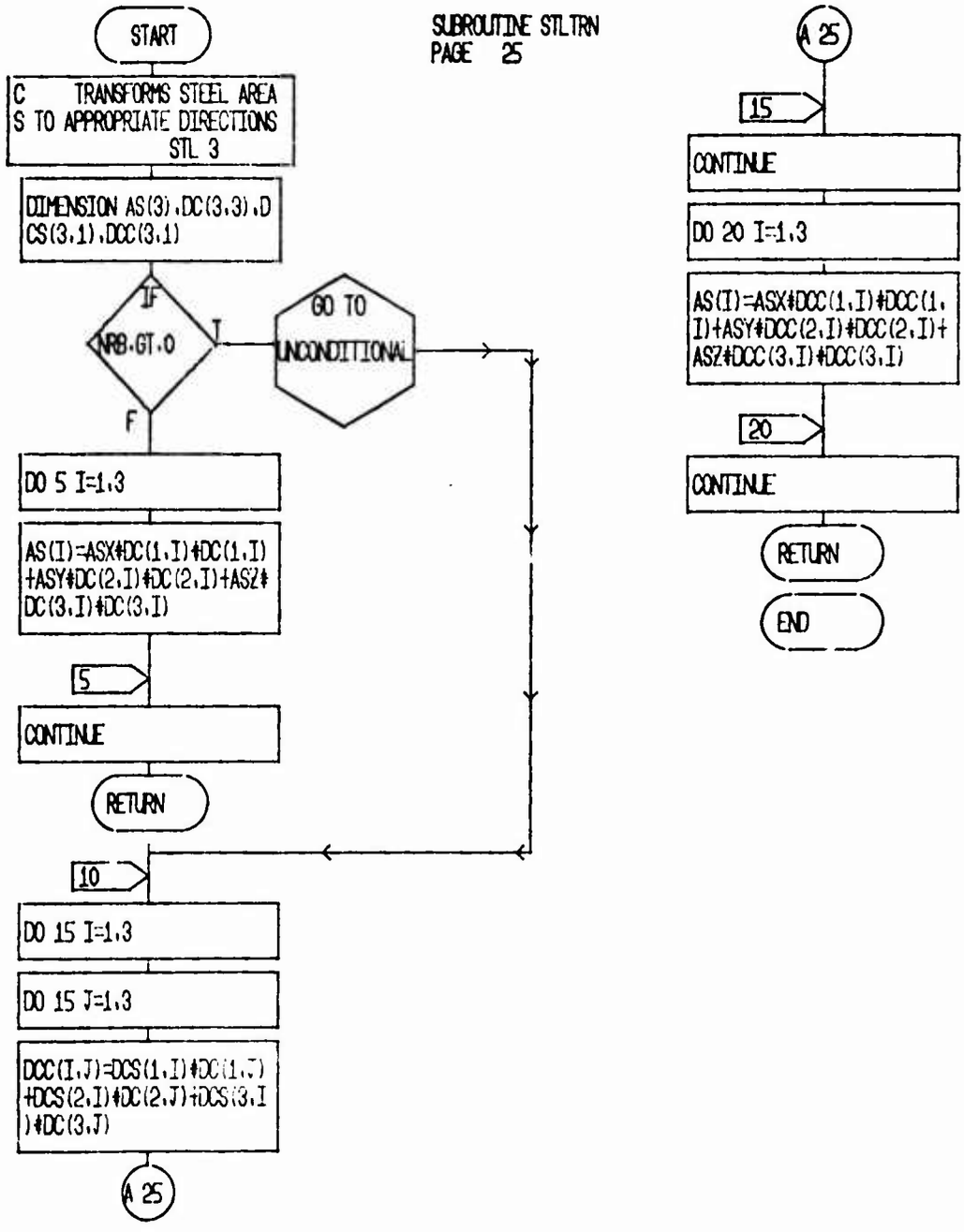
START
SUBROUTINE STLTRN
PAGE 25
C TRANSFORMS STEEL AREA
S TO APPROPRIATE DIRECTIONS
STL 3
DIMENSION AS(3),DC(3,3),D
CS(3,1),DCC(3,1)
IF
NRB.GT.0
T
GO TO
UNCONDITIONAL
F
DO 5 I=1,3
AS(I)=ASX*DC(1,I)*DC(1,I)
+ASY*DC(2,I)*DC(2,I)+ASZ*
DC(3,I)*DC(3,I)
5
CONTINUE
RETURN
10
DO 15 I=1,3
DO 15 J=1,3
DCC(I,J)=DCS(1,I)*DC(1,J)
+DCS(2,I)*DC(2,J)+DCS(3,I
)*DC(3,J)
A 25
A 25
15
CONTINUE
DO 20 I=1,3
AS(I)=ASX*DCC(1,I)*DCC(1,
I)+ASY*DCC(2,I)*DCC(2,I)+
ASZ*DCC(3,I)*DCC(3,I)
20
CONTINUE
RETURN
END

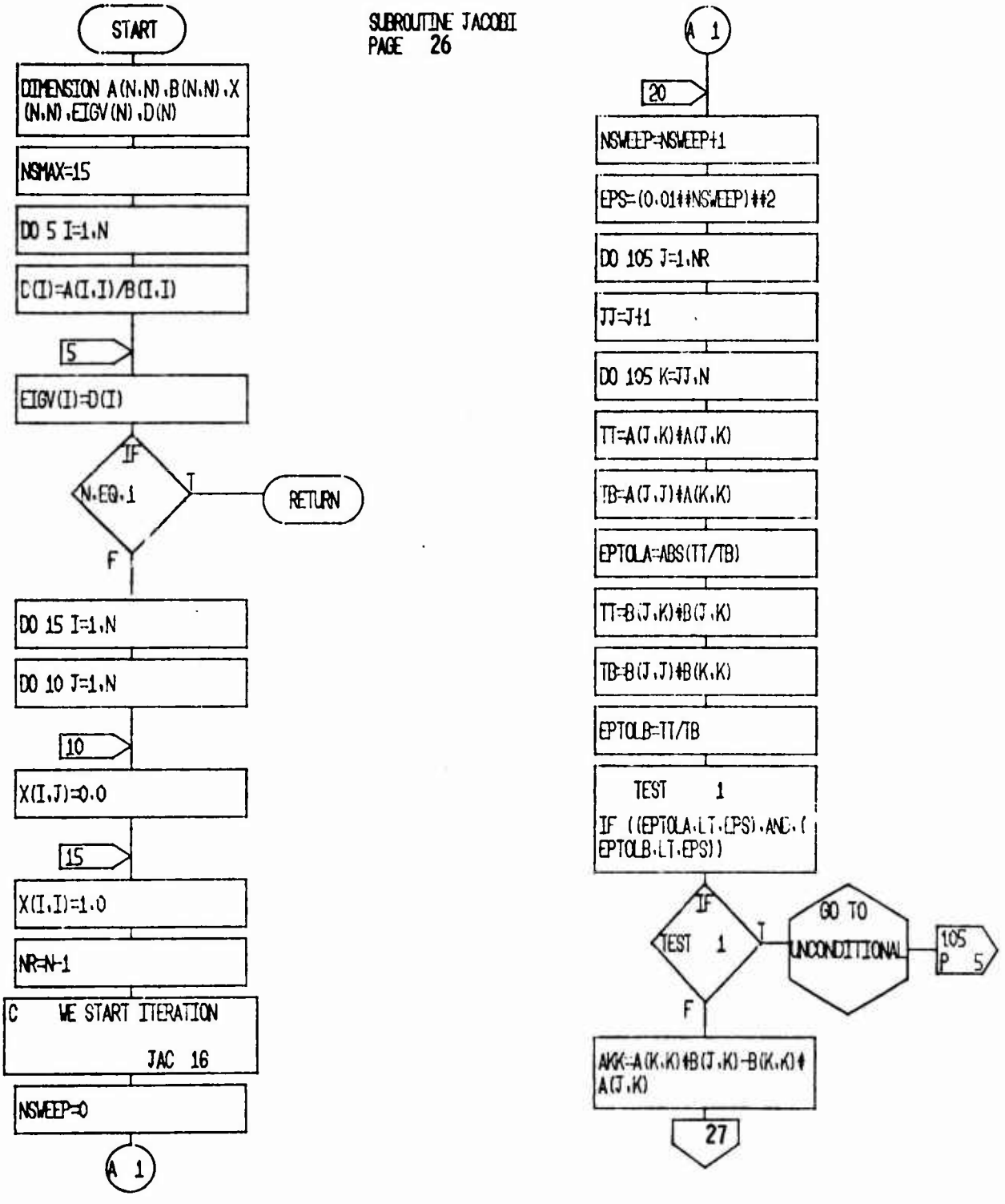
START
DIMENSION A(N,N),B(N,N),X (N,N),EIGV(N),D(N)
NSMAX=15
DO 5 I=1,N
D(I)=A(I,I)/B(I,I)
5
EIGV(I)=D(I)
IF N.EQ.1
T
RETURN
F
DO 15 I=1,N
DO 10 J=1,N
10
X(I,J)=0.0
15
X(I,I)=1.0
NR=N-1
C WE START ITERATION
JAC 16
NSWEEP=0
A 1
A 1
20
NSWEEP=NSWEEP+1
EPS=(0.01**NSWEEP)**2
DO 105 J=1,NR
JJ=J+1
DO 105 K=JJ,N
TT=A(J,K)*A(J,K)
TB=A(J,J)*A(K,K)
EPTOLA=ABS(TT/TB)
TT=B(J,K)*B(J,K)
TB=B(J,J)*B(K,K)
EPTOLB=TT/TB
TEST 1
IF ((EPTOLA.LT.EPS).AND.(EPTOLB.LT.EPS))
IF
TEST 1
T
GO TO
UNCONDITIONAL
105
P 5
F
AKK=A(K,K)*B(J,K)-B(K,K)* A(J,K)
27

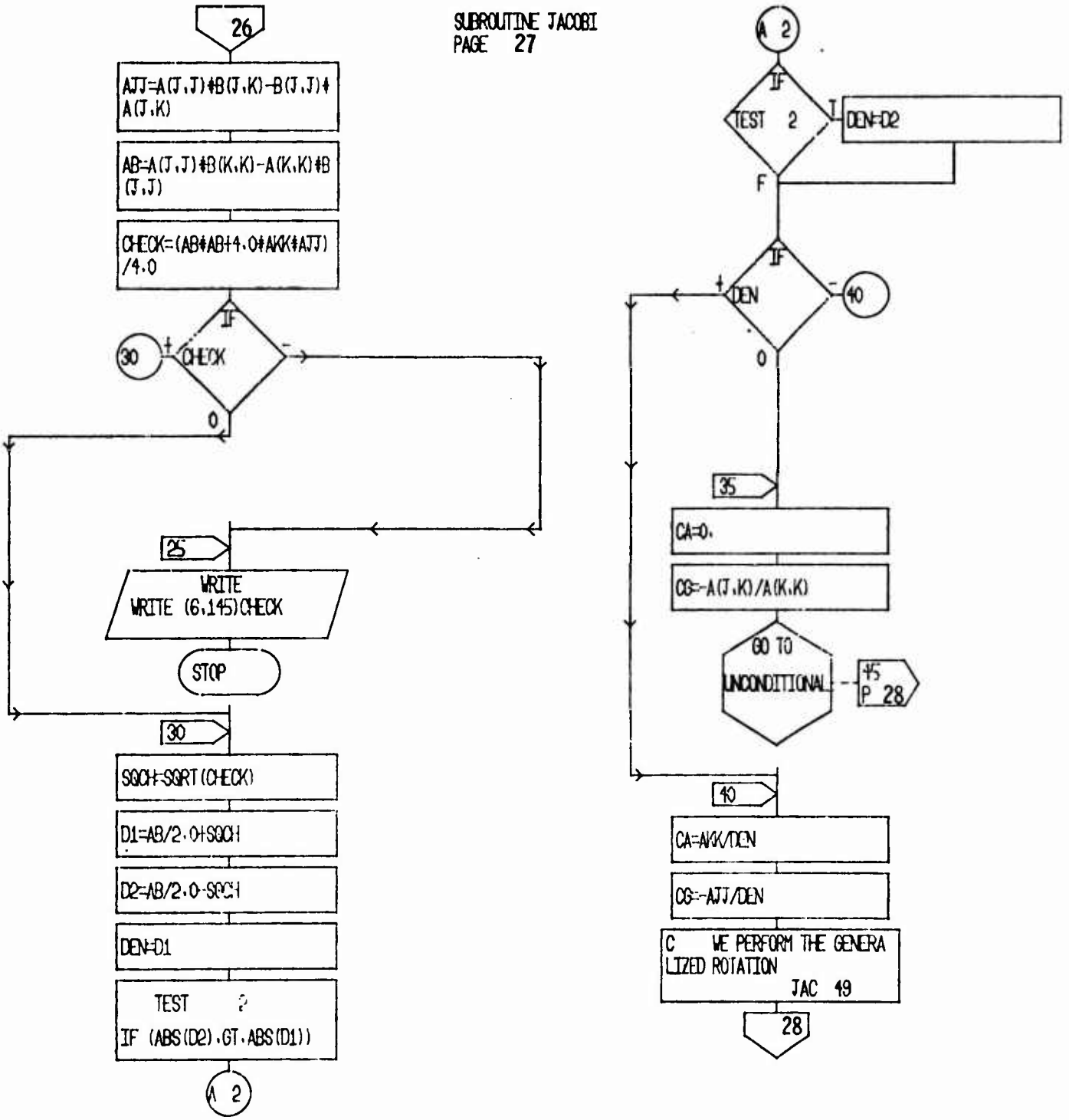
26
AJJ=A(J,J)*B(J,K)-B(J,J)*A(J,K)
AB=A(J,J)*B(K,K)-A(K,K)*B(J,J)
CHECK=(AB*AB+4.0*AKK*AJJ)/4.0
IF
30
+
CHECK
-
0
25
WRITE
WRITE (6,145)CHECK
STOP
30
SQCH=SQRT(CHECK)
D1=AB/2.0+SQCH
D2=AB/2.0-SQCH
DEN=D1
TEST 2
IF (ABS(D2).GT.ABS(D1))
A 2
A 2
IF
TEST 2
I
DEN=D2
F
IF
+
DEN
-
40
0
35
CA=0.
CG=-A(J,K)/A(K,K)
GO TO
UNCONDITIONAL
45
P 28
40
CA=AKK/DEN
CG=-AJJ/DEN
C WE PERFORM THE GENERALIZED ROTATION
JAC 49
28

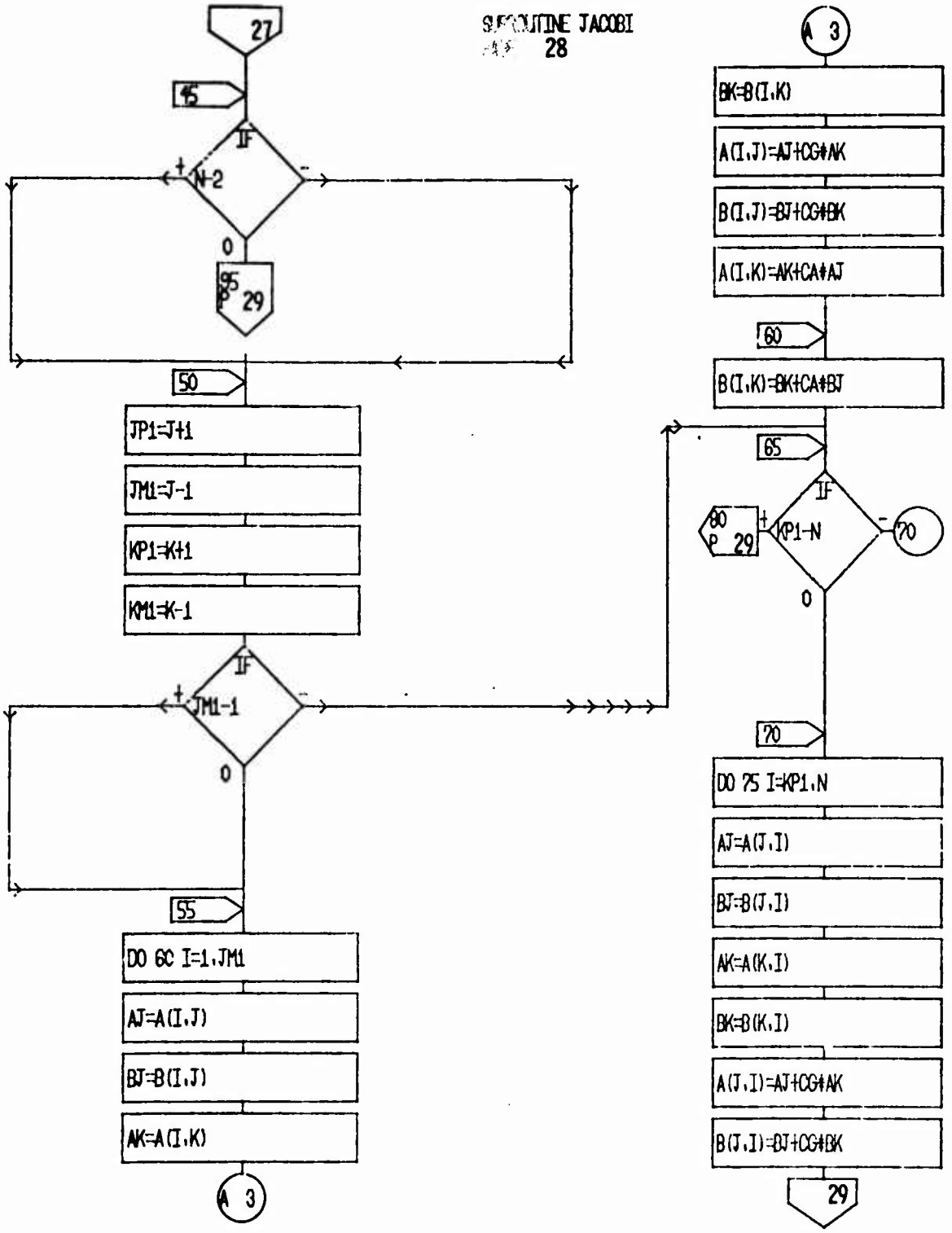
SUBROUTINE JACOBI
28
27
45
IF
N-2
+
-
0
95
P 29
50
JP1=J+1
JM1=J-1
KP1=K+1
KM1=K-1
IF
JM1-1
+
-
0
55
DO 60 I=1,JM1
AJ=A(I,J)
BJ=B(I,J)
AK=A(I,K)
A 3
A 3
BK=B(I,K)
A(I,J)=AJ+CG*AK
B(I,J)=BJ+CG*BK
A(I,K)=AK+CA*AJ
60
B(I,K)=BK+CA*BJ
65
80
P 29
IF
KP1-N
+
-
70
0
70
DO 75 I=KP1,N
AJ=A(J,I)
BJ=B(J,I)
AK=A(K,I)
BK=B(K,I)
A(J,I)=AJ+CG*AK
B(J,I)=BJ+CG*BK
29

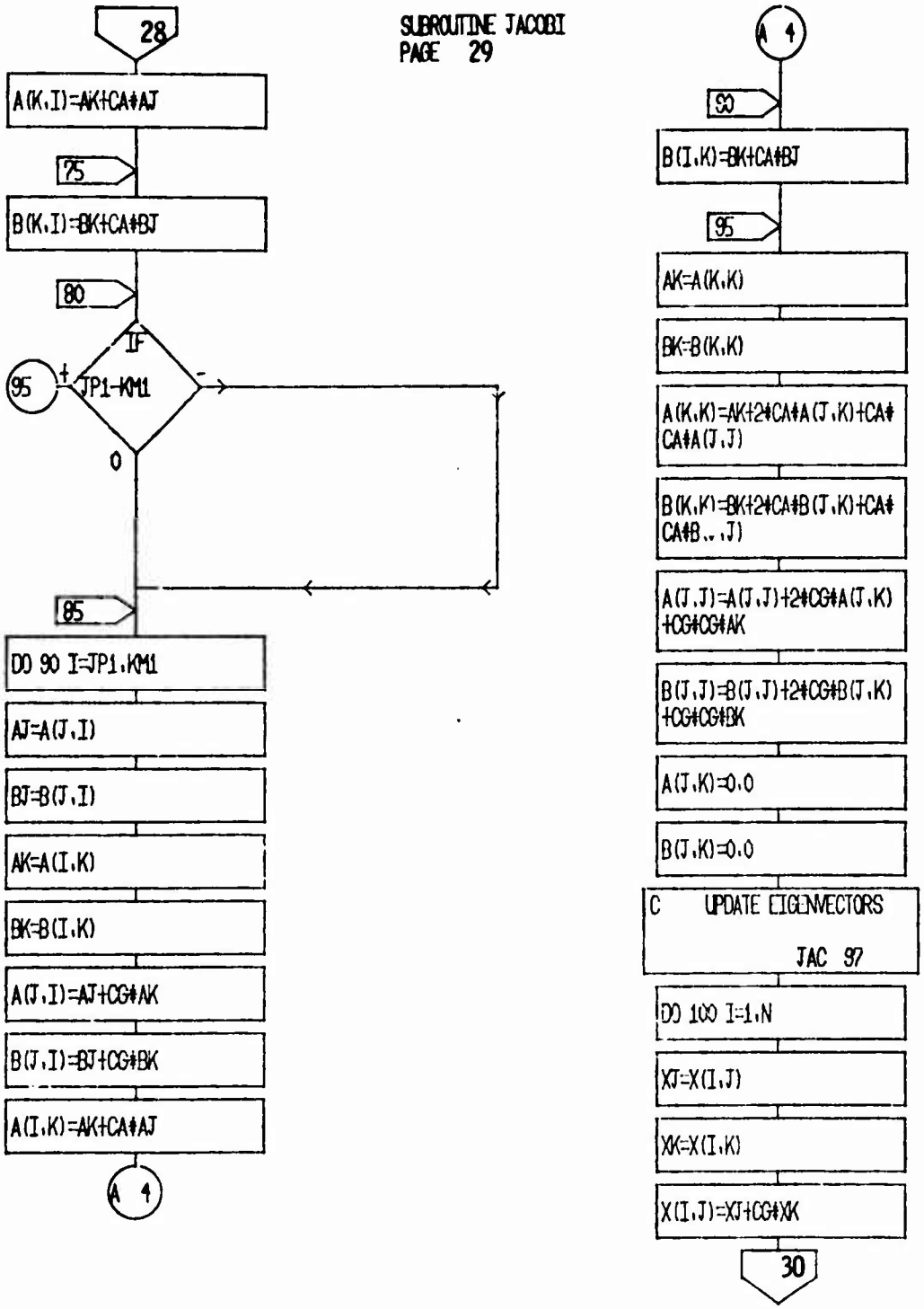
28
A(K,I)=AK+CA*AJ
75
B(K,I)=BK+CA*BJ
80
IF
95
+
JP1-KM1
-
0
85
DO 90 I=JP1,KM1
AJ=A(J,I)
BJ=B(J,I)
AK=A(I,K)
BK=B(I,K)
A(J,I)=AJ+CG*AK
B(J,I)=BJ+CG*BK
A(I,K)=AK+CA*AJ
A 4
A 4
90
B(I,K)=BK+CA*BJ
95
AK=A(K,K)
BK=B(K,K)
A(K,K)=AK+2*CA*A(J,K)+CA*CA*A(J,J)
B(K,K)=BK+2*CA*B(J,K)+CA*CA*B(J,J)
A(J,J)=A(J,J)+2*CG*A(J,K)+CG*CG*AK
B(J,J)=B(J,J)+2*CG*B(J,K)+CG*CG*BK
A(J,K)=0.0
B(J,K)=0.0
C UPDATE EIGENVECTORS
JAC 97
DO 100 I=1,N
XJ=X(I,J)
XK=X(I,K)
X(I,J)=XJ+CG*XK
30

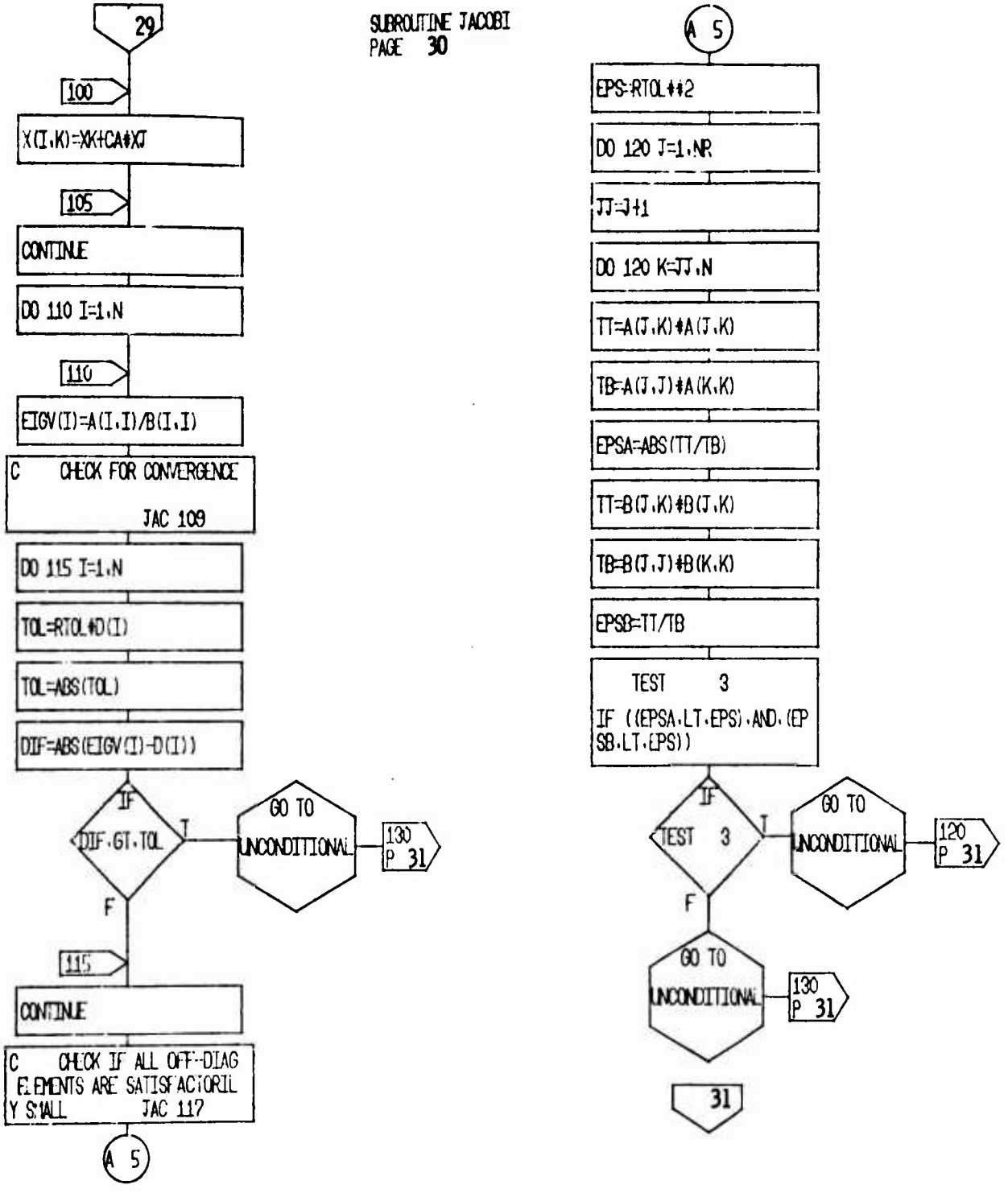
29
100
X(I,K)=XK+CA*XJ
105
CONTINUE
DO 110 I=1,N
110
EIGV(I)=A(I,I)/B(I,I)
C CHECK FOR CONVERGENCE
JAC 109
DO 115 I=1,N
TOL=RTOL*D(I)
TOL=ABS(TOL)
DIF=ABS(EIGV(I)-D(I))
IF
DIF.GT.TOL
T
GO TO
UNCONDITIONAL
130
P 31
F
115
CONTINUE
C CHECK IF ALL OFF-DIAG
ELEMENTS ARE SATISFACTORIL
Y SMALL JAC 117
A 5
A 5
EPS=RTOL**2
DO 120 J=1,NR
JJ=J+1
DO 120 K=JJ,N
TT=A(J,K)*A(J,K)
TB=A(J,J)*A(K,K)
EPSA=ABS(TT/TB)
TT=B(J,K)*B(J,K)
TB=B(J,J)*B(K,K)
EPSB=TT/TB
TEST 3
IF ((EPSA.LT.EPS).AND.(EP
SB.LT.EPS))
IF
TEST 3
T
GO TO
UNCONDITIONAL
120
P 31
F
GO TO
UNCONDITIONAL
130
P 31
31

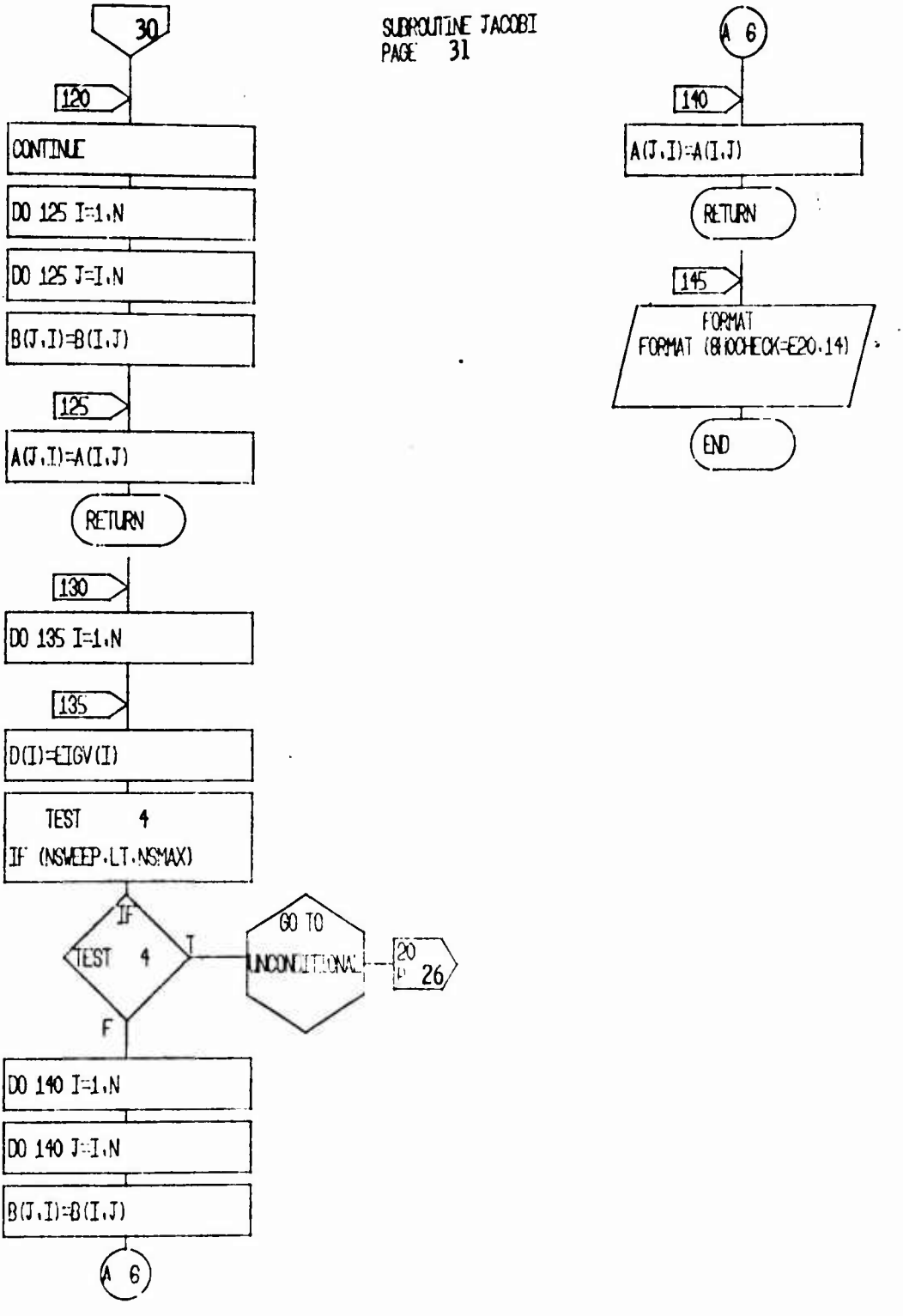
30
120
CONTINUE
DO 125 I=1,N
DO 125 J=I,N
B(J,I)=B(I,J)
125
A(J,I)=A(I,J)
RETURN
130
DO 135 I=1,N
135
D(I)=EIGV(I)
TEST 4
IF (NSWEEP.LT.NSMAX)
IF
TEST 4
T
GO TO
UNCONDITIONAL
20
26
F
DO 140 I=1,N
DO 140 J=I,N
B(J,I)=B(I,J)
A 6
A 6
140
A(J,I)=A(I,J)
RETURN
145
FORMAT
FORMAT (8H0CHECK=E20.14)
END

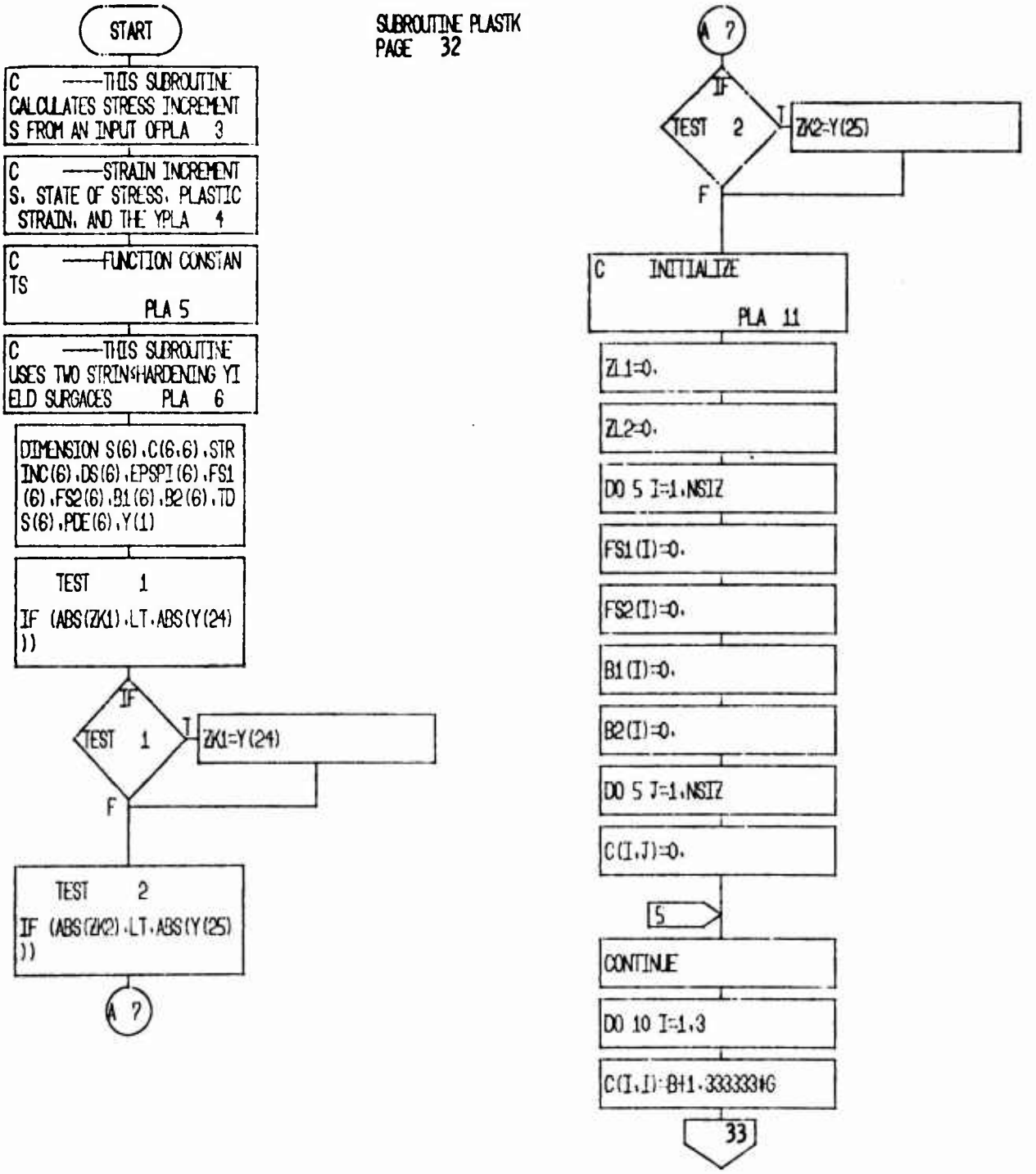
START
C ——THIS SUBROUTINE CALCULATES STRESS INCREMENTS FROM AN INPUT OFPLA 3
C ——STRAIN INCREMENTS, STATE OF STRESS, PLASTIC STRAIN, AND THE YPLA 4
C ——FUNCTION CONSTANTS PLA 5
C ——THIS SUBROUTINE USES TWO STRIN-HARDENING YIELD SURFACES PLA 6
DIMENSION S(6),C(6,6),STRINC(6),DS(6),EPSPI(6),FS1(6),FS2(6),B1(6),B2(6),TDS(6),PDE(6),Y(1)
TEST 1
IF (ABS(ZK1).LT.ABS(Y(24)))
IF
TEST 1
T
ZK1=Y(24)
F
TEST 2
IF (ABS(ZK2).LT.ABS(Y(25)))
A 7
A 7
IF
TEST 2
T
ZK2=Y(25)
F
C INITIALIZE PLA 11
ZL1=0.
ZL2=0.
DO 5 I=1,NSIZ
FS1(I)=0.
FS2(I)=0.
B1(I)=0.
B2(I)=0.
DO 5 J=1,NSIZ
C(I,J)=0.
5
CONTINUE
DO 10 I=1,3
C(I,I)=BH1.3333334G
33

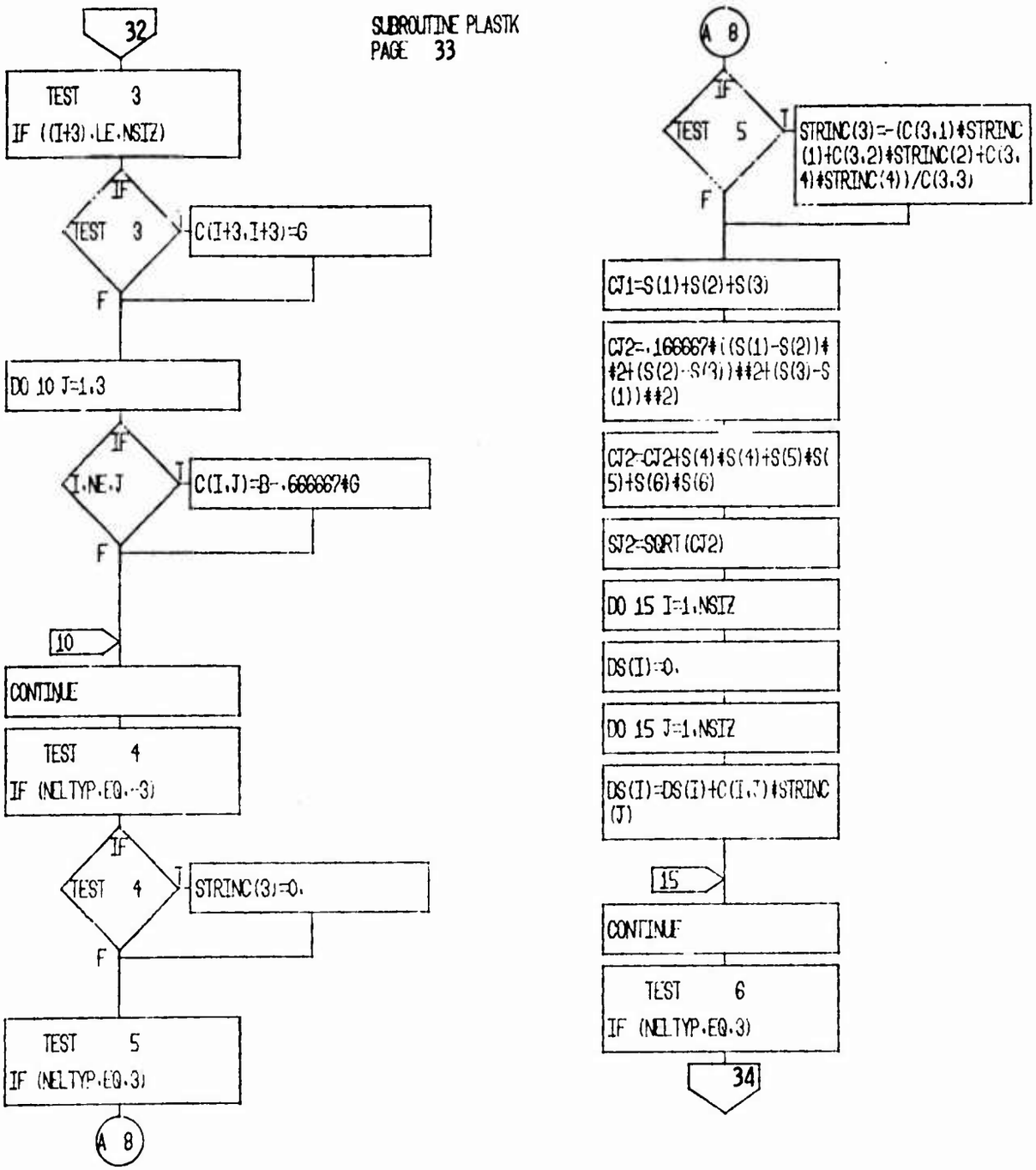
32
TEST 3
IF ((I+3).LE.NSIZ)
IF
TEST 3
T
C(I+3,I+3)=G
F
DO 10 J=1,3
IF
I.NE.J
T
C(I,J)=B-.666667*G
F
10
CONTINUE
TEST 4
IF (NELTYP.EQ.-3)
IF
TEST 4
T
STRINC(3)=0.
F
TEST 5
IF (NELTYP.EQ.3)
A 8
A 8
IF
TEST 5
T
STRINC(3)=-(C(3,1)*STRINC(1)+C(3,2)*STRINC(2)+C(3,4)*STRINC(4))/C(3,3)
F
CJ1=S(1)+S(2)+S(3)
CJ2=.166667*((S(1)-S(2))**2+(S(2)-S(3))**2+(S(3)-S(1))**2)
CJ2=CJ2+S(4)*S(4)+S(5)*S(5)+S(6)*S(6)
SJ2=SQRT(CJ2)
DO 15 I=1,NSIZ
DS(I)=0.
DO 15 J=1,NSIZ
DS(I)=DS(I)+C(I,J)*STRINC(J)
15
CONTINUE
TEST 6
IF (NELTYP.EQ.3)
34

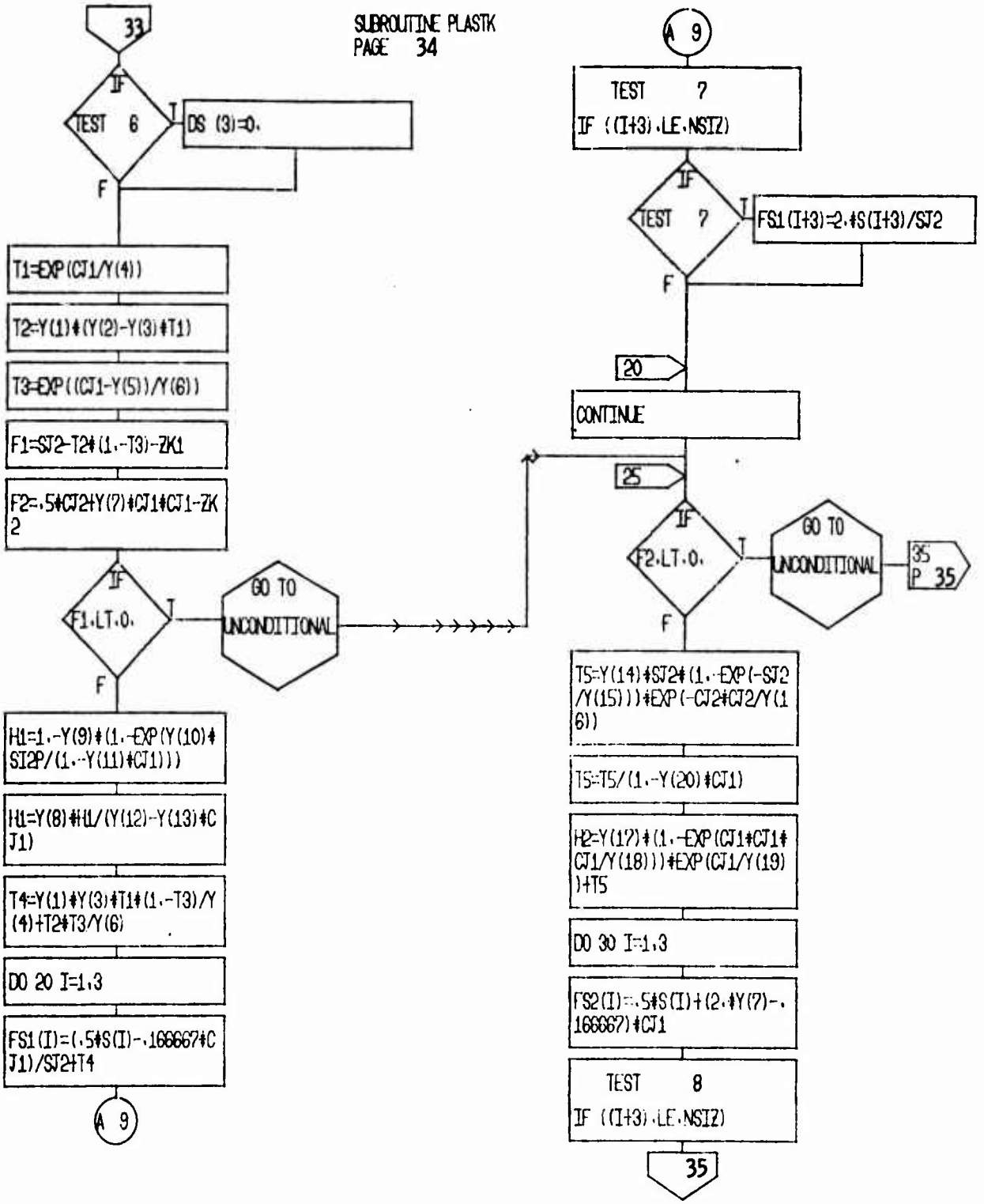
SUBROUTINE PLASTK
PAGE 34
33
IF
TEST 6
T
DS (3)=0.
F
T1=EXP(CJ1/Y(4))
T2=Y(1)*(Y(2)-Y(3)*T1)
T3=EXP((CJ1-Y(5))/Y(6))
F1=SJ2-T2*(1.-T3)-ZK1
F2=.5*CJ2+Y(7)*CJ1*CJ1-ZK2
IF
F1.LT.0.
T
GO TO
UNCONDITIONAL
F
H1=1.-Y(9)*(1.-EXP(Y(10)*SI2P/(1.-Y(11)*CJ1)))
HL=Y(8)*HL/(Y(12)-Y(13)*CJ1)
T4=Y(1)*Y(3)*T1*(1.-T3)/Y(4)+T2*T3/Y(6)
DO 20 I=1,3
FS1(I)=(.5*S(I)-.166667*CJ1)/SJ2+T4
A 9
A 9
TEST 7
IF ((I+3).LE.NSIZ)
IF
TEST 7
T
FS1(I+3)=2.*S(I+3)/SJ2
F
20
CONTINUE
25
IF
F2.LT.0.
T
GO TO
UNCONDITIONAL
35
P 35
F
T5=Y(14)*SJ2*(1.-EXP(-SJ2/Y(15)))*EXP(-CJ2*CJ2/Y(16))
T5=T5/(1.-Y(20)*CJ1)
H2=Y(17)*(1.-EXP(CJ1*CJ1*CJ1/Y(18)))*EXP(CJ1/Y(19))+T5
DO 30 I=1,3
FS2(I)=.5*S(I)+(2.*Y(7)-.166667)*CJ1
TEST 8
IF ((I+3).LE.NSIZ)
35

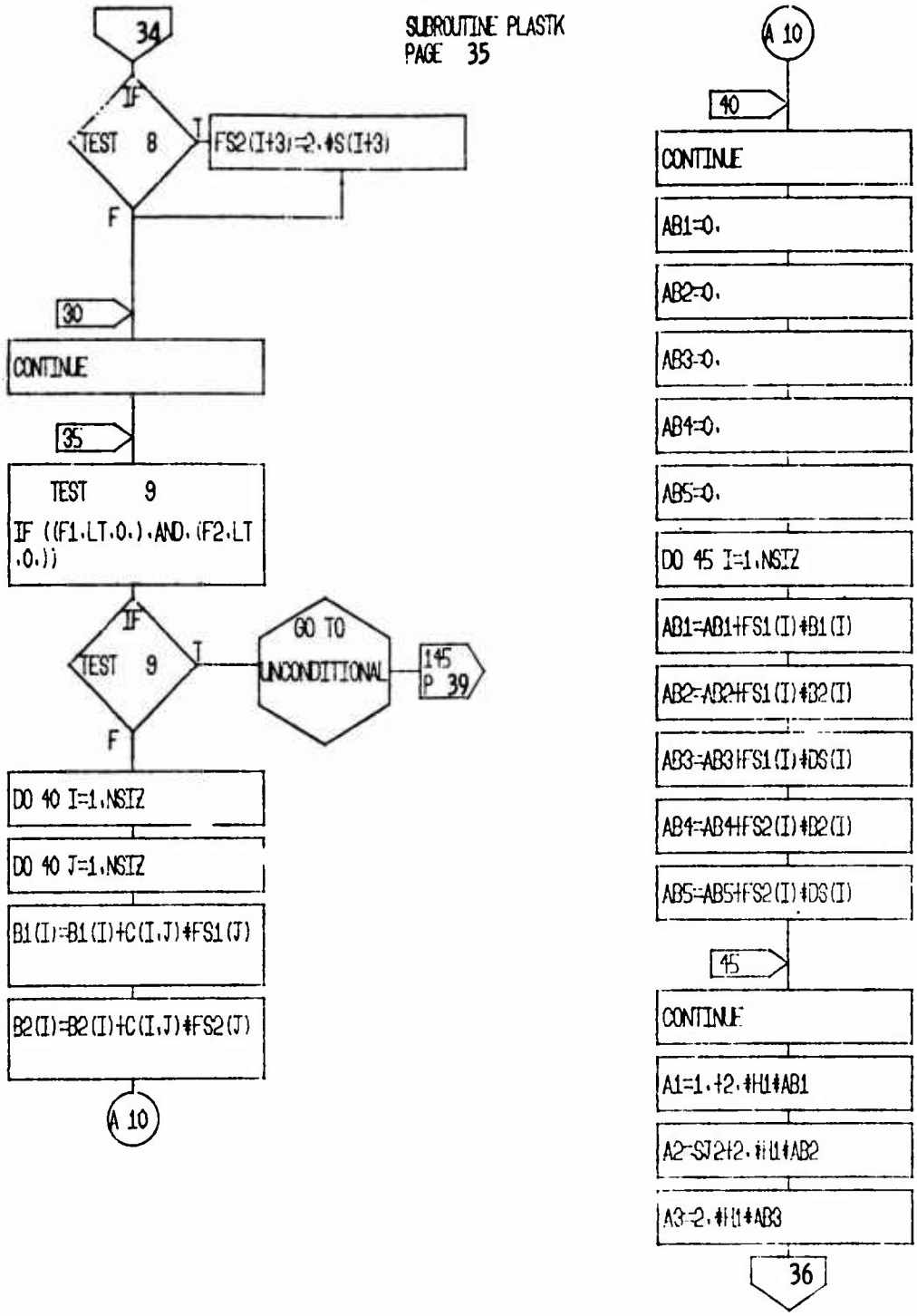
34
IF
TEST 8
T
FS2(I+3)=2.*S(I+3)
F
30
CONTINUE
35
TEST 9
IF ((F1.LT.0.).AND.(F2.LT.0.))
IF
TEST 9
T
GO TO
UNCONDITIONAL
145
P 39
F
DO 40 I=1,NSIZ
DO 40 J=1,NSIZ
B1(I)=B1(I)+C(I,J)*FS1(J)
B2(I)=B2(I)+C(I,J)*FS2(J)
A 10
A 10
40
CONTINUE
AB1=0.
AB2=0.
AB3=0.
AB4=0.
AB5=0.
DO 45 I=1,NSIZ
AB1=AB1+FS1(I)*B1(I)
AB2=AB2+FS1(I)*B2(I)
AB3=AB3+FS1(I)*DS(I)
AB4=AB4+FS2(I)*B2(I)
AB5=AB5+FS2(I)*DS(I)
45
CONTINUE
A1=1.+2.*H1*AB1
A2=SI2+2.*H1*AB2
A3=2.*H1*AB3
36

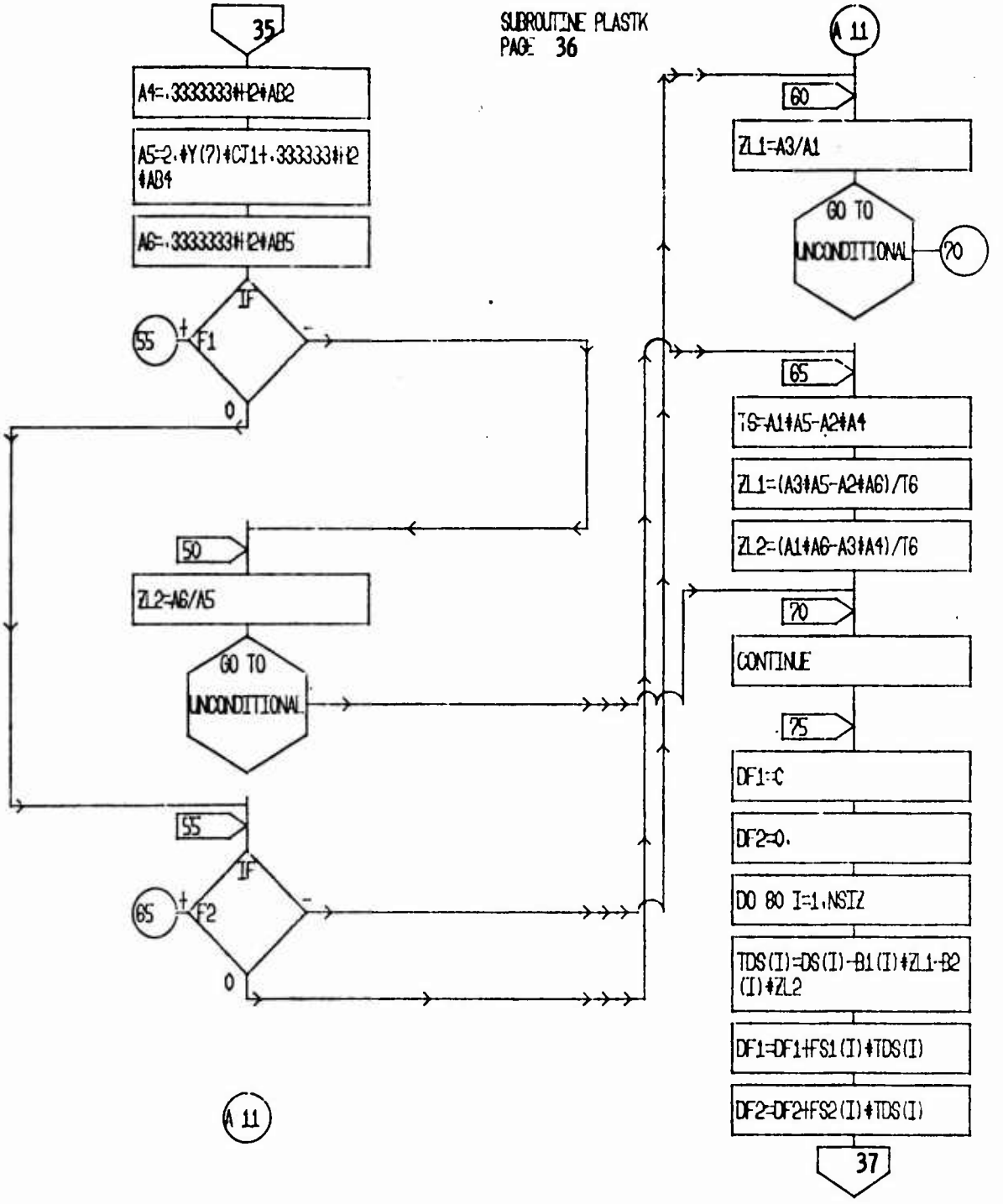
35
A4=.3333333*H2*AB2
A5=2.*Y(7)*(CJ1+.333333*H2*AB4
A6=.3333333*H2*AB5
IF
55
+
F1
-
0
50
ZL2=A6/A5
GO TO
UNCONDITIONAL
55
IF
65
+
F2
-
0
A 11
A 11
60
ZL1=A3/A1
GO TO
UNCONDITIONAL
70
65
TS=A1*A5-A2*A4
ZL1=(A3*A5-A2*A6)/T6
ZL2=(A1*A6-A3*A4)/T6
70
CONTINUE
75
DF1=0
DF2=0.
DO 80 I=1,NSIZ
TDS(I)=DS(I)-B1(I)*ZL1-B2(I)*ZL2
DF1=DF1+FS1(I)*TDS(I)
DF2=DF2+FS2(I)*TDS(I)
37

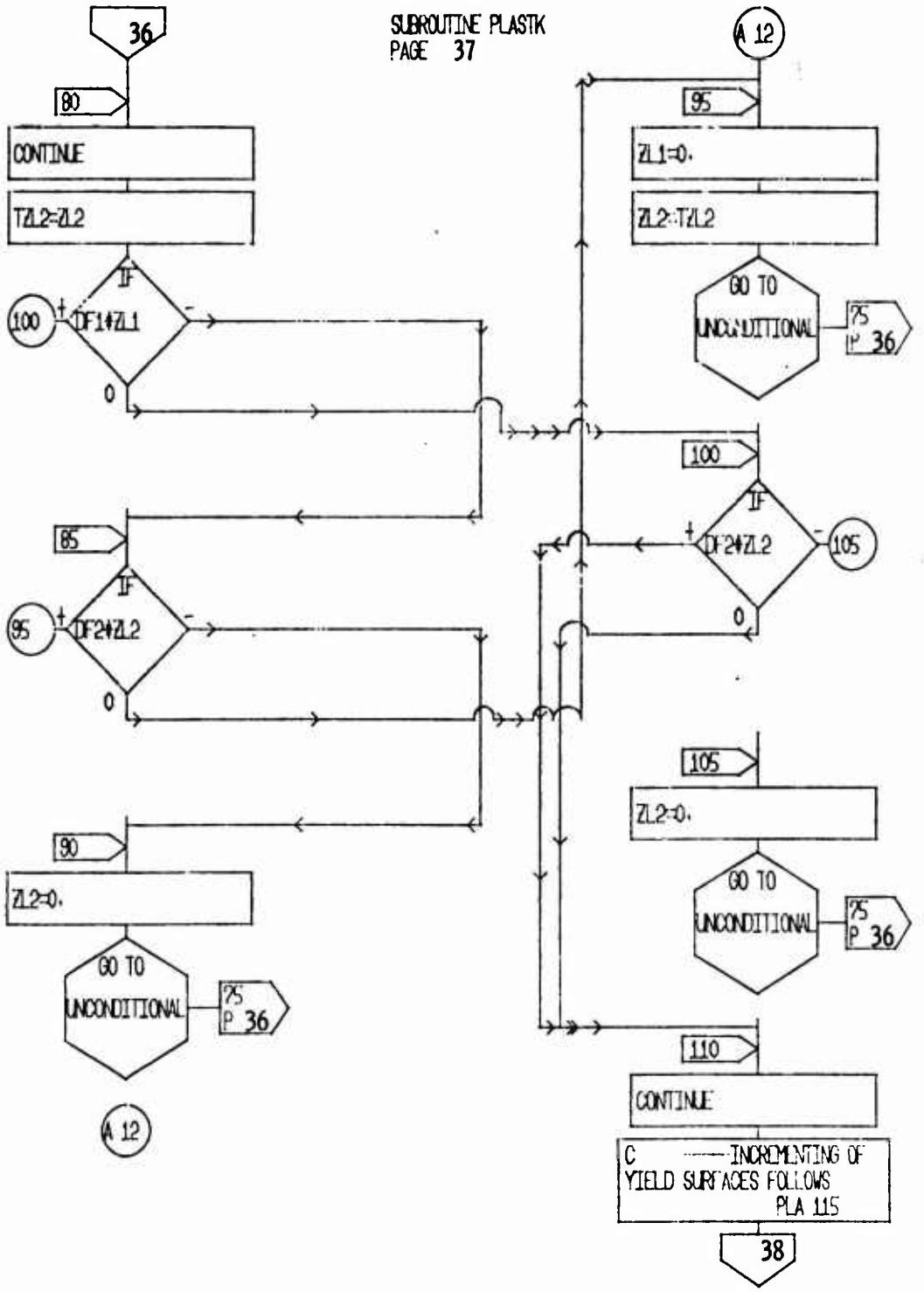
36
80
CONTINUE
TZL2=ZL2
IF
100
+
DF1≠ZL1
-
0
85
IF
95
+
DF2≠ZL2
-
0
90
ZL2=0.
GO TO
UNCONDITIONAL
75
P 36
A 12
A 12
95
ZL1=0.
ZL2=TZL2
GO TO
UNCONDITIONAL
75
P 36
100
IF
+
DF2≠ZL2
105
-
0
105
ZL2=0.
GO TO
UNCONDITIONAL
75
P 36
110
CONTINUE
C ——INCREMENTING OF
YIELD SURFACES FOLLOWS
PLA 115
38

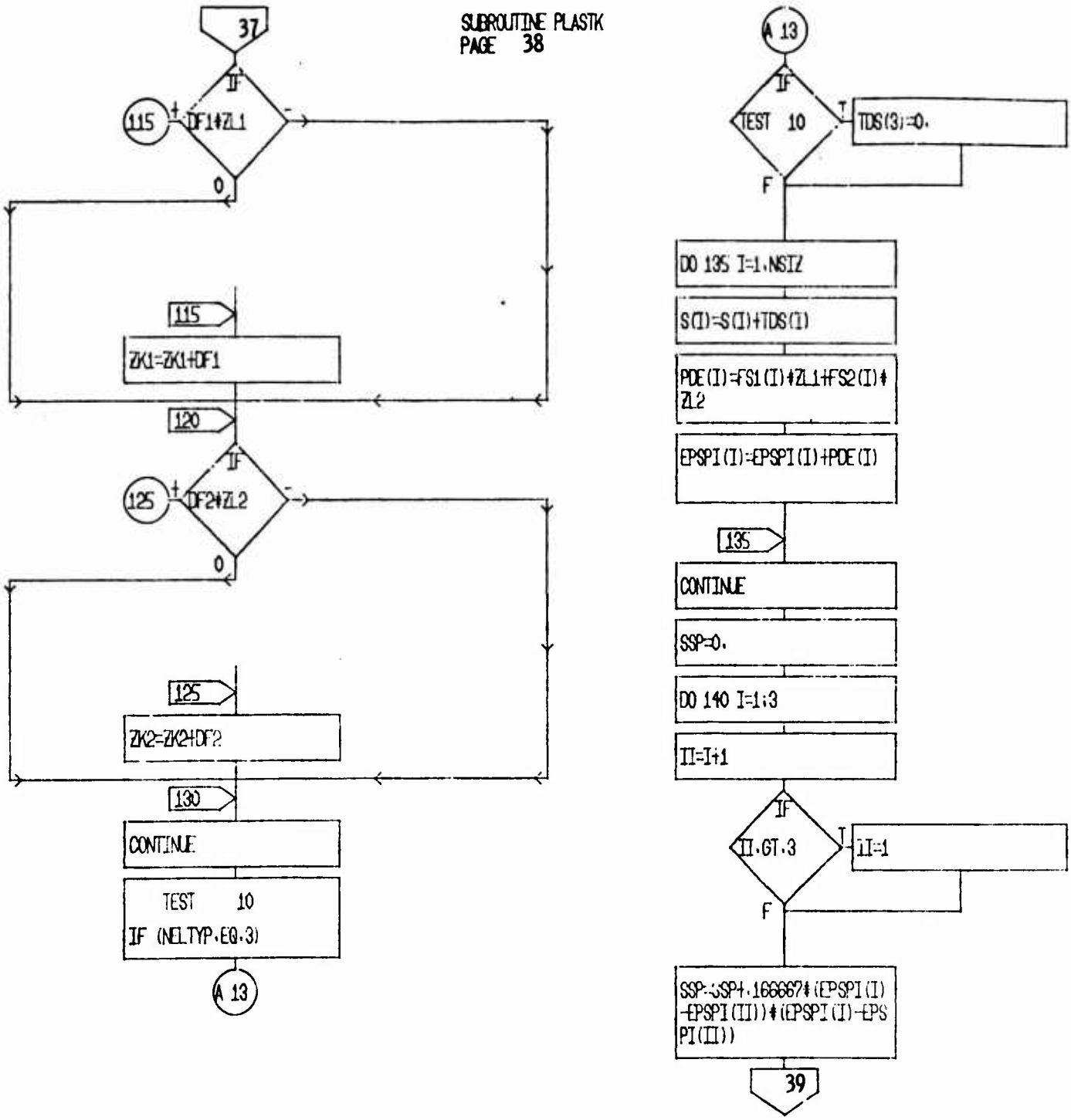
37
IF
115
+
DF1+ZL1
-
0
115
ZK1=ZK1+DF1
120
IF
125
+
DF2+ZL2
-
0
125
ZK2=ZK2+DF2
130
CONTINUE
TEST 10
IF (NELTYP.EQ.3)
A 13
A 13
IF
TEST 10
T
TDS(3)=0.
F
DO 135 I=1,NSIZ
S(I)=S(I)+TDS(I)
PDE(I)=FS1(I)*ZL1+FS2(I)*ZL2
EPSPI(I)=EPSPI(I)+PDE(I)
135
CONTINUE
SSP=0.
DO 140 I=1,3
II=I+1
IF
II.GT.3
I
II=1
F
SSP=.5SP+.166667*(EPSPI(I)-EPSPI(II))*(EPSPI(I)-EPSPI(II))
39

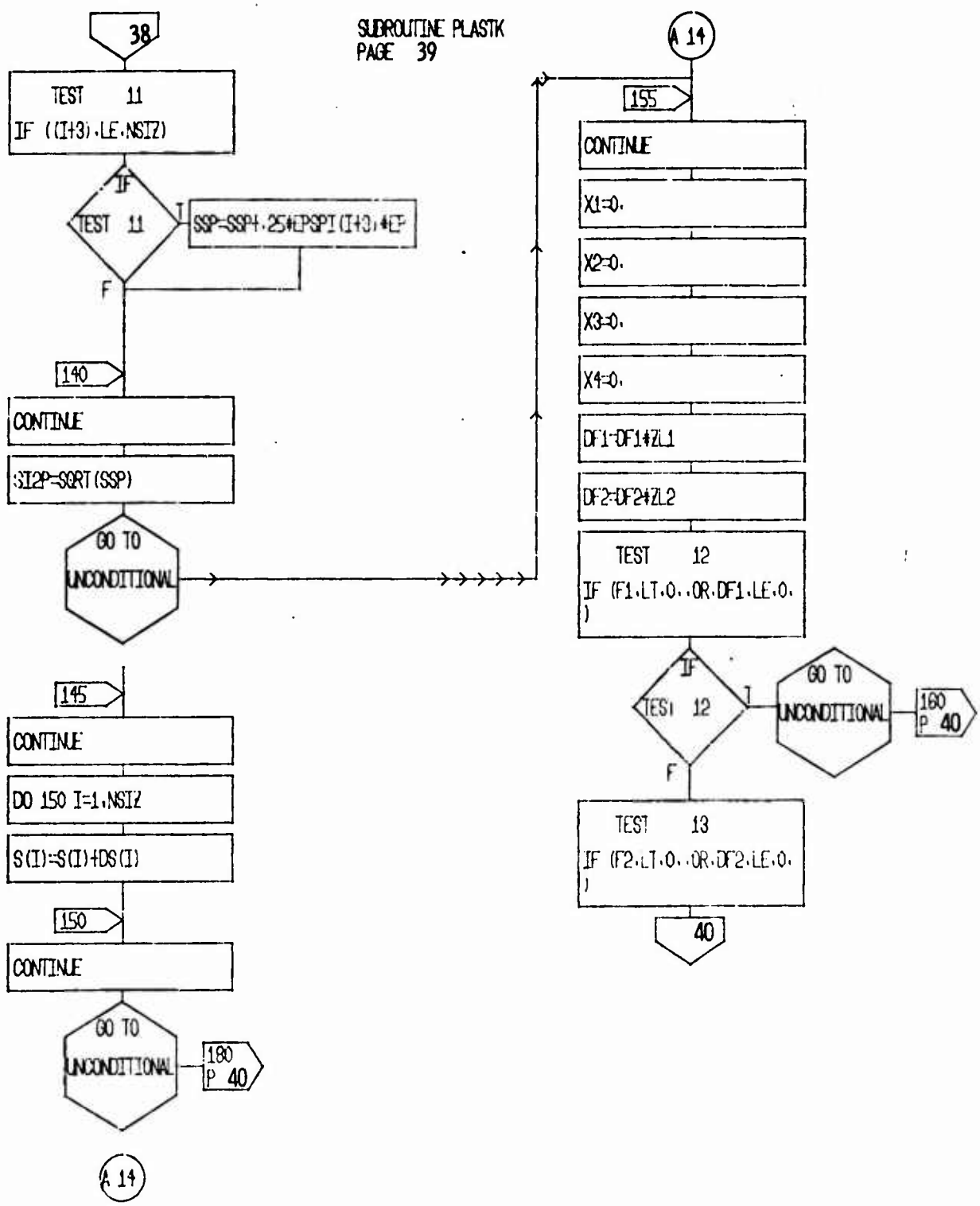
SUBROUTINE PLASTK
PAGE 39
38
TEST 11
IF ((I+3).LE.NSIZ)
IF
TEST 11
T
SSP=SSP+.25*EPSPI(I+3)*EP
F
140
CONTINUE
SI2P=SQRT(SSP)
GO TO
UNCONDITIONAL
145
CONTINUE
DO 150 I=1,NSIZ
S(I)=S(I)+DS(I)
150
CONTINUE
GO TO
UNCONDITIONAL
180
P 40
A 14
A 14
155
CONTINUE
X1=0.
X2=0.
X3=0.
X4=0.
DF1=DF1*ZL1
DF2=DF2*ZL2
TEST 12
IF (F1.LT.0..OR.DF1.LE.0.
)
IF
TEST 12
T
GO TO
UNCONDITIONAL
160
P 40
F
TEST 13
IF (F2.LT.0..OR.DF2.LE.0.
)
40

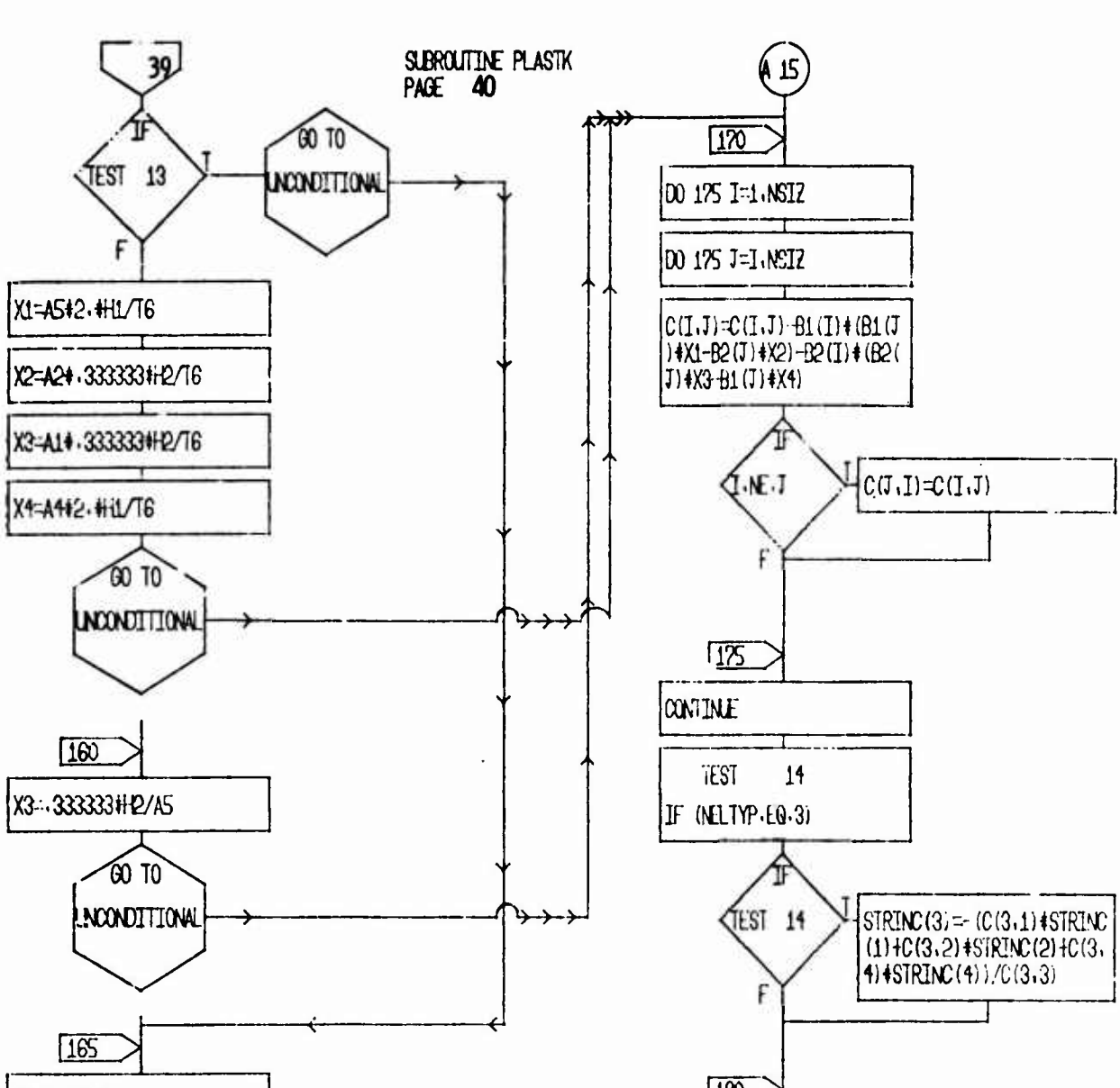
SUBROUTINE PLASTK
PAGE 40
39
IF
TEST 13
T
GO TO
UNCONDITIONAL
F
X1=A5**2.*H1/T6
X2=A2*.333333*H2/T6
X3=A1*.333333*H2/T6
X4=A4**2.*H1/T6
GO TO
UNCONDITIONAL
160
X3=.333333*H2/A5
GO TO
UNCONDITIONAL
165
X1=2.*H1/A1
A 15
A 15
120
DO 175 I=1,NSIZ
DO 175 J=I,NSIZ
C(I,J)=C(I,J)-B1(I)*(B1(J)*X1-B2(J)*X2)-B2(I)*(B2(J)*X3-B1(J)*X4)
IF
I.NE.J
T
C(J,I)=C(I,J)
F
175
CONTINUE
TEST 14
IF (NELTYP.EQ.3)
IF
TEST 14
T
STRINC(3)=-(C(3,1)*STRINC(1)+C(3,2)*STRINC(2)+C(3,4)*STRINC(4))/C(3,3)
F
180
RETURN
END

SUBROUTINE DOWEL 1
PAGE 41

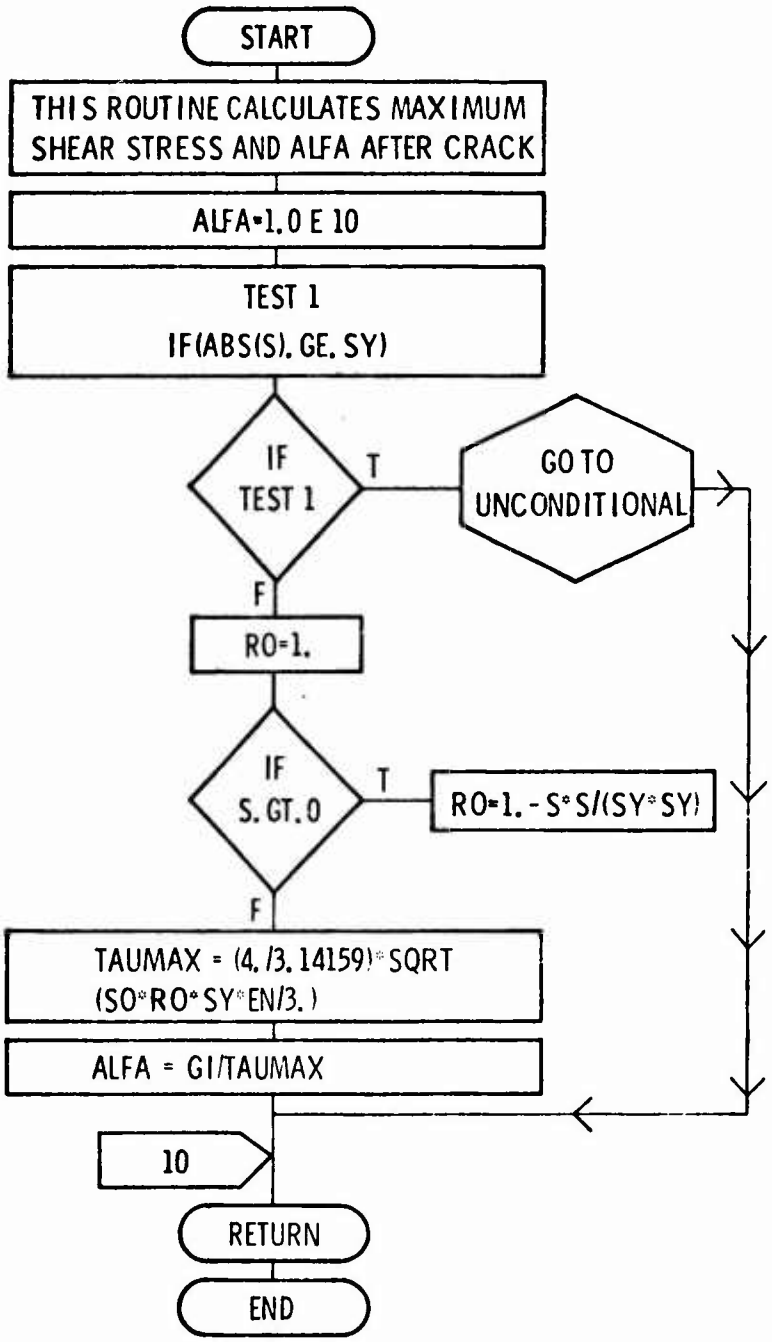

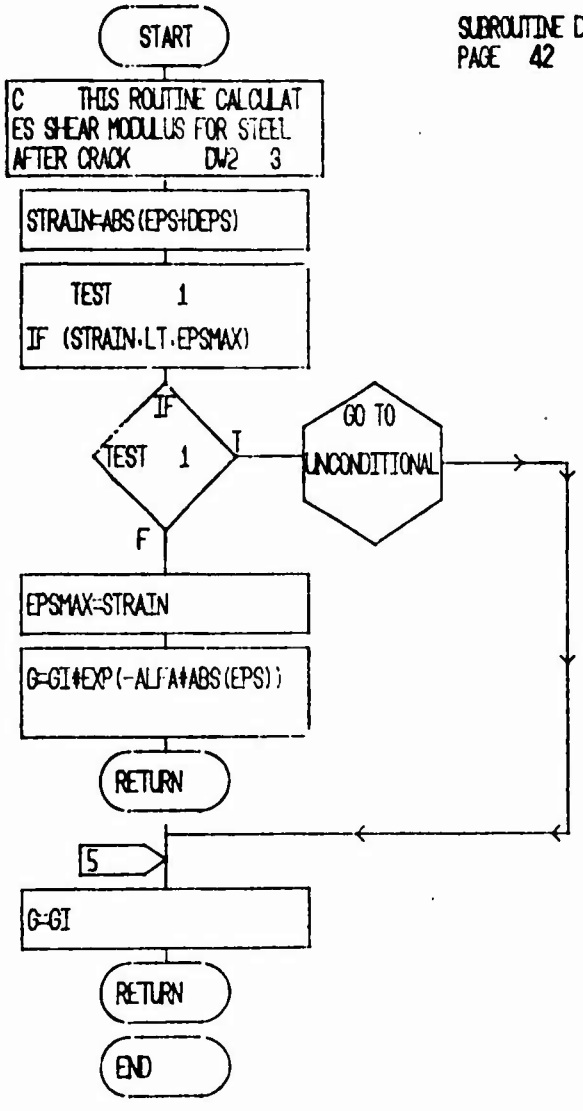

SUBROUTINE DOWEL2
PAGE 42

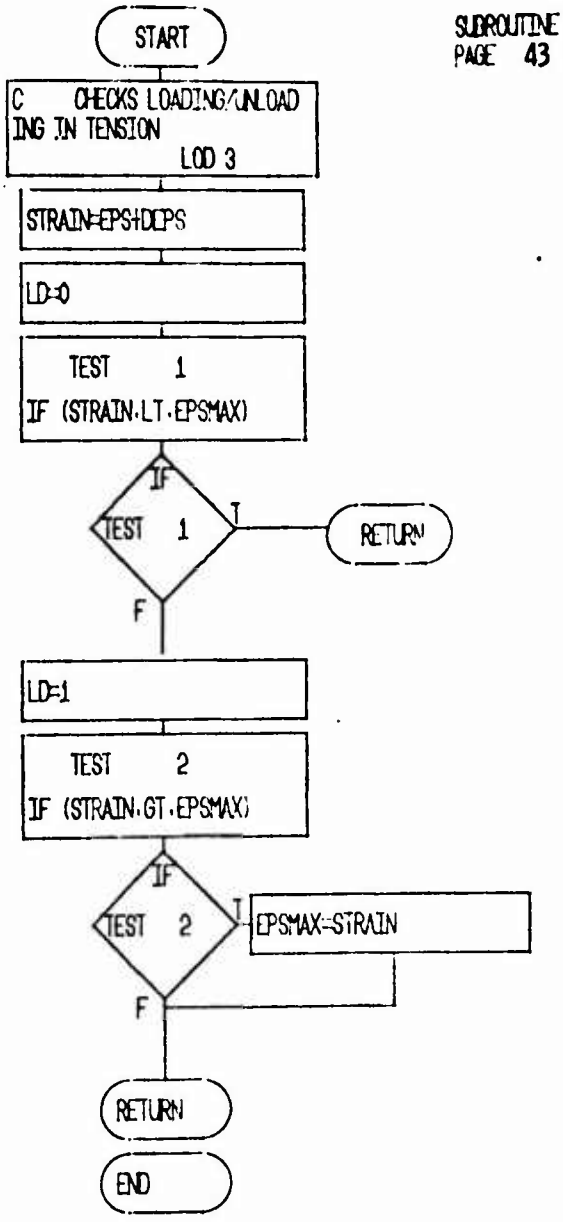
START
C CHECKS LOADING/UNLOAD
ING IN TENSION
LOD 3
STRAIN=EPS+DEPS
LD=0
TEST 1
IF (STRAIN.LT.EPSMAX)
IF
TEST 1
T
RETURN
F
LD=1
TEST 2
IF (STRAIN.GT.EPSMAX)
IF
TEST 2
T
EPSMAX=STRAIN
F
RETURN
END

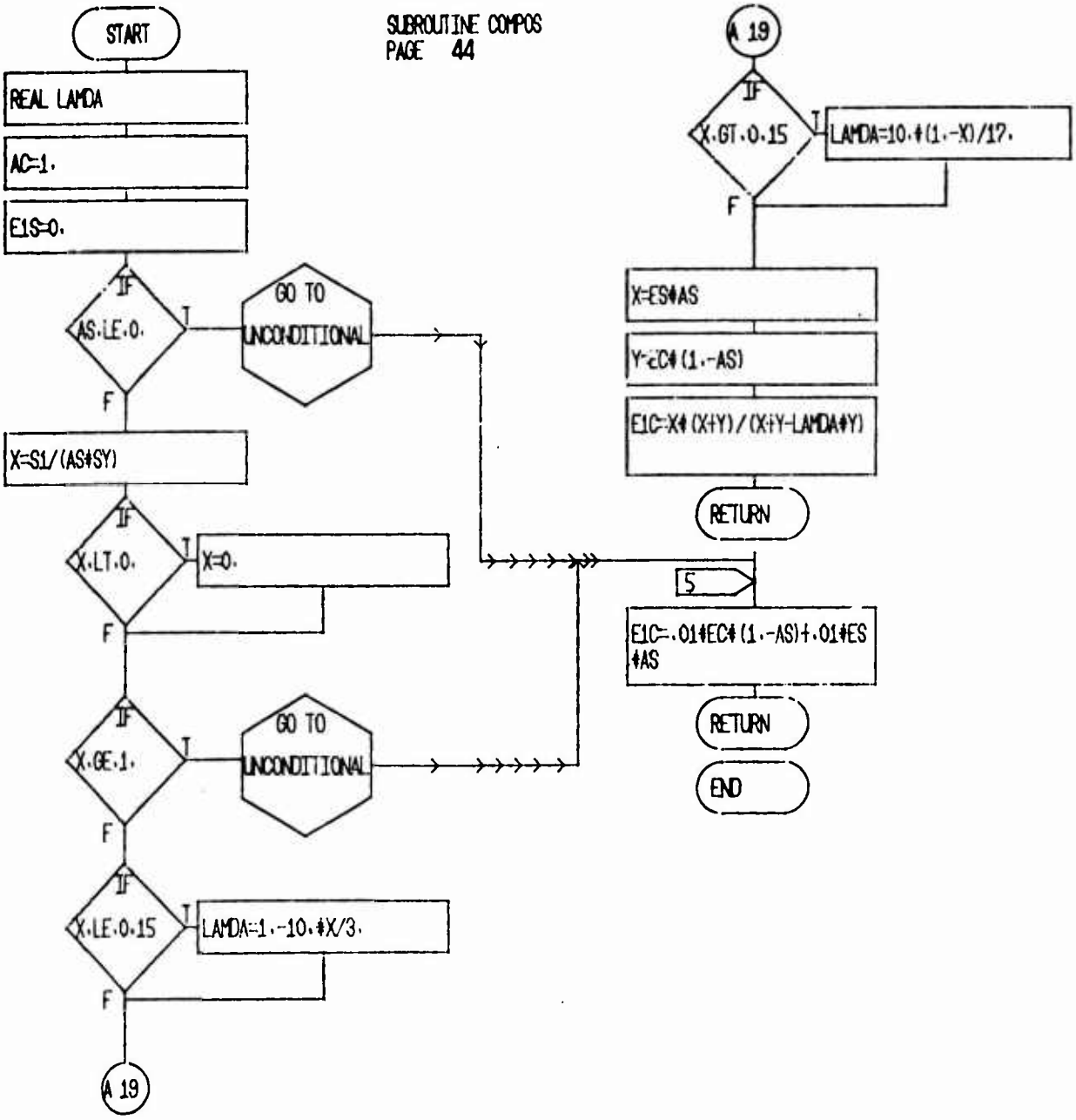
SUBROUTINE COMPOS
PAGE 44
START
REAL LAMDA
AC=1.
E1S=0.
IF
AS.LE.0.
T
GO TO
UNCONDITIONAL
F
X=S1/(AS*SY)
IF
X.LT.0.
T
X=0.
F
IF
X.GE.1.
T
GO TO
UNCONDITIONAL
F
IF
X.LE.0.15
T
LAMDA=1.-10.*X/3.
F
A 19
A 19
IF
X.GT.0.15
T
LAMDA=10.*(1.-X)/17.
F
X=ES*AS
Y=EC*(1.-AS)
E1C=X*(X+Y)/(X+Y-LAMDA*Y)
RETURN
5
E1C=.01*EC*(1.-AS)+.01*ES*AS
RETURN
END

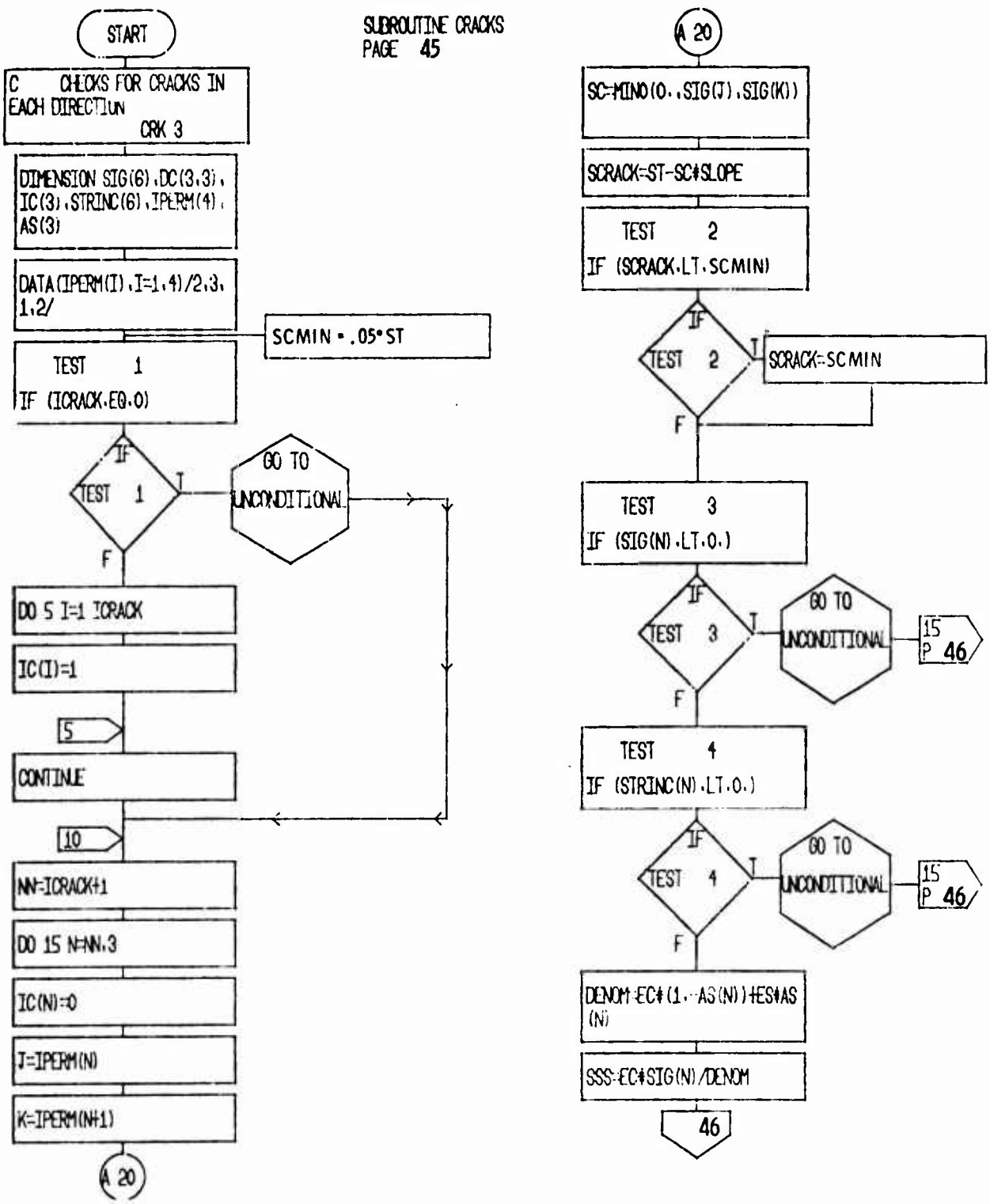
START
SUBROUTINE CRACKS
PAGE 45
C CHECKS FOR CRACKS IN EACH DIRECTION
CRK 3
DIMENSION SIG(6),DC(3,3),IC(3),STRINC(6),IPERM(4),AS(3)
DATA(IPERM(I),I=1,4)/2,3,1,2/
SCMIN = .05*ST
TEST 1
IF (ICRACK.EQ.0)
IF TEST 1
T
F
GO TO UNCONDITIONAL
DO 5 I=1 ICRACK
IC(I)=1
5
CONTINUE
10
NN=ICRACK+1
DO 15 N=NN,3
IC(N)=0
J=IPERM(N)
K=IPERM(N+1)
A 20
A 20
SC=MIN0(0.,SIG(J),SIG(K))
SCRACK=ST-SC*SLOPE
TEST 2
IF (SCRACK.LT.SCMIN)
IF TEST 2
T
F
SCRACK=SCMIN
TEST 3
IF (SIG(N).LT.0.)
IF TEST 3
T
F
GO TO UNCONDITIONAL
15 P 46
TEST 4
IF (STRINC(N).LT.0.)
IF TEST 4
T
F
GO TO UNCONDITIONAL
15 P 46
DENOM=EC*(1.-AS(N))+ES*AS(N)
SSS=EC*SIG(N)/DENOM
46

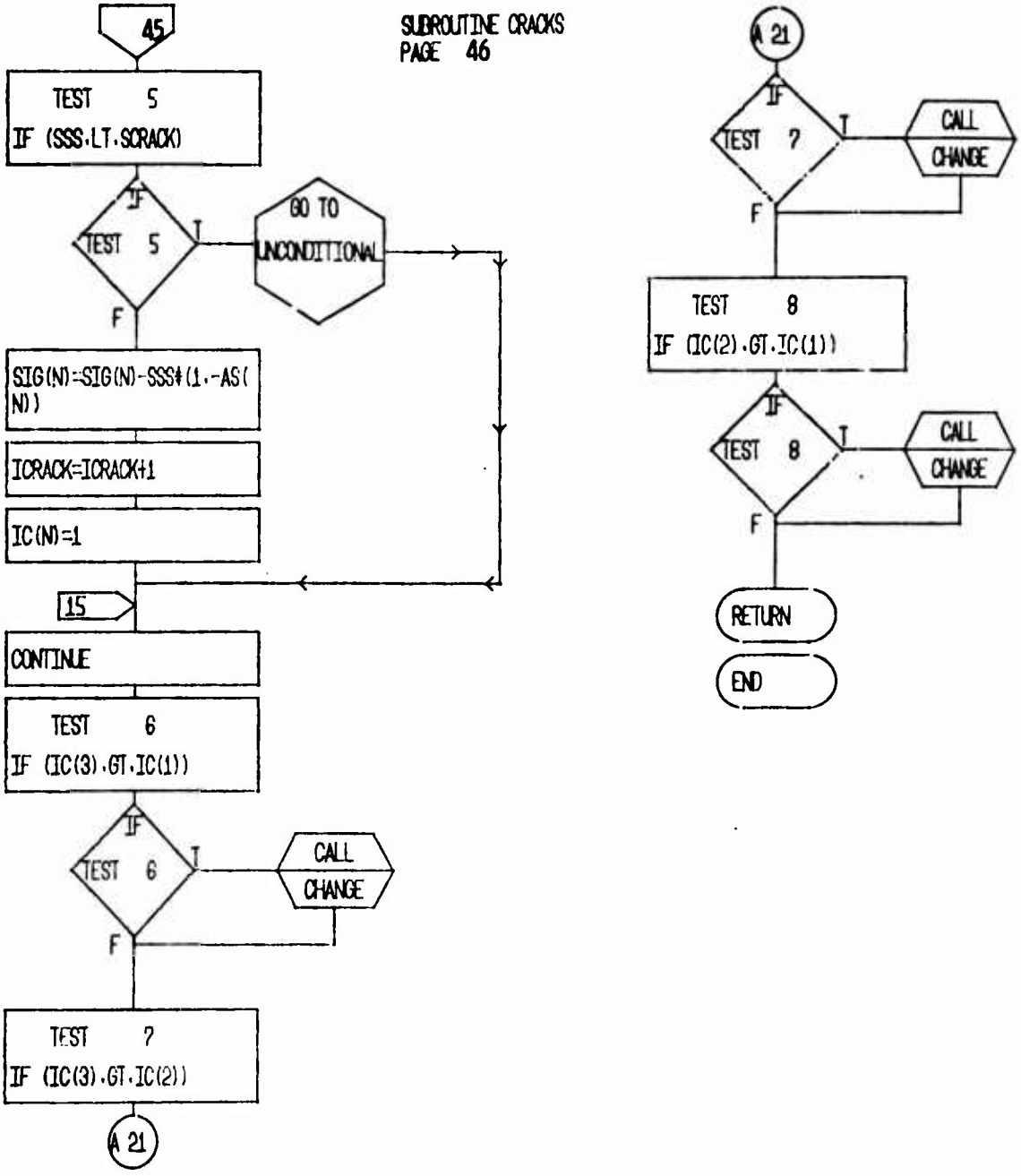
SUBROUTINE CRACKS
PAGE 46
45
TEST 5
IF (SSS.LT.SCRACK)
IF
TEST 5
T
GO TO
UNCONDITIONAL
F
SIG(N)=SIG(N)-SSS*(1.-AS(
N))
ICRACK=ICRACK+1
IC(N)=1
15
CONTINUE
TEST 6
IF (IC(3).GT.IC(1))
IF
TEST 6
T
CALL
CHANGE
F
TEST 7
IF (IC(3).GT.IC(2))
A 21
A 21
IF
TEST 7
T
CALL
CHANGE
F
TEST 8
IF (IC(2).GT.IC(1))
IF
TEST 8
T
CALL
CHANGE
F
RETURN
END

SUBROUTINE MATPAC
PAGE 47

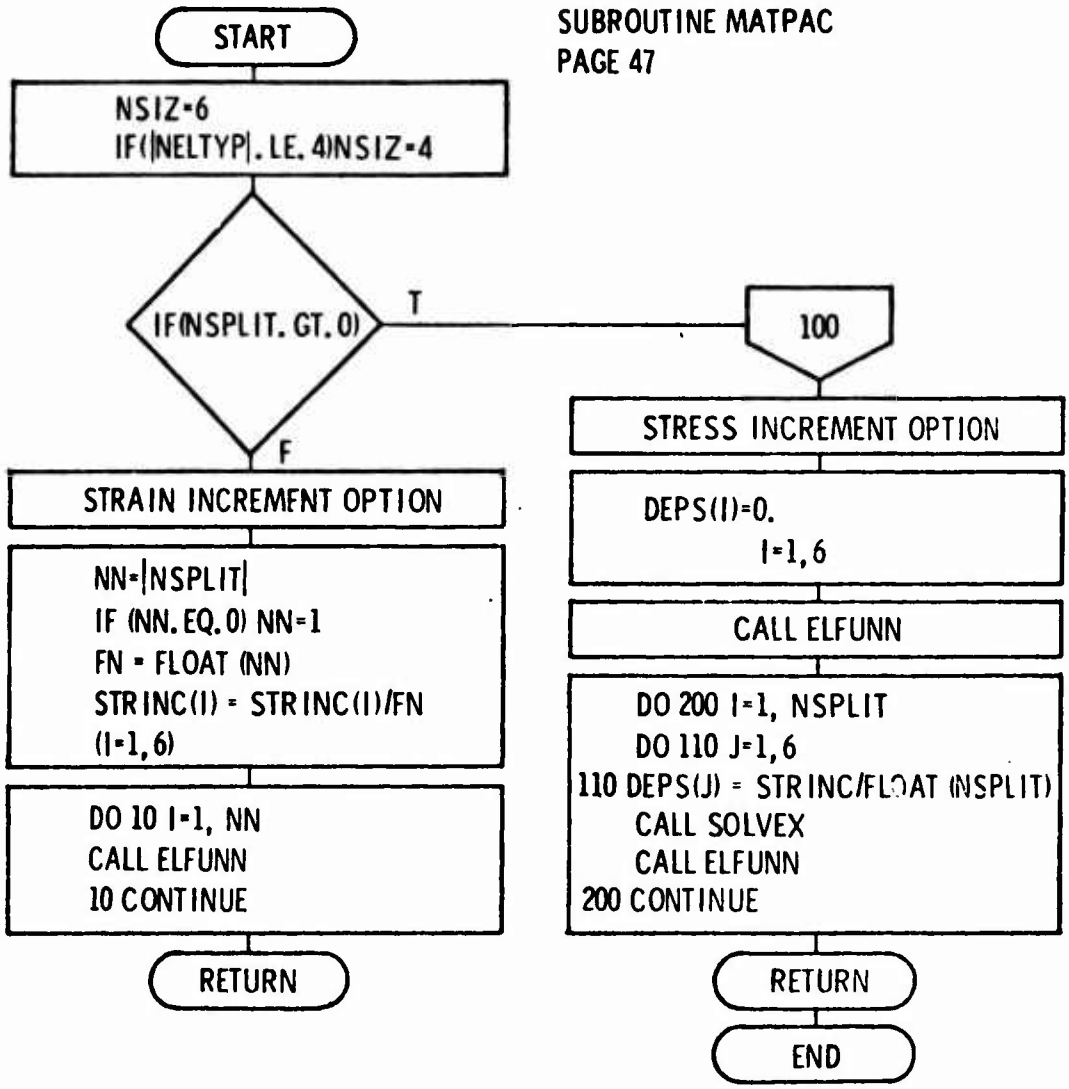

SUBROUTINE SOLVEX
PAGE 48

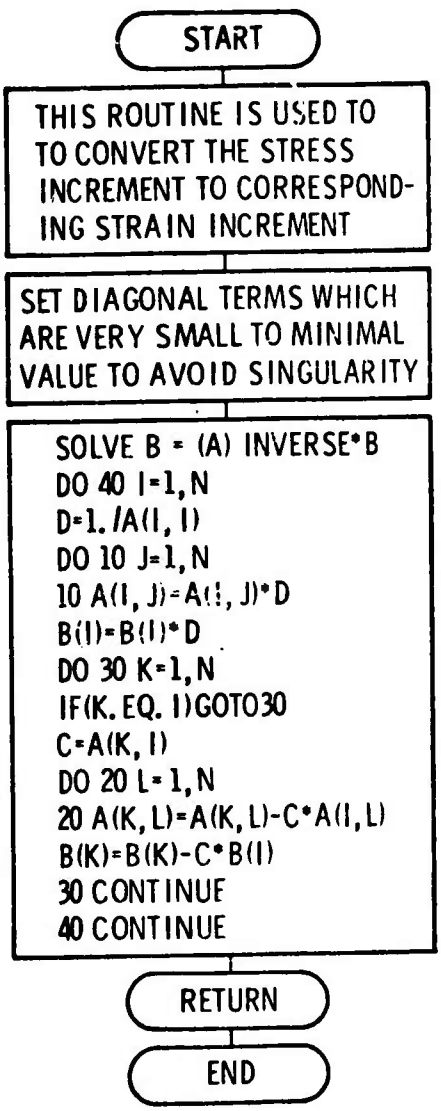

5. LISTING OF MATPAC PROGRAM

```
* T I D Y *
                              SUBROUTINE CADJST (CMAT)

      SUBROUTINE CADJST (CMAT)                                          CAD   1
C     ADJUST C-MATRIX FOR PLANE-STRESS PROBLEMS                         CAD   2
      DIMENSION CMAT(6,6)                                               CAD   3
C                                                                       CAD   4
      DO 15 I=1,4                                                       CAD   5
      IF (I.EQ.3) GO TO 15                                              CAD   6
      DO 5 J=I,4                                                        CAD   7
      IF (J.EQ.3) GO TO 5                                               CAD   8
      CMAT(I,J)=CMAT(I,J)-CMAT(3,I)*CMAT(3,J)/CMAT(3,3)                 CAD   9
      IF (I.NE.J) CMAT(J,I)=CMAT(I,J)                                   CAD  10
5     CONTINUE                                                          CAD  11
      IF (I.NE.4) GO TO 15                                              CAD  12
      DO 10 J=1,4                                                       CAD  13
      CMAT(3,J)=0.                                                      CAD  14
      CMAT(J,3)=0.                                                      CAD  15
10    CONTINUE                                                          CAD  16
15    CONTINUE                                                          CAD  17
      DO 25 I=1,4                                                       CAD  18
      IF (I.EQ.3) GO TO 25                                              CAD  19
      IF (CMAT(I,I).GE.0.) GO TO 25                                     CAD  20
      DO 20 J=1,4                                                       CAD  21
      CMAT(I,J)=0.                                                      CAD  22
      CMAT(J,I)=0.                                                      CAD  23
20    CONTINUE                                                          CAD  24
25    CONTINUE                                                          CAD  25
      RETURN                                                            CAD  26
      END                                                               CAD  27
```

```
* T I D Y *
                    SUBROUTINE CHANGE (DC,SIG,IC,M,N,M1,N1)

      SUBROUTINE CHANGE (DC,SIG,IC,M,N,M1,N1)                          CHA   1
C                                                                      CHA   2
C     INTERCHANGES AXIS TO ORDER CRACKED DIRECTIONS                    CHA   3
C                                                                      CHA   4
      DIMENSION DC(3,3), SIG(6), IC(3)                                 CHA   5
      DUM=SIG(M)                                                       CHA   6
      SIG(M)=SIG(N)                                                    CHA   7
      SIG(N)=DUM                                                       CHA   8
      DUM=SIG(M1)                                                      CHA   9
      SIG(M1)=SIG(N1)                                                  CHA  10
      SIG(N1)=DUM                                                      CHA  11
      DUM=IC(M)                                                        CHA  12
      IC(M)=IC(N)                                                      CHA  13
      IC(N)=DUM                                                        CHA  14
      DO 5 I=1,3                                                       CHA  15
      DUM=DC(I,M)                                                      CHA  16
      DC(I,M)=DC(I,N)                                                  CHA  17
      DC(I,N)=DUM                                                      CHA  18
5     CONTINUE                                                         CHA  19
      RETURN                                                           CHA  20
      END                                                              CHA  21.
```

```
* T I D Y *
                SUBROUTINE COMPOS (S1,SY,AC,AS,EC,ES,E1C,E1S)

      SUBROUTINE COMPOS (S1,SY,AC,AS,EC,ES,E1C,E1S)                    COM   1
      REAL LAMDA                                                       COM   2
      AC=1.                                                            COM   3
      E1S=0.                                                           COM   4
      IF (AS.LE.0.) GO TO 5                                            COM   5
      X=S1/(AS*SY)                                                     COM   6
      IF (X.LT.0.) X=0.                                                COM   7
      IF (X.GE.1.) GO TO 5                                             COM   8
      IF (X.LE.0.15) LAMDA=1.-10.*X/3.                                 COM   9
      IF (X.GT.0.15) LAMDA=10.*(1.-X)/17.                              COM  10
      X=ES*AS                                                          COM  11
      Y=EC*(1.-AS)                                                     COM  12
      E1C=X*(X+Y)/(X+Y-LAMDA*Y)                                        COM  13
      RETURN                                                           COM  14
5     E1C=.01*EC*(1.-AS)+.01*ES*AS                                     COM  15
      RETURN                                                           COM  16
      END                                                              COM  17.
```

```
* T I D Y *
            SUBROUTINE COMPUT (C,STRINC,STRESS,STRSIN,NSIZ,NELTYP)

      SUBROUTINE COMPUT (C,STRINC,STRESS,STRSIN,NSIZ,NELTYP)                COM   1
      DIMENSION C(6,6), STRINC(6), STRESS(6), STRSIN(6)                     COM   2
      IF (NSIZ.EQ.6) GO TO 10                                               COM   3
      IF (NELTYP.EQ.-3) STRINC(3)=0.                                        COM   4
      IF (NELTYP.EQ.3) GO TO 5                                              COM   5
      GO TO 10                                                              COM   6
5     STRINC(3)=-C(3,1)*STRINC(1)-C(3,2)*STRINC(2)-C(3,4)*STRINC(4)         COM   7
      STRINC(3)=STRINC(3)/C(3,3)                                            COM   8
10    DO 20 I=1,NSIZ                                                        COM   9
      STRSIN(I)=0.                                                          COM  10
      DO 15 J=1,NSIZ                                                        COM  11
      STRSIN(I)=STRSIN(I)+C(I,J)*STRINC(J)                                  COM  12
15    CONTINUE                                                              COM  13
      STRESS(I)=STRESS(I)+STRSIN(I)                                         COM  14
20    CONTINUE                                                              COM  15
      IF (NELTYP.EQ.3) STRESS(3)=0.                                         COM  16
      IF (NELTYP.EQ.3) STRSIN(3)=0.                                         COM  17
      RETURN                                                                COM  18
      END                                                                   COM  19
```

```
      SUBROUTINE CRACKS (SIG,DC,ST,SLOPE,ICRACK,STRINC,EC,ES,AS)          CRK   1
C                                                                         CRK   2
C     CHECKS FOR CRACKS IN EACH DIRECTION                                 CRK   3
C                                                                         CRK   4
      DIMENSION SIG(6), DC(3,3), IC(3), STRINC(6), IPERM(4), AS(3)        CRK   5
      DATA (IPERM(I),I=1,4)/2,3,1,2/                                      CRK   6
      SCMIN=.05*ST
      IF (ICRACK.EQ.0) GO TO 10                                           CRK   7
      DO 5 I=1,ICRACK                                                     CRK   8
      IC(I)=1                                                             CRK   9
5     CONTINUE                                                            CRK  10
10    NN=ICRACK+1                                                         CRK  11
      DO 15 N=NN,3                                                        CRK  12
      IC(N)=0                                                             CRK  13
      J=IPERM(N)                                                          CRK  14
      K=IPERM(N+1)                                                        CRK  15
      SC=MIN0(0.,SIG(J),SIG(K))                                           CRK  16
      SCRACK=ST-SC*SLOPE                                                  CRK  17
      IF (SCRACK.LT.SCMIN) SCRACK=SCMIN
      IF (SIG(N).LT.0.) GO TO 15                                          CRK  19
      IF (STRINC(N).LT.0.) GO TO 15                                       CRK  20
      DENOM=EC*(1.-AS(N))+ES*AS(N)                                        CRK  21
      SSS=EC*SIG(N)/DENOM                                                 CRK  22
      IF (SSS.LT.SCRACK) GO TO 15                                         CRK  23
      SIG(N)=SIG(N)-SSS*(1.-AS(N))                                        CRK  24
      ICRACK=ICRACK+1                                                     CRK  25
      IC(N)=1                                                             CRK  26
15    CONTINUE                                                            CRK  27
      IF (IC(3).GT.IC(1)) CALL CHANGE (DC,SIG,IC,3,1,4,5)                 CRK  28
      IF (IC(3).GT.IC(2)) CALL CHANGE (DC,SIG,IC,3,2,4,6)                 CRK  29
      IF (IC(2).GT.IC(1)) CALL CHANGE (DC,SIG,IC,2,1,5,6)                 CRK  30
      RETURN                                                              CRK  31
      END                                                                 CRK  32.
```

```
      SUBROUTINE CTRANF (A,B,C)                                          CTR   1
C                                                                        CTR   2
C     TRANSFORMS C-MATRIX TO GLOBAL COORDINATE SYSTEM                    CTR   3
C                                                                        CTR   4
      DIMENSION A(6,6), B(6,6), C(6,6)                                   CTR   5
      DO 5 I=1,6                                                         CTR   6
      DO 5 J=1,6                                                         CTR   7
      A(I,J)=0.                                                          CTR   8
      DO 5 K=1,6                                                         CTR   9
      A(I,J)=A(I,J)+B(I,K)*C(K,J)                                        CTR  10
5     CONTINUE                                                           CTR  11
      DO 10 I=1,6                                                        CTR  12
      DO 10 J=1,6                                                        CTR  13
      C(I,J)=0.                                                          CTR  14
      DO 10 K=1,6                                                        CTR  15
      C(I,J)=C(I,J)+A(I,K)*B(J,K)                                        CTR  16
10    CONTINUE                                                           CTR  17
      DO 15 I=1,6
      DO 15 J=4,6
      IF(I.EQ.J) GO TO 15
      C(I,J)=0.
      C(J,I)=0.
15    CONTINUE
      RETURN                                                             CTR  18
      END                                                                CTR  19.
```

```
*IT FOR DOUBLI,DOUBLI
      SUBROUTINE DOUBLI (S,SY,SO,ALFA,GAMA,FN,GI)                        DWI
C
C     THIS ROUTINE CALCULATES ALLOWABLE MAXIMUM SHEAR AFTER CRACK
C
      ALFA=1.0E+10
      IF(ABS(S).GE.SY) GO TO 10
      RO=1.
      IF(S.GT.0.) RO=1.-S*S/(SY*SY)
      TAUMAX=(4./3.14159)*SQRT(SO*RO*SY*EN/3.)
      ALFA=GI/TAUMAX
10    RETURN
      END
```

```
* T I D Y *
                SUBROUTINE DOWEL2 (GI,ALFA,EPS,DEPS,EPSMAX,G)

      SUBROUTINE DOWEL2 (GI,ALFA,EPS,DEPS,EPSMAX,G)                    DW2   1
C                                                                      DW2   2
C     THIS ROUTINE CALCULATES SHEAR MODULUS FOR STEEL AFTER CRACK      DW2   3
C                                                                      DW2   4
      STRAIN=ABS(EPS+DEPS)                                             DW2   5
      IF (STRAIN.LT.EPSMAX) GO TO 5                                    DW2   6
      EPSMAX=STRAIN                                                    DW2   7
      G=GI*EXP(-ALFA*ABS(EPS))                                         DW2   8
      RETURN                                                           DW2   9
5     G=GI                                                             DW2  10
      RETURN                                                           DW2  11
      END                                                              DW2  12
```

```
$IT FOR ELFUNN,ELFUNN
      SUBROUTINE ELFUNN (STRESS,STRAIN,STRINC,EPSEL,COEFF,ALKMOD,SHRMOD,
     1YCOF,CC,DCS,AST,NRB,ZK1,ZK2,SIPP,ICOMPS,NELTYP,C,ICRACK)
C
C     CALCULATES STRESS FROM STRAIN INCREMENTS FOR COMPOSITE MATERIALS
C
      DIMENSION STRESS(6),STRAIN(6),STRINC(6),EPSEL(6),COEFF(15),
     1YCOF(25),DC(3,3),DCS(3,3),AST(3),C(6,6),SIG(6),EPS(6),DEPS(6),
     2          AS(6),STRSIN(6),A(6,6),B(6,6),EPSPL(6),FS1(6),FS2(6),
     3R1(6),R2(6),TOS(6),PDE(6),BUFFER(40)
      REAL NU
      EQUIVALENCE (PDE,SIG),(TOS,EPS),(B2,DEPS),(B1,BUFFER),(FS2,AS),
     1(FS1,A),(EPSPL,B)
      NSIZ=6
      IF(IABS(NELTYP).LE.4) NSIZ=4
      IF(ICOMPS.EQ.2) GO TO 200
      EC=COEFF(1)
      ES=COEFF(2)
      SC=COEFF(3)
      SY=COEFF(4)
      NU=COEFF(5)
      ST=COEFF(6)
      SLOPE=COEFF(7)
      EA=COEFF(8)
      GST=COEFF(9)
      ERMOD=COEFF(10)
      IF (ICRACK.EQ.0)
     1CALL PRESTR (BUFFER(1),BUFFER(10),STRESS,DC,SIG,BUFFER(19))
C     CRACKED SECTION.  CONVERT TO PRINCIPAL ORTHOTROPIC DIRECTIONS
      CALL TRANSF (A,B,DC)
      CALL MATPLY (A,STRESS,SIG,1)
      IF(NSIZ.EQ.4.OR.ICRACK.GE.2) GO TO 20
C     CRACK NORMAL TO 1-AXIS, FIND EXTREMUM STRESSES IN 2-3 PLANE
      CALL MAXMIN (SIG(2),SIG(3),SIG(5),THETA)
C     ADJUST DIRECTIONS
      CC=COS(THETA)
      SS=SIN(THETA)
      DO 10 J=1,3
      DUM=DC(J,2)*CC+DC(J,3)*SS
      DC(J,3)=-DC(J,2)*SS+DC(J,3)*CC
      DC(J,2)=DUM
10    CONTINUE
      CALL TRANSF(A,B,DC)
      CALL MATPLY (A,STRESS,SIG,1)
20    CALL MATPLY (B,STRINC,DEPS,-1)
C     CHECK FOR ADDITIONAL CRACKS
      CALL STLTRN (AS,DC,DCS,BUFFER,NRB,AST(1),AST(2),AST(3))
      CALL CRACKS (SIG,DC,ST,SLOPE,ICRACK,DEPS,EC,FS,AS)
      CALL TRANSF (A,B,DC)
      CALL MATPLY (B,STRAIN,EPS,-1)
      CALL MATPLY (B,STRINC,DEPS,-1)
      CALL MATPLY (A,SIG,STRESS,1)
      CALL STLTRN (AS,DC,DCS,BUFFER,NRB,AST(1),AST(2),AST(3))
C
      CALL VARMOD (SIG,EPS,SO,SY,EC,ES,NU,AS,C,ICRACK,NELTYP,DEPS,EPSEL,
     1,ALPA,GAMA,FN,GST,ERMOD)
      CALL CTRANF (BUFFER,B,C)
      CALL COMPUT (C,STRINC,STRESS,STRSIN,NSIZ,NELTYP)
      IF(NELTYP.EQ.3) CALL CADJST (C)
      DO 50 I=1,NSIZ
```

```
      STRAIN(I)=STRAIN(I)+STRINC(I)
50    CONTINUE
      IF(ICRACK.LE.0) RETURN
      CALL MATPLY (A,STRESS,SIG,1)
      DO 60 I=1,ICRACK
      IF (SIG(I).LE.0.) GO TO 55
      S=SY*AS(I)
      IF(SIG(I).GT.S) SIG(I)=S
      GO TO 60
55    CONTINUE
      S=-SY*AS(I)
      IF(EPS(I).GT.0.) SIG(I)=AMAX1(S,SIG(I))
60    CONTINUE
      CALL MATPLY (B,SIG,STRESS,1)
      RETURN
C
C     USE TERTEN MODEL
C
200   DO 250 I=1,NSIZ
      EPSPL(I)=STRAIN(I)-EPSEL(I)
250   CONTINUE
      CALL PLASTK(STRESS,C,YCOF      ,STRINC,STRSIN,EPSPL,FS1,FS2,B1,B2,
     *TOS,POF,ZK1,ZK2,SIZP,PLKMOD,SHRMOD,NSIZ,NELTYP)
      DO 260 I=1,NSIZ
      STRAIN(I)=STRAIN(I)+STRINC(I)
      EPSEL(I)=STRAIN(I)-EPSPL(I)
260   CONTINUE
      IF(NELTYP.EQ.3) CALL CADJST (C)
      RETURN
      END
```

```
* T I D Y *
                SUBROUTINE FORMC (POIS,FC,ES,AC,AS,C,GSTL)
C                                                                       FOR    1
      SUBROUTINE FORMC (POIS,FC,ES,AC,AS,C,GSTL)                        FOR    2
      DIMENSION POIS(3,3), EC(3), ES(3), AC(3), AS(3), C(6,6), NP(5), GSFOR    3
     1TL(3)                                                             FOR    4
      DATA (NP(I),I=1,5)/1,2,3,1,2/                                     FOR    5
C     INITIALIZE                                                        FOR    6
      DO 5 I=1,6                                                        FOR    7
      DO 5 J=1,6                                                        FOR    8
      C(I,J)=0.                                                         FOR    9
5     CONTINUE                                                          FOR   10
      D=1.-POIS(2,3)*POIS(3,2)-POIS(1,2)*POIS(2,1)-POIS(1,3)*POIS(3,1)-PFOR   11
     1OIS(1,2)*POIS(2,3)*POIS(3,1)-POIS(1,3)*POIS(2,1)*POIS(3,2)        FOR   12
      DO 10 I=1,3                                                       FOR   13
      J=NP(I+1)                                                         FOR   14
      K=NP(I+2)                                                         FOR   15
      A=EC(I)*AC(I)/D                                                   FOR   16
      C(I,I)=A*(1.-POIS(J,K)*POIS(K,J))+ES(I)*AS(I)                     FOR   17
      C(I,J)=A*(POIS(I,J)+POIS(I,K)*POIS(K,J))                          FOR   18
      C(I,K)=A*(POIS(I,K)+POIS(I,J)*POIS(J,K))                          FOR   19
      C(I+3,I+3)=POIS(I,I)*AC(I)+GSTL(I)*AB(I)                          FOR   20
10    CONTINUE                                                          FOR   21
      DO 15 I=1,2                                                       FOR   22
      II=I+1                                                            FOR   23
      DO 15 J=II,3                                                      FOR   24
      C(I,J)=C(J,I)                                                     FOR   25
15    CONTINUE                                                          FOR   26
      RETURN                                                            FOR   27*
      END
```

```
* T I D Y *
                    SUBROUTINE JACOBI (A,B,X,EIGV,D,N,RTOL)

      SUBROUTINE JACOBI (A,B,X,EIGV,D,N,RTOL)                          JAC   1
C                                                                      JAC   2
      DIMENSION A(N,N), B(N,N), X(N,N), EIGV(N), D(N)                  JAC   3
C                                                                      JAC   4
      NSWAX=15                                                         JAC   5
      DO 5 I=1,N                                                       JAC   6
      D(I)=A(I,I)/B(I,I)                                               JAC   7
5     EIGV(I)=D(I)                                                     JAC   8
      IF (N.EQ.1) RETURN                                               JAC   9
      DO 15 I=1,N                                                      JAC  10
      DO 10 J=1,N                                                      JAC  11
10    X(I,J)=0.0                                                       JAC  12
15    X(I,I)=1.0                                                       JAC  13
      NR=N-1                                                           JAC  14
C                                                                      JAC  15
C     WE START ITERATION                                               JAC  16
      NSWEEP=0                                                         JAC  17
20    NSWEEP=NSWEEP+1                                                  JAC  18
      EPS=(0.01**NSWEEP)**2                                            JAC  19
      DO 105 J=1,NR                                                    JAC  20
      JJ=J+1                                                           JAC  21
      DO 105 K=JJ,N                                                    JAC  22
      TT=A(J,K)*A(J,K)                                                 JAC  23
      TB=A(J,J)*A(K,K)                                                 JAC  24
      EPTOLA=ABS(TT/TB)                                                JAC  25
      TT=B(J,K)*B(J,K)                                                 JAC  26
      TB=B(J,J)*B(K,K)                                                 JAC  27
      EPTOLB=TT/TB                                                     JAC  28
      IF ((EPTOLA.LT.EPS).AND.(EPTOLB.LT.EPS)) GO TO 105               JAC  29
      AKK=A(K,K)*B(J,K)-B(K,K)*A(J,K)                                  JAC  30
      AJJ=A(J,J)*B(J,K)-B(J,J)*A(J,K)                                  JAC  31
      AB=A(J,J)*B(K,K)-A(K,K)*B(J,J)                                   JAC  32
      CHECK=(AB*AB+4.0*AKK*AJJ)/4.0                                    JAC  33
      IF (CHECK) 25,30,30                                              JAC  34
25    WRITE (6,145) CHECK                                              JAC  35
      STOP                                                             JAC  36
30    SQCH=SQRT(CHECK)                                                 JAC  37
      D1=AB/2.0+SQCH                                                   JAC  38
      D2=AB/2.0-SQCH                                                   JAC  39
      DEN=D1                                                           JAC  40
      IF (ABS(D2).GT.ABS(D1)) DEN=D2                                   JAC  41
      IF (DEN) 40,35,40                                                JAC  42
35    CA=0.                                                            JAC  43
      CG=-A(J,K)/A(K,K)                                                JAC  44
      GO TO 45                                                         JAC  45
40    CA=AKK/DEN                                                       JAC  46
      CG=-AJJ/DEN                                                      JAC  47
C                                                                      JAC  48
C     WE PERFORM THE GENERALIZED ROTATION.                             JAC  49
45    IF (N-2) 50,95,50                                                JAC  50
```

```
* T I D Y *
                SUBROUTINE JACOBI (A,B,X,EIGV,D,N,RTOL)

50      JP1=J+1                                                    JAC  51
        JM1=J-1                                                    JAC  52
        KP1=K+1                                                    JAC  53
        KM1=K-1                                                    JAC  54
C                                                                  JAC  55
        IF (JM1-1) 65,55,55                                        JAC  56
55      DO 60 I=1,JM1                                              JAC  57
        AJ=A(I,J)                                                  JAC  58
        BJ=B(I,J)                                                  JAC  59
        AK=A(I,K)                                                  JAC  60
        BK=B(I,K)                                                  JAC  61
        A(I,J)=AJ+CG*AK                                            JAC  62
        B(I,J)=BJ+CG*BK                                            JAC  63
        A(I,K)=AK+CA*AJ                                            JAC  64
60      B(I,K)=BK+CA*BJ                                            JAC  65
C                                                                  JAC  66
65      IF (KP1-N) 70,70,80                                        JAC  67
70      DO 75 I=KP1,N                                              JAC  68
        AJ=A(J,I)                                                  JAC  69
        BJ=B(J,I)                                                  JAC  70
        AK=A(K,I)                                                  JAC  71
        BK=B(K,I)                                                  JAC  72
        A(J,I)=AJ+CG*AK                                            JAC  73
        B(J,I)=BJ+CG*BK                                            JAC  74
        A(K,I)=AK+CA*AJ                                            JAC  75
75      B(K,I)=BK+CA*BJ                                            JAC  76
C                                                                  JAC  77
80      IF (JP1-KM1) 85,85,95                                      JAC  78
85      DO 90 I=JP1,KM1                                            JAC  79
        AJ=A(J,I)                                                  JAC  80
        BJ=B(J,I)                                                  JAC  81
        AK=A(I,K)                                                  JAC  82
        BK=B(I,K)                                                  JAC  83
        A(J,I)=AJ+CG*AK                                            JAC  84
        B(J,I)=BJ+CG*BK                                            JAC  85
        A(I,K)=AK+CA*AJ                                            JAC  86
90      B(I,K)=BK+CA*BJ                                            JAC  87
95      AK=A(K,K)                                                  JAC  88
        BK=B(K,K)                                                  JAC  89
        A(K,K)=AK+2*CA*A(J,K)+CA*CA*A(J,J)                         JAC  90
        B(K,K)=BK+2*CA*B(J,K)+CA*CA*B(J,J)                         JAC  91
        A(J,J)=A(J,J)+2*CG*A(J,K)+CG*CG*AK                         JAC  92
        B(J,J)=B(J,J)+2*CG*B(J,K)-CG*CG*BK                         JAC  93
        A(J,K)=0.0                                                 JAC  94
        B(J,K)=0.0                                                 JAC  95
C                                                                  JAC  96
C       UPDATE EIGENVECTORS                                        JAC  97
        DO 100 I=1,N                                               JAC  98
        XJ=X(I,J)                                                  JAC  99
        XK=X(I,K)                                                  JAC 100
```

```
* T I D Y *
                SUBROUTINE JACOBI (A,B,X,EIGV,D,N,RTOL)
      X(I,J)=XJ+CG*XK                                                   JAC 101
100   X(I,K)=XK+CA*XJ                                                   JAC 102
C                                                                       JAC 103
105   CONTINUE                                                          JAC 104
C                                                                       JAC 105
      DO 110 I=1,N                                                      JAC 106
110   EIGV(I)=A(I,I)/B(I,I)                                             JAC 107
C                                                                       JAC 108
C     CHECK FOR CONVERGENCE                                             JAC 109
      DO 115 I=1,N                                                      JAC 110
      TOL=RTOL*D(I)                                                     JAC 111
      TOL=ABS(TOL)                                                      JAC 112
      DIF=ABS(EIGV(I)-D(I))                                             JAC 113
      IF (DIF.GT.TOL) GO TO 130                                         JAC 114
115   CONTINUE                                                          JAC 115
C                                                                       JAC 116
C     CHECK IF ALL OFF-DIAG ELEMENTS ARE SATISFACTORILY SMALL           JAC 117
      EPS=RTOL**2                                                       JAC 118
      DO 120 J=1,NR                                                     JAC 119
      JJ=J+1                                                            JAC 120
      DO 120 K=JJ,N                                                     JAC 121
      TT=A(J,K)*A(J,K)                                                  JAC 122
      TB=A(J,J)*A(K,K)                                                  JAC 123
      EPSA=ABS(TT/TB)                                                   JAC 124
      TT=B(J,K)*B(J,K)                                                  JAC 125
      TB=B(J,J)*B(K,K)                                                  JAC 126
      EPSB=TT/TB                                                        JAC 127
      IF ((EPSA.LT.EPS).AND.(EPSB.LT.EPS)) GO TO 120                    JAC 128
      GO TO 130                                                         JAC 129
120   CONTINUE                                                          JAC 130
C                                                                       JAC 131
      DO 125 I=1,N                                                      JAC 132
      DO 125 J=I,N                                                      JAC 133
      B(J,I)=B(I,J)                                                     JAC 134
125   A(J,I)=A(I,J)                                                     JAC 135
      RETURN                                                            JAC 136
C                                                                       JAC 137
130   DO 135 I=1,N                                                      JAC 138
135   D(I)=EIGV(I)                                                      JAC 139
      IF (NS-KEEP.LT.NSMAX) GO TO 70                                    JAC 140
      DO 140 I=1,N                                                      JAC 141
      DO 140 J=I,N                                                      JAC 142
      B(J,I)=B(I,J)                                                     JAC 143
140   A(J,I)=A(I,J)                                                     JAC 144
      RETURN                                                            JAC 145
C                                                                       JAC 146
C                                                                       JAC 147
145   FORMAT (8HOCHECK =E20.14)                                         JAC 148
      END                                                               JAC 149=
```

```
* T I D Y *
                    SUBROUTINE LODUN (EPS,DEPS,EPSMAX,LD)

      SUBROUTINE LODUN (EPS,DEPS,EPSMAX,LD)                          LOD   1
C                                                                    LOD   2
C     CHECKS LOADING/UNLOADING IN TENSION                            LOD   3
C                                                                    LOD   4
      STRAIN=EPS+DEPS                                                LOD   5
      LD=0                                                           LOD   6
      IF (STRAIN.LT.EPSMAX) RETURN                                   LOD   7
      LD=1                                                           LOD   8
      IF (STRAIN.GT.EPSMAX) EPSMAX=STRAIN                            LOD   9
      RETURN                                                         LOD  10
      END                                                            LOD  11
```

```
$IT FOR MATPAC,MATPAC
      SUBROUTINE MATPAC (STRESS,STRAIN,STRINC,EPSEL,COEFF,BLKMOD,SHRMOD,
     1YCOF,DC,DCS,AST,NRH,ZK1,ZK2,SI2P,ICOMPS,NELTYP,C,ICRACK,NSPLIT)
C
C     IF(NSPLIT.LT.0) STRINC =STRAIN INCREMENT
C     IF(NSPLIT.GE.0) STRINC =STRESS INCREMENT
C     IABS(NSPLIT)= NUMBER OF SPLITS FOR STRESS OR STRAIN INCREMENTS
C
      DIMENSION STRESS(6),STRAIN(6),STRINC(6),EPSEL(6),COEFF(15),
     1YCOF(25),DC(3,3),DCS(3,3),AST(3),C(6,6),DEPS(6)
C
      NSIZ=6
      IF(NELTYP.LE.4) NSIZ=4
      IF(NSPLIT.GT.0) GO TO 100
C
C     STRAIN INCREMENT OPTION
C
      NN=IABS(NSPLIT)
      IF(NN.EQ.0) NN=1
      FN=FLOAT(NN)
      DO 5 I=1,6
    5 STRINC(I)=STRINC(I)/FN
      DO 10 I=1,NN
      CALL ELPUNN (STRESS,STRAIN,STRINC,EPSEL,COEFF,BLKMOD,SHRMOD,YCOF,
     1DC,DCS,AST,NRH,ZK1,ZK2,SI2P,ICOMPS,NELTYP,C,ICRACK)
   10 CONTINUE
      RETURN
C
C     STRESS INPUT OPTION
C
  100 CONTINUE
      DO 105 I=1,6
  105 DEPS(I)=0.
      CALL ELPUNN (STRESS,STRAIN,DEPS,EPSEL,COEFF,BLKMOD,SHRMOD,YCOF,
     1DC,DCS,AST,NRH,ZK1,ZK2,SI2P,ICOMPS,NELTYP,C,ICRACK)
      FN=FLOAT(NSPLIT)
      DO 200 I=1,NSPLIT
      DO 110 J=1,6
  110 DEPS(J)=STRINC(J)/FN
      CALL SOLVEX (NSIZ,C,DEPS)
      CALL ELPUNN (STRESS,STRAIN,DEPS,EPSEL,COEFF,BLKMOD,SHRMOD,YCOF,
     1DC,DCS,AST,NRH,ZK1,ZK2,SI2P,ICOMPS,NELTYP,C,ICRACK)
  200 CONTINUE
      RETURN
      END
```

```
* T I D Y *
                        SUBROUTINE MATPLY (A,X,Y,IOPT)

      SUBROUTINE MATPLY (A,X,Y,IOPT)                                    MAT    1
C                                                                       MAT    2
C     MATRIX MULTIPLICATION ROUTINE                                     MAT    3
C     IOPT.GE.1       Y=A*X                                             MAT    4
C     IOPT.LT.1       Y=(A)TRANSPOSE * X                                MAT    5
C                                                                       MAT    6
      DIMENSION A(6,6), X(6), Y(6)                                      MAT    7
      DO 5 I=1,6                                                        MAT    8
      Y(I)=0.                                                           MAT    9
      DO 5 J=1,6                                                        MAT   10
      IF (IOPT.GE.1) Y(I)=Y(I)+A(I,J)*X(J)                              MAT   11
      IF (IOPT.LT.1) Y(I)=Y(I)+A(J,I)*X(J)                              MAT   12
5     CONTINUE                                                          MAT   13
      RETURN                                                            MAT   14
      END                                                               MAT   15
```

```
* T I D Y *
                    SUBROUTINE MAXMIN (XX,YY,XY,THETA)

      SUBROUTINE MAXMIN (XX,YY,XY,THETA)                                  MAX    1
C                                                                         MAX    2
C     EVALUATES PRINCIPAL STRESS DIRECTION IN A PLANE                     MAX    3
C                                                                         MAX    4
      AP=1.E-30                                                           MAX    5
      AM=-1.E+30                                                          MAX    6
      AXY=ABS(XY)                                                         MAX    7
      XXYY=ABS(XX-YY)                                                     MAX    8
      IF (XXYY.LE.AP.OR.AXY.LE.AP) GO TO 20                               MAX    9
      TN=(2.*XY)/(XX-YY)                                                  MAX   10
      ATN=ABS(TN)                                                         MAX   11
      THETA=.5*ATAN(ATN)                                                  MAX   12
      IF ((XX.GT.YY.AND.XX.GT.AP).OR.(YY.LT.XX.AND.YY.LT.AM)) GO TO 5     MAX   13
      GO TO 15                                                            MAX   14
5     IF (XY) 10,20,25                                                    MAX   15
10    THETA=-THETA                                                        MAX   16
      GO TO 25                                                            MAX   17
15    THETA=1.57079-THETA                                                 MAX   18
      IF (XY) 10,20,25                                                    MAX   19
20    THETA=0.                                                            MAX   20
25    RETURN                                                              MAX   21
      END                                                                 MAX   22.
```

```
* T I D Y *
      SUBROUTINE MODULI (S1,S2,S0,EPS1,EC,ES,E1C,E1B,NU,DEPS,EPSMAX)

      SUBROUTINE MODULI (S1,S2,S0,EPS1,EC,ES,E1C,E1B,NU,DEPS,EPSMAX)     MOD   1
      REAL NU                                                           MOD   2
      EMIN=.01*EC                                                       MOD   3
      IF (S1.GE.0.) GO TO 25                                            MOD   4
      IF ((EPS1+DEPS).GE.EPSMAX) GO TO 25                               MOD   5
      EPSMAX=EPS1+DEPS                                                  MOD   6
C     BETA=S2/S1                                                        MOD   7
      BETA=0.                                                           MOD   8
      IF (BETA.LT.0.) BETA=0.                                           MOD   9
      IF (BETA.GE.0.2) GO TO 5                                          MOD  10
      SP=S0*(1.+BETA/(1.2-BETA))                                        MOD  11
      GO TO 20                                                          MOD  12
5     IF (BETA.GT.1.) GO TO 10                                          MOD  13
      SP=1.2*S0                                                         MOD  14
      GO TO 20                                                          MOD  15
10    IF (BETA.GT.5.) GO TO 15                                          MOD  16
      SP=1.2*S0/BETA                                                    MOD  17
      GO TO 20                                                          MOD  18
15    SP=S0*(1.+1./(1.2*BETA-1.))/BETA                                  MOD  19
20    IF (BETA.LE.1.) EPSP=.0025                                        MOD  20
      IF (BETA.GT.1.) EPSP=(-500.+0.55*SP)*1.0E-6                       MOD  21
      X=-EPS1/EPSP                                                      MOD  22
      ESEC=SP/EPSP                                                      MOD  23
      Y=1.+(EC/(ESEC-ESEC*NU*BETA)-2.)*X+X*X                            MOD  24
      Y=Y*Y                                                             MOD  25
      E1B=EC*(1.-X*X)/Y                                                 MOD  26
      IF (E1B.LT.EMIN) E1B=EMIN                                         MOD  27
      E1C=E1B                                                           MOD  28
      RETURN                                                            MOD  29
25    E1B=EC                                                            MOD  30
      E1C=EC                                                            MOD  31
      RETURN                                                            MOD  32
      END                                                               MOD  33-
```

```
* T I D Y *
      SUBROUTINE PLASTK (S,C,Y,STRINC,DS,EPSPI,FS1,FS2,B1,B2,TDS,PDE,ZK1

      SUBROUTINE PLASTK (S,C,Y,STRINC,DS,EPSPI,FS1,FS2,B1,B2,TDS,PDE,ZK1PLA    1
     1,ZK2,SI2P,B,G,NSIZ,NELTYP)                                        PLA    2
C     -----THIS SUBROUTINE CALCULATES STRESS INCREMENTS FROM AN INPUT OFPLA    3
C     -----STRAIN INCREMENTS, STATE OF STRESS, PLASTIC STRAIN, AND THE YPLA    4
C     -----FUNCTION CONSTANTS                                           PLA    5
C     -----THIS SUBROUTINE USES TWO STRIN1HARDENING YIELD SURFACES      PLA    6
      DIMENSION S(6), C(6,6), STRINC(6), DS(6), EPSPI(6), FS1(6), FS2(6)PLA    7
     1, B1(6), B2(6), TDS(6), PDE(6), Y(1)                              PLA    8
      IF (ABS(ZK1).LT.ABS(Y(24))) ZK1=Y(24)                             PLA    9
      IF (ABS(ZK2).LT.ABS(Y(25))) ZK2=Y(25)                             PLA   10
C     INITIALIZE                                                        PLA   11
      ZL1=0.                                                            PLA   12
      ZL2=0.                                                            PLA   13
      DO 5 I=1,NSIZ                                                     PLA   14
      FS1(I)=0.                                                         PLA   15
      FS2(I)=0.                                                         PLA   16
      B1(I)=0.                                                          PLA   17
      B2(I)=0.                                                          PLA   18
      DO 5 J=1,NSIZ                                                     PLA   19
      C(I,J)=0.                                                         PLA   20
5     CONTINUE                                                          PLA   21
      DO 10 I=1,3                                                       PLA   22
      C(I,I)=B+1.333333*G                                               PLA   23
      IF ((I+3).LE.NSIZ) C(I+3,I+3)=G                                   PLA   24
      DO 10 J=1,3                                                       PLA   25
      IF (I.NE.J) C(I,J)=B-.666667*G                                    PLA   26
10    CONTINUE                                                          PLA   27
      IF (NELTYP.EQ.3) STRINC(3)=0.                                     PLA   28
      IF (NELTYP.EQ.3) STRINC(3)=-(C(3,1)*STRINC(1)+C(3,2)*STRINC(2)+C(3PLA   29
     1,4)*STRINC(4))/C(3,3)                                             PLA   30
      CJ1=S(1)+S(2)+S(3)                                                PLA   31
      CJ2=.166667*((S(1)-S(2))**2+(S(2)-S(3))**2+(S(3)-S(1))**2)        PLA   32
      CJ2=CJ2+S(4)*S(4)+S(5)*S(5)+S(6)*S(6)                             PLA   33
      SJ2=SQRT(CJ2)                                                     PLA   34
      DO 15 I=1,NSIZ                                                    PLA   35
      DS(I)=0.                                                          PLA   36
      DO 15 J=1,NSIZ                                                    PLA   37
      DS(I)=DS(I)+C(I,J)*STRINC(J)                                      PLA   38
15    CONTINUE                                                          PLA   39
      IF (NELTYP.EQ.3) DS(3)=0.                                         PLA   40
      T1=EXP(CJ1/Y(4))                                                  PLA   41
      T2=Y(1)*(Y(2)-Y(3)*T1)                                            PLA   42
      T3=EXP((CJ1-Y(5))/Y(6))                                           PLA   43
      F1=SJ2-T2*(1.-T3)-ZK1                                             PLA   44
      F2=.5*CJ2+Y(7)*CJ1*CJ1-ZK2                                        PLA   45
      IF (F1.LT.0.) GO TO 25                                            PLA   46
      H1=1.-Y(9)*(1.-EXP(Y(10)*SI2P/(1.-Y(11)*CJ1)))                    PLA   47
      H1=Y(8)*H1/(Y(12)-Y(13)*CJ1)                                      PLA   48
      T4=Y(1)*Y(3)*T1*(1.-T3)/Y(4)+T2*T3/Y(6)                           PLA   49
      DO 20 I=1,3                                                       PLA   50
```

```
* T I D Y *
      SUBROUTINE PLASTK (S,C,Y,STRINC,DS,FPSPI,FS1,FS2,B1,B2,TDS,PDE,ZK1
C
      FS1(I)=(.5*S(I)-.166667*CJ1)/SJ2+T4                                PLA  51
      IF ((I+3).LE.NSIZ) FS1(I+3)=2.*S(I+3)/SJ2                          PLA  52
20    CONTINUE                                                           PLA  53
25    IF (F2.LT.0.) GO TO 35                                             PLA  54
      T5=Y(14)*SJ2*(1.-EXP(-SJ2/Y(15)))*EXP(-CJ2*CJ2/Y(16))              PLA  55
      T5=T5/(1.-Y(20)*CJ1)                                               PLA  56
      H2=Y(17)*(1.-EXP(CJ1*CJ1*CJ1/Y(18)))*EXP(CJ1/Y(19))+T5             PLA  57
      DO 30 I=1,3                                                        PLA  58
      FS2(I)=.5*S(I)+(2.*Y(7)-.166667)*CJ1                               PLA  59
      IF ((I+3).LE.NSIZ) FS2(I+3)=2.*S(I+3)                              PLA  60
30    CONTINUE                                                           PLA  61
35    IF ((F1.LT.0.).AND.(F2.LT.0.)) GO TO 145                           PLA  62
      DO 40 I=1,NSIZ                                                     PLA  63
      DO 40 J=1,NSIZ                                                     PLA  64
      B1(I)=H1(I)+C(I,J)*FS1(J)                                          PLA  65
      B2(I)=B2(I)+C(I,J)*FS2(J)                                          PLA  66
40    CONTINUE                                                           PLA  67
      AB1=0.                                                             PLA  68
      AB2=0.                                                             PLA  69
      AB3=0.                                                             PLA  70
      AB4=0.                                                             PLA  71
      AB5=0.                                                             PLA  72
      DO 45 I=1,NSIZ                                                     PLA  73
      AB1=AB1+FS1(I)*B1(I)                                               PLA  74
      AB2=AB2+FS1(I)*B2(I)                                               PLA  75
      AB3=AB3+FS1(I)*DS(I)                                               PLA  76
      AB4=AB4+FS2(I)*B2(I)                                               PLA  77
      AB5=AB5+FS2(I)*DS(I)                                               PLA  78
45    CONTINUE                                                           PLA  79
      A1=1.+2.*H1*AB1                                                    PLA  80
      A2=SJ2+2.*H1*AB2                                                   PLA  81
      A3=2.*H1*AB3                                                       PLA  82
      A4=.333333*H2*AB2                                                  PLA  83
      A5=2.*Y(7)*CJ1+.333333*H2*AB4                                      PLA  84
      A6=.333333*H2*AB5                                                  PLA  85
      IF (F1) 50,55,55                                                   PLA  86
50    ZL2=A6/A5                                                          PLA  87
      GO TO 70                                                           PLA  88
55    IF (F2) 60,65,65                                                   PLA  89
60    ZL1=A3/A1                                                          PLA  90
      GO TO 70                                                           PLA  91
65    T6=A1*A5-A2*A4                                                     PLA  92
      ZL1=(A3*A5-A2*A6)/T6                                               PLA  93
      ZL2=(A1*A6-A3*A4)/T6                                               PLA  94
70    CONTINUE                                                           PLA  95
75    DF1=0.                                                             PLA  96
      DF2=0.                                                             PLA  97
      DO 80 I=1,NSIZ                                                     PLA  98
      TDS(I)=DS(I)-B1(I)*ZL1-B2(I)*ZL2                                   PLA  99
      DF1=DF1+FS1(I)*TDS(I)                                              PLA 100
```

```
* T I D Y *
      SUBROUTINE PLASTK (S,C,Y,STRING,DS,EPSPI,FS1,FS2,B1,B2,TDS,PDE,ZK1

      DF2=DF2+FS2(I)*TDS(I)                                              PLA 101
80    CONTINUE                                                           PLA 102
      TZL2=ZL2                                                           PLA 103
      IF (DF1*ZL1) 85,100,100                                            PLA 104
85    IF (DF2*ZL2) 90,95,95                                              PLA 105
90    ZL2=0.                                                             PLA 106
      GO TO 75                                                           PLA 107
95    ZL1=0.                                                             PLA 108
      ZL2=TZL2                                                           PLA 109
      GO TO 75                                                           PLA 110
100   IF (DF2*ZL2) 105,110,110                                           PLA 111
105   ZL2=0.                                                             PLA 112
      GO TO 75                                                           PLA 113
110   CONTINUE                                                           PLA 114
C     *****INCREMENTING OF YIELD SURFACES FOLLOWS                        PLA 115
      IF (DF1*ZL1) 120,120,115                                           PLA 116
115   ZK1=ZK1+DF1                                                        PLA 117
120   IF (DF2*ZL2) 130,130,125                                           PLA 118
125   ZK2=ZK2+DF2                                                        PLA 119
130   CONTINUE                                                           PLA 120
      IF (SELTYP.EQ.3) TDS(3)=0.                                         PLA 121
      DO 135 I=1,NSIZ                                                    PLA 122
      S(I)=S(I)+TDS(I)                                                   PLA 123
      PDE(I)=FS1(I)*ZL1+FS2(I)*ZL2                                       PLA 124
      EPSPI(I)=EPSPI(I)+PDE(I)                                           PLA 125
135   CONTINUE                                                           PLA 126
      SSP=0.                                                             PLA 127
      DO 140 I=1,3                                                       PLA 128
      II=I+1                                                             PLA 129
      IF (II.GT.3) II=1                                                  PLA 130
      SSP=SSP+.166667*(EPSPI(I)-EPSPI(II))*(EPSPI(I)-EPSPI(II))          PLA 131
      IF ((I+3).LE.NSIZ) SSP=SSP+.25*EPSPI(I+3)*EPSPI(I+3)               PLA 132
140   CONTINUE                                                           PLA 133
      SI2P=SQRT(SSP)                                                     PLA 134
      GO TO 155                                                          PLA 135
145   CONTINUE                                                           PLA 136
      DO 150 I=1,NSIZ                                                    PLA 137
      S(I)=S(I)+DS(I)                                                    PLA 138
150   CONTINUE                                                           PLA 139
      GO TO 180                                                          PLA 140
155   CONTINUE                                                           PLA 141
      X1=0.                                                              PLA 142
      X2=0.                                                              PLA 143
      X3=0.                                                              PLA 144
      X4=0.                                                              PLA 145
      DF1=DF1*ZL1                                                        PLA 146
      DF2=DF2*ZL2                                                        PLA 147
      IF (F1.LT.0..OR.DF1.LE.0.) GO TO 160                               PLA 148
      IF (F2.LT.0..OR.DF2.LE.0.) GO TO 165                               PLA 149
      X1=A5*2.*H1/T6                                                     PLA 150
```

```
* T I D Y *
      SUBROUTINE PLASTK (S,C,Y,STRINC,DS,EPSPI,FS1,FS2,B1,B2,TDS,PDE,ZK1

      X2=A2*.333333*H2/T6                                                    PLA 151
      X3=A1*.333333*H2/T6                                                    PLA 152
      X4=A4*2.*H1/T6                                                         PLA 153
      GO TO 170                                                              PLA 154
160   X3=.333333*H2/A5                                                       PLA 155
      GO TO 170                                                              PLA 156
165   X1=2.*H1/A1                                                            PLA 157
170   DO 175 I=1,NSIZ                                                        PLA 158
      DO 175 J=I,NSIZ                                                        PLA 159
      C(I,J)=C(I,J)-B1(I)*(B1(J)*X1-B2(J)*X2)-B2(I)*(B2(J)*X3-B1(J)*X4)      PLA 160
      IF (I.NE.J) C(J,I)=C(I,J)                                              PLA 161
175   CONTINUE                                                               PLA 162
      IF (NELTYP.EQ.3) STRINC(3)=(C(3,1)*STRINC(1)+C(3,2)*STRINC(2)+C(3PLA 163
     1,4)*STRINC(4))/C(3,3)                                                  PLA 164
180   RETURN                                                                 PLA 165
      END                                                                    PLA 166
```

```
* T I D Y *
                    SUBROUTINE PRNSTR (A,B,S,X,SIG,D)
      SUBROUTINE PRNSTR (A,B,S,X,SIG,D)                                 PRN   1
                                                                        PRN   2
C                                                                       PRN   3
C     EVALUATES PRINCIPAL STRESSES AND DIRECTIONS                       PRN   4
C                                                                       PRN   5
      DIMENSION A(3,3), B(3,3), S(6), X(3,3), SIG(6), D(3)              PRN   6
      N=3                                                               PRN   7
      RTOL=.1E-6                                                        PRN   8
      A(1,2)=S(4)                                                       PRN   9
      A(1,3)=S(6)                                                       PRN  10
      A(2,3)=S(5)                                                       PRN  11
      DO 5 I=1,3                                                        PRN  12
      A(I,I)=S(I)                                                       PRN  13
      B(I,I)=1.                                                         PRN  14
      DO 5 J=I,3                                                        PRN  15
      IF (J.EQ.I) GO TO 5                                               PRN  16
      B(I,J)=0.                                                         PRN  17
      B(J,I)=0.                                                         PRN  18
      A(J,I)=A(I,J)                                                     PRN  19
5     CONTINUE                                                          PRN  20
C     CALL JACOBI FOR EIGENVALUES AND EIGENVECTORS (PRINCIPAL STRESSES) PRN  21
      CALL JACOBI (A,B,X,SIG,D,N,RTOL)                                  PRN  22
      DO 10 I=1,3                                                       PRN  23
      C=SQRT(X(1,I)*X(1,I)+X(2,I)*X(2,I)+X(3,I)*X(3,I))                 PRN  24
      SIG(I+3)=0.                                                       PRN  25
      DO 10 J=1,3                                                       PRN  26
      X(J,I)=X(J,I)/C                                                   PRN  27
10    CONTINUE                                                          PRN  28
      RETURN                                                            PRN  29*
      END
```

```
* T I D Y *
                    SUBROUTINE REBOND (EPS,ECC,EC,ERBOND)

      SUBROUTINE REBOND (EPS,ECC,EC,ERBOND)                          REB   1
C     CHECKS FOR REBONDING AFTER CRACK                               REB   2
      ECC=0.01*EC                                                    REB   3
      IF (EPS.LT.0.) ECC=ERBOND*EC                                   REB   4
      RETURN                                                         REB   5
      END                                                            REB   6
```

```
$IT FOR SOLVEX,SOLVEX
      SUBROUTINE SOLVEX (N,A,B)
      DIMENSION A(6,6),B(6)
C
C     B=A-INVERSE * B
C
      TRACE=0.
      DO 5 I=1,N
    5 TRACE =TRACE+ABS(A(I,I))
      TRACE=.001*TRACE
      DO 6 I=1,N
      IF(ABS(A(I,I)).LT.TRACE)A(I,I)=TRACE
    6 CONTINUE
C
      DO 40 I=1,N
      IF(A(I,I).EQ.0.) GO TO 40
      D=1./A(I,I)
      DO 10 J=1,N
   10 A(I,J)=A(I,J)*D
      B(I)=B(I)*D
      DO 30 K=1,N
      IF(K.EQ.I) GO TO 30
      C=A(K,I)
      IF(C.EQ.0.) GO TO 30
      DO 20 L=1,N
   20 A(K,L)=A(K,L)-C*A(I,L)
      B(K)=B(K)-C*B(I)
30    CONTINUE
40    CONTINUE
      RETURN
      END
```

```
* T I D Y *
                SUBROUTINE STLTRN (AS,DC,DCS,DCC,NRB,ASX,ASY,ASZ)

      SUBROUTINE STLTRN (AS,DC,DCS,DCC,NRB,ASX,ASY,ASZ)                  STL   1
                                                                         STL   2
C                                                                        STL   3
C     TRANSFORMS STEEL AREAS TO APPROPRIATE DIRECTIONS                   STL   4
C                                                                        STL   5
      DIMENSION AS(3), DC(3,3), DCS(3,1), DCC(3,1)                       STL   6
C                                                                        STL   7
      IF (NRB.GT.0) GO TO 10                                             STL   8
      DO 5 I=1,3                                                         STL   9
      AS(I)=ASX*DC(1,I)*DC(1,I)+ASY*DC(2,I)*DC(2,I)+ASZ*DC(3,I)*DC(3,I)  STL  10
5     CONTINUE                                                           STL  11
      RETURN                                                             STL  12
C                                                                        STL  13
10    DO 15 I=1,3                                                        STL  14
      DO 15 J=1,3                                                        STL  15
      DCC(I,J)=DCS(1,I)*DC(1,J)+DCS(2,I)*DC(2,J)+DCS(3,I)*DC(3,J)        STL  16
15    CONTINUE                                                           STL  17
      DO 20 I=1,3                                                        STL  18
      AS(I)=ASX*DCC(1,I)*DCC(1,I)+ASY*DCC(2,I)*DCC(2,I)+ASZ*DCC(3,I)*DCCSTL  19
     1(3,I)                                                              STL  20
20    CONTINUE                                                           STL  21
      RETURN                                                             STL  22
C                                                                        STL  23
      END
```

```
* T I D Y *
                    SUBROUTINE TRANSF (A,B,DC)

      SUBROUTINE TRANSF (A,B,DC)                                        TRN   1
C                                                                       TRN   2
C     FORMULATES TRANSFORMATION MATRICIES TO CONVERT STRESS/STRAIN      TRN   3
C     ONE SET OF COORDINATE SYSTEM TO ANOTHER                           TRN   4
C                                                                       TRN   5
      DIMENSION A(6,6), B(6,6), DC(3,3), NP(6)                          TRN   6
      DATA (NP(I),I=1,6)/1,2,2,3,3,1/                                   TRN   7
C     FORM TRANSFORMATION MATRICIES A AND B                             TRN   8
      DO 5 I=1,3                                                        TRN   9
      L1=NP(2*I-1)                                                      TRN  10
      L2=NP(2*I)                                                        TRN  11
      DO 5 J=1,3                                                        TRN  12
      K1=NP(2*J-1)                                                      TRN  13
      K2=NP(2*J)                                                        TRN  14
      B(I,J)=DC(I,J)*DC(I,J)                                            TRN  15
      B(I+3,J+3)=DC(L1,K1)*DC(L2,K2)+DC(L1,K2)*DC(L2,K1)                TRN  16
      B(I+3,J)=DC(L1,J)*DC(L2,J)                                        TRN  17
      B(I,J+3)=DC(I,K1)*DC(I,K2)*2.                                     TRN  18
      A(J,I)=B(I,J)                                                     TRN  19
      A(J+3,I+3)=B(I+3,J+3)                                             TRN  20
      A(J,I+3)=B(I+3,J)*2.                                              TRN  21
      A(J+3,I)=B(I,J+3)/2.                                              TRN  22
5     CONTINUE                                                          TRN  23
      RETURN                                                            TRN  24
      END                                                               TRN  25.
```

```
*IT FOR VARMOD,VARMOD
      SUBROUTINE VARMOD (SIG,EPS,SO,SY,EC,ES,NU,AS,C,ICRACK,NELTYP,DEPS,
     ,EPSEL,ALFA,GAMA,EN,GST,ERBOND)
      DIMENSION SIG(1),EPS(1),AS(1),C(6,6),ECC(3),ESS(3),AC(3),POIS(3,3)
     1,DEPS(1),EPSEL(1),GSTL(3)
      REAL NU
      S1=SIG(1)
      S2=SIG(2)
      S3=SIG(3)
      E1=EPS(1)
      E2=EPS(2)
      E3=EPS(3)
      GI=GST
      DO 5 I=1,3
      GSTL(I)=GST
      POIS(I,I)=0.
      AC(I)=1.-AS(I)
      ESS(I)=ES
      DO 5 J=1,3
      IF(I.NE.J) POIS(I,J)=NU
5     CONTINUE
      IF(ICRACK.EQ.0) GO TO 100
      POIS(2,1)=0.
      POIS(3,1)=0.
      POIS(1,2)=0.
      POIS(1,3)=0.
      GSTL(1)=0.
      GSTL(3)=0.
      S=S2+S3
      CALL LODUM (EPS(1),DEPS(1),EPSEL(1),LD)
      IF (LD.GT.0 ) CALL COMPOS (S1,SY,AC(1),AS(1),EC,ES,ECC(1),FSS(1))
      IF(LD.LE.0) CALL REBOND (EPS(1),ECC(1),EC,ERBOND)
      IF(ICRACK.EQ.1) GO TO 20
      POIS(2,3)=0.
      POIS(3,2)=0.
      GSTL(2)=0.
      S=S1+S3
      CALL LODUM (EPS(2),DEPS(2),EPSEL(2),LD)
      IF(LD.GT.0 ) CALL COMPOS (S2,SY,AC(2),AS(2),EC,ES,ECC(2),FSS(2))
      IF(LD.LE.0) CALL REBOND (EPS(2),ECC(2),EC,ERBOND)
      IF(ICRACK.EQ.2) GO TO 40
      S=S1+S2
      CALL LODUM (EPS(3),DEPS(3),EPSEL(3),LD)
      IF(LD.GT.0 ) CALL COMPOS (S3,SY,AC(3),AS(3),EC,ES,ECC(3),FSS(3))
      IF(LD.LE.0) CALL REBOND (EPS(3),ECC(3),EC,ERBOND)
      GO TO 200
20    CALL MODULI (S2,S3,SO,E2,EC,ES,ECC(2),DUM2,NU,DEPS(2),EPSEL(2))
      CALL MODULI (S3,S2,SO,E3,EC,ES,ECC(3),DUM3,NU,DEPS(3),EPSEL(3))
      POIS(2,2)=DUM2*DUM3/((DUM2+DUM3)*(1.+NU))
      IF (AS(1).LE.0.) GO TO 200
      S=S1/AS(1)
      CALL DOMEL1 (S,SY,SO,ALFA,GAMA,EN,GI)
      CALL DOMEL2 (GI,ALFA,EPS(4),DEPS(4),EPSEL(4),GSTL(1))
      IF(ABS(NELTYP).GT.4) CALL DOMEL2 (GI,ALFA,EPS(6),DEPS(6),EPSEL(6),
     ,GSTL(3))
      GO TO 200
40    S=0.
      CALL MODULI (S3,S,SO,E3,EC,ES,ECC(3),DUM3,NU,DEPS(3),EPSEL(3))
      GO TO 200
100   S=S2+S3
```

```
      CALL MODULI (S1,S ,S0,E1,EC,ES,ECC(1),DUM1,NU,DEPS(1),EPSEL(1))
      S=S1+S3
      CALL MODULI (S2,S ,S0,E2,EC,ES,ECC(2),DUM2,NU,DEPS(2),EPSEL(2))
      S=S1+S2
      CALL MODULI (S3,S,S0,E3,EC,ES,ECC(3),DUM3,NU,DEPS(3),EPSEL(3))
      POIS(1,1)=DUM1*DUM2/((DUM1+DUM2)*(1.+NU))
      POIS(2,2)=DUM2*DUM3/((DUM2+DUM3)*(1.+NU))
      POIS(3,3)=DUM1*DUM3/((DUM1+DUM3)*(1.+NU))
200   CALL FORMC (POIS,ECC,ESS,AC,AS,C,GSTL)
      RETURN
      END
```

6. DEMONSTRATION PROBLEMS

Two simple one-dimensional demonstration cases are included in the following. The first problem is used to demonstrate the capability of the material model to use strain as input to calculate stress. The second problem is used to demonstrate the capability of the material model to accept stress input. The stress calculated from the first example was used as input to the material model in the second example.

a. Demonstration Problem 1

This example has been run to compute the stresses corresponding to several specified strain increments. The input parameters were:

NRB = 0; ICOMPS = 1; NELTYP = 4 (plane strain problem);
NSTEPS = 12; NSPLIT = -1 (indicating strain input)

NRB equal to zero implies that steel is oriented in the global coordinate directions. Thus it is not necessary to provide steel orientation defined by DCS.

CØEFF(1)	= 3×10^6 psi ($20{,}685 \times 10^6$ N/m^2)	= E_c
CØEFF(2)	= 30×10^6 psi ($20{,}685 \times 10^7$ N/m^2)	= E_s
CØEFF(3)	= 6×10^3 psi ($41{,}370 \times 10^3$ N/m^2)	f'_c
CØEFF(4)	= 4.8×10^4 psi ($33{,}096 \times 10^4$ N/m^2)	= f_y
CØEFF(5)	= 0.15	= ν
CØEFF(6)	= 500 psi (34.5×10^5 N/m^2)	= f_t
CØEFF(7)	= -0.083	= η (slope of cracking envelope)
CØEFF(8)	= 4.0	= n (dowel shear coefficient)

CØEFF(9) = 1.2×10^7 psi (8274×10^7 N/m^2) = G_s

CØEFF(10) = 0.5 = Rebonding coefficient

COEFF(11 through 15) = 0.0 (not necessary for this example)

AST(1) = 0.02

AST(2) = 0.0

AST(3) = 0.0

DCS: 0, ..., 0

The element is subjected to compressive loading, then unloading, and then reloading.

Strain increments: 1 through 7 are -5×10^{-4}; 8, 9 are $+5 \times 10^{-4}$; 10 through 14 are -5×10^{-4}.

The resulting stress/strain curve is shown in figure 108(a).

b. Demonstration Problem 2

Using the stress increment shown in figure 108(a) as input, the material program was run again with the following parameters:

NRB = 0; ICOMPS = 1; NELTYP = 4; NSTEPS = 11;
NSPLIT = 5 (indicating stress input)

CØEFF(1 through 15) = Same as for example 1

AST(1 through 3) = Same as for example 1

DCS = Same as for example 1

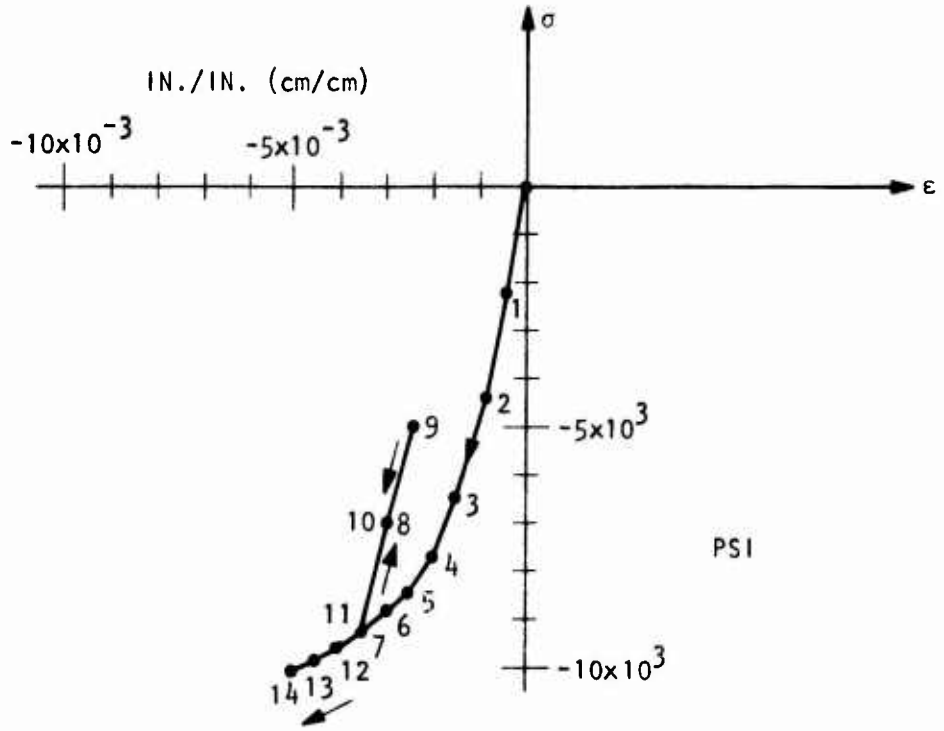

(a) Stress corresponding to specified strain increments

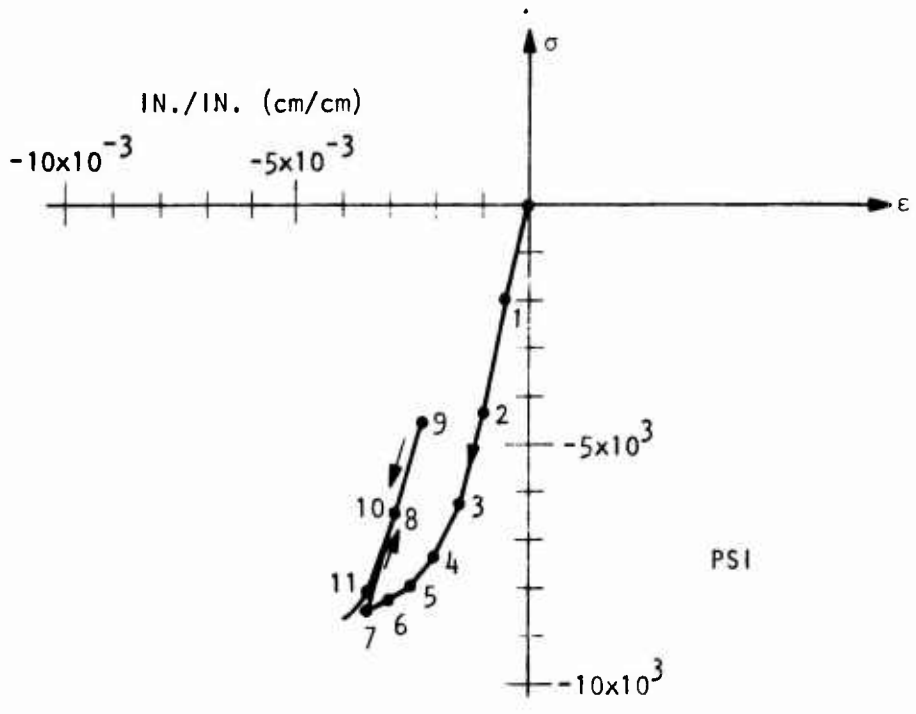

(b) Strain corresponding to specified stress increments

Figure 108. Stress/Strain Diagram for Examples 1 and 2 (English Units)

Stress increments:

-2.110×10^3, -2.303×10^3, -2.009×10^3, -1.382×10^3

-7.478×10^2, -3.181×10^2, -3.181×10^2, $+2.111 \times 10^3$

$+2.111 \times 10^3$, -2.111×10^3, -2.111×10^3

The stress increments for components 2 and 3 are 1 through 7: -3.26×10^2; and 8,9: $+3.26 \times 10^2$; 10,11: -3.26×10^2.

The resulting stress-strain diagram is shown in figure 108(b).

Results of figure 108(b) are in good agreement with those of figure 108(a). A listing of the input and output from these two examples is included in the next pages.

EXAMPLE 1 UNIAXIAL STRAIN (2 PERCENT STEEL) STRAIN INPUT OPTION

NRB	ICOMPS	NELTYP	NSTEPS	NSPLIT
0	1	4	30	-1

```
COEFF
  .35000+07   .30000+08   .60000+04   .48000+05   .15000+00   .50000+03  -.83000-01   .40000+01   .12000+08   .50000+00
  .00000      .00000      .00000      .00000      .00000
AST   .2000-01    .0000       .0000

DCS   .00000      .00000      .00000      .00000      .00000      .00000      .00000      .00000      .00000

STEP=  1
STRINC   -.5000-03    .0000       .0000       .0000       .0000       .0000
STRESS   -.21109+04   -.32609+03  -.32609+03  .00000      .00000      .00000
STRAIN   -.50000-03   .00000      .00000      .00000      .00000      .00000
EPSEL    .00000       .00000      .00000      .00000      .00000      .00000
ICRACK   0
DIRCOS    .10000+01   .00000      .00000      .00000      .10000+01   .00000      .00000      .00000      .10000+01
CMATRIX
  .42217+07   .65217+06   .65217+06   .00000      .00000      .00000
  .65217+06   .36957+07   .65217+06   .00000      .00000      .00000
  .65217+06   .65217+06   .36957+07   .00000      .00000      .00000
  .00000      .00000      .00000      .17313+07   .00000      .00000
  .00000      .00000      .00000      .00000      .15217+07   .00000
  .00000      .00000      .00000      .00000      .00000      .15217+07
STEP=  2
STRINC   -.5000-03    .0000       .0000       .0000       .0000       .0000
STRESS   -.44137+04   -.65217+03  -.65217+03  .00000      .00000      .00000
STRAIN   -.10000-02   .00000      .00000      .00000      .00000      .00000
EPSEL    -.10000-02   .00000      .00000      .00000      .00000      .00000
ICRACK   0
DIRCOS    .10000+01   .00000      .00000      .00000      .10000+01   .00000      .00000      .00000      .10000+01
CMATRIX
  .46056+07   .65217+06   .65217+06   .00000      .00000      .00000
  .65217+06   .36957+07   .65217+06   .00000      .00000      .00000
  .65217+06   .65217+06   .36957+07   .00000      .00000      .00000
  .00000      .00000      .00000      .18064+07   .00000      .00000
  .00000      .00000      .00000      .00000      .15217+07   .00000
  .00000      .00000      .00000      .00000      .00000      .15983+07
STEP=  3
STRINC   -.5000-03    .0000       .0000       .0000       .0000       .0000
STRESS   -.64230+04   -.97826+03  -.97826+03  .00000      .00000      .00000
STRAIN   -.15000-02   .00000      .00000      .00000      .00000      .00000
EPSEL    -.15000-02   .00000      .00000      .00000      .00000      .00000
ICRACK   0
DIRCOS    .10000+01   .00000      .00000      .00000      .10000+01   .00000      .00000      .00000      .10000+01
CMATRIX
  .40187+07   .65217+06   .65217+06   .00000      .00000      .00000
  .65217+06   .36957+07   .65217+06   .00000      .00000      .00000
  .65217+06   .65217+06   .36957+07   .00000      .00000      .00000
  .00000      .00000      .00000      .16883+07   .00000      .00000
  .00000      .00000      .00000      .00000      .15217+07   .00000
  .00000      .00000      .00000      .00000      .00000      .14779+07
STEP=  4
```

```
STRINC   -.5000-03    .0000       .0000       .0000       .0000       .0000
STRESS   -.78049+04   -.13043+04  -.13043+04   .00000      .00000      .00000
STRAIN   -.20000-02    .00000      .00000      .00000      .00000      .00000
EPSEL    -.20000-02    .00000      .00000      .00000      .00000      .00000
ICRACK   0
DIRCOS    .10000+01    .00000      .00000      .00000      .10000+01   .00000      .00000      .00000      .10000+01
CMATRIX
  .27635+07   .65217+06   .65217+06   .00000      .00000      .00000
  .65217+06   .36957+07   .65217+06   .00000      .00000      .00000
  .65217+06   .65217+06   .36957+07   .00000      .00000      .00000
  .00000      .00000      .00000      .13555+07   .00000      .00000
  .00000      .00000      .00000      .00000      .15217+07   .00000
  .00000      .00000      .00000      .00000      .00000      .11383+07
STEP=  5
STRINC   -.5000-03    .0000       .0000       .0000       .0000       .0000
STRESS   -.85527+04   -.16304+04  -.16304+04   .00000      .00000      .00000
STRAIN   -.25000-02    .00000      .00000      .00000      .00000      .00000
EPSEL    -.25000-02    .00000      .00000      .00000      .00000      .00000
ICRACK   0
DIRCOS    .10000+01    .00000      .00000      .00000      .10000+01   .00000      .00000      .00000      .10000+01
CMATRIX
  .14955+07   .65217+06   .65217+06   .00000      .00000      .00000
  .65217+06   .36957+07   .65217+06   .00000      .00000      .00000
  .65217+06   .65217+06   .36957+07   .00000      .00000      .00000
  .00000      .00000      .00000      .83125+06   .00000      .00000
  .00000      .00000      .00000      .00000      .15217+07   .00000
  .00000      .00000      .00000      .00000      .00000      .60332+06
STEP=  6
STRINC   -.5000-03    .0000       .0000       .0000       .0000       .0000
STRESS   -.88704+04   -.19565+04  -.19565+04   .00000      .00000      .00000
STRAIN   -.30000-02    .00000      .00000      .00000      .00000      .00000
EPSEL    -.30000-02    .00000      .00000      .00000      .00000      .00000
ICRACK   0
DIRCOS    .10000+01    .00000      .00000      .00000      .10000+01   .00000      .00000      .00000      .10000+01
CMATRIX
  .63622+06   .65217+06   .65217+06   .00000      .00000      .00000
  .65217+06   .36957+07   .65217+06   .00000      .00000      .00000
  .65217+06   .65217+06   .36957+07   .00000      .00000      .00000
  .00000      .00000      .00000      .26953+06   .00000      .00000
  .00000      .00000      .00000      .00000      .15217+07   .00000
  .00000      .00000      .00000      .00000      .00000      .30133+05
STEP=  7
STRINC   -.5000-03    .0000       .0000       .0000       .0000       .0000
STRESS   -.91889+04   -.22826+04  -.22826+04   .00000      .00000      .00000
STRAIN   -.35000-02    .00000      .00000      .00000      .00000      .00000
EPSEL    -.35000-02    .00000      .00000      .00000      .00000      .00000
ICRACK   0
DIRCOS    .10000+01    .00000      .00000      .00000      .10000+01   .00000      .00000      .00000      .10000+01
CMATRIX
  .63622+06   .65217+06   .65217+06   .00000      .00000      .00000
  .65217+06   .36957+07   .65217+06   .00000      .00000      .00000
  .65217+06   .65217+06   .36957+07   .00000      .00000      .00000
  .00000      .00000      .00000      .26953+06   .00000      .00000
  .00000      .00000      .00000      .00000      .15217+07   .00000
  .00000      .00000      .00000      .00000      .00000      .30133+05
STEP=  8
STRINC    .5000-03    .0000       .0000       .0000       .0000       .0000
STRESS   -.70780+04   -.19565+04  -.19565+04   .00000      .00000      .00000
STRAIN   -.30000-02    .00000      .00000      .00000      .00000      .00000
EPSEL    -.35000-02    .00000      .00000      .00000      .00000      .00000
```

```
ICRACK  0
DIRCOS   .10000+01   .00000      .00000      .00000      .10000+01   .00000      .00000      .00000      .10000+01
CMATRIX
  .42217+07   .65217+06   .65217+06   .00000      .00000      .00000
  .65217+06   .36957+07   .65217+06   .00000      .00000      .00000
  .65217+06   .65217+06   .36957+07   .00000      .00000      .00000
  .00000      .00000      .00000      .17313+07   .00000      .00000
  .00000      .00000      .00000      .00000      .15217+07   .00000
  .00000      .00000      .00000      .00000      .00000      .15217+07
STEP=  9
STRINC    .5000-03    .0000       .0000       .0000       .0000       .0000
STRESS  -.49671+04  -.16304+04  -.16304+04   .00000      .00000      .00000
STRAIN  -.25000-02   .00000      .00000      .00000      .00000      .00000
EPSEL   -.35000-02   .00000      .00000      .00000      .00000      .00000
ICRACK  0
DIRCOS   .10000+01   .00000      .00000      .00000      .10000+01   .00000      .00000      .00000      .10000+01
CMATRIX
  .42217+07   .65217+06   .65217+06   .00000      .00000      .00000
  .65217+06   .36957+07   .65217+06   .00000      .00000      .00000
  .65217+06   .65217+06   .36957+07   .00000      .00000      .00000
  .00000      .00000      .00000      .17313+07   .00000      .00000
  .00000      .00000      .00000      .00000      .15217+07   .00000
  .00000      .00000      .00000      .00000      .00000      .15217+07
STEP= 10
STRINC   -.5000-03    .0000       .0000       .0000       .0000       .0000
STRESS  -.70780+04  -.19565+04  -.19565+04   .00000      .00000      .00000
STRAIN  -.30000-02   .00000      .00000      .00000      .00000      .00000
EPSEL   -.35000-02   .00000      .00000      .00000      .00000      .00000
ICRACK  0
DIRCOS   .10000+01   .00000      .00000      .00000      .10000+01   .00000      .00000      .00000      .10000+01
CMATRIX
  .42217+07   .65217+06   .65217+06   .00000      .00000      .00000
  .65217+06   .36957+07   .65217+06   .00000      .00000      .00000
  .65217+06   .65217+06   .36957+07   .00000      .00000      .00000
  .00000      .00000      .00000      .17313+07   .00000      .00000
  .00000      .00000      .00000      .00000      .15217+07   .00000
  .00000      .00000      .00000      .00000      .00000      .15217+07
STEP= 11
STRINC   -.5000-03    .0000       .0000       .0000       .0000       .0000
STRESS  -.91889+04  -.22826+04  -.22826+04   .00000      .00000      .00000
STRAIN  -.35000-02   .00000      .00000      .00000      .00000      .00000
EPSEL   -.35000-02   .00000      .00000      .00000      .00000      .00000
ICRACK  0
DIRCOS   .10000+01   .00000      .00000      .00000      .10000+01   .00000      .00000      .00000      .10000+01
CMATRIX
  .42217+07   .65217+06   .65217+06   .00000      .00000      .00000
  .65217+06   .36957+07   .65217+06   .00000      .00000      .00000
  .65217+06   .65217+06   .36957+07   .00000      .00000      .00000
  .00000      .00000      .00000      .17313+07   .00000      .00000
  .00000      .00000      .00000      .00000      .15217+07   .00000
  .00000      .00000      .00000      .00000      .00000      .15217+07
STEP= 12
STRINC   -.5000-03    .0000       .0000       .0000       .0000       .0000
STRESS  -.95070+04  -.26087+04  -.26087+04   .00000      .00000      .00000
STRAIN  -.40000-02   .00000      .00000      .00000      .00000      .00000
EPSEL   -.40000-02   .00000      .00000      .00000      .00000      .00000
ICRACK  0
DIRCOS   .10000+01   .00000      .00000      .00000      .10000+01   .00000      .00000      .00000      .10000+01
CMATRIX
  .63622+06   .65217+06   .65217+06   .00000      .00000      .00000
```

```
  .65217+06   .36957+07   .65217+06   .00000      .00000      .00000
  .65217+06   .65217+06   .36957+07   .00000      .00000      .00000
  .00000      .00000      .00000      .26953+06   .00000      .00000
  .00000      .00000      .00000      .00000      .15217+07   .00000
  .00000      .00000      .00000      .00000      .00000      .30133+05
STEP= 13
STRINC   =.5000=03    .0000       .0000       .0000       .0000       .0000
STRESS   =.98251+04   =.29348+04  =.29348+04   .00000      .00000      .00000
STRAIN   =.45000=02   .00000      .00000      .00000      .00000      .00000
EPSEL    =.45000=02   .00000      .00000      .00000      .00000      .00000
ICRACK   0
DIRCOS    .10000+01   .00000      .00000      .00000      .10000+01   .00000      .00000      .00000      .10000+01
CMATRIX
  .63622+06   .65217+06   .65217+06   .00000      .00000      .00000
  .65217+06   .36957+07   .65217+06   .00000      .00000      .00000
  .65217+06   .65217+06   .36957+07   .00000      .00000      .00000
  .00000      .00000      .00000      .26953+06   .00000      .00000
  .00000      .00000      .00000      .00000      .15217+07   .00000
  .00000      .00000      .00000      .00000      .00000      .30133+05
STEP= 14
STRINC   =.5000=03    .0000       .0000       .0000       .0000       .0000
STRESS   =.10143+05   =.32609+04  =.32609+04   .00000      .00000      .00000
STRAIN   =.50000=02   .00000      .00000      .00000      .00000      .00000
EPSEL    =.50000=02   .00000      .00000      .00000      .00000      .00000
ICRACK   0
DIRCOS    .10000+01   .00000      .00000      .00000      .10000+01   .00000      .00000      .00000      .10000+01
CMATRIX
  .63622+06   .65217+06   .65217+06   .00000      .00000      .00000
  .65217+06   .36957+07   .65217+06   .00000      .00000      .00000
  .65217+06   .65217+06   .36957+07   .00000      .00000      .00000
  .00000      .00000      .00000      .26953+06   .00000      .00000
  .00000      .00000      .00000      .00000      .15217+07   .00000
  .00000      .00000      .00000      .00000      .00000      .30133+05
STEP= 15
STRINC   =.5000=03    .0000       .0000       .0000       .0000       .0000
STRESS   =.10461+05   =.35870+04  =.35870+04   .00000      .00000      .00000
STRAIN   =.55000=02   .00000      .00000      .00000      .00000      .00000
EPSEL    =.55000=02   .00000      .00000      .00000      .00000      .00000
ICRACK   0
DIRCOS    .10000+01   .00000      .00000      .00000      .10000+01   .00000      .00000      .00000      .10000+01
CMATRIX
  .63622+06   .65217+06   .65217+06   .00000      .00000      .00000
  .65217+06   .36957+07   .65217+06   .00000      .00000      .00000
  .65217+06   .65217+06   .36957+07   .00000      .00000      .00000
  .00000      .00000      .00000      .26953+06   .00000      .00000
  .00000      .00000      .00000      .00000      .15217+07   .00000
  .00000      .00000      .00000      .00000      .00000      .30133+05
STEP= 16
STRINC   =.5000=03    .0000       .0000       .0000       .0000       .0000
STRESS   =.10779+05   =.39130+04  =.39130+04   .00000      .00000      .00000
STRAIN   =.60000=02   .00000      .00000      .00000      .00000      .00000
EPSEL    =.60000=02   .00000      .00000      .00000      .00000      .00000
ICRACK   0
DIRCOS    .10000+01   .00000      .00000      .00000      .10000+01   .00000      .00000      .00000      .10000+01
CMATRIX
  .63622+06   .65217+06   .65217+06   .00000      .00000      .00000
  .65217+06   .36957+07   .65217+06   .00000      .00000      .00000
  .65217+06   .65217+06   .36957+07   .00000      .00000      .00000
  .00000      .00000      .00000      .26953+06   .00000      .00000
  .00000      .00000      .00000      .00000      .15217+07   .00000
```

```
  .00000      .00000      .00000      .00000      .00000      .30133+05
STEP= 17
STRINC   =.5000-03    .0000       .0000       .0000       .0000       .0000
STRESS   =.11098+05   =.42391+04  =.42391+04   .00000      .00000      .00000
STRAIN   =.65000-02   .00000      .00000      .00000      .00000      .00000
EPSEL    =.65000-02   .00000      .00000      .00000      .00000      .00000
ICRACK   0
DIRCOS    .10000+01   .00000      .00000      .00000      .10000+01   .00000      .00000      .00000      .10000+01
CMATRIX
  .63622+06   .65217+06   .65217+06   .00000      .00000      .00000
  .65217+06   .36957+07   .65217+06   .00000      .00000      .00000
  .65217+06   .65217+06   .36957+07   .00000      .00000      .00000
  .00000      .00000      .00000      .26953+06   .00000      .00000
  .00000      .00000      .00000      .00000      .15217+07   .00000
  .00000      .00000      .00000      .00000      .00000      .30133+05
STEP= 18
STRINC    .5000-03    .0000       .0000       .0000       .0000       .0000
STRESS   =.89867+04   =.39130+04  =.39130+04   .00000      .00000      .00000
STRAIN   =.60000-02   .00000      .00000      .00000      .00000      .00000
EPSEL    =.65000-02   .00000      .00000      .00000      .00000      .00000
ICRACK   0
DIRCOS    .10000+01   .00000      .00000      .00000      .10000+01   .00000      .00000      .00000      .10000+01
CMATRIX
  .42217+07   .65217+06   .65217+06   .00000      .00000      .00000
  .65217+06   .36957+07   .65217+06   .00000      .00000      .00000
  .65217+06   .65217+06   .36957+07   .00000      .00000      .00000
  .00000      .00000      .00000      .17313+07   .00000      .00000
  .00000      .00000      .00000      .00000      .15217+07   .00000
  .00000      .00000      .00000      .00000      .00000      .15217+07
STEP= 19
STRINC    .5000-03    .0000       .0000       .0000       .0000       .0000
STRESS   =.68758+04   =.35870+04  =.35870+04   .00000      .00000      .00000
STRAIN   =.55000-02   .00000      .00000      .00000      .00000      .00000
EPSEL    =.65000-02   .00000      .00000      .00000      .00000      .00000
ICRACK   0
DIRCOS    .10000+01   .00000      .00000      .00000      .10000+01   .00000      .00000      .00000      .10000+01
CMATRIX
  .42217+07   .65217+06   .65217+06   .00000      .00000      .00000
  .65217+06   .36957+07   .65217+06   .00000      .00000      .00000
  .65217+06   .65217+06   .36957+07   .00000      .00000      .00000
  .00000      .00000      .00000      .17313+07   .00000      .00000
  .00000      .00000      .00000      .00000      .15217+07   .00000
  .00000      .00000      .00000      .00000      .00000      .15217+07
STEP= 20
STRINC    .5000-03    .0000       .0000       .0000       .0000       .0000
STRESS   =.47649+04   =.32609+04  =.32609+04   .00000      .00000      .00000
STRAIN   =.50000-02   .00000      .00000      .00000      .00000      .00000
EPSEL    =.65000-02   .00000      .00000      .00000      .00000      .00000
ICRACK   0
DIRCOS    .10000+01   .00000      .00000      .00000      .10000+01   .00000      .00000      .00000      .10000+01
CMATRIX
  .42217+07   .65217+06   .65217+06   .00000      .00000      .00000
  .65217+06   .36957+07   .65217+06   .00000      .00000      .00000
  .65217+06   .65217+06   .36957+07   .00000      .00000      .00000
  .00000      .00000      .00000      .17313+07   .00000      .00000
  .00000      .00000      .00000      .00000      .15217+07   .00000
  .00000      .00000      .00000      .00000      .00000      .15217+07
STEP= 21
STRINC    .5000-03    .0000       .0000       .0000       .0000       .0000
STRESS   =.26541+04   =.29348+04  =.29348+04   .00000      .00000      .00000
```

```
STRAIN  -.45000-02   .00000      .00000      .00000      .00000      .00000
EPSEL   -.65000-02   .00000      .00000      .00000      .00000      .00000
ICRACK  0
DIRCOS   .10000+01   .00000      .00000      .00000      .10000+01   .00000      .00000      .00000      .10000+01
CMATRIX
  .42217+07   .65217+06   .65217+06   .00000      .00000      .00000
  .65217+06   .36957+07   .65217+06   .00000      .00000      .00000
  .65217+06   .65217+06   .36957+07   .00000      .00000      .00000
  .00000      .00000      .00000      .17313+07   .00000      .00000
  .00000      .00000      .00000      .00000      .15217+07   .00000
  .00000      .00000      .00000      .00000      .00000      .15217+07
STEP= 22
STRINC   .2500-03    .0000       .0000       .0000       .0000       .0000
STRESS  -.15990+04  -.27717+04  -.27717+04   .00000      .00000      .00000
STRAIN  -.42500-02   .00000      .00000      .00000      .00000      .00000
EPSEL   -.65000-02   .00000      .00000      .00000      .00000      .00000
ICRACK  0
DIRCOS   .10000+01   .00000      .00000      .00000      .10000+01   .00000      .00000      .00000      .10000+01
CMATRIX
  .42217+07   .65217+06   .65217+06   .00000      .00000      .00000
  .65217+06   .36957+07   .65217+06   .00000      .00000      .00000
  .65217+06   .65217+06   .36957+07   .00000      .00000      .00000
  .00000      .00000      .00000      .17313+07   .00000      .00000
  .00000      .00000      .00000      .00000      .15217+07   .00000
  .00000      .00000      .00000      .00000      .00000      .15217+07
STEP= 23
STRINC   .2500-03    .0000       .0000       .0000       .0000       .0000
STRESS  -.54319+03  -.26087+04  -.26087+04   .00000      .00000      .00000
STRAIN  -.40000-02   .00000      .00000      .00000      .00000      .00000
EPSEL   -.65000-02   .00000      .00000      .00000      .00000      .00000
ICRACK  0
DIRCOS   .10000+01   .00000      .00000      .00000      .10000+01   .00000      .00000      .00000      .10000+01
CMATRIX
  .42217+07   .65217+06   .65217+06   .00000      .00000      .00000
  .65217+06   .36957+07   .65217+06   .00000      .00000      .00000
  .65217+06   .65217+06   .36957+07   .00000      .00000      .00000
  .00000      .00000      .00000      .17313+07   .00000      .00000
  .00000      .00000      .00000      .00000      .15217+07   .00000
  .00000      .00000      .00000      .00000      .00000      .15217+07
STEP= 24
STRINC   .2500-03    .0000       .0000       .0000       .0000       .0000
STRESS   .51225+03  -.24457+04  -.24457+04   .00000      .00000      .00000
STRAIN  -.37500-02   .00000      .00000      .00000      .00000      .00000
EPSEL   -.65000-02   .00000      .00000      .00000      .00000      .00000
ICRACK  0
DIRCOS   .10000+01   .00000      .00000      .00000      .10000+01   .00000      .00000      .00000      .10000+01
CMATRIX
  .42217+07   .65217+06   .65217+06   .00000      .00000      .00000
  .65217+06   .36957+07   .65217+06   .00000      .00000      .00000
  .65217+06   .65217+06   .36957+07   .00000      .00000      .00000
  .00000      .00000      .00000      .17313+07   .00000      .00000
  .00000      .00000      .00000      .00000      .15217+07   .00000
  .00000      .00000      .00000      .00000      .00000      .15217+07
STEP= 25
STRINC   .2500-03    .0000       .0000       .0000       .0000       .0000
STRESS   .47705+03  -.24457+04  -.24457+04   .00000      .00000      .00000
STRAIN  -.35000-02   .00000      .00000      .00000      .00000      .00000
EPSEL   -.35000-02   .00000      .00000      .00000      .00000      .00000
ICRACK  1
DIRCOS   .10000+01   .00000      .00000      .00000      .10000+01   .00000      .00000      .00000      .10000+01
```

```
CMATRIX
  .16031+07   .00000      .00000      .00000      .00000      .00000
  .00000      .35806+07   .53708+06   .00000      .00000      .00000
  .00000      .53708+06   .35806+07   .00000      .00000      .00000
  .00000      .00000      .00000      .24000+06   .00000      .00000
  .00000      .00000      .00000      .00000      .15217+07   .00000
  .00000      .00000      .00000      .00000      .00000      .00000
STEP= 26
STRINC    .1000-03    .0000       .0000       .0000       .0000       .0000
STRESS    .55725+03  -.24457+04  -.24457+04   .00000      .00000      .00000
STRAIN   -.34000-02   .00000      .00000      .00000      .00000      .00000
EPSEL    -.34000-02   .00000      .00000      .00000      .00000      .00000
ICRACK    1
DIRCOS    .10000+01   .00000      .00000      .00000      .10000+01   .00000      .00000      .00000      .10000+01
CMATRIX
  .80200+06   .00000      .00000      .00000      .00000      .00000
  .00000      .35806+07   .53708+06   .00000      .00000      .00000
  .00000      .53708+06   .35806+07   .00000      .00000      .00000
  .00000      .00000      .00000      .24000+06   .00000      .00000
  .00000      .00000      .00000      .00000      .15217+07   .00000
  .00000      .00000      .00000      .00000      .00000      .00000
STEP= 27
STRINC    .1000-03    .0000       .0000       .0000       .0000       .0000
STRESS    .63320+03  -.24457+04  -.24457+04   .00000      .00000      .00000
STRAIN   -.33000-02   .00000      .00000      .00000      .00000      .00000
EPSEL    -.33000-02   .00000      .00000      .00000      .00000      .00000
ICRACK    1
DIRCOS    .10000+01   .00000      .00000      .00000      .10000+01   .00000      .00000      .00000      .10000+01
CMATRIX
  .75953+06   .00000      .00000      .00000      .00000      .00000
  .00000      .35806+07   .53708+06   .00000      .00000      .00000
  .00000      .53708+06   .35806+07   .00000      .00000      .00000
  .00000      .00000      .00000      .24000+06   .00000      .00000
  .00000      .00000      .00000      .00000      .15217+07   .00000
  .00000      .00000      .00000      .00000      .00000      .00000
STEP= 28
STRINC    .1000-03    .0000       .0000       .0000       .0000       .0000
STRESS    .70553+03  -.24457+04  -.24457+04   .00000      .00000      .00000
STRAIN   -.32000-02   .00000      .00000      .00000      .00000      .00000
EPSEL    -.32000-02   .00000      .00000      .00000      .00000      .00000
ICRACK    1
DIRCOS    .10000+01   .00000      .00000      .00000      .10000+01   .00000      .00000      .00000      .10000+01
CMATRIX
  .72327+06   .00000      .00000      .00000      .00000      .00000
  .00000      .35806+07   .53708+06   .00000      .00000      .00000
  .00000      .53708+06   .35806+07   .00000      .00000      .00000
  .00000      .00000      .00000      .24000+06   .00000      .00000
  .00000      .00000      .00000      .00000      .15217+07   .00000
  .00000      .00000      .00000      .00000      .00000      .00000
STEP= 29
STRINC    .1000-03    .0000       .0000       .0000       .0000       .0000
STRESS    .77471+03  -.24457+04  -.24457+04   .00000      .00000      .00000
STRAIN   -.31000-02   .00000      .00000      .00000      .00000      .00000
EPSEL    -.31000-02   .00000      .00000      .00000      .00000      .00000
ICRACK    1
DIRCOS    .10000+01   .00000      .00000      .00000      .10000+01   .00000      .00000      .00000      .10000+01
CMATRIX
  .69181+06   .00000      .00000      .00000      .00000      .00000
  .00000      .35806+07   .53708+06   .00000      .00000      .00000
  .00000      .53708+06   .35806+07   .00000      .00000      .00000
```

```
  .00000       .00000       .00000       .24000+06    .00000       .00000
  .00000       .00000       .00000       .00000       .15217+07    .00000
  .00000       .00000       .00000       .00000       .00000       .00000
STEP= 30
STRINC     .1000+03     .0000        .0000        .0000        .0000        .0000
STRESS     .84113+03   -.24457+04   -.24457+04    .00000       .00000       .00000
STRAIN    -.30000-02    .00000       .00000       .00000       .00000       .00000
EPSEL     -.30000-02    .00000       .00000       .00000       .00000       .00000
ICRACK  1
DIRCOS     .10000+01    .00000       .00000       .00000       .10000+01    .00000       .00000       .00000       .10000+01
CMATRIX
  .66418+06    .00000       .00000       .00000       .00000       .00000
  .00000       .35806+07    .53708+06    .00000       .00000       .00000
  .00000       .53708+06    .35806+07    .00000       .00000       .00000
  .00000       .00000       .00000       .24000+06    .00000       .00000
  .00000       .00000       .00000       .00000       .15217+07    .00000
  .00000       .00000       .00000       .00000       .00000       .00000
```

EXAMPLE 2 UNIAXIAL STRAIN (2 PERCENT STEEL) STRESS INPUT OPTION

NRB	ICOMPS	NELTYP	NSTEPS	NSPLIT
0	1	4	11	5

```
COEFF
  .35000+07   .30000+08   .60000+04   .48000+05   .15000+00   .50000+03  -.83000-01   .40000+01   .12000+08   .90000+00
  .00000      .00000      .00000      .00000      .00000
AST    .2000-01    .0000       .0000

DCS   .00000      .00000      .00000      .00000      .00000      .00000      .00000      .00000      .00000

STEP=  1
STRINC   -.2113+04   -.3261+03   -.3261+03    .0000       .0000       .0000
STRESS   -.2140B+04  -.32613+03  -.32613+03   .00000      .00000      .00000
STRAIN   -.4823-03   -.26019-05  -.26019-05   .00000      .00000      .00000
EPSFL    -.4823-03   -.26019-05  -.26019-05   .00000      .00000      .00000
ICRACK   0
DIRCOS    .10000+01   .00000      .00000      .00000      .10000+01   .00000      .00000      .00000      .10000+01
CMATRIX
  .46006+07   .65258+06   .65258+06   .00000      .00000      .00000
  .65258+06   .3A98?+07   .65258+06   .00000      .00000      .00000
  .65258+06   .65258+06   .3A980+07   .00000      .00000      .00000
  .00000      .00000      .00000      .18059+07   .00000      .00000
  .00000      .00000      .00000      .00000      .15227+07   .00000
  .00000      .00000      .00000      .00000      .00000      .15979+07
STEP=  2
STRINC   -.2303+04   -.3261+03   -.3261+03    .0000       .0000       .0000
STRESS   -.44515+04  -.65221+03  -.65221+03   .00000      .00000      .00000
STRAIN   -.10010-02   .15153-06   .15153-06   .00000      .00000      .00000
EPSEL    -.10010-02  -.26019-05  -.26019-05   .00000      .00000      .00000
ICRACK   0
DIRCOS    .10000+01   .00000      .00000      .00000      .10000+01   .00000      .00000      .00000      .10000+01
CMATRIX
  .42168+07   .65217+06   .65217+06   .00000      .00000      .00000
  .65217+06   .3A957+07   .65217+06   .00000      .00000      .00000
  .65217+06   .65217+06   .36957+07   .00000      .00000      .00000
  .00000      .00000      .00000      .17303+07   .00000      .00000
  .00000      .00000      .00000      .00000      .15217+07   .00000
  .00000      .00000      .00000      .00000      .00000      .15207+07
STEP=  3
STRINC   -.2009+04   -.3261+03   -.3261+03    .0000       .0000       .0000
STRESS   -.43271+04  -.97829+03  -.97829+03   .00000      .00000      .00000
STRAIN   -.15383-02   .57466-05   .57466-05   .00000      .00000      .00000
EPSEL    -.15383-02  -.26019-05  -.26019-05   .00000      .00000      .00000
ICRACK   0
DIRCOS    .10000+01   .00000      .00000      .00000      .10000+01   .00000      .00000      .00000      .10000+01
CMATRIX
  .29949+07   .65217+06   .65217+06   .00000      .00000      .00000
  .65217+06   .3A957+07   .65217+06   .00000      .00000      .00000
  .65217+06   .65217+06   .36957+07   .00000      .00000      .00000
  .00000      .00000      .00000      .14272+07   .00000      .00000
  .00000      .00000      .00000      .00000      .15217+07   .00000
  .00000      .00000      .00000      .00000      .00000      .12114+07
STEP=  4
```

```
STRINC   -.1382+04   -.3261+03   -.3261+03    .0000       .0000       .0000
STRESS   -.74780+04  -.13044+04  -.13044+04   .00000      .00000      .00000
STRAIN   -.20944-02   .14173-04   .14173-04   .00000      .00000      .00000
EPSEL    -.20944-02  -.26019-05  -.26019-05   .00000      .00000      .00000
ICRACK   0
DIRCOS    .10000+01   .00000      .00000      .00000      .10000+01   .00000      .00000      .00000      .10000+01
CMATRIX
  .16180+07   .65217+06   .65217+06   .00000      .00000      .00000
  .65217+06   .36957+07   .65217+06   .00000      .00000      .00000
  .65217+06   .65217+06   .36957+07   .00000      .00000      .00000
  .00000      .00000      .00000      .89443+06   .00000      .00000
  .00000      .00000      .00000      .00000      .15217+07   .00000
  .00000      .00000      .00000      .00000      .00000      .66779+06
STEP=  5
STRINC   -.7478+03   -.3261+03   -.3261+03    .0000       .0000       .0000
STRESS   -.80277+04  -.16305+04  -.16305+04   .00000      .00000      .00000
STRAIN   -.27513-02   .37703-04   .37703-04   .00000      .00000      .00000
EPSEL    -.27513-02  -.26019-05  -.26019-05   .00000      .00000      .00000
ICRACK   0
DIRCOS    .10000+01   .00000      .00000      .00000      .10000+01   .00000      .00000      .00000      .10000+01
CMATRIX
  .63622+06   .65217+06   .65217+06   .00000      .00000      .00000
  .65217+06   .36957+07   .65217+06   .00000      .00000      .00000
  .65217+06   .65217+06   .36957+07   .00000      .00000      .00000
  .00000      .00000      .00000      .26953+06   .00000      .00000
  .00000      .00000      .00000      .00000      .15217+07   .00000
  .00000      .00000      .00000      .00000      .00000      .30133+05
STEP=  6
STRINC   -.3181+03   -.3261+03   -.3261+03    .0000       .0000       .0000
STRESS   -.84065+04  -.19565+04  -.19565+04   .00000      .00000      .00000
STRAIN   -.31022-02   .24345-04   .24345-04   .00000      .00000      .00000
EPSEL    -.31022-02  -.26019-05  -.26019-05   .00000      .00000      .00000
ICRACK   0
DIRCOS    .10000+01   .00000      .00000      .00000      .10000+01   .00000      .00000      .00000      .10000+01
CMATRIX
  .63622+06   .65217+06   .65217+06   .00000      .00000      .00000
  .65217+06   .36957+07   .65217+06   .00000      .00000      .00000
  .65217+06   .65217+06   .36957+07   .00000      .00000      .00000
  .00000      .00000      .00000      .26953+06   .00000      .00000
  .00000      .00000      .00000      .00000      .15217+07   .00000
  .00000      .00000      .00000      .00000      .00000      .30133+05
STEP=  7
STRINC   -.3181+03   -.3261+03   -.3261+03    .0000       .0000       .0000
STRESS   -.85854+04  -.22826+04  -.22826+04   .00000      .00000      .00000
STRAIN   -.35732-02   .10986-04   .10986-04   .00000      .00000      .00000
EPSEL    -.35732-02  -.26019-05  -.26019-05   .00000      .00000      .00000
ICRACK   0
DIRCOS    .10000+01   .00000      .00000      .00000      .10000+01   .00000      .00000      .00000      .10000+01
CMATRIX
  .63622+06   .65217+06   .65217+06   .00000      .00000      .00000
  .65217+06   .36957+07   .65217+06   .00000      .00000      .00000
  .65217+06   .65217+06   .36957+07   .00000      .00000      .00000
  .00000      .00000      .00000      .26953+06   .00000      .00000
  .00000      .00000      .00000      .00000      .15217+07   .00000
  .00000      .00000      .00000      .00000      .00000      .30133+05
STEP=  8
STRINC    .2111+04    -.3260+03    .3260+03    .0000       .0000       .0000
STRESS   -.64745+04  -.19566+04  -.19566+04   .00000      .00000      .00000
STRAIN   -.30731-02   .10984-04   .10984-04   .00000      .00000      .00000
EPSEL    -.35732-02  -.26019-05  -.26019-05   .00000      .00000      .00000
```

```
ICRACK  0
DIRCOS   .10000+01   .00000      .00000      .00000      .10000+01   .00000      .00000      .00000      .10000+01
CMATRIX
  .42217+07   .65217+06   .65217+06   .00000      .00000      .00000
  .65217+06   .36957+07   .65217+06   .00000      .00000      .00000
  .65217+06   .65217+06   .36957+07   .00000      .00000      .00000
  .00000      .00000      .00000      .17313+07   .00000      .00000
  .00000      .00000      .00000      .00000      .15217+07   .00000
  .00000      .00000      .00000      .00000      .00000      .15217+07
STEP=  9
STRINC    .2111+04    .3260+03    .3260+03    .0000       .0000       .0000
STRESS  -.43634+04  -.16306+04  -.16306+04   .00000      .00000      .00000
STRAIN  -.25731-02   .10942-04   .10942-04   .00000      .00000      .00000
EPSEL   -.35732-02  -.26019-05  -.26019-05   .00000      .00000      .00000
ICRACK  0
DIRCOS   .10000+01   .00000      .00000      .00000      .10000+01   .00000      .00000      .00000      .10000+01
CMATRIX
  .42217+07   .65217+06   .65217+06   .00000      .00000      .00000
  .65217+06   .36957+07   .65217+06   .00000      .00000      .00000
  .65217+06   .65217+06   .36957+07   .00000      .00000      .00000
  .00000      .00000      .00000      .17313+07   .00000      .00000
  .00000      .00000      .00000      .00000      .15217+07   .00000
  .00000      .00000      .00000      .00000      .00000      .15217+07
STEP= 10
STRINC   -.2111+04   -.3260+03   -.3260+03    .0000       .0000       .0000
STRESS  -.64746+04  -.19566+04  -.19566+04   .00000      .00000      .00000
STRAIN  -.30732-02   .10967-04   .10967-04   .00000      .00000      .00000
EPSEL   -.35732-02  -.26019-05  -.26019-05   .00000      .00000      .00000
ICRACK  0
DIRCOS   .10000+01   .00000      .00000      .00000      .10000+01   .00000      .00000      .00000      .10000+01
CMATRIX
  .42217+07   .65217+06   .65217+06   .00000      .00000      .00000
  .65217+06   .36957+07   .65217+06   .00000      .00000      .00000
  .65217+06   .65217+06   .36957+07   .00000      .00000      .00000
  .00000      .00000      .00000      .17313+07   .00000      .00000
  .00000      .00000      .00000      .00000      .15217+07   .00000
  .00000      .00000      .00000      .00000      .00000      .15217+07
STEP= 11
STRINC   -.2111+04   -.3260+03   -.3260+03    .0000       .0000       .0000
STRESS  -.82269+04  -.22826+04  -.22826+04   .00000      .00000      .00000
STRAIN  -.35732-02   .10989-04   .10989-04   .00000      .00000      .00000
EPSEL   -.35732-02  -.26019-05  -.26019-05   .00000      .00000      .00000
ICRACK  0
DIRCOS   .10000+01   .00000      .00000      .00000      .10000+01   .00000      .00000      .00000      .10000+01
CMATRIX
  .63622+06   .65217+06   .65217+06   .00000      .00000      .00000
  .65217+06   .36957+07   .65217+06   .00000      .00000      .00000
  .65217+06   .65217+06   .36957+07   .00000      .00000      .00000
  .00000      .00000      .00000      .26953+06   .00000      .00000
  .00000      .00000      .00000      .00000      .15217+07   .00000
  .00000      .00000      .00000      .00000      .00000      .30133+05
```

7. LISTING OF MAIN PROGRAM FOR TESTING MATPAC PACKAGE

```
$IT FOR MAIN1,MAIN1
C       MATERIAL PACKAGE TEST PROGRAM
        DIMENSION STRESS(6),STRAIN(6),EPSEL(6),STRINC(6),COEFF(15),
       *YCOF(25),DC(3,3),DCS(3,3),AST(3),C(6,6),TITLE(12)
        READ(5,50) TITLE,NRM,ICOMPS,NELTYP,NSTEPS,NSPLIT
   50 FORMAT(12A6/5I5)
        WRITE(6,60)TITLE
   60 FORMAT(//25X,12A6//)
        WRITE(6,70) NRM,ICOMPS,NELTYP,NSTEPS,NSPLIT
   70 FORMAT(    50H       NRM    ICOMPS    NELTYP    NSTEPS    NSPLIT/
      15I10/)
        IF(ICOMPS.EQ.2) GO TO 200
        READ(5,80) COEFF
        WRITE(6,90) COEFF
   80 FORMAT(8F10.0)
   90 FORMAT(// 6H COEFF/(10E12.5) )
        READ(5,80) AST
        IF(NRM.GT.0.) READ (5,80) DCS
        WRITE(6,100) AST,DCS
  100 FORMAT(4H AST, 3E12.4//4H DCS,9E12.5/)
        GO TO 300
  200 READ(5,80)BLKMOD  ,SHRMOD
        READ(5,80)YCOF
        WRITE(6,110) BLKMOD,SHRMOD ,YCOF
  110 FORMAT(10H....BLKMOD,E12.5,10H....SHRMOD,E12.5//6H  YCOF/
      *(10E12.5))
  300 DO 400 N=1,NSTEPS
        READ(5,80) STRINC
        WRITE(6,130)N,STRINC
        CALL MATPAC (STRESS,STRAIN,STRINC,EPSEL,COEFF,BLKMOD ,SHRMOD,
      *YCOF,DC,DCS,AST,NRM,ZK1,ZK2,S12P,ICOMPS,NELTYP,C,ICRACK,NSPLIT)
  130 FORMAT(6H STEP=,I3,/7H STRINC,6E12.4)
        WRITE(6,140) STRESS,STRAIN,EPSEL,ICRACK,DC,C
  140 FORMAT(7H STRESS, 6E12.5/7H STRAIN,6E12.5/6H EPSEL, 6F12.5/7H ICRA
      *CK,I3/7H DIRCOS,9F12.5/8H CMATRIX/(6E12.5))
  400 CONTINUE
        END
```

APPENDIX II

PROCEDURE FOR SETTING UP INPUT FOR ANALYTICAL MODEL

1. INTRODUCTION

Several factors need to be included in the procedure of setting up finite element input for the present analytical model:

a. Element size should be small enough to allow for a better description of stress and/or strain gradients.

b. Elements should be divided to provide an area of steel not to exceed 5 percent of the area of concrete.

c. Element width should be large enough to provide full bond at the start of loading and allow primary cracks to develop within the element (width should be greater than twice thickness of concrete cover).

d. Integration time-step in a dynamic solution should be small enough to allow for better description of sharp rise time of the dynamic input.

e. Element and nodal point numbers and integration time-step requirements are subject to computer budget limitations.

To illustrate the procedure followed to set up input for both static and dynamic cases, two examples were selected. Detailed description of the input will be given in the following subsections. The numerical results and discussions are included in section VI of this report.

2. STATIC EXAMPLE

The geometry of beam 2S1.6-1 of static case S-1 is given in figure 109(a). The finite element mesh used in the analysis was shown in figure 56 and is reproduced as figure 109(b). Sizes and location of elements were chosen such that reinforcing bars were approximately in the center of the elements. The area of tension steel in Elements 1 through 8 is about 5 percent of the

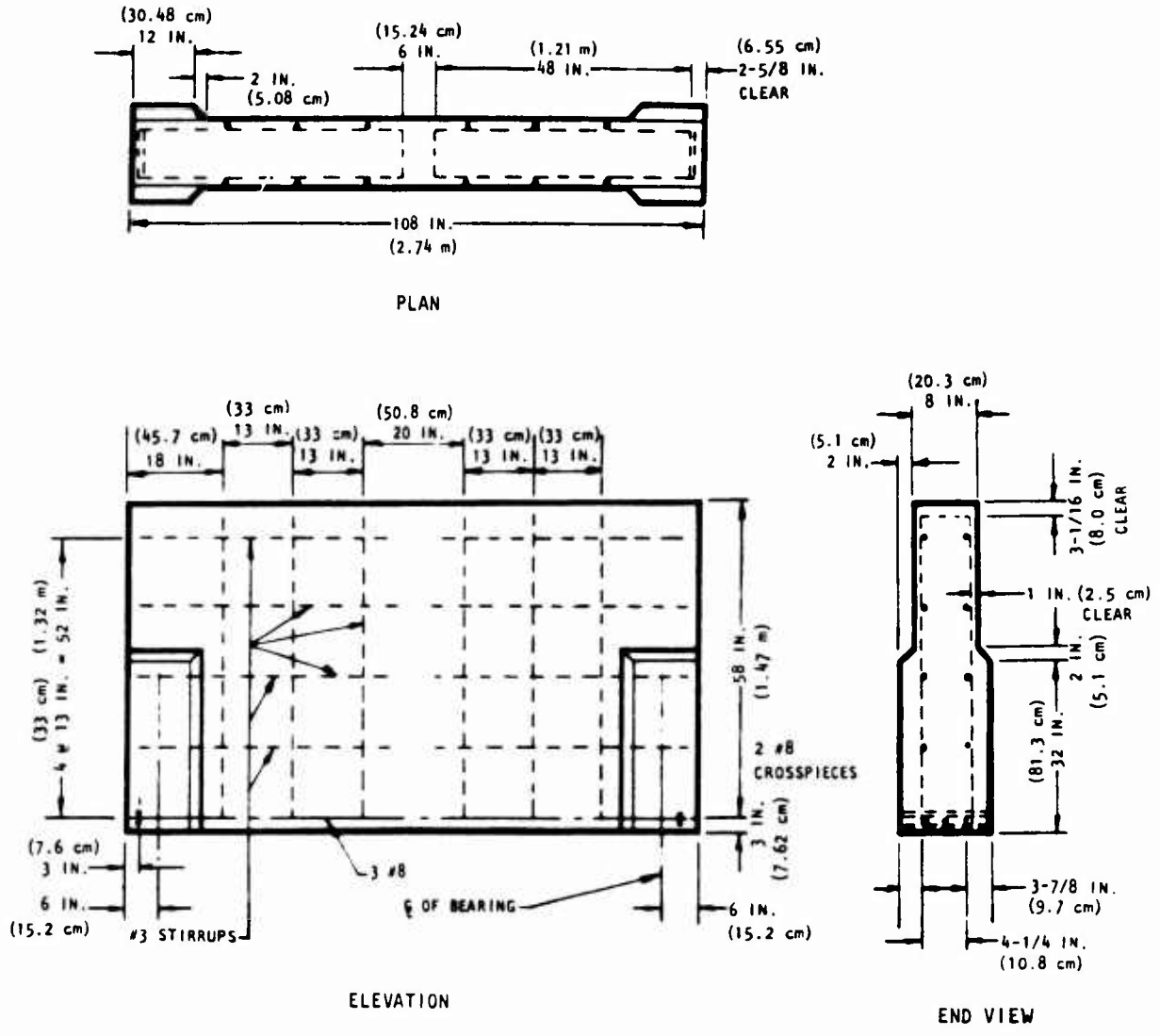

(a) Geometry of beam

Figure 109. Static Beam 251.6-1, Case S-1 (Ref. 89)

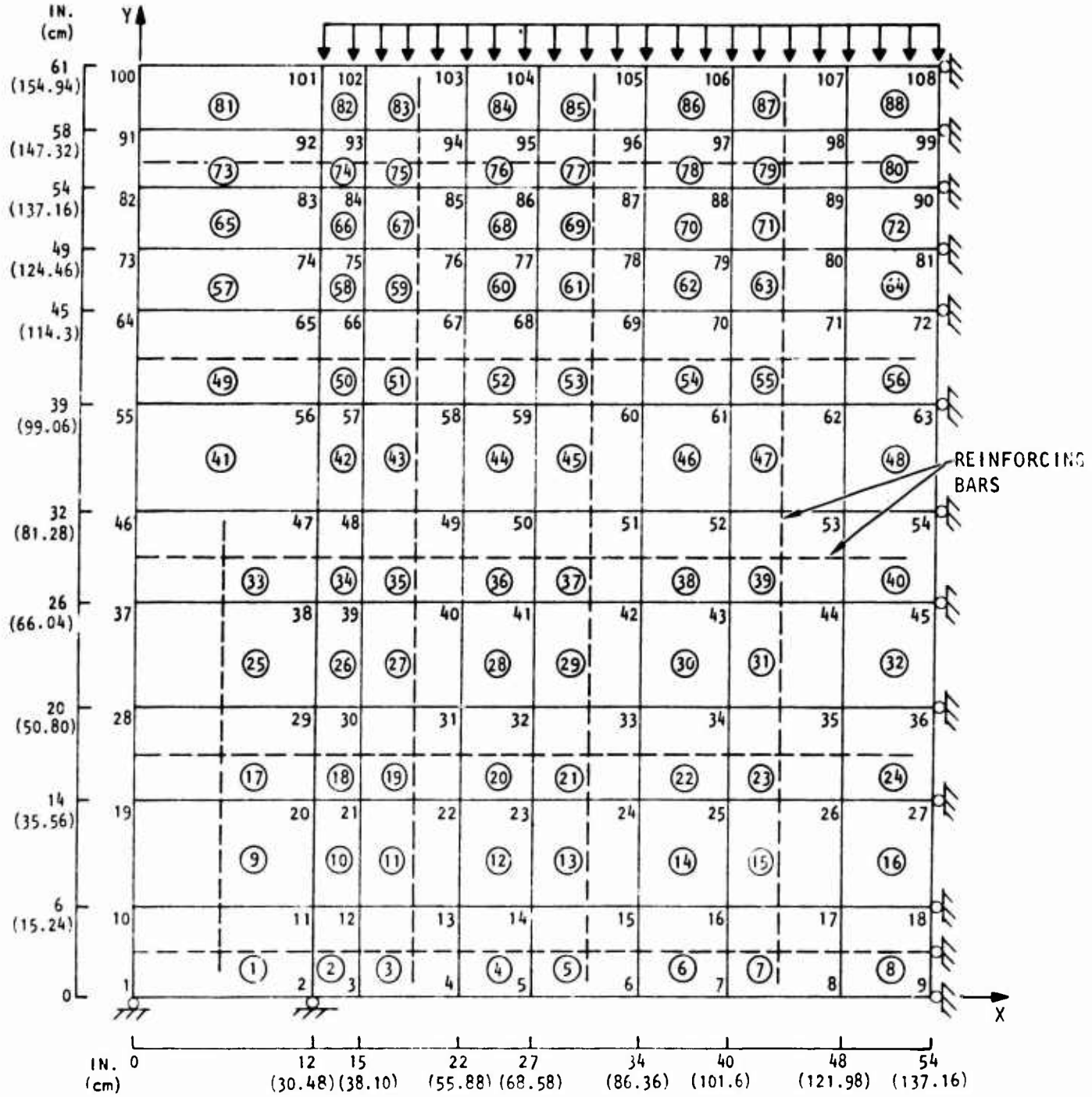

(b) Finite element representation of beam

Figure 109. Static Beam 251.6-1, Case S-1 (Ref. 89) (concluded)

cross-sectional area of the elements (in the x-direction). Area of steel in the other two perpendicular directions ranges between 0.15 and 0.4 percent. These percentages do not exceed the 5 percent that is recommended for satisfactory distribution of steel in elements. The width of elements in the cracking zone ranges from 3 in. (7.6 cm) for Element 2 to 8 in. (20.3 cm) for Element 7. This width was dictated by the location of steel in the vertical direction and the need to monitor stress and/or strain gradient in the x-direction. The width is less than the 18 in. (45.7 cm) required for developing full bond. Therefore, the interpretation of the analytical results should account for this choice. The properties of steel and concrete were based on the data given in reference 89. Young's modulus was calculated using equation 13 as follows:

$$E = 33\, W^{3/2} \sqrt{f'_c} \tag{108}$$

where

W = 145 lb per cubic ft (645 Kg/m^3)

f'_c = 4160 psi (1992×10^4 N/m^2)

Therefore

$$E_c = 3.00 \times 10^6 \text{ psi } (20685 \times 10^6 \text{ N/m}^2) \tag{109}$$

The steel directions coincide with the global directions. Therefore both NRB and DCS will be specified as zero values.

A sample of area of steel calculated for Elements 1 to 8 is given in table IX.

Table IX. Calculated Areas of Steel

A_s/A_c \ Element No.	1	2	3	4	5	6	7	8
x-direction	0.0330	0.05	0.050	0.050	0.050	0.050	0.0500	0.050
y-direction	0.0015	0.0	0.0040	0.000	0.004	0.000	0.0030	0.000
z-direction	0.0	0.0	0.0050	0.000	0.005	0.000	0.0045	0.000

The input parameters were:

NRB = 0 ICOMPS = 1 (for variable modulus model)
NELTYP = 3 (plane stress problem)

NSTEPS = 32 (number of static load steps)

NSPLIT = -1 (indicating strain input to material package)

The material properties in array COEFF are arranged as follows:

CØEFF(1) = 3 x 10^6 psi (20,685 x 10^6 N/m^2) = E_c

CØEFF(2) = 30 x 10^6 psi (20,685 x 10^7 N/m^2) = E_s

CØEFF(3) = 4.16 x 10^3 psi (28,683 x 10^4 N/m^2) = f'_c

CØEFF(4) = 4.8 x 10^4 psi (33,096 x 10^4 N/m^2) = f_y

CØEFF(5) = 0.2 = ν

CØEFF(6) = 365 psi (2517 x 10^3 N/m^2) = f_t

CØEFF(7) = -0.088 = n (slope of cracking envelope)

CØEFF(8) = 4.0 = n (dowel shear coefficient)

CØEFF(9) = 1.20 x 10^7 psi (8274 x 10^7 N/m^2) = G_s

CØEFF(10) = Rebonding coefficient not needed for this example

CØEFF(11 through 15) = 0.0 (not necessary for this case)

3. DYNAMIC EXAMPLE

The geometry of the beam of case D-4 was given in figure 89. The finite element mesh used in the analysis was also shown in the same figure. Sizes and location of elements were chosen such that, whenever possible, reinforcing bars were approximately in the center of the elements. The width of element in the tension cracking zone along the x-axis ranges between 2.125 in. (5.4 cm) for Element 141 to 5.375 in. (13.7 cm) for Element 91. This width was dictated by the location of the vertical steel, the applied vertical loads, the location of beam supports, and the need to monitor stress and/or strain gradient in the x-direction. Since the width of the element in the cracked zone is less than the width recommended for developing full bond, the analytical model is expected to overestimate the stiffness at the early stages of the loading.

The division of the height of the beam, in the y-direction, into 10 elements was mainly dictated by budget limitations. This choice resulted in a bandwidth of 26, 176 nodal points, and 150 elements.

The area of steel in various elements is given in table X and indicates that a high steel ratio of 18 percent of cross-sectional area is used in the row of elements in the tension zone starting with Element 2 (Fig. 89).

This steel ratio is well above the 5 percent recommended for steel distribution, and the effect of its variation should be investigated in future work.

The properties of steel and concrete were based on data given in reference 91.

Since the steel directions coincide with the global directions, both NRB and DCS were specified as zero values.

The selection of integration time step Δt was guided by the rise time t_r of the dynamic input given in figure 90. A rise time of 18 msec was indicated in this figure. The time step Δt is related to the rise time t_r by the empirical relationship

Table X. Steel Ratio for Dynamic Example Case D-4

Element No.	Steel Ratio, A_s/A_c			Element No.	Steel Ratio, A_s/A_c		
	x	y	z		x	y	z
2	0.1802	0.0063	0.0206	82	0.1802	0.0039	0.0127
3 - 8	0	0.0063	0	83 - 88	0	0.0039	0
9	0.1333	0.0063	0.0254	89	0.1333	0.0039	0.0157
12	0.1802	0.0049	0.0160	92	0.1802	0.0031	0.0101
13 - 18	0	0.0049	0	93 - 98	0	0.0031	0
19	0.1333	0.0049	0.0198	99	0.1333	0.0031	0.0124
22	0.1802	0.0033	0.0105	102	0.1802	0.0053	0.0173
23 - 28	0	0.0033	0	103 - 108	0	0.0053	0
29	0.1333	0.0033	0.0130	109	0.1333	0.0053	0.0213
32	0.1802	0.0039	0.0127	112	0.1802	0.0039	0.0127
33 - 38	0	0.0039	0	113 - 118	0	0.0039	0
39	0.1333	0.0039	0.0157	119	0.1333	0.0039	0.0157
42	0.1802	0.0039	0.0127	122	0.1802	0.0039	0.0127
43 - 48	0	0.0039	0	123 - 128	0	0.0039	0
49	0.1333	0.0039	0.0157	129	0.1333	0.0039	0 0157
52	0.1802	0.0039	0.0127	132	0.1802	0.0039	0.0127
53 - 58	0	0.0039	0	133 - 138	0	0.0039	0
59	0.1333	0.0039	0.0157	139	0.1333	0.0039	0.0157
62	0.1802	0.0039	0.0127	142	0.1802	0.0039	0.0127
63 - 68	0	0.0039	0	143 - 148	0	0.0039	0
69	0.1333	0.0039	0.0157	149	0.1333	0.0039	0.0157
72	0.1802	0.0039	0.0127				
73 - 78	0	0.0039	0				
79	0.1333	0.0039	0.0157				

$$\Delta t \cong \frac{t_r}{15} \text{ to } \frac{t_r}{20} \tag{110}$$

or

$$\Delta t = \frac{t_r}{18}$$

$$= 0.001 \text{ sec} \tag{111}$$

The input parameters were:

NRB = 0 ICOMPS = 1 (for variable modulus)

NELTYP = 3 (plane stress problem) NSTEPS = 50

NSPLIT = -1 (indicating strain input to material package)

The material properties in array COEFF are arranged as follows:

CØEFF(1) = 3.74×10^6 psi ($25,787 \times 10^6$ N/m^2) = E_c

CØEFF(2) = 30×10^6 psi ($20,685 \times 10^7$ N/m^2) = E_s

CØEFF(3) = 3.26×10^3 psi ($22,478 \times 10^3$ N/m^2) = f'_c

CØEFF(4) = 4.58×10^4 psi ($31,759 \times 10^4$ N/m^2) = f_y

CØEFF(5) = 0.2 = ν

CØEFF(6) = 450 psi (3103×10^3 N/m^2) = f_t

CØEFF(7) = -0.138 = n (slope of cracking envelope)

CØEFF(8) = 4.0 = n (dowel shear coefficient)

CØEFF(9) = 1.2×10^7 psi (8274×10^7 N/m^2) = G_s

CØEFF 10) = 0.5 = rebonding coefficient

CØEFF 11 through 15) = 0.0 (not needed for this case)

REFERENCES

1. ISENBERG, J.; and ADHAM, S. "Analysis of Orthotropic Reinforced Concrete Structures," *J. of the Structural Div., Proc. ASCE*, 96:ST12 (December 1970).

2. NGO, D.; and SCORDELIS, A. C. "Finite Element Analysis of Reinforced Concrete Beams," *Proc. ACI Journal*, 64:3 (March 1967).

3. NILSON, A. H. "Finite Element Analysis of Reinforced Concrete," Ph.D. dissertation, Div. of Structural Eng. and Structural Mech., Univ. of California, Berkeley, March 1967.

4. SCORDELIS, A. C. "Finite Element Analysis of Reinforced Concrete Structures," paper presented at the Specialty Conference on the Finite Element Method in Civil Engineering, June 1-2, 1972, sponsored by the Bridge and Structural Division of the Engineering Institute of Canada and McGill University, Montreal, Canada.

5. BAGGE, C. F.; and LEE, Y. C. "Applicability of Continuum Models for Jointed Rock-Structure Interaction," *Applications of the Finite Element Method in Geotechnical Engineering*, C. S. Desai (ed.), Proc. of the Symposium held at Vicksburg, Mississippi, May 1-4, 1972.

6. CLOUGH, R. W. "Finite Element Method in Plane Stress Analysis," *Proc., 2nd ASCE Conference on Electronic Computation*, Pittsburgh, September 1960.

7. WILSON, E. L. *Finite Element Analysis of Two-Dimensional Structures*, Report No. 63-2. Berkeley: Univ. of California, Structural Engineering Laboratory, June 1963.

8. ARGYRIS, J. M. "Continua and Discontinua," *Conf. on Matrix Methods in Structural Mechanics*. Wright Patterson AFB: Air Force Inst. of Tech., October 1965.

9. ZIENKIEWICZ, O. C. *The Finite Element Method in Engineering Science*, London: McGraw-Hill, 1971.

10. DESAI, C. S.; and ABEL, J. F. *Introduction to the Finite Element Method, a Numerical Method for Engineering Analysis*. New York: Van Nostrand Reinhold, 1972.

11. CLOUGH, R. W.; and RASHID, Y. "Finite Element Analysis of Axi-Symmetric Solids," *Proc. ASCE, J. of the Engineering Mech. Div.*, 31:EM1 (February 1965) pp. 71-85.

References (Continued)

12. CLOUGH, R. W.; and WOODWARD, R. J. *Analysis of Embankment Stresses and Deformations*, Report No. TE-66-4. Berkeley: Univ. of California, Soil Mech. Lab., September 1966.

13. CLOUGH, R. W., and CHOPRA, A. K. *Earthquake Stress Analysis in Earth Dams*, Report No. 65-S. Berkeley: Univ. of California, Dept. of Civil Eng., July 1965.

14. WILSON, E. L. *A Computer Program for the Dynamic Stress Analysis of Underground Structures*, Report No. 68-1. Berkeley: Univ. of California, Structural Eng. Lab., January 1968.

15. ADHAM, S. A.; and MALTHAN, J. A. *The Finite Element Method for Investigating Edge Effects in the High-Explosive Simulation Technique (HEST), Project HEST Test V*, Technical Report No. AFSWC-TR-68-26. Kirtland AFB, New Mexico: Air Force Special Weapons Center, February 1969.

16. FELIPPA, C. A. *Refined Finite Element Analysis of Linear and Nonlinear Two-Dimensional Structures*, Report No. 66-22. Berkeley: Univ. of California, Structural Eng. Lab., 1966.

17. ZIENKIEWICZ, O. C.; VALLIAPPAN, S.; and KING, I. P. "Elasto-Plastic Solutions of Engineering Problems 'Initial Stress,' Finite Element Approach," *Int. J. for Numerical Methods in Eng.*, 1:1 (1969) pp. 75-100.

18. NGO, D.; SCORDELIS, A. C.; and FRANKLIN, H. A. *Finite Element Study of Reinforced Concrete Beams with Diagonal Tension Cracks*, UCSESM Report No. 70-19. Berkeley: University of California, December 1970.

19. NILSON, A. H. "Nonlinear Analysis of Reinforced Concrete by the Finite Element Method," *Proc. ACI Journal*, 65:9 (September 1968).

20. FRANKLIN, H. A. "Non-linear Analysis of Reinforced Concrete Frames and Panels," Ph.D. dissertation, Div. of Structural Eng. and Structural Mech., University of California, at Berkeley, March 1970.

21. CERVENKA, V., "Inelastic Finite Element Analysis of Reinforced Concrete Panels Under In-Plane Loads," Ph.D. dissertation, Dept. of Civil Eng., Univ. of Colorado, Boulder, 1970.

22. PETER, J. *Zur Bewehrung von Scheiben nud Schalen fur Haptspanning schiefwinkelig zur Bewehrungsrichtung*, thesis presented to the Technishe Hochschule, Stuttgart, in 1964 in partial fulfillment of the Ph.D. requirements.

References (continued)

23. BARNARD, P. R. "Researches into the Complete Stress-Strain Curve for Concrete," *Magazine of Concrete Research*, 16:49 (December 1964).

24. KABAILA, A., Discussion of a paper by Desayi and Krishnan "Equation for the Stress-Strain Curve of Concrete," *ACI Journal*, 61:9 (September 1964) pp. 1227-1235.

25. BALMER, G. C. "Shearing Strength of Concrete Under High Triaxial Stress-Computation of Mohr's Envelope as a Curve," *Structural Research Laboratory Report No. SP-23*. U. S. Dept. of the Interior: Bureau of Reclamation, October 28, 1949.

26. ISENBERG, J. "Inelasticity and Fracture in Plain Concrete," Ph.D. dissertation, University of Cambridge, England, June 1967.

27. ----, "Properties of Concrete Change when Microcracking Occurs," *Symposium on Causes, Mechanism and Control of Cracking in Concrete*, Publication SP-20. Detroit: American Concrete Institute, 1968.

28. ROBINSON, G. S. "Behavior of Concrete in Biaxial Compression," *Proc. ASCE*, 93:ST1 (February 1967) pp. 71-86.

29. TODD, J. D. "The Determination of Tensile Stress/Strain Curves for Concrete," *Proc. of the Institute of Civil Engineers*, Part 1, Vol. 4 (March 1955) pp. 201-211.

30. MC HENRY, D.; and KARNI, J. "Strength of Concrete Under Combined Tensile and Compressive Stress," *ACI Journal*, 54:10 (April 1958) pp. 829-840.

31. BRESLER, B.; and PISTER, K. S. "Strength of Concrete Under Combined Stress," *ACI Journal*, 55 (September 1968) pp. 321-346.

32. RICHART, F. E., et al. "A Study of Failure of Concrete under Combined Compressive Stresses," Bulletin No. 185. Urbana-Champaign: Univ. of Illinois, Experimental Station, November 20, 1928.

33. BROMS, B. B. "Crack Width and Crack Spacing in Reinforced Concrete Members," *ACI Journal, Proc.*, 62:10 (October 1965) pp. 1237-1255.

34. BRESLER, B.; and BERTERO, V. "Behavior of Reinforced Concrete under Repeated Load," *Proc. ASCE*, 94:ST6 (June 1968).

35. SELNA, L. G. *Time-Dependent Behavior of Reinforced Concrete Structures,* SESM Report No. 67-19. Berkeley: Univ. of California, August 1967.

36. ----, "Creep, Cracking, and Shrinkage in Concrete Frame Structures," *J. Struct. Div., ASCE,* 95:ST12 (December 1969).

37. SANDHU, R. S.; WILSON, E. L.; and RAPHAEL, J. M. *Two-Dimensional Stress Analysis with Incremental Construction and Creep,* SESM Report No. 67-34. Berkeley: Univ. of California, December 1967.

38. VALLIAPPAN, S.; and DOOLAN, T. "Nonlinear Stress Analysis of Reinforced Concrete," *J. Struct. Div., ASCE,* 98:ST4 (April 1972).

39. YUZUGULLU, O.; and SCHNOBRICH, W. C., "Finite Element Approach for the Prediction of Inelastic Behavior of Shear Wall-Frame Systems," Structural Research Series No. 386, UILU-Eng-72-2007. Urbana-Champaign: Univ. of Illinois, May 1972.

40. TAYLOR, M. A.; ROMSTAD, K. M.; HERMAN, L. R.; and RAMEY, M. R. "A Finite Element Computer Program for the Prediction of the Behavior of Reinforced and Prestressed Concrete Structures Subject to Cracking," AD-749-998. Davis, California: Univ. of California, June 1972.

41. JOFRIET, J. C.; and McNIECE, G. M. "Finite Element Analysis of Reinforced Concrete Slabs," *J. Struct. Div., ASCE,* 97:ST3 (March 1971).

42. BELL, J. C.; and ELMS, D. "Partially Cracked Finite Elements," *J. Struct. Div., ASCE,* 97:ST7 (July 1971).

43. WAHL, H. W.; and KASIBA, R. J. "Design and Construction Aspects of Large Prestressed Concrete (PWR) Containment Vessels," *ACI Journal,* 66:5 (May 1969).

44. RASHID, Y. R. "Ultimate Strength Analysis of Prestressed Concrete Pressure Vessels," *Nucl. Eng. Design,* 7 (1968) pp. 334.

45. ENDEBROCK, E. G., and TRAINA, L. A. *Static Concrete Constitutive Relations Based on Cubical Specimens, Part I,* Report No. AFWL-TR-72-59. Kirtland AFB, New Mexico: Air Force Weapons Laboratory, December 1972.

46. POPOVICS, S. "A Review of Stress-Strain Relationships for Concrete," *ACI Journal,* 67:3 (March 1970).

47. COWAN, H. J. "The Strength of Plain, Reinforced, and Prestressed Concrete Under the Action of Combined Stresses," *Magazine of Concrete Research,* 5:14 (1953).

48. BRESLER, B., and PISTER, K. "Failure of Plain Concrete Under Combined Stresses," *Trans., ASCE,* 122 (1957).

49. NEWMAN, K. "Criteria for the Behavior of Plain Concrete Under Complex States of Stress," *Proc., International Conference on the Structure of Concrete*, London, 1965.

50. KUPFER, H.; HILSDORF, H.K.; and RUSCH, H. "Behavior of Concrete Under Biaxial Stresses," *ACI Journal*, 66:8 (August 1969).

51. GREEN, S. J.; SWANSON, S. R.; GRIFFIN, R. M.; BUTTERS, S. W.; and PRATT, H. R. *Static Constitutive Relations for Concrete*, AFWL-TR-72-244. Kirtland AFB, New Mexico: Air Force Special Weapons Laboratory, (April 1973).

52. BUYOKOZTURK, O.; NILSON, A. H.; and SLATE, F. O. *Stress-Strain Response and Fracture of a Model of Concrete in Biaxial Loading*, Report No. 337. Ithaca: Cornell University, Dept. of Structural Eng., May 1970.

53. LIU, T. C. Y.; NILSON, A. H.; and SLATE, F. O. "Biaxial Stress-Strain Relations for Concrete," *J. of the Structural Division, Proc. ASCE*, 98:ST5 (May 1972).

54. SAENZ, L. P. "Discussion of 'Equation for the Stress-Strain Curve of Concrete' by P. Desayi and S. Krishman,' " *ACI Journal, Proc.* 61 (September 1964) pp. 1229-1235.

55. DESAYI, P.; and KRISHNAN, S. "Equation for the Stress-Strain Curve of Concrete," *ACI Journal, Proc.*, 61:3 (March 1964) pp. 345-350.

56. PAUW, A. "Static Modulus of Elasticity of Concrete as Affected by Density," *J. of the American Concrete Institute*, 57:6 (December 1960).

57. JONES, R. "The Ultimate Strength of Reinforced Concrete Beams in Shear," *Magazine of Concrete Research*, London, England, 8:23 (August 1956) pp. 69-84.

58. PARMELEE, R. "A Study of the Ultimate Shear Strength of Reinforced Concrete Beams," Graduate Student Report No. 11. Berkeley: Univ. of California, Dept. of Civil Eng., January 1961.

59. KREFELD, W.; and THURSTON, C. *Studies of the Shear and Diagonal Tension Strength of Simply Supported Reinforced Concrete Beams*. New York: Columbia Univ., Dept. of Eng. and Eng. Mech., June 1962.

60. LORENTSEN, M. "Shear and Bond in Prestressed Concrete Beams Without Shear Reinforcement," *Trans., Handlingar No. 47*, National Swedish Council for Building Research, Stockholm, Sweden (1964).

61. BRESLER, B.; and MacGREGOR, J. G. "Review of Concrete Beams Failing in Shear," *J. of the Structural Division*, ASCE, 93:ST1 (February 1967) pp. 343-372.

References (continued)

62. HOFBECK, J. A.; IBRAHIM, I. A.; and MATTOCK, Alan H. "Shear Transfer in Reinforced Concrete," *ACI Journal, Proc.*, 66:2 (February 1969) pp. 119-128.

63. JOHNSTON, D. W.; and ZIA, P. "Analysis of Dowel Action," *J. of the Structural Division, ASCE*, 97:ST5 (May 1971) pp. 1611-1630.

64. ACI-ASCE Committee 426, *The Shear Strength of Reinforced Concrete Members*, Preliminary Draft Report, July 1972.

65. DULACSKA, H. "Dowel Action of Reinforcement Crossing Cracks in Concrete," *ACI Journal*, Digest No. 69-70 (December 1972) pp. 754-757.

66. ISMAIL, M. A. F.; and JIRSA, J. O. "Bond Deterioration in Reinforced Concrete Subject to Low Cycle Loads," *ACI Journal*, 69 (June 1972).

67. TANNER, J. A. "An Experimental Investigation of Bond Slip in Reinforced Concrete," M.S. Thesis, Cornell University, Ithaca, New York, November 1971.

68. BERNANDER, K. G. "Vidhaftningens beroende av kamarea och kamavstand hos armeringsstal," *Betong*, No. 1 (1952).

69. BRICE, L. D. "Adherance des Barres d'Acier dans le Beton," *Annales*, l'Institute Technique du Batiment et des Travaux Publics, Paris, No. 179 (1951).

70. CLARK, A. P. "Cracking in Reinforced Concrete Flexural Members," *ACI Journal, Proc.*, 52:10 (April 1956) pp. 851-862.

71. EFESEN, A.; and KRENCHEL, H. "Prognosis of the Crack Problems in Reinforced Concrete Based on Statistical Investigations," *Proc.*, Symposium on Bond and Crack Formation in Reinforced Concrete (Stockholm, 1957), RILEM, Paris (Published by Tekniska Hogskolans Rotaprinttryckeri, Stockholm, 1958).

72. GASTON, J. R.; and HOGNESTAD, E. "High Strength Bars as Concrete Reinforcement. 3--Tests of Full Scale Roof Girder," *Journal*, PCA Research and Development Laboratories, 4:2 (May 1962) pp. 10-23.

73. HOGNESTAD, E. "High Strength Bars as Concrete Reinforcement. 1--Introduction to a Series of Experimental Reports," *Journal*, PCA Research and Development Laboratories, 3:3 (September 1961) pp. 23-38.

74. ----, "High Strength Bars as Concrete Reinforcement. 2--Control of Flexural Cracking," *Journal*, PCA Research and Development Laboratories, 4:1 (January 1962) pp. 46-62.

References (continued)

75. KAAR, P. H.; and MATTOCK, A. H. "High Strength Bars as Concrete Reinforcement. 4--Control of Cracking," *Journal*, PCA Research and Development Laboratories, 5:1 (January 1963) pp. 15-38.

76. KUUSKOSKI, V. "Uber die Haftung zwischen Beton und Stahl," Publication No. 19, The State Institute for Technical Research, Finland: Helsinki, 1950.

77. REHM, G. "Uber die Grundlagen des Verbundes zwischen Stahl und Beton," Bulletin No. 138, Deutscher Ausschuss fur Stahlbeton, Berlin, 1961.

78. WATSTEIN, D. "Distribution of Bond Stress in Concrete Pull-Out Specimens," *ACI Journal, Proc.*, 43:9 (May 1947) pp. 1041-1052.

79. WATSTEIN, D.; and MATHEY, R. B. "Widths of Cracks at the Surface of Reinforcing Steel Evaluated by Means of Tensile Bond Specimen," *ACI Journal, Proc.*, 56:1 (July 1959) pp. 47-56.

80. BASE, G. D., et. al. "An Investigation of the Crack Control Characteristics of Various Types of Reinforced Concrete Beams," Research Report No. 18, Part 1 and Part 2, Cement and Concrete Association, London, December 1966.

81. HUSSAIN, S. I. "Flexural Crack Width by Epoxy Injection into Reinforced Concrete Beams," thesis presented to the University of Texas at Austin, Texas in 1968, in partial fulfillment of the requirements for the Ph.D. degree.

82. LUTZ, L. A.; and GERGELY, P. "Mechanics of Bond and Slip of Deformed Bars in Concrete," *Journal of the American Concrete Institute, Proc.*, 64 (November 1967) pp. 711-721.

83. LUTZ, L. A. "Analysis of Stresses in Concrete Near a Reinforcing Bar Due to Bond and Transverse Cracking," *J. of the American Concrete Institute*, 67 (October 1970) p. 778.

84. VENKATESWARLU, B. "Bond Slip and Cracking in Reinforced Concrete Beams," thesis presented to the University of Kentucky at Lexington, Kentucky, in 1970, in partial fulfillment of the requirements for the Ph.D. degree.

85. LEVI, F. "Work of the European Concrete Committee," *ACI Journal, Proc.*, 57:9 (March 1961) pp. 1041-1070.

86. ODMAN, S. T. A. "Slip Between Reinforcement and Concrete," *Proc.*, Symposium on Bond and Crack Formation in Reinforced Concrete (Stockholm, 1957), RILEM, Paris (Published by Tekniska Hogskolans Rotaprinttryckeri, Stockholm, 1958).

References (concluded)

87. MAINS, R. M. "Measurement of the Distribution of Tensile and Bond Stresses Along Reinforcing Bars," *JACI*, 23:3 (November 1951) pp. 225-252.

88. *1972 Annual Book of ASTM Standards*, Part 4. Philadelphia: American Society for Testing and Materials, 1972.

89. CRIST, Robert "Static and Dynamic Shear Behavior of Uniformly Loaded Reinforced Concrete Deep Beams," Report No. AFWL-TR-71-74. Kirtland AFB, New Mexico: Air Force Weapons Laboratory, November 1971.

90. LANE, E. G. "Static Behavior of Reinforced Concrete Beams," to be published by Air Force Weapons Laboratory, Kirtland AFB, New Mexico, 1974.

91. FELDMAN, A.; KEENAN, W. A.; and SIESS, C. P. "Investigation of Resistance and Behavior of Reinforced Concrete Members Subjected to Dynamic Loading, Part III," Report No. DASA-1259, D74-174. Urbana, Illinois: Univ. of Illinois, February 1962.